THE STATIC ANALYSIS OF COMPOSITE AIRCRAFT WING-BOX STRUCTURE

Asst. Prof. Dr. Ahmed A. Ali
Mechanical Eng. Dept. , College of Eng.
Baghdad University, Bagdad, Iraq

Asst. Lect. Azhar K. Farhood
Mechanical Eng. Dept. , College of Eng.
Baghdad University, Bagdad, Iraq

ABSTRACT

In this paper, the static analysis for finding the best location of boxes inside the composite wing-box structure has been performed. A software ANSYS (ver.11) was used to analyses the Aluminum wing to find the maximum stresses reached in.

These results are used as a base for the composite wingbox to find the numbers of layers and location of the box beam and its dimensions so that the composite wingbox may carry the same loading conditions in the Aluminum wing. Analysis showed that a composite wingbox having two boxes is better than the single or triple boxes wing based on stress to weight ratio. Mass saving of (40%) had been achieved when composite wing-box is used instead of Aluminum wing.

الخلاصة

يتضمن البحث ايجا د افضل موقع للصندوق داخل الجناح الصندوقي المركب من خلال التحليل السكوني للهيكل. أستخدم برنامج (ANSYS11) لايجاد اعلى اجهاد يتحمله جناح الالمنيوم.

هذه النتائج استخدمت كأ ساس في تصميم الجناح الصندوقي المركب لايجاد عدد الطبقات وموقع وابعاد الصندوق وبذلك سوف يتعرض النموذج لنفس الحمل المسلط على الجناح القياسي. بينت التحاليل بأن الجناح المركب الحاوي على صندوقين افضل من الأحادي و الثلاثي و ذلك اعتمادا على النسبة بين الإجهاد / الوزن وان النقصان الواضح في قيمه الكتله عند استخدام الجناح الصندوقي المركب بدل من جناح الالمنيوم القياسي كان بمقدار(40%).

Keywords: wing-box, aircraft structure, composite wing

1. Introduction

As today's military aircraft are required to fly faster, higher and a further, the trend in the wing boxes of such aircraft is towards lighter and thinner structures. One factor which is helping to achieve these aims is the emerging use of composite materials in the primary structure of aircraft because they have a greater strength/weight ratio than conventional aluminum alloys. The use of a multi box wing for the wing box helps meet the requirement for thinness by allowing low wing box depths while still achieving the necessary bending rigidity.

Snell and Bartholomew 1987 studied the minimum weight design of multidirectional carbon fiber reinforced plastic (CFRP) plates under uniaxial compression was first considered. The results of this study were applied to the optimization of multi-spar wing bend boxes under bending and vertical shear loading, using geometric programming. Based on the present simplified modeling, overall weight savings proportional to the material densities of the order of 40% can therefore be expected from the use of composite materials in corrugated spars.

Greenhalgh et-al 1993 Concluded that beneficial twist-bend coupling can be induced in wing box-beam members using conventional continuous fiber fabrication processes. Experimental tests were conducted on five beams to determine beam twist and bend as a function of load at various fiber angle layups. The maximum twist-bend coupling was exhibited at a layup angle of approximately 17°.

Astonused and Williams 1994 presented the buckling analysis of multi-spar wing boxes made from composite materials. Used the lower bound method and the repetitive analysis method. Both methods were illustrated by using the computer program VICONOPT to analyze six variants of a laboratory test specimen of the type used when developing multi-spar wing boxes. The results indicate that the lower bound method usually achieves accuracy well within 10%.

Peter et-al. 2000 established the aeroelastic effects of variation of composite fiber orientation, root flexibility, and stacking of plies for a rectangular closed thin-walled wing box. Used the finite element code ASTROS. The research showed that the root stiffness had a significant influence on the modal response of a wing. It also showed that this behavior influenced the aeroelastic properties of the lifting surface.

Guo et-al. 2003 presented an analytical study on optimization of a laminated composite wing structure for achieving a maximum flutter speed and a minimum weight without strength penalty. Results from a thin-walled wing box made of laminated composite material show that up to 18 per cent increase in flutter speed and 13 per cent reduction in weight can be achieved without compromising the strength. The investigation shows that a careful choice of initial lay-up and design variables leads to a desirable bending, torsional and coupling rigidities, with the provision of an efficient approach when achieving a maximum flutter speed with a minimum mass of a composite wing.

Koundouros et-al. 2004 used the finite element method in conjunction with the Soutis-Fleck model to predict the residual strength after impact of a carbon-fiber reinforced plastic wingbox subjected to a cantilever type loading. The maximum stress failure criterion further validates the Soutis-Fleck model predictions. The Soutis-Fleck model predicts that the wingbox fails at approximately 5.5% less than the experimental observation.

Rohani 2004 presented an investigation on the design and optimization of a thin composite wing box structure for a civil tilt-rotor aircraft. Two different concepts are considered for the cantilever wing: (a) a thin monolithic skin design and (b) a thick sandwich skin design. The global-local

technique was used in the analysis and optimization of the six design models. The optimum skin ply pattern for the monolithic skin concept is found to be ((0/±45/90/ (0/90)2) s) s while for the sandwich skin concept the optimal ply pattern was found to be ((0/±45/90)2s)s.

Buchanan 2007 investigated the use of a structural design optimization process to develop an alternative light weight design for a wing box rib. The approach utilized accepted finite element analysis procedures in two iterative loops to derive structures by formulation of a design optimization problem. Definition of a CAD model of the final concept provided indication that a weight saving of approximately 10% over traditional design approaches could be obtained.

Ryu et-al. 2008 noticed the deformation of the composite wing box under bending load was monitored in real time by using the built-in fiber Bragg grating strain sensors. The measured strains showed good agreement with those by twenty electrical strain gages. Also, the experimental results were analyzed and compared with the results simulated by a finite element method. Bending-induced buckling occurred in the wing box and the embedded fiber Bragg gration sensors successfully monitored the buckling behaviors of the top skin and front spar.

The objective of this paper built up the best boxes inside the wing box structure by using software (ANSYS11), based on changing the number of layers, orientation and number of boxes, manufacturing a composite wing box from (E-glass) that may carry the same loading condition for the standard Aluminum wing and having a less weight than the Aluminum wing.

2. Wing Specification

In this work an Aluminum model is constructed to obtain the maximum load that may be carried by the standard wing that makes the stress reaches its maximum or ultimate value in the root of the wing. This value of load is used in the composite wingbox model design to estimate the best location (as shown in **Fig.1)** of the boxes inside wing section. **Table 1** and **Fig.2** shows the wing body configuration data [11].

3. Beam Used in The Wing Standard Structure.

Properties of the beam section used in building the wing longitudinal stiffeners are shown in **Table 2.**

4. Materials Used in the Wing Structure.

The properties of the isotropic materials used in building the wing structure are shown in **Table 3.**

5. Finite Element Analysis of Standard Aircraft Wing

The finite element analysis will be used to obtain the displacement, stress, as they are considered the main design parameters. The wing will be divided into elements for the isotropic shell structure the element (4-node quadrilateral element) had been used. The elements shell 63 and beam 4 are used for wing standard as Shown in **Table 4** .

6. Structural Model

The structural model used in this work is in the form of a two boxes, fiber-reinforced composite wingbox shown in **Fig.3**.The considered structure model is similar to that developed in Ref.[12].**Table 5** shows experimental mechanical properties of woven glass fibers.

7. Element Type of the Model

The composite wingbox of the aircraft consists of box, ribs, as well as lower and upper skin, so the wing will be divided into elements for the orthotropic shell structure, where the element (8-node octeral element) as shown in **Fig.4** had been used for modeling.

Each node on this element has six degree of freedom (three translation and three rotation). The region of the wing root are built in so (u = v = w = $\theta_x = \theta_y = \theta_z = 0$). For the analysis of the three dimensional model, the finite element tool (ANSYS 11) is used. The element shell 99 is used for wing model. A convergence in the numerical results calculated by ANSYS is achieved after using (29374)D.O.F , where the value of stress shows a good stability in this range as shown in **Fig.5**.

8. Experimental work

The primary objective of the methodology is to obtain the deflection of the composite wing box model structure, subjected to transverse static load and calculating the deflection at the tip end of the wing using an LCD CAMERA (12 mega pixel) having a resolution of 0.001474 mm/pixel for each image captured by the camera, the rig for the experimental work as illustrated in **Fig.6** .The load is applied as a concentrated force on the tip end from 1to 11 kg by steps of 1kg each as shown in **Fig.7**, images are captured for each step of loading and where analyzed to calculate the difference in pixels between each step of loading. This difference is multiplied by the resolution to obtain the deflection for each step of loading. The results are compared with the tradition way of monitoring deflection using DIAL GAGE having a accuracy of 0.01mm as shown in **Fig.8**. The results shows a good agreement, these results are compared with the numerical results obtained by ANSYS11 and little difference between them was observed this difference is due to the miss contact between some parts in the experimental model which plays a big part in reducing the stiffness of the model.

9. Results

Structure analysis Package ANSYS was used to examine the best box (one box, two boxes and three boxes) and better location of the boxes inside the wing from the less stress to weight Ratio, as well as the less stress of fiber orientation and number of layer for composite material under static load. Experimental program was used to estimate the deflection and to compare it with the numerical results.

10. The Best Location of Boxes inside the Wing

A structure analysis was achieved by using ANSYS11 in order to study wingbox in static loading condition. The analysis results for one box of composite material and its results are shown in **Table 6** and **Fig. 9**, In case 40% for cord length(C) can be noticed that this ratio gives the best location of one box because the stress to weight ratio is (7.628129) which is less than the other ratios.

Also **Tables 7** and **8** show the best location of two and three boxes, where the case 31%cord is the better for two boxes while the results for three boxes is at 35%cord.

Figs. 9, 10 and **11** shows the smaller ratio of the one box, two boxes and three boxes inside the wing, where in **Table 9** the ratio for the two boxes is the best because the minimum value is (6.873) at 31%cord, as well as the deflection which are less than the one boxes at 40%cord and three boxes at 35%cord.

11. The Effect of Fiber Orientation for The Two Boxes Wing

An optimization analysis based on varying the orientation of the four layers of woven fiber for the two box section is done in this work. That the fiber orientation (90/0/0/90) has a minimum value of stresses which is (74.5Mpa) at the root for composite wingbox as shown in **Fig.12** when compared with other fiber orientation, therefore it is a good orientation.

12. Structural Testing

A tailored composite wing box for methodology was subjected to transverse static load at the tip. **Tables 10** and **11** show the experimental and numerical results for six

layers (two layers for skin and four layers for the box), of the two boxes with over all thickness (4mm). When changing the load for each case there is a little deference between the value of the displacements measured numerically and experimentally, this is due to the miss in contact between the various parts of the wing as shown in **Figs. 13** and **14**.

Fig. 15 shows the deflection shape for the wing box model obtain from numerical analysis by ANSYS at maximum loading.

13. Conclusions

The main conclusions obtained from the present work can be summarized as follow:

1. From the results obtained from ANSYS software it's found that the wingbox with double boxes section is better than the single and triple boxes section from the side that the double boxes section has a stress to weight ratio (9.9% and 1.0196%) less than the other sections respectively.
2. The composite double box wing section has a (40%) less weight than the traditional Aluminum wing which carries the same loading condition.
3. The orientation of the woven fibers (90, 0, 0, 90) for the inside boxes gives the minimum stress compared with the other orientations.
4. In the case of the single box section the dimensions of the box should be 40% of cord length to give the minimum stress /weight ratio, whereas for double box section the ratio is 31% of the cord length and for the triple section the ratio is 35%.
5. In calculating the minimum number of layers needed in constructing the interior boxes that will carry the same load, the Aluminum wing results show that choosing two or three layers makes the stress reach the region of ultimate stress. Therefore, four layers had been chosen to make the stress within the range of allowable value.
6. The use of digital LCD camera in measuring deflection is more accurate from the dial gage where an accuracy of 0.001474 mm/pixel had been achieved.
7. The use of tapered composite wingbox section is easier in constructing and manufacturing from a rectangular composite wingbox section.

14. References

Chi-Young Ryu, Jung-Ryul Lee, Chun-Gon Kim and Chang-Sun Hong "Buckling behavior monitoring of a composite wing box using multiplexed and multi-channeled built-in fiber bragg grating strain sensors", NOT&International 41, (2008), 534-543.

E. S. Greenhalgh, C. M. Pastore and M. Garfinkle "A continuous-fiber composite wing box-beam exhibiting twist-bend coupling", composite engineering, vol.3, Nos 7-8, pp.691-697, 1993.

G. Aston and F. W. Williams "Simplified methods for the buckling analysis of composite multi-spar wing boxes", Composite Structures28, (1994), 215-223.

Guo S.J., Bannerjee J.R. and Cheung C.W. "The effect of laminate lay-up on the flutter speed of composite wings", Journal of aerospace engineering, vol.217, No.(3), pp115-122, 2003.

Lie Qiu and Shenfang Yuan "On development of a multi-channel PZT array scanning system and its evaluating application on UAV wing box", Sensors and Actuators A 151 (2009) 220–230.

M. B. Snell and P. Bartholomew "The engineering optimization of hybrid composite/metallic wing boxes for buckling and strength constraints", Composite Structures7, (1987), 21-58.

MasoudRais-Rohani "Global-local analysis and optimization of a composite civil tilt-rotor wing", NASA Langley grant NAG 1-1571,2004.

Megson T.H.G "Aircraft structure for engineering students" Arnold, 1999.

Michael Koundouros, Brian G. Falzon, Costas Soutis and Steven J.Lord "Predicting the ultimate load of a CFRP wing box", composite: part A35, (2004), 895-903.

Peter W. G. De Baets, Rupinder S. Battoo and Dimitri N. Mavris "Aeroelastic analysis of a Composite wing box with varying root flexibity", AIAA-2000-1623.

Shijun Guo "Aeroelastic optimization of an aerobatic aircraft wing structure", Aerospace Science and Technology 11 (2007) 396–404.

Sid Buchanan "Development of a wing box rib for a passenger Jet aircraft using design optimization and constrained to traditional design and manufacture requirements", Altair Engineering, 2007.

Table (1) Wing body configuration data.

Wing span(m)	4.6
Aspect ratio	6.7
Taper ratio	0.44
Root chord(m)	2.03
Tip chord(m)	0.8932
Wing root section profile	NACA 23015
Wing tip section profile	NACA 23012
Wing shape	Trapezoidal

Table (2) Properties of beam section [11].

Beam section type	**Representation**	**Cross sectional area(m^2)**	**I_{xx}(m^4)**	**I_{yy}(m^4)**
	stringers	$69*10^{-6}$	$0.75418*10^{-8}$	$0.13387*10^{-8}$

Table (3) Properties of the isotropic material [11].

Material	**Young modulus(Gpa)**	**Yield stress(Mpa)**	**Poisson Ratio**	**Density(kg/m3)**
[AL]7075-T6	71	470	0.33	2800

Table (4) Finite element of the wing

Parts	Type of element(ANSYS11)
Surface(isotropic)	Shell63(4-node quadrilateral element)elastic shell
Ribs	Shell63(4-node quadrilateral element)elastic shell
Spars	Shell63(4-nodequadrilateral element)elastic shell
Stringers	Beam 4(3-D elastic beam)

Table (5) Experimental mechanical properties.

composite	E_x (Gpa)	E_y (Gpa)	σ_{yeild} (Mpa)	υ_{xy}	υ_{yz}	G_{xy} (Gpa)
Woven fiber	38	38	227.1	0.23	0.053	5.3

Table (6) Results of optimization for one box section.

One box					
cases	**%c**	**Deflection (m)**	**Stress (Mpa)**	**Weight (kg)**	**Ratio (σ/w)**
1	9	0.395724	143	17.20267	8.312663
2	18	0.394092	146	17.6276	8.282466
3	22	0.395176	145	17.4785	8.295906
4	31	0.401061	131	17.1381	7.643788
5	40	0.413952	128	16.76	7.628129
6	49	0.429199	176	16.45	11.6991
7	58	0.457167	231	16.1414	14.311
8	76	0.517133	159	15.38111	10.3373355

Table (7) Results of optimization for two boxes sections.

Two box					
cases	**%c**	**Deflection (m)**	**Stress (Mpa)**	**Weight (kg)**	**Ratio (σ/w)**
1	18	0.372529	128	18.53	6.91
2	31	0.37535	124	18.0416	6.873
3	36	0.37765	130	17.872	7.274
4	45	0.387795	134	17.5422	7.639
5	49	0.3912926	135	17.353	7.78

Table (8) Results of optimization for three boxes sections.

Three box					
cases	**%c**	**Deflection (m)**	**Stress (Mpa)**	**Weight (kg)**	**Ratio (σ/w)**
1	27	0.381653	129	18.21203	7.08323
2	35	0.382764	126	18.14568	6.9438
3	67	0.38509	137	17.1743	7.977035

Table (9) A comparison between the three types of wings showing the stress to weight ratios and box dimensions relative to cord

Types	Stress(Mpa)	Weight(kg)	Ratio (Mpa/kg)	Dimension relative to cord length %
One box	128	16.76	7.62813	40%
Two boxes	124	18.0416	6.873	31%
Three boxes	126	18.14568	6.9438	35%

.

Table (10) Experimental determination of the deflection at the tip of the composite wingbox experimentally using (camera) and Ansys, (2skin layers and 4layers for box),4mm thickness.

		Deflection(mm)		
case	Load(kg)	Experimental(Camera)	ANSYS(ver.11)	Error%
1	1	0.1322	0.118	10.74%
2	2	0.26532	0.236	11.05%
3	3	0.39	0.354	9.23%
4	4	0.50434	0.472	6.4%
5	5	0.66	0.59	10.6%
6	6	0.8	0.708	11.5%
7	7	0.9125	0.826	9.48%
8	8	1.06	0.964	10.9%
9	9	1.15	1.062	7.65%
10	10	1.3	1.18	9.23%
11	11	1.4	1.298	7.28%

Table (11) Experimental determination of the deflection at the tip of the composite wingbox experimentally using (camera) and dial gage ,(2skin layers and 4layers for box),4mm thickness.

		Deflection(mm)		
case	Load(kg)	Dial gage	Camera	Error%
1	1	0.145	0.1322	8.8276%
2	2	0.292	0.26532	9.137%
3	3	0.4	0.39	2.5%
4	4	0.55	0.50434	8.3%
5	5	0.695	0.66	5.036%
6	6	0.86	0.8	6.977%
7	7	0.95	0.9125	3.95%
8	8	1.18	1.06	10.17%
9	9	1.25	1.15	8%
10	10	1.4	1.3	7.143%
11	11	1.52	1.4	7.9%

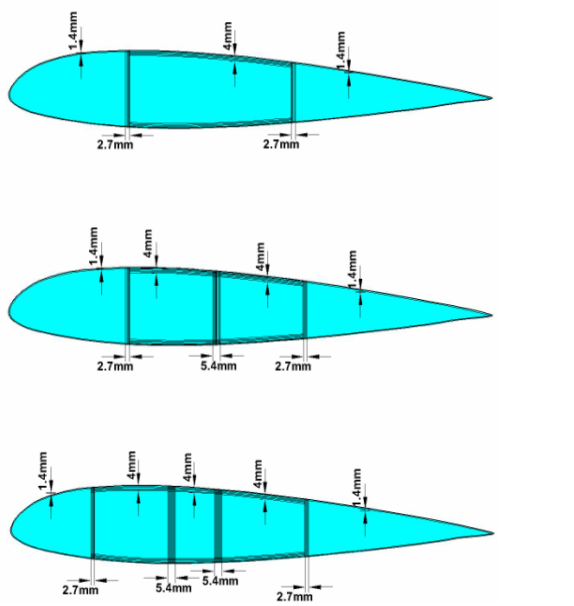

Figure (1) Types of the wing box sections.

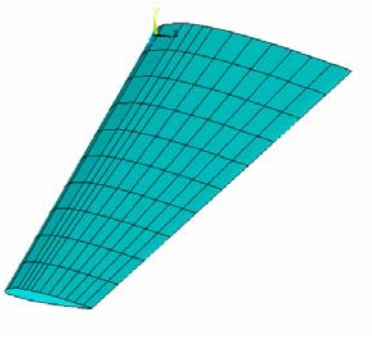

Figure (2) Shape of standard wing.

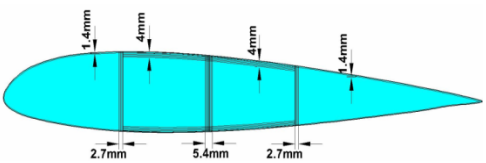

Figure (3) Composite wingbox.

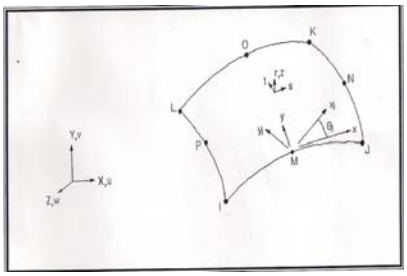

Figure (4) Element - 8nodes.

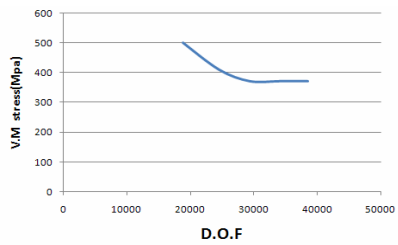

Figure (5) Stability of results for taper wingbox.

Figure (6) Using digital camera for calculating deflection.

Figure (7) Rig used for the experimental work

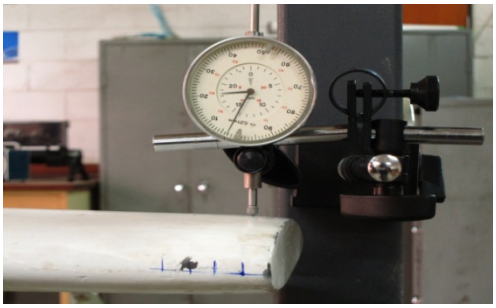

Figure (8) Dial Gage for measuring tip deflection.

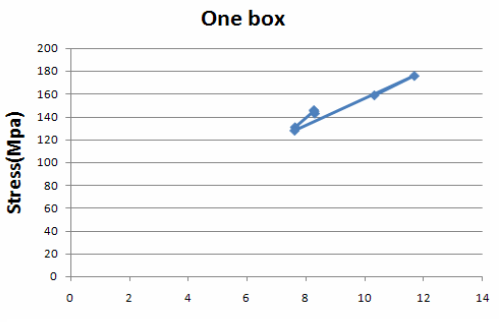

Figure (9) Stress to weight ratio for one box section.

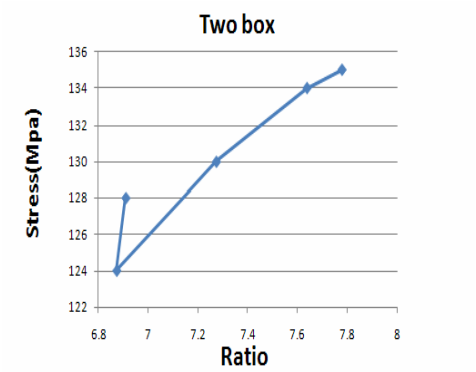

Figure (10) Stress to weight ratio for two boxes section.

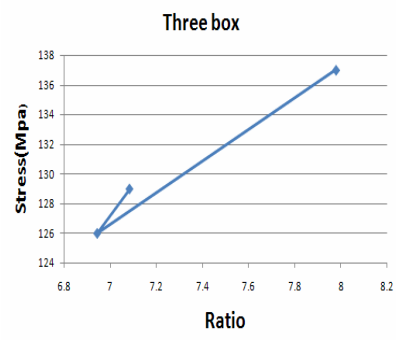

Figure (11) Stress to weight ratio for three boxes section.

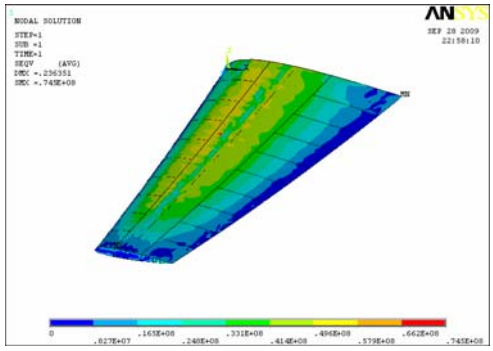

Figure (12) Minimum value of stress at the wing root with (90/0/0/90) fibers orientation.

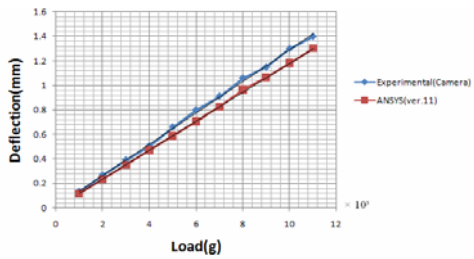

Figure (13) Measured deflection by the camera and ANSYS.

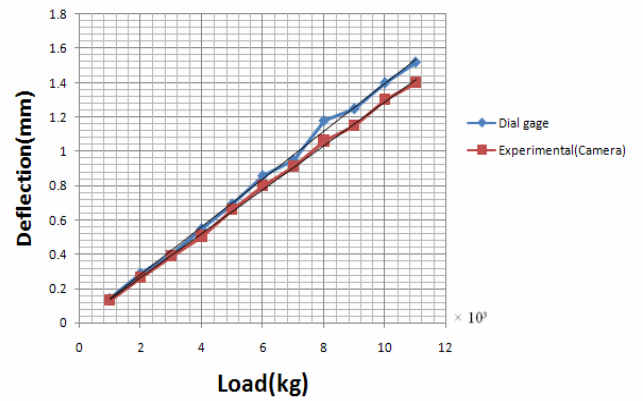

Figure (14) Measured deflection by the camera and Dial gage.

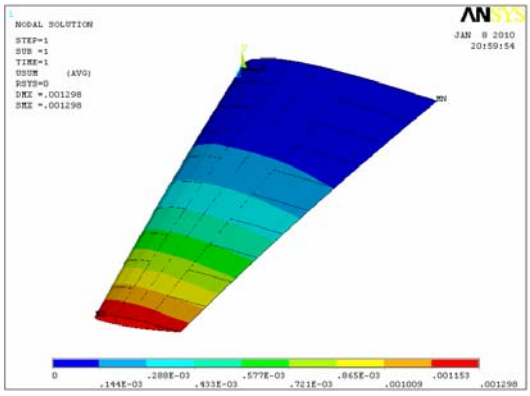

Figure (15) Deflected shape of model at maximum load for.

An Experimental Investigation on Fatigue Properties of AA3003-H14 Aluminum alloy Friction Stir Welds

Dr.Ayad M. Takhakh
ayadtakak@yahoo.com

Asmaa M. Abdullah
rx_am@yahoo.com

Al- Nahrain University
Baghdad -Iraq

ABSTRACT

AA3003-H14 aluminum alloy plates were welded by friction stir welding and TIG welding. Fatigue properties of the welded joints were evaluated based on the superior tensile properties for FSW at 1500 rpm rotational speed and 80 mm/min welding speed. However, there is not much information available on effect of welding parameters with evolution of fatigue life of friction stir welds. The present study experimentally analyzed fatigue properties for base, FSW, and TIG welds of AA 3003-H14 aluminum alloy. Fatigue properties of FSW joints were slightly lower than the base metal and higher than TIG welding.

الخلاصة

تم لحام سبيكة المنيوم نوع AA3003-H14 باستخدام طريقة اللحام الاحتكاكي بالمزج FSW وكذلك باستخدام طريقة اللحام بغاز التنكستن الخامل TIG . وقد تم دراسة خواص الكلال للملحومات و للمعدن الاساس، وبالنسبة لملحومات FSW تم اختيار افضل كفاءة لحام عند سرعة دورانية 1500 دورة/دقيقة وسرعة لحام 80 ملم/دقيقة ، و لعدم توفر معلومات كافية حول تأثير متغيرات لحام FSW على خواص الكلال تم في هذا البحث دراسة خواص الكلال لملحومات FSW ومقارنتها بالمعدن الاساس وبطريقة اللحام TIG وبينت النتائج من خلال معادلة العمر ان ملحومات FSW تمتلك خواص كلال اقل قليلاً من المعدن الاساس واعلى من ملحومات TIG .

Keywords: AA3003-H14 aluminum alloy, Friction stirs welding, Fatigue properties,

INTRODUCTION

Friction stir welding (FSW) is a solid state joining process suitable for joining aluminum alloys developed by The Welding Institute (TWI), UK in 1991 . The process consists of a spinning cylindrical pin with a stepped shoulder, which is pressed against the seam line of the two parts to be welded .As the pin rotates, it penetrates the plates inducing a plastic deformation and then translates along the weld line .The friction between the tool and the parts produces material stirring motion that results in the weld .Thus far, the FSW process has been successfully developed and applied in various cases, but the process itself is not yet fully understood [M. Awang, et al 2005]. Friction stir welding has been applied to metals with moderate melting points .Initially, FSW was applied primarily to aluminum alloys, which could be easily welded due to the relatively low softening temperatures of these alloys . Other relatively soft metals, such as copper, lead, zinc, and magnesium, have also been welded .In contrast, for a number of years it was difficult to weld ferrous alloys and other high softening- temperature metals due to the lack of suitable tool materials [Carl and Tracy 2007].

MIG welding is a flexible and productive method and is therefore widely used for welding aluminum alloys in shipbuilding . However, two disadvantages with MIG welding are the deformation of the base material and a decrease in the strength of the heat affected zone.

Other fusion welding techniques like TIG and plasma welding are also widely used . However, these methods have the same weakness as MIG welding .An alternative to other fusion welding methods is the recently introduced Friction Stir Welding technique [Helena and Leif Karlsson 2000, L. Fratini et al 2007,and Vladvoj et al 2005].

Welding parameters and stirrer geometry effect, and tool effect on FSW have been studied [D .Booth and I .Sinclair 2000, P. Cavaliere et al 2008, Mustafa Boz and Adem Kurt 2004]. The typical welding defects and welding material aspects and the Effect of Friction Stir Welding on Dynamic Properties of some aluminum alloys also have been investigated [Hua-Bin et. al 2006, Bogdan Radu et. Al 2007,and Tomotake Hirato et. al 2007]. For many applications, like aerospace structures, transport vehicles, platforms, and bridge constructions, fatigue properties are critical. Therefore, it is important to understand the fatigue characteristics of FSW welds due to potentially wide range of engineering applications of FSW technique. This has led to increasing research interest on evaluating the fatigue behavior of FSW welds, including stress–number of cycles to failure (S–N) behavior and Fatigue Crack Propagation (FCP) behavior [Eui I. Lim 2006, Lemmen et al 2009, Omar et al 2009, G. Padmanaban and V. Balasubramamian 2010, N .Jayaraman et. al 2002]. However; there is not much information available on correlation of welding parameters with evolution of defect-free weld.

In order to produce a defect-free weld the optimization of welding parameters is extremely important .In this investigation fatigue properties of 3003-H14 aluminum alloy was studied after determined the optimization values of rotational speed and welding speed to produce best welding efficiency.

EXPERIMENTAL SET-UP

Friction stir welds were produced in AA 3003 aluminum using different combinations of rotational and welding speeds, as shown in Table 1 .Alloy AA 3003 is a non-heat-treatable Al-Mn alloy 1.04%Mn, 0.4%Fe, 0.192%Si with good weldability/formability and very good corrosion resistance lead to applications such

as food and chemical handling, tanks, trim, litho sheet, pressure vessels, and piping.

A clamping fixture was utilized in order to fix the specimens to be welded on a milling machine, Fig. 2. The tool was made in X38 tool steel cylindrical pin d with the following geometrical characteristics: shoulder diameter equal to 22 mm, pin diameter equal to 7 mm and pin height equal to 2.8 mm.

Two aluminum plates were utilized as base materials: AA3003-H14. The sheet metals were received in 100 mm×150 mm, with 3mm thick plate.

Fatigue tests were conducted at room temperature and with a constant amplitude in tensile testing The load ratio R =(min stress/max stress) was -1 .The fatigue samples were in the as-welded condition without machining the weld top and root faces, Fig. 3.

RESULTS AND DISCUSSION

FSW made a sound joint without voids, cracks or distortion. Fig .4 shows the macrostructure of the welded joint. The tensile strength of FSW joints for AA 3003-H14 material was carried out. Tensile specimens had been examined at room circumstances conditions, Fig.5. Tensile results shown in Fig 6 . Optimum value obtained at 1500 rpm and 80 mm/min and the efficiency 89 % of the base metal Al 3003 H14.

In Figures 7 to 9, the fatigue properties of FSW weldments are presented and compared with, TIG welding, and base metal. All the tested samplesof FSW showed very good fatigue behavior .Welds in base material AA 30033 showed better fatigue properties, compared with TIG welds .The scatter was also larger for welds in TIG than for welds in FSW, Fig. 10

From measured strength levels it would therefore be expected that fracture would occur in the weld region .This is in good agreement with the metal, equiaxed microstructure in the center of the nugget zone .It was difficult to predict where to expect fracture in AA 3003 from strength comparisons .

This investigation shows good fatigue properties for FSW samples Figure 8, and several investigations were conducted on the S–N curve behavior of FSW 3003-H14.

The Endurance limit of FSW weld at 2×10^6 cycles was lower than that of the base metal, i.e., the FSW welds are susceptible to fatigue crack initiation. However, the fatigue strength of the FSW weld was higher than that of TIG welds, as shown in Table 2. Typical S–N curves for FSW weld, TIG weld, and base metal of 3003-H14 are shown in Fig .10 .The finer and uniform microstructure after FSW leads to better properties as compared to fusion TIG welds. Surface quality of the FSW welds exerted a significant effect on the fatigue strength of the welds [N .Jayaraman et. Al 2002]. Overall, the fatigue results for FSWaluminum alloys are very encouraging.

The FSW joint has better mechanical properties than TIG joint, because of the differences between the two welding method should be considered. FSW is a solid state joining technology. The friction heat softens the welded material at a temperature less than its melting point. The softened material underneath the shoulder is also subjected to extrusion by the tool rotational. It is expected that this process will inherently produce a weld with relatively few residual stress and distortion. TIG is a fusion welding technology. The alloy is melt under high temperature during the welding process and then solidified. The weld of TIG joint is as-cast structure, which means work hardening disappears. Therefore the fatigue strength of TIG joints is lower than FSW joints [Juan Zhao, et al 2010].

CONCLUSIONS

The fatigue properties of 3003-H14 aluminum alloy friction stir welds in 3mm plates were studies in this paper. The main results can be summarized as following:

- AA 3003H-14 aluminum alloy was successfully joined without visual defects by friction stir welding under the following

parameters: 1500 rpm rotational speed and 80 mm/min welding speed with 89% welding efficiency.

• Good mechanical properties included fatigue properties of FSW joint are attributed to the well preservation of cold working microstructure.

• The fatigue strength of the FSW weld was higher than that of fusion TIG welds, the endurance limits were 52 MPa and 41 MPa for FSW joint and TIG joint respectively.

REFRENCES

Bogdan Radu et. al., “Aspects of the Material Flow during Friction Stir Welding of 5754 Al Alloy” , Institute for welding and Material Testing, Romania, IIW DOC., pp.1-10, 2007.

Brian M. Salerno, et. al., "Buckling Collapse Testing of Friction Stir Welded Aluminum", Technical Report, Ship Structure Committee, PP.7-9, 2009.

Carl D. Sorensen and Tracy W. Nelson, "Friction Stir Welding of Ferrous and Nickel Alloys ", Friction Stir Welding and Processing, ASM International, pp.111-121, 2007.

D .Booth and I .Sinclair, "Fatigue of Friction Stir Welded 2024-T351 Aluminium Alloy", Trans Tech Publications, pp.1-6, 2000.

Eui I. Lim, ” Fatigue Crack Propagation and Stable Tearing in Friction-Stir-Welded Aluminum Sheet”, ASIP, pp.1-29, 2006.

G. Padmanaban and V. Balasubramamian, "An experimental investigation on friction stir welding of AZ31B magnesium alloy, Int. J. Adv. Manuf. Technol.., vol.49, pp.111-121, 2010.

H. J. K. Lemmen et. al., ” Detailed strain field analyses of fatigue cracks in friction stir welded joints”, Aerospace structures and materials, pp.1-23, 2009.

Helena Larsson and Leif Karlsson, "Friction Stir welding of AA 5083 and AA 6082 aluminium", A welding review published by ESAB AB, Sweden, vol.54, No .2, pp.6-10, 2000.

Hua-Bin et. al., ”The investigation of typical welding defects for 5456 aluminum alloy friction stir welds”, Materials Science and Engineering A, pp.61-69, 2006.

Juan Zhao, et. al., "Comparative investigation of tungsten inert gas and friction stir welding characteristics of Al-Mg-Sc alloy plates", Materials and design, vol. 31,, pp. 306-311,2010

L Fratini, et. al., "Friction stir spot welding of AA6082-T6 :influence of the most relevant process parameters and comparison with classic mechanical fastening techniques", Proc .IMechE Vol .221 Part B :J .Engineering Manufacture, 2007.

M. Awang, et. al., " Thermo-Mechanical Modeling of Friction Stir Spot Welding (FSSW) Process :Use of an Explicit Adaptive Meshing Scheme". SAE International, PP.1-6, 2005.

Mustafa Boz and Adem Kurt, “The influence of stirrer geometry on bonding and mechanical properties in friction stir welding process”, Material and Design, vol.25, pp.343-347, 2004.

N .Jayaraman et. al., "Fatigue life improvement of an aluminum alloy FSW with low plasticity burnishing", Lambda Technologies, pp.1-10, 2002.

Omar Hatamleh et. al., “Fatigue Crack Growth of Peened Friction Stir-Welded 7075 Aluminum Alloy under Different Load Ratios” , Journal of materials Engineering and performance, 2009.

P. Cavaliere et. al., ” Effect of welding parameters on mechanical and microstructural properties of dissimilar AA6082–AA2024 joints produced by friction stir welding”, Material and Design, vol.25, pp.1-8, 2008.

Tomotake Hirato, et. al., “Influence of friction stir welding parameters on grain size and formability in 5083 aluminum alloy”, Materials Science and Engineering A, vol.456, pp.344-349, 2007.

Vladvoj Očenášek, et. al., "Microstructure and properties of friction stir welded aluminum alloys", Hradec nad Moravicí, pp.1-8, 2005.

Table 1: FSW process parameters variables

Sample No.	Weld speed (mm/min)	Rotational speed RPM
F1	20	1000
F2	20	1250
F3	20	1500
F4	20	2000
F5	40	1000
F6	40	1250
F7	40	1500
F8	40	2000
F9	60	1000
F10	60	1250
F11	60	1500
F12	60	2000
F13	80	1000
F14	80	1250
F15	80	1500
F16	80	2000

Table 2: Life equation and endurance limit of AA 3003 Aluminum alloy

Welding Process	Life Equation at 2×10^6 Cycle	Endurance Limit (Mpa)
Base metal	$\sigma = 1168.5N_f^{-0.204}$	62
FSW	$\sigma = 773.42N_f^{-0.189}$	52
TIG	$\sigma = 617.68N_f^{-0.191}$	41

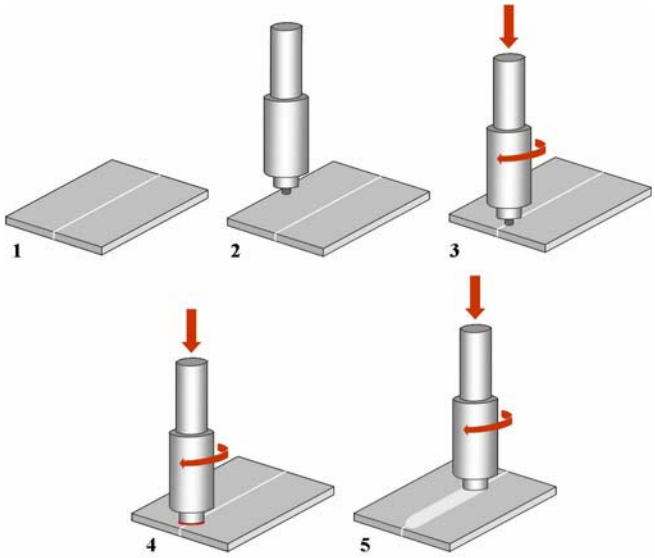

Figure 1: Steps of the FSW process [Brian M. et al 2009]

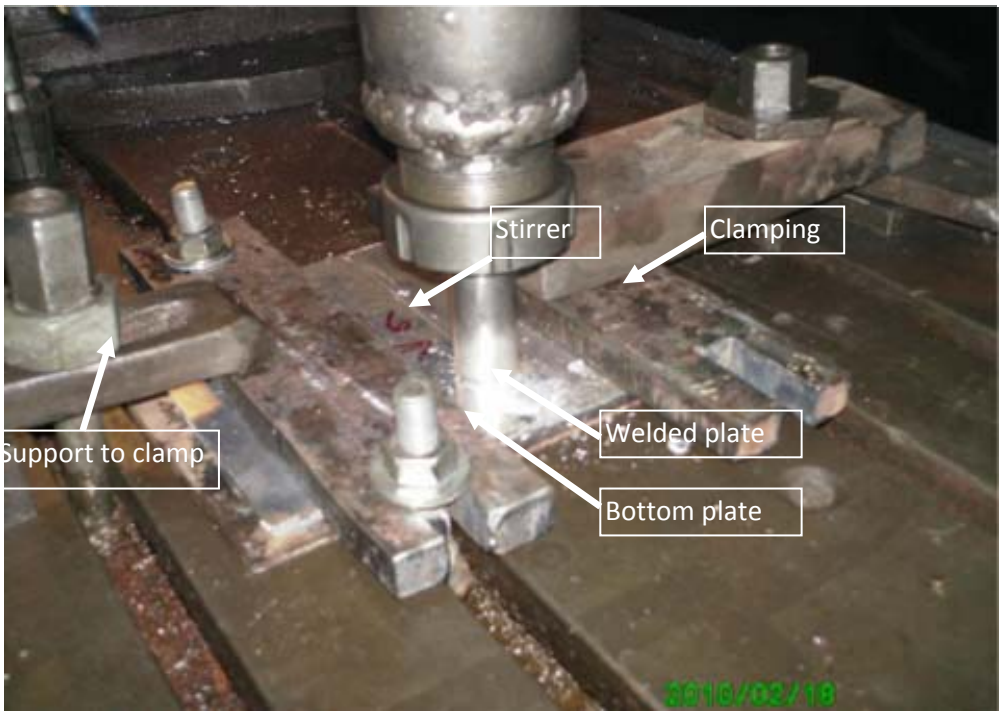

Figure 2: Experimental setup

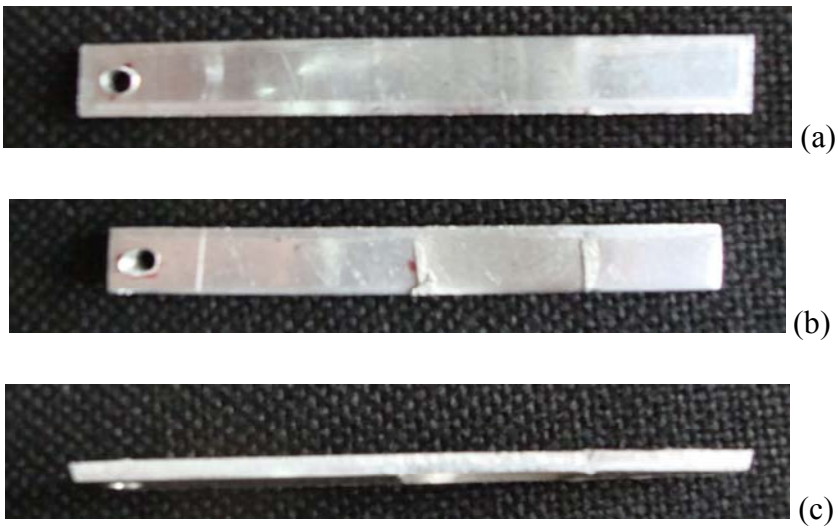

Figure 3: Fatigue sample of friction stir weld, a- Bottom surface of weld region, b- Top surface of weld region, c- Side view

Figure 4: Friction stir weld in 3 mm AA 3003, welded at 80 mm/min and 1500 rpm rotational speed.

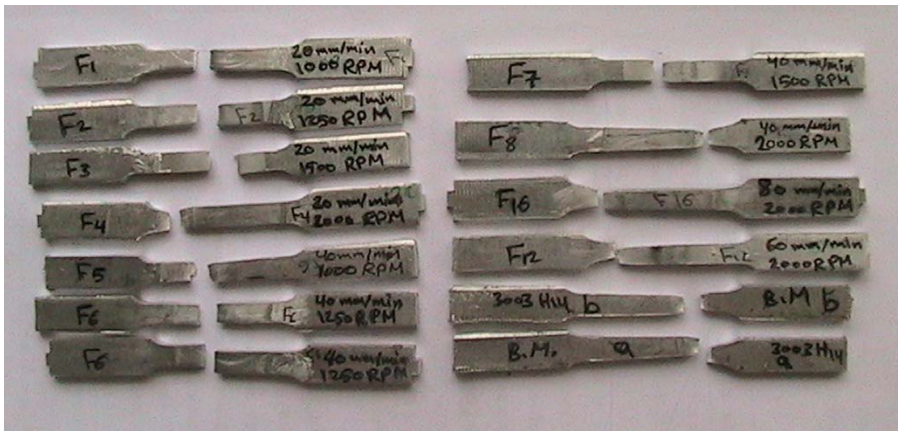

Figure 5: Some of tensile specimens after test

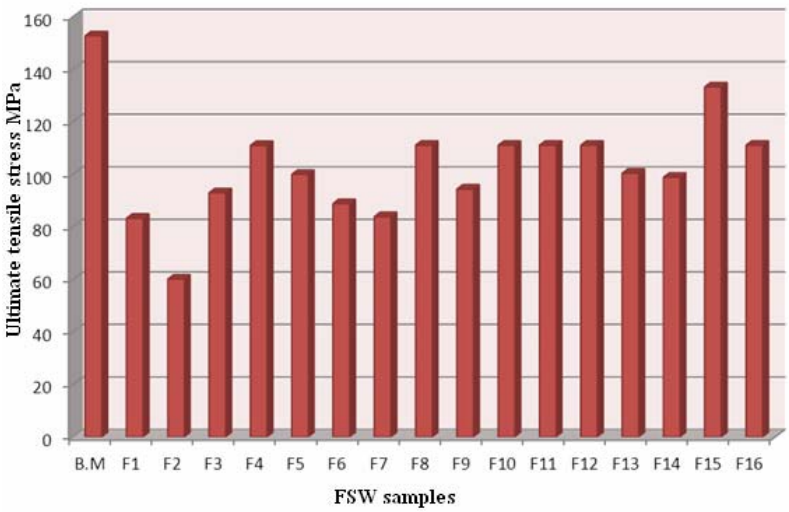

Figure 6: Tensile test results

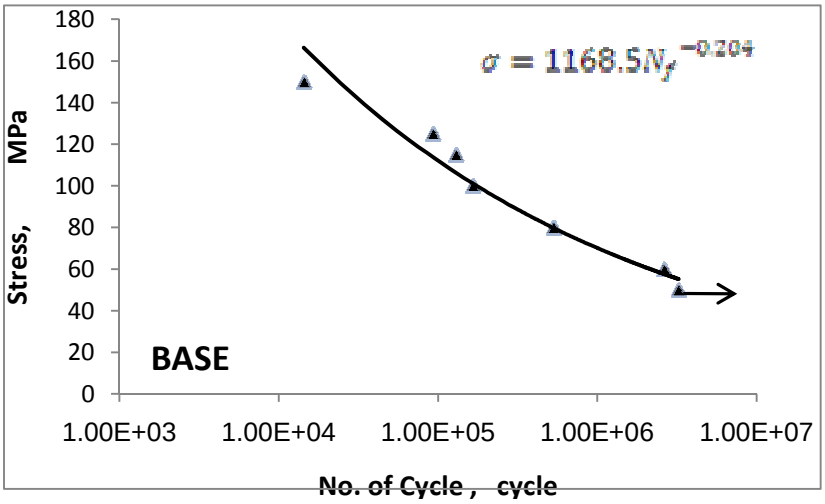

Figure 7: Base metal AA 3003-H14 S-N curve

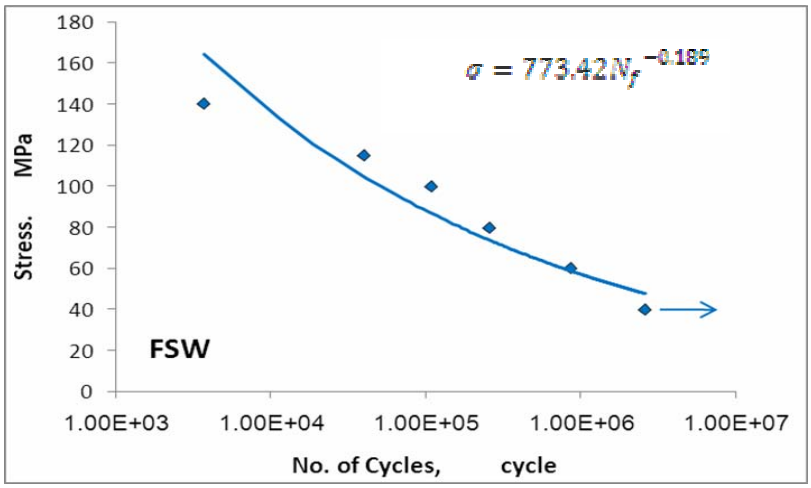

Figure 8: Friction stir welding AA 3003-H14 S-N curve

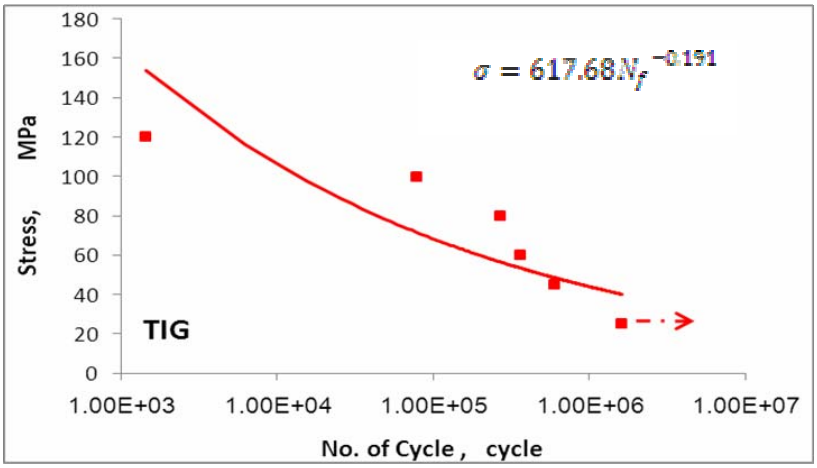

Figure 9: TIG welding AA 3003-H14 S-N curve

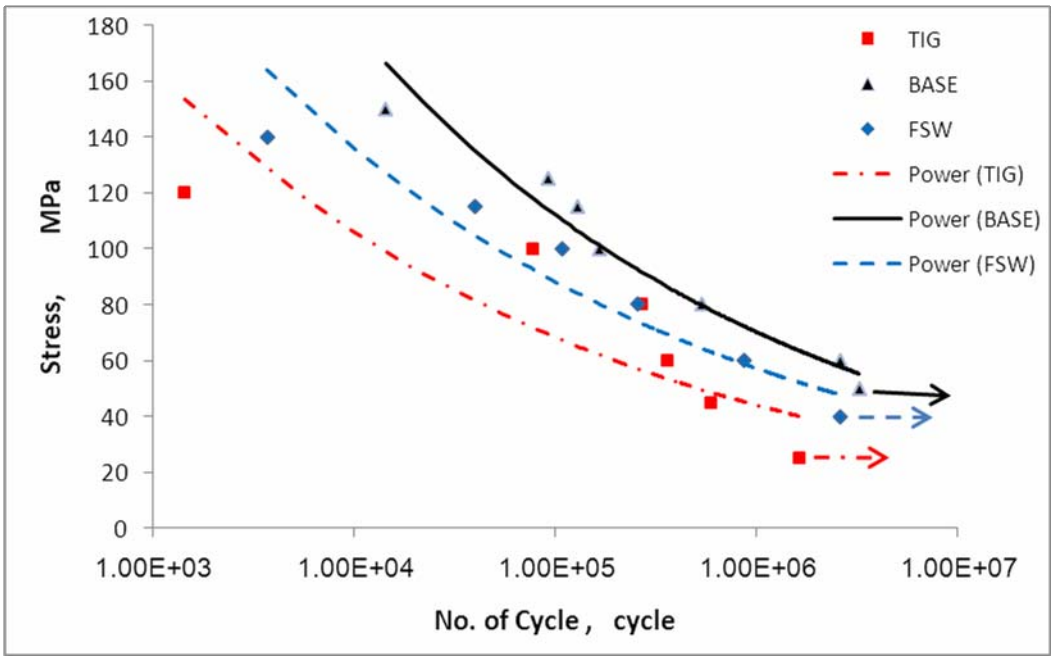

Figure 10: Comparison between base metal, TIG welding and FSW

SIMULATION OF FLIGHT THROUGH GUST

Asst. Lect. Kareem Jawad Kadhum
Univ. of Baghdad, College of Eng., Mech. Dept.

ABSTRACT

A flight simulation programme has been developed on a personal computer using Microsoft FORTRAN to simulate flight trajectories of a light aircraft by using Six-Degree-of-Freedom equation of motion. The simulation has been made realistic through pre-programmed the input to the control surfaces, atmospheric gust during the flight mode. The programme plays an important role in the evaluation and validation of the aircraft design process. A light aircraft (Cessna 182T) has been tested through free flight, gliding flight, flight with gust. The results show good trend and show that the programme could be dependent as a realistic flight test programme.

الملخص:

تم تطوير برنامج محاكاة الطيران على الحاسبة باستعمال لغة الفورتران لمحاكاة مسارات الطيران لطائرة خفيفة الوزن من خلال استخدام معادلات الحركة الحرة ذات الدرجة السادسة. لقد تم جعل المحاكاة اقرب الى الحقيقة من خلال البرمجة المسبقة للتحكم بسطوح التحكم، وعند وجود عاصفة جوية اثناء الرحلة الجوية. يلعب البرنامج دور مهم خلال تقييم وتحقيق عملية التصميم للطائرة. الطائرة الخفيفة (سيزنا) تم اختبارها من خلال البرنامج للطيران الحر، والطيران الانزلاقي، والطيران خلال عاصفة جوية. اظهرت النتائج اتجاه جيد كذلك اظهر البرنامج انه من الممكن الاعتماد عليه كبرنامج اختبار للطيران الحقيقي.

Keywords: six degree of freedom, flight simulation, equations of motion

INTRODUCTION:

With the advent of the new state-of-the-art computers capable of performing several million floating point operations per second, computer simulation provides an inexpensive, powerful and flexible tool to simulate the various aspects of flight. A software has been developed in Fortran language using power station compiler to simulate flight trajectories of a light aircraft .situation that might ask for a simulation are for example Wind effects, Dynamic effects, Transition between different flight stages and needing simulating data of an aircraft part (e.g. lift force on the stabilizer). Wind effects and motion of the atmosphere can be discrete or random; in any case they are usually characterized by only the three velocity orthogonal components. Therefore, to account for atmospheric disturbances such as winds, gust or turbulence, the forces and moments must be related to the relative motion with respect to the atmosphere. This is accomplished by expressing the velocities used in calculating the aerodynamics in terms of inertial and gust velocities.

Many references deal with equation of motion in a non uniform atmosphere, one of the important references is (**Roskam 1972)**, some of the analytical techniques are available to flight control engineers to study the dynamic response of an airplane to control deflection or atmospheric disturbances. Gust, wind shear and turbulence have been studied and outlined to improve flight safety. (**McRuer 1973),** discuses the effects causes by non uniform atmosphere where there are a large scale changes in wind speed and direction with altitude which will produce force and moment perturbations on the diving or climbing aircraft. He assumed that the atmospheric properties such as density or speed of

sound are considered negligible for the small altitude perturbations of the usual interest. **(Khare 1992),** software has been constructed with automatic sortie simulation feature through multiple way points to predict the trajectories of aircraft.

In the present work, six degree of freedom equation of motion has been integrated to predict the trajectories of a light aircraft with new discretization discussed in the next section. This type of discretization simplifies the problem by adding different components to the aircraft model and its effect on the whole motion of aircraft like landing gear or canopy etc. The non uniform atmosphere like gusts is also considered in this study with input command to control surfaces of the aircraft.

MATHEMATICAL FORMULATION:

Firstly some of the assumptions of the problem can be summarized as follows;

- Flat earth surface (no rotation).
- Thrust will be in axial direction through center of gravity.
- Rigid body motion (mass will be constant through flight).
- Wind has no acceleration (constant velocity).

To implement a real-time flight simulator, a new procedure will be done in this work. To calculate the lift and drag forces on aircraft model, the aircraft will be discretized into number of smaller element sections then collect the geometric and performance data for each section. It must be note that the relative air velocity and angle of attack over each element section must be calculated. The wing may be divided into four sections fitted with aileron and flap as shown in **Fig (1)** and the other sections are the elevator and rudder. Finally you can lump the entire components with the fuselage together as one additional section. The summations of all components contributions are to find the resultant forces and moments with thrust and gravity. The performance data for each section must be presented by using experimental data as a function of angle of attack which is calculated by evaluating the relative velocity in each section **(Hoerner 1985)** presented many wing shape experimental data of lift and drag.

There are two right-handed coordinate system that are commonly used to characterize the forces and moments applied to the airframe and the resulting aircraft motion. The primary coordinate systems used are the North-West-Up, or NWU axes (some references used NED which are North, East and Down body axes (**Roskam 1972**), and the body axes. The NWU axes are defined with the origin at the aircraft center of gravity, x-axis positive north, y-axis positive east, and z-axis positive upward. For purposes of this discussion, "upward" represents the direction from the aircraft center of gravity upward along and reverse in the direction of the local gravity vector. In this simulation, the Earth is considered flat. Therefore, the local gravity vector always points to the earth. The body axes are defined with the center at the aircraft's center of gravity, the x-axis positive through the nose of the aircraft, the y-axis positive through the left wing, and the z-axis positive through the upper of the aircraft. The plane on which the body x-axis and body z-axis lie is called the plane of symmetry. The angle between the body x-axis and the horizontal plane is called the elevation angle, θ, and its sense is positive nose up. The angle between the body y-axis and the horizontal plane is called the bank angle, φ, and its sense is positive starboard wing down. The angle between the projection of the body x-axis on the horizontal plane and the north axis of the NWU coordinate system is called the azimuth angle, ψ, which ranges from 0 to 360° with 0 being magnetic north and increasing from north to east. The body axes are useful as an aircraft-fixed reference system for thrust and forces acting upon the control surfaces. The NWU axes are a useful frame for calculating the aircraft motion with respect to the earth and for developing wind velocity profiles.

The angle between the body x-axis and the projection of V in the plane of symmetry is called the angle-of-attack, denoted α. The angle between the stability x-axis and V is called the sideslip angle, β. These coordinate systems are suitable for these calculations because the forces are normal to the airflow across the airframe.

The relative velocity compensates from linear velocity and rotational one. The formula may be used as;

$$v_R = v_{cg} + (\omega \times r) \qquad (1)$$

Where v_{cg} represents the vector of air speed and flight direction of the aircraft, ω is the angular velocity vector of the aircraft and r is the distance between the component and the centre of gravity of airplane. It must be noted that any additional velocity like gusts, shear or turbulence could be added to the above equation to account for

atmospheric effects after transformed to the body coordinates.

Preceding by calculation the angle of attack for each wing section is done by evaluation the normal vector for the specified section. The angle between the lift vectors which is perpendicular to the velocity vector represents the angle of attack and this involves taking the dot product between these two vectors.

Once the angle of attack has been evaluated, the resultant forces at each element are calculated from data tables referred previously for each element section. The data sheet for every section consist stall angle where the lift forces are falls down and the drag increased at these points. By assuming the thrust vector in the x-direction only and passes through centre of gravity (it could be made vectoring in any direction and the landing gear drag may be added). Moments at center of gravity can be calculated by multiplying the force vector at each element with aerodynamic center measured from center of gravity of airplane. Thrust will be added to the resultant force. All these forces and moments have been referenced in the body fixed coordinate system. The body forces vector must first rotated from the body space to earth space coordinates and then apply the gravity force.

There is a problem with using three Euler angles in rigid body simulations. So, when numerical pitch angle reaches plus or minus 90° roll and yaw become ambiguous and since Euler angles involving cosines in the denominator the equations becomes singular. One must use some other means of keeping track of orientation in your simulation which is called *Quaternions* (**Douglas B. Sweetser**).

The loads on the airplane are completed; so that, the next step is to integrate the equations of motion to simulate progressing through time. The integration scheme in this work is simple Euler method. One can advance the work by using fourth order Range-Kutta method.

It must be noted that the angular motion is to calculate the new angular velocity using Euler integration. This is done in body coordinates by using the equation of motion,

$$M_{cg} = \frac{dH_{cg}}{dt} = I\left(\frac{d\omega}{dt}\right) + [\omega \times (I\omega)] \qquad (2)$$

The next step is done by another integration to update the airplane's orientation, which is expressed as a quaternion. Since the linear velocity was previously calculated in global coordinates and loads need to velocity in the body coordinates system, the velocity vector must be rotated to the body coordinate.

The aircraft responses are done by adding disturbances inputs due to gust in the body axes, then,

$$u_{disturb} = u_{gust}$$
$$v_{disturb} = v_{gust} \qquad (3)$$
$$w_{disturb} = w_{gust}$$

Incorporating constant wind (generated in global NWU coordinate) and total disturbance input (transformed to the global NWU coordinate) to get the total resultant velocity in the global coordinates of reference. The body velocity components of the total velocity can be obtained by transforming the component velocity from global NWU coordinate to local coordinates.

The discrete gust formulation can be summarized as follows (**McRuer 1973) (**It could be get the data sheets for the wind gust records and put it as a discrete data).

$$w_{gust} = \begin{bmatrix} 0 & 0 \le x < x1 \\ \frac{Vm}{2} * \left(1 - \cos\left(\frac{\pi(x-x1)}{dm}\right)\right) & x1 \le x < x2 \\ Vm & x2 \le x < x3 \\ \frac{Vm}{2} * \left(1 + \cos\left(\frac{\pi(x3-x)}{dm}\right)\right) & x3 \le x < x4 \\ 0 & x \ge x4 \end{bmatrix}$$

(4)

Where,
dm = V/2f,
V_T = Aircraft velocity
$x_2=x_1+dm$
$x_3=x_2+dx$
$x_4=x_3+dm$,
dx is the desired gust width
f is the characteristic aircraft frequency,
x_1 is the position of start of gust along global x- axis,
V_m is the maximum gust velocity.

In the present work the gust is divided into two branches the first one is the velocity in the z-direction which is presented in the equ (4) and the other what is called shear velocity (velocity in the direction of y), the same equ (4) is use d in the y-direction. The most important note that the gust must be transformed from global

velocity to body coordinates (it represents vertical velocity only with specified distribution). Gust velocity will be calculated at each element section of the aircraft. This gives more realistic to the flight simulation. Of course you can add cockpit, landing gear and winglets to the model of aircraft and by this way one can get more accurate results (the loads coefficient of these parts must known to be added to the total forces of the aircraft).

NUMERICAL SOLUTION:

As mentioned before in the mathematical procedure the integration will be done using simple Euler Method which needs small time interval to get accurate integration results. Six degree of freedom equation of motion are considered and integrated to predict aircraft trajectories which consisting of three displacements and three orientations of the aircraft. The steps for calculations can be summarized as follows;

1- Input geometric information (number of elements of the aircraft and its position, setting angle, mass, moment of inertia, projected area and flap, aileron, elevator and rudder angles).
2- Initial conditions with position, flight velocity, maximum gust velocity if consist, angular velocity, thrust force, external forces and/or moments vectors if consist and roll, pitch and yaw angles for the aircraft.
3- Summations all global velocities like flight velocity and constant wind velocity and transformed from global NWU coordinate to the body coordinate.
4- Evaluate the mass properties like total mass, center of gravity, moment of inertia with respect to the center of gravity. Then compute the inverse of the inertia matrix.
5- Time loop begins with appropriate time step.
6- Calculation of aircraft load and moments which are done by calculate the normal vector at every section and then calculate the local velocity from equ.(1) with disturbance velocities in equs.(3,4) at each section. The drag force vector will be along the local velocity vector in opposite direction. The dot product between a unit drag vector and normal vector will give angle of attack at any sections.
7- The normal force can be calculated by evaluate the vector normal to the local velocity vector.
8- With help of angle of attack, area of each section, velocity and density at known altitude the lift force and drag force will be evaluated at each section from data sheets of aircraft components.
9- By multiplying the resultant force with the distances between each component and center of gravity the moment vector at center of gravity is evaluated.
10- The resultant force will be summed with thrust force and this force transformed in to the global NWU coordinate to accumulate the gravity force. (Transformation matrix is done by using quaternion).
11- The force will be divided by the total mass of the aircraft to find the linear acceleration and the multiply by the time step to find new velocity vector. The velocity vector will be multiplied by the time step to find the new position of the aircraft.
12- Using equ (2) to find the angular acceleration vector by multiply the moment and initial angular velocity vector by inverse moment of inertia matrix.
13- The new angular velocity and orientation of the aircraft are evaluated by multiplying by time step.
14- The loop continues for a specified condition like time interval, specified position etc.

The above procedure is programmed in FORTRAN language and compiled with Microsoft power station compiler. The results are tabled in different files consisting time history of position, orientation, velocities and accelerations, the other data is the force and moment data along flight simulation. All these data are discussed in the next section. The procedure presented here provides a low time consuming because it deals with vectors.

RESULTS AND DISCUSSIONS:

In this section the time history results will be discussed and some of them will be compared with other previously published data.

The properties of the aircraft which is chosen to test the programme result can be found in the (**Paul Jackson 2005) Fig (3).**

The first group of figures are figures (4 to 7) they show the response of aircraft when the aircraft cruse at speed near 42 m/s (M=0.124) and thrust equal to 2560 N and there is no control for flaps, aileron, rudder or elevator. First two figures show the distance that will be travelled by the aircraft, it could be seen that the aircraft moved forward and increasing its height due to lift force as the time progress. All fluctuation at the beginning are due to unsteady behaviour of flight since the aircraft did not takeoff from ground. So that, after this period the aircraft becomes stable and its motion becomes steady. Another thing that the star board motion was not happens because the aircraft in this case have two components only (no gyroscopic motion). Same notes are cleared for the velocity components in x and y-direction.

The most important note is illustrated in the figures 6 for the acceleration components where x and z-direction is shown in this figures, these components became zero for steady state flight (i.e. Cruse flight) this mean the thrust force equal to the drag force and lift nearly equal to the weight of the aircraft. In figure 7 the pitch angle is nose up when the right hand applied to the left side of the aircraft the positive direction when the aircraft pitch angle is nose down. The angular acceleration in yawing and rolling are zero while the pitching is equal to zero after a period of time this make the aircraft has a constant pitch angle.

Figures from 8 to 11 show the response of the aircraft when the thrust increased. The response is going to unstable state and the fluctuation of the aircraft increased and again no control available during the flight. The velocity component in the x-direction was increased and also the pitch angle. The motion will be damped out and steady motion may be obtained after a period of time.

Flaps were tested to illustrate the response of the aircraft for the figures between: 12-15, these devices gives a reasonable stability to the aircraft and also increasing the lift force, so that the elevation of the aircraft increased as shown in figures.

Two type of gust are considered, the first is normal gust velocity with equations shown previously and shear gust represented by same equation with only one difference where the velocity in the y-direction instead of z-direction. It could be seen that z-direction gust could be controlled by aircraft if it affected by this type of gust. But shear wind could not, and the third motion appears in this case (mean in y-direction). The figures from 16 to 26 illustrate the behaviour of aircraft during these effects. **Fig. (27)** shows the flow chart of the programme.

CONCLUSIONS:

The programme is a useful tool in simulation of flight trajectories of a light aircraft. It is aid for flight visualization during gust and constant wind for various flight conditions within the flight envelope of the light aircraft. A new approach has been developed in this work which simplifies the solution by discrediting the aircraft into component and treats these components separately. This procedure provides to add a multiple component into the model. Input angles of control surfaces gives realistic feel to any flight simulation and the programme provides this facility by pre-programmed inputs to control surfaces. The programme is under development to account for atmospheric turbulence or wind shear and augmented through an autopilot for sortie simulation.

NOMENCLATURE:

u	Velocity in x-direction (m/s)
v	Velocity in y-direction (m/s)
w	Velocity in z-direction (m/s)
M	Moment vector
H	Momentum vector
I	Mass moment of inertia matrix
t	Time (sec)
ω	Angular velocity vector
r	Distance to the center of gravity vector

REFERENCES:

1- Roskam J., "**Flight Dynamics of Rigid and Elastic Airplanes**", Published by Roskam aviation and engineering corporation, Kansas, 66044, 1972.

2- McRuer D., Ashkenas I., Graham D., "**Aircraft Dynamics and Automatic Control**", Princeton University Press, New Jersey, 1973.

3- Khare Alok, Madhuranath Padma, "**SOFT–Simulation of Flight Trajectories**", NAL-PD-FC-9209, National Aeronautical Laboratory, Bangalore, December 1992.

4- S. F. Hoerner, "**Fluid-Dynamic Lift Practical Information for Aerodynamic and Hydrodynamic Lift**", 2nd edition, published by Mrs. Liselotte A. Hoernoer, 1985.

5- S. F. Hoerner, "**Fluid-Dynamic Drag Practical Information for Aerodynamic and**

Hydrodynamic Drag", 2nd edition, published by Mrs. Liselotte A. Hoernoer, 1985.

6- Douglas B. Sweetser, "**Doing Physics with Quaternions**", http://quaternions.com

7- Paul Jackson, "**Jane's All the World's Aircraft 2004-2005**", http://Jawa.janes.com.

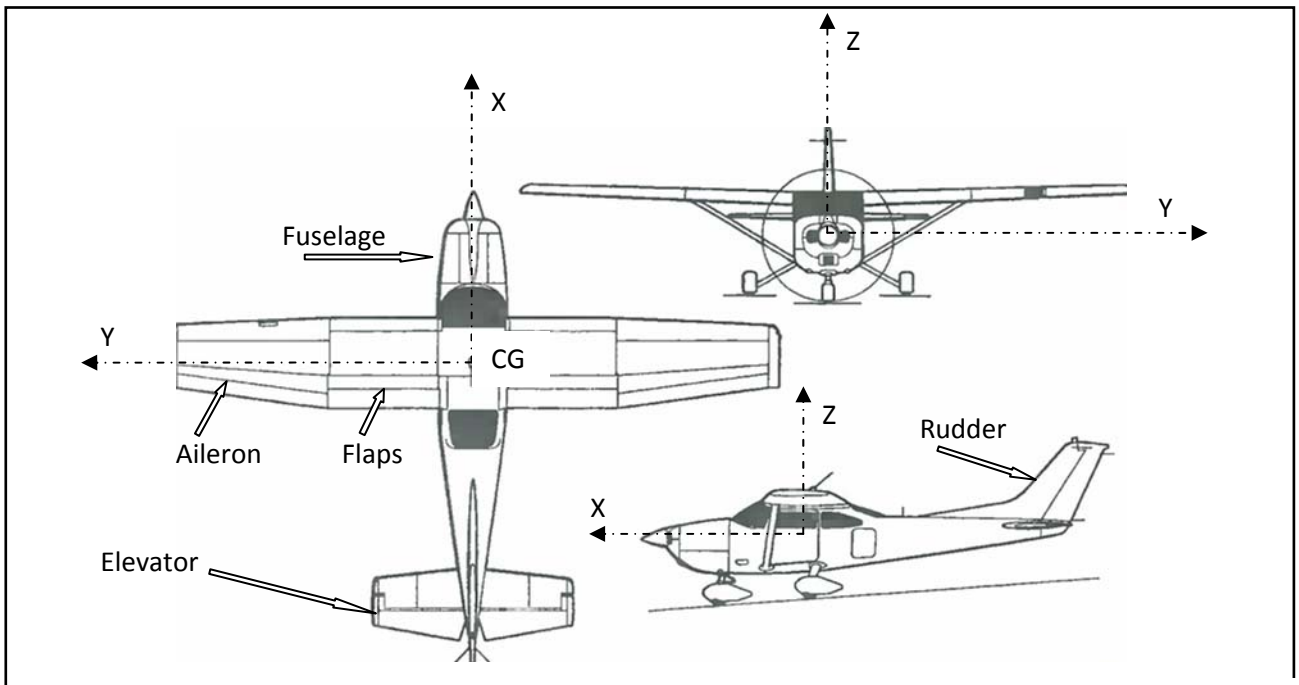

Figure 1: Element Sections of (Cessna 182T) Airplane.

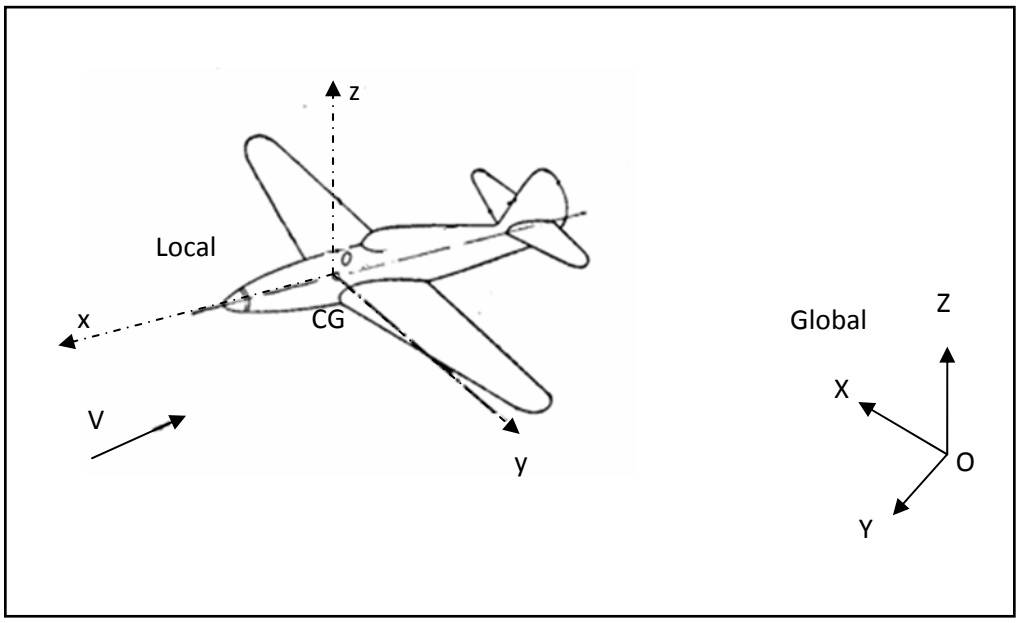

Figure 2: Coordinate Systems.

Cessna 172R Skyhawk *(Paul Jackson)* NEW/0568389

Performance

Maximum level speed	227 km/h
Cruising speed at 80% power at FL80	226 km/h
Stalling speed, power off	
Flap up	95 km/h
Flap down	87 km/h
Max rate of climb at S/L	219 m/min
Service ceiling	4,115 m
T-O run	288 m
T-O to15 m	514 m
Landing from 15 m	395 m
Range at 80% power at FL80	1.074 km
Endurance	6 h 36 min

Dimension and weight

Wing span	11 m
Wing aspect ratio	7.5
Propeller diameter	1.9 m
Length overall	8.28 m

Weight and loading

Weight empty	745 kg
Baggage capacity	45 kg
Max ramp: Normal	1,114 kg
Utility	956 kg
Max T-O and landing weight	
Normal	1,111 kg
Utility	952 kg
Max wing loading	68.7 kg/m2
Max power loading	9.32 kg/kW

Figure 3: Aircraft Dimensions and Properties.

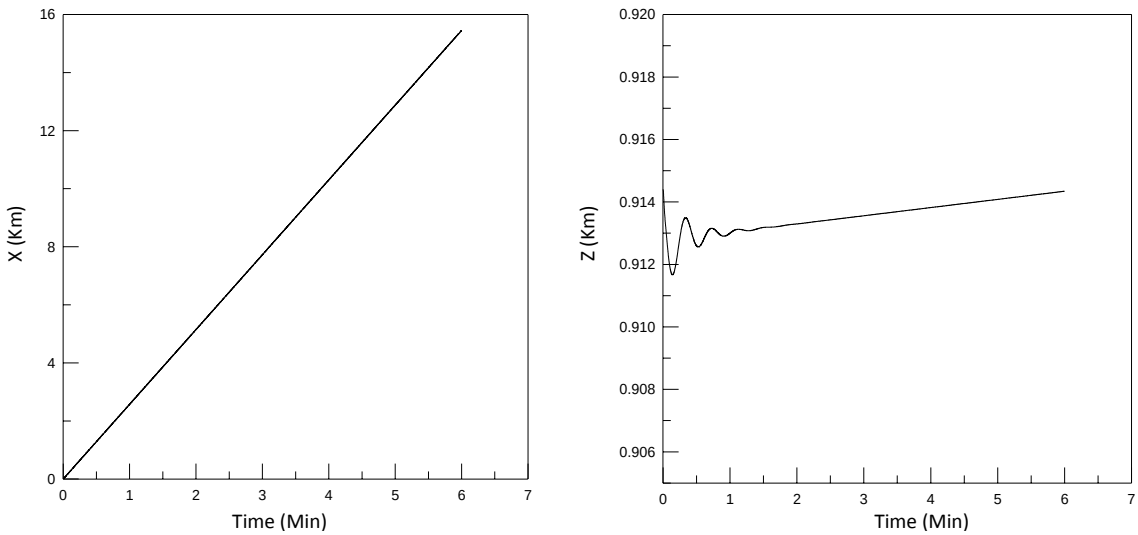

Figure 4: Time History of Aircraft Distance in X and Z-Direction in Cruise Flight.

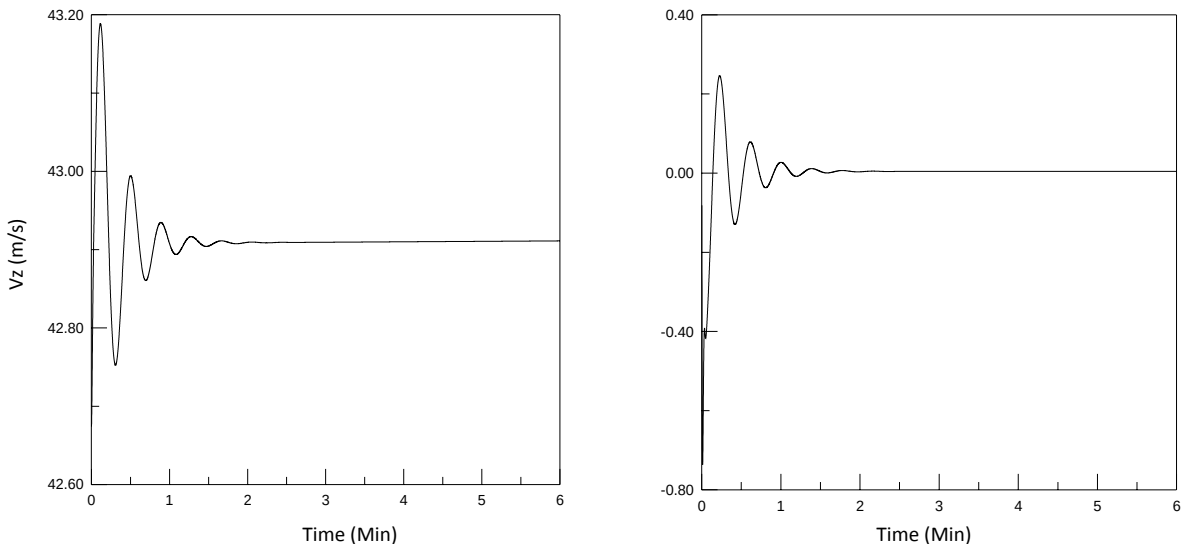

Figure 5: Time History of Aircraft Velocity in X and Z-Direction in Cruise Flight.

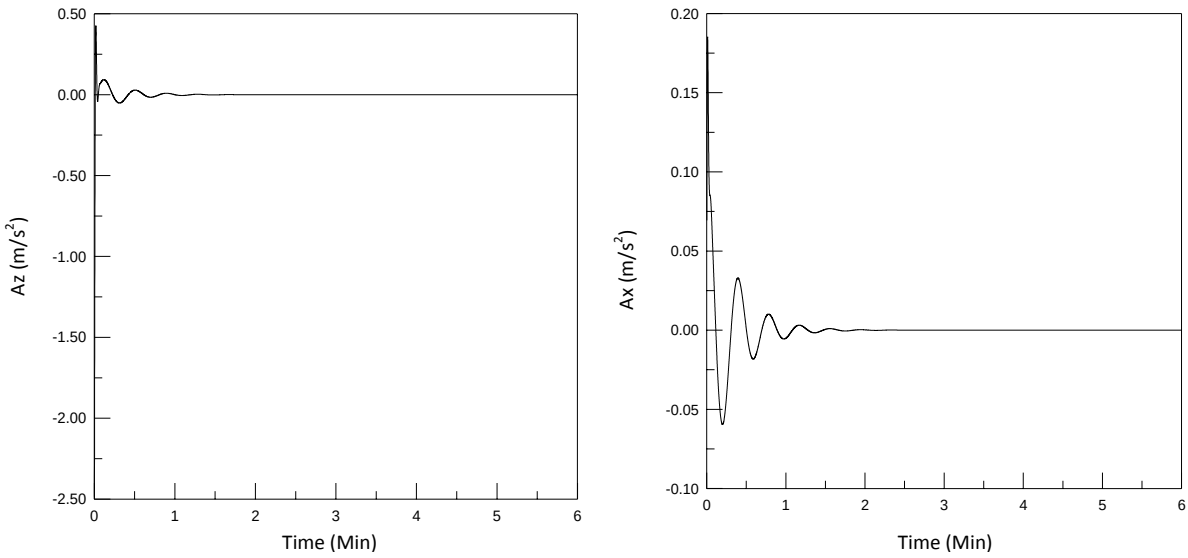

Figure 6: Time History of Aircraft Acceleration in X and Z-Direction in Cruise Flight.

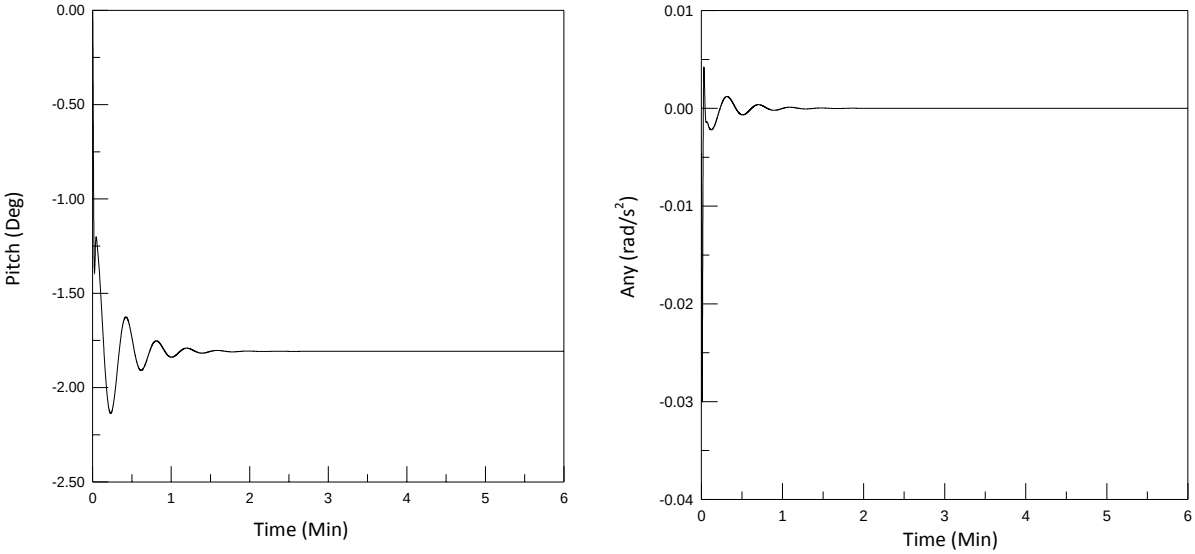

Figure 7: Time History of Pitch and Angular Acceleration of Aircraft in Cruise Flight.

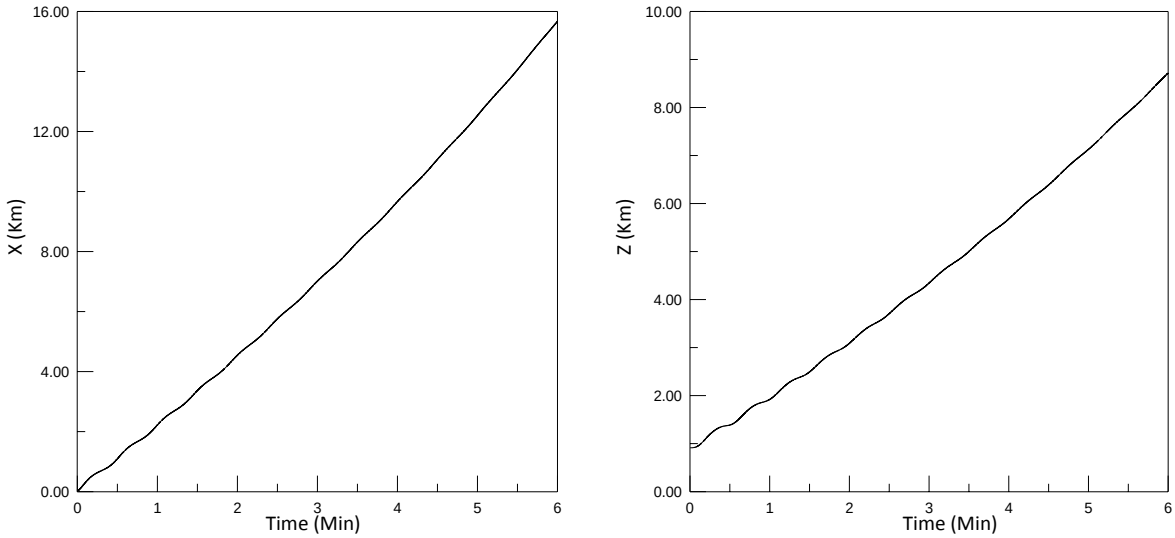

Figure 8: Time History of Aircraft Distance in X and Z-Direction when the thrust increased.

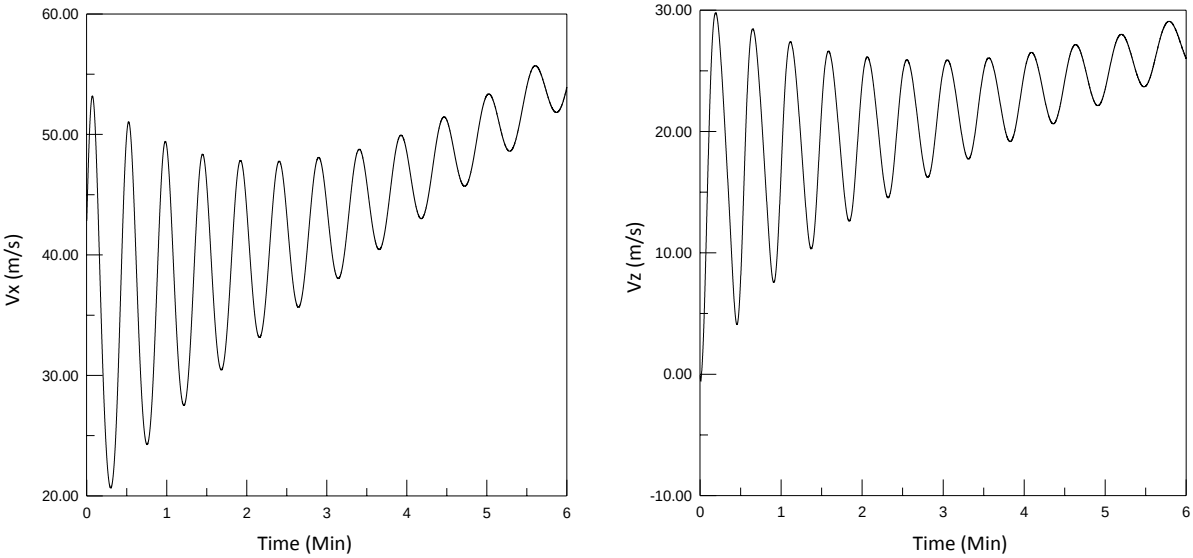

Figure 9: Time History of Aircraft Velocity in X and Z-Direction when the thrust increased.

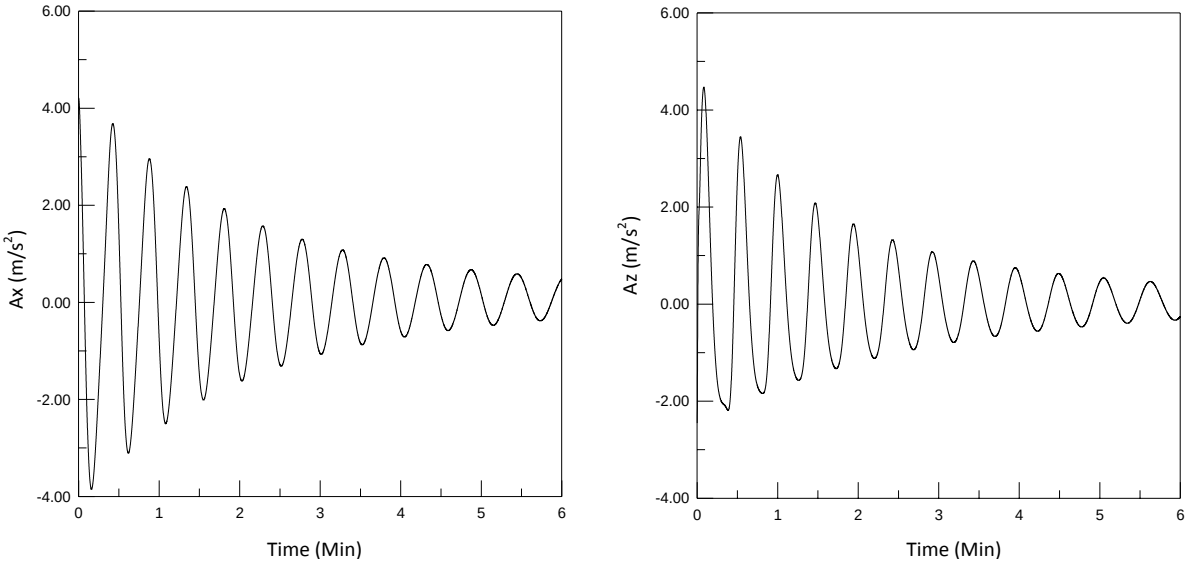

Figure 10: Time History of Aircraft Acceleration in X and Z-direction when the thrust increased.

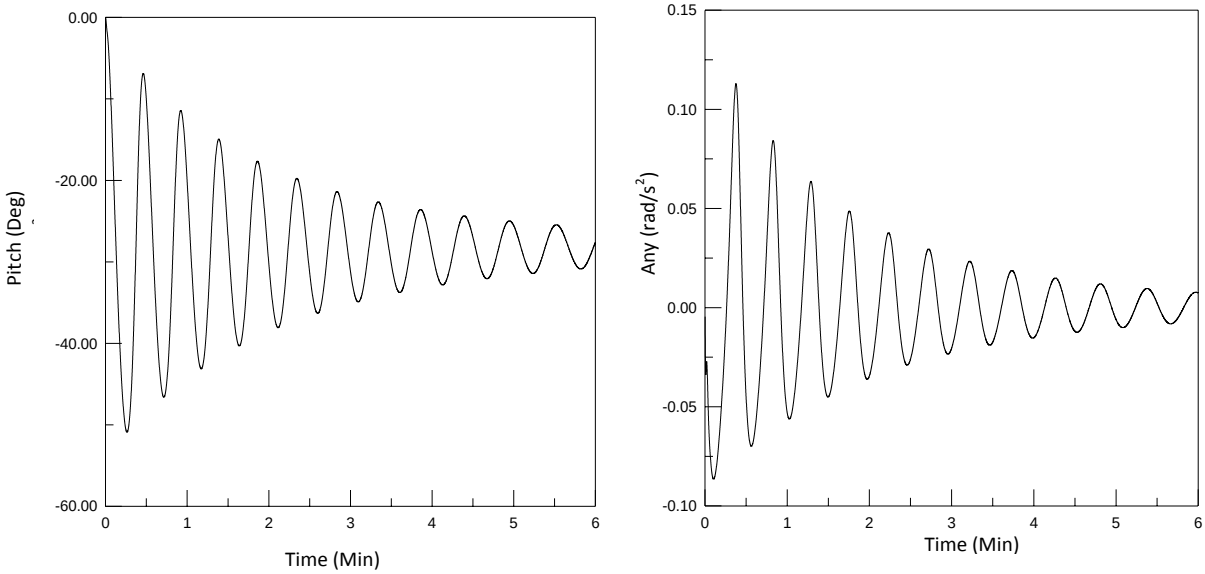

Figure 11: Time History of Pitch and Angular acceleration of Aircraft when the thrust increased.

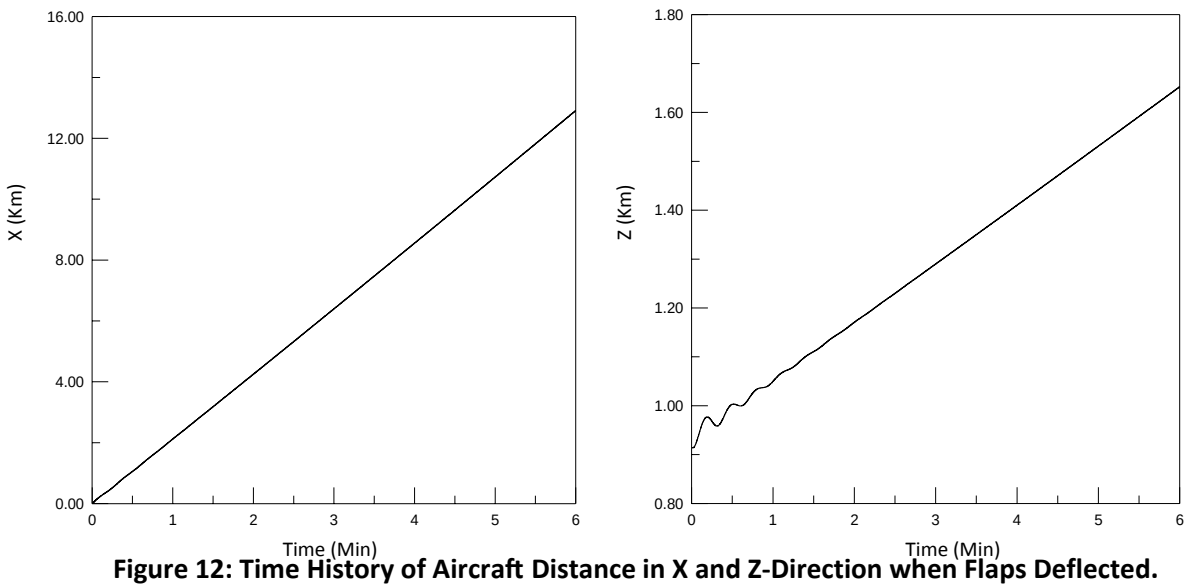

Figure 12: Time History of Aircraft Distance in X and Z-Direction when Flaps Deflected.

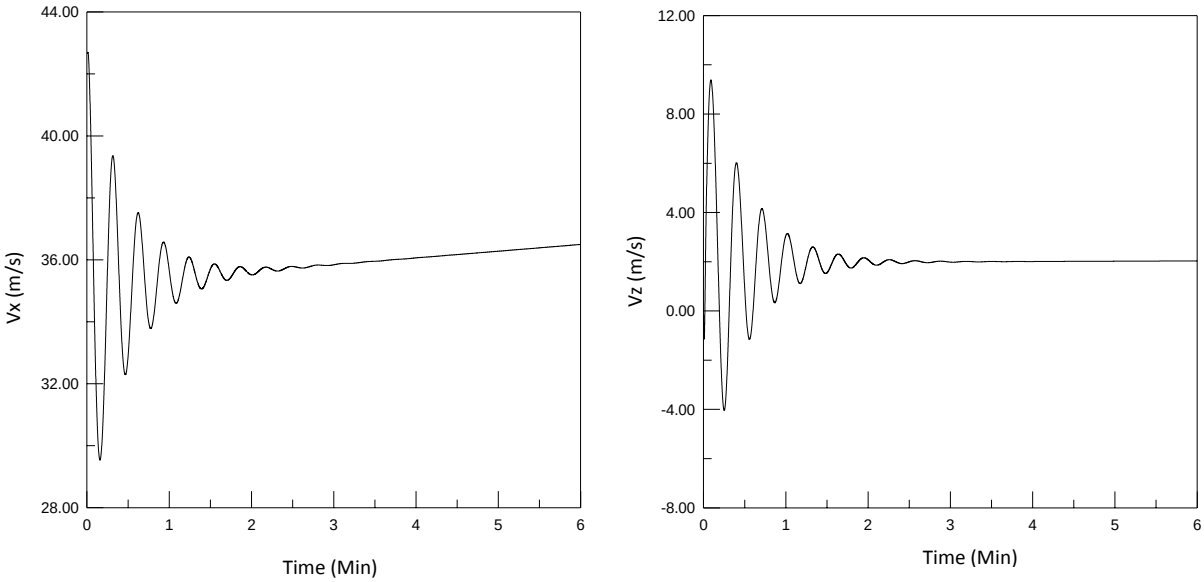

Figure 13: Time History of Aircraft Velocity in X and Z-Direction when Flaps Deflected.

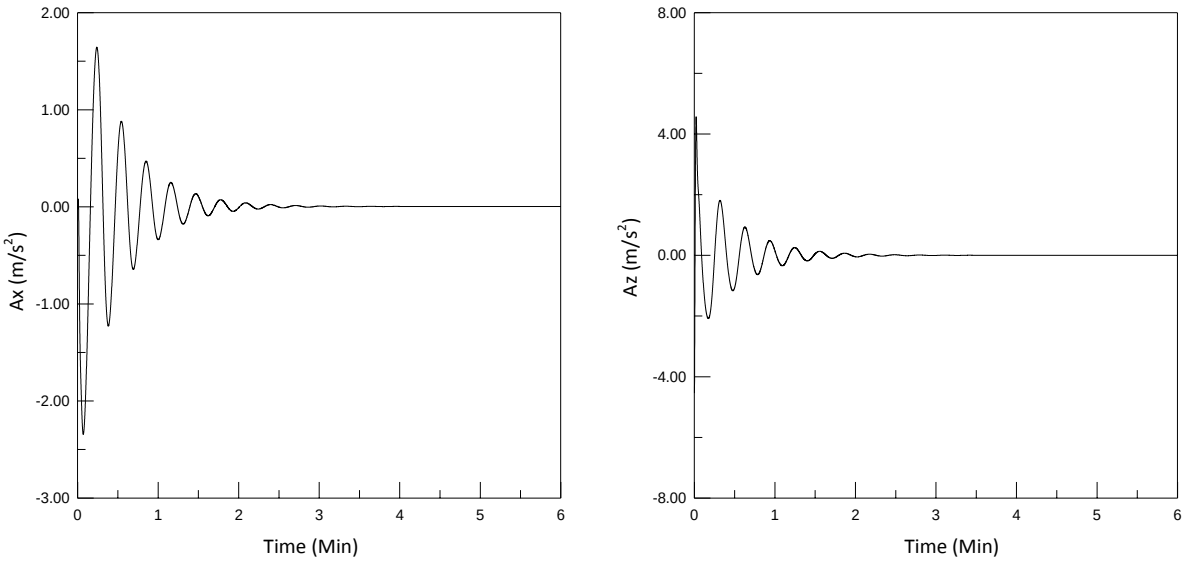

Figure 14: Time History of Aircraft Acceleration in X and Z-direction when Flaps Deflected.

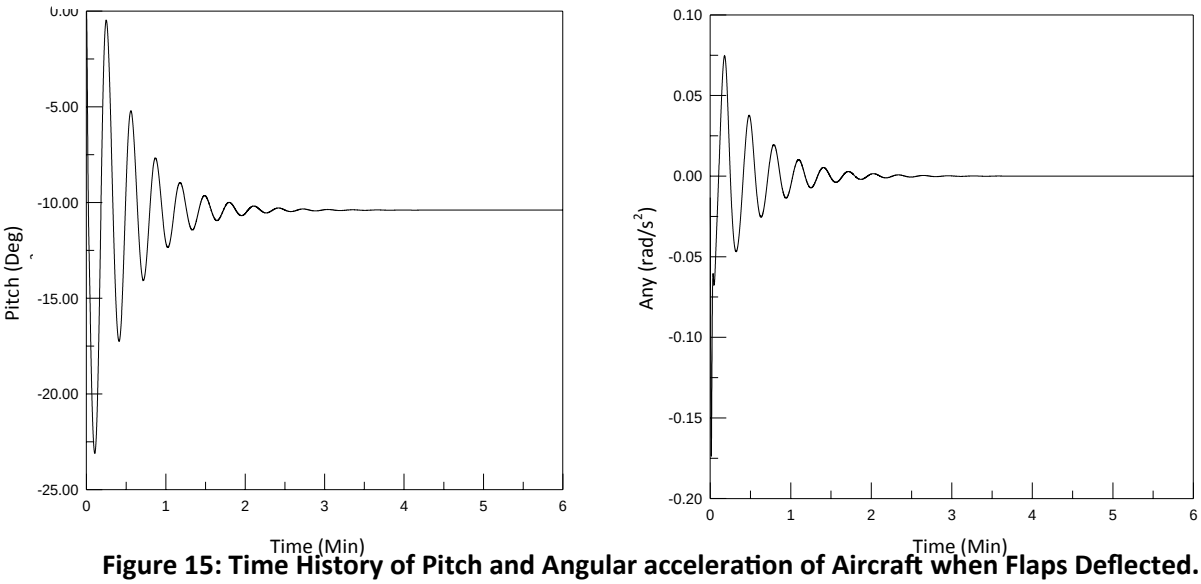

Figure 15: Time History of Pitch and Angular acceleration of Aircraft when Flaps Deflected.

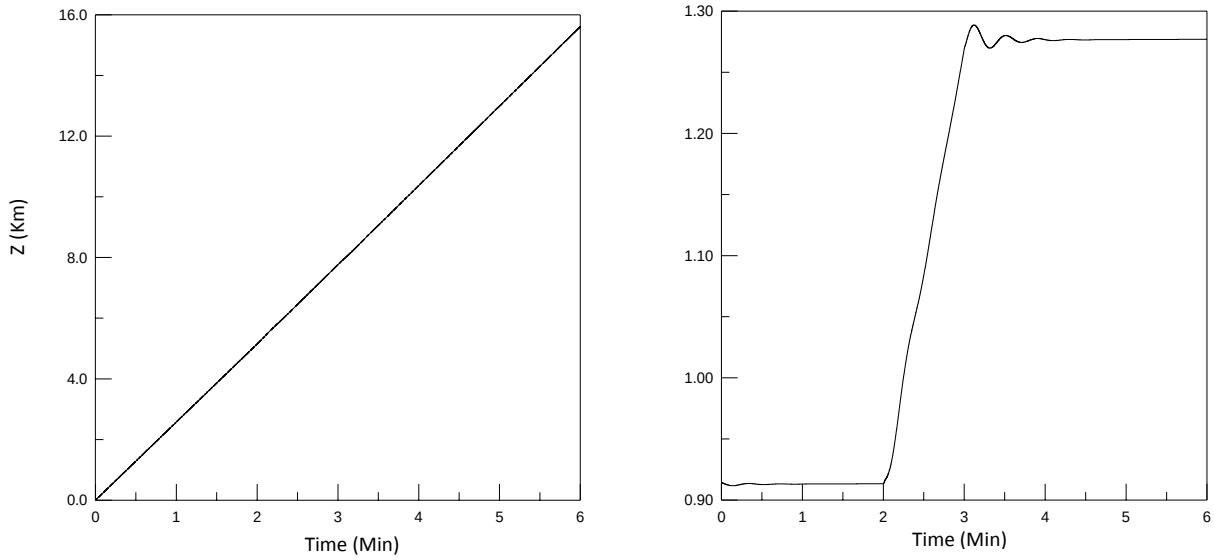

Figure 16: Time History of Aircraft Distance in X and Z-Direction with Normal Gust.

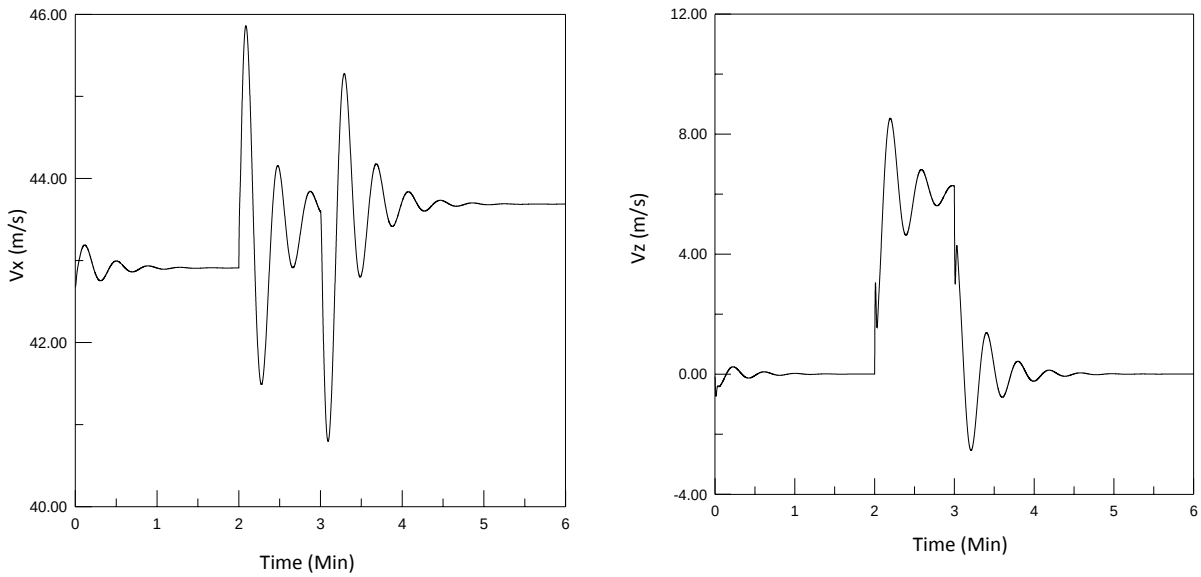

Figure 17: Time History of Aircraft Velocity in X and Z-Direction with Normal Gust.

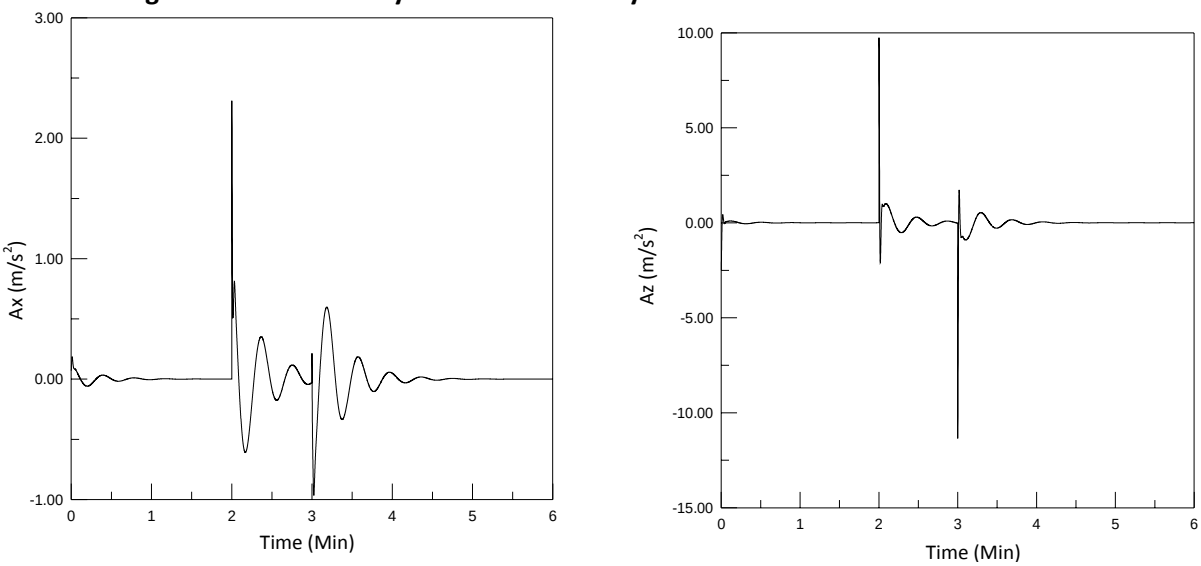

Figure 18: Time History of Aircraft Acceleration in X and Z-Direction with Normal Gust.

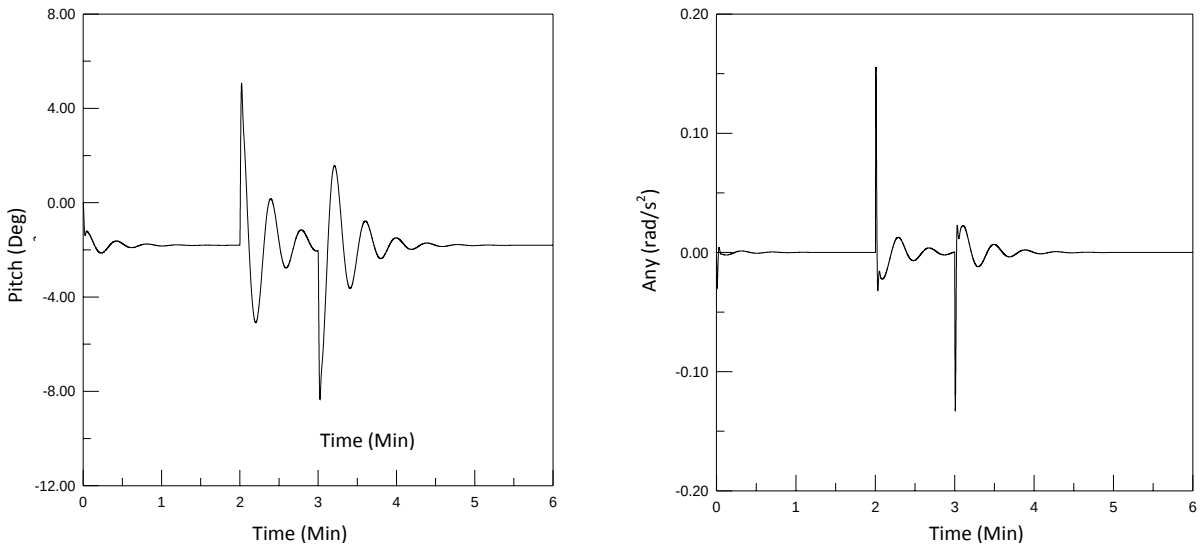

Figure 19: Time History of Pitch and Angular acceleration of aircraft with Normal Gust.

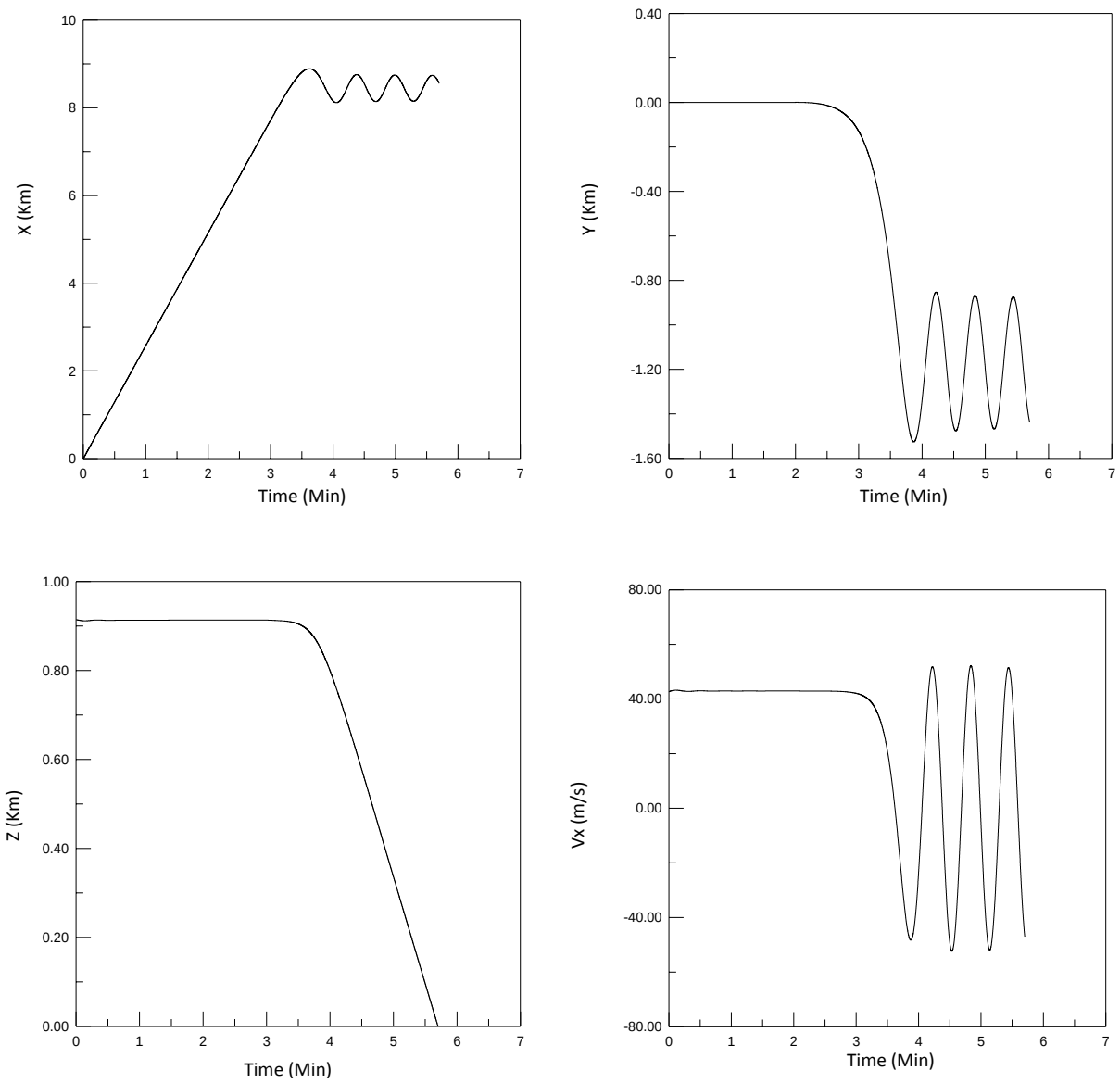

Figure 20: Time History of Aircraft Distances in X and Y-Direction with Shear Gust.

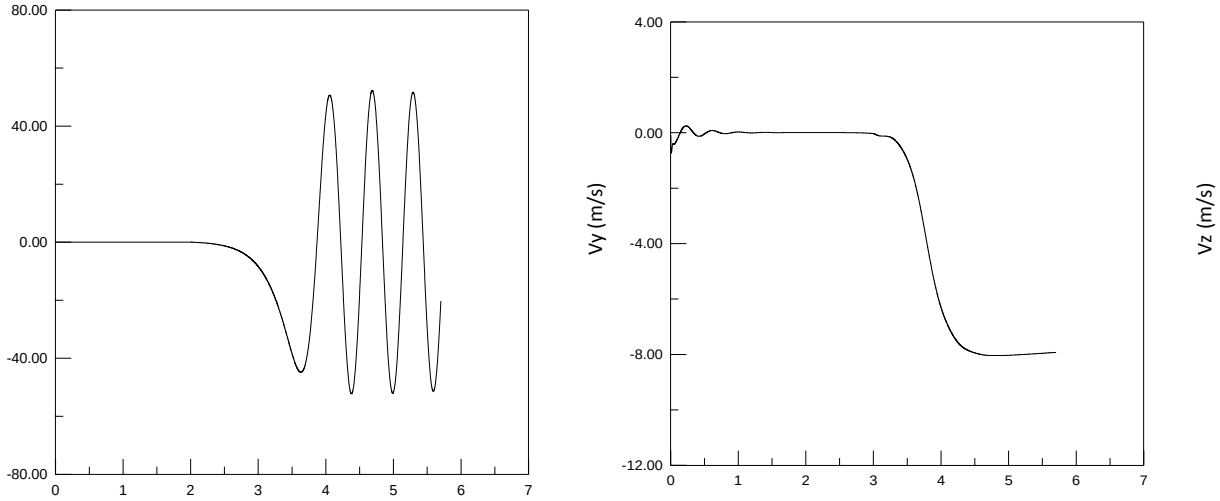

Figure 21: Time History of Aircraft Distance in Z-Direction and Velocity in X-Direction with Shear

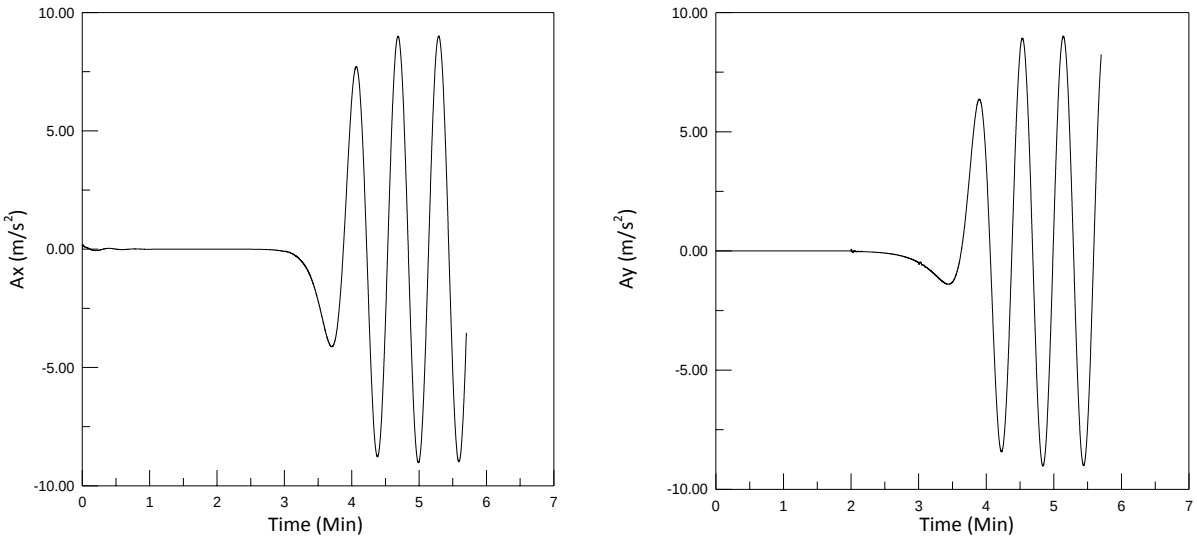

Figure 22: Time History of Aircraft Velocity in Y and Z-direction with Shear Gust.

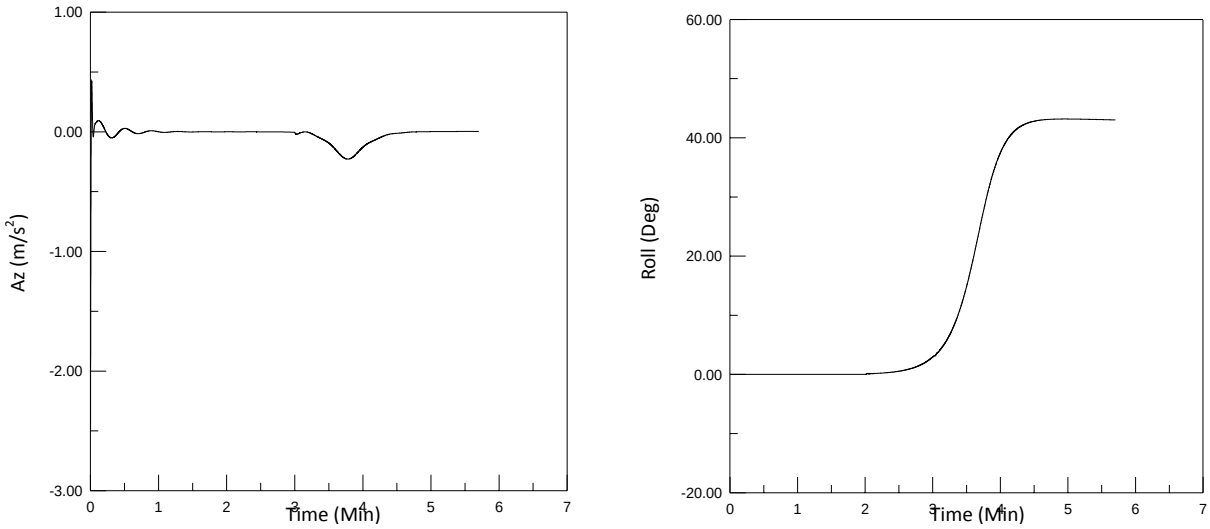

Figure 23: Time History of Aircraft acceleration in X and Y-Direction with Shear Gust.

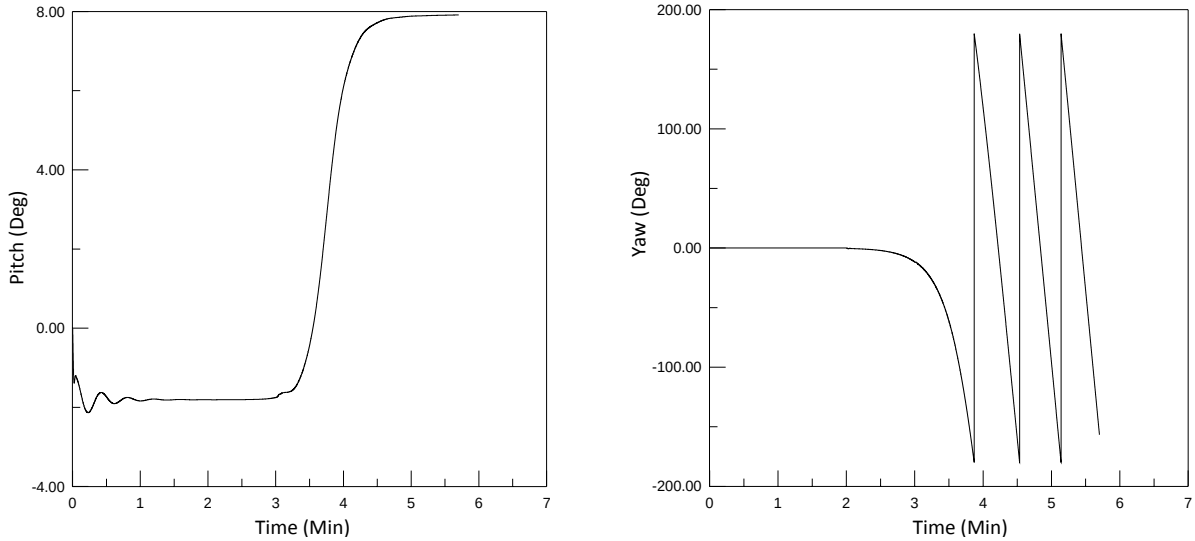

Figure 24: Time History of Aircraft acceleration and Roll angle with Shear Gust.

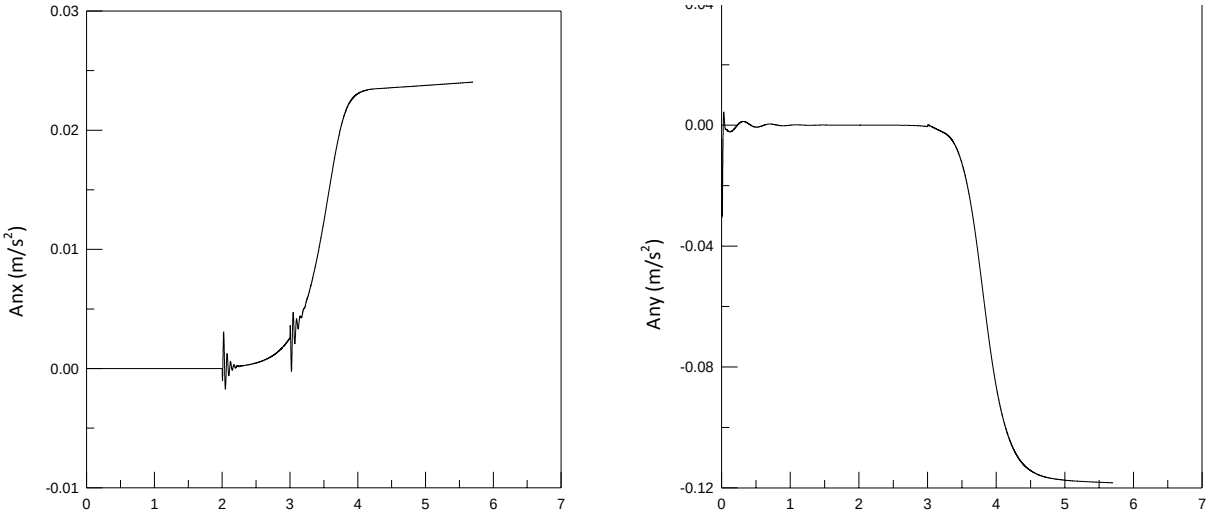

Figure 25: Time History of Aircraft Pitch and Yawing angles with Shear Gust.

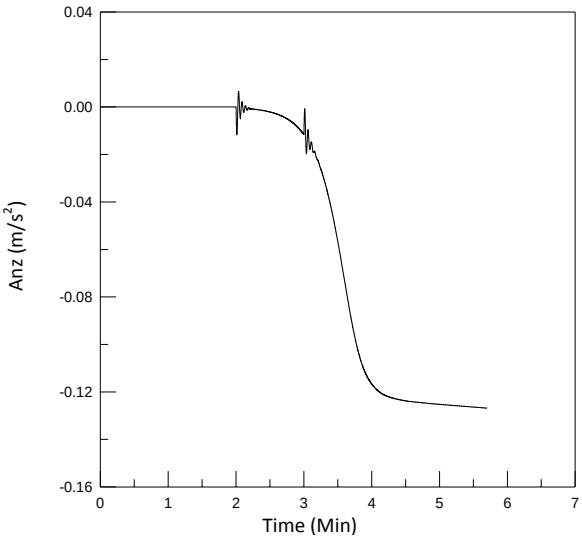

Figure 26: Time History of Aircraft Angular acceleration in X, Y and Z-Directions

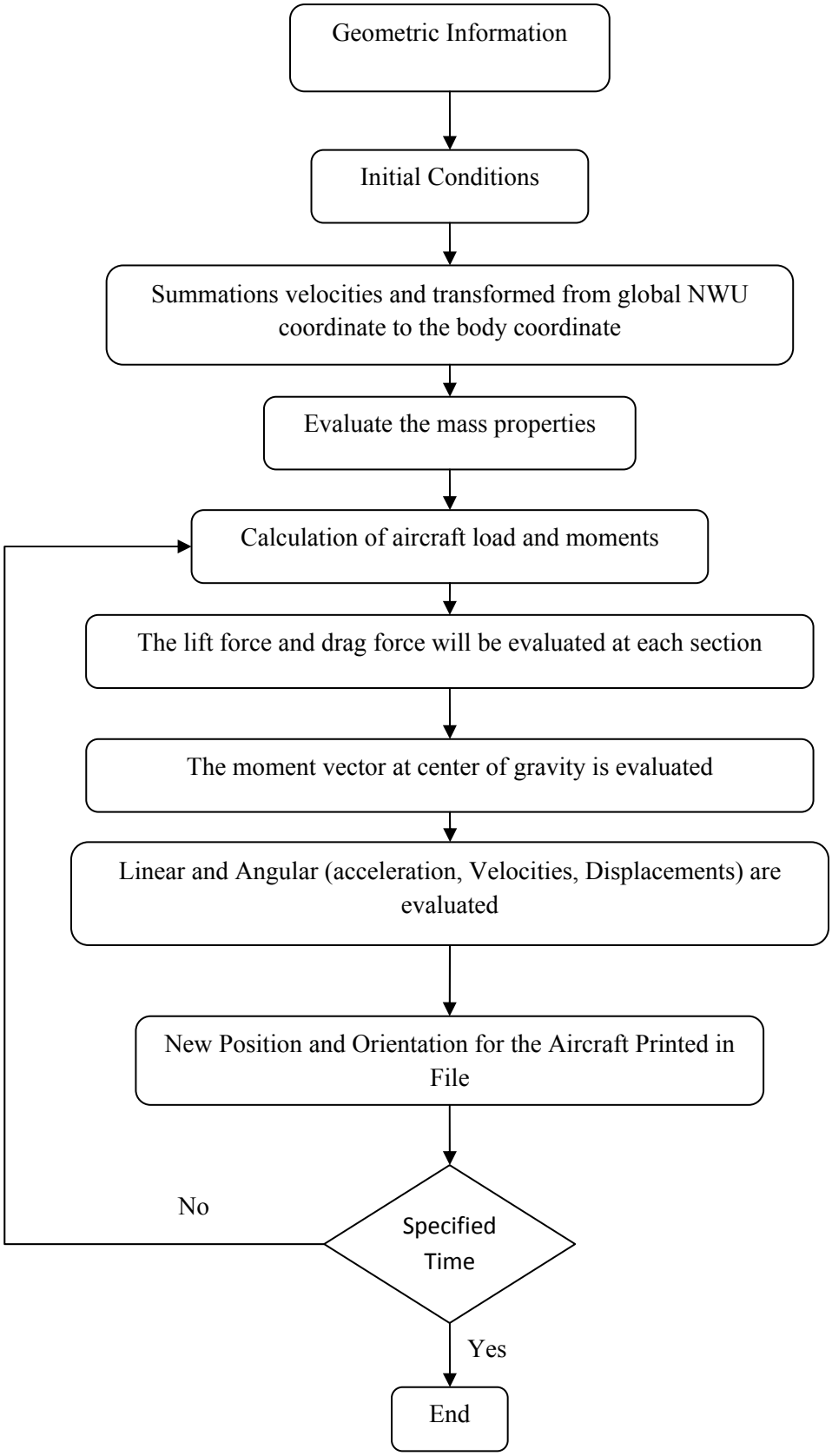

Figure 27: Flow Chart of Programme.

ORGANIZATION OF MEMORY CHIPS IN MEMORY SYSTEMS THAT HAVE WORD SIZE WIDER THAN 8-BIT

Omar W. Abdul-Wahab
University of Baghdad
College of Engineering
Computer Engineering Department

ABSTRACT
This paper presents a method to organize memory chips when they are used to build memory systems that have word size wider than 8-bit. Most memory chips have 8-bit word size. When the memory system has to be built from several memory chips of various sizes, this method gives all possible organizations of these chips in the memory system. This paper also suggests a precise definition of the term "memory bank" that is usually used in memory systems. Finally, an illustrative design problem was taken to illustrate the presented method practically.

الخلاصة
هذا البحث يقدم طريقة لتنظيم رقائق الذاكرة المستخدمة لبناء انظمة الذاكرة التي يكون عرض الكلمة فيها اكبر من 8 خانات. معظم رقائق الذاكرة يكون عرض كلمتها 8- خانات. عندما يراد بناء نظام ذاكرة باستخدام عدة رقائق ذاكرة ذات حجوم مختلفة فان هذه الطريقة تعطي كل التنظيمات الممكنة لهذه الرقائق في نظام الذاكرة. هذا البحث يقترح ايضا تعريفاً دقيقاً لمصطلح (صف الذاكرة) الذي يستخدم عادةً في انظمة الذاكرة. أخيراً تم اخذ مسألة تصميم توضيحية لشرح الطريقة المقدمة عملياً.

KEYWORDS
Data bank, address bank, *p*-tuple $(n_1, n_2, ..., n_p)$, combinations with repetition.

INTRODUCTION
Microprocessors are categorized into 4-bit, 8-bit, 16-bit, 32-bit, and 64-bit microprocessors. There are two points of views in identifying the category of a microprocessor. The first one, which is adopted in (Brey 2009) (Antonakos 2006) (Rafiquzzaman 1995) (Rafiquzzaman 2008) (Tischer and Jennrich 1996) (Triebel 1996) considers the internal architecture, i.e. the width of the internal data bus of the microprocessor, while the second one, which is adopted in (Protopapas 1988) (Godse 2007) (Antonakos 1999) considers the width of its external data bus. The difference becomes clear for microprocessors which have internal data bus wider than their external data bus, as in Intel 8088 and Motorola 68000. From the first point of view the 8088 is a 16-bit microprocessor and the 68000 is a 32-bit microprocessor, while from the second point of view the 8088 is an 8-bit microprocessor and the 68000 is a 16-bit microprocessor. Some references, such as (Mathur 1989), comprises between the two points of views so that they categorize the 8088 as a hybrid 8/16-bit microprocessor and the 68000 as a hybrid 16/32-bit microprocessor. To avoid any confusion, the phrase "microprocessor with d-bit external data bus" is used throughout this paper.

In many memory applications the required memory capacity or word size cannot be satisfied by one memory chip. Instead, several memory chips must be combined to provide the capacity and/or the word size (Tocci and Widmer 2001). The concept of building a memory device from smaller memories is called *memory banking* (Page 2009) or *memory array design* (Rafiquzzaman 2008), and the collection of smaller memories is called *memory bank*. There are two main advantages of memory banking. Firstly, from the memory designers' point of view, it prevents scale from becoming a problem. Secondly, the use of banked memory allows improving memory access performance for microprocessors that have external data bus wider than 8-bit (Page 2009). The second advantage is achieved by implementing the physical address space of the microprocessor as a number of independent byte-wide banks and each bank supplies just eight lines of the microprocessor's data

bus (Triebel 1996). In this way, all the bytes of a d-bit aligned word that are scattered amongst the banks can be accessed in parallel.

Memory locations are still numbered byte-wise either from the low order bank to the high order bank (little endian) such as the Intel family of microprocessors or from the high order bank to the low order bank (big endian) such as the Motorola family of microprocessors (Tanenbaum 2006) (Berger 2005) (Balch 2003). Since contiguous memory addresses represent memory locations lying in contiguous banks, the sizes of the memory banks must be equal.

A memory system generally consists of several memory chips. Generally, the word size of the memory system is determined by the width of the external data bus of the microprocessor (Mathur 1989). In (Shiva 2008), a method is given to design a memory system using memory chips. However, this method assumes equal size memory chips and does not handle memory systems that have word size wider than 8-bit. The method presented in this paper is a general method to design memory systems that have 8-bit word size or wider from different size memory chips.

DATA BANK AND ADDRESS BANK

The presented method needs a precise definition of the term *memory bank*. As defined in (Page 2009), a memory bank is a collection of memory devices. The system shown in **Fig. 1** is a 256 KB memory system built from eight 32 KB memory chips and interfaced to the 80486 microprocessor (Brey 2009). From one point of view there are four memory banks: chip collection (U6, U10), chip collection (U5, U9), chip collection (U4, U8), and chip collection (U3, U7). From another point of view there are two memory banks: chip collection (U3, U4, U5, U6) and chip collection (U7, U8, U9, U10). To distinguish between the two points of views, the term bank can be given a more descriptive definition which results in classifying it into *data bank* and *address bank*. Data bank is defined as the collection of memory chips that are connected to the same 8-bit data bus lines. On the other hand, address bank is defined as the collection of memory chips for which the maximum number of the higher address lines in the memory map of the memory system remain constant. Thus, the memory system shown in **Fig. 1** consists of four data banks and two address banks. The data banks are as follows: chip collection U6 and U10 which are connected to $D_0 - D_7$, chip collection U5 and U9 which are connected to $D_8 - D_{15}$, chip collection U4 and U8 which are connected to $D_{16} - D_{23}$, and chip collection U3 and U7 which are connected to $D_{24} - D_{31}$. The address banks are as follows: chip collection U3, U4, U5, and U6 for which the address lines A_{17} through A_{31} in the memory map of the memory system remain constant, and chip collection U7, U8, U9, and U10 for which the same address lines remain constant. **Fig. 2** shows a 128 KB memory system built from two 32 KB and one 64KB memory chips and interfaced to the 8086 microprocessor. For this memory system, there are two data banks and one address bank. The first data bank is chip collection U1 and U2 which are connected to $D_0 - D_7$ and the second data bank consists of chip U3 only which is connected to $D_8 - D_{15}$. To identify the address bank, memory chips U1 and U2 are considered as one unit so that the sum of their sizes equals to the size of U3. For chips U1 and U2, address lines A_{17} through A_{19} in the memory map remain constant. For chip U3, the same address lines have the same value as that of U1 and U2. Hence, U1 and U2 together with U3 constitute the address bank. This means that the largest memory chip in any data bank is considered as a reference in constructing address banks.

The address of any memory location determines the address bank and the data bank that contain this memory location. While the higher address lines determine the address bank, the $\log_2 \frac{d}{8}$ lower address bits (which are encoded internally by the microprocessor) determine the data bank. Therefore, a data bank does not contain memory locations that have arbitrary addresses; rather, it contains memory locations that have the same value of the $\log_2 \frac{d}{8}$ lower address bits. Thus, for a given memory location, its data bank is determined by:

$$i = (\text{Address of memory location}) \ \text{MOD} \left(\frac{d}{8}\right) \qquad (1)$$

where i is the index of the data bank.

CONSTRUCTION OF DATA BANKS

To design an M KB memory system whose word size is d-bit using N_1 memory chips of size M_1 KB and N_2 memory chips of size M_2 KB up to N_p memory chips of size M_p KB (so that $\sum_{i=1}^{p} N_i \times M_i = M$), there may be more than one possible arrangement of these memory chips among data banks. The following procedure can be used to determine these arrangements:

1- Since the size of the data banks in a memory system must be equal, the amount of memory in each data bank is

$$D = \frac{\text{Total amount of memory}}{\text{Word size of the memory subsystem}/8} = \frac{M}{d/8} \quad (2)$$

2- For each data bank, all the possible p-tuples $(n_1, n_2, ..., n_p)$ must be determined, where n_i are nonnegative integers that represent the number of memory chips of size M_i and satisfy the equation

$$M_1 \times n_1 + M_2 \times n_2 + ... + M_p \times n_p = D \quad (3)$$

This step results in **Table 1.**

If eq. (3) has no nonnegative integer solution, then any data bank cannot be constructed using the desired sizes of memory chips and hence the memory system cannot be designed.

Since the amount of memory in each data bank is the same (D KB), step 2 need not be repeated for all data banks. Instead, **Table 1** holds for all data banks.

3- Since there are $\frac{d}{8}$ data banks, therefore, $\frac{d}{8}$ p-tuples $(n_1, n_2, ..., n_p)$ must be chosen from **Table 1** to implement the total memory system. The number of ways of choosing a set of size $\frac{d}{8}$ from a set of size r that may be repeated any number of times is the combinations with repetition (Stirzaker 2003) (Kreyszig 2006). It is given by

$$C = \binom{r + \frac{d}{8} - 1}{\frac{d}{8}} = \frac{(r + d/8 - 1)!}{\frac{d}{8}! \times (r-1)!} \quad (4)$$

However, not all of these combinations satisfy the requirements of the total number of memory chips. From these combinations, the only possible ones are those satisfying the following summations

$$\sum_{j=1}^{d/8} n_{1i(j)} = N_1 \quad , \quad \sum_{j=1}^{d/8} n_{2i(j)} = N_2 \quad , \ .... \ , \text{ and}$$

$$\sum_{j=1}^{d/8} n_{pi(j)} = N_p \quad (5)$$

where $i(j)$ is the index of the ordered tuple in the combinations mentioned above. If there is no combination satisfies the above summations, then the memory system cannot be designed using the desired number of memory chips. **Fig. 3** shows a flow chart of an algorithm that determines these combinations.

CONSTRUCTION OF ADDRESS BANKS

After constructing data banks, address banks must be constructed. A suitable construction of address banks helps in simplifying the design of the decoder of the memory system.

A suitable way for constructing address banks is to sort the memory chips in each data bank in an ascending order according to their sizes. Then, looking at the first memory chip in each data bank, if all of these memory chips are of the same size, they would compose the first address bank; otherwise, the largest memory chip among these memory chips would be considered as a reference and in each data bank the remaining memory chips are collected with the first one so that they compose the same amount of memory as that of the reference one. The resultant memory chips in all data banks would compose the first address bank. This procedure is repeated for constructing other address banks (if any) with the remaining memory chips. The sizes of the address banks need not be equal.

DESIGN OF A 512 KB MEMORY SYSTEM WHOSE WORD SIZE IS 32-BIT

To illustrate the presented method practically, a 512 KB memory system whose word size is 32-bit is to be designed using eight 32 KB and four 64 KB memory chips. Here, $M = 512$, $N_1 = 8$, $M_1 = 32$, $N_2 = 4$, $M_2 = 64$, and $d = 32$. The amount of memory in each data bank, according to eq. (2), is

$$D = \frac{M}{d/8} = \frac{512}{32/8} = 128 \text{ KB.}$$

Substituting $M_1 = 32$ and $M_2 = 64$ in eq. (3) yields

$$32 \times n_1 + 64 \times n_2 = 128 \qquad (6)$$

and for each data bank the ordered pair (n_1, n_2) must satisfy eq. (6). **Fig. 4** shows the graph of eq. (6) which is a line in the $n_1 n_2$-plane. However, since n_1 and n_2 are nonnegative integers, only three points on this line satisfy eq. (6), which are (0,2), (2,1), and (4,0). Listing (1) is a C program that determines these solutions. The result is shown in **Table 2.**

There are $\frac{d}{8} = \frac{32}{8} = 4$ data banks, therefore, four ordered pairs (n_1, n_2) must be chosen from **Table 2** with the possibility of repetition. The number of combinations when repetition is possible, according to eq. (4), is

$$C = \binom{r + \frac{d}{8} - 1}{\frac{d}{8}} = \binom{3+4-1}{4} = \binom{6}{4} = \frac{6!}{4! \times 2!} = 15$$

From these 15 combinations we pick only those satisfying eq. (5), i.e., those satisfying

$$\sum_{j=1}^{4} n_{1i(j)} = N_1 = 8 \quad \text{and} \quad \sum_{j=1}^{d/8} n_{2i(j)} = N_2 = 4.$$

Listing (2) is a C program implementation of the algorithm shown in **Fig. 3** with $p = 2$, $r = 3$, and $d = 32$. Running this program gives the combinations {(2,1),(2,1),(2,1),(2,1)}, {(0,2), (0,2),(4,0),(4,0)}, and {(0,2),(2,1),(2,1),(4,0)}.

Fig.5 through **Fig. 7** show the schematic diagrams of the memory system for these three combinations of the data banks after constructing the address banks for each case.

CONCLUSIONS

From the presented method it is obvious that designing a memory system whose word size is wider than 8-bit is not as simple and straightforward as designing a memory system whose word size is 8-bit wide. The existence of more than one data bank raises the problem of distributing the memory chips among them so that they have the same amount of memory. This makes some restrictions on the size and number of the memory chips so that in some cases it is impossible to design a memory system from a given set of memory chips either because of their sizes or because of their number. On the other hand, the existence of more than one data bank makes the design of the decoder of the memory system more complex since the chip select signal must activate all the data banks simultaneously. This illustrates the need to suitably construct the address banks to simplify the design of the decoder. Finally, this method can be included in references that cover the subject of memory interface with advanced microprocessors.

Listing (1)

```
#include<stdio.h>
main()
{
        int n1,n2;
        for(n1=0;n1<=8;n1++)
        for(n2=0;n2<=4;n2++)
        if((32*n1+64*n2)==128)
        printf("%d\t%d\n",n1,n2); }
```

Listing (2)

```
#include<stdio.h>
main()
{       int i,j,k,m,sumn1,sumn2, n[5][5];
        n[1][1]=0;n[2][1]=2;n[1][2]=2;n[2][2]=1;
        n[1][3]=4;n[2][3]=0;
        for(i=1;i<=3;i++)    for(j=1;j<=3;j++)
        for (k=1;k<=3;k++) for (m=1;m<=3;m++)
{       if((m>=k)&&(k>=j)&&(j>=i))
```

```
{       sumn1=n[1][i]+n[1][j]+n[1][k]+n[1][m];
        sumn2=n[2][i]+n[2][j]+n[2][k]+n[2][m];
        if((sumn1==8)&&(sumn2==4))
{       printf("\n %d %d",n[1][i],n[2][i]);
        printf("\n %d %d",n[1][j],n[2][j]);
        printf("\n %d %d",n[1][k],n[2][k]);
        printf("\n %d %d",n[1][m],n[2][m]);
} } } }
```

REFERENCES

Antonakos, J. L., "The Intel Microprocessor Family", Delmar Thomson Learning, 2006.

Antonakos, J. L., "The 68000 Microprocessor", Prentice-Hall, 1999.

Balch, M., "Complete Digital Design", McGraw-Hill, 2003.

Berger, A. S., "Hardware and Computer Organization", Elsevier, 2005.

Brey, B. B., "The Intel Microprocessors", Prentice-Hall, 2009.

Godse, A. P. and Godse, D. A., "Microprocessor Interfacing Techniques", Technical Publications pune, 2007.

Kreyszig, E., "Advanced Engineering Mathematics", John Wiley and Sons, 2006.

Mathur , A. P., "Introduction to Microprocessors", Tata McGraw-Hill, 1989.

Page, D., "A Practical Introduction to Computer Architecture", Springer, 2009.

Protopapas, D. A., "Microcomputer Hardware Design", Prentice-Hall, 1988.

Rafiquzzaman, M., "Microprocessors and Microcomputer-Based System Design", 1995.

Rafiquzzaman, M., "Microprocessor Theory", John Wiley & Sons, 2008.

Shiva, S. G., "Computer Organization, Design and Architecture", Marcel Dekker, 2008.

Stirzaker, D., "Elementary Probability", Cambridge University Press, 2003.

Tanenbaum, A. S., "Structured Computer Organization", Pearson Education, 2006.

Tischer, M. and Jennrich B., "PC Intern", Abacus, 1996.

Tocci, R. J. and Widmer, N. S., "Digital Systems", Prentice-Hall, 2001.

Triebel, W. A., "The 80386, 80486, and Pentium Processors", Prentice Hall, 1996.

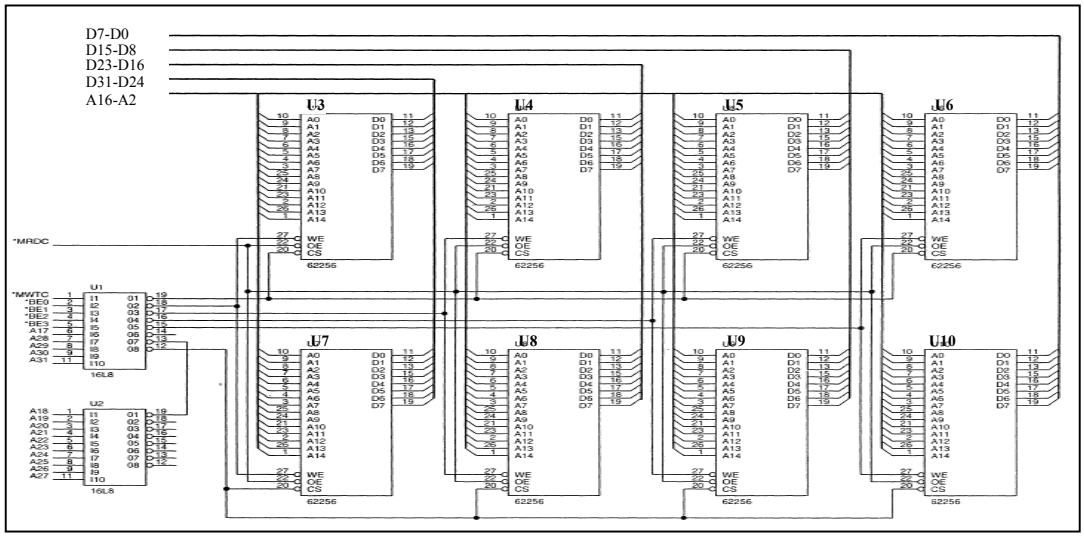

Fig. 1: A 256 KB memory system interfaced to the 80486 microprocessor.

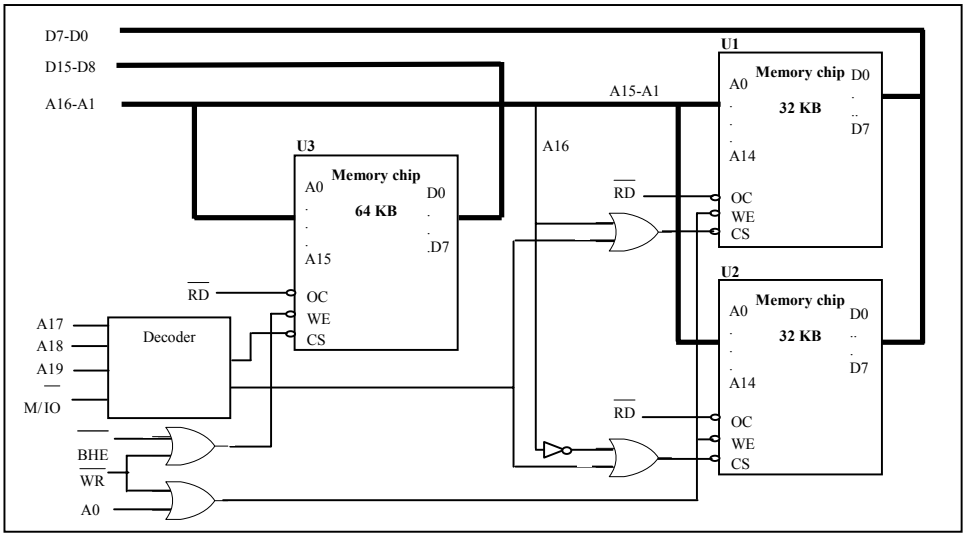

Fig. 2: A 128 KB memory system interfaced to the 8086 microprocessor.

Table 1: Nonnegative integer solutions of eq. (3)

$(n_1$	n_2	$\cdots$	$n_p)$
$(n_{11}$	n_{21}	$\cdots$	$n_{p1})$
$(n_{12}$	n_{22}	$\cdots$	$n_{p2})$
$\vdots$	$\vdots$	$\cdots$	$\vdots$
$(n_{1r}$	n_{2r}	$\cdots$	$n_{pr})$

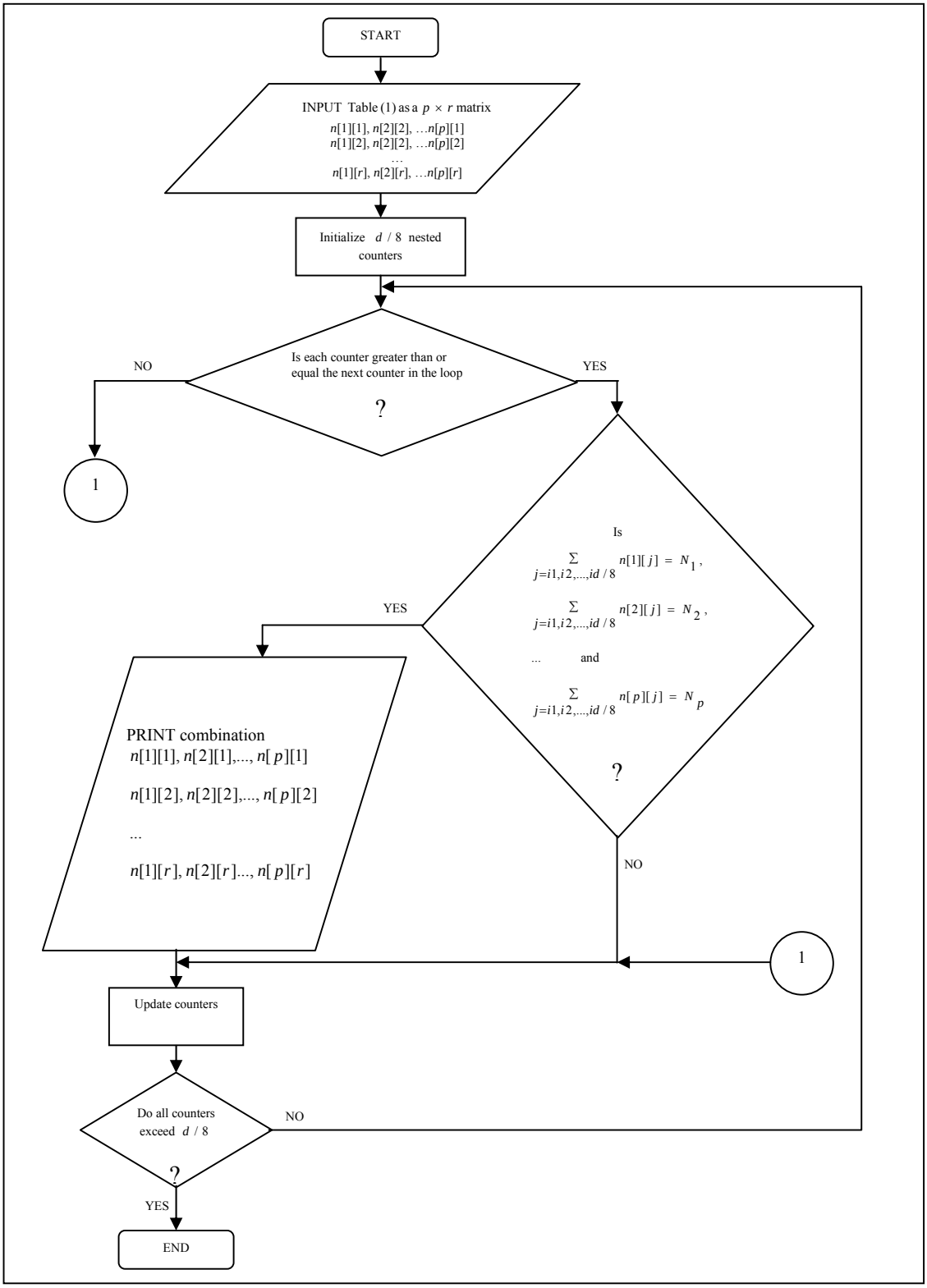

Fig. 3: Flow chart of an algorithm that determines the combinations that represents all the possible arrangements of memory chips among data banks

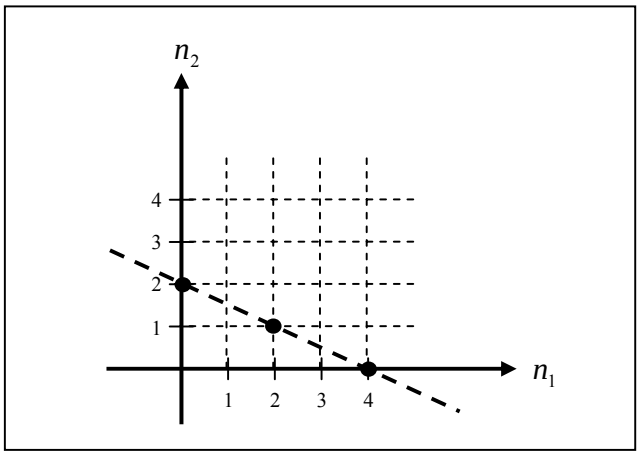

Fig. 4: Graph of eq. (6) with its nonnegative integer solutions.

Table 2: Nonnegative integer solutions of eq. (6).

$(n_1$	$n_2)$
(0	2)
(2	1)
(4	0)

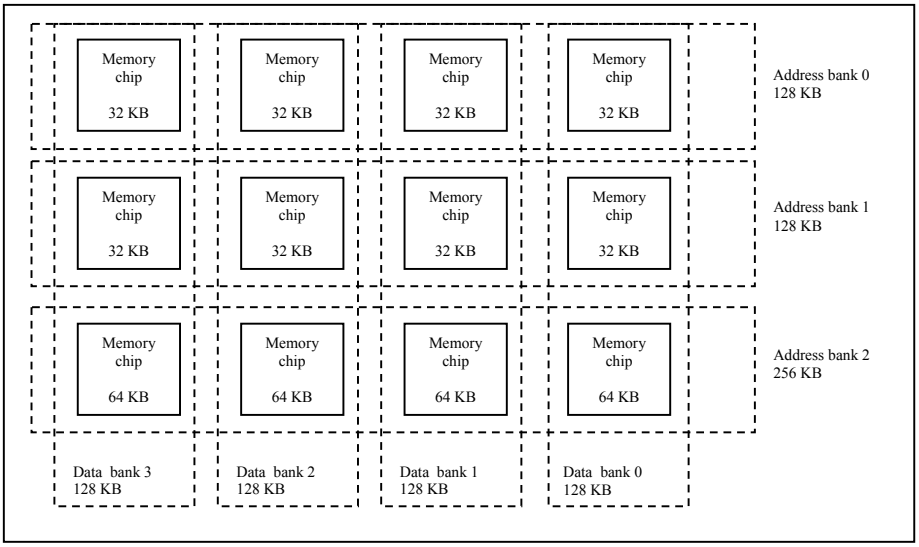

Fig. 5: Data banks arranged as $\{(2,1),(2,1),(2,1),(2,1)\}$

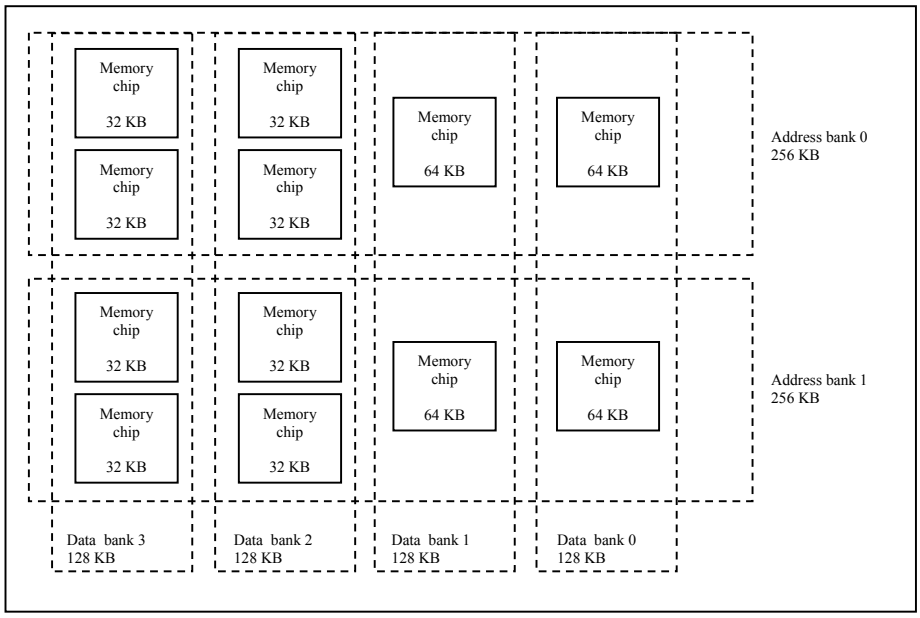

Fig. 6: Data banks arranged as $\{(0,2),(0,2),(4,0),(4,0)\}$

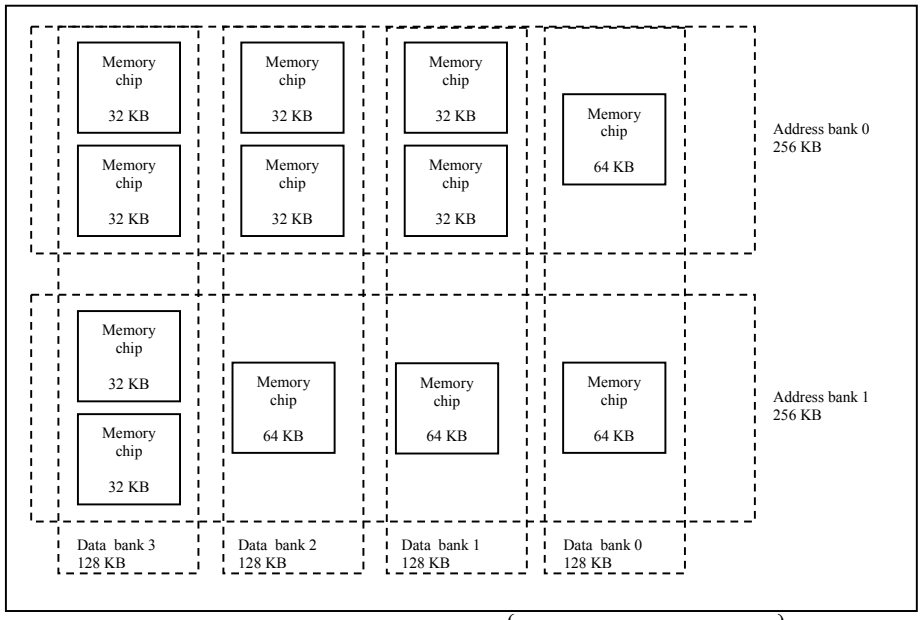

Fig. 7: Data banks arranged as $\{(0,2),(2,1),(2,1),(4,0)\}$

ESTIMATION THE 7 AND 28- DAY NORMAL COMPRESSIVE STRENGTH BY ACCELERATED TEST METHODS IN CONCRETE

Dr. Prof. R.S. Al Rawi **Dr. Dr.Firas F. Abdul-Hameed** **Dr. Zena K. Abbas**

ABSTRACT

Curing of concrete is the maintenance of a satisfactory moisture content and temperature for a period of time immediately following placing so the desired properties are developed. Accelerated curing is advantages where early strength gain in concrete is important. The expose of concrete specimens to the accelerated curing conditions which permit the specimens to develop a significant portion of their ultimate strength within a period of time (1-2 days), depends on the method of the curing cycle.

Three accelerated curing test methods are adopted in this study. These are warm water, autogenous and proposed test methods. The results of this study has shown good correlation between the accelerated strength especially for the proposal curing test method and normal strength using normal curing method at ages 7 and 28 day for the five different chemical composition of cement with different water to cement ratios equal to 0.45, 0.55, 0.65 and 0.75. Linear and nonlinear regression analysis show high correlation for the different types of the accelerated curing methods with coefficient of correlation (R^2) more than 0.9.

تخمين مقاومة الانضغاط الاعتيادية بعمر 7 و 28 يوم بأستخدام طرق الفحص المعجلة في الخرسانة

أ.د. رياض شفيق الراوي د. فراس فيصل عبد الحميد د. زينة خضير عباس

الخلاصة

معالجة الخرسانة هي من أجل المحافظة على كمية الماء المناسبة و درجة الحرارة لفترة من الزمن مباشرة بعد عملية الوضع من أجل تطوير الخصائص المطلوبة. المعالجة بالطريقة المعجلة هي مفيدة عندما يكون من المهم الحصول على القوة المبكرة. تم دراسة النماذج الخرسانية المعرضة الى المعالجة المعجلة من أجل الحصول على الجزء الاكبر من قوتها النهائية خلال فترة تتراوح بين يوم و يومين بالاعتماد على طريقة المعالجة.

أعتمدت ثلاثة طرق في المعالجة المعجلة و هي طريقة الحمام الدافئ ، طريقة التعجيل الذاتي و الطريقة المقترحة. أظهرت النتائج علاقة جيدة بين المقاومة المعجلة و خاصة الطريقة المقترحة مع 7 و 28 يوم للخرسانة المعجلة أعتياديا للخمس أنواع سمنت مختلفة التركيب الكيمياوي و لنسبة ماء الى سمنت تساوي 0.45، 0.55 ، 0.65 و 0.75. الموديلات الاحصائية الخطية و غير الخطية أظهرت علاقة جيدة للطرق المختلفة للمعالجة المعجلة مع معامل أرتباط لا يقل عن 0.9.

Keywords: accelerated strength, normal strength, warm test method, autogenous test method, proposed test method, compressive strength, regression analysis

1.0 INTRODUCTION

Accelerated curing of concrete is used extensively in the production of the precast concrete structural members such as pipes and prestressed products are used to get a high early strength enough to transfer the prestress force to concrete and lift the precast element. The acceptance of concrete in the site depends on the 28 days strength, at that time, usually a considerable concrete work has been done on the first casting which makes the remedy for the weak concrete is very difficult and complicated, also if it was too strong, the mix proportion used will be uneconomical. Thus, the production control with 28 days delay is not sensible **[Neville (1995)].** Concrete specimens are exposed to accelerated curing conditions that permit the specimens to develop a significant portion of their ultimate strength within a time period of (1-day to 2-day depends on the method of curing cycle).The accelerated curing procedure provides at the earliest practical time, an indication of the potential strength of a specific concrete mixture.

The accelerated strength tests used in the experimental work is presented below:

1.1 Warm Water Method.

This test method is applied according to the **ASTM C684-99 (method A)** and **BS 1881: Part 112:1983**

1.2 Autogenous Method.

This test method is applied according to the **ASTM C 684-99 (method C)** except that the satisfactory containers are unavailable in the lab, and the average temperature lab test is approximately 30°C.

1.3 Proposed Method

The cycle includes the delay period, the temperature rise period, and the period of the curing at the maximum temperature. It is designed to enable a turnover of one batch per one day, allowing for cooling, demolding, cleaning, oiling, and assembling molds for the next batch. Then cubes are tested. The curing cycle is adopted below after casting the concrete in 100mm cube mold in the normal way. The molds are covered with a top plate in good contact with the top face of the mold:

1. Delay period (Presteaming period): The curing cycle is also designed to minimize the destructive processes in the structure of the accelerated –cured concrete by using an adequate delay period and a medium rate of temperature rise. **Mamillian (1982)** as reported by **Al Qassab (2006)** concluded that the loss in the 28-day strength can be reached 40% for the steam cured concrete at 75ºC with no delay period.

Results obtained by **Lewis (1968)** using 100mm cube specimens show that the optimum initial maturity prior to the steam curing and corresponding to maximum strength is about 80˚C. A study done by **Al Rawi (1974)** concludes that the use of a short delay period 1hr resulted in an appreciable in a1-day accelerated curing plus 27-day normal curing compressive strength of concrete, as compared with the strength obtained when 5 to 11-hr delay periods are used. Therefore, such short delay periods should not be used unless the large expansion of the liquid phase is counteracted by some means such as closed rigid molds. Assuming the temperature of the mix prior to steam curing was 20˚C, the optimum delay period will be 4-hr. Therefore, a delay period of 4-hr is used.

2. Rate of temperature rise: After a delay period of 4-hr, the molds are placed in a water tank at a temperature of 20˚C, the water temperature is raised to 70˚C±4˚C in about 2-hr, with rate of temperature rise about 25˚C per hour. As a practical method operation, a maximum rate of temperature rise is 22˚C to 33˚C **[ACI 517.2R-80]**.

3. Maximum curing temperature and duration: Several investigators have found that the most effective results are obtained when the concrete is cured at a temperature between 66˚C and 82˚C, lower temperature are advantageous if steaming is continued for more than 24-hr **[ACI 517.2R-80].**

The temperature is chosen 70˚C±4˚C for 16-hr which is in confidence by the results of **Al-Rawi (1977)** for choice of cured concrete. He also finds that there is no such difference

between 70˚C and 90˚C. For 80˚C and above the hydration of the C_3A will form the cubic C_3AH_6 phase, instead of hexagonal phases. High steam – curing temperatures always require longer presteaming periods. Early strengths are higher, but 28-day strengths are generally lower with high steaming temperatures **[ACI 517.2R-80]** as explained above.

The desired maximum temperature within the enclosure and the concrete is approximately 66˚C. It has been shown that the strength will not increase significantly if the maximum steam temperature is raised from 66˚C to 79˚C, and the steam temperatures above 82˚C should be avoided because of the wasted energy and potential reduction in ultimate concrete strength **[Kosmatka and Panarese (1994)].**

4. Cooling period: Rapid changes during the cooling period should be avoided so as to reduce the cracking of the members from the effects of restraints **[ACI 517.2R-80]**. The temperature of the water tank dropped approximately to 21˚C within about 2-hr.

This 24-hr curing cycle is shown in the Figure (1) and Figure (2) for typical idealized atmospheric steam-curing cycle for pipe [**ACI 517.2R-80**]. The molds then are removed from water tank and the cubes are tested in half an hour.

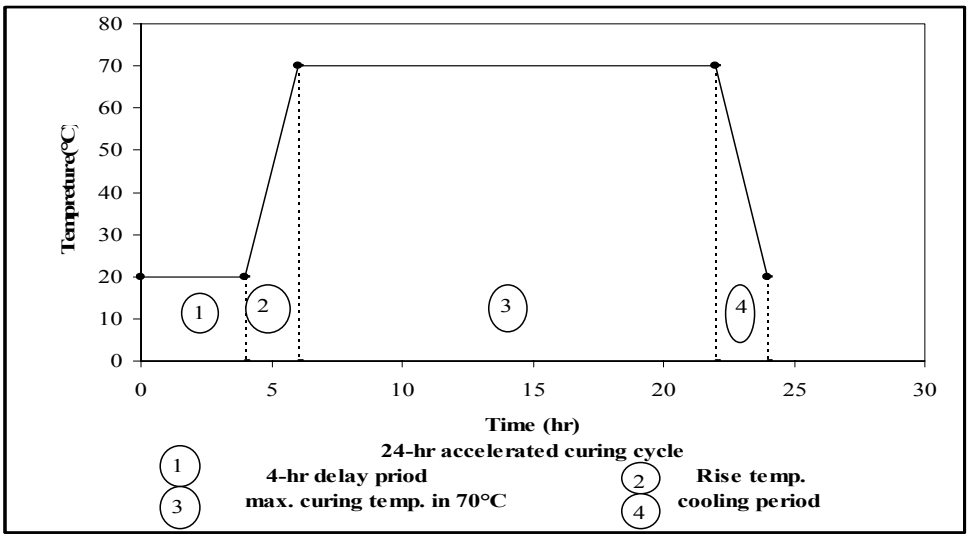

Fig. 1: Proposed accelerated curing cycle.

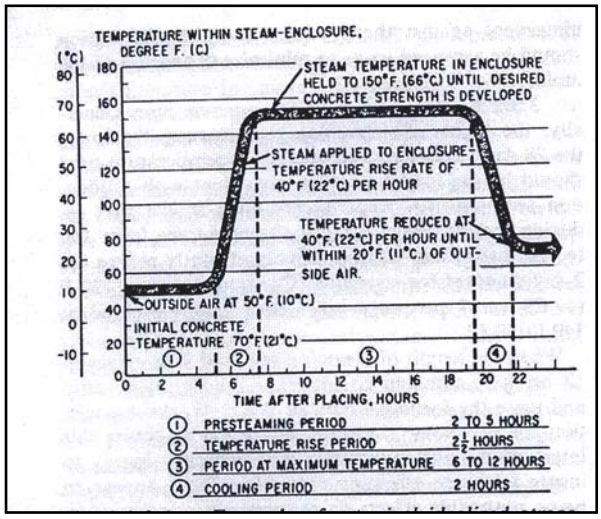

Fig. 2: Typical idealized atmospheric steam-curing cycle for pipe- **ACI 517.2R-80**.

2.0 EXPERIMENTAL PROGRAM

2.1 Materials

2.1.1 Cement

Five different chemical composition Portland cements, conforming to the **IQS 5/1984** were used. Three ordinary Portland cement (Iraqi, Lebanese and Turkish) and two sulfate resisting Portland cement (Lebanese and Kuwaiti).

The chemical analysis and physical properties of these cements are listed in Tables 1 and 2 respectively.

Table 1: Chemical composition of cement used

Oxide Content %	Iraqi (OPC)	Turkish (OPC)	Lebanese (OPC)	Lebanese (SRPC)	Kuwaiti (SRPC)
SiO_2	20.49	20.63	20.4	21.25	19.65
Al_2O_3	4.56	4.77	4.94	3.10	3.78
Fe_2O_3	4.35	4.64	3.84	4.00	3.89
CaO	61.82	61.89	60.34	59.08	63.93
SO_3	2.31	2.14	2.68	2.11	2.30
MgO	2.59	2.13	4.58	2.02	3.30
L.O.I	2.23	1.47	2.35	3.10	2.45
I.R	1.12	1.50	0.62	1.74	1.56
L.S.F	0.92	0.904	0.89	0.86	0.85
Compound Composition (Bogue` s Equation)					
C_3S	52.44	50.32	44.22	46.39	72.76
C_2S	19.27	21.27	25.21	26.01	1.53
C_3A	4.73	4.80	6.60	1.45	3.44
C_4AF	13.22	14.10	11.67	12.16	11.82

- Chemical and Physical tests are conducted by the Central Organization for Standardization and Quality Control, Ministry of Planning

Table 2: Physical properties of cements used

Properties	Iraqi (OPC)	Turkish (OPC)	Lebanese (OPC)	Lebanese (SRPC)	Kuwaiti (SRPC)
Specific surface (Air permeability test),m^2/kg	340	380	340	360	350
Autoclave expansion,%	0.01	0.04	0.07	0.04	0.04
Setting time (vicate apparatus),					
a. Initial - hr:min	2:30	3:35	3:30	1:40	2:25
b. Final - hr:min	4:0	4:35	5:30	4:40	4:30
Compressive strength MPa(N/mm^2):					
a. 3-days	30.96	32.12	27.99	30.5	31.5
b. 7-days	35.71	33.99	29.6	31.5	32.5

- Chemical and Physical tests are conducted by the Central Organization for Standardization and Quality Control, Ministry of Planning

- L.O.I: Loss on ignition, I.R: Insoluble residue, L.S.F: lime saturation factor.

2.1.2 Fine Aggregate

Fine aggregate from Al-Ukhaider region was used. The grading satisfy the Iraqi specification **IQS 45/1984** and failed in the zone two. The sieve analysis is shown in Table 3. The sulfate content and the physical properties of fine aggregate are shown in Table 4.

2.1.3 Coarse Aggregate

The maximum size of 20mm of natural coarse aggregate from Al-Niba`ee quarry (crushed) was used. The aggregate satisfies the Iraqi specification **IQS 45/1984**. The sieve analysis for the crushed aggregate is shown in Table 5. The sulfate content and the physical properties are shown in Table 6.

Table 3: Sieves analysis of fine aggregate.

Sieve size	% passing by weight	Limits of IQS 45/1984 (Zone 2)
10mm	100	100
4.75mm	96	90-100
2.36mm	82	75-100
1.18mm	69	55-90
600µm	47	35-59
300µm	21	8-30
150µm	5	0-10

Fineness modulus = 2.8

Table 4: Physicals properties and sulfate content of fine aggregate used in experimental work.

Properties	results	Specification	IQS 45/1984
Grading zone	Zone 2	IQS 45/1984	
Fineness modulus	2.8	ASTM C125-03	
Specific gravity	2.6	ASTM C128-01	
Absorption ,%	1.5	ASTM C128-01	
Moisture content,%	0.3	ASTM C566-97	
Passing sieve size 75µm%	2.2	IQS No. 45-84	Max. 5% for natural fine aggregate
Sulfate content (SO_3), %	0.2	IQS No. 33-89	Max. 0.5%

- Tests are carried out in the Material Laboratory of the College of Engineering-Baghdad University

Table 5: Sieves analysis of coarse aggregate with 20mm maximum size.

Sieve size	% passing by weight	Limits of IQS 45/1984
37.5mm	100	100
20mm	96	95-100
10mm	41	30-60
5mm	2	0-10

Table 6: Physical properties and sulfate content of coarse aggregate with 20mm maximum size.

Properties	results	Specification	IQS 45/1984
Dry rodded unit weight,kg/m^3	1680	ASTM 29/C29M/97	--
Specific gravity (Saturated surface dry)	2.67	ASTM C127-01	--
Absorption ,%	0.8	ASTM C127-01	--
Moisture content ,%	0.2	ASTM C566-97	--
Passing sieve size 75µm,%	0.9	IQS No. 45-84	Max. 3% for natural coarse aggregate
Sulfate content (SO_3),%	0.02	IQS No. 33-89	Max. 0.1%

- Tests are carried out in the Material Laboratory of the College of Engineering-Baghdad University

2.1.4 Mixing Water

Ordinary water is used for mixing and curing of the concrete, according to the **IQS 1703/1992**. The PH equal to 7.4 and the TDS (total dissolve solids means the sum of all the minerals, metals, salts dissolved in the water) equal to 389ppm.

2.2 Mix Proportion

The ACI **211.1-91** mix design method recommended specifies both the maximum and minimum value for the slump which is based on the type of construction. So, it is decided to select (75-100) mm as a range for slump in all the experimental work.

In this method, the required water/cement ratio is determined by the compressive strength and the durability requirement. In the present work, four water/cement ratios are used (0.45, 0.55, 0.65 and 0.75) by weight as an attempt to use low, medium and high W/C ratios. The mix proportions and adjustment to keep the effective W/C constant used in preparing the test specimens according to **ACI 211.1-91** method is presented below in Table (7).

Table (7): The mix proportions used in preparing the test specimens according to **ACI 211.1-91** method

W/C	Water (kg/m^3)	Cement (kg/m^3)	Fine aggregate (kg/m^3)	Coarse aggregate (kg/m^3)
0.45*	203	451	639	1036
0.45**	209	464	628	1036
0.55	203	369	706	1036
0.65	203	312	754	1036
0.75	203	270	788	1036

* Trial batch adjustment (before adjusting)
** After adjusting

2.3 Mixing, Casting, Curing of Concrete

The cement was passed through the sieve No.14 (1.18mm) and the lumps were removed. The mixing of ingredients is done by hand in a plastic pan. Cast iron cube moulds, with dimensions of 100x100x100mm are prepared, cleaned and oiled before starting mixing of concrete.

Casting was made in two layers; the compaction of concrete was done by a vibrating table for 10 to 15 second for each layer. For the normal curing, after casting (30-

45minutes), the molds were covered with Nylon bag and polyethylene sheets and for the 3-cubes accelerated curing test the procedure was mentioned in the curing cycle. For the normal curing the concrete specimen was kept their moulds for nearly 24hr, then they are demolded and placed in the curing tank filled with water until the time of testing (7 and 28-day according to test procure), and for accelerated curing test the procedure was mentioned in the curing cycle.

2.4 Tests Performed

The following are the standard tests that were carried out on the fresh concrete, and hardened concrete.

2.4.1 Fresh Concrete

A slump test is the most usual test used in Iraq for testing the workability of the fresh concrete. The **ACI 116-90** describes it as a measure of consistency. The slump test of fresh concrete is according to **ASTM C143/C143M– 00**. The present experimental work is based on the mix proportion method with a slump range (75-100mm).

2.4.2 Compressive Strength Test

The compressive strength test of concrete cubes of (100) mm was carried out in the present work according to the **BS 1881: Part 116: 1983**, because it is the most suitable test for the compressive strength used in Iraq. The cubes of concrete were tested at accelerated curing test (warm water method, autogenic curing method and proposal method) with the 7, 28, 90, 180-day for normal curing strength according to the test procedure.

At each test age, three cubes of concrete are taken from the curing tank and were placed in the testing machine. The load at failure was recorded and calculates the average of compressive strength for the 3-cubes at each age test.

3. RESULTS AND DISCUSSION

3.1 Fresh Concrete –Slump Test

The slump result for different chemical compositions of the 5-cements is presented in Table 8. Figure 3 illustrates that the Turkey cement is the lowest slump result for different W/C ratios, then the Lebanese(SRPC), that is compatible with a high specific surface area of cement for Turkish- 380 m^2/kg and Lebanese(SRPC)-360 m^2/kg compared with the others lead to reduce the slump test result.

Table 8: Slump test for different types of cement and W/C ratios.

Type of cement	Slump (cm)			
	W/C= 0.45	W/C= 0.55	W/C= 0.65	W/C= 0.75
Iraqi (OPC)	8.5	9.5	10.0	11.5
Turkish (OPC)	7.0	7.5	8.0	9.0
Leb. (OPC)	8.0	9.5	10.5	11.0
Leb. (SRPC)	7.75	8.5	9.5	10.5
Kuwait(SRPC)	8.5	9.0	10.0	11.0

3.2 Hardened Concrete -Compressive Strength Test

The development of the compressive strength with the age (accelerated strength for different methods, 7and 28-day normal strength) for the twenty mixes used through the first part of this study is shown in the Table 9. Figures 4 to 9 show the relation between water to cement ratios (0.45, 0.55, 0.65 and0.75) with the compressive strength (accelerated strength for different methods and 7, 28 day normal strength).

The curves indicate that the proposed method is the closer to the 7-day normal then the autogenous then the warm water method for the same water to cement ratio at a given

age. The difference is related to the effect of the method of the accelerated test.

The mixes for the Kuwaiti cement (SRPC) show a high rate of gaining strength relative to the other mixes. This cement has relatively a high C_3S to a C_2S ratio, Sr = 47.4. Meanwhile ,the mixes for the Iraqi and Turkish cements (OPC) are more faster gaining strength than the Lebanese cement (OPC) , this could be attributed to a high content of the C_3S = 52.44% and 50.32% with Sr = 2.72 and 2.365 for Iraqi and Turkey cements respectively, and the C_3S = 44.22 with Sr = 1.754 for the Lebanese cement (OPC).

Finally the mixes for the Lebanese cement (SRPC) gained strength faster than the Lebanese cement (OPC) with closer Sr = 1.78 and 1.754 respectively, although, the reviewed literature shows that the (OPC) cements often have high early strength and gain strength faster than the SRPC cement and this can be attributed to the failure of the Lebanese mixes (OPC) to achieve the minimum average strength for different water to cement ratios.

Table 9: Accelerated strength (warm, autogenous and proposed method) with normal strength (7 and 28 day) for different type of cement -Reference mixes

Mix. No.	Cement Type	Sr.	W/C	Accelerated strength MPa			Normal strength MPa	
				Warm method 1-day	Autogenous method 1-day	Proposed method 2-day	7-day	28-day
1	Iraqi (OPC)	2.72	0.45	15.0	16.75	25.5	28.25	40.5
2			0.55	13.75	15.75	23.75	25.75	37.5
3			0.65	10.25	13.0	19.0	21.5	28.0
4			0.75	8.25	9.5	14.25	14.75	21.5
5	Turkish (OPC)	2.365	0.45	14.75	16.5	25.0	27.75	40.25
6			0.55	13.0	14.75	22.25	24.75	35.5
7			0.65	9.75	11.25	17.25	19.75	27.0
8			0.75	8.0	8.75	12.75	14.25	20.75
9	Leb. (OPC)	1.754	0.45	13.25	15.25	22.75	26.5	38.25
10			0.55	10.25	12.25	18.0	20.25	30.5
11			0.65	7.25	9.5	13.5	16.75	22.5
12			0.75	6.25	7.25	10.75	12.0	19.5
13	Leb. (SRPC)	1.78	0.45	14.25	16.25	24.5	27.0	39.0
14			0.55	12.25	14.25	21.0	23.75	34.5
15			0.65	9.0	11.0	16.25	18.5	26.5
16			0.75	7.75	8.25	12.25	14.0	20.0
17	Kuwaiti (SRPC)	47.4	0.45	16.75	17.75	26.0	29.0	42.75
18			0.55	14.75	16.25	24.25	26.5	39.5
19			0.65	11.5	13.5	20.5	22.5	30.75
20			0.75	9.25	10.0	15.0	15.25	24.5

Sr. = C_3S/C_2S

Figures 10 to 13 show the relation between the accelerated strength (warm water method compared to proposed method) with the 7and 28-day normal strength for the OPC and the SRPC. The linear line is closer to each other for the OPC and the SRPC in 28- day normal

strength than for the 7-day normal strength and it is approximately the same in the proposed method and that is referred to the proposed method correlation which is more reasonable for a less difference between the OPC and the SRPC.

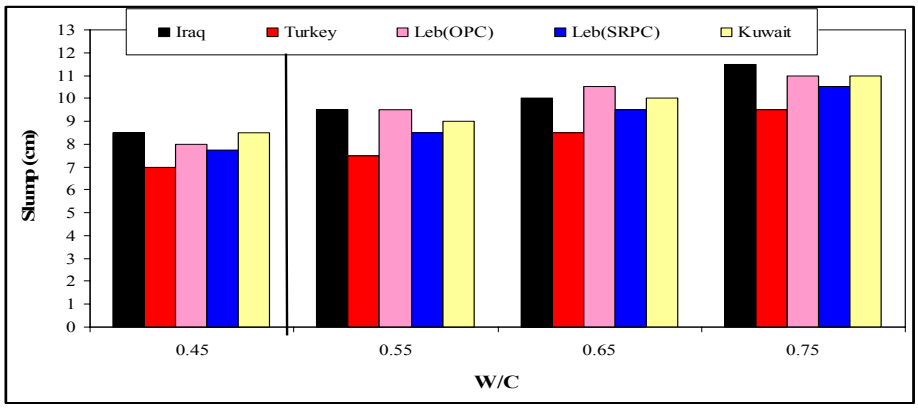

Fig. 3: Histogram for slump test for different W/C ratios.

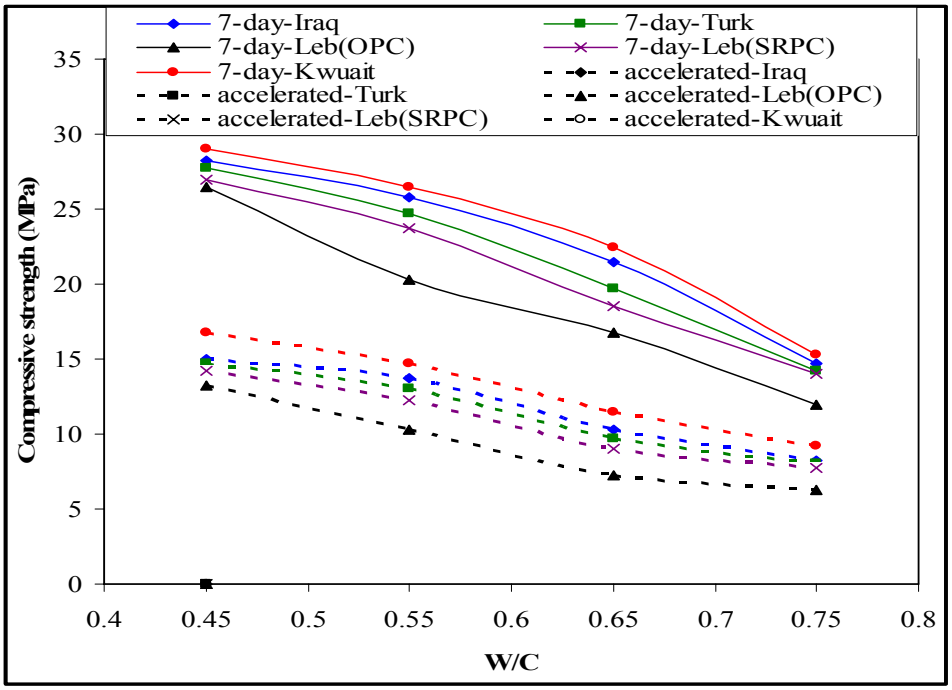

Fig. 4: Relationship between water to cement ratio and compressive strength of concrete (7-day normal strength and accelerated strength –warm water method)

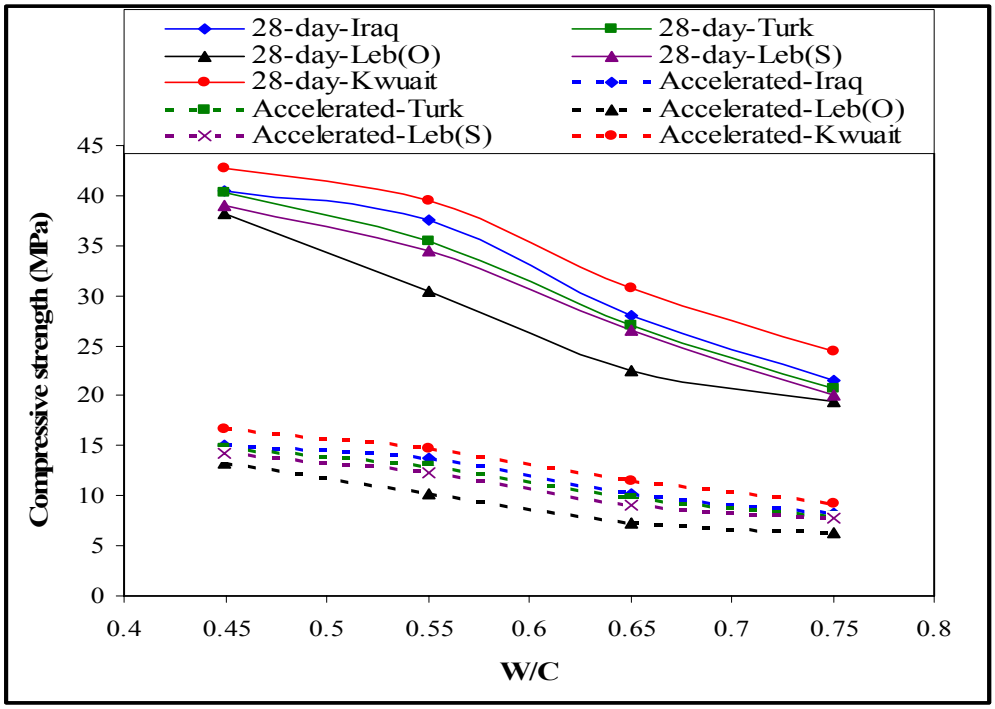

Fig. 5: Relationship between water to cement ratio and compressive strength of concrete (28-day normal strength and accelerated strength –warm water method)

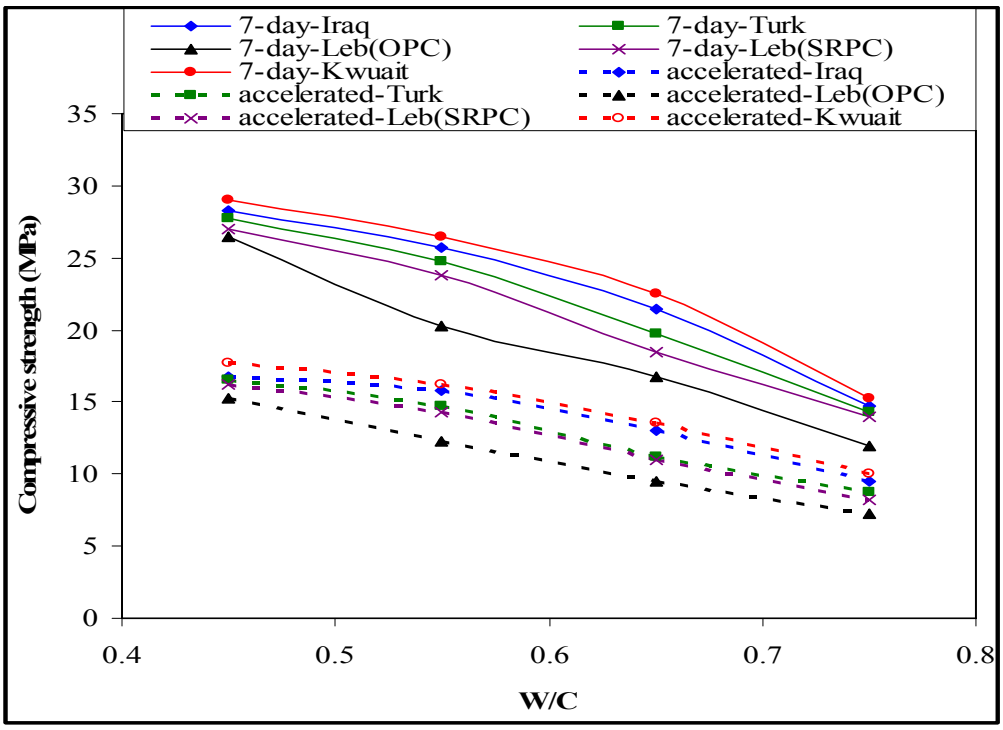

Fig. 6: Relationship between water to cement ratio and compressive strength of concrete (7-day normal strength and accelerated strength –autogenous method)

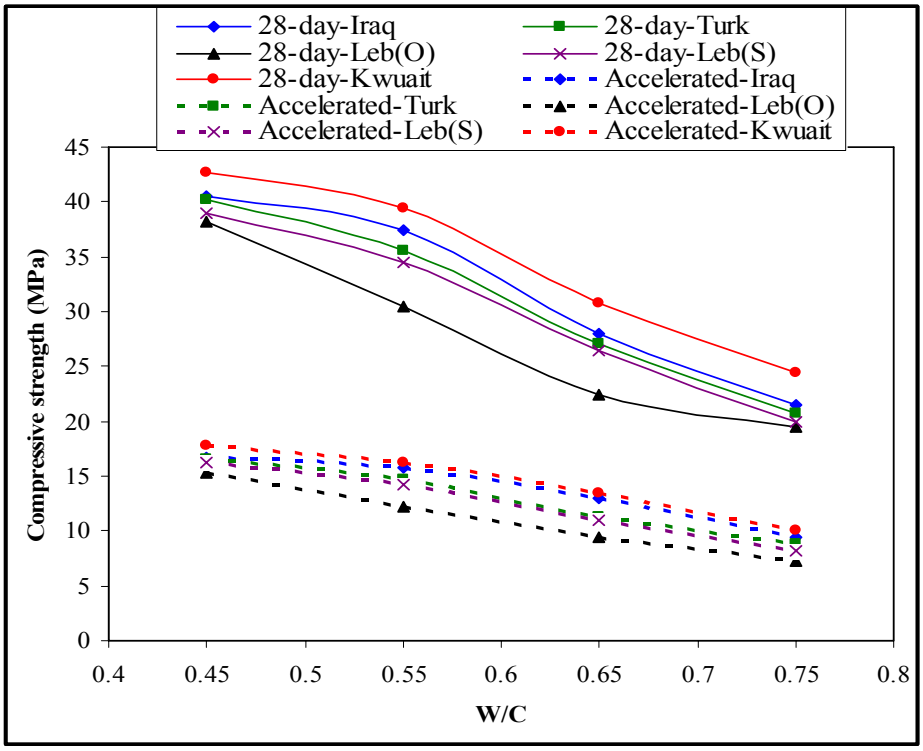

Fig. 7: Relationship between water to cement ratio and compressive strength of concrete (28-day normal strength and accelerated strength –autogenous method)

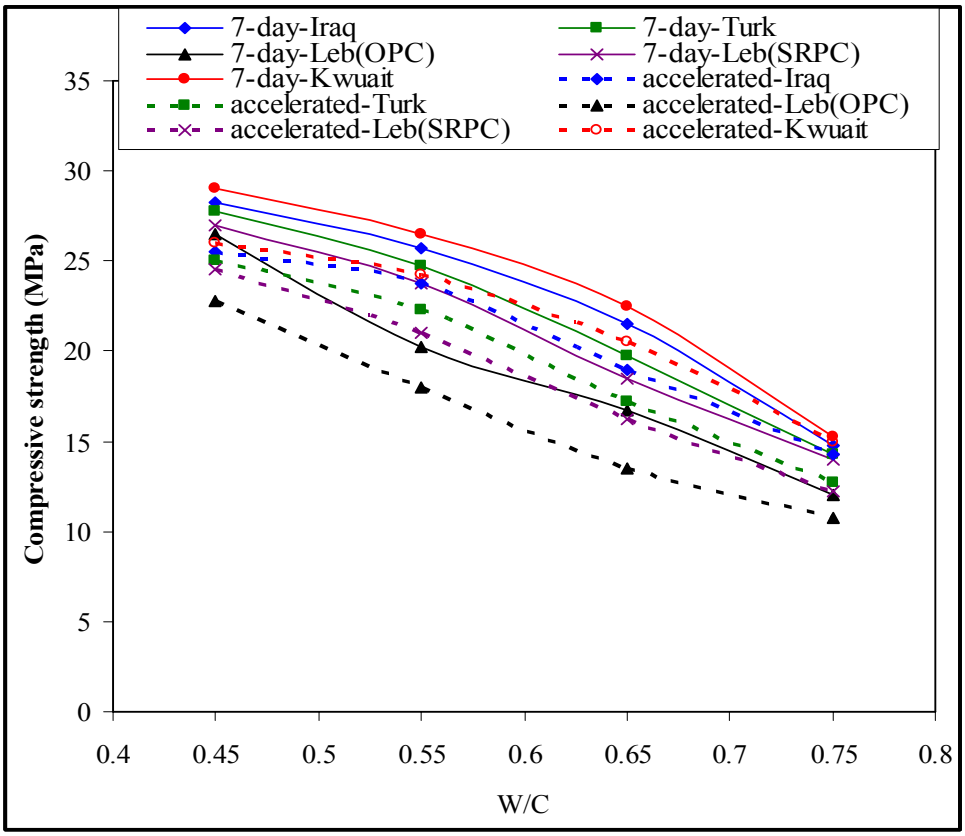

Fig. 8: Relationship between water to cement ratio and compressive strength of concrete (7-day normal strength and accelerated strength –proposed method)

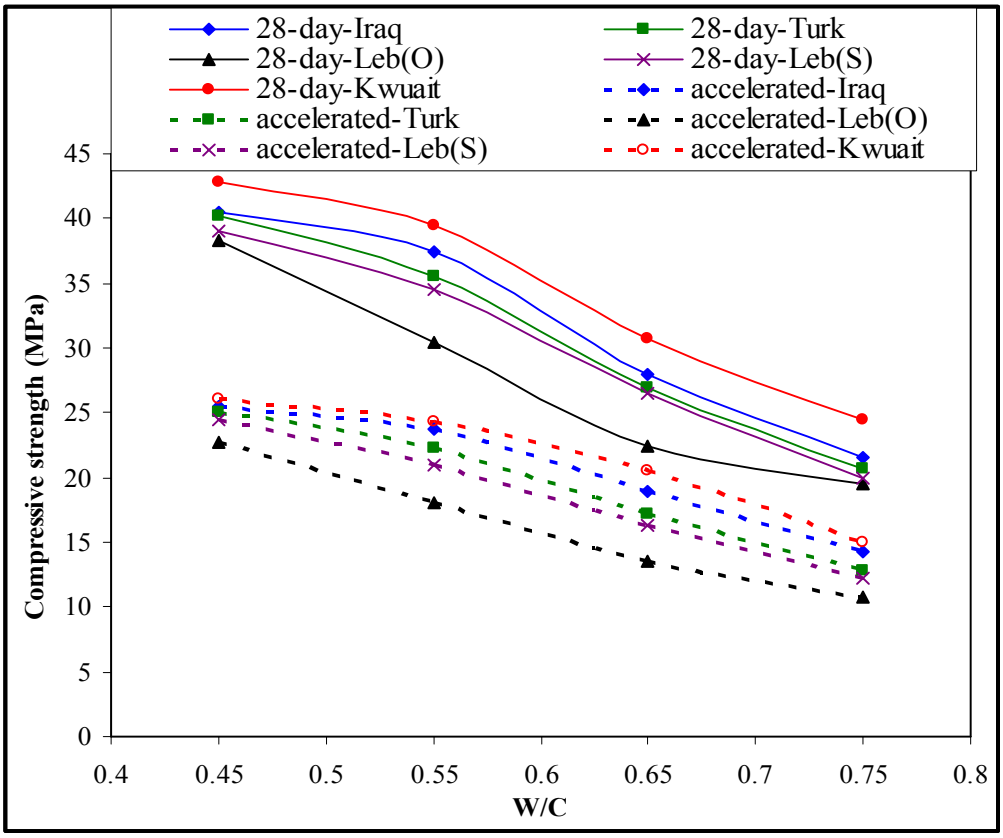

Fig. 9: Relationship between water to cement ratio and compressive strength of concrete (28-day normal strength and accelerated strength –proposed method)

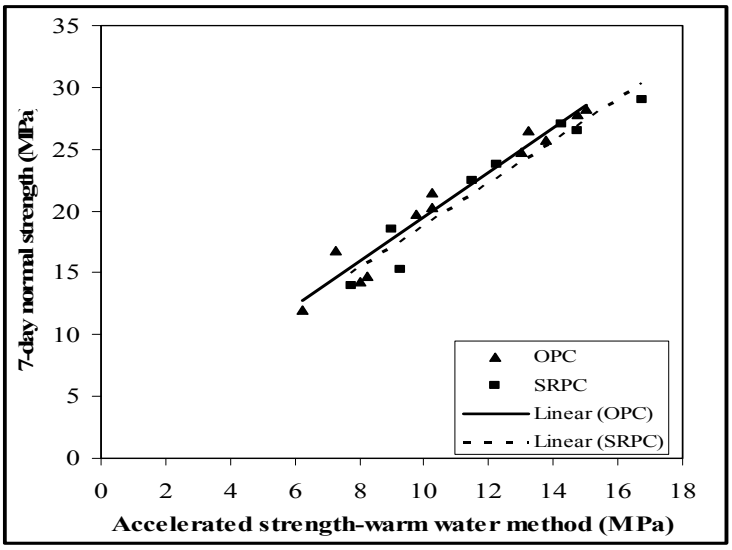

Fig. 10: Relationship between 7-day normal strength and accelerated strength using warm water method for (OPC) and (SRPC) cements.

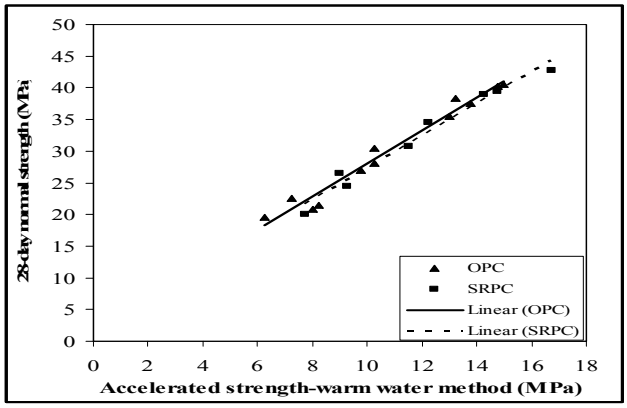

Fig. 11: Relationship between 28-day normal strength and accelerated strength using warm water method for (OPC) and (SRPC) cements.

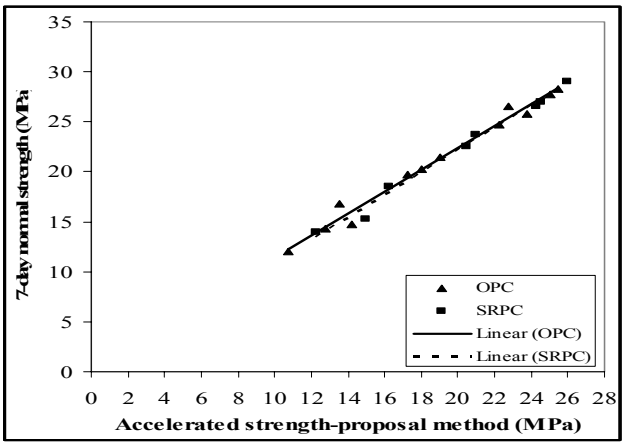

Fig. 12: Relationship between 7-day normal strength and accelerated strength –proposed method (OPC) and (SRPC) cements.

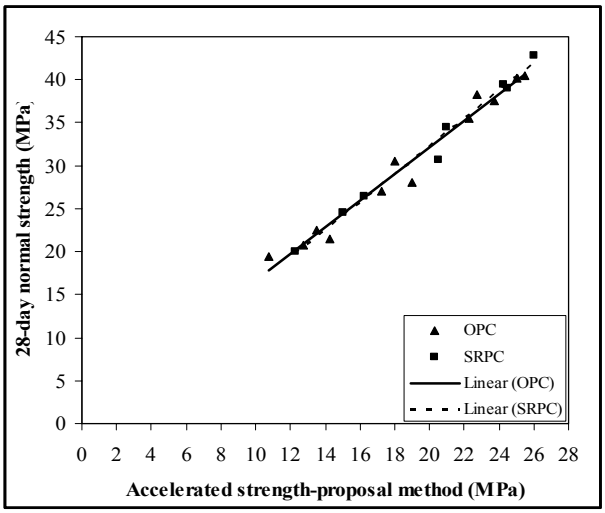

Fig. 13: Relationship between 28-day normal strength and accelerated strength using proposal method for (OPC) and (SRPC) cements.

4. REGRESSION ANALYSIS MODELS

The 7 and 28-day normal curing is used as the dependent variable and the accelerated curing strength is the independent variable (warm water, autogenous and proposed method). The experimental data are presented in Table 8, numbers of data enters the model is 20 in each model.

4.1 Descriptive Statistical Analysis

The calculated measures of central tendency and dispersion are presented in Table 10 for data enters the models.

Table 10: Descriptive statistics analysis-experimental work

	Accelerated strength –Warm water (MPa)	Accelerated strength – Autogenous (MPa)	Accelerated strength – Proposed (MPa)	7-day normal strength (MPa)	28-day normal strength (MPa)
No. of data	20	20	20	20	20
Mean	11.26	12.89	19.23	21.44	30.96
Standard deviation	3.06	3.26	4.98	5.50	7.90
Variance	9.39	10.64	24.77	30.29	62.42
Minimum	6.25	7.25	10.75	12.00	19.50
Maximum	16.75	17.75	26.00	29.00	42.75

No. of data = 20

4.2 Regression Model –Warm Water, Autogenous and Proposed Accelerated Curing Test

The regression models for linear and non linear relationship between accelerated strength (warm water, autogenous and proposed method) and 28-day normal curing strength is presented in Tables 11, 12 and 13 respectively. Tables (14), (15) and (16) respectively presents the ANOVA, R^2, root mean square of error and T= $\sum$residual$\times$predicted 7 or 28-day normal strength for all models.

Table 11: Linear and non linear models for 7 and 28-day normal strength – warm water method

Model	ANOVA					R^2	Root mean square of error	T value
	Source	D.F.	Sum of squares	Mean square	F value			
1-L-Au.	Model(Reg.)	1	568.06	568.06	1355.7	0.987	0.805	-1.73
	Error(Res.)	18	7.542	0.419				
2-Q-Au.	Model(Reg.)	2	568.22	284.11	654.0	0.987	0.812	7.79
	Error(Res.)	17	7.385	0.4344				
3-P-Au.	Model(Reg.)	1	1.431	1.431	1135.18	0.984	0.188	18.3
	Error(Res.)	18	.0226	0.001				
4-L-Au.	Model(Reg.)	1	1161.6	1161.63	856.93	0.979	1.079	-2.46
	Error(Res.)	18	24.400	1.355				
5-Q-Au.	Model(Reg.)	2	1165.9	582.97	493.55	0.983	1.042	-43.37
	Error(Res.)	17	20.08	1.181				
6-P-Au.	Model(Reg.)	1	1.321	1.321	685.82	0.974	0.209	46.08
	Error(Res.)	18	.0346	0.002				

Table 12: Statistical analysis for 7 and 28-day normal strength – warm water method

Model No.	Equation
1-L-Wr.	7-day normal strength = 1.797+ 1.744x accelerated strength(warm)
2-Q-Wr.	7-day normal strength = -6.173+ 3.250x accelerated strength (warm) - 0.066x accelerated strength(warm)^2
3-P-Wr.	7-day normal strength = 2.199x accelerated strength(warm)^ 0.941
4-L-Wr.	28-day normal strength = 2.357+ 2.540x accelerated strength(warm)
5-Q-Wr.	28-day normal strength = -2.237+ 3.408x accelerated strength(warm) - 0.038 x accelerated strength(warm)^2
6-P-Wr.	28-day normal strength = 3.321 x accelerated strength(warm)^ 0.922

No. of data = 20

Model 1-L-Wr. is the best for the 7-day normal strength since F value (292.77) is more than F tabulated (4.41), high R^2 (0.942), low root mean square of error (1.166) and the lowest T value (-0.62). Model 4-L-Wr. is the best for the 28-day normal strength since F value (578.95) is highest than others and more than F tabulated (4.41), high R^2 (0.969), low root mean square of error (1.187) and the lowest T value (-0.84).

Table 13: Linear and non linear models for 7 and 28-day normal strength – autogenous method

Model No.	Equation
1-L-Au.	7-day normal strength = -0.171+ 1.677x accelerated strength(autogenous)
2-Q-Au.	7-day normal strength = -1.784+ 1.951x accelerated strength (autogenous) - 0.011x accelerated strength(autogenous)^2
3-P-Au.	7-day normal strength = 1.605x accelerated strength(autogenous)^ 1.013
4-L-Au.	28-day normal strength = 0.062+ 2.398x accelerated strength(autogenous)
5-Q-Au.	28-day normal strength = 8.524+ 0.967x accelerated strength(autogenous) +0.057x accelerated strength(autogenous)^2
6-P-Au.	28-day normal strength = 2.567 x accelerated strength(autogenous)^ 0.974

Table 14: Statistical analysis for 7 and 28-day normal strength – autogenous method

Model	ANOVA					R^2	Root mean square of error	T value
	Source	D.F.	Sum of squares	Mean square	F value			
1-L-Wr.	Model(Reg.)	1	542.27	542.27	292.77	0.942	1.166	-0.62
	Error(Res.)	18	33.33	1.852				
2-Q-Wr.	Model(Reg.)	2	547.68	273.84	166.68	0.951	1.132	-15.7
	Error(Res.)	17	27.928	1.643				
3-P-Wr.	Model(Reg.)	1	1.352	1.352	241.6	0.931	0.273	-11.36
	Error(Res.)	18	0.101	0.006				
4-L-Wr.	Model(Reg.)	1	1150.2	1150.27	578.95	0.969	1.187	-0.84
	Error(Res.)	18	35.762	1.986				
5-Q-Wr.	Model(Reg.)	2	1152.0	576.03	288.31	0.971	1.189	-16.93
	Error(Res.)	17	33.96	1.997				
6-P-Wr.	Model(Reg.)	1	1.3015	1.301	431.24	0.959	0.234	48.64
	Error(Res.)	18	0.0543	0.003				

Table 15: Linear and non linear models for proposed method 7 and 28-day normal strength – proposed method

Model No.	Equation
1-L-Pr.	7-day normal strength = 0.349+ 1.097x accelerated strength(proposed)
2-Q-Pr.	7-day normal strength = -0.492+ 1.193x accelerated strength (proposed) -0.003x accelerated strength(proposed)^2
3-P-Pr.	7-day normal strength = 1.164x accelerated strength(proposed)^ 0.985
4-L-Pr.	28-day normal strength = 0.792+ 1.569x accelerated strength(proposed)
5-Q-Pr.	28-day normal strength = 9.250+ 0.602x accelerated strength(proposed) +0.026x accelerated strength(proposed)^2
6-P-Pr.	28-day normal strength = 1.873x accelerated strength(proposed)^ 0.949

No. of data = 20

Table 16: Statistical analysis for 7 and 28-day normal strength – proposal method

Model	ANOVA					R^2	Root mean square of error	T value
	Source	D.F.	Sum of squares	Mean square	F value			
1-L-Pr.	Model(Reg.)	1	566.24	566.24	1088.3	0.984	0.849	-0.63
	Error(Res.)	18	9.364	0.520				
2-Q-Pr.	Model(Reg.)	2	566.28	283.14	516.44	0.984	0.860	82.11
	Error(Res.)	17	9.320	0.548				
3-P-Pr.	Model(Reg.)	1	1.422	1.422	827.08	0.978	0.203	17.08
	Error(Res.)	18	.0309	0.002				
4-L-Pr.	Model(Reg.)	1	1159.0	1159.01	772.11	0.977	1.107	4.25
	Error(Res.)	18	27.019	1.501				
5-Q-Pr.	Model(Reg.)	2	1163.5	581.75	438.88	0.981	1.073	-56.94
	Error(Res.)	17	22.53	1.325				
6-P-Pr.	Model(Reg.)	1	1.3195	1.319	654.42	0.973	0.212	52.97
	Error(Res.)	18	.03629	0.002				

No. of data = 20

Model 1-L-Au. is the best for the 7-day normal strength since F value (1355.7) is highest than others and more than F tabulated (4.41) , high R^2 (0.987), low root mean square of error (0.805) and the lowest T value (-1.73). Model 4-L-Au. is the best for the 28-day normal strength since F value is highest than others and more than F tabulated (4.41), high R^2 (0.979), low root mean square of error (1.079) and the lowest T value (-2.46).

Model 1-L-Pr. is the best for the 7-day normal strength since F value (1088.3) is highest than others and more than F tabulated (4.41), high R^2 (0.984), low root mean square of error (0.849) and the lowest T value (-0.64). Model 4-L-Pr. is the best for the 28-day normal strength since F value (772.11) is highest than others and more than F tabulated (4.41), high R^2 (0.977), low root mean square of error (1.107) and the lowest T value (4.25).

5.0 CONCLUSIONS

1. A good correlation has been obtained between a 1-day accelerated test (proposed test method) and 28 days normal curing test using a period of curing at the maximum temperature 70°C with a delay period of 4 hours, and a cooling period of 2 hours.

2. Proposed test methods give the highest accelerated strength than the others and the closer to the 7-days, due to its cycle of curing.
3. A good correlation has been obtained between a 1-day accelerated test (warm water method) and a 28 days normal curing test, with respect to the easy cycle preparation.
4. A good correlation has been obtained between a 2-day accelerated test (autogenous test method) and a 28 days normal curing test, taking into consideration that this method needs a two day accelerated curing compared with the warm water and the proposal methods.
5. Linear and nonlinear regression analysis between accelerated strength (warm water , autogenouse and proposed curing test) and normal curing strength for 7 and 28-day shows high correlation with R^2 more than 0.94 for different models.

REFERENCES

ACI 517.2R, (1987) revised (1992)," Accelerated curing of concrete at atmospheric pressure –state of the art".

Al Anbori, Z.K.,(2010) , "Factors effecting accelerated strength testing of concrete" PhD. Thesis, University of Baghdad , College of Engineering, Iraq.

Al Qassab, F.F.,(2006) , "Development of concrete mix design method with reference to Iraqi conditions" PhD. Thesis, University of Baghdad , College of Engineering, Iraq.

Al Rawi, R.S., (1974), "The effect of composition and fineness of cement in accelerated testing of concrete", ASTM, Journal of Testing and Evaluation, Vol.2, No.2, pp.102-106.

ASTM C684 -99: Standard test method for making accelerated curing, testing.

ASTM C 143/C 143M – 00: Standard test method for slump of hydraulic-cement concrete.

BS 1881: Part 112: 1983: Methods of accelerated curing of test cubes.

BS 1881: Part 116: 1983: Methods for determination of compressive strength of concrete cubes.

IQS 5-1984: Iraq standard specification for Portland cement.

IQS 7-1981: Standard methods for chemical analysis of Portland cement.

IQS 8-1989: Standard method for physical test of Portland cement.

IQS 33-1989: Sulfate content for fine and coarse aggregate.

IQS 45-1984: Aggregate from natural sources for concrete and building construction.

IQS 1703/1992: Water used in concrete.

Kosmatka and Panarese (1994),"Design and control of concrete mixtures", 13th e.d., Portland cement Association.

Lewis, R.K., (1968),"A summery of investigation of steam curing of concrete related to cement characteristics", Constructional Review, Vol. 41, No. 3, pp. 18-25.

Mamillian, M. Traitement thermique des b'etons, (1982), "presses de L'Ecole Nationale des Ponts de chausse'es ", in Le b'eton hydraulique, pp 261-269, Paris.

Neville, A.M. (1995), "Properties of concrete", 4th Edition and final edition, London.

MECHANISTIC EVALUATION OF LIME-MODIFIED ASPHALT CONCRETE MIXTURES

Dr. Amjad H. Albayati, (Civil Eng. Dept.) / Baghdad Univ.
Email: sirtransportation@yahoo.com

ABSTRACT

Frequently, Load associated mode of failure (rutting and fatigue) as well as, occasionally, moisture damage in some sections poorly drained are the main failure types found in some of the newly constructed road within Baghdad as well as other cities in Iraq. The use of hydrated lime in pavement construction could be one of the possible steps taken in the direction of improving pavement performance and meeting the required standards.

In this study, the mechanistic properties of asphalt concrete mixes modified with hydrated lime as a partial replacement of limestone dust mineral filler were evaluated. Seven replacement rates were used; 0, 0.5, 1, 1.5, 2, 2.5 and 3 percent by weight of aggregate. Asphalt concrete mixes were prepared at their optimum asphalt content and then tested to evaluate their engineering properties which include moisture damage, resilient modulus, permanent deformation and fatigue characteristics. These properties have been evaluated using indirect tensile strength, uniaxial repeated loading and repeated flexural beam tests. Mixes modified with hydrated lime were found to have improved fatigue and permanent deformation characteristics, also showed lower moisture susceptibility and high resilient modulus. The use of 2 percent hydrated lime as a partial replacement of mineral filler has added to local knowledge the ability to produce more durable asphalt concrete mixtures with better serviceability.

الخلاصة

أظهرت بعض الطرق المبلطة حديثا بالخرسانة الاسفلتية قي بغداد وباقي محافظات القطر تدهورا مبكرا بالاداء نتيجة فشل الكلل والتشوهات الدائمية وفي بعض الاحيان نتيجة الفشل تحت تاثير الدور المخرب للماء. ان استخدام الجير المطفأ ($Ca(OH)_2$) في انتاج الخرسانة الاسفلتية ممكن ان تكون واحدة من الخطوات التي يمكن اتخاذها في اتجاه تحسين الخصائص المتعلقة بالاداء للتبليط الاسفلتي لجعله يطابق متطلبات المواصفة من خلال توفير المقاومة اللازمة لانواع الفشل المذكورة انفا. لقد تم في هذه الدراسة تقييم الخصائص الميكانيكية لخلطات الخرسانة الاسفلتية والتي تحوي على نسب مختلفة من الجير المطفأ وهذه النسب هي (0.0 ، 0.5 ، 1.0، 1.5، 2.0 ، 2.5 و 3 % من وزن الركام)، وتمت الاضافة عن طريق الاستبدال الجزئي للمادة المالئة التقليدية (مطحون حجر الكلس). حيث تم اجراء فحوصات الشد غير المباشر، المرونة الاستردادية، الحمل المحوري المتكرر وكذلك فحص الانحناء المتكرر للنماذج المختبرية والتي اعدت باستخدام النسب المثلى للاسفلت لتقييم الخصائص المتعلقة بضرر الماء ، معامل المرونة الاستردادي، التشوهات الدائمية وكذلك خاصية الكلل.

لقد بينت النتائج بان استخدام الجير المطفأ يحسن الى حد كبير خصائص الاداء المتعلقة بضرر الماء وكذلك يحسن معامل المرونة الاستردادي ومقاومة التشوهات الدائمية والكلل. ان استخدام نسبة 2% من الجير المطفأ كاستبدال جزئي للمادة المالئة التقليدية قد أضاف إلى الخبرة المحلية المتوفرة في هذا المجال إمكانية أنتاج خرسانة إسفلتية لاغراض التبليط بديمومة أعلى ومستوى خدمة أفضل.

Key words: Asphalt concrete, Hydrated lime, Mechanical properties

1-INTRODUCTION

In the recent five years, some of the newly constructed asphalt concrete pavements in Baghdad as well as other cities across Iraq have shown premature failures with consequential negative impact on both roadway safety and economy. Frequently, Load associated mode of failure (rutting and fatigue) as well as, occasionally, moisture damage in some sections poorly drained are the main failure types found in those newly constructed road. Investigations on the reasons beyond these failure showed that it can be grouped into two categories, extrinsic and intrinsic, the first one due to the heavy axle loading coupled with relentless high summer temperatures (ambient air temperature for nearly three month can reach 50 degree Celsius and pavement surface temperature can reach up to 60 degree Celsius) , whereas the second category is limited to the mixture itself , improper gradients, excess use of natural sand and lack of mineral filler all of these factors acts either in collect or in single manner for the deterioration in the mix strength and also loss of durability of asphalt concrete pavement.

Based on the preceding it is clear that there is a real need to the development of modified asphalt concrete mixtures to improve the overall performance of pavements. The use of hydrated lime in pavement construction could be one of the possible steps taken in this direction. In the United States of America, Hydrated lime has been added to hot mix asphalt pavements for over 30 years, improving the mixtures in many ways and increasing the life of highways. Extensive experimental studies have revealed that the use of hydrated lime in Hot-Mix Asphalt (HMA) mixtures can reduce permanent deformation, long-term aging, and moisture susceptibility of mixtures. In addition, it increases the stiffness and fatigue resistance of mixtures. The structure of hydrated lime consists of different size fractions. The larger size fraction performs as a filler and increases the stiffness of the bituminous mixture. The smaller size fraction increases binder film thickness enhancing viscosity of the binder, and improving the binder cohesion and stiffness.

In view of this , the primary objective of this study is to evaluate the mechanical properties of asphalt concrete mixtures containing hydrated lime (as a partial replacement of limestone filler) based on the following tests, Marshall properties (Mix Design), Indirect tensile test (Moisture susceptibility) , uniaxial repeated load test (Resilient Modulus and permanent deformation) and repeated flexural beam test (fatigue characteristics).

2-BACKGROUND

Hydrated lime which is also known as calcium hydrate (Ca(OH)2) has been used in asphalt mixes for a long time, both as mineral filler and as an antistripping additive. Researchers observed that when hydrated lime coats an aggregate particle, it induces polar components in asphalt cement to bond to the aggregate surface. This effect also inhibits hydrophilic polar groups in the asphalt from congregating on the aggregate surface (McGennis et al. 1984). In addition, lime can neutralize acidic aggregate surfaces by replacing or coating acidic compounds and water-soluble salts on the aggregates and can react pozzolanically to remove deleterious materials (Epps et al. 2003).

Petersen et al. [1987] selected four AC-10 asphalts on the basis of variable chemical composition and geographical usage in paving industries and evaluated the effects of hydrated lime on asphalt concrete performance. A comparative study was also carried out by replacing lime with a high-calcium limestone, pulverized to match the physical fineness of the hydrated lime. It was reported that hydrated lime treatment reduced asphalt age hardening, increased the high-temperature stiffness of both unaged and aged asphalts, and also increased the asphalt tensile-elongation at low temperatures. They also stated that the relative response to hydrated lime treatment varied as a function of asphalt cement source. Furthermore, the comparison study between limestone powder and hydrated lime showed that hydrated lime outperformed the limestone powder considering age hardening, tensile strength, and the elongation to break properties of asphalt binder.

Al-Suhaibani [1992] evaluated the mineral filler properties of hydrated lime and other local fillers available in Saudi Arabia. The mechanical properties of the mixes were studied using tests such as the resilient modulus test, the indirect tensile strength test, Hveem stability, and Marshall criteria. The research results revealed that the amount and characteristics of the mineral fillers can have an effect on the rutting susceptibility of flexible pavements, and that the use of hydrated lime can improve resistance of the mixes to rutting. The lime showed improved stiffening properties when incorporated into the mixture.

Shahrour and Saloukeh [1992] conducted a research study to evaluate the influence of ten types of different fillers (including hydrated lime) on the physical properties of filler-bitumen mixtures and two types of asphalt mixtures namely- Asphaltic concrete (AC) and Dense Bitumen Macadam (DBM)

commonly used Dubai, U.A.E. The mixtures were designed using Marshall mix design method, and the fillers were incorporated in various ratios to the mixtures. Marshal parameters (% VFB, % VIM, % VMA, and Bulk Specific Gravity) for asphalt mixtures were reported to be not significantly affected by changing the type of filler at specific filler contents. On the other hand, Penetration, Ring and Ball Softening point, Viscosity, and Kinematic Viscosity tests on the filler-binder mixtures (mastics) showed that all types of mineral fillers acted as an extender to the binder with minimal stiffening effect. But comparing to others, hydrated lime showed superior stiffening performance. The authors also recommended to use hydrated lime as a mineral filler in a ratio of 0.5 to 0.8 of the bitumen content in the asphalt mixtures. Afterwards Paul, 1995; Khosla et al., 2000; McCann and Sebaaly, 2003; Khattak and Kyatham, 2008 conducted numerous researches to evaluate the influence of hydrated lime on the moisture damage of HMA pavements. In those studies, hydrated lime was reported to improve the resistance against the moisture induced damages of HMA mixtures. By maintaining a good adhesion between the aggregate and the asphalt cement in the presence of water, hydrated lime worked successfully as an antistripping agent. Its ability to reduce viscosity building polar components in the asphalt binder enabled hydrated lime to show effect as an oxidation reducing agent. Also, its ability to increase mixture stiffness by filling air voids in the mixture with its tiny particles makes it effective mineral filler

Baig et al. [1998] conducted a study to investigate the effectiveness of using hedmanite (rockwool natural fibers) and lime as filler in improving the performance of HMA mixtures that could withstand the major pavement distress problems in the desert climate of Saudi Arabia. Locally used quarried limestone and the 60/70 penetration grade asphalt were used while the Marshall mix design method was implemented to produce mixtures. Resilient modulus test, Marshall stability test, Split tensile strength test, and Fatigue and permanent deformation test were conducted and the results indicated that the use of these fillers improved the resilient modulus, fatigue property, and resistance to rutting compared to the control mix. Among two fillers, the stability loss and tensile strength loss were higher in hedmanite mixes while lime modified mixes showed better resistance to rutting and the adverse effect of water. Consequently, the researchers opted for lime as filler than hedmanite to produce better quality asphalt concrete mixtures.

Lime-treated mixtures also showed cost efficiency in terms of pavement life. Sebaaly et al. [2003] conducted a research to quantify the improvements of pavement performance that contained lime. Performances of HMA mixtures from the northwestern part of Nevada were evaluated both in the laboratory and in the field. In the laboratory evaluation, both lime treated and untreated sections were sampled and then evaluated through laboratory test. On the other hand, pavement performance data from pavement management system (PMS) were used to assess field performance of lime treated and untreated sections. The study showed that lime treatment on HMA mixtures significantly improved their moisture resistance and resistance to multiple freeze-thaw cycles than that of untreated HMA mixtures. From the long-term pavement performance data it was also evident that under similar environmental and traffic conditions, lime treated mixtures provided better performance with lesser maintenance and rehabilitation activities. Again, the analysis of the impact of lime on pavement life indicated that lime treatment extended the performance life of HMA pavements by an average of 3 years which represented an average increase of 38% in the expected pavement life.

Hydrated lime can be introduced into asphalt mixes by several methods: lime slurry to dry or wet aggregate, dry lime to wet aggregate, dry lime to dry aggregate and dry lime to asphalt. Although little research has been done to quantify the difference in effects of these methods, it is sufficient to say that asphalt mixes benefit from the addition of hydrated lime, no matter how it is introduced into the mix (Epps et al. 2003). Typically, the amount of hydrated lime added is 1 to 2 percent by weight of the mix, or 10 to 20 percent by weight of the liquid asphalt binder but If an aggregate has more fines present, it may be necessary to use more lime additive due to the increased surface area of the aggregate.

3- MATERIAL CHARACTERAZATION

The materials used in this work, namely asphalt cement, aggregate, and fillers were characterized using routine type of tests and results were compared with State Corporation for Roads and Bridges specifications (SCRB, R/9 2003)

3-1 Asphalt Cement

The asphalt cement used in this work is a 40-50 penetration grade. It was obtained from the Dora

refinery, south-west of Baghdad. The asphalt properties are shown in Table (1) below.

Table 1 Properties of Asphalt Cement

Property	ASTM designation	Penetration grade 40-50	
		Test results	SCRB specification
1-Penetration at 25C,100 gm,5 sec. (0.1mm)	D-5	47	40-50
2- Rotational viscosity at 135◦C (cP.s)	D4402	519	……
2- Softening Point. (◦C)	D-36	47	……
3-Ductility at 25 C, 5cm/min,(cm)	D-113	>100	>100
4-Flash Point, (◦C)	D-92	289	Min.232
5-Specific Gravity	D-70	1.041	……
6- Residue from thin film oven test - Retained penetration,% of original - Ductility at 25 C, 5cm/min,(cm)	D-1754 D-5 D-113	 59.5 80	 >55 >25

3-2 Aggregate

The aggregate used in this work was crushed quartz obtained from Amanat Baghdad asphalt concrete mix plant located in Taji, north of Baghdad, its source is Al-Nibaie quarry. This aggregate is widely used in Baghdad city for asphaltic mixes. The coarse and fine aggregates used in this work were sieved and recombined in the proper proportions to meet the wearing course gradation as required by SCRB specification (SCRB, R/9 2003). The gradation curve for the aggregate is shown in Figure (1).

Routine tests were performed on the aggregate to evaluate their physical properties. The results together with the specification limits as set by the SCRB are summarized in Table (2). Tests results show that the chosen aggregate met the SCRB specifications.

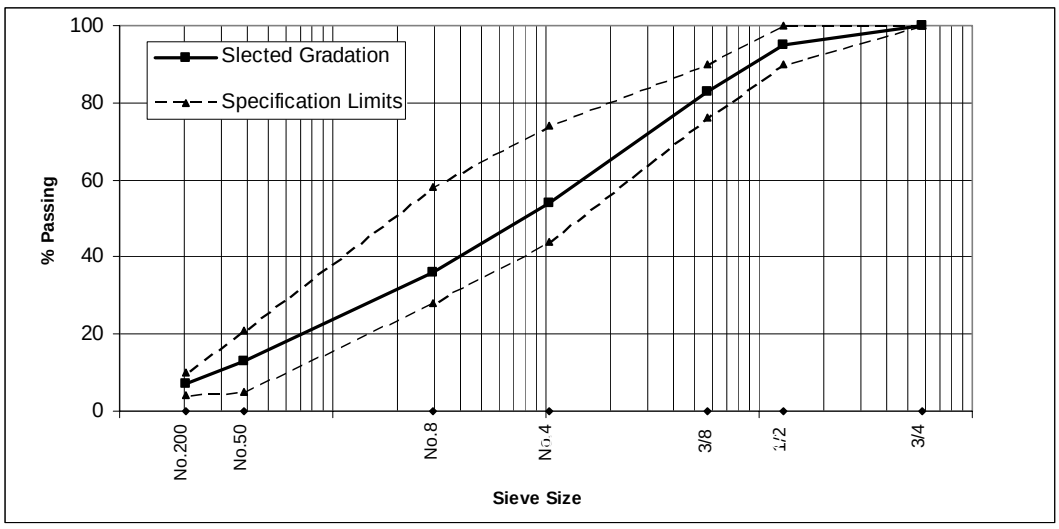

Fig. 1 Aggregate Gradation

Table (2) Physical Properties of Aggregates

Property	ASTM designation	Test results	SCRB specification
Coarse aggregate			
1. Bulk specific gravity	C-127	2.614	……
2. Apparent specific gravity		2.686	……
3. Water absorption,%		0.441	……
4. Percent wear by Los Angeles abrasion ,%	C-131	17.5	30 Max
5. Soundness loss by sodium sulfate solution,%	C-88	3.4	10 Max
6. Fractured pieces, %		98	90 Min
Fine aggregate			
1. Bulk specific gravity	C-127	2.664	……
2. Apparent specific gravity		2.696	……
3. Water absorption,%		0.724	……
4. Sand equivalent,%	D-2419	57	45 Min.

3-3 Filler

The filler is a non plastic material that passing sieve No.200 (0.075mm). In this work, the control mixes were prepared using limestone dust as a mineral filler at a content of 7 percent, this content represent the mid-range set by the SCRB specification for the type IIIA mixes of wearing course. Mixes in which the limestone dust was partially replaced by a hydrated lime were also prepared. The replacement percentages were 0, 0.5, 1.0, 1.5, 2, 2.5 and 3% by total weight of aggregate. The limestone dust and hydrated lime were obtained from lime factory in Karbala governorate, south east of Baghdad. The chemical composition and physical properties of the fillers are presented in Table (3) below:

Table (3) Properties of Fillers

Filler type	Chemical Composition ,%							Physical Properties		
	Cao	Sio_2	Al_20_3	Mgo	Fe_2o_3	So_3	L.O.I	Specific gravity	Surface area* (m^2/kg)	% Passing sieve No. 200(0.075)
Limestone Dust	68.3	2.23	-	0.32	-	1.20	27.3	2.41	244	94
Hydrated Lime	56.1	1.38	0.72	0.13	0.12	0.21	40.6	2.78	398	98

* Blain air permeability method (ASTM C204)

4- EXPERIMENTAL WORK

The experimental work was started by determining the optimum asphalt content for all the asphalt concrete mixes using the Marshall mix design method. To investigate the stiffening effect of hydrated lime on the filler-asphalt mortar, filler-asphalt mixes were then prepared and tested using the conventional binder tests, penetration and softening point. Also, asphalt concrete mixes were made at their optimum asphalt content and tested to evaluate the engineering properties which include moisture damage, resilient modulus, permanent deformation and fatigue characteristics. These properties have been evaluated using indirect tensile strength, uniaxial repeated loading and repeated flexural beam tests.

4-1 Marshall Mix Design

A complete mix design was conducted using the Marshall method as outlined in AI's manual series No.2 (AI, 1981) using 75 blows of the automatic Marshall compactor on each side of specimen. Based upon this method, the optimum asphalt content is determined by averaging the three values shown below:

Asphalt content at maximum unit weight
Asphalt content at maximum stability
Asphalt content at 4% air voids

For each percentage of hydrated lime content, six Marshall specimens were prepared with a constant increments rate in asphalt cement content of 0.2 percent. The selected asphalt cement content starts from 4.2 percent for the control and 0.5 percent hydrated lime mixes and increased 0.2 percent for each 1 percent increase in hydrated lime content, so for the mixes with 3 percent hydrated lime, the starting value for asphalt cement content was 4.8 percent. This procedure is followed since it was found earlier in this work that the use of low asphalt content was not sufficient to provide proper coating for the aggregate with high content of hydrated lime. The complete summary of Marshall test data is shown in appendix A.

4-2 Conventional Binder Test

To investigate the stiffening effect of hydrated lime upon the filler- asphalt mixture, the penetration as well as softening point tests was conducted according the ASTM –D5 and ASTM D 36, respectively for the mixes prepared using 7 percent filler but with different hydrated lime contents as a partial replace of limestone filler and corresponding optimum asphalt cement content.

4-3 Indirect Tensile Test

The moisture susceptibility of the asphalt concrete mixtures was evaluated using ASTM D 4867. The result of this test is the indirect tensile strength (ITS) and tensile strength ratio (TSR). In this test, a set of specimens were prepared for each mix according to Marshall procedure and compacted to 7±1 % air voids using different numbers of blows per face that varies from (34 to 49) according to the hydrated lime replacement rate. The set consists of six specimens and divided into two subsets, one set (control) was tested at 25°C and the other set (conditioned) was subjected to one cycle of freezing and thawing then tested at 25°C. The test (shown below in fig. (2)) involved loading the specimens with compressive load at a rate of (50.8mm/min) acting parallel to and along the vertical diametrical plane through 0.5 in. wide steel strips which are curved at the interface with specimens. These specimens failed by splitting along the vertical diameter. The indirect tensile strength which is calculated according to (Eq.1) of the conditioned specimens (ITSc) is divided by the control specimens (ITSd), which gives the tensile strength ratio (TSR) as the following (Eq.2).

$$ITS = \frac{2P}{\pi t D} \qquad \text{eq. (1)}$$

$$TSR = \frac{ITS_c}{ITS_d} \qquad \text{eq. (2)}$$

where
ITS= Indirect tensile strength
P = Ultimate applied load
t = Thickness of specimen
D = Diameter of specimen
Other parameters are defined previously

Fig. 2 Photograph for ITS test

4-4 Uniaxial repeated loading test

The uniaxial repeated loading tests were conducted for cylindrical specimens, 101.6 mm (4 inch) in diameter and 203.2 mm (8 inch) in height, using the pneumatic repeated load system (shown below in fig.(3)). In these tests, repetitive compressive loading with a stress level of 20 psi was applied in the form of rectangular wave with a constant loading frequency of 1 Hz (0.1 sec. load duration and 0.9 sec. rest period) and the axial permanent deformation was measured under the different loading repetitions. All the uniaxial repeated loading

tests were conducted at 40°C (104°F). The specimen preparation method for this test can be found elsewhere (Albayati, 2006).

The permanent strain (εp) is calculated by applying the following equation:

$$\varepsilon_p = \frac{p_d \times 10^6}{h} \qquad \text{eq. (3)}$$

where
εp= axial permanent microstrain
pd= axial permanent deformation
h= specimen height

Also, throughout this test the resilient deflection is measured at the load repetition of 50 to 100, and the resilient strain (εr) and resilient modulus (Mr) are calculated as follows:

$$\varepsilon_r = \frac{r_d \times 10^6}{h} \qquad \text{eq. (4)}$$

$$M_r = \frac{\sigma}{\varepsilon_r} \qquad \text{eq. (5)}$$

where
εr= axial resilient microstrain
rd= axial resilient deflection
h= specimen height
Mr= Resilient modulus
σ = repeated axial stress
εr= axial resilient strain

Fig. 3 Photograph for the PRLS

The permanent deformation test results for this study are represented by the linear log-log relationship between the number of load repetitions and the permanent microstrain with the form shown in Eq.6 below which is originally suggested by Monismith et. al., (1975) and Barksdale (1972).

$$\varepsilon_p = aN^b \qquad \text{eq. (6)}$$

where
εp= permanent strain
N=number of stress applications
a= intercept coefficient
b= slope coefficient

4-5 Flexural Beam Fatigue Test

Within this study, third-point flexural fatigue bending test was adopted to evaluate the fatigue performance of asphalt concrete mixtures using the pneumatic repeated load system, this test was performed in stress controlled mode with flexural stress level varying from 5 to 30 percent of ultimate indirect tensile strength applied at the frequency of 2 Hz with 0.1 s loading and 0.4 s unloading times and in rectangular waveform shape. All tests were conducted as specified in SHRP standards at 20°C (68°F) on beam specimens 76 mm (3 in) x 76 mm (3 in) x 381 mm (15 in) prepared according to the method described in (Al-khashaab, 2009). In the fatigue test, the initial tensile strain of each test has been determined at the 50th repetition by using (Eq.7) shown below and the initial strain was plotted versus the number of repetition to failure on log scales, collapse of the beam was defined as failure, the plot can be approximated by a straight line and has the form shown below in (Eq. 8).

$$\varepsilon_t = \frac{\sigma}{Es} = \frac{12h\Delta}{3L^2 - 4a^2} \qquad \text{eq. (7)}$$

$$N_f = k_1(\varepsilon_t)^{-k2} \qquad \text{eq. (8)}$$

where
ε_t = Initial tensile strain
σ =Extreme flexural stress
Es =Stiffness modulus based on center deflection.
h =Height of the beam
Δ =Dynamic deflection at the center of the beam.
L = Length of span between supports.
a =Distance from support to the load point (L/3)
N_f= Number of repetitions to failure
k_1= fatigue constant, value of Nf when ε_t=1
k_2= inverse slope of the straight line in the logarithmic relationship

5- TEST RESULTS AND DISCUSSION

5-1 Effects of Hydrated Lime on Filler-Asphalt Mixes

The consistency of filler-asphalt mixes with different percentage contents of hydrated lime as partial replacement of limestone dust was determined using the penetration and softening point tests, the result of tests are presented in table (4) and shown graphically in figures (4) and (5).

Table (4) Penetration and softening point tests result

Hydrated Lime Content* , %		0	0.5	1.0	1.5	2.0	2.5	3.0
Optimum Asphalt Content, %		4.73	4.75	4.88	4.92	5.07	5.13	5.34
Test Results	Penetration at 25C,100 gm,5 sec. (0.1mm) (original=47)	34	32	29	28	26	22	19
	Softening Point, (◦C) (original=47°C)	51.0	54.2	58.0	59.6	61.3	64.4	69.0

* As partial replacement of limestone dust, 7 percent filler content is constant.

As can be seen from the presented data, hydrated lime content has a substantial influence on the the consistency of filler-asphalt mixes. With respect to the penetration test, the penetration decreases with increasing hydrated lime content, for example, the penetration value for 1.5 percent hydrated lime content is 0.875 times the value of 0.5 percent, the constant of proportionality which can be driven from figure (4) is approximately -4.857 (1/10 mm) for each 1 percent increase in hydrated lime content. By contrast, the softening point increases with increasing the hydrated lime content and the constant of proportionality is +5.55 (◦C) for each 1 percent increase in hydrated lime content. From the above results, it may be possible to argue that the higher the replacement rate of limestone dust with hydrated lime, the higher the stiffness of the resulted filler-asphalt mixes.

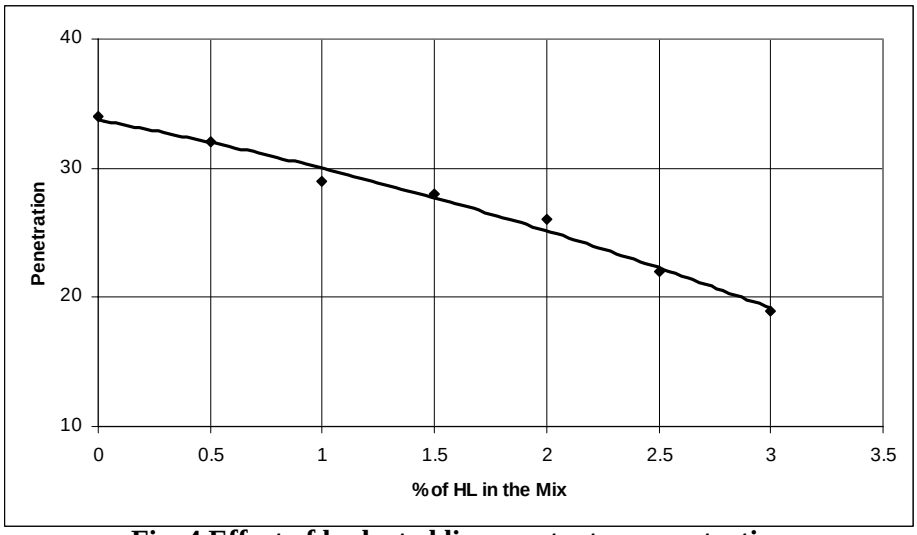

Fig. 4 Effect of hydrated lime content on penetration

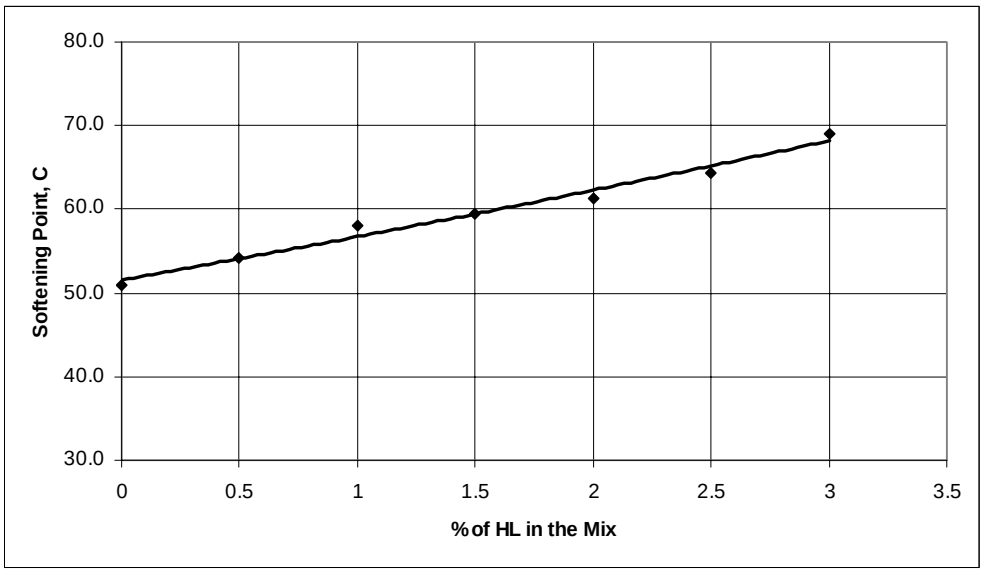

Fig. 5 Effect of hydrated lime content on softening point

5-2 Effects of Hydrated Lime on Marshall Properties

The variation of Marshall properties with hydrated lime content is shown in figure (6) which is based on the data presented in Table (5). Examinations of the presented data suggest that the mixes with higher hydrated lime content possess higher optimum asphalt cement content, the highest value of optimum asphalt content (5.34%) was obtained with 3% hydrated lime, while the lowest value (4.73%) was obtained with 0% hydrated lime which is the case that the mineral filler entirely consists of limestone dust.

Table (5) Summary of the Marshall properties of asphalt concrete mixes at optimum asphalt content

Hydrated Lime Content* , %		0	0.5	1.0	1.5	2.0	2.5	3.0
Optimum Asphalt Content, %		4.73	4.75	4.88	4.92	5.07	5.13	5.34
Marshall Properties	Stability, kN	8.65	8.87	9.76	10.3	11.05	11.14	11.2
	Flow, mm	3.23	3.5	3.62	3.73	3.8	3.53	3.41
	Density, gm/cm^3	2.320	2.329	2.333	2.336	2.348	2.337	2.331
	Air Voids, %	4.3	4.14	4.03	3.94	3.71	4.21	4.7
	VMA , %	15.83	15.45	15.49	15.42	15.12	15.57	15.97

* As partial replacement of limestone dust, 7 percent filler content is constant.

These differences can be attributed to the higher surface area of hydrated lime as compared to that of limestone dust. As shown earlier in this study, the surface area of hydrated lime is 1.63 times that of limestone dust, and hence the demand for asphalt has increased with increasing the replacement rate of limestone dust with hydrated lime. With respect to stability, the results indicate that the stability increases with increasing hydrated lime content, also the increment rate varies with hydrated lime content, the maximum rate obtained is 1.09 kN/1 percent for the hydrated lime content ranged from 0.5 to 2 percent, whereas for the hydrated lime content ranged from 0 to 0.5 percent and from 2 to 3 percent the rate was 0.44 and 0.15 kN/1 percent, respectively. From the stability plot, it may be possible to argue that the maximum benefit can be obtained with the use of 2 percent hydrated lime since further increase in hydrated lime content associated with just slight increases in stability value and require

more asphalt cement content as compared to mixes with 2 percent hydrated lime.

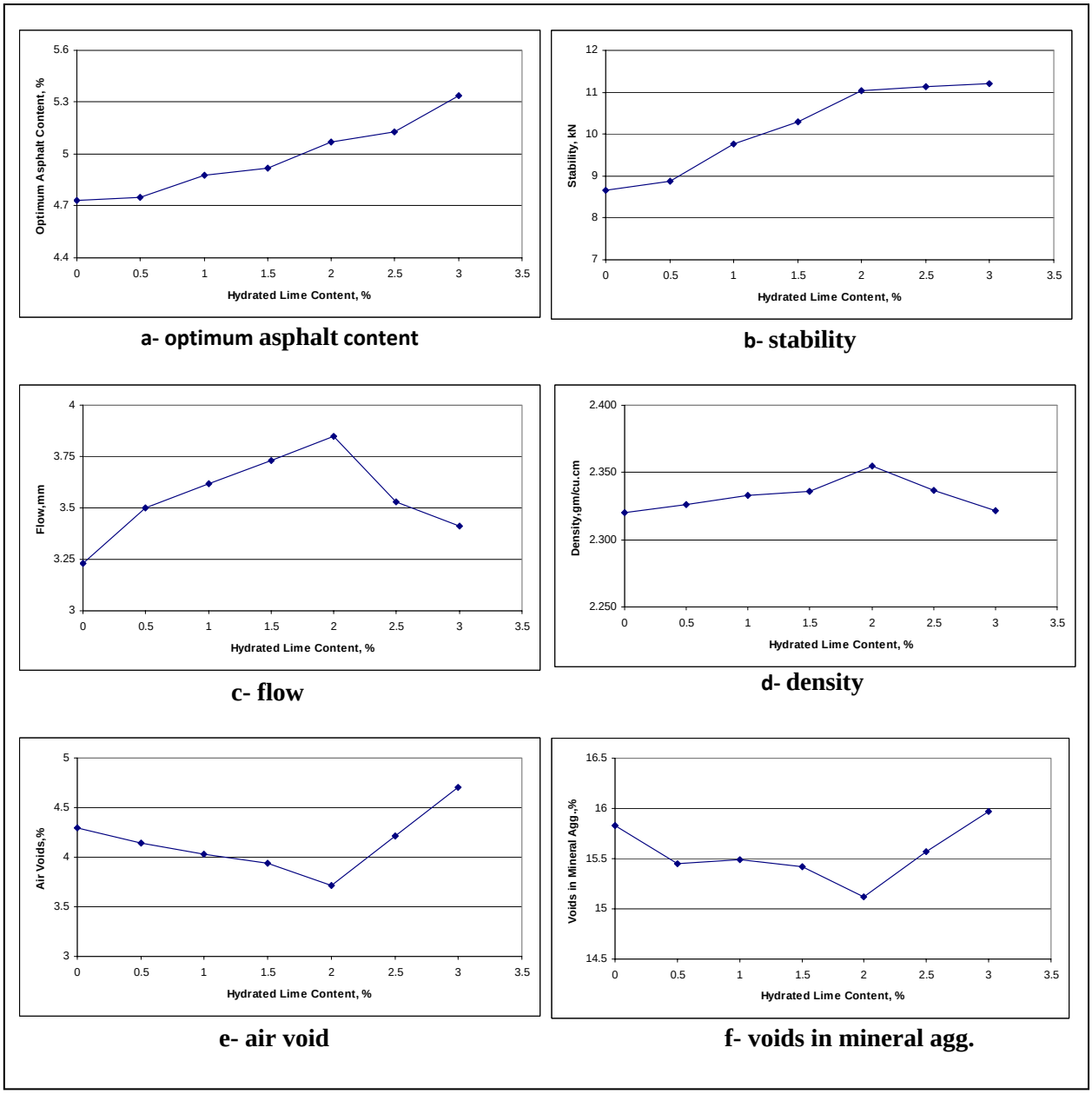

Fig. 6 Effect of hydrated lime content on Marshall properties

The results of flow as a function of varying the hydrated lime content is shown in plot "c", its obvious that the flow value increases as the hydrated lime content increases from 0 to 2 percent, and then decreases as the hydrated lime content increases. This is due to the fact that air voids are too low at 2 percent hydrated lime content, addition of hydrated lime higher than this value tend to increase air voids due to insufficient compaction effort so the flow value decrease. The relationship between hydrated lime content and density which is shown in plot "d" follow the same trend of that between the hydrated lime content and Marshall flow, an optimum hydrated lime content which yields the highest Marshall density is 2 percent, further increases in hydrated lime content tend to decrease the Marshall density. As demonstrated in plot "e", the trend observed for the effect of hydrated lime content on air voids values is exactly opposite to that observed between hydrated lime content and flow , for a hydrated lime content from 0 to 2 percent, the air voids decreases with a rate of -0.295 percent for

each 1 percent change in hydrated lime content, beyond 2 percent, the air voids content increases rapidly with a rate of +0.99 percent for each 1 percent change in hydrated lime content, this can be easily explained by the fact that the hydrated lime is finer than limestone dust so it can efficiently fill the voids pockets and stiffens the mixes for a certain amount beyond which there will be a lack in the compaction effort resulting in high air voids content. Plot "f" demonstrates the effect of hydrated lime content on voids in mineral aggregate (VMA), as its clear from the plot until a 2 percent of hydrated lime content the VMA decreases as the hydrated lime content increases, the minimum VMA value corresponding to 2 percent hydrated lime is 15.12 percent which means less spaces to be accommodated by asphalt cement, after 2 percent hydrated lime content, an addition of hydrated lime result in increasing the VMA values.

5-3 Effects of Hydrated Lime on Moisture Susceptibility

Based on the data shown in Table (6) and Figure (7), it appears that the examined hydrated lime contents have influence on the moisture susceptibility of the asphalt concrete mixes. The indirect tensile strength results for both control and conditioned mixes approximately linearly proportional to the hydrated lime content with constants of proportionality of +92.5 for the former and +150.5 kPa per 1 percent change in hydrated lime content for the latter. It is interesting to note that the improvement rate in the indirect tensile strength for the mixes with hydrated lime, added as part of the mineral filler, is higher in the case of conditioned mixes than that of control mixes. These findings beside that related to tensile strength ratio shown in figure (7) confirm that the resistance to moisture induced damage is enhanced in asphalt concrete pavement modified with hydrated lime.

Table (6) Moisture susceptibility test results

Hydrated Lime Content, %	ITS, kPa		TSR, %
	Control	Conditioned	
0	1290	1051	81.5
0.5	1342	1053	78.4
1.0	1373	1124	81.9
1.5	1441	1200	83.3
2.0	1496	1281	85.6
2.5	1532	1405	91.7
3.0	1554	1467	94.4

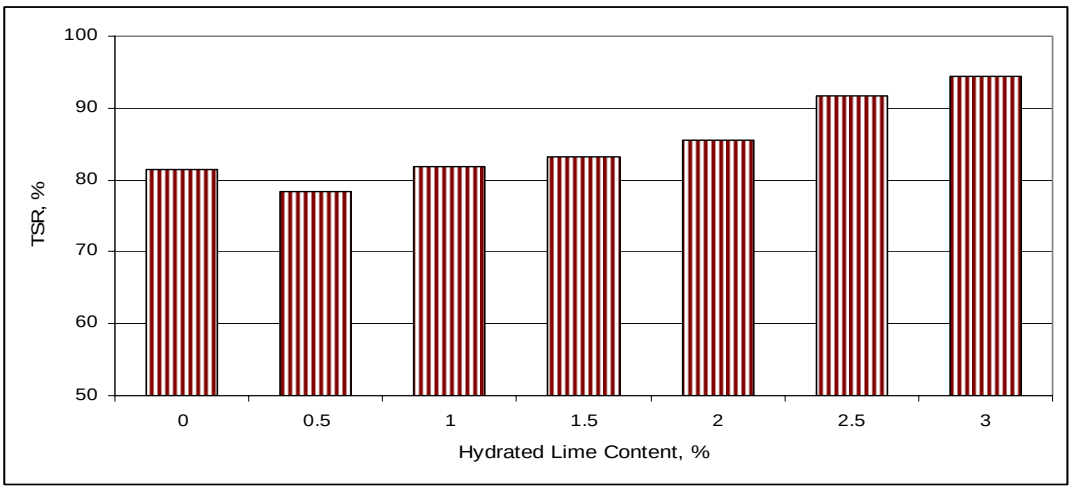

Fig. 7 Effect of hydrated lime content on tensile strength ratio

5-4 Effects of Hydrated Lime on Resilient Modulus

Table (7) as well as figure (8) exhibits the variation of the resilient modulus values with the hydrated lime content. The relation is in reverse order up to 1 percent content of hydrated lime (i.e., as the hydrated lime content increases the resilient modulus decreases), but further increase in hydrated lime content reflects this relation, the resilient modulus of the mixes with 3 percent hydrated lime (159165 psi) is 1.4 times the value for mixes with 1 percent hydrated lime which was 112995 psi. these results can be explained as follow; since the test was conducted under relatively high temperature (40°C (104°F)), so the low level of hydrated lime content (below 1 percent) is insufficient to stiffening the asphalt concrete mixes whereas the higher values of resilient modulus resulted from the high level of hydrated lime content (above 1 percent) indicate that the hydrated lime did increase the stiffness of the asphalt concrete mix.

Table (7) Resilient modulus test results

Hydrated Lime Content , %	0	0.5	1.0	1.5	2.0	2.5	3.0
Resilient Modulus, psi	121500	115425	112995	126360	143370	151875	159165

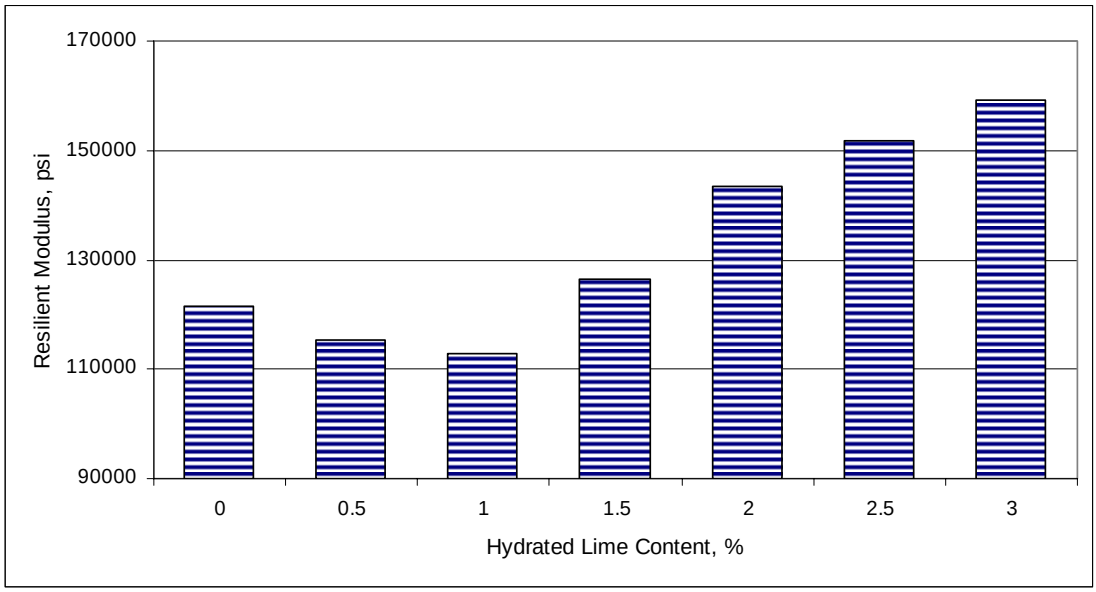

Fig. 8 Effect of hydrated lime content on resilient modulus

5-5 Effects of Hydrated Lime on Permanent Deformation

The result of permanent deformation tests is shown in figure (9) which is based on the data presented in table (8), Examinations of the presented data suggests that the permanent deformation parameters intercept and slope generally improved with the use of hydrated lime, for mixes containing 0 percent hydrated lime, the slope value which reflects the accumulation rate of permanent deformation is approximately 20 percent higher than that of mixes with 3 percent hydrated lime. For the intercept, the value is slightly increase as the hydrated lime content increases from the 0 to 0.5 percent, but then the addition of extra amount of hydrated lime tend to decrease the intercept value in a rate of 19.7 microstrain per each 1 percent change in hydrated lime content. This finding confirms that the rutting mode of failure in asphalt concrete pavement which is enhanced at hot summer temperature can be reduced into large extent with the introduction of hydrated lime to asphalt concrete mixtures.

Table (8) permanent deformation test results

Hydrated Lime Content , %	0	0.5	1.0	1.5	2.0	2.5	3.0
Intercept	108	113	102	95	80	70	66
Slope	0.372	0.366	0.355	0.341	0.324	0.312	0.300

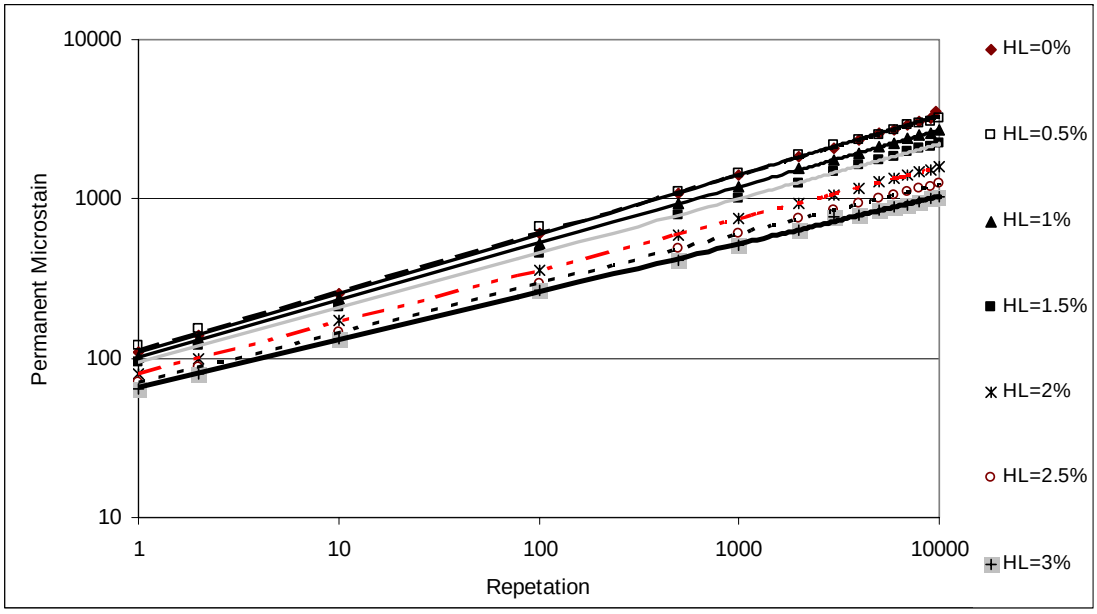

Fig. 9 Effect of hydrated lime content on resilient modulus

5-6 Effects of Hydrated Lime on Fatigue Performance

The fatigue characteristic curves for all mixtures are presented in Fig. 10. The fatigue parameters k1 and k2 are shown in Table 9. Values of k1 and k2 can be used as indicators of the effects of hydrated lime on the fatigue characteristics of a paving mixture. The flatter the slope of the fatigue curve, the larger the value of. k_2 If two materials have the same k_1 value, then a large value of k_2 indicates a potential for longer fatigue life. On the other hand, a lower k_1 value represents a shorter fatigue life when the fatigue curves are parallel, that is, $k_2$is constant. Test results indicate that the use of hydrated lime with a rate of content ranged from 0 to 1 percent does not have significant effect on fatigue life but the mixes with more than 1 percent hydrated lime showed better fatigue performance, the k_2 value for mixes with 2 and 3 percent hydrated lime was more than that of 1 percent hydrated lime by 54.4 and 30.6 percent, respectively. Considering k_1, it can be concluded from the data shown in table (9) that there is an agreement between the results of k_1 and k_2 in the field of fatigue resistance, k_1 has the smallest value (9.561x E-12) when the hydrated lime content was 3 percent and it was increase as the hydrated lime content decreased from 3 to 1 percent, but for the mixes with 0.5 percent hydrated lime content, k_1 value was more than that of 0 percent hydrated lime.

Table (9) Fatigue test results

Hydrated Lime Content , %	0	0.5	1.0	1.5	2.0	2.5	3.0
k_1	1.339 x E-7	4.162 x E-7	1.780 x E-7	1.555 x E-8	1.822 x E-9	5.499 x E-11	9.561 x E-12
k_2	2.74	2.56	2.61	3.08	3.41	3.83	4.03

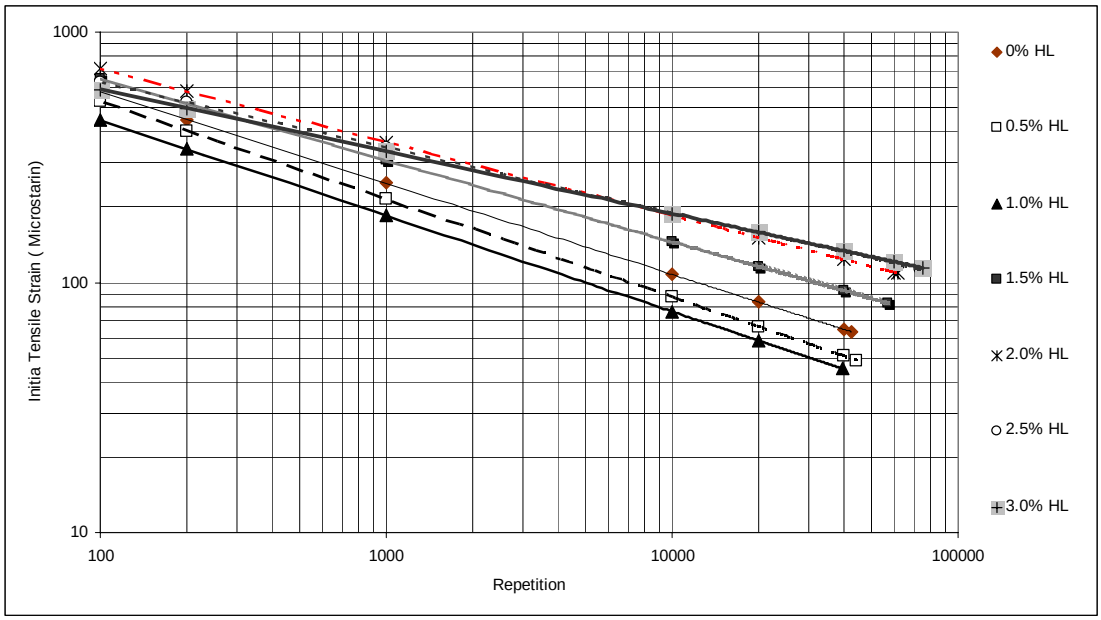

Fig. 10 Effect of hydrated lime content on fatigue performance

6- CONCLUSIONS AND RECOMMENDATIONS

The following conclusions and recommendations are based on the results of the laboratory tests and analysis presented in this study:

1. In the filler-asphalt mixes, hydrated lime has shown significant stiffening properties when mixed with asphalt cement as partial replacement for limestone dust. For each 1 percent increase in hydrated lime, the penetration value decreases at a rate of 4.857 (1/10 mm) whereas the softening point increases at a rate of +5.55 (°C).
2. The addition of different percentages of hydrated lime as a filler substitute has a significant effect on volumetric mixture properties, some of the obtained results can be summarized as follow:

- The mixes with higher hydrated lime content possess higher optimum asphalt content, the highest value of optimum asphalt content (5.34%) was obtained with 3 percent hydrated lime, while the lowest value (4.73%) was obtained with 0 percent hydrated lime
- An optimum hydrated lime content which yields the highest density is 2 percent, further increases in hydrated lime content tend to decrease the density
- For mixes with a hydrated lime content ranged from 0 to 2 percent, the air voids decreases with a rate of -0.295 percent for each 1 percent change in hydrated lime content. Beyond 2 percent, the air voids content increases rapidly with a rate of +0.99 percent for each 1 percent change in hydrated lime content

3. The addition of hydrated lime has improved the indirect tensile strength for both control and conditioned mixes with a rate of +92.5 and +150.5 kPa per 1 percent increase in hydrated lime content, respectively. The resistance to moisture induced damage is enhanced in asphalt concrete pavement modified with hydrated lime
4. The addition of hydrated lime as a filler substitute with a rate ranged from 1.5 to 3 percent has shown an increase in resilient modulus. The resilient modulus for mixes with 3 percent hydrated lime was 1.31 times that for mixes with 0 percent hydrated lime.
5. The permanent deformation parameters, slope and intercept, was significantly effected with the addition of deferent percentages of hydrated lime. The modified mixes show higher resistance to permanent deformation when the percentage of hydrated lime is increased as a filler substitute.
6. The use of hydrated lime as a filler substitute within a range of 1.5-3 percent has improved the fatigue property of the asphalt concrete mixes as determined by flexural test. The k_2 value (inverse slope of fatigue line) for mixes with 2 and 3 percent hydrated lime was more than that of 0 percent hydrated lime by 53.6 and 24.4 percent, respectively.
7. The use of 2 percent hydrated lime has shown a significant improvement of asphalt concrete behavior, and has added to the local knowledge the possibility of producing more durable mixtures with higher resistance to distresses.

7-REFERENCES

AI (1981), “Thickness Design-Asphalt Pavements for Highways and Streets”, Asphalt Institute, Manual Series No.1, College Park, Maryland, USA.

Albayati, A.H., (2006),"Permanent Deformation Prediction of Asphalt Concrete Under Repeated Loading" Ph.D. Thesis, Baghdad University.

Alkhashab. Y.Y.,(2009), "Development of Fatigue Prediction Model for Local Asphalt Paving Materials" Ph.D. Thesis, Baghdad University.

Al-Suhaibani, AbdulRahman, Al-Mudaiheem, Jamal, and Al-Fozan, Fahd, "Effect of Filler Type and Content on Properties of Asphalt Concrete Mixes," Effects of Aggregates and Mineral Fillers on Asphalt Mixture Performance, ASTM STP 1147, Richard C. Meininger, Editor, American Society for Testing and Materials, Philadelphia , pp. 107-130.

Atud, T.J., Kanitpong, K., and Martono, W. 2007. “Laboratory Evaluation of Hydrated Lime Application Process in Asphalt Mixture for Moisture Damage and Rutting Resistance.” *Transportation Research Board 86th Annual Meeting CD-ROM*, Paper No. 1508, Washington, D.C.

Baig, M.G. and Wahhab, H.I.A. 1998. “Mechanistic Evaluation of Hedmanite and Lime Modified Asphalt Concrete Mixtures.” *Journal of Materials of Civil Engineering*, Vol. 10, No. 3, pp. 153-160.

Barksdale, R. (1972). “Laboratory Evaluation of Rutting in Base Course Materials”, Proceedings, Third International Conference on the Structural Design of Asphalt Pavements, London.

Epps, J., Berger, E., and Anagnos, J. N. (2003). “Treatments.” Moisture Sensitivity of Asphalt Pavements, A National Seminar, Transportation Research Board, Miscellaneous Report, Transportation Research Board, Washington D. C., pp. 117-186.

Khattak, M.J. and Kyatham, V. 2008. “Visco-Elastic Behavior of Asphalt Matrix & HMA under Moisture Damage Condition.” Transportation Research Board 87th Annual *Meeting CD-ROM*, Washington, D.C.

Khosla, N.P., Birdshall, B.G., Kawaguchi, S. 2000. “Evaluation of Moisture Susceptibility of Asphalt Mixtures, Conventional and New Methods.” Transportation Research Record: Journal of the Transportation Research Board, No. 1728, Transportation Research Board of the National Academies, Washington, D.C., pp.43-51.

Little, D.N. and Petersen, J.C. 2005. “Unique Effects of Hydrated Lime Filler on the Performance-Related Properties of Asphalt Cements: Physical and Chemical Interactions Revisited.” Journal of Materials in Civil Engineering, Volume 17, No. 2, pp.207-218.

McCann, M. and Sebaaly, P.E. 2003. "Evaluation of Moisture Sensitivity and Performance of Lime in Hot Mix Asphalt: Resilient Modulus, Tensile Strength, and Simple Shear Tests." Transportation Research Record: Journal of the Transportation Research Board, No. 1832, Transportation Research Board of the National Academies, Washington, D.C., pp.9-16.

McGennis, R. B., Kennedy, T. W., and Machemehl, R. B. (1984). "Stripping and moisture damage in asphalt mixtures." Center for Transportation Research, Bureau of Engineering Research, The University of Texas at Austin.

Mohammad, L.N., Abadie, C., Gokmen, R. and Puppala, A.J. 2000. "Mechanistic Evaluation of Hydrated Lime in Hot-Mix Asphalt mixtures" Transportation Research Record: Journal of the Transportation Research Board, No. 1723, pp.26-36.

Monismith, C., Ogawa, N. and Freeme, C. (1975). "Permanent Deformation Characteristics of Subgrade Soils due to Repeated Loadings", TRR 537.

Paul, Harold R. 1995. "Compatibility of Aggregate, Asphalt Cement and Antistrip Materilas." Louisiana Transportation Research Center, Report No. FHWA/LA-95-292.

Petersen, J.C., Plancher, H. and Harnsberger, P.M. 1987. "Lime Treatment of Asphalt to Reduce Age Harding and Improve Flow Properties." Journal of the Association of Asphalt Paving Technologists, Volume 56, pp.633-653.

SCRB/R9 (2003). General Specification for Roads and Bridges, Section R/9, Hot-Mix Asphalt Concrete Pavement, Revised Edition. State Corporation of Roads and Bridges, Ministry of Housing and Construction, Republic of Iraq.

Sebaaly, P.E., Hitti, E. and Weitzel, D. 2003. "Effectiveness of Lime in Hot Mix Asphalt Pavements." Transportation Research Record: Journal of the Transportation Research Board, No. 1832, Transportation Research Board of the National Academies, Washington, D.C., pp.34-41.

Shahrour, M.A., and Saloukeh, B.G. 1992 "Effect of Quality and Quantity of Locally Produced Filler (Passing Sieve No. 200) on Asphaltic Mixtures in Dubai," Effects of Aggregates and Mineral Fillers on Asphalt Mixture Performance, ASTM STP 1147, Richard C. Meininger, Editor, American Society for Testing and Materials, Philadelphia, pp.187-208.

APPENDIX A

Table (A1) Mix design data

Marshall Properties	Stability, kN	Flow, mm	Density, gm/cm^3	Air voids, %	Voids in Mineral Aggregate, %
Asphalt Content, % (by wt. of total mix)	Hydrated Lime content = 0.0 %*				
4.2	7.85	2.88	2.281	6.57	16.79
4.4	8.18	3	2.294	5.76	16.49
4.6	8.78	3.1	2.311	4.62	16.04
4.8	8.08	3.25	2.325	3.97	15.71
5.0	7.43	3.4	2.316	4.22	16.21
5.2	7.13	3.65	2.309	4.06	16.64
Asphalt Content, % (by wt. of total mix)	Hydrated Lime content = 0.5%*				
4.2	8.37	2.93	2.293	6.26	16.35
4.4	8.76	3.22	2.307	5.42	16.01
4.6	9.45	3.31	2.322	4.53	15.64
4.8	8.69	3.6	2.331	3.96	15.49
5.0	8.12	3.81	2.314	4.30	16.29
5.2	7.58	3.93	2.308	3.91	16.68
Asphalt Content, % (by wt. of total mix)	Hydrated Lime content = 1%*				
4.4	8.91	3.1	2.311	5.35	15.87
4.6	9.36	3.32	2.319	4.75	15.75
4.8	9.88	3.56	2.321	4.40	15.86
5.0	9.69	3.78	2.334	3.59	15.56
5.2	9.49	3.88	2.325	3.69	16.07
5.4	9.23	3.94	2.32	3.77	16.42
Asphalt Content, % (by wt. of total mix)	Hydrated Lime content = 1.5%*				
4.4	9.35	2.99	2.301	6.05	16.23
4.6	10.14	3.12	2.318	5.08	15.79
4.8	10.46	3.64	2.332	4.24	15.46
5.0	10.19	3.75	2.336	3.80	15.49
5.2	10.12	3.8	2.328	3.86	15.96
5.4	9.97	3.98	2.322	3.93	16.35
Asphalt Content, % (by wt. of total mix)	Hydrated Lime content = 2%*				
4.6	9.45	3.44	2.327	5.18	15.46
4.8	10.19	3.65	2.333	4.66	15.42
5.0	11.19	3.76	2.342	4.02	15.27
5.2	9.99	3.86	2.351	3.38	15.13
5.4	9.72	3.94	2.33	3.97	16.06
5.6	9.31	3.98	2.312	4.45	16.89
Asphalt Content, % (by wt. of total mix)	Hydrated Lime content = 2.5%*				
4.6	9.84	3.21	2.319	5.88	15.75
4.8	9.95	3.44	2.331	5.01	15.49
5.0	11.29	3.6	2.336	4.54	15.49
5.2	10.76	3.74	2.342	3.94	15.45
5.4	9.64	3.82	2.322	4.13	16.35
5.6	8.29	3.89	2.306	4.59	17.10
Asphalt Content, % (by wt. of total mix)	Hydrated Lime content = 3%*				
4.8	10.35	3.2	2.319	6.09	15.93
5.0	11.09	3.3	2.323	5.66	15.96
5.2	11.4	3.4	2.331	5.07	15.85
5.4	10.99	3.6	2.332	4.03	15.99
5.6	10.59	3.7	2.322	4.13	16.53
5.8	10.11	3.9	2.319	3.98	16.81

MODELING HOUSEHOLD TRIP GENERATION FOR SELECTED ZONES AT AL-KARKH SIDE OF BAGHDAD CITY

Prof. Saad Issa Sarsam
Civil Engineering Department
University of Baghdad

Su'ad Saba' Al-Hassani
Civil Engineering Department
University of Baghdad

ABSTRACT

Trip generation is the first phase in the travel forecasting process. It involves the estimation of the total number of trips entering or leaving a parcel of land per time period (usually on a daily basis); as a function of the socioeconomic, locational, and land-use characteristics of the parcel.
The objective of this study is to develop statistical models to predict trips production volumes for a proper target year. Non-motorized trips are considered in the modeling process. Traditional method to forecast the trip generation volume according to trip rate, based on family type is proposed in this study. Families are classified by three characteristics of population social class, income, and number of vehicle ownership. The study area is divided into 10 sectors. Each sector is subdivided into number of zones so; the total number of zones is 45 zones based on the administrative divisions. The trip rate for the family is determined by sampling. A questionnaire is designed and interviews are implemented for data collection from selected zones at Al-Karkh side of Baghdad city. Two techniques have been used, full interview and home questionnaire. The questionnaire forms are distributed in many institutes, intermediate, secondary and, commercial schools. The developed models are total person trips /household, work trips /household, education trips/household, shopping and social/recreational trips/household and, person trips/person. These models are developed by using stepwise regression technique after the collected data being fed to SPSS software.
Results show that total persons trips/household are related to family size and structure variables such as number of person more than 6 year age, number of male, total number of workers, total number of students in the household, number of private vehicles. This model has coefficient of determination equal to 0.669 for the whole study area. Also the results show that the home-based work trips are related to number of worker in the household, number of male workers in the household, number of female workers in the household and number of persons of (25-60) year age; this model has coefficient of determination equal to 0.82 for the whole study area. Home-based education trips are strongly related to number of students in the household and this model has coefficient of determination equal to 0.90 for the whole study area.

المستخلص

تعد مرحلة تولد الرحلة أول مراحل تخمين الطلب المروري. و تتضمن هذه المرحلة تخمين العدد الكلي للرحلات الداخلة أو الخارجة من منطقة معينة من الأرض خلال فترة زمنية (عادة خلال يوم)؛ كعلاقة مع الخصائص الاجتماعية اقتصادية، المكانية، و خصائص استخدام الأرض لتلك المنطقة. أن هدف الدراسة هو لبناء نماذج إحصائية لتخمين حجوم الرحلات المنتجة لمناطق مختارة لجهة الكرخ من بغداد ولسنة هدف مناسبة. أخذت هذه الدراسة رحلات المشي بنظر الاعتبار عند

عملية بناء النماذج. تناولت هذه الدراسة تخمين حجوم الرحلات المتولدة من كل قطاع مروري في منطقة الدراسة و ذلك بنمذجة عدد الرحلات المتولدة باليوم لكل أسرة بالطريقة التقليدية.

صنفت الأسر حسب الخصائص الاجتماعية الاقتصادية المؤثرة على معدل الرحلات لكل أسرة مثل حجم الأسرة، معدل الدخل الشهري للأسرة، و تملك المركبة. تم تقسيم منطقة الدراسة إلى 10 قطاعات مرورية و قسم كل قطاع إلى عدد من المناطق المرورية و بذلك فإن عدد المناطق المرورية هو 45 منطقة بالاعتماد على التقسيمات الإدارية لمدينة بغداد. بعد ذلك صممت استمارة الاستبيان لغرض جمع المعلومات و بعدها أجريت عملية المسح لمناطق مختارة لجهة الكرخ من بغداد. وزعت الاستمارات بطريقة مسح المقابلة البيتية وكذلك وزعت الاستمارات على المدارس الإعدادية والتجارية في المدينةَ وقدم شرح مركز عن كيفية ملئ الاستمارات قبل ملئ الاستمارة من قبل الباحثة. تم بناء العلاقات الإحصائية آلاتية، عدد رحلات الأشخاص الكلية /عائلة، رحلات العمل/عائلة، رحلات الدراسة/ عائلة، رحلات التسوق و الرحلات الاجتماعية/ترفيهية /عائلة، رحلات الفرد/فرد و ذلك باستخدام طريقة الانحدار الخطي المتعدد بعد إدخال البيانات في برنامج SPSS.

أوضحت النتائج إن عدد رحلات الأشخاص /عائلة(Y) يرتبط بمتغيرات حجم الأسرة و تركيبتها و خصوصا عدد الأشخاص الذين بسن أكبر من 6 سنوات ، العدد الكلي للعاملين في الأسرة، العدد الكلي للطلاب في الأسرة، عدد الذكور، و عدد المركبات الخصوصية و أن معامل الحساب لهذا النموذج هو 0.669 لعموم منطقة الدراسة؛ بينما رحلات العمل تتأثر بعدد العاملين في الأسرة و عدد الذكور العاملين في الأسرة و عدد الإناث العاملات في الأسرة و عدد الأشخاص الذين بعمر(25-60) و أن معامل الحساب لهذا النموذج هو 0.82 لعموم منطقة الدراسة. و تتأثر رحلات الدراسة بصورة كبيرة بالعدد الكلي للطلاب في الأسرة و أن معامل الحساب لهذا النموذج هو 0.9 لعموم منطقة الدراسة.

Key Word: - Household, Modeling, Trip Generation, Travel Demand.

INTRODUCTION

Urban transportation planning is the process which represents the integration of many interacting characteristics of the urban environment (Brain et al, 1974). It is carried out to develop a program of high way and transit projects that should be completed in the future. As motorization is progressed, it has become increasingly evident that the traffic congestion "problem" cannot be solved by building more road infrastructure.

Forecast of demand for the system at the various levels of facility provision considered is one of the basic elements of long-term transportation planning. It is consist of the following steps (Wright, 1998):

1. Population and economic analysis.
2. Land use analysis.
3. Trip generation.
4. Trip distribution.
5. Mode choice (or model split).
6. Traffic assignment.

Population and economic activity predictions generally are derived by specialist demographic and economic projections outside the scope of the transportation study.

There has been considerable debate on the land use. A number of models have been developed that relate changes in land use to such independent variables as: accessibility to employment, land value, intensity of land use …etc (Wright, 1998).

The population of Baghdad urban area according to the previous census is given in Table 1, whereas Fig.1 is illustrate the land uses for Baghdad city.

The four remaining steps are of considerable interest and the whole four steps are refer to as (Traditional Method) for prediction travel demand (Venigalla et al, 1999).

Trip generation involves the estimation of the total number of trips entering or leaving a parcel of land per time period (usually on a daily basis); as a function of the socioeconomic, locational, and land-use characteristics of the parcel. Usually multi-mode and purpose journeys are simplified into trip identified by a principal mode and purpose, ignoring intermediate stages and stops for secondary purposes (Hobbs, 1979). The reliability of forecasting results influences the following steps such as trip distribution, mode split, and traffic assignment. Therefore, improved trip generation models are needed to improve forecasting precision (Liya and Hongzahi, 2008).

Table 1 Population of Baghdad City (Ref. BCTS 1980, 1977 Census, 1987 Census, 1997 Census).

Census year	population
1947	666000
1957	785000
1977	2023242
1987	3841269
1997	4083258

The ultimate purpose of the trip generation analysis is to arrive at an estimate of the trip ends generated at each analysis unit of the study area.

Traditionally, trip generation forecasts are established independently of any direct consideration of the transportation network. This assumes that trips produced at or attracted to a zone are a function only of the attributes of the zone itself and are not directly a function of the transportation network on which the trips are made (NTL, 2006).

The study of trip generation attempts to identify and quantify the trip ends related to various urban activities without describing other trip characteristics such as direction, length or duration. Usually, the interest is in trips per average weekday, but may be for weekend or special purpose travel (FHWA, 1975).

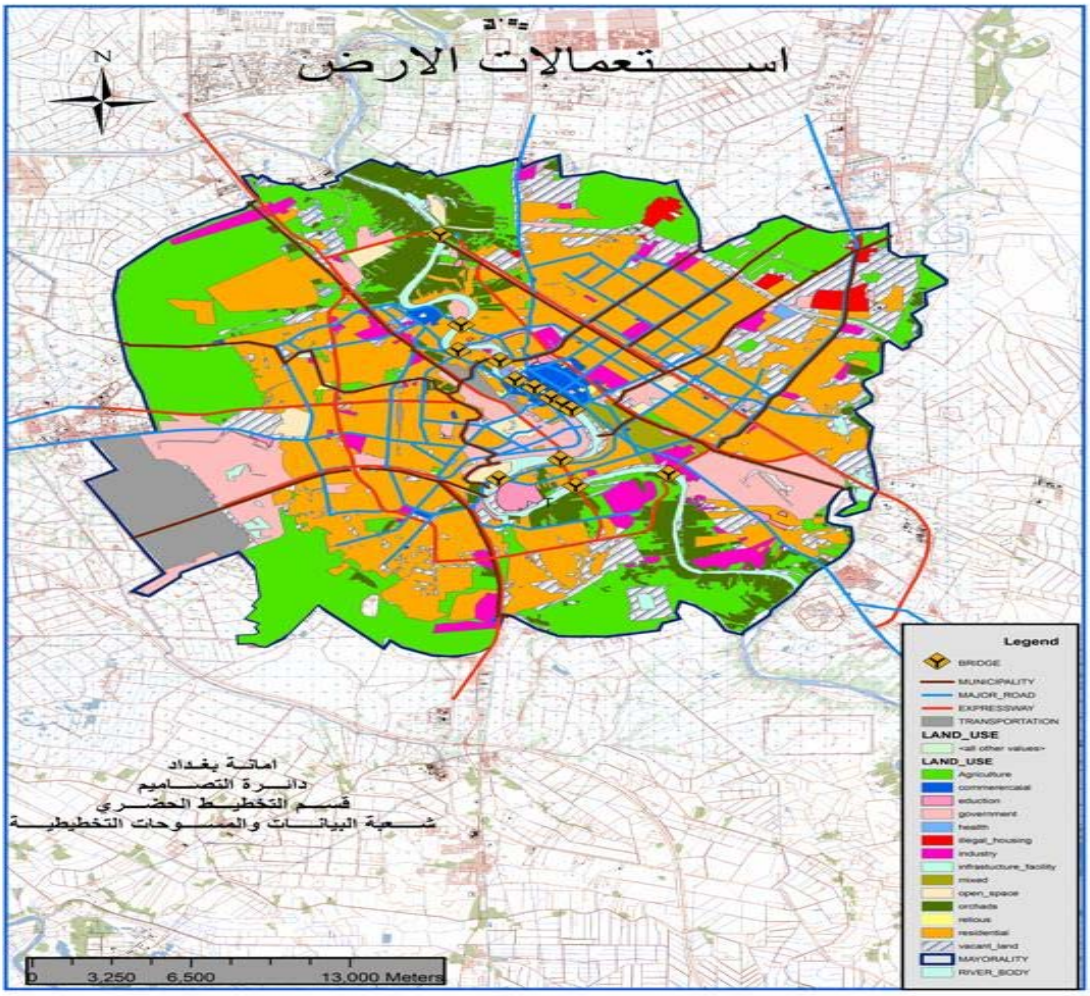

Fig.1 Land Uses of Baghdad City

Methodology

The models start with defining the study area and dividing them into a number of zones and considering the entire transport network in the system. The database also includes the current (base year) levels of population, economic activity like employment, shopping space, educational, and leisure facilities of each zone.

The following steps are convenient to be followed:

-Selection and Zoning the study area.
-Design of the questionnaire form.
-Sample sizes calculation and selection
-Data collection and processing

1.0 Selection and Zoning the study area

The study area is bounded between the left bank of Tigris River and the external west boundaries of Baghdad city. The population of Al-Karkh urban area reached to 1,010,408 inhabitants in 1977 census and 1,365,057 inhabitants in 1987 census and 1,797,557 inhabitants in 1997 census (Census Results,1977),(Census Results,1987),(Census Results,1997).

Because of the mass of data collected relates to individual journeys, households and, centers of employment, and in its crude form, is difficult to analyze and interpret, the area being surveyed is divided into zones for the purpose of grouping the data so as to make it intelligible, amenable to analysis (Bruton, 1985).

The zoning procedure requires the division of the survey area into spatial units suitable as a basis for data collection, and later for aggregate analysis purposes. In certain cases, it may be desirable to set up two complete zoning patterns. The first of these would be the zoning pattern to be used in data collection , and would divided the area up to spatial unit best suited to be treated as individual element in sampling process. The

second set of zones would comprise the zones to be used for analysis purposes (Stopher, 1977). In large study area it is more convenient to divide the study area into sectors. The zoning system used in this analysis is based on the administration divisions shown in Fig.2. Study area zoning is shown in Fig.3

2.0 Design of the Questionnaire Form

Traditional household survey has five sections; dwelling unit information, household characteristics, car ownership characteristics, personal characteristics and, trip details (Mathew and Rao, 2007).

Dwelling unit characteristics; this section includes a set of questions designed to obtain information about the dwelling unit. Information includes:

Dwelling unit type
Dwelling unit ownership
Availability of garage
The Household characteristics; include
Average monthly income
Number of persons in the household (stratified into male and female)

Trip data; this part of the survey aims at detecting and characterizing all trips made by the household members include:

Number of trips
Purpose of each trip
Mode of trips
Origins and destinations of trips
Time of starting and ending of trips
Cost of trips

Purposes of trips considered here are work, education (school or college), shopping, social/recreational, change mode and, return to

Number of workers in the household (stratified into male and female).
Number of students in the household (stratified into male and female).
Number of persons less than school age
Number of persons in each age group
Car ownership characteristics; include:
Number of available cars
Type of each car
Nature of use

Often, cars are classified according to type and size (BCTS, 1980), therefore cars are classified into private, taxi, bus, minibus, truck, pickup and, others.

Personal characteristics; this part includes questions designed to classify the household members (older than 6 year) according to the following aspects:

Gender, Age
Profession
Winning or official
Educational level
Number of residence year
Location of the work or education
Time waiting the transportation mode in minute

home. It may necessary to combine some of these purposes at modeling stage (BCTS, survey report, August 1980).

Travel modes used are:

Private (salon, taxi, bus, truck).
Government bus.
Taxi.
Mini bus.
Bus.
Motor cycle
Bicycle.
Walking.

Fig.2 Council Municipals of Baghdad City

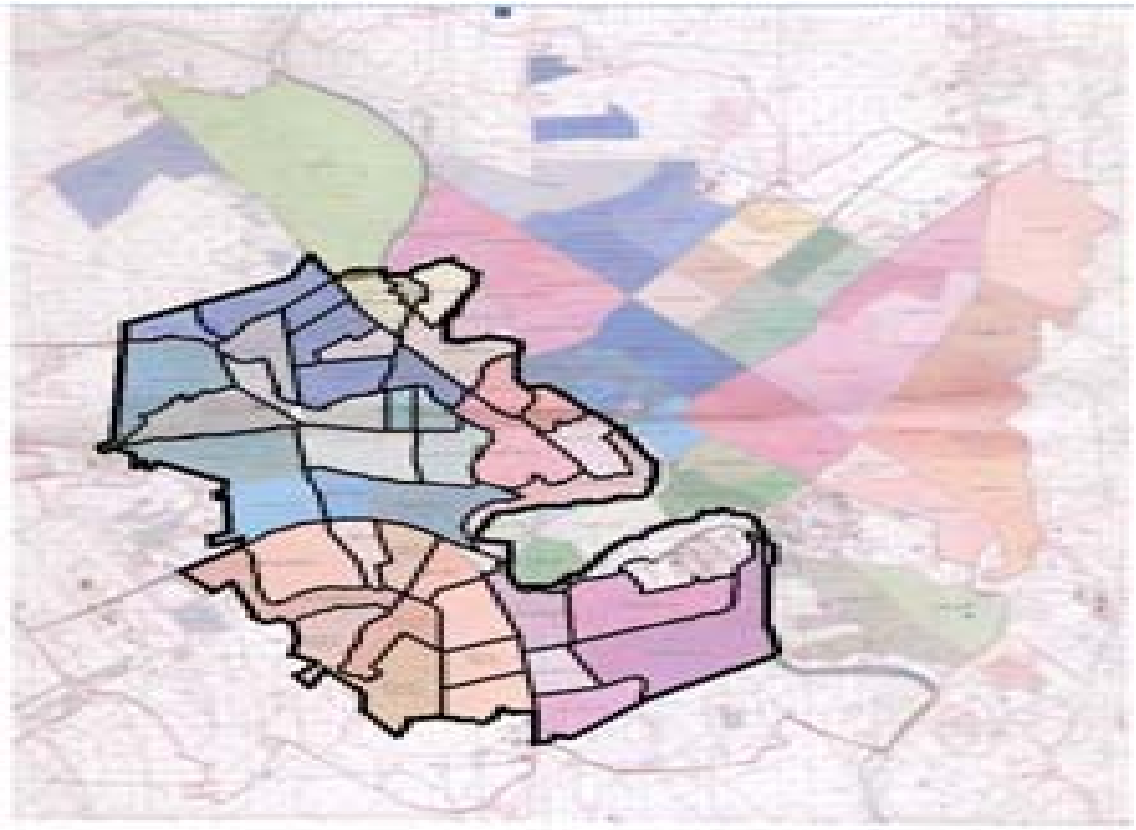

Fig. 3 Study Area Zoning

Table 2 Sample Size for Home Interview Survey

Study Area Population	Sample Size	
	Minimum	Recommended
Under 50 000	1 in 10	1 in 5
50 000 –150 000	1 in 20	1 in 8
150 000 – 300 000	1 in 35	1 in 10
300 000 – 500 000	1 in 50	1 in 15
500 000 – 1 million	1 in 70	1 in 20
Over 1 million	1 in 100	1in 25

Table 3 Executed Samples

No. of sector	Executed size	Sample Rate
1	451	0.112300797
2	116	0.028884462
3	519	0.129233068
4	451	0.112300797
5	479	0.119272908
6	490	0.122011952
7	225	0.056025896
8	550	0.136952191
9	551	0.137201195
10	300	0.074701195
Total	4016	1

3.0 Sample Sizes Calculation and Selection

The methods used to calculate the sample size for this analysis are:

1. The National Committee on Urban Transportation (NCUT) Method: The method is recommended for conducting home interviews, sample sizes is given in the table above.
2. Smith formula method: smith formula specify the use of coefficient of variation in determining the sample size as shown in the following formula:

$$n = C.V^2 Z^2 / E^2 \qquad \text{eq.1}$$

Where C.V = coefficient of variation (For a given variables),
E = accuracy level,
Z = normal variants, and

n = number of samples.

Table 3 shows the executed sample for each sector in the study area.

4.0Data Collection and Processing

The collection and processing of the Household Interview Survey data will follow a set of carefully considered and approved methods and procedures. To develop accurate trip production models, a large number of data is needed. Most of the necessary data are needed to relate the amount and character of urban activity. Typically, these data come from large-scale of household travel surveys and inventories of existing land-use characteristics. Census data are also a valuable source of information for transportation planners (Wallace and Shadoff, 1998) The methods used in home interview survey are:

a-Full interview technique: Involves interviewing as many members of the household as possible in directly recording all the information.

b-Home questionnaire technique: The interviewer collects details of the household characteristics leaving forms for household residents to be completed, regarding travel information. The completed forms are collected by the interviewer after day or two (Safa-Eldeen, 2006). This study uses two methods as shown in Table 4.

Table 4 The Distribution of Types of Survey Methods

Sector No.	Full Interview		Questionnaire		Total	
	No.	%	No.	%	No.	%
1	187	41.46	264	58.54	451	100
2	31	26	85	74	116	100
3	193	37.18	326	62.82	519	100
4	151	33.48	300	66.52	451	100
5	100	20.87	379	79.13	479	100
6	*0	*0	490	100	490	100
7	*0	*0	225	100	225	100
8	105	19.09	445	80.91	550	100
9	101	18.33	450	81.67	551	100
10	44	14.66	256	85.34	300	100
Total	820	21.93	3196	78.07	4016	100

Development of Trip Production Models

The dependent and independent variables for this analysis are as follow:

Dependent Variables

Y = Total Persons trips/HH
Y_1 = Home-Base-Work trips
Y_2 = Home-Base-Education trips
Y_3 = Home-Base-Social/Recreational & Shopping trips
Y_p = Person trips /person

Independent Variables

1. Dwelling Unit Characteristics and Income

X_{101} = Dwelling unit type (House=1, other=0)
X_{102} = Dwelling unit Ownership (Owned=1, Rented=0)
X_{103} = Availability of Garage (Yes=1, No=0)
X_{104} = Household mean income in (ID 1000)

2. Household Size and Structure

X_{201} = Number of Males
X_{202} = Number of Females
X_{203} = Household size
X_{204} = Number of Male workers in the Household
X_{205} = Number of Female workers in the Household
X_{206} = Total Household workers
X_{207} = Number of Male students in the Household
X_{208} = Number of Female students in the Household
X_{209} = Total Household students

3. Household by Age Groups

X_{301} = No. of Person Less than (6) years
X_{302} = No. of Person (6 – 18) years
X_{303} = No. of Person (19 – 24) years
X_{304} = No. of Person (25 – 60) years
X_{305} = No. of Person more than (60) years
X_{306} = No. of Person more than (6) years

4. Vehicle Ownership

X_{401} = No. of Available Vehicles
X_{402} = No. of Private Vehicles
X_{403} = No. of Taxi Vehicles
X_{404} = No. of Other Vehicles

5. Person Characteristics

X_{501} = Age
X_{502} = Gender (Male =1, Female =0)
X_{503} = Education Level "Educated" (Yes=1, No=0)
X_{504} = Education Level "School*" (Yes=1, No=0)

X_{505} = Education Level "Collage or Institute" (Yes=1, No=0)
X_{506} = Profession Status (Work=1, Do Not Work=0)
X_{507} = Profession "Official" (Yes=1, No=0)
X_{508} = Profession "Winner" (Yes=1, No=0)
X_{509} = No. of Years in the Residence
X_{510} = Time waiting the transport mode in minute
X_{511} = Mode of Travel (Private) (Yes=1, No=0)
X_{512} = Mode of Travel (Taxi) (Yes=1, No=0)
X_{513} = Mode of Travel (Bus) (Yes=1, No=0)
X_{514} = Mode of Travel (Walk or biking) (Yes=1, No=0)

Prior to model development, there are many steps should be carried out. These steps are followed in this study and shown graphically in the figure 4 below:

Test Variables for Multi-co linearity

Table 5 represents the partial correlation matrix controlling for Y for the whole data of Al-Karkh. If the correlation coefficient between two variables is high, then one variable has the larger correlation coefficient with the dependent variable should be included in the models but not both the variables. For example, by inspecting Table 5 the correlation coefficient between number of female (X_{202}) and number of female student per household(X_{208}) is 0.606 and the correlation between total trips/HH and X_{202} and X_{208} are 0.507 and 0.434 respectability therefore only X_{202} should be included in the model.

Error Tests

The distribution of error must be normal. This assumption can be tested by normal probability plot. If 95% of points lies in the range (-2,2) then the errors are normally distributed. Fig. 5 shows the 45 line plot of errors for whole data of the study area. It can be noted that the points lies between the range of (0,1) and errors are normaly distributed.

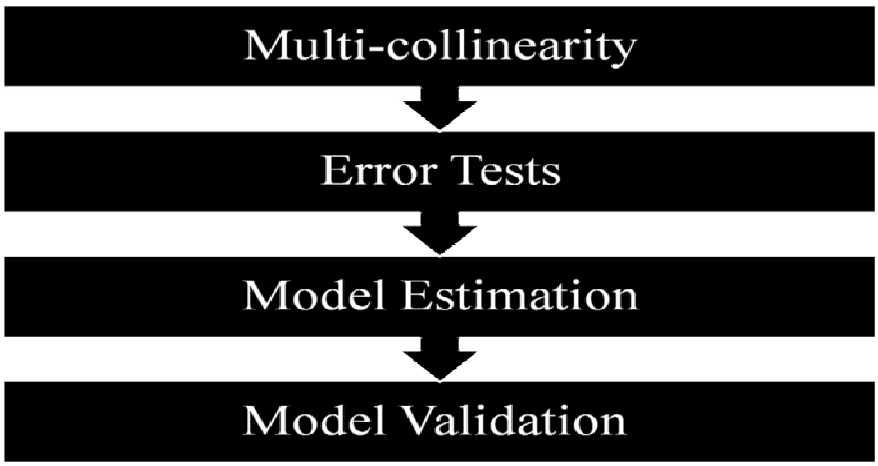

Fig.4 Statistical Methodology for model estimation

Table 5 Partial Correlation Matrix Controlling for Y

variables	X_{104}	X_{202}	X_{205}	X_{208}	X_{301}	X_{303}	X_{304}	X_{306}	X_{401}	X_{402}	X_{403}
X_{104}	1										
X_{202}	-0.071	1									
X_{205}	0.303	0.008	1								
X_{208}	-0.161	0.606	-0.124	1							
X_{301}	0.006	0.519	-0.064	0.258	1						
X_{303}	-0.024	0.324	-0.089	-0.105	-0.023	1					
X_{304}	0.139	0.125	0.064	-0.079	0.362	-0.091	1				
X_{306}	0.167	0.184	0.077	-0.188	0.345	0.158	0.015	1			
X_{401}	0.284	-0.030	0.087	-0.058	0.024	0.029	0.069	0.127	1		
X_{402}	0.280	-0.019	0.104	-0.016	-0.008	-0.004	0.052	0.097	0.839	1	
X_{403}	-0.019	0.010	-0.022	-0.040	0.032	0.073	0.029	0.009	0.134	-0.126	1

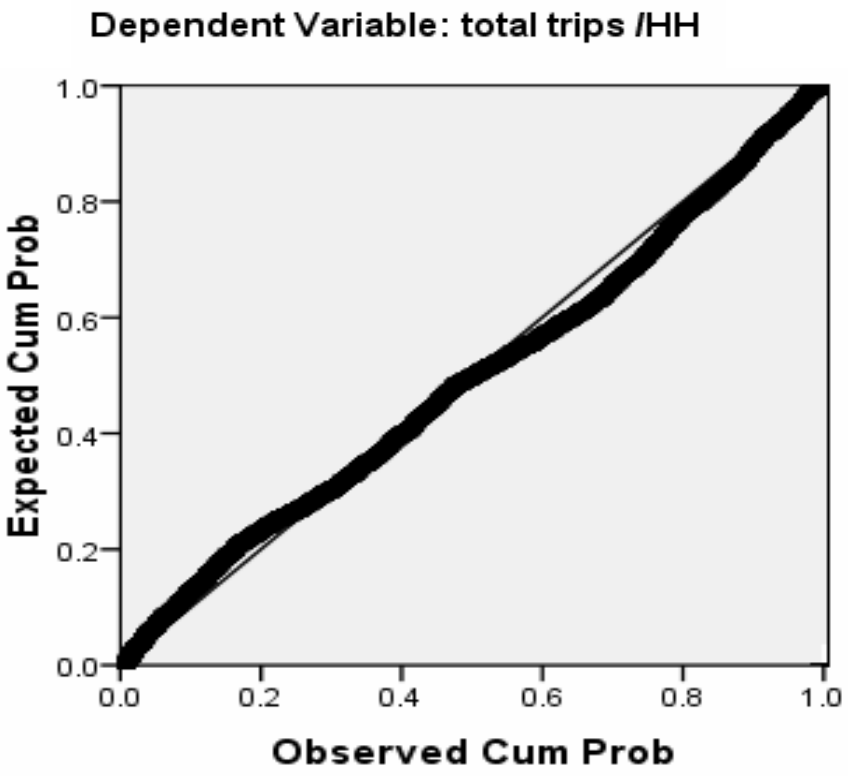

Fig. 5 45 line Plot of Errors

Models Estimation

Many methods of linear regression are available, they are:

Enter, Stepwise, Remove, Backward, Forward

The best and commonly method used to determine parameter of prediction model is

stepwise method (Abed, 2010). This method computes the simple regression model for each independent variable. The independent variable that has the largest F-statistic is chosen as the first entering variables. If at least one variable exceeds the standard, the procedure continues. The procedure considers whether the model will be improved by adding a second independent variable and so on. It examines all variables to determine which has the F-statistic which suite the selected F-statistic to enter criteria (Al-Zaidy, 2005). Either F value or probability of F are used as enter criteria. Probability of F equal to 0.05 is used in the analysis, this correspond to 3.84 F value.

Table 6 shows the resulted models with coefficient of determination R^2 for whole data of the study area

Table 6 Stepwise Regression Results for Y

Dependent Variable	Models	R^2
Y	$3.019+1.362X_{306}+0.758X_{209}+0.493X_{206}+0.356X_{201}+0.243X_{402}$	0.669
Y1	$0.182+0.478X_{206}+1.194X_{204}+1.26X_{205}+0.08X_{304}+0.035X_{303}+0.07X_{305}$	0.82
Y2	$0.378+1.792X_{209}$	0.900
Y3	$2.789+0.13X_{203}+0.243X_{201} - 0.533X_{205} +0.326X_{103} +0.23X_{303} +0.362X_{304} - 0.452X_{204}+0.352X_{305}+0.182X_{401} - 0.202X_{102}$	0.089
Yp	$0.43+1.034X_{502}+0.283X_{505}+1.297X_{514}+1.141X_{513}+1.128X_{511} +1.097X_{512}+0.003X_{501} +0.353X_{504}$	0.478

Conclusions

Major conclusions found in the trip production analysis are that the first model (Y) is the preferred from the rest models because of the preferred statistical results and the simplicity of the application. On the other hand, purposes trip models (Y1, Y2, and Y3) cannot be use in application because all purposes trips models must be applicable to use. Work and education trip models are good from the statistical point of view, while shopping and social/recreational trip models are poor from the statistical point of view. Whereas person trip models (Yp) are weak. It may be due to the non linear relationship between Yp and person's variables.

Other conclusions found are:

1. Most of the household variables have statistically significant relationships to each trip purpose, apparently due to multiple collinearities between a household's numbers of person's workers, and vehicles.
2. In general, the strongest single predictor of trips in a given purpose is the number of persons eligible or most expected to make such trips. For work trips, this is the number of employed persons; for education trips, it is the number of school-age children and persons in a college age group. For shop and other trips, this is simply the number of persons counted as trip makers such as number of male, number of female workers per household.
3. The most effective independent variables on total trips/HH are household size variables, from these variables the most notable effect is number of person more than 6 year. The most effective independent variables on person trips/person are gender and modes of travel.
4. In many models the constant and income parameters have (t) value less than 2 and hence these parameters are insignificant. Therefore, the constant and income are eliminating from these models.

References

AL-Zaidy M.A., "Influence of Socio-Economic Factors on Trip Generation of a Selected District in Baghdad ", MSC. Thesis, University of Baghdad, 2005.

Abed, A. H., "Required Criteria for Implementation of the Superpave System; Local Pavement Design" PHD thesis, University of Baghdad, 2010, Ch.6.

Brain; Memmott; and Bone, "Principles And Technique of Predicting Future Demand for Urban Area Transportation", M.I.T. Report No. 3, 1974.

Bruton, M. J. , " Introduction to transportation planning ", Hutchinson, London, 1985

Baghdad Comprehensive Transportation Study (B.C.T.S), Scott Wilson Kirkpatrick & Partiners, Amanat-Al-Assima "Survey Report , August 1980".

Federal Highway Administration , "Trip Generation Analysis ", U.S. Department of Transportation, Washington, D.C. August 1975

Hobbs F.D. , " Traffic Planning And Engineering " Cox &Wyman Ltd , London ,1979

Liya Y.; Hongzahi G ; and Hai Y. , "Trip Generation Model Based on Destination Attractiveness " , TSINGHUA Science And Technology ISSN 1007 -0214 , Vol.13 , No.5, October 20

Mathew, V. and Rao, K.V., "Introduction to Transportation Engineering", NPTEL, May3, 2007.

National Transportation Library ,"Travel Model Development and Refinement –trip Generation" Final Report ,US Department of Transportation Research and Innovative Technology Administration, 2006.

Quade, P.B. and Douglas, " Travel Demand Model Development and Application Guidelines " , Oregon Department Of Transportation , Planning Section, Transportation Planning Analysis Unit , September 1994

Simek, C. ; Turner, A.; and Greenman, B. ,"Bicycle and Pedestrian Travel : Exploration of Collision Exposure in Florida " , Center of Urban Transportation Research CUTR , Final Report , September 2002

Stopher, P. R. and Myburge A.H. , " Urban Transportation Modeling and Planning " , Lexington Books, D.C. Heath and Company , Lexington, Massachusetts ,Toronto ,London ,1977 .

Smith, M.E.," Design of Small-Sample Home Interview Travel Surveys", Transportation Research Board TRB No.701, 1979.

Safa-Eldeen G.I., "Trip Generation Model for Kirkuk City", MSC thesis, University of Technology, 2006.

Wright, P. H. and Ashford, N. J.," Transportation Engineering Planning and Design", John Wiley & sons, 4th Edition United State of America 1998.

Wallace, B.P. and Shadoff, J. " Evaluation of Travel Demand Management Strategies in the Trip Generation Phase of a Network-Based Modeling Approach " , Washington State Transportation Center TRAC , July 1998 .

BEARING CAPACITY OF SHALLOW FOOTING ON SOFT CLAY IMPROVED BY COMPACTED FLY ASH

Dr. Mosa J. Aziz Al-Mosawe
Professor, Civil Eng. Department
Head of Baghdad University

Dr. Bushra S. Albusoda
Lecturer, Civil Eng.Departement
University of Baghdad
E−Mail:albusoda@yahoo.com

Azhar S. Yaseen
B.Sc.,Civil Eng. Department.
University of Baghdad
E-Mail: azharealhilo@yahoo.com

ABSTRACT

Low bearing capacity of weak soil under shallow footings represents one of construction problems. Kaolin with water content converges to liquid limit used to represent the weak soil under shallow footing prototype. On the other hand, fly ash, which can be defined as undesirable industrial waste material, was used to improve the bearing capacity of the soft soil considered in this research. The soft soil was prepared in steel box (36×36×25) cm and shallow square footing prototype (6×6) cm were used .Group of physical and chemical tests were conducted on kaolin and fly ash. The soft soil was improved by a bed of compacted fly ash placed under the footing with dimensions equal to that of footing but with different depth ratios. The results show that there is a noticeable improvement in the behavior of footing when improved by compacted fly ash. The improvement showed a decrease in settlement and increase in bearing capacity. The improvement ratio in bearing capacity was calculated by comparing the ultimate bearing capacity value when testing the kaolin alone with its value of kaolin improved with compacted fly ash at the same value of eccentricity. It is important to note that eccentricity values were chosen according to the rule of middle third of footing base(i.e.,e≤B/6). The improvement ratio was about (130%) in average value, that represent a good ratio of improvement.

الخلاصة

تمثل قابلية التحمل الواطئة للترب الضعيفة اسفل الاسس الضحلة من أهم مشاكل الانشاء. استخدمت تربة الكاؤولين بمحتوى رطوبة يقترب من حد السيولة لتمثيل التربة الضعيفة اسفل نموذج الاساس الضحل كما تم استعمال مادة الفحم المتطاير وهي من مواد المخلفات الصناعية . تم استعمالها في تحسين قابلية تحمل التربة الضعيفة الممثلة بمادة الكائولين التجاري في هذا البحث.تم تحظير التربة داخل صندوق من الحديد بأبعاد(36×36×25)سم مع نموذج لاساس مربع ضحل(6×6)سم . أجريت مجموعة من الفحوص الفيزيائية والكيميائية لمادة الكائولين ومادة الفحم المتطاير وتمت عملية التحسين من خلال عمل شق اسفل انموذج ألأساس الضحل وبنفس طول وعرض ألأساس وتم حدل مادة الفحم المتطاير فيه (عند محتوى الرطوبة ألأمثل) ولثلاثة اعماق مختلفة (D=B,D=2B,D=3B)، علما ان B تمثل عرض ألأساس.أ جريت مجموعة من فحوص التحميل على التربة قبل وبعد التحسين وبتحميل مركزي ولامركزي مع الأخذ بنظر الأعتبار قاعدة منتصف ثلث قاعدة الأساس اي (e≤B/6)في التحميل اللامركزي.

أستخدمت العلاقة بين الضغط المسلط على الأساس مع الهبوط الحاصل في الأساس لإيجاد مقاومة التحمل القصوى للتربة تحت تأثير الاحمال المسلطة ولكل انواع الفحوص. تم احتساب نسبة التحسين في مقاومة التحمل من خلال مقارنة مقاومة التحمل القصوىلتربة الكاؤولين بمفردها مع مقاومة التحمل القصوى لتربة الكاؤولين مع مادة الفحم المتطاير ولنفس مسافة التحميل اللامركزي .اعتمد البحث على عدة معادلات خطية تقريبية لتفسير النتائج العملية للفحوص، وصل معدل نسبة التحسين الى حوالي (130%) وهو ما يعتبر نسبة تحسين جيدة بالنسبة الى مقاومة التحمل.

Keywards: bearing capacity, improvement of soft clay, fly ash, shallow footing, eccentric loading

Introduction

the transfer of load to the soft clay was arranged through a model footing. It was revealed from the Many researchers studied the improvement and stabilization of soft soil using different methods and procedures.

Chakrabrti and Bhandri (2004) worked on improvement of settlement behavior and vertical stress dispersion of soft clay using compacted pulverized fuel Ash. They showed in most of cases the ground improvement becomes expensive, increasing the total project cost. Pulverized fuel Ash (PFA) is waste material from thermal power plants and creates problems during its disposal. The research was conducted using normally consolidated commercial kaolin (soft clay) in a test tank and results that the improvement of load carrying capacity could be remarkably increased, using compacted PFA layer on soft clay. The percentage of improvement of bearing capacity has been revealed in two ways. The first by increase of diameter wells with the depth of compacted PFA, though the improvement is more in case of increment of depth (Z) of PFA bed, rather than increment of diameter (D'). The percentage of improvement of bearing capacity, for different depths and diameter of compacted PFA varies from 12 to 390. The stress dispersion was also improved for different depths and diameters of compacted PFA bed.

Deschamps (1998) used FBC and stoker Ashes as roadway fill. It was noticed that approximately 100,000 m^3 of atmospheric fluidized bed combustion (FBC) ash and stoker ash were used as structural fill in the construction of a large roadway embankment. The embankment is ~ 200 m long and 10m high, and it supports an extension of a street across a gravel quarry in waste Lafayette, Ind. An over view of the project and construction operation is described, and the results of geotechnical laboratory tests and field monitoring presented. Instruments used in the monitoring of fill behavior include settlement plates, vertical and horizontal inclinometers, seismic cross-hole tests, and preconstruction standard penetration tests.

MAERITAL PROPERTIES

Kaolin

The kaolin clay used in this research was of commercial grade. It was from North of Hussainiat, AL-Anbar Governorate, Iraq.

Physical properties of kaolin, shear strength and compressibility parameters could be shown in **Table 1**

It was obvious from results shown in **Table 1** that the clay was classified as low plasticity clay (CL) according to the Unified soil classification system.

Chemical tests were carried out on kaolin with assistance of the state of geologic surveying and mining and the chemical composition of kaolin can be shown in **Table 2**

White kaolin which selected was provided by (The state of geologic surveying and mining) from Dewielca lies in the west of Iraq.

Fly ash

The fly ash used in this research was from station of south Baghdad electricity ,Baghdad ,Iraq. Specific gravity test, standard Proctor and direct shear test were conducted on fly ash. The results are shown in **Table 3** .

Chemical tests were conducted for fly ash with the assistance of NCCLR. The results could be shown in **Table 4**

EXPERIMENTAL WORK

In order to simulate the behavior of shallow footing on weak soil, special techniques were used to achieve this purpose. These techniques include the manufacturing of steel box having the dimensions (36×36×25) cm.This box was filled with kaolin prepared at water content near its liquid limit. Also,a steel plate of (6×6 × 0.5)cm was used to simulate the shallow footing. A trench was made under the footing that resting on soft kaolin. The trench had the same dimensions of footing and excavated at different depths (D=B, D=2B, D=3B), where B represents footing width. Then, the trench filled with compacted fly ash (at its optimum moisture content) to the desired depth. **Fig. 1** shows a simple section in model loading test and the detail of footing and fly ash column which support it.

Then, the footing is loaded at the beginning of the test until failure is reached. The settlement at centre and edge of the footing is recorded with the use of video camera.

Compacted fly ash (C.F.A)

The fly ash was prepared at optimum moisture content ($\omega_{opt.}$=24%) three depths of C.F.A. (H=6,H=12,H=18cm) were used. The sample of soft soil was prepared by putting the first layer of kaolin .Then; scaled steel mold was put and centered in length and width of steel box at the desirable depth which worked on. Then the trench under the footing was filled with compacted fly ash at its maximum dry density and optimum water content. It is compacted to the desired depth.

Results of load –settlement tests

Typical load (kN) vs. foundation settlements at edge and centre of foundation diagrams were obtained from loading tests as shown in **Fig.2** to **Fig.4**. The ultimate bearing capacity is defined as the point where a maximum value of q_u is clearly arrived, or where slope Δs/Δq becomes maximum and the load vs. settlement not remains practically linear thereafter Vesic (1973).

Effect of (H/B) ratio on Bearing Capacity

In general, the ultimate bearing capacity incrased as H/B ratio increased. This behavoir was expected due to the increase in strength of soil under the footing as the (H/B) ratio, of the fly ash used for improvement, increased . In addtion, the ratio of improvement increased as the (H/B) ratio increased . The largset ratio of improvement getten for soil improved by fly ash at H/B=3,see **Fig.5** and **Table 4** . This behavoir may be explained accoring to the shear strength prameters, where the cohesion and angle of internal friction of cement dust were (5 kPa, 30^0) respectively.

Effect of Eccentricity on Bearing Capacity

The eccentricity has large effect on ultimate bearing capacity. Generaly the ultimate bearing capacity decreased as the eccenricity increased as shown in figure **Fig.6** .This behavior may be attributed to the reduction in effictive area as eccentrisity increased.

Improvement ratio in the ultimate bearing capacity

Foundation was reaching to failure if the settlement would be greater than (10%) from footing width, ASTM (D1194-94) so the bearing capacity at this ratio was equal to the ultimate bearing capacity. **Fig.5** shows the variation of improvement ratio with eccentricity

at different (H/B) ratios. It is important to know that the improvement ratio is defined as:-

$$\text{Ratio of improvement (r) \%} = \frac{Q_{improved} - Q_{without\ Improvement}}{Q_{without\ improvement}} * 100\%$$

Equations obtained from experimental results

Ratio of improvement in bearing capacity for cement dust used in improvement at different values of eccentricity were varied with the change in H/B ratio ,see **Fig.8**. In general, acceptable equations were obtained that simulate the incrase in r % with incrase of the H/B ratio for different values of eccentricity.

Table 5 shows the all equations can be use to predict the improvement ratio for any (H/B) ratio given, all equations was linear and have acceptable values of (R^2) (difference between the experimental results and the fitting equation results).

CONCLUSIONS

Number of laboratory loading tests of shallow square footing supported by **(C.F.A.)** columns made in soft clay have been presented, based on the these results the following conclusions can be drawn:-

1. There are acceptable improvement ratios for square footing prototype can be obtained (233%) maximum value of improvement ratio(r %).
2. Bearing capacity of soft soils under the shallow footing can be increased by making square trench under the footing with the same dimensions of it and for different depths. This trench is filled with compacted fly ash at optimum water content.
3. The maximum improvement ratios in ultimate bearing capacity was appeared at maximum values of the (H/B) ratio which equal to (3).
4. Acceptable ratios can be used for (H/B) ratios less than (3).
5. Many fitting equations were obtained to estimate the improvement ratio from H/B ratio, most of equation are linear and have acceptable values of (R^2).

REFERENCES

ASTM D854-02 Standard Test Methods for Specific Gravity of Soil Solids by Water Pycnometer.

ASTM D698-00 a Standard Test Methods for Laboratory Compaction Characteristics of Soil Using Standard Effort (12,400 ft-lbf/ft3 (600 kN-m/m3)).

ASTM D1194-94 Standard Test Method for Bearing Capacity of Soil for Static Load and Spread footings.

ASTM D2166-80 Standard Test Method for Unconfined compression Test of Soils.

ASTM D2435-80 Standard Test Method for Standard Consolidation Test of Soils.

ASTM D3080-98 Standard Test Method for Direct Shear Test of Soils under Consolidated Drained Conditions.

ASTM D4318-00 Standard Test Methods for Liquid Limit, Plastic Limit, and Plasticity Index of soils.

Chakrabrti and Bhandri,(2004), “Improvement of Settlement Behavoir and Vertical Dispersion of Soft Clay Using

Compacted Pulverised Fuel Ash", Department of Civil engineering , Both at Jadavpur University, Kolkata 700 032. IE(I) Journal- CV, Vol 84, February

Das B.M. and Hanna A.M,(1988),"Model tests for shallow strip foundation on granular trench" (GSP 16), ED BM Das, ASCE, New York,.110-124.

Deschamps, R.J. (1998), " Using FBC and Stoker Ashes as Roadway Fill: A Case Study". Journal of Geotechnical and Geoenviromental Engineering. Vol.124, No.11 /November.

Vesic A.S., (1973),"Analysis of Ultimate loads of Shallow Foundations", J. soil Mech. Found. Div. (ASCE), 99(1), 45-73.

NOTATIONS

Symbol	Meaning
C.F.A.	Compacted fly ash
C_u	Undrained shear strength
H/B	Ratio between the depth of fly ash column to the footing width
L.O.I	Loss Of Ignition
NCCLR	National Centre of Construction Laboratories
PFA	Pulverized fuel Ash
Q_u	Ultimate bearing capacity
R^2	difference between the experimental data and fitting equation
r %	Improvement ratio in ultimate bearing capacity

Table 1 Physical properties, shear strength and compressibility parameters of kaolin

Property	Value	Type of test	Standard
LL%	44%	Atterberge limits	*ASTM 4318*
PI	25%		
G_s	2.77	Specific gravity of solids	*ASTM D854*
e_o	0.819	Standard Consolidation test	*ASTM D2435*
n	0.45		
Cc	0.34		
ϕ_u	0	Unconfined compression test	*ASTM 2166*
C_u	13 kPa		
C_v	$5.608*10^{-8}$ m^2/s	Standard Consolidation test	*ASTM D2435*

Table 2 Chemical composition of kaolin

Chemical composition				
L.O.I.*	TiO_2	Fe_2O_3	SiO_3	Al_2O_3
13.4-15.1%	1.4-2.96%	0.5-1.96%	38-45%	35.5-41.4%

*L.O.I: Loss of Ignition

Table 3 Results of physical, standard Proctor and direct shear test for fly ash.

Material Properties	Value	Type of test	standard
G_s	2.78	Specific gravity	*ASTM D854*
$\gamma_{d\,max}$	16.5 kN/m^3	Standard Procter test	*ASTM D698*
$\omega_{opt.}$	24%		
C_u at ω_{opt}.	5kPa	Direct shear test	*ASTM D3080*
ϕ_u at ω_{opt}.	30°		

Table 4 Results of chemical tests for fly ash.

SO_3 %	1.72
Organic matter %	0.98
$CaCo_3$ %	4
Cl %	0.18
pH	7.14

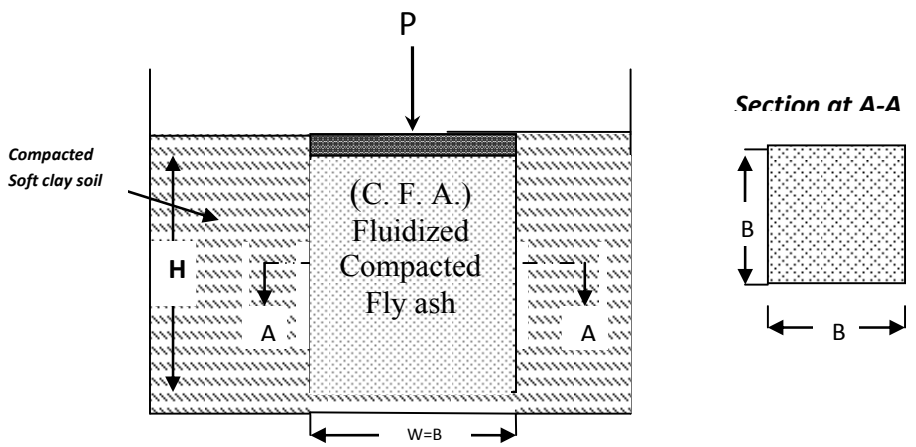

Fig.1 Rectangular footing on **C.F.A.,** note that: width of compacted fly ash column **C.F.A.** =W, width of footing = B, W=B

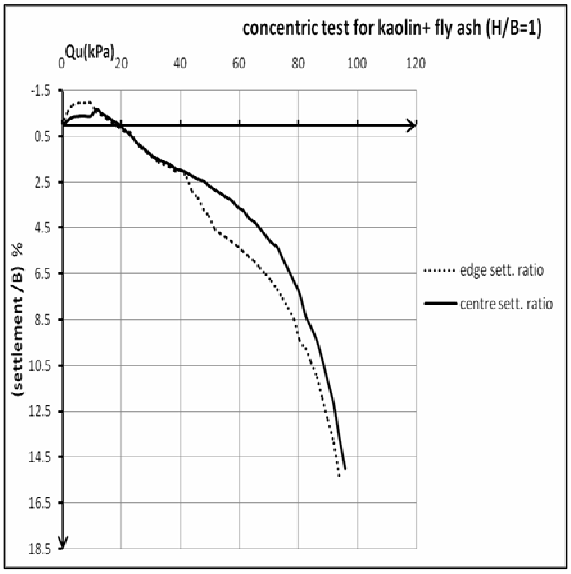

Fig.2 Pressure-settlement ratio curve for kaolin with fly ash (H/B=1), concentric loading

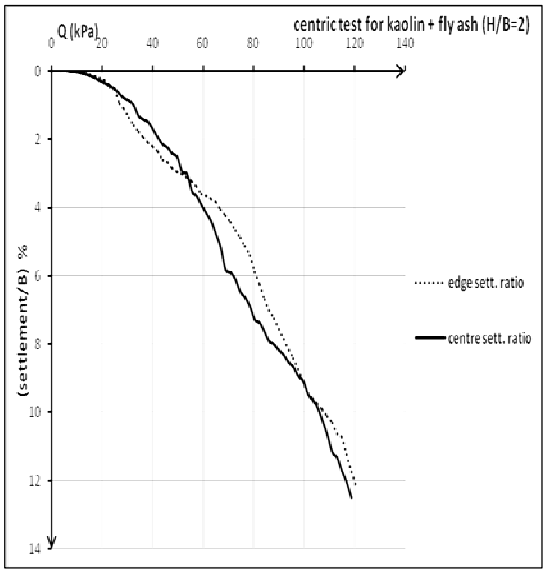

Fig.3 Pressure-settlement ratio curve for kaolin with fly ash (H/B=2), concentric loading

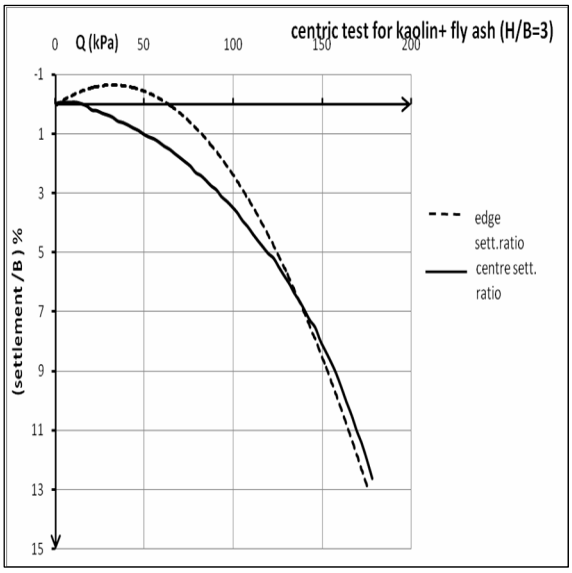

Fig.4 Pressure-settlement ratio curve for kaolin with fly ash (H/B=3), concentric loading

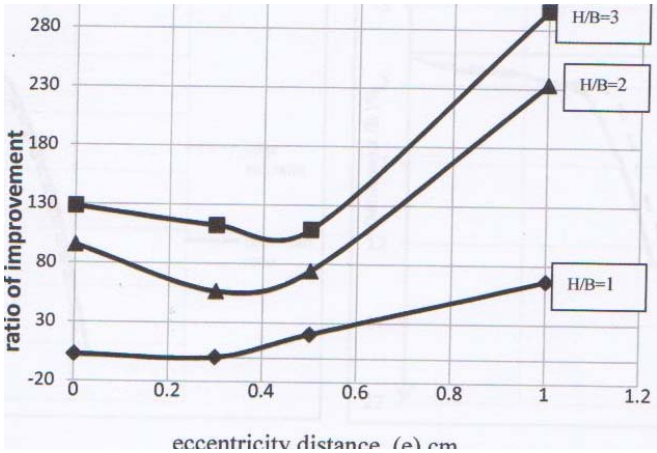

Fig.5 Ratio of improvement and eccentricity relationship at different values of H/B ratio,"kaoline- fly ash"

Table 4 Type of the tests and the ultimate bearing capacity values

ype of material used	Qu(kPa)	H/B	e(cm)	percent of improvement ratio%	Test no.
kaolin	82	0	0	0	1
kaolin +fly ash	84	1	0	2.4	2
kaolin + fly ash	105	2	0	28	3
kaolin + fly ash	160	3	0	95	4
kaolin	84	0	0.3	0	5
kaolin + fly ash	78	1	0.3	0	6
kaolin + fly ash	74	2	0.3	-	7
kaolin + fly ash	95	3	0.3	13	8
kaolin	57	0	0.5	0	9
kaolin + fly ash	57	1	0.5	-	10
kaolin + fly ash	62	2	0.5	8.8	11
kaolin + fly ash	98	3	0.5	71.9	12
kaolin	24	0	1	0	13
kaolin + fly ash	40	1	1	66.7	14
kaolin + fly ash	71	2	1	195.8	15
kaolin + fly ash	80	3	1	233.3	16

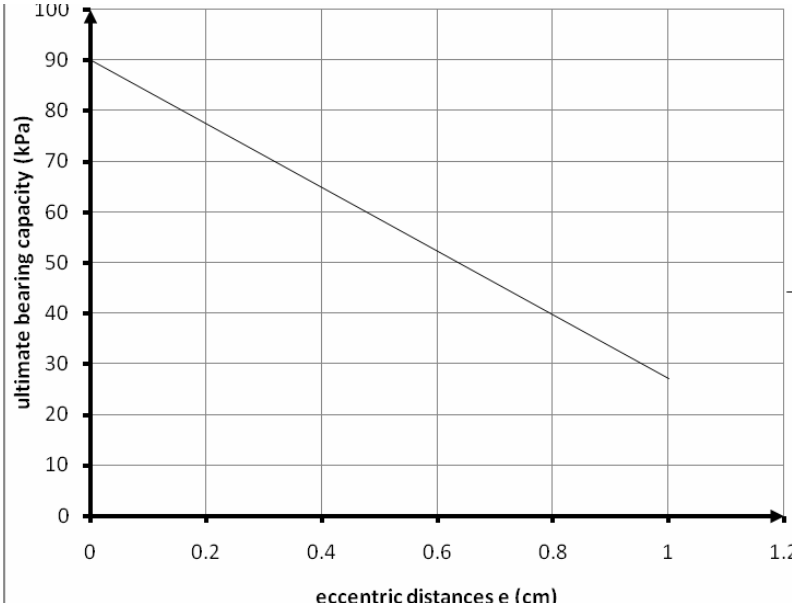

Fig.6 Ultimate bearing capacity vs. eccentric distance relationship**.**

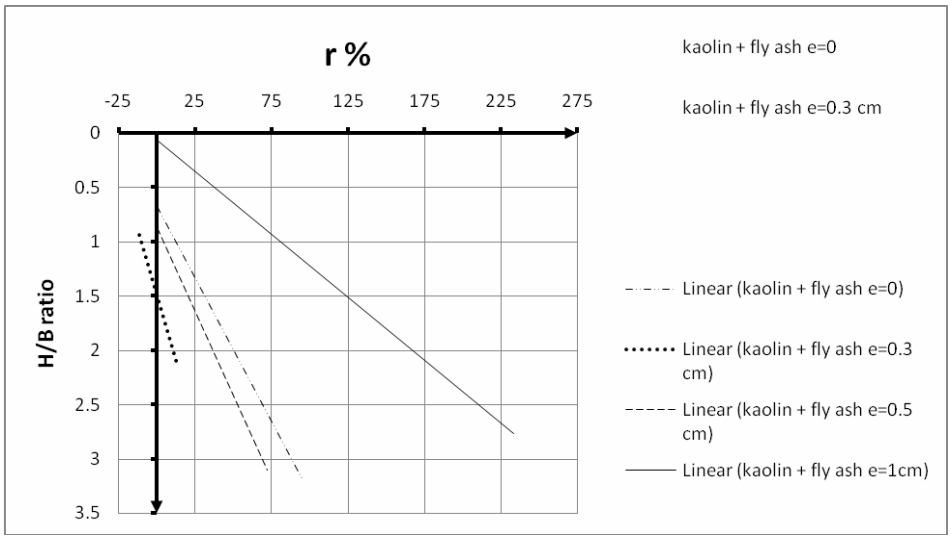

Fig.7 Ratio of improvement and H/B relationship at different values of eccentricity, “kaolin improved by fly ash"

Table 5 Predicted equations for estimating improvement ratio from depth ratio

Type of material and test	Equations	R^2
Kaolin+ fly ash , e=0	r %= 38(H/B) -25.7	0.82
Kaolin+ fly ash, e=0.05B	r %= 21(H/B) -32	0.16
Kaolin+ fly ash, e=0.85B	r %= 27(H/B) -24	0.693
Kaolin+ fly ash, e=0.167B	r %= 90(H/B) -6	0.96

REMOVAL OF COPPER ION FROM WASTEWATER BY FLOTATION

Ahmed A. Mohammed and Farah I. Abed

Environmental Engineering Department

University of Baghdad Iraq

ABSTRACT

Several industrial wastewater streams may contain heavy metal ions, which must be effectively removal before the discharge or reuse of treated waters could take place. In this paper, the removal of copper(II) by foam flotation from dilute aqueous solutions was investigated at laboratory scale. The effects of various parameters such as pH, collector and frother concentrations, initial copper concentration, air flow rate, hole diameter of the gas distributor, and NaCl addition were tested in a bubble column of 6 cm inside diameter and 120 cm height. Sodium dodecylsulfate (SDS) and Hexadecyl trimethyl ammonium bromide (HTAB) were used as anionic and cationic surfactant, respectively. Ethanol was used as frothers and the optimal removal conditions have been established. Successful removals about (98%) and (76%) could be achieved for copper ions with SDS and HTAB, respectively. Copper removal reached about 80% under the optimum conditions at low pH; at high pH it became as high as 98% probably due to the contribution from the flotation of precipitated copper. It was found that the presence of NaCl in the solution reduced the recoveries. Adding ethanol at 1% concentration increased the removal efficiency. From the results the rate of flotation was found to be first order.

Key words: bubble column, copper ions, flotation.

1. Introduction:

Water pollution is nowadays a matter of deep apprehension. Many industrial wastewaters contain numerous toxic metals, such as chromium, mercury, cadmium, lead, copper, which must be removed before reuse of the water or its discharge to the environment. According to environmental regulations, there is an increasing concern about the removal of metal in the effluent streams. Therefore, the scientific research is being directed towards the implementation of novel approaches dealing with the efficient removal of toxic metals from wastewater (Zhang et al., 2009).

The wastewater treatments used for removal of toxic metals include the convention a physicochemical treatment of addition of inorganic coagulants and polymers, subsequent precipitation, aeration, and final neutralization. However, the final step, which should involve the treatment and safe disposal of toxic sludge, has been largely ignored (Matis et al., 2001).

In the treated industrial wastewaters, depending on reuse/recycling options; some of the values often exceed legal limits. Therefore, the necessity of innovative, simple, and economical treatment methods for the final polishing step or tertiary treatment are needed (Matis et al., 2001).

Copper has received considerable attention owing to its uses in metallurgy, chemical industries and is necessary for other many biological important functions (Ghazy et al., 2008). The primary sources of copper in industrial wastewaters are metal process pickling baths and plating baths (Eckenfelder et al. 2009).Copper may also be present in wastewaters from a variety of chemical manufacturing processes employing copper salts or a copper catalyst in different range from 0.12 mg/l to 183 mg/l such as mining acid, mine

drainage, paint and pigment manufacturing and motor vehicle (Metcalf and Eddy, 2003).

There are various methods for removing metals from water and wastewater, e.g., chemical precipitation, ion exchange, reverses osmosis. These methods are relatively expensive, involving either costly equipment or elaborate procedures, and with some techniques, large volumes of secondary wastes are generated (Sabti et al., 2002).Flotation is one of the adsorptive bubble separation techniques which have many advantage such as high selectivity to remove contaminants, high overflow ,low detention periods and low operating costs(Sulaymon and Mohammed,2010).

Several researches have been done on the copper removal from wastewater using foam separation techniques. A thermodynamic approach was investigated to model the removal of cupric ion using different surfactant types and ion flotation systems by liu et al., 2001.

Doyle et al., 2003 reported that the effect of a neutral chelating ligands, triethylenetetraamine (Trien) on the ability to separate copper (II) and calcium (II) ions.

A study concerning the kinetics of Cu^{+2} ion separating by precipitate flotation using alkyl amine type and alkylammonium salt as cationic collectors and alkylsulphate and alkylcarboxilic type as anionic collectors was presented by Stoica et al., 2003.

Lazaridis et al., 2004 was investigated the recovery of copper ions from wastewater. They used three different mechanisms: ion flotation using xanthates, precipitate flotation generating copper hydroxide and sorptive flotation using zeolites as a sorbent material.

Ghazy et al., 2008 developed a simple, rapid and economic procedure for copper (II) and lead (II) removal under the optimum conditions. It was based on the complex formation between Cu^{+2} and Pb^{+2} ions and diphenylcarbazone (HDPC) followed by flotation with oleic acid (HOL) surfactant.

Liu et al.,2009 Investigated the Ion Flotation of Co^{+2}, Ni+2, and Cu^{+2} using Dodecyldiethylenetriamine(Ddien),They obtained that a chelating surfactant, dodecyldi-ethylenetriamine (Ddien), could selectively remove one metal ion over others at different pH values.

A system for removal of Cu^{+2} from aqueous solution by foam fractionation using Dodecyl Benzenesulfonic acid (the anionic surfactant) was proposed by Zhang et al., 2009.

Abryutin et al., 2010 investigated the regularities of the ion flotation of copper by using sodium diethyldithiocarbamate (DEDTK) as the collector.

2. Experimental Apparatus and Procedure:

The foam flotation tests were carried out in a bubble column (acrylic) of 6 cm inside diameter and 120 cm in height. **Fig. (1)** Show a schematic diagram of experimental apparatus. Air supplied by the compressor was fed to the column through a pre-calibrated rotameter. Air entered the column was dispersed as bubbles in to liquid. Feed inter with different metal concentration (25 up to 200 ppm) was poured gently at the top of the column. At the same time, the column was pressurized so as not to weep the liquid through the holes. Two perforated plates of the air distributor were used. The first one has 20 holes with 0.1 cm diameter, and the second one has 25 holes with 0.05 cm diameter. The holes are arranges in the equilatered triangular pitch through the whole area which are located inside the column. The column was operated at batch mode as far as the liquid phase and continuous flow with respect to air. This column contains six taps of 0.2 cm inside diameter, these taps arranged at interval of 15cm and used to draw samples from the column. Synthetic polluted water samples containing maximum concentration of copper (200mg/l) were prepared by dissolving ($CuCl_2.2H_2O$) in distilled water. Surfactants and ethanol were added to the synthetic polluted water. Solution pH was adjusted to a desired value using H_2SO_4 or NaOH. Then the solution was placed in the flotation column. Foam samples were taken at preset time intervals as 5, 10, 15, 20, 25, 30, 35 and 40 minutes. A port 0.45 m above the base was used for periodic

sampling. About 3ml of solution was drained from the port before withdrawing each sample; samples were withdrawn slowly, to minimize entrainment of air bubbles.Between experiments, the column was cleaned using HNO_3, and then rinsed three times with double distilled water.

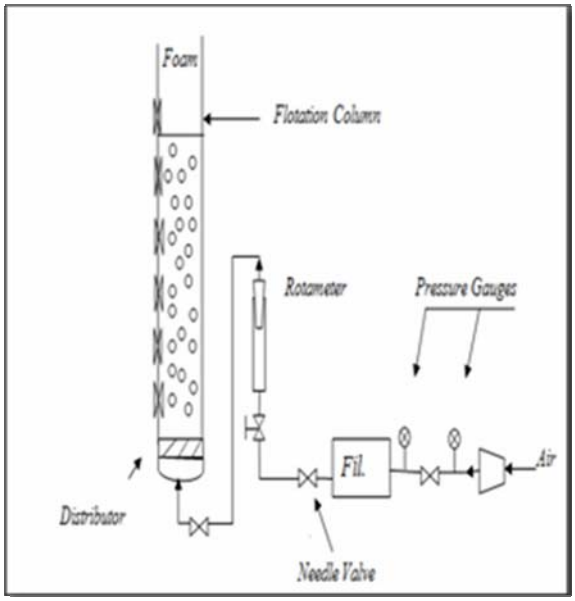

Figure (1): Schematic diagram of experiment system.

3. Results and Discussion

3.1 Effect of pH

The effect of pH on the recovery of copper by bubble column is shown in **Fig. (2)** by plotting the removal ratios versus time at various pH values .As shown in this figure the removal ratios decreases suddenly after approximately ten minute from the beginning of the run, then, these ratios began to decrease slowly with time. It was found that the highest removal achieved when the pH of the solution was 10. This results are in accordance with Polat and Erdogan (2007) that suggested that the charge of copper ion was positive Cu^{+2}, $CuOH^{+}$ at pH below 10 whereas they are negatively charged $Cu(OH)^{-3}$ and $Cu(OH)_4^{-2}$ at pH values greater than 10. At and around pH 10, precipitation of neutral $Cu(OH)_2$ takes place. The formation of the precipitation of $Cu(OH)_2$ can explain the higher recovery for pH values at and around 10.

3.2 Effect of surfactant type

The removal rate of copper from water was studied at two different types of surfactant (sodium dodecyl sulfate and Hexadecyltrimethyl ammonium bromide) in order to show the effect of adding anionic and cationic surfactant on the removal rate of copper ions. The effect is shown in **Fig. (3)** at the two surfactant types. From this figure, it can be seen that the anionic surfactant (SDS) is more efficient than the cationic surfactant (HTAB) and at pH lower than 10 no significant removal rate was obtained using (HTAB) and the removal rate increases for pH more than 10.

3.3 Effect of surfactant concentration

The effect of different sodium dodecyl sulfate (SDS) concentration in the copper removal was shown in **Fig. (4)**. It can be seen that there is no significant difference in removal rates with increasing SDS concentration from 25 mg/l to 75 mg/l. Further increasing in surfactant concentration results in decreasing in the copper removal .The decreasing in the copper removal for raised collector concentration can be due to competition between coligend-collector complex and free ion collectors for a place in the surface of the bubble (Medina et al., 2005).

3.4 Effect of initial copper concentration

The removal rate of copper at various initial copper concentrations is shown in **Fig. (5)** by plotting (C/C_0) rate versus time. From these figures, it was found that there is no significant difference in removal rate with increasing copper concentration from 100mg/l to 200mg/l. However at low copper concentration (25mg/l) the removal rate decreased because of large

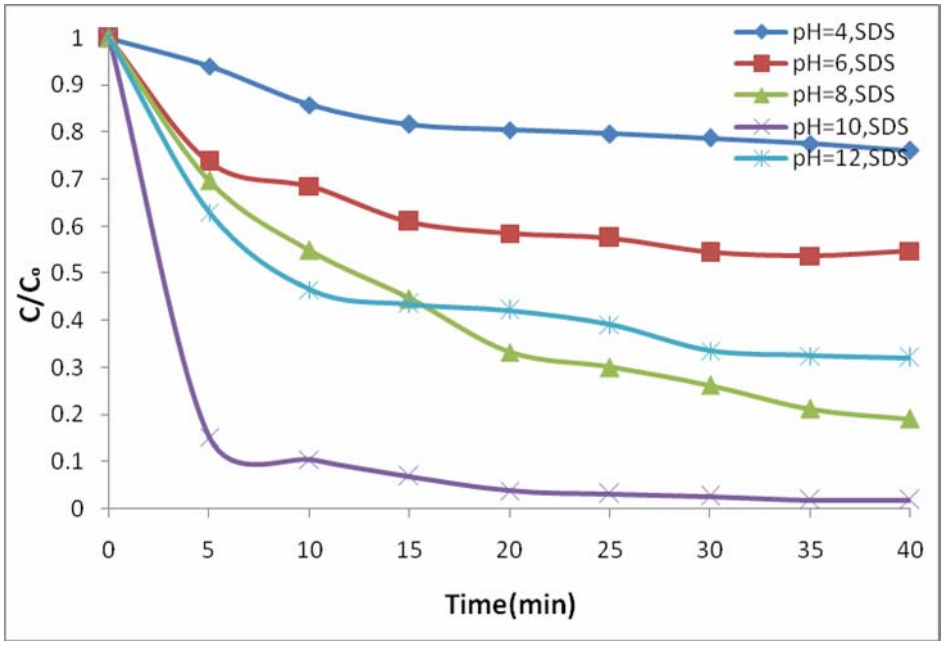

Figure 2. Effect of pH on the removal ratio of copper ions (C_o=100mg/l; SDS=75 mg/l; Q =250 ml/min; ethanol=1%, do=1mm).

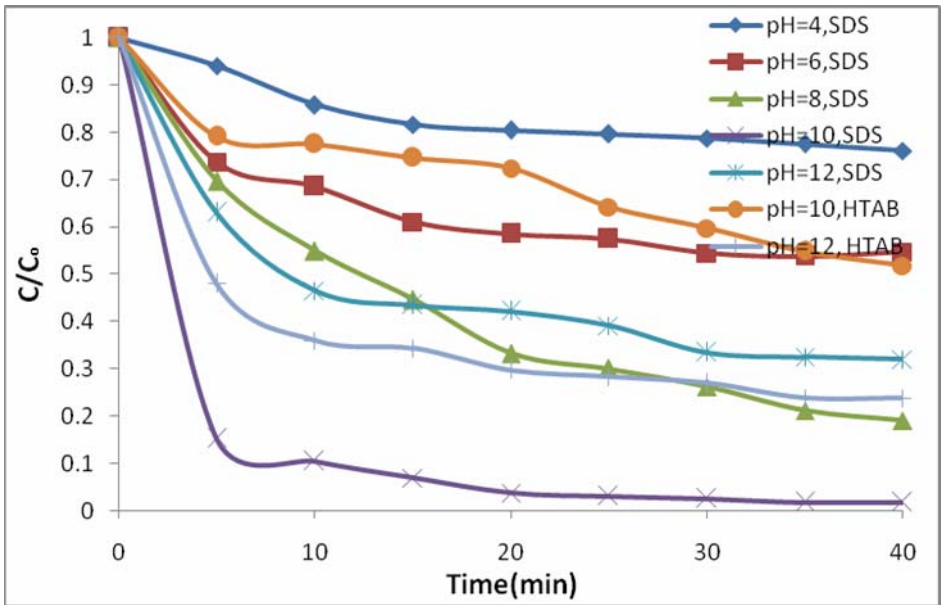

Figure 3. Effect of surfactant type on the removal ratio of copper (Co=100 mg/l; Q = 250 ml/min; SDS=75mg/l; HTAB=75mg/l; ethanol = 1 %, do =1 mm).

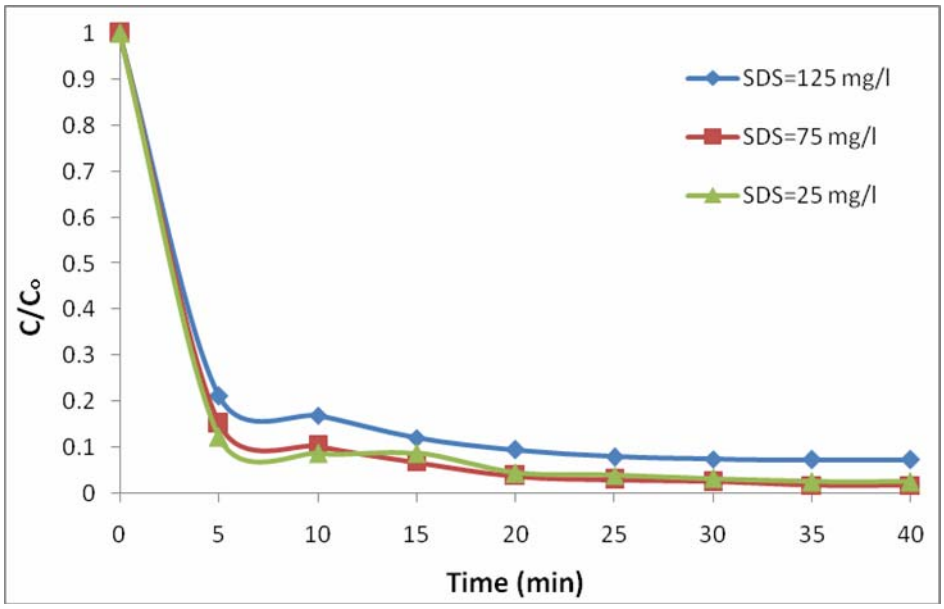

Figure 4. Effect of surfactant concentration on the removal rate of copper (pH=10; Co=100 mg/l; Q=250 ml/min; ethanol=1%; do=1mm).

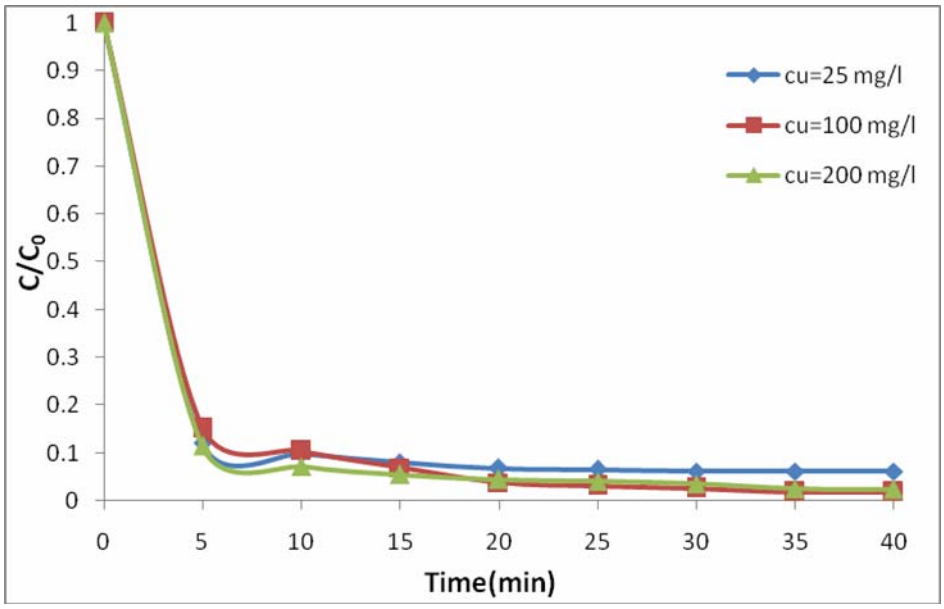

Figure 5 Effect of copper concentration on the removal rate (pH=10; SDS =75mg/l; Q =250 ml/min; Ethanol=1%, do=1mm).

Surfactant: copper ion ratio which cause competition, for bubble surface, between the metal–collector product and free collector ions (Shakir et al., 2010).

3.5 Effect of air flow rates

The effect of gas flow rate (100,250 and 500ml/min) on the removal efficiency of copper in the bubble column was investigated .The results are shown in **Fig. (6)**. The removal rate was highly affected by the gas flow rate. As gas flow rate increased, the removal ratio increased, This is because increased gas flow rate causes early bubble detachment, large fluid activities (stress)at the bottom section and bubble coalescence and (mostly) break up (Sulaymon and Mohammed, 2010).This results in a large number of small bubbles which leads to increasing surface area available for adsorption metal-collector.

3.6 Effect of frothers

The effect of adding ethanol to the copper ions removal is shown in **Fig. (7)**. The figure show that adding ethanol leads to increase removal rate of copper ions and at higher ethanol concentration the efficiency decreased. Increasing the removal efficiency with increasing in ethanol concentration in the solution is presumably attributed to decrease of degree of coalescence of gas bubbles leading to formation of more fine bubbles (Cho and Laskowski, 2002). Consequently, the surface area of the gas phase increases leading to improvement in flotation efficiency. However, an increase in ethanol concentration over a certain value results in reduction in the removal efficiency. This reduction in removal is attributed to that on elevation of frother concentration over a particular concentration (the critical coalescence concentration) the bubble size becomes no longer controlled by coalescence but will strongly depend on the sparger geometry and hydrodynamic conditions (Shakir et al.,2010). Also at the higher ethanol concentrations, the number of sites on the interface liquid-gas available for metal- collector complex adsorption will be reduced due to adsorption of alcohol molecules, which may lower metal removal (Medina et al., 2005).

3.7 Effect of ionic strength

The effect of adding NaCl to the copper ions removal was shown in **Fig. (8)** .It can be seen that the removal rate decreases with increasing NaCl concentration. The explanation of this improvement is that Na ions compete with copper ions so the metal ions cannot find enough dodecyl sulfate molecules to attach to (Choi et al., 1998).

4. Flotation kinetics

Flotation kinetics studies the variation of floated concentration according to flotation time.
Chemical kinetics principles are used in the modeling of flotation processes, particularly in the formulation of the basic rate eq.(1):

$$\frac{dc}{dt} = -kc^n \qquad (1)$$

where, (C) is the residual concentration of chromium at time t, (t) is the flotation time,(n) is the order of the flotation process, and k is the flotation rate constant, C_o is the initial concentration of copper . The results suggest that the process of copper(II) removal by precipitate flotation follows kinetics of first order being represented by equation(1): The integration of Eq. (1) gives:

$$\ln\left(\frac{C}{Co}\right) = kt \qquad (3)$$

The values for $\ln(C/C_o)$ plotted against flotation time gives a straight line with a slope equal to 0.092 and n equal to 0.944.

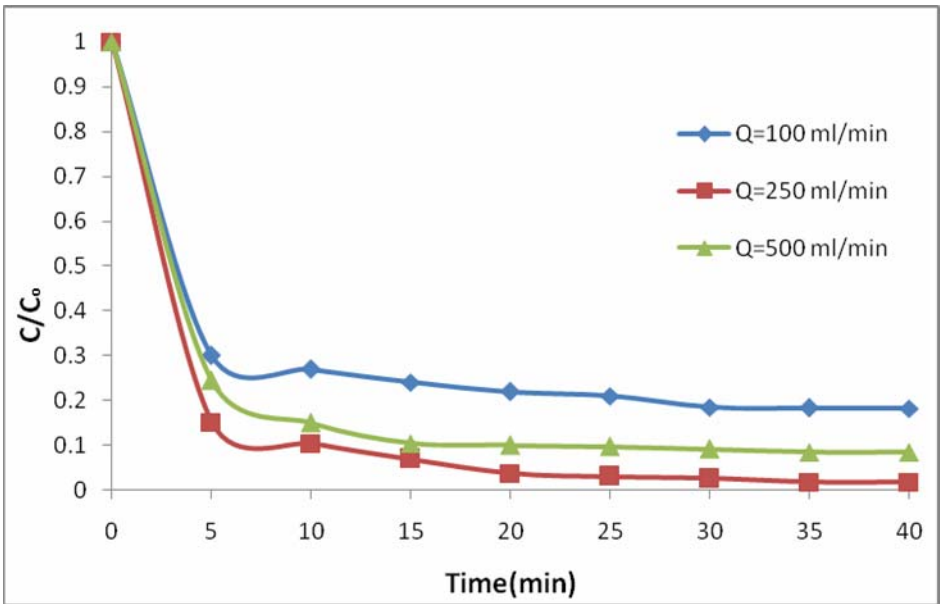

Figure 6. Effect of gas flow rate on the removal rate of copper (pH=10; Co = 100 mg / l; SDS=75 mg/l; ethanol=1%, do=1mm).

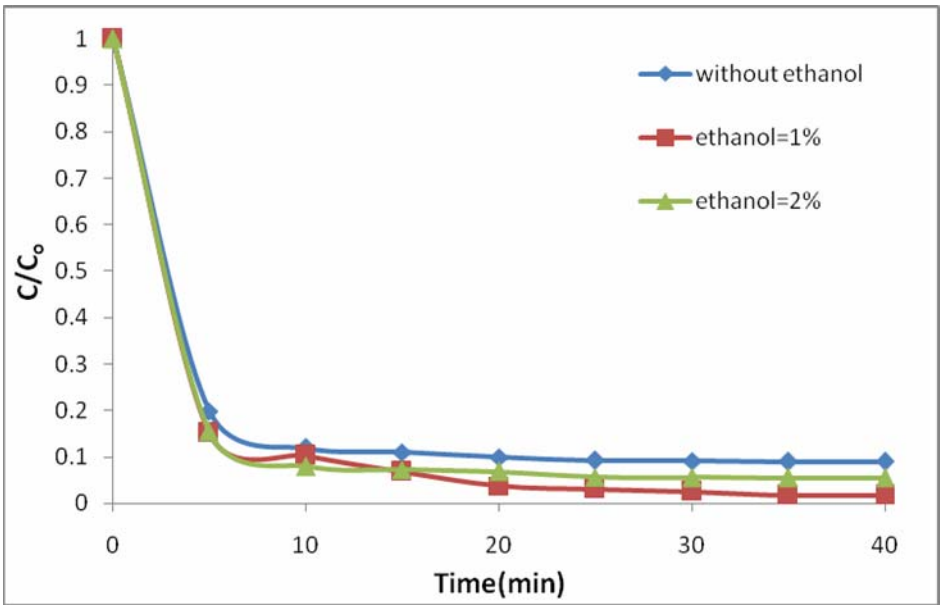

Figure 7. Effect of ethanol concentration on the removal rate of copper (pH=10; Co =100 mg/l; SDS=75 mg/l; Q =250 ml/min, d_o=1mm).

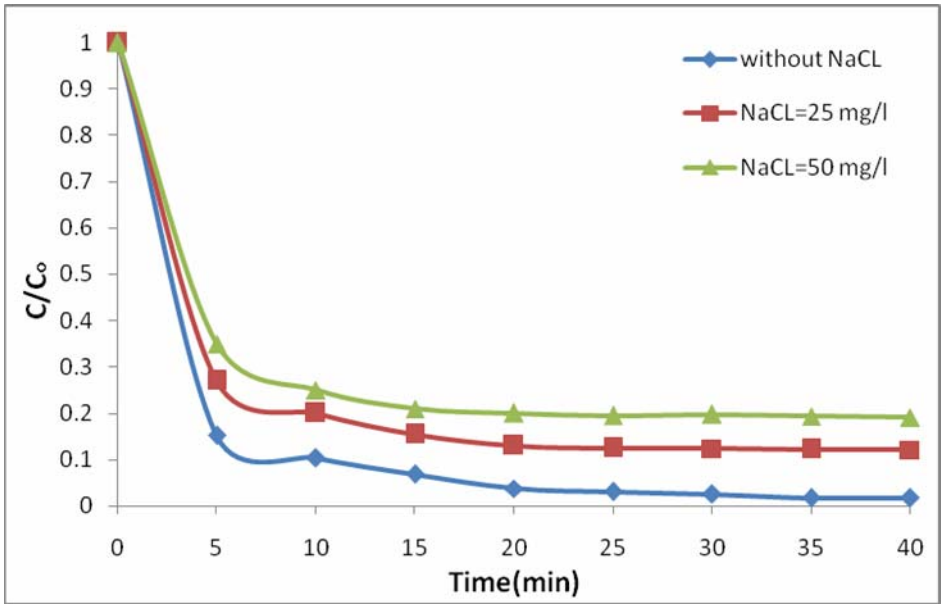

Figure 8. Effect of NaCl concentration on the removal rate of copper (pH=10; Co = 100 mg/l; SDS=75 mg/l; Q =250 ml/min; ethanol = 1 %, d_o=1mm).

References

Abryutin, D., and Strel, K., Investigation of regularities of ion flotation of copper with the use of sodium diethyldithiocarbamate, Russian Journal of Non-Ferrous Metals, 51, 85–88(2010).

Cho, Y.S., and Laskowski, J.S., Effect of flotation frothers on bubble size and foam stability, Int. J. Miner. Process, 64, 69-80 (2002).

Choi, S.J., and KIM, K.H., The improvement of the removal efficiency of foam flotation by synergistic effect of mixed surfactant solutions, Environment Technology, 19, 1151-1156(1998).

Doyle, M.F., Ion flotation—it is potential for hydrometallurgical operations, Int. J. Mineral Process, 72, 387–399(2003).

Eckenfelder, W., and Ford, D.L., Industrial water quality, 4th edition, McGraw-Hill, New York (2009).

Ghazy, S. E., El-moray, S. M., and Ragab, A. H., Ion flotation of copper (II) and lead (II) from environmental water samples, J. Appl. Sci. Environ. Manage. 12, 75 – 82(2008).

Lazaridis, N.K. , Peleka, E.N. , Karapantsios, T.D. ,and Matis, K.A. ,Copper removal from

effluents by various separation techniques, Hydrometallurgy,74 ,49–156(2004).

Liu, Z., and Doyle, M.F., A thermodynamic approach to ion flotation, Colloids Surf. , 178, 79–92(2001).

Liu, Z.,and Doyle, M.F.,Ion Flotation of Co^{+2}, Ni^{+2}, and Cu^{+2} using dodecyldiethylenetriamine (Ddien), Langmuir, 25, 8927–8934(2009).

Matis, K.A., and Zouboulis, A.I., Flotation techniques in water technology for metals recovery: the impact of speciation, Separation Science and Technology, 36, 3777–3800, (2001).

Medina, P., Torem, M., and Mesquita, L., on the kinetics of precipitate flotation of Cr III using sodium dodecylsulfate and ethanol, Minerals Engineering, 18 225–231(2005).

Polat, H., and Erdogan, D., Heavy metal removal from waste waters by ion flotation, Journal of Hazardous Materials, 148, 267–273(2007).

Sabti,H.,Brooks,R.R.,Stewart,R.B.and Hossain ,M., Adsorbing colloid flotation for removal of metal ions in waters from base metal mines, Environmental progress ,21, 63-69(2002).

Shakir, K., and Ahmed, F. , Removal of rhodamine (a basic dye) and thoron (An acidic dye) from dilute aqueous solutions and wastewater stimulants by ion flotation, Water Research, 44, 1449– 1461(2010).

Stoica, L., Oproiu, G.C., Cosmeleata, R. , and Dinculescu, M., Kinetics of Cu^{2+} separation by flotation, Sep. Sci. Technol., 38, 613–632 (2003).

Sulaymon, A., and Mohammed, A., Separation and hydrodynamic performance of air – kerosene-water system by bubble column, International journal of chemical reactor engineering, 8, 1-15 (2010).

Tchobanoglous, G., and Burton, F.L., and Stensel, D.H., Wastewater engineering treatment and reuse, McGraw-Hill Companies (2003).

Zhang, J., and Jing, Y., Removal of trace Cu^{2+} from aqueous solution by foam fractionation, Desalination, 249, 503–506 (2009).

PERFORMANCE CHARACTERISTICS OF METHANOL-DIESEL BLENDS IN CI ENGINES

Khalil Ibrahim Abaas
Assistant lecturer-Mechanical Engineering Dep.-University of Technology

ABSTRACT

Owing to the energy crisis and pollution problems of today, investigations have concentrated on decreasing fuel consumption and on lowering the concentration of toxic components in combustion products by using non-petroleum, renewable, sustainable and non-polluting fuels. While conventional energy sources such as natural gas, oil and coal are non-renewable, alcohol can be coupled to renewable and sustainable energy sources.

In this study, the combustion characteristics of diesel fuel and methanol blends were compared. The tests were performed at steady state conditions in a four-cylinder DI diesel engine at full load at 1500-rpm engine speed. The experimental results showed that diesel methanol blends provided 12.7% increase in brake-specific fuel consumption due to its lower heating value. The results indicated that methanol may be blended with diesel fuel to be used without any modification on the engine.

مواصفات أداء خلائط ديزل- ميثانول في محركات الاشتعال بالانضغاط

خليل إبراهيم عباس
مدرس مساعد- قسم هندسة المكائن والمعدات- الجامعة التكنولوجية

الخلاصة

أهتمت الأبحاث العلمية الحديثة بتقليل استهلاك الوقود وتقليل الملوثات السامة الناتجة من الاحتراق، بسبب الأزمة العالمية الخاصة بالطاقة ومشاكل التلوث، وذلك باستخدام أنواع من الوقود المتجدد، المتوفر وغير مسبب للتلوث، ويمكن اعتبار الكحول مصدر طاقة متجددة ومتوفرة، بينما أنواع الوقود التقليدي مثل الغاز الطبيعي، النفط والفحم غير متجددة.

في هذة الدراسة، تمت مقارنة مواصفات أداء وقود ديزل وخلائط من الديزل-الميثانول، وأجريت التجارب باستخدام محرك رباعي الاسطوانات ذي حقن مباشروعند حمل كلي وسرعة 1500 rpm، وبينت النتائج أن خلائط الديزل-الميثانول تسبب ارتفاع في استهلاك الوقود النوعي المكبحي بحدود 12.7 %، بسبب انخفاض القيمة الحرارية له، وبينت النتائج أن الميثانول يمكن استخدامه باضافتة الى وقود الديزل بدون عمل أي تحويرات في المحرك.

KEY WORDS

Methanol, diesel, equivalence ratio, engine speed, brake power, specific fuel consumption, indicated thermal efficiency, exhuast gas temperature.

INTRODUCTION

The higher efficiency of compression ignition direct injection diesel engines compared to spark ignited gasoline engines makes them desirable for automotive and truck vehicles, especially now with ever increasing crude oil prices, driven mainly by significant increases in demand (Bertoii, 1997).

As for the fuels in diesel engines, research has been conducted to identify the effects of fuel properties on diesel combustion and exhaust emissions. For example, sulfur content in fuels has been reduced in order to improve the acid rain problem and its reduction to 0.05 wt-% has been set as regulations to reduce particulate levels (Huang, 2003). Other fuel properties related to the improvement include aromatic content, ignitability, oxygen content, and viscosity and distillation temperature (Akasaka, 1996). As for oxygen content or oxygenates, the addition of lower alcohols such as methanol and ethanol to diesel fuel was effective in reducing particulate emissions without sacrificing other emission components (Nabil, 2006).

Practically, adding some oxygenated compounds to fuels to reduce engine emissions without engine modification seems to be a more attractive proposition. Methanol is regarded as one of the promising alternative fuels or oxygen additives for diesel engines with its advantages of low price and high oxygen content. However, due to the difficulty in forming a stabilized diesel/methanol blend, few reports found on this topic, and previous work was mainly concentrated on the application of diesel/ethanol blends in a compression ignition engine (Huang, 2004 & Fleisch, 1995). Therefore, much work is needed in the application of diesel/methanol blends in compression-ignition engine for clarifying the basic combustion and emission characteristics and providing an approach for attaining a stabilized diesel/methanol blend with some solvent, and the study could be expected to supply more information on engine combustion when operating on oxygenated fuels and provide more practical measures for the improvement of combustion and reduction of emissions (Huang, 2005).

However, there were problems as the methanol has inherently poor solubility to diesel fuel and poor lubricity, and its lower ignitability made it impossible to use neat alcohols or high blending ratios in conventional diesel fuel without special measures to improve ignition (Huang, 1999).

Methanol is also known as methyl alcohol and its chemical formula is CH_3OH. Commercially, methanol is most commonly produced by steam reforming of natural gas. In this process, the natural gas is first transformed into CO and hydrogen. Methanol is then produced by combining the CO and hydrogen under high temperature and pressure in the presence of special catalysts. Methanol was once made from the destructive distillation of wood (hence it's other common name, “wood alcohol”), but this process is no longer economically viable (Shi, 2005).

Methanol is poisonous and prolonged exposure to vapors and wetting of the skin are to be avoided. Methanol is more corrosive than gasoline and requires that minor changes be made in gasoline fuel system materials to be compatible (McCormic, 2000). Methanol was the alternative fuel that first received attention and serious funding from state agencies and engine manufacturers. The results of several demonstrations have been documented in a number of interim and final reports Issues related to transit vehicle characteristics that are often considered for methanol transit bus operation include performance and acceleration, vehicle range, vehicle weight limits, compatibility of fuel system materials with methanol, and travel through tunnels (Tsolakis, 2007 & Kajitani, 1997).

Because methanol is corrosive to some metals and damaging to rubber and some plastics, fuel storage tanks and dispensing

equipment must be corrosion and damage resistant. These include the fuel tank, fuel lines, fuel injectors, fuel pumps, and filters. Also, because methanol is water soluble, it could be quickly diluted in large bodies of water to levels that are safe for organisms. Environmental recovery rates for methanol spills are often faster than for petroleum spills (Kapus, 1995).

Instead of the octane number, the cetane number is the key parameter for a diesel fuel. For a conventional diesel fuel, the cetane number is around 40-55. Fuels with high cetane numbers result in smoother engine operation and reduced emissions of NOx, particulate matter, hydrocarbons, and CO. Cetane numbers of 15 to18 for ethanol and methanol, is considered very low cetane numbers. In addition to the cetane number, flash point and pour point temperatures are also important parameters for a diesel fuel (Hu, 2008). Even though some cetane improving additives are capable of reducing NOx level, the amount of reduction is reported to be inadequate. Moreover, most of the additives are expensive and can promote auto-oxidation in biodiesel (Miyamoto, 1998).

The volumetric energy density of the fuel is an important parameter since it directly affects the size of the fuel storage system of tile vehicle. Unfortunately, all of the alternative fuels are less energy dense per volume compared to gasoline or diesel (Table 1). It is noticed that diesel fuel is the only fuel better than gasoline, which accounts for 12 per cent of the higher fuel economy (mpg) associated with the disel-powered vehicle (Jacobs, 2003).

Liquid fuels have a better volumetric energy density than gaseous fuels. They also are the most compatible fuels with existing distribution systems and engines. i.e. they require the least departure from the technologies in place today both the vehicle and the refueling infrastructure (Puhan, 2009).

Since methanol is not only corrosive but also insufficient in lubricating ability (Wang, 2008), elemental research has been needed to so1ve these issues. However, elemental research can be explained at another opportunity and this paper describes the operating performance of a methanol diesel engine without touching elemental research.

The objectives of this study was to form the oxygenated blends by adding methanol and solvent in diesel fuel and then study the performance characteristics in a compression ignition engine fueled with the oxygenated blends.

EXPERIMENTAL SETUP

Experimental apparatus of engine under study is DI, water cooled four cylinders, in-line, natural aspirated FIAT diesel engine whose major specifications are shown in Table 1. The engine was coupled to a hydraulic dynamometer through which load was applied by increasing the torque. The cylinder pressure was obtained by a Kistler piezoelectric sensor type 6125A, the output of the pressure transducer was amplified by a Kistler charge amplifier type 5015A, and then converted to digital signals and recorded by a data acquisition apparatus (Yokogawa: GP-IB), which was used to calculate the rate of heat release and analyze the combustion characteristics. **Fig.1** represents photo of the used engine.

Three kinds of diesel/methanol blends with different methanol additions were selected for the study. Due to the low solubility of the methanol in diesel fuel, a solvent consisting of oleic and iso-butanol was added into the diesel/methanol blends to develop the stabilized diesel/ methanol blends. Fuel properties and the constitutions of three blends are given in **Tables 2, 3** and **Fig. 2**, and the oxygen fraction in the fuel blends ranged from 5.87 to 11.1 as shown in **Table 3** and **Fig. 3**. It can be seen that the oxygen in the fuel blends come mainly from methanol addition although the mass fraction of methanol and solvent has the same level, so it is reasonable to regard the influence of oxygen in the fuel blends to be the influence of oxygen from the addition of methanol. The solvent was added to methanol in the exact wanted ratefirst. Then the mixture was added

to diesel fuel to perform the combustible mixture.

The following equations were used in calculating engine performance parameters:

1- Brake power

$$bp = \frac{2\pi * N * T}{60 * 1000} \quad kW$$

2- Brake mean effective pressure

$$bmep = bp \times \frac{2 * 60}{V_{sn} * N} \quad kN/m^2$$

3- Fuel mass flow rate

$$\dot{m}_f = \frac{v_f \times 10^{-6}}{1000} \times \frac{\rho_f}{time} \quad kg/sec$$

4- Air mass flow rate

$$\dot{m}_{a.act.} = \frac{12\sqrt{h_o * 0.85}}{3600} \times \rho_{air} \quad \frac{kg}{sec}$$

$$\dot{m}_{a,theo} = V_{s.n} \times \frac{N}{60 * 2} \times \rho_{air} \quad \frac{kg}{sec}$$

5- Brake specific fuel consumpotion

$$bsfc = \frac{\dot{m}_f}{bp} \times 3600 \quad \frac{kg}{kW.hr}$$

6- Total fuel heat

$$Q_t = \dot{m}_f \times LCV \quad kW$$

7- Brake thermal efficiency

$$\eta_{bth.} = \frac{bp}{Q_t} \times 100 \quad \%$$

The fuel properties show that methanol has high oxygen content, while the heat value is low, and cetane number is low compared to diesel fuel. In the experiment, the above three fuel blends with different methanol proportions were operated on the engine; meanwhile combustion characteristics were measured and analyzed at the same brake mean effective pressure (bmep), and same injection timing (38˚BTDC). Furthermore, these parameters were compared with those of pure diesel combustion in order to clarify the effect of an oxygenated additive on combustion.

DISCUSSION

The BSFC is defined as the ratio of mass fuel consumption to the brake power. The percent variation in the BSFC with methanol–diesel fuel blends compared to diesel fuel is shown in **Fig. 4**. The obtained BSFC results for different diesel/methanol blends. Due to low energy content of the methanol, there is an increasing trend in BSFC with increasing methanol content in the fuel mixture compared to diesel fuel, at low and meduim loads.

Among the tested fuels the lowest BSFC values were obtained with diesel fuel because of low fuel consumption rate. The results showed that BSFC increases significantly when the engine is fueled with the blends having high methanol content due to lower heating value and density of methanol. As shown in **Fig. 4**, BSFC values increased with about 12.7% with M05 (5% methanol), about 15.1% increament with M10 (10% methanol), and increased 22.3% with M15 (15% methanol).

Volumatric efficiency improved with increasing methanol portion in the fuel mixture, due to OH ion in its structure, as **Fig. 5** shows. This efficiency reduced with

increasing load, due to injected fuel increament inside the combustion chamber.

Brake thermal efficiency (BTE) of an engine is the efficiency in which the chemical energy of a fuel is turned into useful work. Compared to diesel fuel, the changes in the BTE of the engine using methanol–diesel fuel blends are shown in **Fig. 6**. There are very slight decreases in BTE with the use of M5 and M10 compared to diesel fuel. In the test operations with the fuel blends, the engine yields relatively high BTE values for the blends up to 10%, which can be attributed to the promoted combustion due to the oxygen content of the blends.

(Irshad, 2001) stated that the fuel blends up to 10% do not cause a significant decrease in the energy content and cetane number of the fuel. In BTE, a noticeable decrease was observed in the case of M15, which results from the considerable increase in BSFC as seen in **Fig. 4**, the change in BTE relative to M0 is 6.2%, 9.3% and 23.4% for M5, M10 and M15, respectively, at constant injection timing.

Exhaust gas temperatures increased with load increase, and increased by increasing methanol percentage in the fuel mixture by 5.9% and 11.6% for M5 and M10 respectively, and reduced by 8.7% for M15 as **Fig. 7** repersents. Increasing load needs more fuel to be burned, and burning more fuel means more released heat and higher exhaust gas temperatures as a result. Increasing methanol portion in the blends M5 and M10 improve combustion charactristics, and increased the released heatby using excess oxygen in thecombustion chamber. The reduction accompanied with M15 was due to the reduction in the heating value of methanol which effect start to appear, the resulting was lower exhaust gas temperatures.

Engine speed effect on resulted brake power (bp) emplaced in **Fig. 8**, bp increased from low to meduim speeds and reduced at high speeds. Bp went down with methanol addition, M10 exhabited improvement compared to other blends, and the reduction in bp for this blend was very limitted. For the other blends the reduction was clear. The improvement when M10 was used due to volumatric efficiency amelioration, while the deterioration of bp with other blends was due to lower heating value effect which overcome the effect of better volumatric efficiency.

BSFC increased with increasing engine speed, as **Fig. 9** shows, as well as it increased with increasing methanol percentage in the blends. Increasing engine speeds means increasing injected fuel, which means BSFC increament, and as mintioned before, because of lower methanol heating value, BSFC increased with increasing methanol perentage in the blends.

Exhaust gas temperature increased with increasing engine speed and increased by using M5 and M10 and reduced for M15, as **Fig. 10** represents. Increasing engine speed needs more power which will be drawn from burning fuel, this cause more fuel to be burned and more resulted exhuast gas temperatures. These temperatures reduced with increasing methanol percentage to 15% depending on reduction of fuel total heating value, and the increaments with M5 and M10 were due to improvements in released energy because of increasing fuel oxygem content, which overcame the reduction in heating value.

CONCLUSION

Environmental protection is an important issue for the future of the world. Because of the reducing amount of petroleum reserves and its rising price, alternative fuels are intensively investigated for the full or partial replacement with diesel fuel. Therefore, in this study, the effect of methanol addition on the performance of a DI diesel engine has been experimentally investigated during the usage of methanol-blended diesel fuel. The tests were conducted at variable loads and at constant and variable engine speed. The following conclusions can be drawn from the present paper:

(1) When methanol-blended-diesel fuel was used, BSFC increased due to the lower energy content of methanol.
(2) All fuel blends yielded a decreased BTE in proportional to the methanol amount in the blend.

(3) Volumatric efficiency improved with methanol addition due to oxygen in its structure.
(4) Exhaust gas temperature increased for M5 and M10, and reduced with increasing methanol percentage to M15 in the blended fuel.
(5) M10 exhabited higher bp compared to other blends, approched nearly to diesel fuel.

REFERANCES

Akasaka Y, Sakurai Y, 1996. Effect of oxygenated fuel on exhaust emission from DI diesel engines. Transactions of JSME, Series B, vol. 63, No. 609, pp: 1833–1839.

Bertoii C, Giacomo N D, Beatrice C, 1997. Diesel combustion improvements by the use of oxygenated synthetic fuels. SAE Transactions vol. 106, No. 4, pp: 1557–1567.

Fleisch T, McCarthy C and Basu A, 1995. A new clean diesel technology: demonstration of ULEV emissions on a Navistar diesel engine fueled with dimethyl ether. SAE Transactions, vol. 104, No. 4, pp: 42– 53.

Hu Chen, Jianxin Wang, Shijin Shuai, Wenmiao Chen, 2008. Study of oxygenated biomass fuel blends on a diesel engine. Fuel, vol. 87, pp: 3462-3468.

Huang Z H, Wang H W and Chen H Y, 1999. Study on combustion characteristics of a compression ignition engine fuelled with dimethyl ether. Proceedings of the Institution of Mechanical Engineers, Part D, Journal of Automobile Engineering, vol. 213 (D6), pp: 647–652.

Huang Z H, Jiang D M, Zeng K, Liu B and Yang Z L, 2003. Combustion characteristics and heat release analysis of a DI compression ignition engine fuelled with diesel-dimethyl carbonate blends. Proceedings of the Institution of Mechanical Engineers, Part D, Journal of Automobile Engineering, vol. 217 (D7), pp: 595–605.

Huang Z, Hongbing Lu, Jiang D, Ke Zeng, Bing Liu, Zhang J and Wang X, 2004. Combustion behaviors of a compression-ignition engine fuelled with diesel/methanol blends under various fuel delivery advance angles, Bioresource Technology, vol.95, pp: 331–341.

Huang Z, Hongbing Lu, Jiang D, Ke Zeng, Bing Liu, Zhang J and Xibin Wang, 2005. Performance and Emissions of a Compression Ignition Engine Fueled with Diesel/Oxygenate Blends for Various Fuel Delivery Advance Angles, Energy & Fuels, vol. 19, pp: 403-410.

Irshad A, 2001. Oxygenated diesel: emissions and performance characteristics of methanol–diesel blends in CI engines. SAE Paper no. 2001-01-2475.

Jacobs T, Assanis d and Filipi Z, 2003. The impact of exhaust gas recirculation on performance and emission of a heavy-duty diesel engine. SAE paper no. 2003-01-1068.

Kajitani Z, Chen L, Konno M, 1997. Engine performance and exhaust characteristics of direct-injection diesel engine operated with DME. SAE Transactions, vol. 106, N0. 4, pp: 1568–1577.

Kapus P and Ofner H, 1995. Development of fuel injection equipment and combustion system for DI diesels operated on dimethyl ether. SAE Transactions, vol. 104, No. 4, pp: 54–69.

McCormic R L, Ross J D, Graboski M S, 2000. Effect of several oxygenates on regulated emissions from heavy-duty diesel engines. Environ Science Technology, vol. 34, pp: 933-939.

Miyamoto N, Ogawa H and Obata K, 1998. Improvements of diesel combustion and emissions by addition of oxygenated agents to diesel fuels: influence of properties of diesel fuels and kinds of oxygenated agents. JSAE Review, vol. 19, No. 2, pp: 154–156.

Nabil N & Chowdhury W, 2006. Iprovement of engine performance using diethelne glycol dimethyl ether (DGM) as additive, Jurnal Teknologi, vol. 44 (A), pp: 1–12, Universiti Teknologi Malaysia.

Puhan S, Jegan R, Balasubbramanian K and Nagarajan G, 2009. Effect of injection pressure on performance, emissions, and combustion characteristics of high linolenic linseed oil methyl ester in a DI diesel engine. Renew Energy; vol. 34, pp: 1227–33.

Shi X, Yu Y, He H, Shuai S, Wang J and Li R, 2005. Emission characteristics using methyl soyate-ethanol-diesel fuel blends on a diesel engine, Fuel, vol. 84, pp: 1543-1549.

Tsolakis A, Megaritis A, Wyszynski M L, Theinnoi K, 2007. Engine performance and emission of a diesel engine operating on diesel-RME (rapeseed methyl ester) blends with exhaust gas recirculation (EGR). Energy, vol. 32, pp: 2072- 2080.

Wang L J, Song R Z, Zou HB, Liu S H, Zhou L B, 2008. Study on combustion characteristics of a methanol–diesel fuel compression ignition engine. Proc Inst Mech Eng D – J Auto 2008; vol. 222, pp: 619–27.

NOMENCLATURE

TDC	top dead centre
BDC	bottom dead centre
BMEP	brake mean effictive pressure
BSFC	brake specific fuel consumption
BTE	brake thermal efficiency
$m^o_{a,\,act.}$	actual air mass flow rate
$m^o_{a,theo}$	theoratical air mass flow rate
Q_t	total fuel heat
LCV	lower calorific value

Fig.1, a photographic picture of the exprimintal rig.

Table 1, Tested engine specifications

Engine type	4cyl., 4-stroke
Engine model	TD 313 Diesel engine reg
Combustion type	DI, water cooled, natural aspirated
Displacement	3.666 L
Valve per cylinder	two
Bore	100 mm
Stroke	110 mm
Compression ratio	17
Fuel injection pump	Unit pump 26 mm diameter plunger
Fuel injection nozzle	Hole nozzle 10 nozzle holes Nozzle hole dia. (0.48mm) Spray angle= 160° Nozzle opening pressure=40 Mpa

Table 2, Fuel properties of diesel, methanol and blended fuel consititions

property	diesel	methanol	Solvent	
			Oleic	Iso-butanol
Chemical formula	$C_{10.8}H_{18.7}$	CH_3OH	$C_{18}H_{34}O_2$	$C_4H_{10}O$
Mole weight (g)	148.3	32	282	74
Density (g/cm^3)	0.86	0.796	0.8905	0.802
Lower heating value (MJ/kg)	44.40	19.68	38.65	33.14
Heat of evaporation (kJ/kg)	260	1110	200	580
Self-ignition temperature (^{o}C)	200-220	470	335	385
Cetane number	45	5	40	10
C wt%	86	37.5	76.6	64.8
Hwt%	14	12.5	12	13.5
O wt%	0	50	11.4	21.7
Blended fuel 1 wt%	79.86	8.96	10.1	1.08
Blended fuel 2 wt%	71.28	13.33	14.47	0.92
Blended fuel 3 wt%	63.94	17.66	16.6	1.8

Table 3, fuel properties of diesel/methanol blended fuel consititutions

Property	Blended fuel 1	Blended fuel 2	Blended fuel 3
Lower heating value (MJ/kg)	41.73	39.89	38.64
Heat of evaporation (kJ/kg)	333.53	367.57	405.94
Cetane number	40.41	38.4	36.21
C wt%	80.47	77.98	75.5
Hwt%	13.66	13.5	13.4
O wt%	5.87	8.52	11.1
O wt% contributed from methanol	4.48	6.67	8.83
O wt% conntributed from solvent	1.39	1.85	2.27

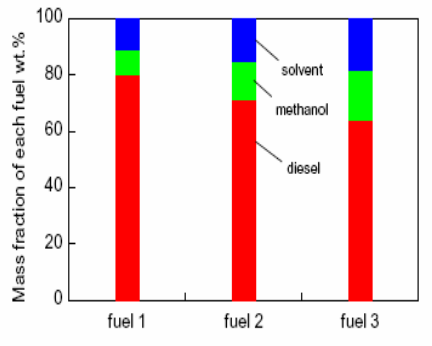

Fig 2, Consititution of the fuel blends.

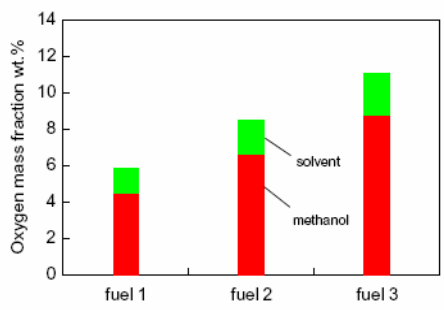

Fig 3, Oxygen mass fraction in the fuel blends

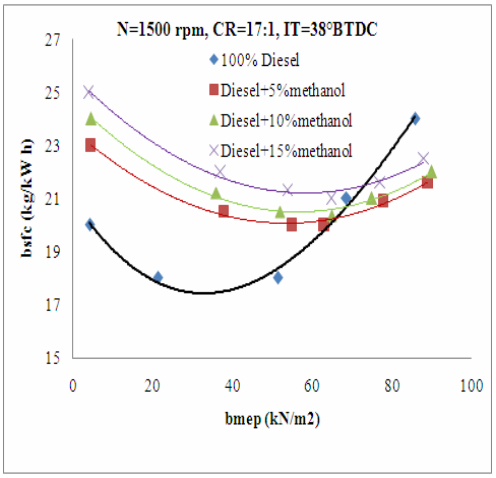

Fig 4, Methanol addition effect on BSFC for different bmep of the tested blends.

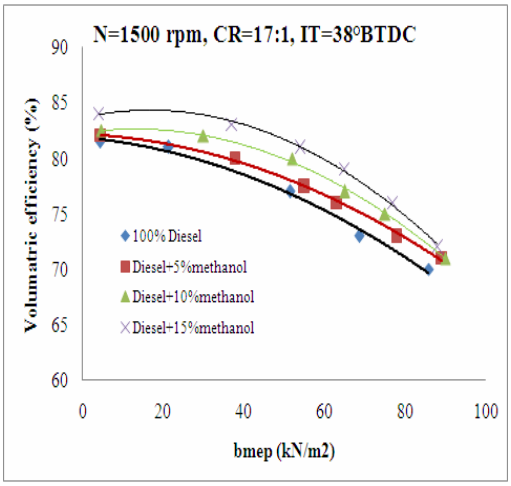

Fig 5, the effect of methanol addition on volumatric efficiency for different bmep

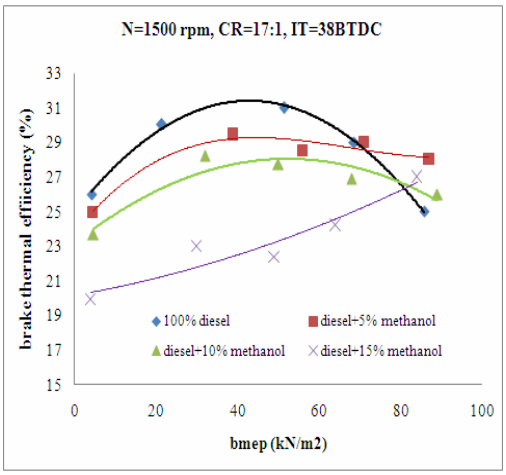

Fig 6, the effect of methanol addition on brake thermal efficiency for different bmep

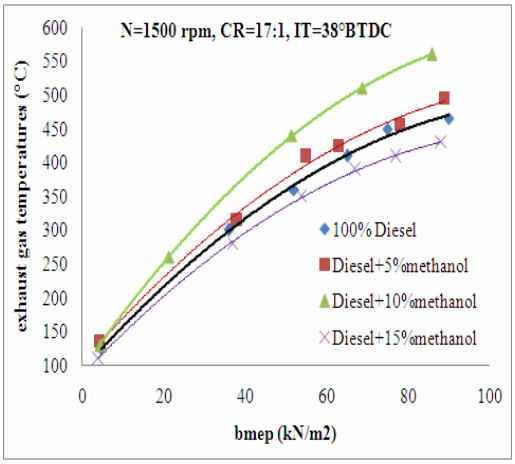

Fig 7, the effect of methanol addition on exhaust gas temperatures for different bmep

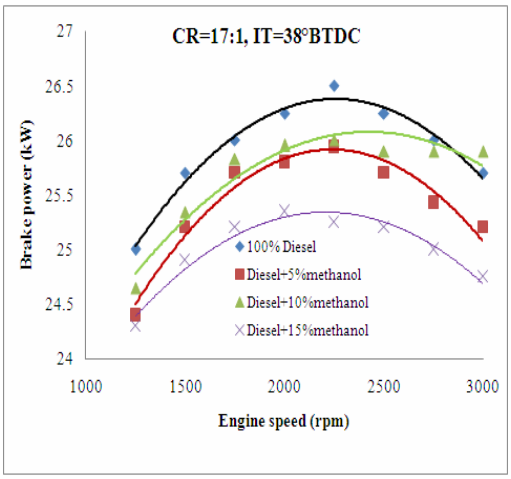

Fig 8, the effect of methanol addition on brake power for different engine speeds

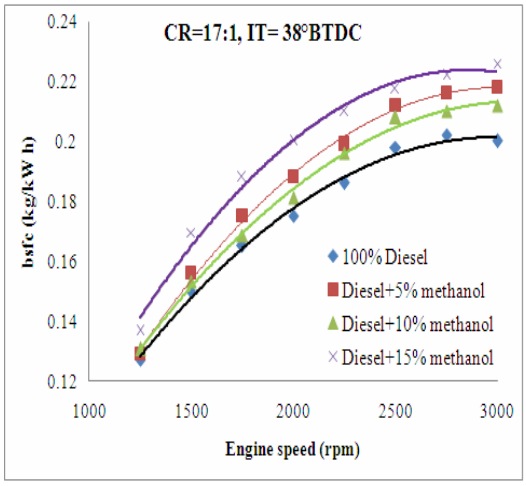

Fig 9, the effect of methanol addition on BSFC for different engine speeds

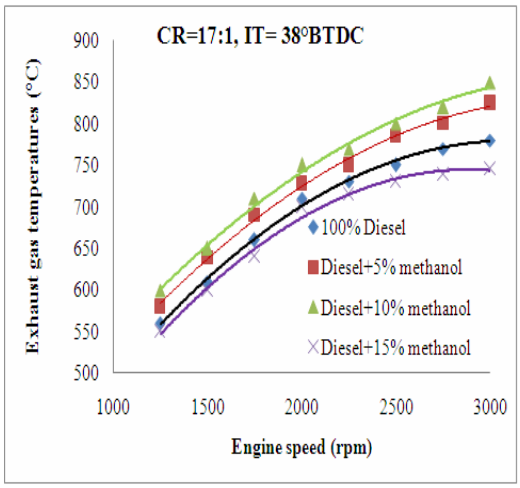

Fig 10, the effect of methanol addition on exhaust gas temperatures for different engine speeds

OPEN CIRCUIT HEAT EXCHANGER DYNAMICS DURING FLOW REDUCTION TRANSIENT IN THEIR SECONDARY LOOPS

Dr. Akram. W. Ezzat
Mechanical Engineering Department
University of Baghdad
Email: akramwahbi@yahoo.ie

ABSTRACT

An experimental and theoretical analysis was conducted for simulation of open circuit cross flow heat exchanger dynamics during flow reduction transient in their secondary loops. Finite difference mathematical model was prepared to cover the heat transfer mechanism between the hot water in the primary circuit and the cold water in the secondary circuit during transient course. This model takes under consideration the effect of water heat up in the secondary circuit due to step reduction of its flow on the physical and thermal properties linked to the parameters that are used for calculation of heat transfer coefficients on both sides of their tubes. Computer program was prepared for calculation purposes which cover all the variables that affect such type of transient mechanisms. The effect of the power density in the primary circuit and the water flow reduction percentage on the average temperature build up of the water in the primary circuit was investigated. The elapsed time required for the primary circuit average temperature to reach a steady state value was also calculated. These calculations were supported with experimental measurements conducted on a standard cross flow heat exchanger apparatus. The experimental results were compared with the theoretical results for certain power density value at different flow reduction percentages which show a reliable agreement. This relative agreement was necessary to consider the mathematical model with certain assurance for calculating transient parameters for higher power densities that are out of apparatus ranges. The results proved that water average temperature build up in the primary circuit has sharp tendency when the percentage of flow reduction in the secondary circuit reach 25% of its nominal values.

الخلاصة

تم أجراء تحليل عملي ونظري لمحاكاة ديناميكية المبادل الحراري من نوع الجريان المتقاطع أثناء الحالات غير المستقرة لنقصان جريان المبرد في دوراتها الثانوية. حيث تم أعداد موديل رياضي مبني على الفروقات المحددة لتغطية ميكانيكية عملية التبادل الحراري ما بين الماء الحار في الدورة الأساسية والماء البارد في الدورة الثانوية. أخذ الموديل بنظر الأعتبار تأثير زيادة تسخين الماء في الدورة الثانوية بسبب النقصان الدرجي لجريانه على الخصائص الفيزياوية والحرارية ذات العلاقة بالحدود المستخدمة في أحتساب معاملات التبادل الحراري على جانبي أنابيب المبادل الحراري. تم أعداد برنامج حسابي على الحاسوب الذي يغطي جميع العوامل المؤثرة لمثل هكذا نوع من ميكانيكية الحالات غير المستقرة.

تم بحث تأثير كثافة الطاقة في الدورة الأساسية والنسبة المئوية لنقصان معدل جريان المبرد في الدورة الثانوية على زيادة معدل درجة حرارة الماء في الدورة الأساسية. تم كذلك حساب الزمن المستغرق لوصول معدل درجة حرارة الماء في الدورة الأساسية الى قيم مستقرة. هذه الحسابات تم تدعيمها بقياسات عملية تم اجرائها على جهاز مختبري لمبادل حراري من نوع الجريان المتقاطع. تم أجراء مقارنة بين الحسابات العملية والنظرية لكثافة طاقة معينة لنسب أنخفاض في معدلات جريان مختلفة وكانت نتائج المقارنة مقبولة. هذا التطابق النسبي كان ضروريا لأعتماد الموديل والبرنامج الرياضي في أحتساب النتائج لقيم كثافات طاقة أعلى من حدود تحمل الجهاز. النتائج برهنت أن زيادة معدل درجة حرارة الماء في الدورة الأساسية تأخذ ميلا حادا عند وصول قيم النسب المئوية لأنخفاض معدل الجريان الى 25% من قيمها الطبيعية.

Keywords: open circuit heat exchanger, cross flow, flow reduction, transient

I NTRODUCTION

In process industries, heat is transferred by radiation, by the mixing of hot and cold fluids or most frequently, by conduction through the walls of heat exchanger.

For our purposes, the characteristic feature of these devices, heat exchangers, is that the capacities on one or both sides are distributed along the length of the exchanger.

Because the exchanger parameters are distributed and interacting the exact dynamic equations for an ordinary exchanger are quite complex, and lengthy calculations are required just to get the open -loop frequency response. In general, heat exchangers are fairly easy to control, and except where very close control is needed, simplified methods of dynamic analysis give answers that are accurate enough for the practicing engineer.

The approach taken here is to present exact transferred functions for a few of simpler cases in order to show the parameters that determine the lags and to explain the resonance effects sometimes found with distributed systems.

Types of Heat Exchangers

One type of heat exchanger is that of a double pipe arrangement with either counter or parallel flow and with either the hot or cold fluid occupying the annular space and the other fluid occupying the inside of the inner pipe type of them. Heat exchangers are widely used in the chemical process industries is that of the shell and tube arrangement.

One fluid flows in the inside of the tubes, while the other fluid is forced through the shell and over the outside of the tubes to insure that the shell side fluid will flow across the tubes and thus induce higher heat transfer, baffles are placed in the shell.

Cross flow heat exchangers are commonly used in air or gas heating and cooling applications where a gas may be forced across a tube bundle, while another fluid is used inside the tubes for heating or cooling purposes. In the relevant study the cross heat exchanger used water in both their primary and secondary circuits.

Loss of Heat Sink

Loss of heat sink occurs due to a decrease in heat removal by the secondary cooling system due to pump failure, blockage in piping or heat exchanger, valve failure or a break in the main pipe of the secondary cooling system.

Sequence of Events and System Operation

In case of pump failure due to loss of electrical power or pump over heat, the secondary pump failure relay will open without time delay and the heat source device is shut down automatically by proper protection system.

If this relay failed closed or in case of other causes to loss of heat sink, the primary coolant temperature would continue to rise, then the primary coolant temperature protection channel will shutdown the heat source device when its corresponding trip value is reached.

If the safety system related to the heat source device failed to shutdown the heat source, the operator can shutdown it manually when he realize that there is an abnormal condition in the system, i.e insufficient cooling, by monitoring the different signals and indications in the control room.

System Performance

During the transient of loss of heat sink the water temperature in the primary circuit will rises up until heat source device is shutdown, then these temperature starts to decrease after heat source device shutdown. The maximum increase in these temperatures above the normal operational values depends on the time lag between loss of reduction of flow in the secondary circuit and the heat source device shutdown.

The attempt of this study is to simulate the response of the primary circuit temperature build up according to the reduction or completely loss of secondary circuit flow during the failure of the safety systems to mitigate such type of transients. Such type of transients plays an important role in the evaluation of heat generation system safety and integrity specially those related to nuclear reactors in which self control is a dominant factor due to the effect of negative temperature factor on the reactivity of the reactor core.

Ezzat & Taki (1987) investigated in the final safety analysis report, FSAR related to the Iraqi research reactor IRT 5000 on 1987 loss of flow incidents on both primary and secondary circuits and their effect on the reactor safety

Gvozdenac (1992) applied Laplace Transform Method to solve the transient response of the counter flow heat exchanger with finite wall capacitance problem. The mathematical model is based on three local energy balance equations which are solved assuming that only the fluid 1 inlet condition is perturbed (step change). As any counter flow problem could be reduced to an adequate integral equation, collocation method is used for solving such equation in the presented case.

Housiadas (2000) investigated the course of loss-of-flow transients in pool-type research reactors, with scram disabled. The analysis is performed with a customized version of the code PARET. The focus was on determining the two-phase flow stability boundaries as function of initial reactor conditions, recognizing that flow instability is the basic mechanism responsible for core damage in such type of transients. A useful chart was provided, which describes the stability region in terms of initial reactor power, initial pool temperature, peaking factor, and flow-decay time constant.

Abdelfatah and Galanis (2000) Calculated the transient temperature field in a parallel flow heat exchanger numerically assuming fully developed hydrodynamic conditions. This approach uses fewer assumptions than published analytical studies. It shows the influence of physical and operational characteristics on experimentally defined parameters that describe the transient response of heat exchangers.

Srihari et al. (2004) focused on the effects of flow mal distribution and conventional heat exchanger parameters on the temperature transients of both U-type and Z-type configurations. It is found that the effect of flow mal distribution is significant and it deteriorates the thermal performance as well as the characteristic features of the dynamic response of the heat exchanger. In contrast to the previous studies, here the axial dispersion describes the in channel back mixing alone, not mal distribution, which is physically more appropriate. Present method is an efficient and consistent way of describing mal distribution and back mixing effects on the transient response of plate heat exchangers using an analytical method without performing intensive computation by complete numerical simulation.

Manish et al. (2005) Presented results of temperature response to step and ramp

change in flow rate of hot and cold fluids, and step, ramp, exponential and sinusoidal variation in hot fluid inlet temperature transient temperature response of cross flow heat exchangers having finite wall capacitance with both fluids unmixed is This investigation is conducted numerically for perturbations provided in both temperature and flow. Results are presented for step and ramp change in flow rate of hot and cold fluids, and step, ramp, exponential and sinusoidal variation in hot fluid inlet temperature.

Thirumarimurugan et al. (2008) presented the performance evaluation of cross flow plate fin heat exchanger with several different Gas-Liquid systems. Experimental results such as exchanger effectiveness, overall heat transfer coefficients were calculated for the flow systems of Cross flow Heat Exchangers. A steady state model for the outlet temperature of both the cold and hot fluid and overall heat transfer coefficient of a plate-fin cross flow heat exchanger was developed and simulated using MATLAB, which was verified with the experiments conducted.

THEORITECAL ANALYSIS

Determination of Heat Convection Coefficient between Water Flows and Tube Surfaces

Heat transfer coefficient for both inner surface and surface of tube bundles could be calculated using the following procedure. This procedure could be conducted for the inner surface and then repeated for the outer surface using the appropriate formula.

The formulas adopted for calculating heat transfer coefficient in our case are recommended by the supplier company for the type of the heat exchanger selected for experimental work, **PRODIT**.

1. Laminar Flow

As far as the laminar flow concerned, there are two zones where the flow is quite different with respect to the other one.

a. Entrance length whose length is given by the following:

$Li = (Re.Pr.d)/20$

Where we can use:

$Nu = 1.86.[Re.Pr.(d/L)]^{0.33} . (\mu/\mu_w)^{0.14}$

For $Re.Pr.(d/L) > 10$, $L/d>2$, $100<Re<2100$, $0.48<Pr<16700$

μ: The dynamic viscosity at average temperature.

μ_w: The dynamic viscosity at wall temperature.

b. The zone where the steady state is generated completely .Here as the convective flow is constant. We have:

$Nu = 3.66$ for constant wall temperature

$Nu = 4.53$ for constant heat flux.

2. Turbulent Flow

a. Entrance length whose length is given always by the previous formula where you can apply:

$Nu = 0.036\ Re^{0.8}.Pr^{0.33}.(d/L)^{0.125}$

With:

$10 < (L/d) < 400$, $Re > 10000$, $0.7 < Pr < 16700$.

b. The zone where steady state is generated completely. Here you can obtain the convective coefficient by:

$$Nu = 0.023\ Re^{0.8}.\ Pr^{0.4}\ [1+(d/L)^{0.7}]$$

$$H_{av.} = [(h_m\ .\ L_m) + (h_g + L_g) / (L_m + L_G)]\ .$$

For $10000 < Re < 120000$, $0.7 < pr < 120$, $(L/d) > 60$

Where
h_m = mouth zone coefficient convection, (W/m. C).

h_g= Steady state completely generated zone coefficient convection .

L_m= Mouth zone length.

L_G= Steady state completely generated zone length.

The thermal and physical properties of the water flowing in both primary and secondary circuits are obtained by interpolation among their values listed in specified tables.
Interpolation is conducted at mean water temperature between input and output values for each of primary and secondary circuits.

$$T_m = (T_{inlet} + T_{outlet})/ 2$$

Assumption Studied Case
We assume that the total mass of water in the primary circuit is (M). Then balance between the heat added to this amount of water by electrical heater and the heat rejected to the secondary circuit could be represented by the following equation:

$$Qi - Qc = M_{pr} * C_{pr} *.(dT_{pa}/dt) \quad (1)$$

$$Qc = U_o * A_o * (T_{pa} - T_{sa}) \quad (2)$$

$$T_{pa} = (T_{pi} + T_{po}) / 2 \quad (3)$$

$$T_{sa} = (T_{si} + T_{so}) / 2 \quad (4)$$

Where**:**
Ao: Heat transfer area between primary side and secondary side of the heat exchanger base on outer surface.
U_o: Overall heat transfer coefficient of the heat exchanger based on the outer surface.

$$U_o = 1 / [(1/h_i).(r_o/r_i) + [r_o.\ln(r_o/r_i)] / K_c + (1/h_o)] \quad (5)$$

Where:
h_i: Heat transfer coefficient between the tube wall and primary circuit water inside the tube.
h_o: heat transfer coefficient between the tube wall and the secondary circuit water outside the tube.
r_i & r_o: The inner and outer radius of the tube respectively.
K_c: Thermal conductivity of the copper tube.

According to the range of the experimental work the calculations in the secondary side is based on the laminar flow. Nusselt No. is calculated using following equation:

$$Nu_o = 1.86 * [Re_o*Pr_o*d_o/L]^{0.33} * (\mu_o / \mu wo)^{0.14} \quad (6)$$

$$Nu_o = 1.86 * [(\rho_o * d_o^2/\mu_o)^{.33} * (Pr_o/L)]^{0.33} * (V_s)^{0.33} * (\mu_o/\mu_{wo})^{0.14} \quad (7)$$

$$h_o = (K_o * Nu_o) / d_o \quad (8)$$

The range of experimental work ensures turbulent flow in the primary circuit of the heat exchanger. Nusselt No. is calculated according to the following equation:

$$Nu_i = 0.023 * (Re_i)^{0.8} * (Pr_i)^{0.4} * (1+d_i/L)^{0.7} \quad (9)$$

$$Nu_i = 0.023 * (\rho_i . d_i/\mu_i)^{0.8} * (Pr_i)^{0.4} * V_p^{0.8} * (1+d_i/L)^{0.7} \quad (10)$$

$$h_i = (K_i * Nu_i)/d_i \quad (11)$$

Here we assume the following:

1. The secondary circuit is open loop i.e. the inlet temperature of the water in the circuit is constant.
2. The heat source (power input) is constant during transient period and this source is continuous during the transient course of secondary flow reduction..
3. The average water temperature in the secondary side of the heat exchanger is calculated based on the temperature difference across the secondary side of the heat exchanger.

$$\Delta T_s = T_{so} - T_{si} = Qi / (m_s * C_s) \quad (12)$$

Where:
ms: mass flow rate of the water in the secondary circuit.
Cps: heat capacity of the water in the secondary circuit.

$$T_{sa} = (T_{si} + T_{so}) / 2 = T_{si} + \Delta T_s / 2$$

$$T_{sa} = T_{si} + (1/2 * Qi) / (m_s * C_s) \quad (13)$$

4. The heat exchanger selected for this calculation is the same that will be used in the test unit. The type of flow selected is parallel.

Using proper notifications for the multiple variables and after necessary substitutions the following set of equations were used to calculate the steady state and transient water average temperature in the primary circuit based on its steady state values:

$$d\theta_p(t)/dt * [C11*V_s(t)^{1.33} + C12*V_s(t)] = [C13*V_s(t)^{1.33} + C14*V_s(t)] - [C3*\theta_p(t)*V_s(t)^{1.33}] + [C9*V_s(t)^{1.33}] + [C10*V_s(t)^{0.33})] \quad (14)$$

For steady state case:
$d\theta_p(t) / dt = 0$

Then we can use equation (14) to find primary side average temperature, θ_{ps} as a function of steady state secondary side velocity, V_{ss}:

$$\theta_{ps} = \frac{C13*V_{ss}^{1.33} + C14*V_{ss} + C9*V_{ss}^{1.33} - C10*V_{ss}^{0.33}}{C3*V_{ss}^{1.33}} \quad (15)$$

Formulate equation (14) to finite difference equation:

$$\theta_p(i+1)=\theta_p(i)+\Delta t*[(C13*V_{si}^{1.33}+C14*V_{si}-C3*\theta_p(i)*V_{si}^{1.33}+C9*V_{si}^{1.33}+C10*V_{si}^{0.33}) / (C11*V_{si}^{1.33}+C12*V_{si})] \quad (16)$$

Where:
$\theta_p(i) = \theta_{ps}$ when i = 0

Suitable computer program was prepared for iterative calculations of the steady state and transient values of water average temperature in the primary and secondary circuits. The structure of the program allows easy interpolation among the values of the physical properties based on the values of water temperature in both circuits.
The empirical formulas adapted for the recent case study could be easily adapted for investigating cases that covers other type of heat exchangers.

EXPERIMENTAL APPROACH

System Description

The test rig consists of shell type cross flow heat exchanger. The hot water flows in shell side, primary side, while the cold water flows in tubes, secondary side. The secondary side consists of 4 tubes.
Thermal conductivity of the copper tubes, k=349 W/m. C. The outer radius of the tubes, ro=8 mm, the inner radius of the tubes, ri=7mm. The total heat exchange area Ah= 67380 mm. Shell diameter=50 mm. Heat exchanger length=355 mm.
Water flow in both primary and secondary sides are ensured by 2 circulating pumps, one in each side which ensures a maximum flow rate of 300l /hr. Each side consists of water flow meter for volumetric flow measurement. Water added and drained from both sides using proper isolation valves.
Water heating in the primary circuit is ensured by electrical heater that is adjusted by proper resistances from 0-800 Watt. Fig. (1) show the main components of the test rig.

Test Procedure

1. The heat exchanger package is connected to the water source. Both primary and secondary circuits are filled of water. Air is relieved from the circuits using the specified air relief valves fixed on both circuits. The primary circuit inlet and outlet pipes are isolated from the water source and drain using the specified valves, while the secondary circuit side is kept connected to the water source to ensure open circuit condition during transient course.
2. The circulation pumps of both circuits are put on to circulate the water inside the circuits. Water flow rates in both circuits are fixed at their operational values using the specified valves. The volumetric flow rate of the water in each circuit is monitored using the specified volumetric flow meters fixed in each circuit.
3. The electrical heaters are turned on to heat up the water in the primary circuit to its operational steady state values. The steady state heat input is controlled using the specified knobs.
4. After the water in the primary and the secondary circuits reach their steady state values, the water flow rate in the secondary circuit is reduced to 0.83 of its steady state value and water input and output temperate to the heat exchanger on both circuits are measured versus time using stop watch till they reach their steady state values.

5. Step no. 4 is repeated by reducing the water flow rate in the secondary circuit to 0.5 & 0.33 of its steady state value. Temperature buildup in both primary & secondary circuits is measured using the stop watch.

RESULTS AND DISCUSSION

All the results and graphs are based on constant water inlet temperature to the secondary circuit equals 25°C and constant water flow rate in the primary circuit equals 190 liter/ hr.

Fig. (2, 3 and 4) show the behavior of the water average temperature in the primary circuit versus time at different percentage of flow reduction in the secondary circuit and constant flow rate in the primary circuit. The graphs show reliable coincidence between the experimental and theoretical results. The negative slop of the plotted graphs within the first 60 seconds of the transient course is justified by the effect of flow turbulence in the secondary side of the heat exchanger accompanies the step decrease of the secondary flow which in turn enhance the heat transfer coefficient in that side and decrease the temperature difference for a short period.

Fig. (5) illustrate the relationship between the elapsed time required for the water temperature in the primary circuit to reach its steady state values after the end of the transient course versus the percentage of flow reduction in the secondary side of the heat exchanger. The graphs show reliable coincidence between the experimental and theoretical results. It is clear that the elapsed time is proportional to the percentage of flow reduction due to the increase of temperature differences between the steady state values of the water in the primary circuit before and after the transient courses.

Fig. (6) show theoretical relationship between average temperature build up of the water in the primary circuit during transient course normalized to its value when the flow reduction percentage is 0% versus the percentage of flow reduction in the secondary circuit. The results show sharp slop of such increase when the percentage of flow reduction reaches 25% of its nominal values.

Fig. (7) show theoretical relationship between the average temperature build up in the primary circuit during transient course normalized to its value at 0% percent flow reduction versus the specific power rate added to the water in the primary circuit at flow reduction percentage in the secondary circuit equals 33%.

CONCLUTIONS

Investigation of heat exchangers transient conditions during operation is very important in the design of safety engineering feature systems related to any power production or chemical process industries. According to this point of view the following were concluded from the research.

1. The results obtained from this study proved reliable modeling for such transients based on the coincidence between the results obtained from both experimental and theoretical analysis.
2. The analysis shows that the slop of temperature buildup in the primary circuit reaches critical values for flow reduction percentage in the secondary circuits above 25% of their nominal values.
3. The investigation and the mathematical modeling takes under consideration the effect of power adding rate to the primary circuit on the temperature build in this

circuit during flow reduction course in the secondary circuit which ensures coverage of this study for wider range of heat exchangers used in power plants.

4. From other hand this study gives an indication to the estimated mission time required for the operation of safety systems based on the elapsed time of each transient course to avoid the heat generation systems from approaching the boiling crisis accompanied by the poor heat transfer mechanisms.

REFERENCES

Abdelfatah Lahzazi and Nicolas Galanis, Thermal transients in parallel flow heat exchanger research, Faculté de genie, Université de Sherbrooke, 2000.

Christos Housiadas , Simulation of loss of flow transients in research reactors, Annals of Nuclear Energy, 27, 1683-1693, 2000.

EL-Wakel, M. M. , Nuclear Power Engineering, McGraw-Hill, New York, 1962.

Ezzat A. W. and Taki H. M., Final analysis report for IRT 5000 research nuclear reactor, 1987.

Gvozdenac D. D., Analytical solution for transient response of counter flow heat exchanger with finite wall capacitance**,** Institute of Thermal Energy and Process Engineering, University of Novi Sad, 21000 Novi Sad, Yugoslavia**,** 1992.

Manish Mishra, P.K. Das and Sunil Sarangi , Transient behavior of cross flow heat exchangers due to perturbations in flow and temperature, Department of Mechanical Engineering, Indian Institute of Technology, Kharagpur 721 302, India 2005.

M. Thirarimurugan, T. Kannadasan and E. Ramasamy, Simulation studies on a cross flow plate fin heat exchanger, American Journal of Applied Sciences 5 (10): 1318-1321, 2008.

N. Srihari, B. Prabhakara Rao, Bengt Sunden and Sarit K. Das, Transient response of plate heat exchangers considering effect of flow mal distribution, department of Mechanical Engineering, Indian Institute of Technology, 2004.

PRODIT, Heat exchangers test unit with water / water cross flow shell and tube heat exchanger exercise book, Reference 28301, Torinto, Italy.

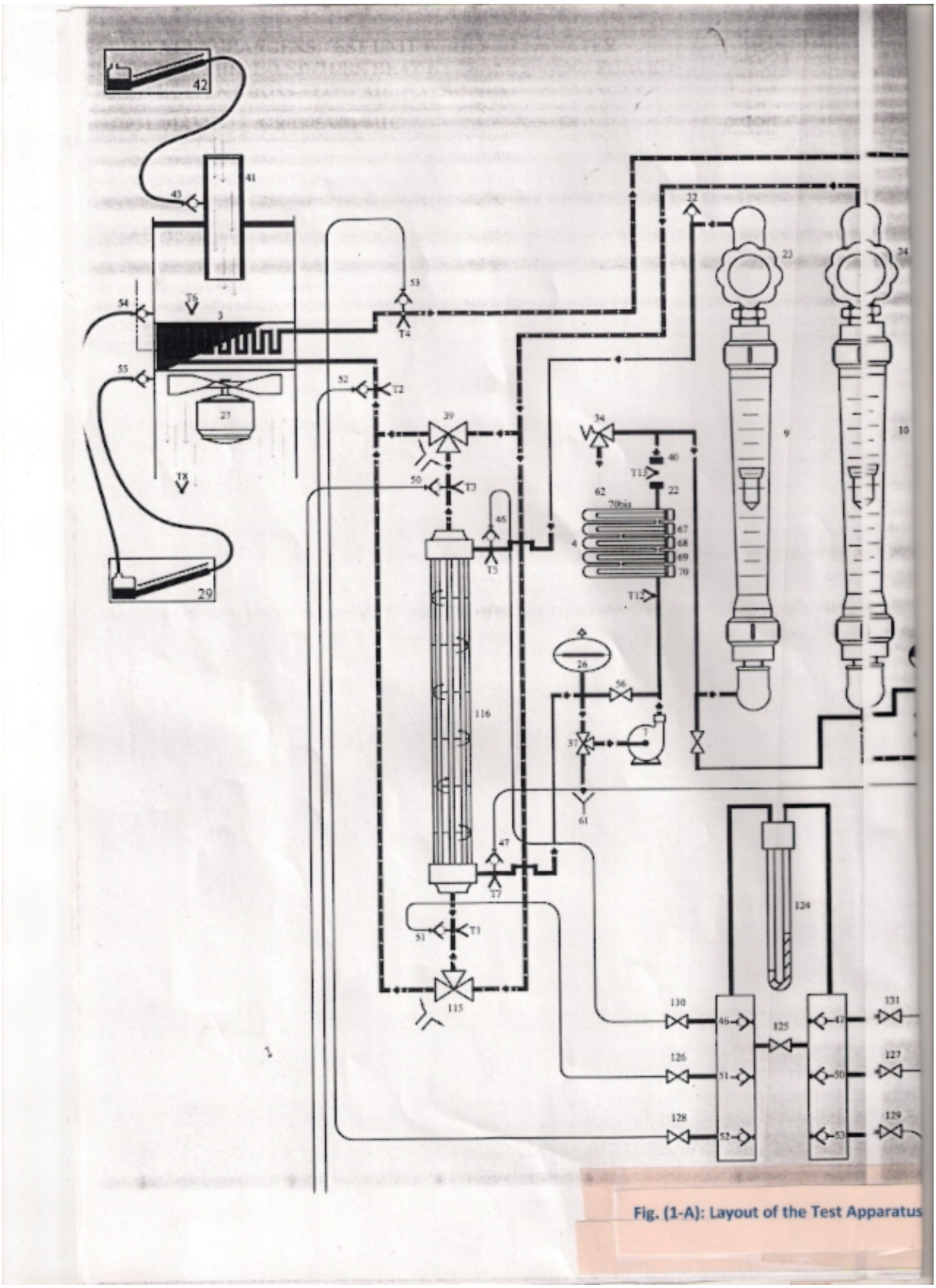

Fig. (1-A): Layout of the Test Apparatus

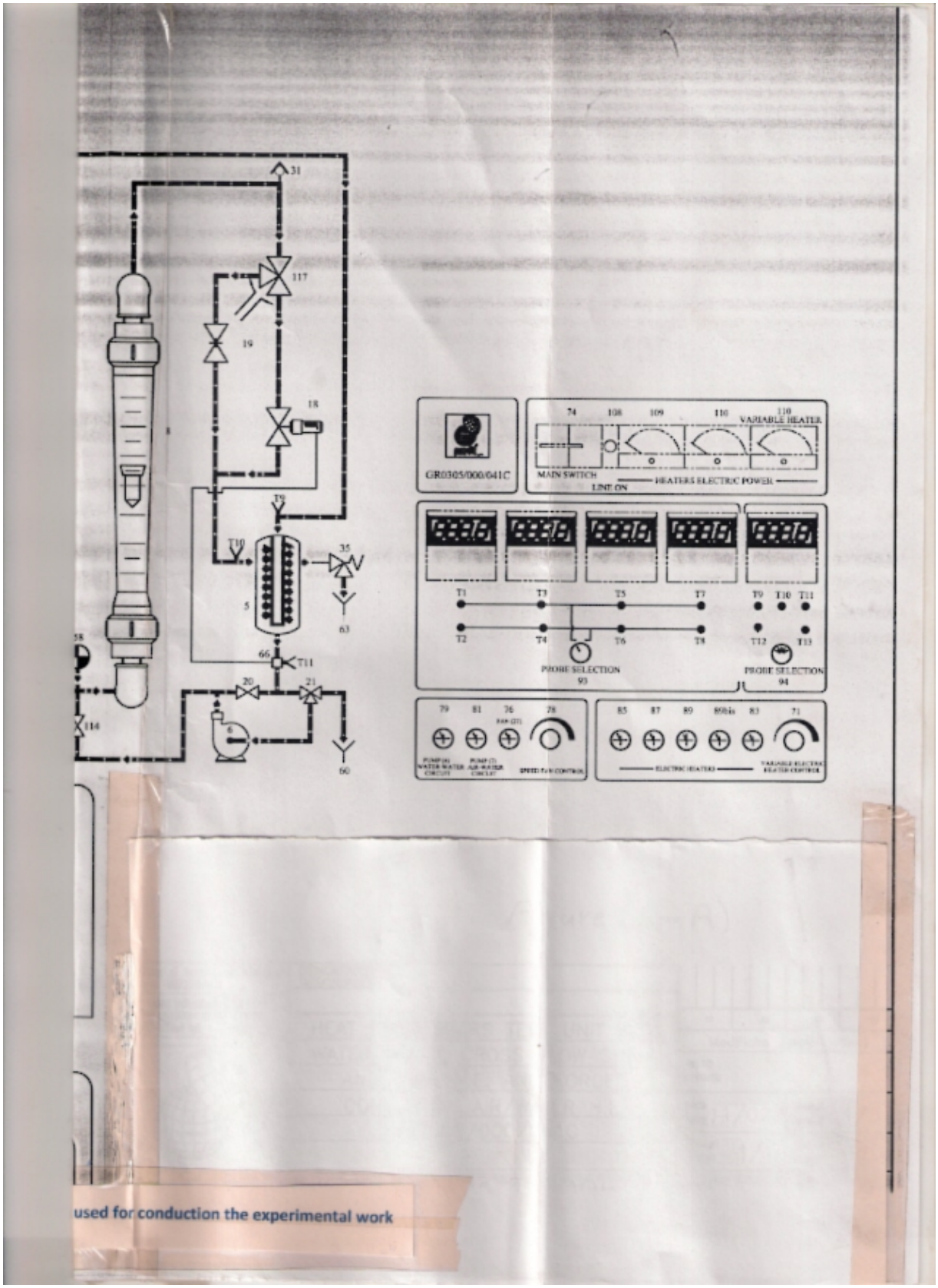

used for conduction the experimental work

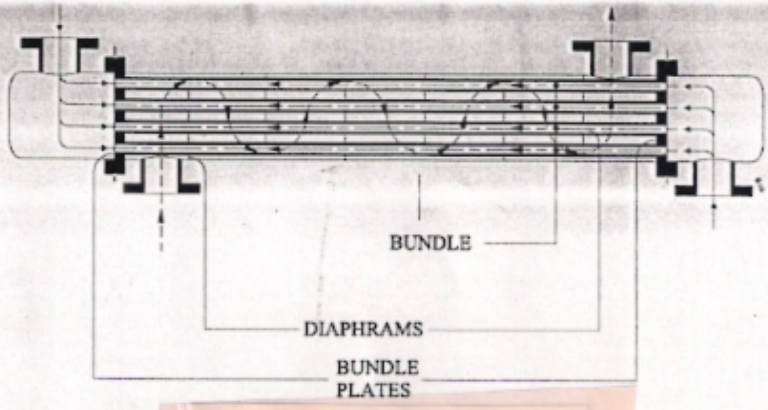

Fig. (1-B): Cross Flow Heat Exchanger

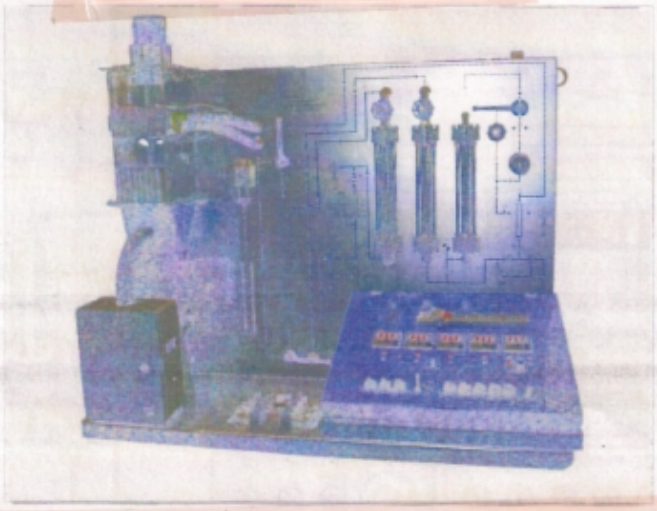

Fig. (1-C): Test Apparatus used for conduction the experimental work

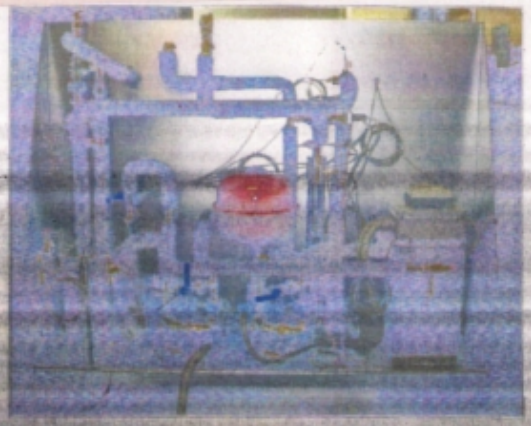

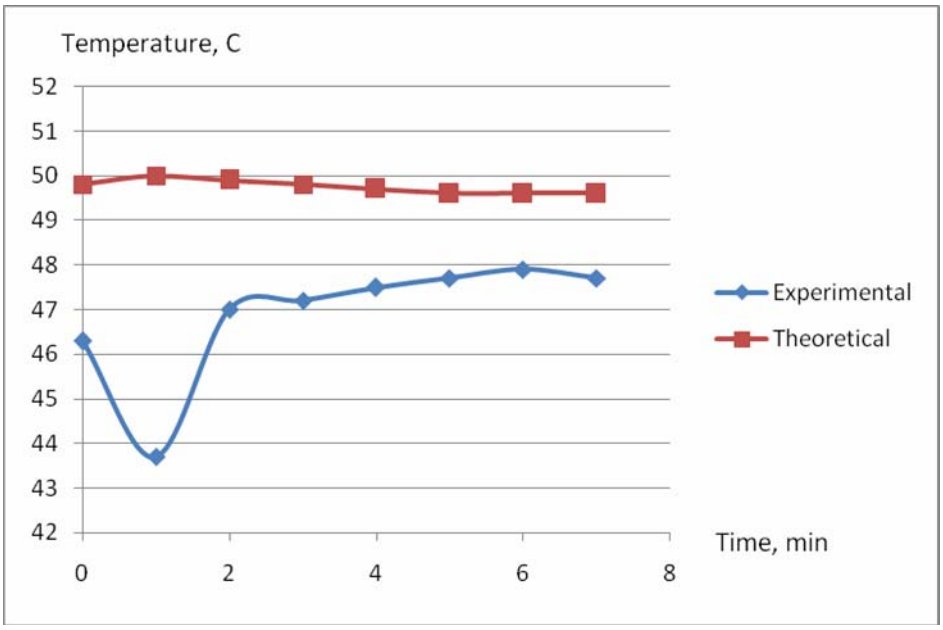

Fig. (2): Experimental & Theoretical average water temperature, T_{pa} buildup in the primary circuit of the heat exchanger versus time during secondary circuit flow reduction from (300 l/hr to 250 l/hr).

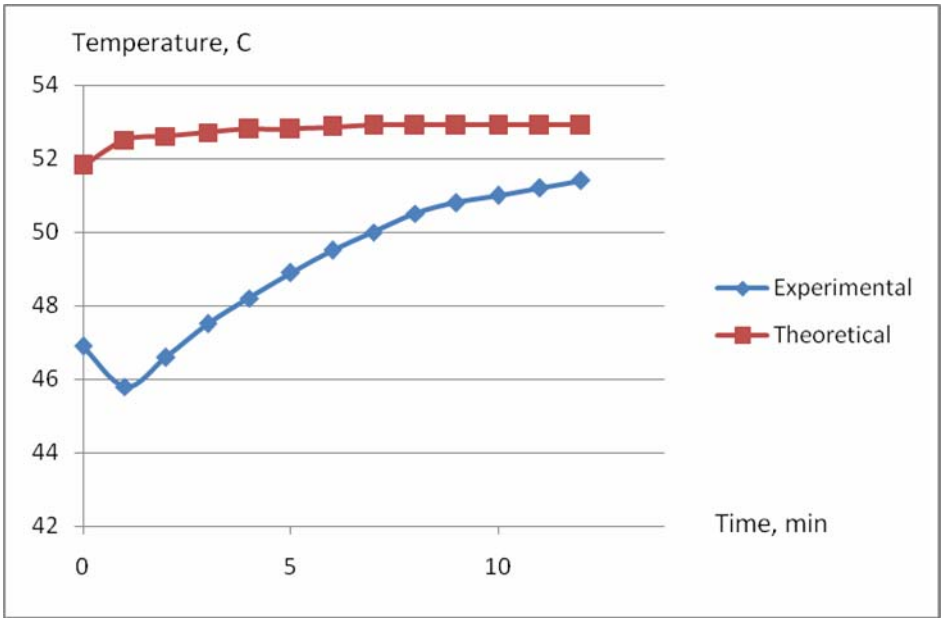

Fig. (3): Experimental & Theoretical average water temperature buildup, T_{pa} in the primary circuit of the heat exchanger versus time during secondary circuit flow reduction from (300 l/hr to 150 l/hr).

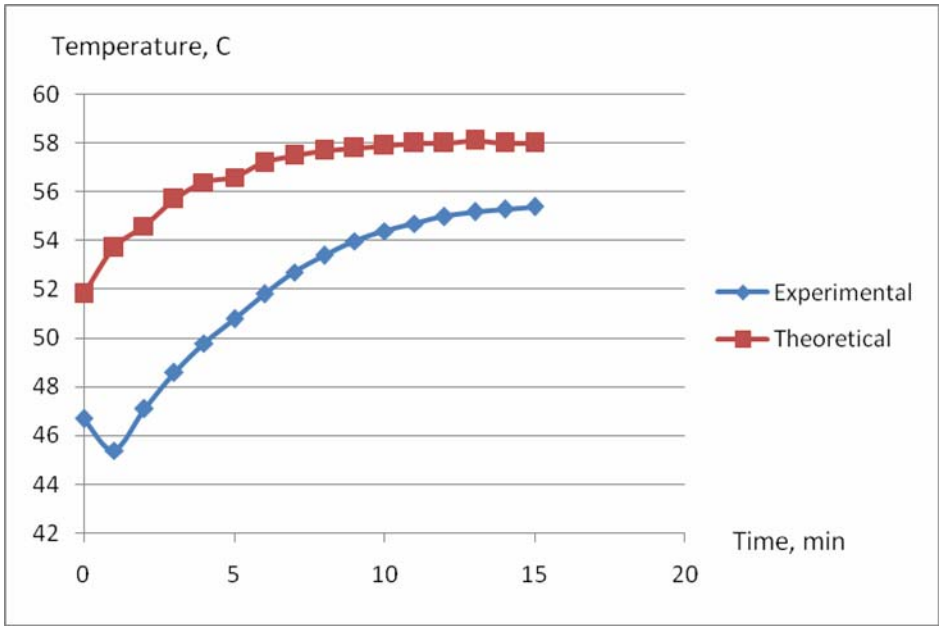

Fig. (4): Experimental & Theoretical average water temperature, T_{pa} buildup in the primary circuit of the heat exchanger versus time during secondary circuit flow reduction from (300 l/hr to 100 l/hr).

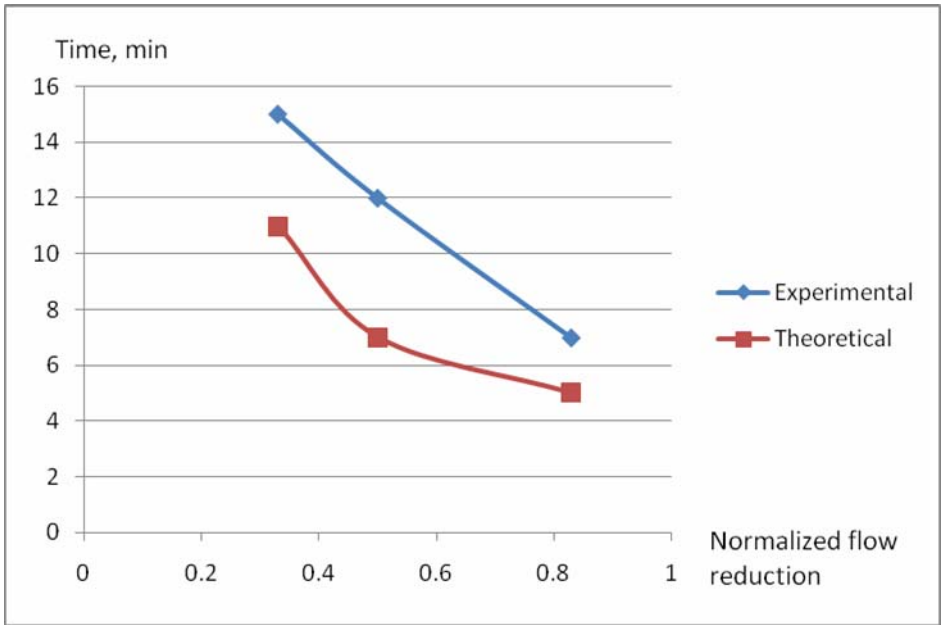

Fig. (5): Experimental & Theoretical results for the elapsed time required to settle the average water temperature in the primary circuit versus normalized flow reduction in the secondary circuit based on its steady state value (300 l/hr).

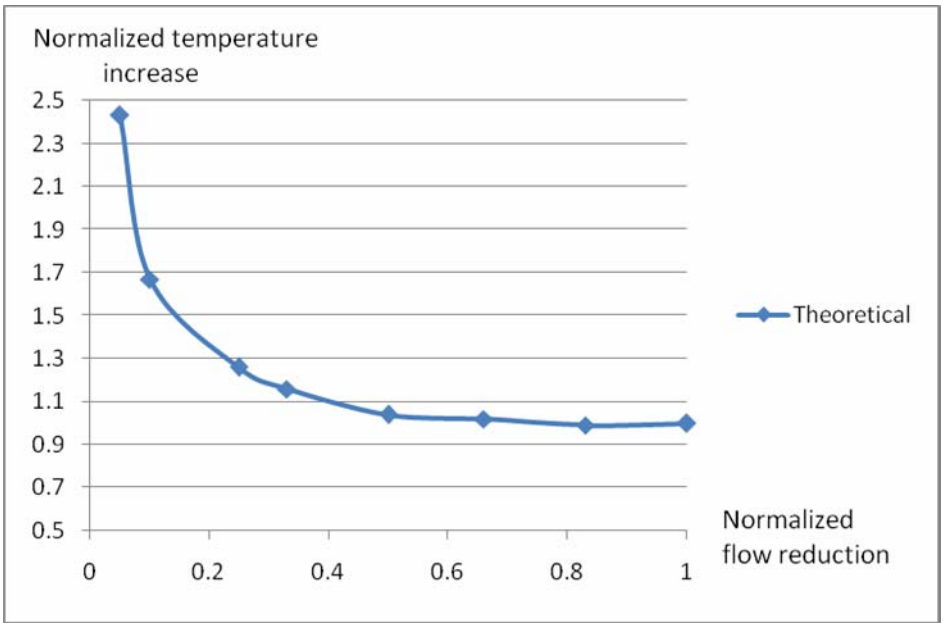

Fig. (6): Theoretical results for the normalized water average temperature increase at the end of transient course with reference to its increase during steady state operation fixed parameters versus normalized flow reduction in the secondary circuit based on its steady state value (300 l/hr).

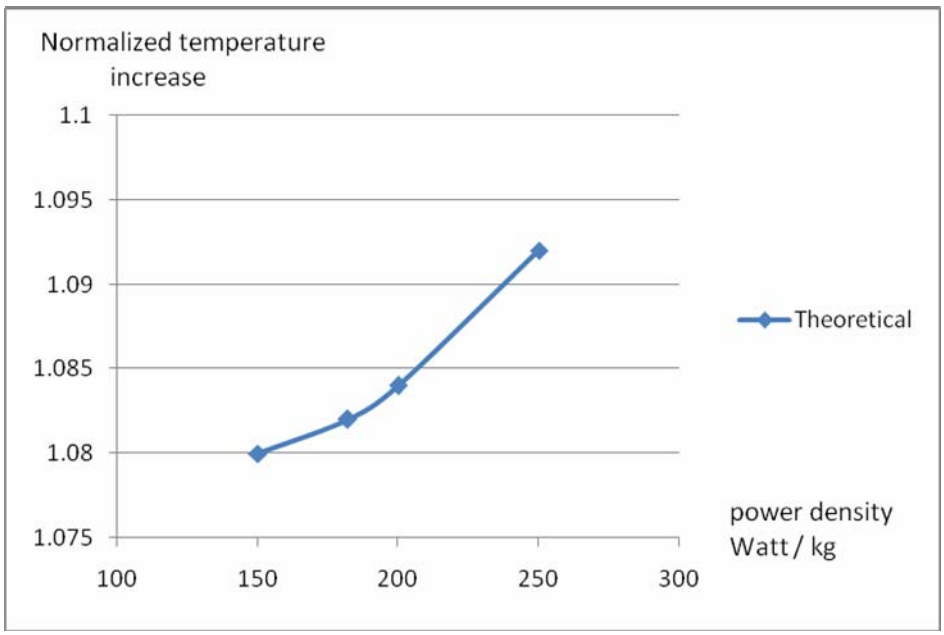

Fig. (7): Theoretical results for the normalized water average temperature increase at the end of transient course with reference to its increase during steady state operation fixed parameters versus power density input to the primary circuit.

EFFECT OF TOOL SHOULDER DIAMETER ON THE MECHANICAL PROPERTIES OF 1200 ALUMINUM FRICTION STIR SPOT WELDING

Dr.Ayad M. Takhakh, samer J. AL-Jodi, Mohamed A. Al-khateeb.

Nahrain University, Iraq Baghdad.

ABSTRACT

A friction stir spot welding (FSSW) process is an emerging solid state joining process in which the material that is being welded does not melt. In this investigation an attempt has been made to understand the effect of tool shoulder diameter on the mechanical properties of the joint. For this purpose four welding tools diameter (10, 13, 16 and 19) mm at constant preheating time and plunging time were used to carry out welding process.

Effect of tool diameter on mechanical properties of welded joints was investigated using shear stress test and Microhardness of joint which welded was studied.

Based on the stir welding experiments conducted in this study the results show that aluminum alloy (1200) can be welded using (FSSW) process with maximum welding efficiency (80%) shear strength using tool diameter(19mm) with rotation speed (900rpm).

الخلاصة.

اللحام النقطي بالخلط والاحتكاك من طرق الحالة الصلبة والتي تكون فيها حالة المعدن الملحوم ليست منصهرة. في هذا البحث محاولة لفهم تاثير قطر العدة على الوصلات. لهذا الغرض استخدمت اربع عدد لحام باقطار (10,13، 16,19) ملم لاجراء عملية اللحام في وقت تسخين وغرس ثابتين.

تاثير قطر العدة وقت اللحام على الخصائص الميكانيكية لوصلات اللحام تم بحثها باستخدام فحوصات الشد والصلادة المجهرية لوصلات اللحام . بناء على التجارب المختلفة في هذة الدراسة اتضح بان سبيكة الالمنيوم (1200) قابلة للحام النقطي بالخلط والاحتكاك مع الحصول على اقصى كفاءة لحام وصلت الى (80%) اعتمادا على مقاومة القص باستخدم قطر اداة (19) ملم مع سرعة دورانية (900 دورة بالدقيقة).

Keywords: friction stirs welding; aluminum; spot welding.

1-Introduction.

Friction stir welding (FSW), a solid-state welding process invented out at TWI (Cambridge, United Kingdom) in 1991 [Moustafa,2004]. The basic concept of FSW is remarkably simple. A non consumable-consumable rotating tool with specially designed pin and shoulder is inserted into the butting edges of sheets or plates to be joined and transverse along the line of joint. After which the tool is extracted from the workpiece. Heat produced at the tool/workpiece interface from friction and interfacial shear is sufficient to locally soften the workpieces. The rotation of the tool aids in 'stirring' the workpieces together to form a potentially defect-free bond. [Joshua,2005]. FSSW is a variant of FSW where the traverse part of the FSW process is eliminated, i.e. the tool is only plunged into the material and retracted **(Figure 1).** The resulting weld is a point or spot weld. FSSW can typically be used in applications where less strength is required, material is thin, and parts are highly contoured. Thus, it is very similar to resistance spot welding (RSW). It is also similar to RSW and other spot joining processes (e.g. riveting) in that FSSW requires significant forces.

FSSW has some distinct potential advantages on aluminum over other welding processes such as RSW, MIG-Spot and Laser - spot as well as performing better than mechanical joining techniques such as Toggle-loc. FSSW tends to have much lower operating costs due to improved energy efficiency and a virtual lack of a consumable. Additionally, FSSW equipment requires significantly less surrounding infrastructure. That is, FSSW requires no water, no compressed air, nor complex electrical transforming equipment [J.F.Hinrichs,2007].

In a previous report [Yasunari,2007], the authors indicated the effect of tool geometry on microstructure and static strength in friction stir spot welds of 6061 aluminum alloy sheets. The tool geometry such as probe length, probe shape and shoulder size is also a key parameter because it would effect the heat generation and the plastic material flow.

In this study, FSSW was performed to join 1200 aluminum alloy sheets to understand the effect of tool shoulder diameter on the mechanical properties of the joint. The aluminum alloy like 1200 commercially pure aluminum, highly resistant to chemical attack and weathering. They are easily worked, but the lowest strength aluminum. They are also excellent for chemical processing equipment and other uses where product purity is important and for metal pressings of all types where ductility is critical.

2- Experimental details

Friction spot stir welding in Aluminum 1200 plate of thickness,(1.5mm). The chemical composition of base material used in this study is given in **(Tables: 1).**

The nominal dimensions of weld samples are 130*25*1.5 mm as shown in **(Figure 2)** according to standards [ASTM,1988].

The stirrer tools were made by special tool steel X38 Cr Mo V 5 1 (DIN 1.2343) as shown in **(Figure 3).**

The welds were made on the Milling machine (Bridgeport CNC series 1 boss 5) with different shoulder

diameters 10, 13, 16 and 19 mm. At constant preheating time, plunging time and depth as shown in **(Table 2),** to carry out FSSW process two aluminum plates were placed overlap on a flat steel plate. These two plates then clamped with special clamps so that they would not separate during welding process, (**Figure 4).**

By using the determined welding parameters three different samples (successfully samples), were used for tensile shear by using uniaxial tensile testing device(INSTRON 1159) and Hardness measurements as mechanical tests(MICROMET, ADOLPH 1. BUEHLER INC).
All samples produced with constant preheating time 20 sec, plunging time 60 sec, and plunging depth 2.7 mm. The influence of shoulder diameter was investigated; shoulder 10, 13, 16 and 19 mm.

3- Results and Discussion.

When rotating pin touches surface of metal, friction had been occur. Friction generates heat which rise temperature of metal, if shoulder diameter less than appointed value the joining area will be not enough to let the two pieces still connected. [k.Elangovan,2008]
As shoulder diameters increase from 10 to 19 mm for a given preheating and plunging time causing increase in shear force (weld force). The highest shear weld failure force 2200 N was obtained at tool shoulder diameter 19 mm **(Figure5).**

The increase in shoulder diameter improves welding force, because with the increasing shoulder diameter stirring area increases and metal mixing increases therefore joining area will increase and the welding become stronger. The results of welding process shown in **(Table 3).** The hardness decreases gradually from the base material through heat affected zone (HAZ) to thermo affected zone (TMAZ) then increase slightly at nugget zone because of metallurgical and amount of plastic deformation. In the stir zone, the hardness is the highest, dropping down in the TMAZ and then rising up to the hardness level of the base material [T.Rosendo,2009], **(Figure 6).**

4- Conclusion.

In this study the effect of shoulder diameter on welding strength of FSSW of aluminum alloy 1200 using simple experimental technique. The result derived from these experiments lead to the following conclusion:

1- Aluminum alloy 1200 is wieldable by using different (FSSW) tool shoulder diameter, it gave different welding efficiencies.

2- The weld joint fabricate with tool of 19 mm diameter showed better mechanical properties than the others.

3- The hardness decreases gradually from the base material through heat affected zone (HAZ) to thermo affected zone (TMAZ) then increase slightly at nugget zone because of friction heat and amount of plastic deformation.

4- Increasing tool shoulder diameter from (10mm to 19mm) step 3mm for a fixed other welding parameter caused increasing

mechanical properties of the welds joint.

5- When the tool shoulder diameter had increase more than 19mm diameter it did not probably for the mechanical properties to be increased.

References.

-Moustafa Boz and Adem Kurt" The Influence of Stirrer Geometry on Bonding and Mechanical Properties of Friction Stir Welding Process, Materials and Design 25 (2004) 343-347.

- Joshua L. Covington" Experimental and Numerical Investigation of Tool Heating during Friction Stir Welding ", M.Sc Thesis, Brigham Young University, .2005.

-J. F. Hinrichs, C. B. Smith, B. F. Orsini, R. J. DeGeorge, B. J. Smale, P. C. Ruehl" Friction Stir Welding for the 21st Century Automotive Industry" Waukesha, WI USA,2007.

- Yasunari Tozaki, Yoshihiko Uematsu, Keiro Tokaji "Effect of tool geometry on microstructure and static strength in friction stir spot welded aluminum alloys" Machine Tools & Manufacture, Vol.47, No.7,PP.2230-2236,2007.

-M. Awang, V. H. Mucino, Z. Feng, and S. A. David" Thermo-Mechanical Modeling of Friction Stir Spot Welding (FSSW) Process: Use of an Explicit Adaptive Meshing Scheme" SAE International, 2005.

- ASM"Properties and Selection: Nonferrous Alloys and Special – Purpose Materials", ASM Internationnal, Volume 2.

-ASTM"Metals-Mecanical Testing Elevated and Low – Temperature Tests; Metallography"Annual Book of ASTM Standards, Volume 03.01,1988.

- K. Elangovan, and V. Balasubramanian''Influences of tool pin profile and tool shoulder diameter on the formation of friction stir processing zone in AA6061 aluminum alloy' Materials and Design 29 362–373 (2008)

-T. Rosendo1, 2, J. Mazzaferro1, 3, C. Mazzaferro1, 2, M. Tier1, 4, F. Ramos1, 2, A. Reguly2, T. Strohaecker2, J. dos Santos1" Friction Spot Processes-FSSW and FSpW –"AEM, 2009.

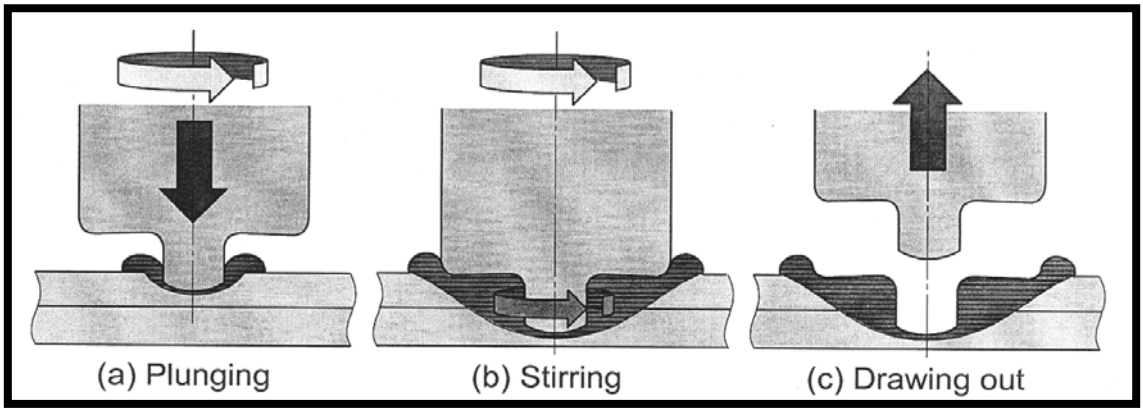

Figure (1) Frictions Stir Spot Welding Process [M.Awang,2005].

Table 1: Chemical Composition of Aluminum 1200 [ASM].

Zn%	Cu%	Fe%	Pb%	Mn%	Si%	Al%
0.0237	0.0986	0-9537	0.0253	0.0324	0.489	Bal.

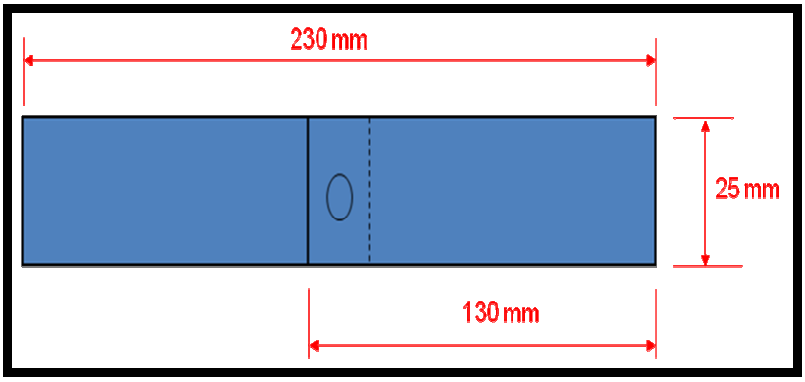

Figure (2) Nominal dimensions of weld sample.

Fig (3) the stirrer tools were made by special tool steel X38.

Figure (4) Clamping and Welding.

Table 2: Friction Spot Stir Welding Parameters.

Shoulder diameter D (mm)	Preheat dwell time (sec)	Plunging time (sec)
10	20	60
13	20	60
16	20	60
19	20	60

Table 3: The Results of Welding Process.

Shoulder diameter (mm)	Preheat dwell time (sec)	Plunging time (sec)	Shear force (N)
10	20	60	Failed
13	20	60	800
16	20	60	1800
19	20	60	2200

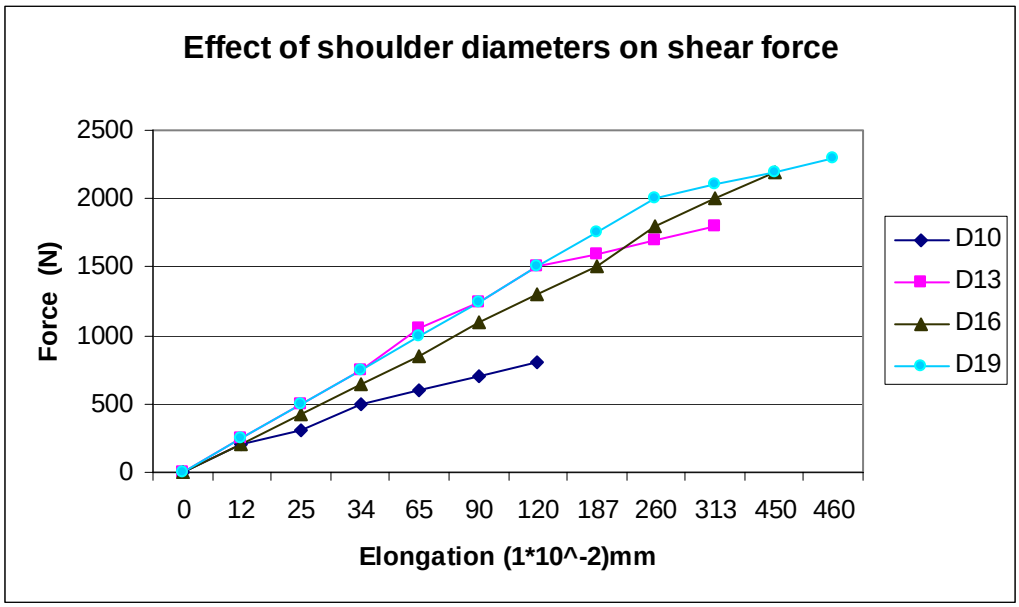

Figure (5) shear force change with shoulder diameter.

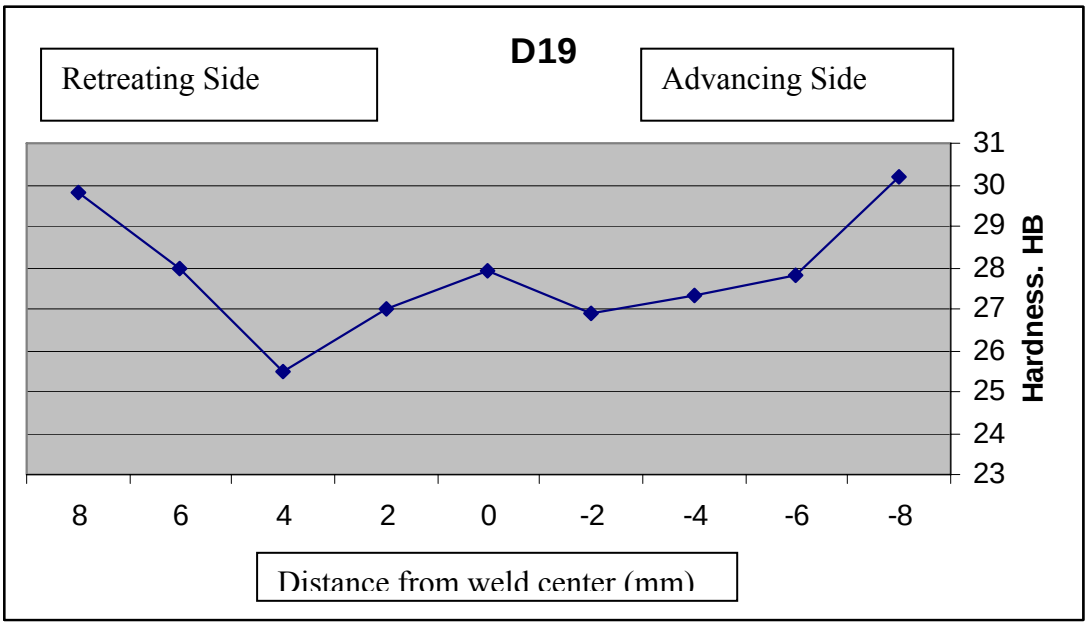

Figure (6) Microhardness at shoulder diameter 19 mm result.

FREE VIBRATION ANALYSIS OF NOTCHED COMPOSITE LAMINATED CANTILEVER BEAMS

Assist. Lecture: Ahmed N. Ouyed
University of Anbar / College of Eng.
Mechanical Eng. Dept.

ABSTRACT

The present work divided into two parts, first the experimental side which included the measuring of the first natural frequency for the notched and unnotched cantilever composite beams which consisted of four symmetrical layers and made of Kevlar- epoxy reinforced. A numerical study covers the effect of notches on the natural frequencies of the same specimen used in the experimental part. The mathematical model for the beam contains two open edges on the upper surface. The effect of the location of cracks relative to the restricted end, depth of cracks, volume fraction of fibers and orientation of the fiber on the natural frequencies are explored. The results were calculated using the known engineering program (ANSYS), the results obtained has been compared with those calculated analytically by (Sierakowski RL.), which have expressed the closest well also the comparison between the experimental results with that calculated by (ANSYS) has very well. The study shows that the highest difference in frequencies occur when the value of the fiber orientation equal to 0^odegree, the effect of location of the cracks decrease when the cracks moving toward the free end and also shows that an increase of the depth of the cracks leads to a decrease in the values of natural frequencies.

الخلاصة:

يقسم البحث الى جزئين ، الأول الجانب العملي والذي يتضمن قياس التردد الطبيعي الاول لعتبة ناتئة من الألواح المركبة محززة و غير محززة مؤلفة من أربعة طبقات متناظرة مصنوعة من مادة (Kevlar- epoxy). الدراسة العددية تبين تأثير الحزوز على الترددات الطبيعية لنفس النموذج المستخدم في الجانب العملي. النموذج الرياضي للعتبة يحتوي على شقيق على السطح العلوي. تم بحث تأثير موقع الحزوز با النسبة الى النهاية المقيدة، تأثير العمق، الكسر ألحجمي للألياف وكذلك زاوية الليف على الترددات الطبيعية. تم حساب النتائج باستخدام البرنامج الهندسي المعروف (ANSYS)، أن النتائج المحسوبة تمت مقارنتها مع تلك المحسوبة بالطريقة التحليلية لـ (Sierakowski RL.) والتي أبدت تقارباً جيدا و كذلك المقارنة بين النتائج العملية و تلك المحسوبة بالبرنامج كانت جيدة ايضاً. أن البحث يظهر أن أعظم اختلاف في الترددات يحدث عندما تكون زاوية اتجاه الليف مساوية 0° وأن تأثير موقع الحزوز يقل بتحرك الحزوز باتجاه النهاية الحرة للعتبة و كذلك تظهر الدراسة أن زيادة عمق الحزوز يؤدي إلى النقصان في قيم الترددات الطبيعية.

KEY WORDS
Vibration, Finite element, Cantilever beams, Laminate, Natural frequencies.

1. INTRODUCTION

During operation, all structures are subjected to degenerative effects that may cause initiation of structural defects such as cracks which, as time progresses, lead to the catastrophic failure or breakdown of the structure. Thus, the importance of inspection in the quality assurance of manufactured products is well understood. Cracks or other defects in a structural element influence its dynamical behavior and change its stiffness and damping properties. Consequently, the natural frequencies of the structure contain information about the location and dimensions of the damage.

The first group of studies have been performed for long times and the most concepts related to the crack detection have been well established from mathematical theory **(Chondros TG,1998)** to impact echo method**(Cam E,2005, Ratcliffe CP1997)** . When a structure suffers from damages, its dynamic properties can change, especially, crack damage can cause a stiffness reduction, with an inherent reduction in natural frequencies, an increase in modal damping, and a change of the mode shapes. Consequently, there would also be a change in the dynamic response of the structure **(Matveev VV, 2002 Kim M-B,2005).**

Over the past decade, several techniques have been explored for detecting and monitoring of the defects in the composite materials. **(Adams RD,1978)** showed that any defect in fibre-reinforced plastics could be detected by reduction in natural frequencies and increase in damping. **(Nikpour K, Dimarogonas AD,1988)** studied the variation of the mixed term in the energy release rate for various angles of inclination of the material axes of symmetry and they derived the local compliance matrix of a prismatic beam with a central crack.

(Nikpour K,1990) studied the buckling of cracked composite columns and showed that the instability increases with the column slenderness and the crack depth. **(Oral S,1991**) developed a shear flexible finite element for non-uniform laminated composite beams. He tested the performance of the element with isotropic and composite materials, constant and variable cross-sections, and straight and curved geometries.

In the last years, the effort is focused on the vibration analysis of structural members using breathing crack models to simulate real fatigue cracks. Several researchers have studied the problem of beams having a breathing crack by employing different approaches. In that **(Saavedra PN,2001)** proposed a new modeling approach for cracked beam structures. They used finite elements for the beam, while for the cracked element a new finite element matrix based on an energy density function was employed. Recently, **(Sinha JK,2002)** developed an alternative finite element approach, where the phase relationship between the first and second response components is simulated correctly. **(Pugno N,2000)** studied the dynamic response of a beam with several breathing cracks subjected to harmonic excitation. Assuming that cracks open and close continuously and using finite elements to model the beam, a system of non-line a algebraic equations was obtained and solved by numerical integration.

Recently, **(Song O,2003)** investigated the dynamics of anisotropic composite cantilevers. They presented an exact solution methodology utilising Laplace traform technique to study the bending free vibration of cantilever composite beams with multiple open cracks.

The present search presented numerical and experimental study for the effect of the cracks on the natural frequencies of cantilever composite beams. The lamination angle of the fiber, volume fraction of fibers and the location of notches relative constrain end are studied.

2. MATHMATICAL MODEL

The model chosen is a cantilever composite beam of uniform cross-section area

A, having two open – edge transverse cracks at a variable positions $L1$ and $L2$. The width , length and height of the beam are B, L and H , respectively as shown in Fig.(1).The beam consist of four symmetric layers.

2.1. The Stiffness Matrix For Crack

According to the St. Venant's principle, the stress field is influenced only in the region near to the crack. The additional strain energy due to crack leads to flexibility coefficients expressed by stress intensity factors derived by means of Castigliano's theorem in the linear elastic range. The compliance coefficients C_{ij} induced by crack are derived from the strain energy release rate, J, developed**(Tada H, Paris PC, 1985)**theory. J can be given as:

$$J = \frac{\partial U(P_i, A)}{\partial A} \tag{1}$$

Where A is the area of the crack section, P_i are the corresponding loads, U is the strain energy of the beam due to crack and can be expressed as **(Nikpour K, Dimarogonas AD,1988)** :

$$U = \int_A \left(D_1 \sum_{i=1}^{i=N} K_{Ii}^2 + D_{12} \sum_{i=1}^{i=N} K_{Ii} \sum_{j=1}^{j=N} K_{IIi} + D_2 \sum_{i=1}^{i=N} K_{IIi}^2 \right) dA, \tag{2}$$

Where K_I and K_{II} are the stress intensity factors for fracture modes of I and II. D_1, D_{12} and D_2 are the coefficients depending on the materials parameters**(Nikpour K, Dimarogonas AD,1988)** :

$$D_1 = -0.5\bar{b}_{22} \ \mathrm{Im} \ \frac{s_1 + s_2}{s_1 s_2} \tag{3}$$

$$D_{12} = \bar{b}_{11} \ \mathrm{Im}(s_1 s_2) \tag{4}$$

$$D_2 = 0.5\bar{b}_{11} \ \mathrm{Im}(s_1 + s_2) \tag{5}$$

The coefficients s_1, s_2 are complex constant and $\bar{b}_{ij}$ are constant. The mode I and II stress intensity factors, K_I and K_{II}, for a composite beam with a crack are expressed as **(Nikpour K,1990)**.

$$K_{ij} = \sigma_i \sqrt{\pi a} Y_j(\zeta) F_{ji}(a/H) \tag{6}$$

Where σ_i is the stress for the corresponding facture mode, is the correction factor for the finite specimen size, $Y_j(\zeta)$ is the correction factor for the anisotropic materia**(Nikpour K, Dimarogonas AD,1988)**, a is the crack depth and H is the element height. Castigliano's theorem [**Tada H,Paris PC, Irwin GR.1985**] implies that the additional displacement due to crack, according to the direction of the P_i, is:

$$u_i = \frac{\partial U(P_i, A)}{\partial P_i} \tag{7}$$

Substitution of this energy rate J into Eq. (7), the relation between displacement and strain energy release rate J can be written as follows:

$$u_i = \frac{\partial}{\partial P_i} \int_A J(P_i, A) dA. \tag{8}$$

The flexibility coefficients, which are the functions of the crack shape and the stress intensity factors, can be introduced as follows**(Tada H, Paris PC, 1985)**:

$$c_{ij} = \frac{\partial u_i}{\partial P_j} = \frac{\partial^2}{\partial P_i \partial P_j} \int_A J(P_i, A) dA = \frac{\partial^2 U}{\partial P_i \partial P_j} \quad (9)$$

The compliance coefficients matrix, after being derived from above equation, can be given according to the displacement vector $\delta = \{u, v, \theta\}$ as

$$C = \lfloor c_{ij} \rfloor_{(3\times3)} \quad (10)$$

Where c_{ij} (i, j = 1, 2, 3) are derived by

using Eqs. (1-9).

The inverse of the compliance coefficients matrix, C^{-1}, is the stiffness matrix due to crack. Considering the cracked node as a cracked element of zero length and zero mass**(Ratcliffe CP1997)**, the crack stiffness can be represented as equivalent compliance coefficients. Finally, resulting stiffness matrix for the crack can be given as:

$$K_c = \begin{bmatrix} [C]^{-1} & -[C]^{-1} \\ -[C]^{-1} & [C]^{-1} \end{bmatrix}_{(6\times6)} \quad (11)$$

2.2. Component Mode Analysis

The equation of motion of a mid-plane symmetrical composite beam is **(Vinson JR, 1991)**:

$$IS_{11}\partial^4 y(x,t)/\partial x^4 + \rho A \partial^2 y(x,t)/\partial t^2 = f(t) \quad (12)$$

Where I, ρ, A and y (x, t) are geometrical moment of inertia of the beam cross-section, material density, cross sectional area of the beam and transverse deflection of the beam, respectively. Now, consider the component A_1, for undamped vibration analysis, Eq. (12), in matrix notation, can be given as:

$$M_{A1}\ddot{q}_{A1} + K_{A1}q_{A1} = f_{A1}(t) \quad (13)$$

where M_{A1} and K_{A1} are the mass and stiffness matrices of the component A_1, respectively, q_{A1} and f_{A1} (t) are the generalized displacement and external force vectors, respectively. Assuming that:

$$\{q_{A1}\} = \{\phi_{A1}\}\sin(\omega_{A1}t + \beta) \quad (14)$$
$$\{\ddot{q}_{A1}\} = -\omega_{A1}^2\{\phi_{A1}\}\sin(\omega_{A1}t + \beta)$$

and substituting them into Eq. (13), one ends up with the Standard free vibration equation for the component A_1 as,

$$\omega_{A1}^2 M_{A1}\phi_{A1} = K_{A1}\phi_{A1} \quad (15)$$

Which gives eigen values $\omega_{A1}^2,...,\omega_{A1n}^2$ and modal matrix ϕ_{A1} for the component A_1. Making the transformation

$$q_{A1} = \phi_{A1}p_{A1} \quad (16)$$

where P_{A1} is the principal coordinate vector. By premultiplying ϕ_{A1}^T and substituting Eq. (16), Eq. (13) becomes:

$$\left(\phi_{A1}^T M_{A1}\phi_{A1}\right)\ddot{p}_{A1} + \left(\phi_{A1}^T K_{A1}\phi_{A1}\right)p_{A1} = \phi_{A1}^T f_{A1}(t) \quad (17)$$

Where

$$\phi_{A1}^T M_{A1}\phi_{A1} = [m_m]$$
$$\phi_{A1}^T K_{A1}\phi_{A1} = [K_m] \quad (18)$$

where $[m_m]$ and $[Kn]$ are modal mass and stiffness matrices, respectively. Mass normalising the modal matrix by:

$$\psi_{ij} = \frac{\phi_{ij}}{\sqrt{m_{ij}}} \tag{19}$$

where ψ_{ij} is mass normalized mode vector. By using the transformation

$$q_{A1} = \psi_{A1} s_{A1} \tag{20}$$

by premultiplying ψ_{A1}^T and substituting Eq. (20), Eq. (13) becomes

$$I\ddot{s}_{A1} + \omega_{A1}^2 s_{A1} = \psi_{A1}^T f_{A1}(t) \tag{21}$$

where ω_{A1}^2 is. a diagonal matrix comprising the eigenvalues of A_1.

Consider components. A_1, A_2,…, A_N, Joined together by means of springs capable of carrying axial, shearing and bending effects. The kinetic and-strain energy of the components, in terms of principal modal coordinates, can be given as:

$$T = \frac{1}{2}\dot{s}^T M \dot{s}$$

$$U = \frac{1}{2} s^T K s \tag{22}$$

Where T and U are kinetic and strain energy, respectively. M and K in Eq. (22) are:

$$M = \begin{bmatrix} 1 & 0 & \dots & 0 \\ 0 & 1 & \dots & 0 \\ \dots & \dots & \dots & \dots \\ 0 & 0 & \dots & 1 \end{bmatrix},$$

$$K = \begin{bmatrix} \omega_{A1}^2 & 0 & \dots & 0 \\ 0 & \omega_{A2}^2 & \dots & 0 \\ \dots & \dots & \dots & \dots \\ 0 & 0 & \dots & \omega_{AN}^2 \end{bmatrix} \tag{23}$$

The strain energy of the connectors, in terms of principal modal coordinates, is:

$$Uc = \frac{1}{2} s^T \psi^T Kc \psi s \tag{24}$$

Where Kc is the stiffness matrix of the cracked nodal element and can be calculated by using Eq. (9) ψ in Eq. (24) can be written as:

$$\psi = \begin{bmatrix} \psi_{A1} & 0 & \dots & 0 \\ 0 & \psi_{A2} & \dots & 0 \\ \dots & \dots & \dots & \dots \\ 0 & 0 & \dots & \psi_{AN} \end{bmatrix} \tag{25}$$

The total strain energy of the system is, therefore:

$$U_T = \frac{1}{2} s^T \left(K + \psi^T Kc \psi\right) s, \tag{26}$$

Where K has been given by Eq. (23). The equation motion of the complete structure is:

$$\ddot{s} + \left(K + \psi^T Kc \psi\right) s = \psi^T f(t) \tag{27}$$

Where ψ has been given by Eq. (25), f (t) is the global force vector for the system. From Eq. (27), the eigenvalues and mode shapes of the cracked system can be determined. After solving these equations, the displacement for each component are calculated by using Eq. (20).

3.RESULTS AND DISCUSSION

3.1. Validation Of The Current Work

In order to check the accuracy of the present method , the results found by using the finite element method (ANSYS 5.4) are compared with the analytical solution of (cracked unidirectional beam), found by Sierakowski RL. **(Vinson JR, Sierakowski RL, 1991)**, as shown in Fig.(1). The beam assumed to be made of graphite fiber reinforced polyamide which contains four notches of triangle shape. The numerical results show a good agreement compared with analytical solution.

3.2. Vibration Of The Laminate Beam

The geometrical characteristics of the beam used in experimental and theoretical analysis are the length (L)= 0.75 m, height (H) =0.03 m and width(B)=0.03 m as shown in Fig.(2) . The material properties of the kevlar- epoxy are**(kawczuk M, 1997)**:

$E1$ =221 Gpa, $E2$ = 23 Gpa ,

$G12$ =8.6 Gpa,

$G23$ = 6.5 Gpa,

$\upsilon 12$ = 0.2,

$\upsilon 23$ = 0.3.

3.2.1 Experimental Side:

Experimental work presents the measurement the first natural frequency of the Specimens shown in Fig.(2). Experimental configuration shown in Fig.(3), used to measured the natural frequency. An accelerometer with a mass of 3 gm attached on the top edge of the beam using a wax at distance of about of 100mm from the clamped end. The accelerometer is connected by an amplifier. The charge amplifier is analyzed by an FFT analyzer which enable to readout the peaks from the digital analyzer.Tables (1,2) show the effect of the fibers orientation and cracks size on the first natural frequency for the cantilever composite beams which contents two cracks which were located as L_1 / L = 0.1, L_2 / L = 0.25 and the volume of fiber (V) was 0.8. It can be clearly seen from table (1) that, the high decreasing in the natural frequency occur until angle of fiber 50° and greater than it the change is very low. Table (2) shows that the first natural frequency of the un notched beams equal to (45.2 Hz) and also shows that increasing the depth of the of cracks lead to decreasing in the value of the first natural frequency.

3.2.2 Theoretical Analysis:

To more deeply analysis, theoretical analysis using the finite element (ANSYS). Figs.(4, 5 and 6) show the first three natural frequencies as a function of the fiber orientation (α) for different crack ratios (a/H). In the model, the composite beam has two cracks which were located as L_1 / L = 0.1, L_2 / L = 0.25 and the volume of fiber (V) was 0.8. It is noticeable that a decrease in the natural frequencies become more intensive with the growth of the crack depth. The most difference in frequencies occur when the value of the fiber (α) is 0°. When the value of the angle of fiber is greater than 55°, the effects of the cracks on the frequencies decrease. This can be explained as the flexibility due to crack is negligible when the angle of the fiber is greater than 55°, especially when the crack ratio is relatively low.

In Figs. (7, 8 and 9), the variation of the three lowest natural frequencies of the composite beam with two cracks is shown as a function of fiber orientation (α) for different cracks locations. In these figures, three cases, labeled as E, F and G, were considered .The cracks locations (L_1/ L , L_2 /L) for the cases E, F and G, where chosen as (0.2, 0.35), (0.5, .65), (0.8,0.95) respectively. From the previous figures it can be clearly seen that , when the cracks are placed near the fixed end the decreases in the first natural frequency are highest , when the cracks are located near the free end ,This observation leads to the conclusion that, the first, second and third natural frequencies are most

affected when the cracks located at the near of the fixed end, the middle of the beam and the free end .

Figs. (10, 11 and 12) present the first three natural frequencies as a function of the volume of fiber (V) for several values of the crack ratios L_1/L = 0.2, L_2/L = 0.35 and the angle of fiber (α) is 0°. As can be seen from the figures, the natural frequencies are affected by the values of the volume of fiber (V) and the crack ratios (a/H), as expected. The flexibility due to cracks is high when the volume of fiber is between 0.2 and 0.8.

4.CONCLUSION

From the previous discussion, the following can be concluded

1. The effect of notches decrease as the notches moved toward the free end.
2. The natural frequencies decrease as the depth of notches are growth.
3. As increase the angle of fibers orientation the change on natural frequencies is negligible.
4. The high flexibility of cracks due at volume of fiber range (0.2 – 0.8).

5. REFRENCES

- Adams RD, Cawely P,Pye CJ, Stone J. A vibration testing for non- destructively assessing the integrity of the structures. J. Mech.Eng.Sci. 1978;20:93-100.
- Chondros TG, et al. A continuous cracked beam vibration theory. J Sound Vib. 1998;215:17–34.
- Cam E, et al. An analysis of cracked beam structure using impactecho method. NDT & E Int. 2005;38:368–73.
- Kim M-B, Zhao M. Study on crack detection of beam using harmonic responses. In: Proceedings of the 2004 international conference on intelligent mechatronics and automation, August2004, Chengdu, China, p.72–6.
- kawczuk M, Ostachowicz W, Zak A. Modal analysis of cracked unidirectional composite beam. Compos Part B 1997; 28:641-50.
- Matveev VV, Bovsunovsky AP. Vibration-based diagnostics of fatigue damage of beam-like structures. J Sound Vib 2002;249(1): 23–40.
- Nikpour K, Dimarogonas AD. Local complains of composite cracked bodies. Composite Sci. Technol. 1988; 32:209-23.
- Nikpour K, Buckling of cracked composite columns. Int.J.Solids Struc. 1990; 26(12):1371-86.
- Oral S. A shear flexible finite element for non uniform laminated composite beam. Comput. Struct. 1991; 38(3) : 353-60..
- Pugno N, Surace C, Ruotolo R. Evaluation of the non-linear dynamic response to harmonic excitation of a beam with several breathing cracks. J Sound Vib 2000;235:749–62.
- Przemieniecki JS. Theory of matrix structural analysis. 1 st ed. London; McGraw – Hill;1967.
- Ratcliffe CP. Damage detection using a modified Laplacian operatoron mode shape data. J Sound Vib 1997;204(3):505–17.
- Sinha JK, Friswell MI. Simulation of the dynamic response of acracked beam. Comput Struct 2002;80:1473–6.

- Saavedra PN, Cuitino LA. Crack detection and vibration behavior of cracked beams. Comput Struct 2001;79:1451–9.

- Song O, Ha TW, Librescu L. Dynamic of an isotropic cantilevers weakened by multiple transverse open cracks. Eng. Fract. Mech. 2003; 70:105-23.

- Tada H, Paris PC, Irwin GR. The stress analysis of cracks handbook. 2nd ed. St. Louis, MO: Paris production incorporated and Del Research Corporation;1985.

- Vinson JR, Sierakowski RL. Behavior of structures composed of composite materials. 1 st ed. Dordrecht: Martinus Nijhoff; 1991.

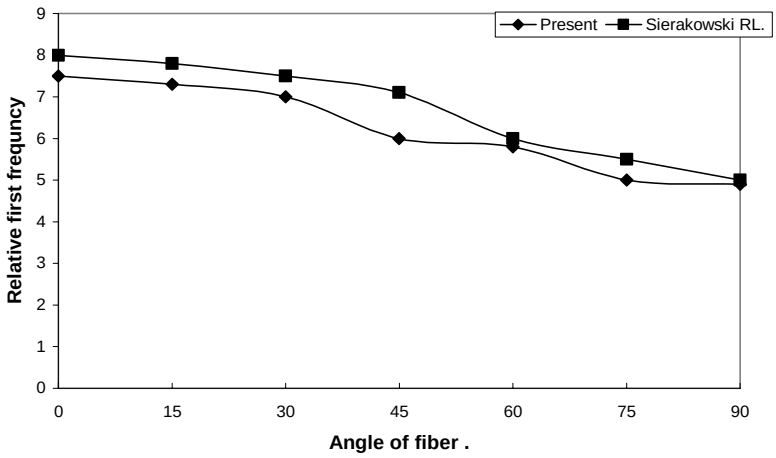

Fig. (1) The relation between the relative first natural frequany and the angle o f the fiber.

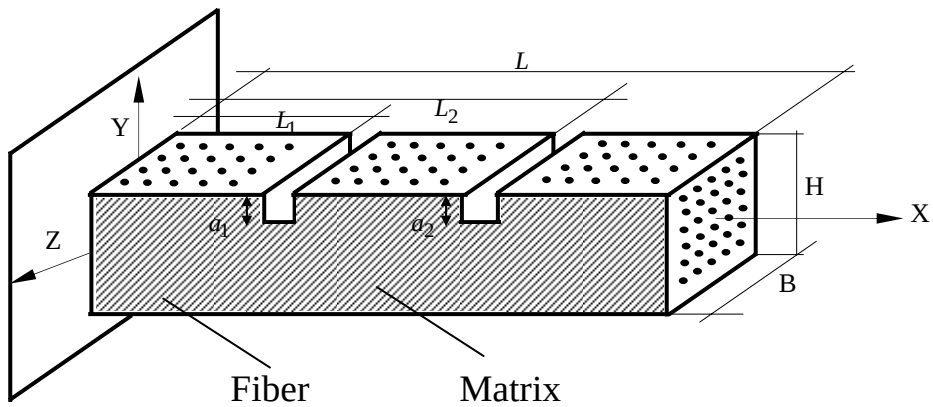

Fig (2)
Geometry of the cantilever composite beam with two cracks.

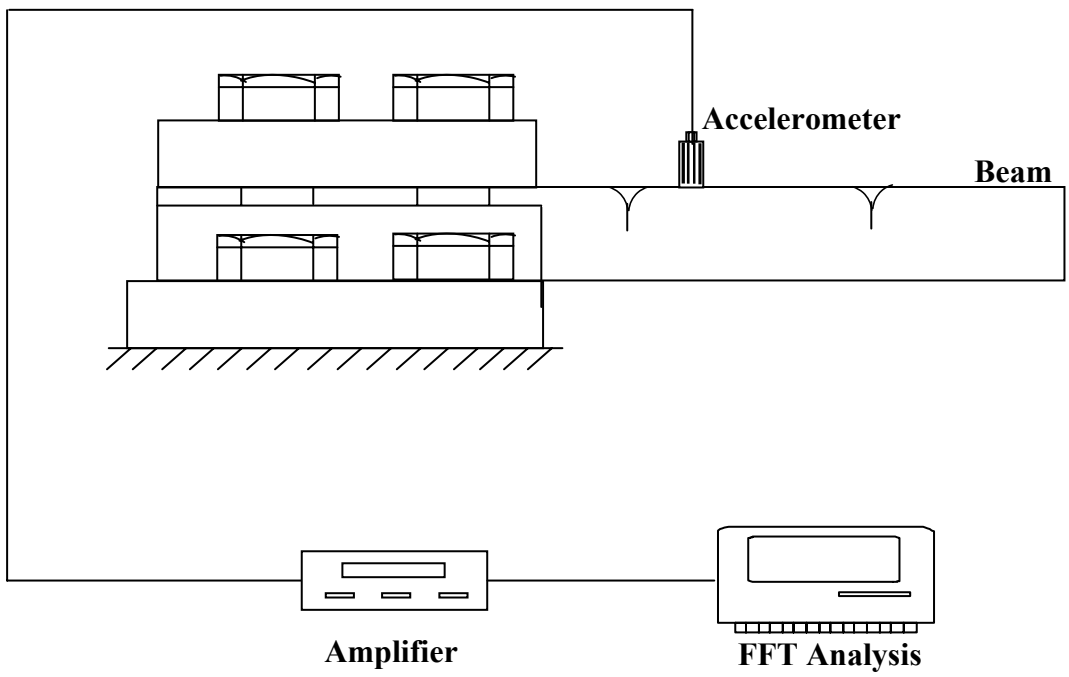

Fig.(3) Experimental configuration

Table (1): The effect of the fibers orientation on the first natural frequency for the notched cantilever plates.

θ^o (Degree)	Experimental ω_1 (HZ)	Present Work (ANSYS) ω_1 (HZ)
0	30	31.4
10	28.5	30.5
20	27	28.6
30	25	26.1
40	22	23.2
50	21.9	22.8
60	21.5	22.51
70	21.4	22.3
80	21.1	22.25
90	20	22

Table(2): The effect of the size of the notches on the first natural frequency for the notched cantilever plates. first natural frequency for the notched cantilever plates.

ratio (a/h)	Experimental First Natural Frequency (HZ)	ANSYS First Natural Frequency (HZ)
0	45.2	46.5
0.1	43	44
0.2	41	42
0.3	36	37
0.4	33	34.5
0.5	30	33
0.6	25	26
0.7	21.9	23

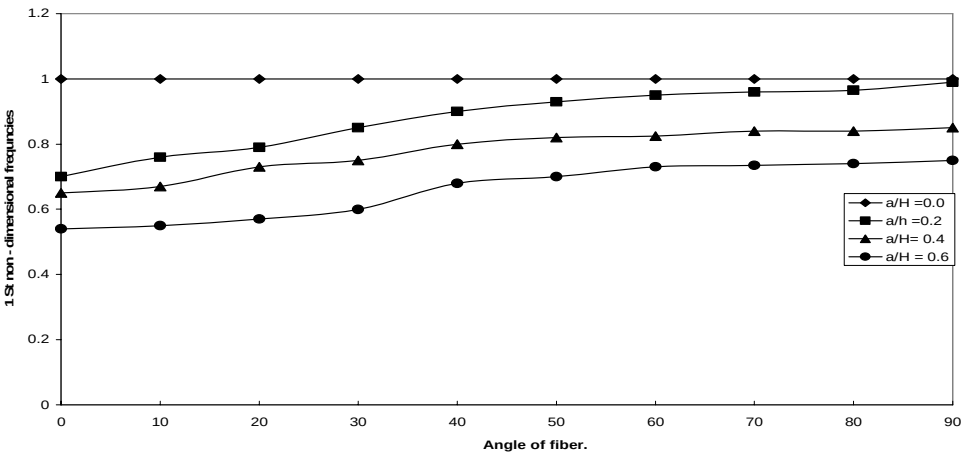

Fig. (4) First non- dimensional natural frequancies as a function of fiber orintation for different crack ratios a/H =0.2, 0.4, 0.6, and volume of the fiber V is 0.8.

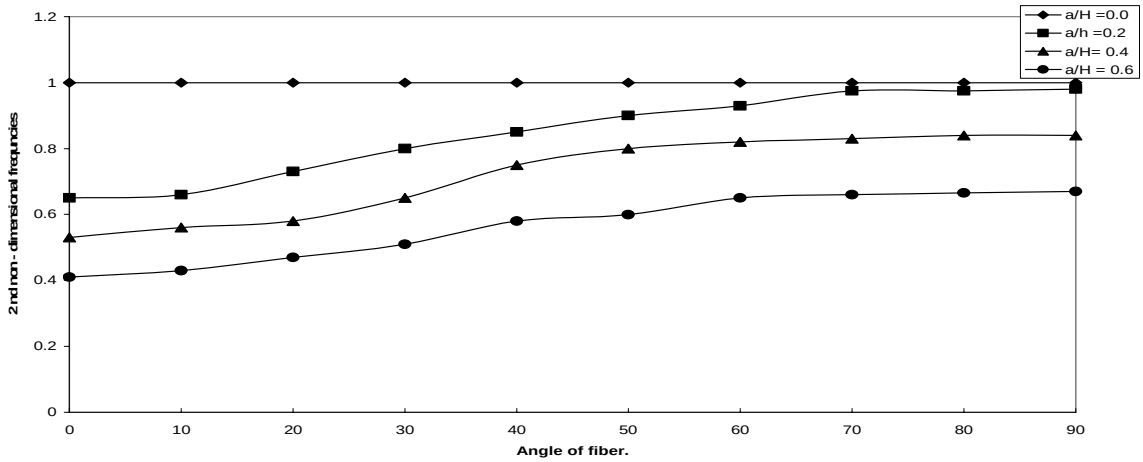

Fig. (5) second non- dimensional natural frequancies as a function of iber orintation for different crack ratios a/H =0.2, 0.4, 0.6, and volume of the fiber V is 0.8.

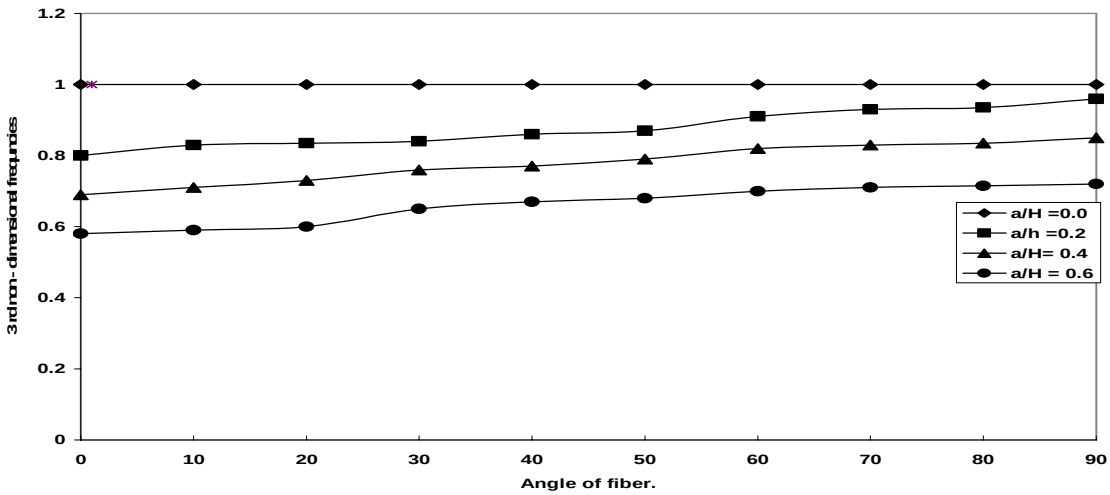

Fig. (6) Third non- dimensional natural frequancies as a function of iber orintation for different crack ratios a/H =0.2, 0.4, 0.6, and volume of the fiber V is 0.8.

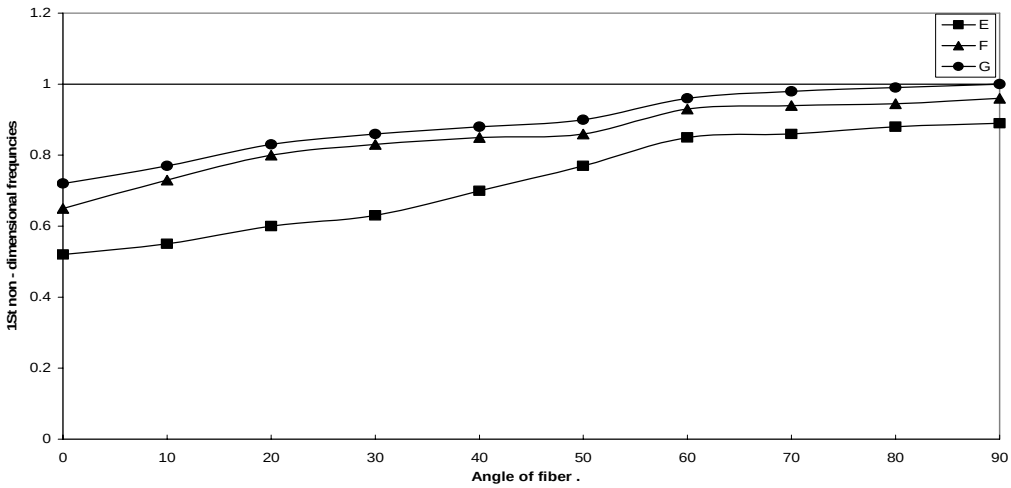

Fig. (7) First non- dimensional natural frequancies as a function of fiber orintation for different crack locations for the cases E, F and G, and volume of the fiber V is 0.8.

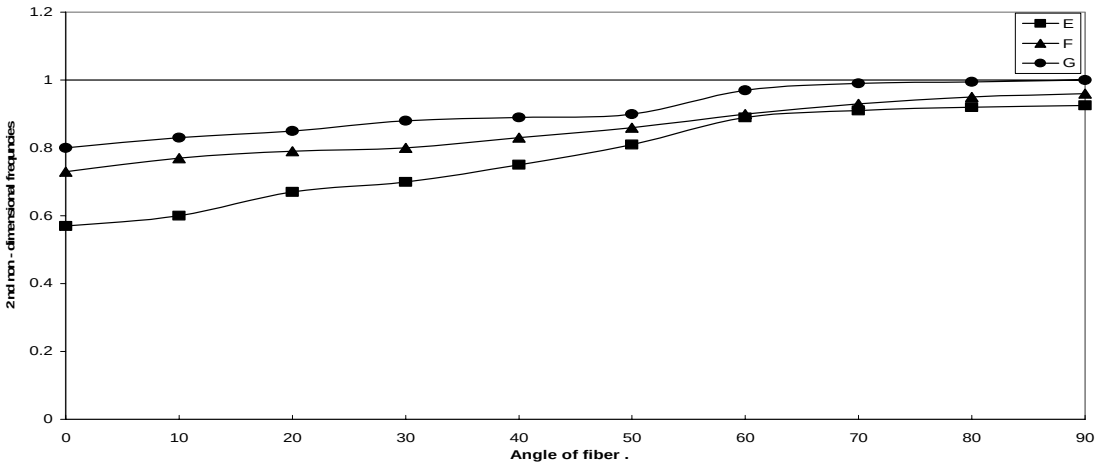

Fig. (8) Second non- dimensional natural frequancies as a function of fiber orintation for different crack locations for the cases E, F and G, and volume of the fiber V is 0.8.

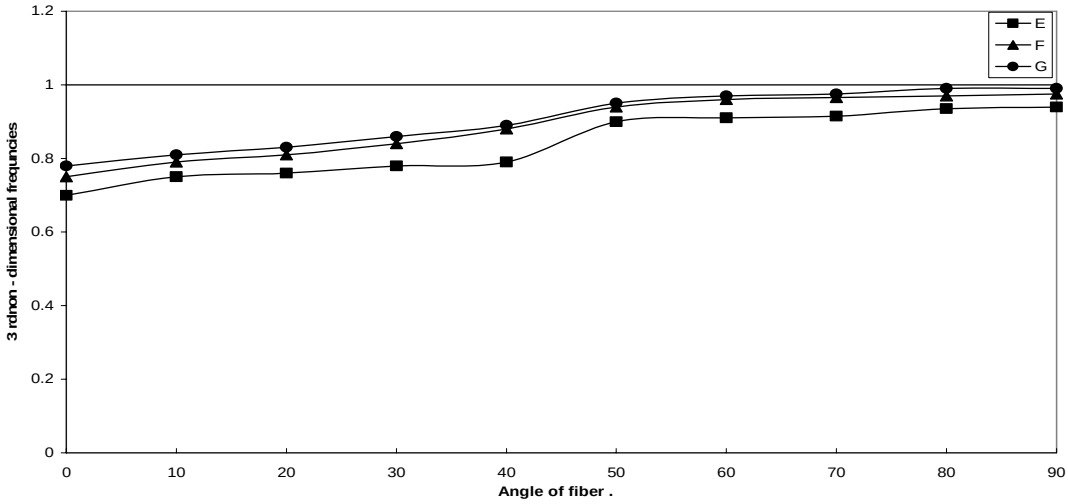

Fig. (9) Third non- dimensional natural frequancies as a function of fiber orintation for different crack locations for the cases E, F and G, and volume of the fiber V is 0.8.

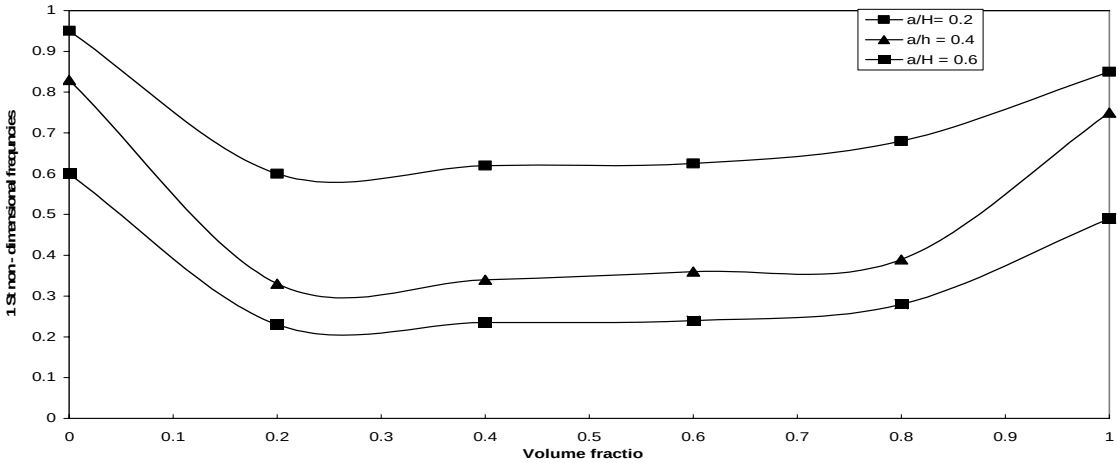

Fig. (10)First non- dimensional natural frequancies as a function of the fiber volume fraction for different crack ratios a/H = 0.2, 0.4, 0.6.

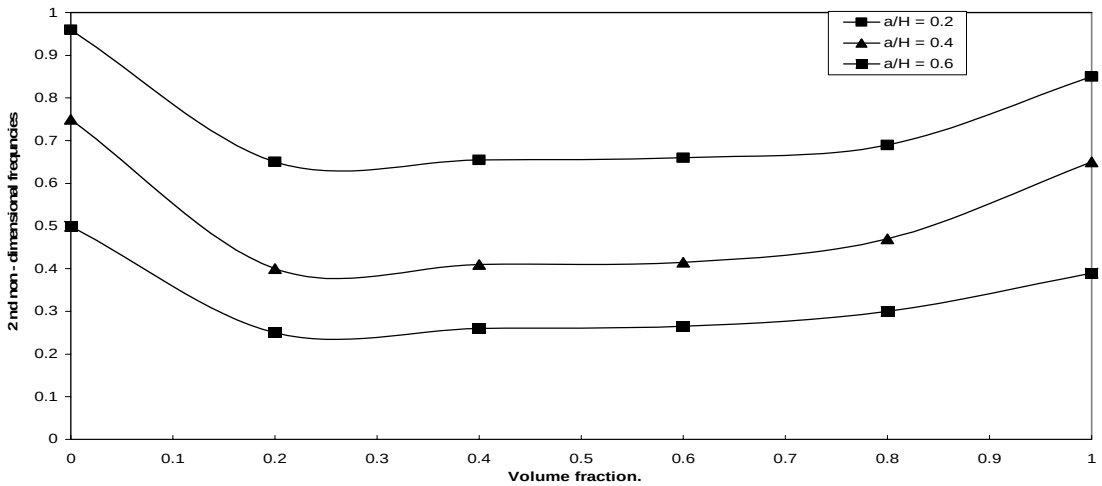

Fig. (11) Second non- dimensional natural frequancies as a function of the fiber volume fraction for different crack ratios a/H = 0.2, 0.4, 0.6.

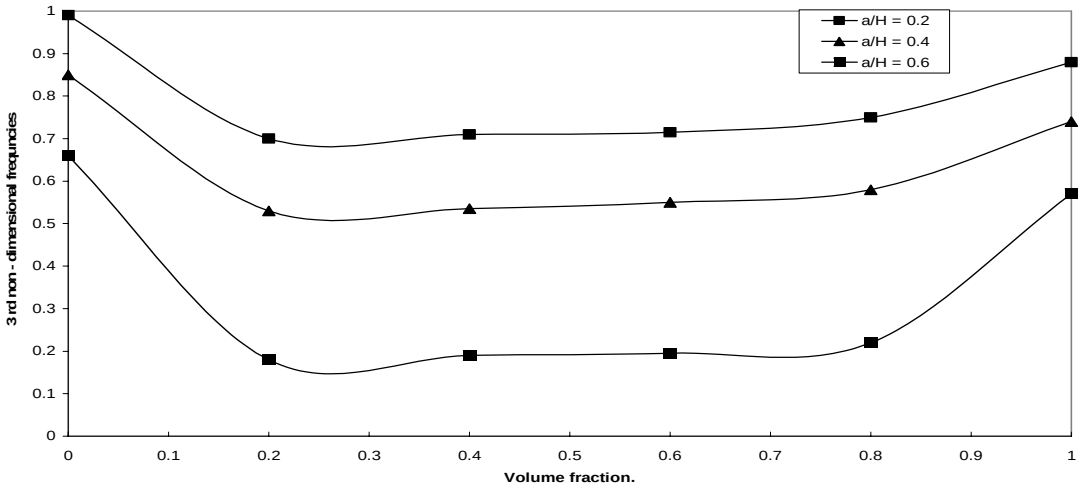

Fig. (12)Third non- dimensional natural frequancies as a function of the fiber volume fraction for different crack ratios a/H = 0.2, 0.4, 0.6.

Effect of Steering Wheel Vibration on drivers Hands in a Two-Wheel Drivers Hand tractor

* Ahmed Abd Ali Hamid
Dr. Mudhfer Kareem Abdullah
** Dr. Ahmed Abdul Hussein Ali
***Ali Fahad Fahem
* Department of Agricultural Mechanization, Collage of Agriculture, Baghdad University, Iraq.
** Department of Mechanical Engineering, Collage of Engineering, Baghdad University.
***Department of Mechanical Engineering, Collage of Engineering, Qadeseaia University.

Abstract

The paper presents research results of the vibration transmitted from the steering wheel of the tractor with a 2-wheel drive to the driver's hands. The vibration measurements were carried out on the tractor randomly chosen from the collage of agriculture / university of Baghdad. Before testing the tractor was examined and adjusted following the producer's recommendations. The vibration levels were measured during the operation tillage at idling and at full load .The field was 31.7 m above level sea. Soil was treated at soil constant moisture (17-20 %) with depth of plowing (17 cm). During operation the weather temperature was measured (15 C) and humidity was (27 %) The vibration level on the steering wheel was measured and analyzed .The frequency-weighted acceleration(RMS) , given in $m/\sec^2$, was calculated. The vibration total value was defined as the root-mean-square of the three component value

الخلاصة :

البحث يوضح تأثير الاهتزاز المنقول من عجلة القيادة إلى أيدي سائق جرار ثنائي الدفع . تم قياس الاهتزاز لجرار اختير عشوائياً من جرارات كلية الزراعة – جامعة بغداد . قبل أجراء التجربة تم تحضير الجرار حسب التوصيات المصنعية . مستويات الاهتزاز قيست خلال أجراء عملية حراثة عند تحميل المحرك الكامل والقليل . حقل التجربة يرتفع 31.7 متر فوق سطح البحر . أجريت معاملة التربة عند رطوبة ثابتة (17- 20 %) وبعمق حراثة (17 سم) . درجة الحرارة كانت (15مئوي) والرطوبة النسبية (27%) . مستوى الاهتزاز المنقول من عجلة القيادة تم قياسه وتحليله . وقياس تردد التعجيل المثقل (جذر مربع المتوسطات) بوحدة متر / ثانية تربيع . قيمة الاهتزاز الكلي عُرفت كجذر مربع المتوسطات للاتجاهات الرئيسة الثلاث .

Keywords: Ergonomics, Hand-transmitted vibration, Tractor, vibration exposure, steere wheel .

Introduction

The operators of the single-axle tractors (also known as two-wheel, walking or hand tractors) are especially exposed to hand-arm transmitted vibrations.

Farm tractors and other earth-moving equipment contribute to some of the most common, prolonged, and severe occupational exposures of vehicle vibration among equipment operators. The recognition of potential hazards has resulted in standards concerned with the vibration transmitted by the seats (ISO 5007, 2003) of these vehicles and the vibration exposure (ISO 5008, 2002) of vehicle operators (Griffin, 1990).

Exposure to whole-body vibration (WBV) and the postural requirements of the job have been identified as important risk factors in the development of musculoskeletal disorders (MSD) of the spine among workers exposed to a vibratory environment (Kittusamy and Buchholz, 2004; Kittusamy, 2002, 2003. Several investigators (Wikstrom et al., 1994; Seidel, 1993; have reported on the adverse health effects of WBV. NIOSH compiled a comprehensive body of epidemiological research presenting risk factor exposures for MSD, such as repetition, force, posture, and WBV. Acute health effects include loss of visual acuity, postural stability and manual control; whereas chronic health effects include low-back pain, early degeneration of the spine, herniated discs, and digestive and circulatory disorders. Long-term exposure to WBV may also contribute to disorders of female reproductive organs and disturbances of pregnancy (Seidel, 1993; Seidel and Heide, 1986). Furthermore, WBV may synergistically affect the development of noise-induced hearing loss (Seidel, 1993).

From experiments using percutaneous pin-mounted accelerometers, they determined resonances at fairly uniform frequencies for all subjects tested, first within a band of 4.5–5.5 Hz and subsequently in the 9.4–13.1-Hz range. They concluded posture, seating, and seat-back inclination affected the frequency response and that rocking of the pelvis essentially determined the response.

Vibration can produce a wide variety of different effects to the operators. Machine operators are usually exposed to two types of vibration: whole-body vibration transmitted via the seat or via the floor and feet, and hand-arm-transmitted vibration(Issever 2003). Both forms of vibration contribute to operator fatigue and can have a detrimental effect on job performance and health. To asses the effect of vibration, the vibration intensity and frequency must be taken into account together with exposure time. To quantify vibration exposure, measurements must be taken under representative conditions. Guidelines for measuring and evaluating human exposure and details of different analysis methods are given in ISO 2631-1-1997 for the whole-body vibration and ISO 5349-1 -2001 for the hand-arm-transmitted vibration. Excessive exposure to hand-transmitted vibration can induce disturbances in finger blood flow, and in neurological and motor functions of the hand and arm. It has been estimated that 1.7–3.6% of the workers in the European countries and USA are exposed to potentially harmful hand-transmitted vibration (Kacian, 1997).

These disorders are also included in a European list of recognized occupational diseases (ISO 5349-2001). The term ‘‘hand-arm vibration syndrome’’ (HAVS) is commonly used to refer to the complex of peripheral vascular, neurological and musculoskeletal disorders associated with exposure to hand-transmitted vibration. Although it is a very serious problem in several countries, Small attention is paid to it.

Almost any operator of forestry and agricultural mechanization is exposed to whole-body vibration and/or hand-arm-transmitted vibration. Even operators on jobs that seem easy, such as tractor driver, can be exposed to unexpected vibration. Specially unexpected are vibration transmitted from the

steering wheel to the driver's hands. This vibration was already recognized as a problem (Goglia and

Gospodaric 2002). The research which is presented in this paper was carried out on the tractor with a 2-wheel drive.

Material and methods

In the ISO 5349 recommendations, the most important quantity used to describe the magnitude of the vibration transmitted to the driver's hands is root-mean square frequency-weighted acceleration expressed in $m/\sec^2$. In addition, it is strongly recommended that for additional purposes frequency spectra should be obtained. Acceleration values from one-third-octave band analysis can be used to obtain the frequency-weighted acceleration ahw: It shall be obtained using (ISO 5008 :2002) :

$$a_{h.w} = \left[\sum_{j=1}^{n} (W_j a_{w.j})^2 \right]^{1/2} \quad (1)$$

Where $a_{w.i}$ is the acceleration measured in the i th one third-octave band in $m/\sec^2$, and W_j is the weighting factor for the ith one-third-octave band as shown in fig.1.

It is known that the vibration entering the hand contains contributions from all three measurement directions. Therefore, the measurement should preferably be made for all three directions simultaneously. In accordance with ISO 8727 the three directions of an orthogonal coordinate system in which the vibration acceleration should be measured is shown in Fig.2. For practical measurements, the orientation of the coordinate system may be defined with reference to an appropriate basicentric coordinate system originating in vibrating handle (steering wheel) gripped by the hand.

The evaluation of vibration exposure in accordance with ISO 5349-2001 is based on a quantity that combines all three axes. This is the vibration total value ahv and it is defined as the root-mean-square of the three component values:

$$a_{hv} = \sqrt{a_{hwx}^2 + a_{hwy}^2 + a_{hwz}^2} \quad (2)$$

Where a_{hwx}; a_{hwy}; a_{hwz} are frequency-weighted acceleration values for the single axes.

As it was mentioned before, the vibration exposure depends on the magnitude of the vibration total value and on the duration of the exposure. Daily exposure duration is the total time for which the hand(s) is (are) exposed to vibration during the working day. It is very important to base estimates of total daily exposure duration on appropriate representative samples for the various operating conditions.

The daily vibration exposure shall be expressed in terms of the (8 hours) energy equivalent frequency-weighted vibration total value as

$$A(8) = a_{hv} \sqrt{\frac{T}{To}} \quad (3)$$

Where T is the total daily duration of the exposure expressed in sec to the vibration ahv ; and $T0$ is the reference duration of 8 h (28 800 sec).

If the work is such that the total daily vibration exposure consists of several operations with different vibration magnitudes, than the daily vibration exposure, A (8 hours) shall be obtained using:

$$A(8) = \sqrt{\frac{1}{To} \cdot \sum_{i=1}^{n} a_{hvi}^2 \times T_i} \quad (4)$$

Where *ahvi* is the vibration total value for the *i*th operation, *n* is the number of individual vibration exposures, and T*i* is the duration of the *i*th operation.

The intention of the research was to define the vibration exposure level of the hand-arm-transmitted vibration from the tractor steering wheel to the driver's hands. The research was carried out on the tractor with a 2-wheel drive. Condition of tractor rebated be recommended ISO 5008 : 2002 , the tractor shall be in working order with full tank and radiator , but without optional front and rear weight , tire ballast, The tire used in test was stander size for tractor .Mold board plow with Massy Ferguson MF285tractor as one machinery unit figure.3and table1 and 2 .

The vibration levels transmitted to the driver's hands were measured under two operating conditions:

*** At idling.**

*** At full load**.

The measurement procedure was in accordance with ISO 5349-2001. The vibration levels were measured in all three axes simultaneously. For all three axes in both operating conditions the frequency spectra were obtained.

The arithmetic mean value of the acceleration values from one-third-octave band analysis was calculated. The frequency-weighted acceleration was calculated from the arithmetic mean value of the acceleration recommended in ISO 5349-2-2001 (see Fig. 4) The vibration meter have one accelerometer (one sensor) and we take five readers and we calculated the Mean value to each directions X, Y and Z (see table 3)

Calibration vibration meter

The vibration meter which used was type (VB-8201HA) and we make calibration with another vibration meter and gave the same results in each reading

Results

Measurement results can be grouped as follows:

1- frequency-weighted accelerations and the vibration total values for both operating conditions - weighted acceleration sum (WAS) values and their presentation in accordance with ISO 5349-1,-2001, table 3 .

2- The daily vibration exposure was obtained using Eq. (4).During an ordinary working day the driver spends approximately 6.5 h in effective work. The effective work consists of two dominant operations during which the tractor is either idling or at full load. The duration of idling is approximately 1.5 h. Thus, tractor is at the full load for 5 h per working day.

3- Vibration acceleration (R.M.S) increased with increasing velocity of tractor and in full load and decrease at idling and low velocity

Therefore, the total daily vibration exposure can be calculated as follows:

$$A(8)\,For\ .L1 = \sqrt{\frac{1}{To}\sum_{i=1}^{n} a_{hvi}^{2}\,Ti}$$

$$= \sqrt{\frac{1}{28800}(5400 \times 14.4^2 + 18000 \times 25.2^2)}$$

$$= 20.875\, m/\sec^2$$

$$A(8)\,ForL\,3 = \sqrt{\frac{1}{28800}(5400 \times 19.1^2 + 18000 \times 33.7^2)}$$

$$= 27.896\ m/\sec^2$$

Conclusion

Results of the study showed that the levels of vibration transmitted from steering wheel to hand a driver during the experiment was high comparing with ISO 5349-1: 2001.Velocity of tractor has a strong effect on transmitted vibration to hands driver from steering wheel all three perpendicular axes. Like these value acceleration (rms) effect on driver and caused

discomfort, will produce finger blanching, tired, less performance and not completely control operation to the tractor by driver. Therefore, it is necessary that persons who are responsible for occupational health and safety take preventive measures. It is presumed that vibration hazards are reduced when continuous vibration exposures over long period are avoided like take rest period after 2 – 4 hours from beginning work. Therefore, work schedules should be arranged to include vibration-free periods. We can reduce vibration transmit by use Hydraulic steeren wheel and use rubber material to connection steeren parts .

EN ISO 5349-2, 2001. Mechanical vibration—measurement and Evaluation of Human Exposure to Hand-Transmitted Vibration—Part 2: practical guidance for measurement at the workplace.

Goglia, V., Gospodari!c, Z., 2002. Driver's exposure to hand transmitted vibration from the steering wheel of the LPKT 40tractor, The 30th International Symposium on Agricultural Engineering, Opatija.

Griffin, M.J., 1990. Handbook of Human Vibration. Academic Press, New York.

ISO 5349-1-, 2001. Mechanical vibration—measurement and evaluation of human exposure to hand-transmitted vibration—Part 1: general Requirements, ISO, Geneva.

ISO. 5008:2002 Agricultural Wheeled Tractors and Field Machinery - Measurement of Whole-Body Vibration of the Operator. International Standardization Organization

Issever H, Aksoy C, Sabuncu H, Karan A: Vibration and itseffects on the body. *Med Princ Pract* 2003, 12, 34-38.

Kacian, N., 1997. A statistical report on occupational diseases in Croatia. Work and Safety 2.

Kittusamy, N., 2002. Ergonomic risk factors: a study of heavy earth moving machinery operators. Professional Safety Journal of the American Society of Safety Engineers October, 38 45.

Kittusamy, N., 2003. Self reported musculoskeletal symptoms among operators of heavy construction equipment. In: Proceedings of the XVth Triennial Congress of the International Ergonomics Association, Seoul, South Korea, /www.iea.orgS.

Kittusamy, N.K., Buchholz, B., 2004. Whole body vibration and postural stress among operators of construction equipment: a literature review. Journal of Safety Research 35, 255 261.

Pope, M.H., Wilder, D.G., Magnusson, M., 1998. Possible mechanisms of low back pain due to whole body vibration. Journal of Sound and Vibration 215 (4), 687 697.

Seidel, H., 1993. Selected health risks caused by long term, whole body vibration. American Journal of Industrial Medicine 23, 589 604.

Seidel, H., Heide, R., 1986. Long term effects of whole body vibration: a critical survey of the literature. International Archives of Occupational and Environmental Health 58, 1 26.

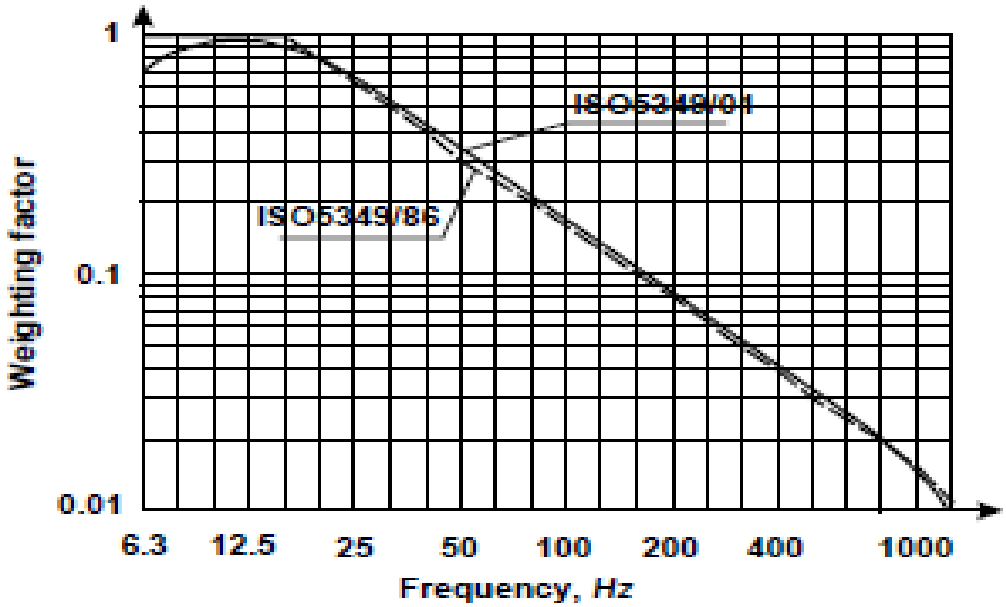

Fig. 1. Frequency-weighting factor curve for hand-transmitted vibration.

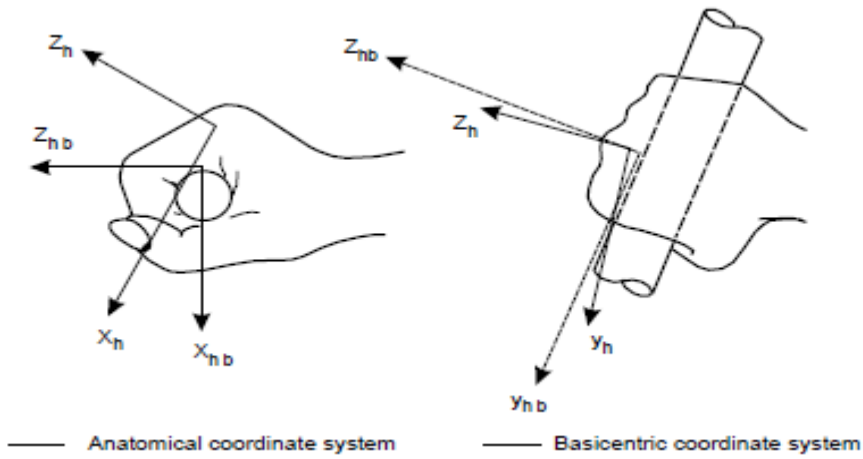

Fig. 2. Coordinate system for the hand (according to ISO 5349).

Fig. 3. Tractor Massy Ferguson MF285 and mold board plow as one machinery unit

Table 1 Tasted tractor – technical characteristics.

Technical characteristics	
Type	Massy Ferguson MF285
Power drive	2- wheel
Type engine	Perkins A4.248 / 4-stroke diesel with direct fuel injection
Cylinders no	4
Stroke length (mm)	115
Bore diameter (mm)	104
Engine power (H.P)	75
Cooling system	liquid force feed with thermostat
Maximal r.p.m	2000
Weight tractor unballasted (KN)	27.30
Tires front size	7-50 R16
Tires front pressure (psi)	35 *
Tires rear size	18-4 R30
Tires rear pressure (psi)	25

* Tires pressure during the operation.

Table 2 Three furrow mould board plough – specification.

Working width (mm)	1050
Max working depth (mm)	270
Weight (kg)	280

A - Measure longitudinal direction X

B - Measure lateral direction Y

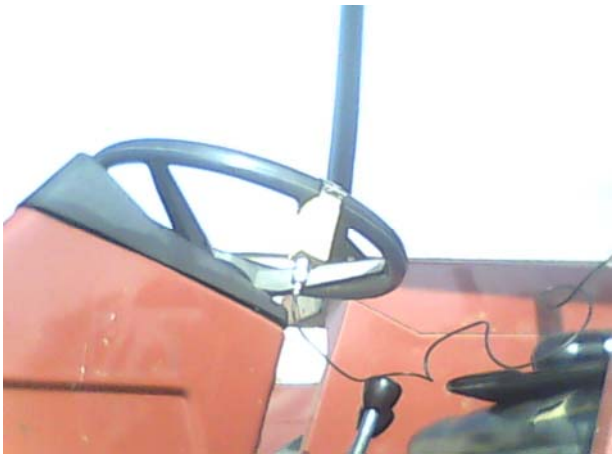

C - Measure vertical direction Z

Fig. 4. Accelerometer locations on steering wheel during measurement.

.

Fig. 5 Vibration meter & sensor

Table 3. Frequency-weighted accelerations and WAS values (weighted acceleration sum) for both operating conditions, $m/\sec^2$.

Gear box No	Acceler direction	Measuring No 1	2	3	4	5	Mean value
L1*	(a)**						
	X	5.4	5.2	5.6	5.8	5.4	5.5
	Y	4.3	4.1	4.5	4.4	4.3	4.3
	Z	12.5	13.6	12.2	12.0	12.7	12.6
	WAS						14.4
	(b)***						
	X	13.2	14.1	14.0	13.5	13.8	13.7
	Y	11.1	10.5	10.6	11.3	10.9	10.9
	Z	19.6	17.0	17.5	17.8	18.6	18.1
	WAS						25.2
L3	(a)						
	X	6.4	6.2	6.8	7.1	7.4	6.8
	Y	5.4	5.2	5.1	5.8	5.6	5.4
	Z	17.6	16.5	16.8	17.2	17.0	17.0
	WAS						19.1
	(b)						
	X	16.7	16.1	16.3	17.2	17.5	16.8
	Y	11.9	11.6	12.0	12.4	12.8	12.1
	Z	25.3	26.2	26.0	27.5	28.0	26.6
	WAS						33.7

* L1 is referring to gear number One from the gear box.
L3 is referring to gear number three from the gear box
** (a) at idling without operation tillage.
*** (b) at full load with operation tillage.

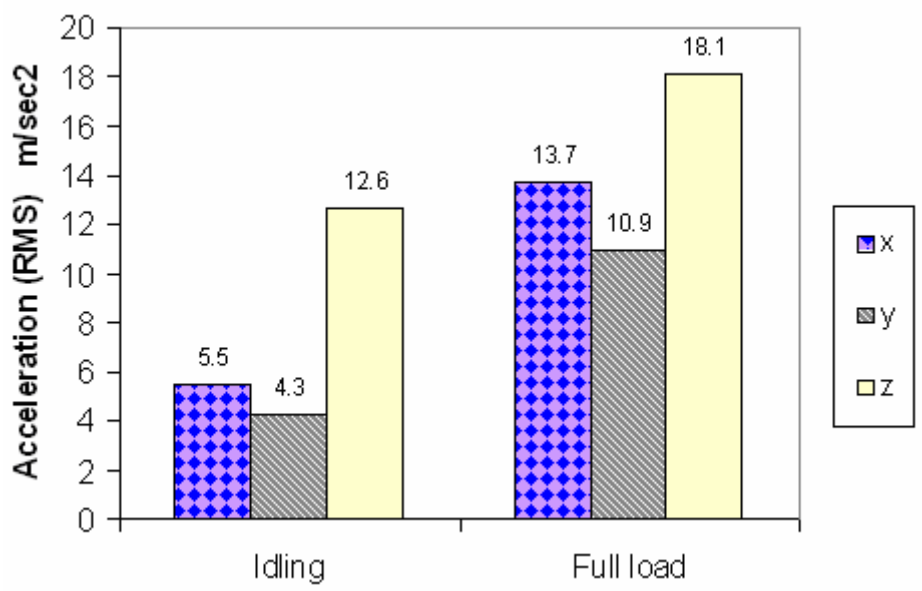

Fig.6. Mean Values of Acceleration (RMS) of three measurements of both operation conditions (X-Y-Z direction) on L1 GEAR BOX.

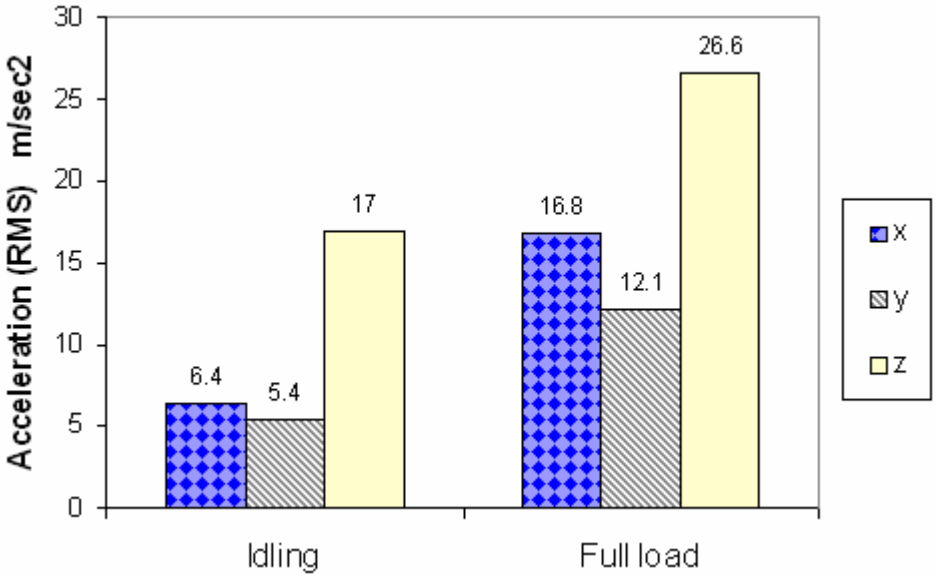

Fig.7. Mean Values of Acceleration (RMS) of three measurements of both operation conditions (X-Y-Z direction) on L3 GEAR BOX.

DESIGN, CONSTRUCTION AND TESTING OF LOW SPEED WIND TUNNEL WITH ITS MEASUREMENT AND INSPECTION DEVICES

Prof. Dr. Ihsan Y. Hussain* **Asst. Lect. Maki H. Majeed***

Lect. Anmar H. Ali* **Lect. Wail S. Sarsam***

* Mech. Engr. Dept., College of Engineering, University of Baghdad

ABSTRACT

A low speed open circuit wind tunnel has been designed, manufactured and constructed at the Mechanical Engineering Department at Baghdad University - College of Engineering. The work is one of the pioneer projects adapted by the R & D Office at the Iraqi MOHESR. The present paper describes the first part of the work; that is the design calculations, simulation and construction. It will be followed by a second part that describes testing and calibration of the tunnel. The proposed wind tunnel has a test section with cross sectional area of (0.7 x 0.7 m^2) and length of (1.5 m). The maximum speed is about (70 m/s) with empty test section. The contraction ratio is (8.16). Three screens are used to minimize flow disturbances in the test section. The design philosophy is discussed and methods for wind tunnel calculation are outlined. Simulation of wind tunnel using ANSYS shows no separation of flow along wind tunnel. Construction steps are also included in present work.

الخلاصة:

تم تصميم و تصنيع و بناء نفق هوائي مفتوح واطى السرعة في قسم الهندسة الميكانيكية في كلية الهندسة – جامعة بغـداد. يمثل العمل احد المشاريع الريادية التي تبنّتها دائرة البحث و التطوير في وزارة التعليم العالي و البحث العلمي العراقية. يتطرق البحث الحالي الى الجزء الاول من العمل و هو الحسابات التصميمية ، التمثيل على الحاسبة والتصنيع، و سوف يتبعه جزء ثاني يتطرق الـى اختبار و معايرة النفق. للنفق الهوائي المقترح مقطع اختبار مساحته (7,. x 7,. م^2) و طول (1,5 م). سرعة الهواء القصوى فـي مقطع الاختبار و هو فارغ تبلغ (70 م / ثا). نسبة التخفيض في المساحة هي (8,16). تم استخدام ثلاثة مشبكات لتقليل الاضطراب في مقطع الاختبار. سوف تتم مناقشة فلسفة التصميم و طرق الحسابات المتبعة في البحث. تم تمثيل النفق علـى الحاسـبة باسـتخدام برنامج (الانسيز) وقد بينت النتائج عدم حصول انفصال للجريان على طول النفق الهوائي. تضمن البحث الحالي ايـضا خطـوات البناء للنفق الهوائي.

Key Words: Wind Tunnel, Low Speed, Design, Simulation and Construction

INTRODUCTION

The development of fluid mechanics involves observation and study of the physical phenomena which form the basis of the theory. Experimental aerodynamics serves to check the existing theory and also its extension. On the other hand, theoretical developments strongly influence experimental ones.

The wind tunnel is an important available device for experimental work in aerodynamics and it can be considered the main tool for aerodynamics design of aircrafts, rockets, turbo-machines…etc; its main function is to provide a uniform and controllable air flow through the test section.

At low speed, dynamic similarity requires the equivalence of Reynolds number, but since the model is visually a scaled down body, this equivalence is difficult to achieve unless a pressurized tunnels are used. However if the Reynolds number exceeds 10^5, it is assumed that the exact equivalence is not essential **(Raikan 2001)**. The basic tunnel type is an open circuit tunnel with suction or blowing as shown in **Fig.1**. The air flows in straight path from the entrance through a settling chamber with contraction to the test section, followed by a diffuser, a fan section and an exhaust of the air. In suction wind tunnel the closed test section pressure is less than that in the surrounding medium, this make it more difficult to carry out test, and introduces inaccuracies into the determination of the forces acting on the model, since atmospheric air enters through the walls of the test section.

The design of the open circuit wind tunnel selected in the present work will be done by analyzing the flow through each component such as the contraction section, test section, and diffuser section. The available literatures that deal with the design of wind tunnel or those components are illustrated firstly. **(Pope and Harper 1966)** pointed out the most important recommendations and presented guide lines for the design of low speed wind tunnel, also by using empirical correlations they presented a design procedure for the fan required for the wind tunnel.**(Milan Valajinac 1970)** summarized the design, construction and calibration of a subsonic wind tunnel. The design philosophy is discussed and methods for wind tunnel calculations are outlined. Comparisons of measured wind tunnel parameters are shown to be in excellent agreement with design calculations. **(Bradshaw and Mehta 1979)** presented design guide lines for the main components of a wind tunnel, the fan, wide angle diffuser, settling chamber, contraction, screens, honey combs and exit diffuser for small low speed wind tunnels, also in similar way as in **(Pope and Harper 1966)**. In **(Raikan 2001),** a subsonic wind tunnel design of closed circuit type for a range of Mach No. in the test section up to 0.7 has been carried out and a mathematical models describe the flow in each component of the wind tunnel are made. The comparisons between the results obtained from their design and the literature were done and they showed that a good agreement exist with these results. In the present work the dynamic pressure in the test section was originally chosen to be more than 3 kpa as a basis for a power requirement and performance calculations, so that the particular fan and power plant selection must match the calculated wind tunnel requirements.

WIND TUNNEL DESIGN CONSIDERATIONS

Mathematical models describing the flow analysis through all components of low-speed wind tunnel are made in this article. The flow field is assumed incompressible throughout the tunnel, and the model for each part is then linked to predict power requirements. The chosen tunnel and its components are also investigated. The wind tunnel shown in **Fig.1** is to be designed and analyzed for its dimensions. It has a square cross section with side equal to (0.7 m) and length is taken to be (1.5 m), since it may be sufficient for testing large models. The total divergence angle (2α) of (1.28°) for one pair of walls is chosen as will be shown later during analysis to maintain approximately constant average Mach number along the test section.

POWER REQUIREMENTS

The power required to maintain steady flow through the wind tunnel is equal to the total losses occurring in the flow through the tunnel. These losses are due to kinetic energy being dissipated by vortices and turbulence. The loss in kinetic energy, which appears as a decrease in total pressure must be compensated by pressure rise usually provided by a fan. The power input to the fan is the motor shaft output, and the fan has efficiency (η). The equation balancing the energy input to the stream to the energy losses in the tunnel is:

$$\eta \square = \sum \text{circuit losses} \quad (1)$$

As pointed-out previously the tunnel can be divided into sections with energy loss of each section written as a drop in pressure Δp or a pressure drop in coefficient $K_i = \Delta p_i / q_o$, Where q_o is the test section dynamic pressure ($1/2\rho_0 v_0^2$). The flow energy through the test section is:

$$E_0 = 1/2\rho_0 v_0^3 A_0 \quad (2)$$

For subsonic flow with M<0.4, $\rho_0/\rho i=1$ (within 1% error) and **eq. (1)** becomes **(Milan Valajinac 1970)**:

$$\eta = 1/2\rho_0 v_0^3 A_0 \sum_i K_i \quad (3)$$

The required power for a given test section size and flow conditions depend on the sum of the pressure drop coefficients (K_i) in various tunnel sections and a reduction in their coefficients improves the tunnel efficiency. The energy ratio defined as:

$$E.R = \frac{1/2\rho_0 v_0^3 A_0}{\eta} = \frac{1}{\sum_i K_i} \quad (4)$$

And is a measure of the tunnel efficiency.

1. The Contraction Section

It has a square cross section of (2x2) m^2 at inlet with an area ratio of (8.16: 1). The contraction wall shape profile, see **Fig.2**, consists of two elliptic arcs matching at a point; the position of maximum slope. The dimensions have been scaled so that the width at the entrance is unity. The arcs are then uniquely specified by the length L. the equations for the arcs in Y and Z direction are given by;

$$y_w = \left(a_w - b_w\sqrt{1 - \frac{x^2}{c_w^2}}\right) \qquad 0 \le x \le \overline{p_w}$$

$$y_w = \left(d_w - e_w\sqrt{1 - \frac{(x^2 - L)}{f_w^2}}\right) \qquad \overline{p_w} \le x \le L$$

$$z_h = \left(a_h - b_h\sqrt{1 - \frac{x^2}{c_h^2}}\right) \qquad 0 \le x \le \overline{p_h}$$

$$z_h = \left(d_h - e_h\sqrt{1 - \frac{(x^2 - L)}{f_h^2}}\right) \qquad \overline{p_h} \le x \le L$$

$$a = \left(\frac{\bar{H}^2 - \bar{p}\bar{T}\bar{H} - \frac{1}{(4ra)^2}}{2\bar{H} - \bar{p}\bar{T} - \frac{1}{ra}}\right)$$

$$b = \left(a - \left(\frac{1}{2ra}\right)\right)$$

$$c^2 = \left(\frac{\bar{p}b^2}{\bar{T}(a - \bar{H})}\right)$$

$$d = \left(\frac{\bar{H}^2 + \bar{T}\bar{H}(L - \bar{p}) - \frac{1}{4}}{\bar{T}(L - \bar{p}) + 2\bar{H} - 1}\right)$$

$$e = \frac{1}{2} - c$$

$$f^2 = e^2(L - \bar{p})/\bar{T}(\bar{H} - d)$$

$$ra_w = \left(\frac{w1}{w2}\right)$$

$$ra_h = h_1/h_2$$

$$\bar{p} = (L/(1 + ra))$$

$$\bar{H} = \left(\frac{1}{ra + 1}\right)$$

$$\bar{T} = \left(\frac{2(ra - 1)}{Lra}\right)$$

(5)

Once separation is assured not to exist, simple procedure to predict performance is the regular one-dimensional flow method. The final differential equation which describes this flow affected by area change and friction is given by **(Shapiro 1953)** as follows;

$$\frac{dM^2}{M^2} = \left[\frac{1 + \frac{(\gamma - 1)M^2}{2}}{1 - M^2}\right]\left\{-2\frac{dA}{A} + \gamma M^2 \frac{4fdx}{DH}\right\} \quad (6)$$

The friction factor in this equation will be calculated from the following relation mounted by **(Shapiro 1953)**, for the subsonic flow:

$$f = \left[1 - \frac{1.12}{\log_{10}(R_{e)}}\right] \tag{7}$$

Where:

$$C_D = \frac{0.42}{\log_{10}(R_e)\left[1 - \frac{\gamma - 1}{2} M^2\right]}$$

$$\text{and Re} = \frac{\rho v_{av} D_H}{\mu} \tag{8}$$

$$D_H = \frac{4 y_w z_h}{(y_w + z_h)}$$

$$A = 4 Y_w Z_h$$

Also, the Sutherland law of viscosity **(Schlichting 1979)**, is used to calculate viscosity:

$$\frac{\mu}{\mu_0} = \left[\frac{T}{T_0}\right]^{3/2} \left[\frac{T_0 + S_1}{T + S_1}\right] \tag{9}$$

Where T_0 is reference temperature taken to be equal to (273.6 K) and μ_0 denotes the viscosity at reference temperature which is (1.708×10^{-5} Pa.s), and S_1 is constant whose value for air is (110 K).

2. Test Section

The main purpose in the design of the test section is to maintain approximately constant static pressure with slightly small change in the average Mach number throughout the test section. Therefore; the cross sectional area should gradually increases in the flow direction to compensate for the thickening of the boundary layer which cause the reduction in the static pressure along the test section, so divergence angle for one pair of the walls will be made, and this may be calculated by assuming the test section as fully turbulent and the boundary layer begins at entrance. For turbulent layer, the displacement thickness could be calculated as **(Schlichting 1979)**;

$$\delta^* = 0.479 * x / (R_x)^{1/5} \tag{10}$$

By considering the test section with constant height, the upper and lower walls are deflected to prevent boundary layer growth. This design provides good view to users. To find losses inside wind tunnel test section, the only losses comes from friction losses so that the losses are:

$$\frac{\Delta P}{1/2 \rho_0 v_0^2} = K_{ts} = f \frac{L}{D_0} \tag{11}$$

where Do represents hydraulic diameter of test section and f is a friction factor, and it is assumed constant along test section and approximately equals to (f = 0.01).

3. Diffuser

The diffuser is used to reduce the power losses due to high flow velocity. Generally; the velocity must decrease with distance without any separation of boundary layer at walls. One of the side effects of separation is the vibration of the fan which then causes change in velocity at test section. The divergence angle is:

$$\theta = \tan^{-1}\left(\frac{R_2 - R_1}{L}\right) = \tan^{-1}\left(1/2 \frac{\sqrt{AR} - 1}{L / D_1}\right) \tag{12}$$

Where $A_R = A_2 / A_1$

One of the most important aspects in diffusers design is that the divergence angle must be small to ensure no separation of boundary layer at wall. But this mean long diffuser for high aspect ratio and may be costly inefficient. **Fig.3** shows the relation between 2θ and aspect ratio for two type of diffusers 2D and axisymmetric diffuser, From **(Wallis 1983).** The pressure losses in diffuser can be calculated with the same equations used in contraction section and same procedure or by using equation listed in **(Pope and Harper 1986):**

$$k_f = \left(1+\frac{1}{AR^2}\right)\frac{f}{8 \quad \sin\theta}$$
$$k_{ex} = k_e(\theta)*\left(\frac{AR-1}{AR}\right)^2 \qquad (13)$$

$$K_e=0.1709-0.117\theta+0.0326\theta^2+0.0010078\theta^3-0.0009076\theta^4-0.000013310\theta^5+0.000013450\theta^6$$
$$1.5^\circ \le \theta \le 5^\circ \qquad (14)$$
$$K_d = k_f + k_{ex}$$

4. Settling Chamber and Straighteners

The two sections are used to decrease the turbulence in flow and make it straight by using honeycombs and screens. The velocity at these sections must be low to decrease the pressure losses in wind tunnel. Screens reduce the axial turbulence more than the lateral turbulence; they have a relatively large pressure drop in the flow direction. Honeycombs have small pressure drop and this have less effect on the axial velocities but they reduce lateral turbulence. **(Pope and Harper 1986)** presents a method for calculating these components depending on semi-empirical equations which used in the coming sections to calculate the pressure drop on the settling section.

5. Entrance

The entrance may be divided into two components. The first called (bell mouth) and the other is a converged duct as show in **Fig.1**. Bell month is an important part in wind tunnel because it improves air flow entrance which decreases the energy losses and increase the amount of air enters the wind tunnel. The design equation of the entrance given by **(Bleier 1997)** is (r = 0.14 D). Same equations and procedure used in contraction section and diffuser are used for the entrance to find energy losses.

NUMERICAL SOLUTION

The numerical solution procedure to solve the governing differential equations and auxiliary relations which are derived in mathematical model for wind tunnel component is described here.

The contraction section consists of a square cross section and with two elliptical cross-sectional areas which represent the wall shape profiles, also two parallel ducts are connected upstream of the contraction toward the last screen and downward to the test section. The flow through the contraction is considered. One dimensional compressible flow affected by area change and friction is used. The final equation which describes the one dimensional flow affected by area change and friction is given by **eq. (6)**. The numerical solution of this equation is done by dividing the contraction section into a number of equal small elements each of length Δx, and the conditions at the inlet are known, the calculation proceeds step by step using a forward finite difference scheme. So **eq. (6)** is written in forward finite difference form. The problem here is that the conditions at the inlet are unknown, but they are known at the exit, and hence the forward finite difference scheme cannot be used, so **eq. (6)** will be written in a backward finite difference form. Solution of this equation step by step gives the inlet conditions. Then the forward finite difference scheme is used with these inlet conditions to obtain the new exit conditions. The friction factor is calculated from **eq. (7)**. Three of wind tunnel parts are calculated by this procedure (Entrance, contraction section and diffuser). In the diffuser the inlet conditions are known, so that, backward difference is not needed.

A computer program was developed to perform the numerical solution formulated and described above. The computer program was written in FORTRAN language and designed to give the distribution of the flow quantities along the wind tunnel. The flow chart of the program is shown in **Fig.8.**

DESIGN CALCULATIONS

The numerical results obtained from the developed computer program in the present work which describe the flow analysis through the all wind tunnel components mentioned previously are presented here.

Test Section

The conditions at the test section are;

- Square inlet area (700*700 mm^2)
- Test section length (1500 mm)
- The dynamic pressure (3000 Pa) and velocity (70 m/s)

From **eq.(10),** the displacement thickness based on Reynolds number of ($3.3*10^6$) is calculated to be equal to (δ^*=3.55 mm). So, the longitudinal direction with width constant along the test section becomes (7.01 mm), it can be approximated to (10 mm) so that the test section dimensions become:

- test section entrance→ (700*700 mm^2)
- test section exit→ (700*710 mm^2)
- test section length→ (1500 mm)

The pressure losses occur at test section could be calculated by assuming constant cross section and the friction factor also constant. So that, from **eq. (11)** (kts = 0.021) for friction factor (f = 0.01).

Contraction Section

For the contraction ratio (8.16: 1) where inlet area is (2000x2000 mm^2) and exit area equal to (700x700 mm^2), the numerical solution was made with the following parameters see **Fig.2**:

- Number of divisions equal to 1000 small elements.
- Convergence limit is 1.0E-5

```
TUNNEL NOZZLE DIMENSIONs:-
=========================
L =        1.5000      m

W1=        2.0000      m
H1=        2.0000      m

W2=        0.7000      m
H2=        0.7000      m

LW =       1.7030      m
LZ =       1.7030      m
CR =       8.1633

OUTPUT PROPERTIES:-
===================
M_OUT = 0.2022
V_OUT = 70.0000          m/s
P_OUT = 98510.0000       Pa
T_OUT = 298.4000         K
RO_OUT = 1.1503          Kg/m3
PO_OUT = 101357.0715     Pa
TO_OUT = 300.8390        K

INPUT PROPERTIES:-
==================
M_IN = 0.0241
V_IN = 8.3979 m/s
P_IN = 101307.2628       Pa
T_IN = 300.8039          K
RO_IN = 1.1735           Kg/m3
PO_IN = 101340.1849      Pa
TO_OUT = 300.8390        K

CONTRACTION LOSSES K:-
======================
Kn = 0.0060          this represent nozzle pressure losses.
```

Diffuser

The energy losses at any point in the wind tunnel depend on the cubic velocity at that point. So that, the diffuser works to decrease the velocity with minimum losses and higher back pressure. Generally it must decrease the velocity without boundary layer separation at the wall.

The relation between divergence angle 2θ and ratio of inlet diameter to length of the diffuser for two type of diffuser (2D and cone diffusers).The following are the diffuser dimensions:

- Inlet diffuser diameter D_1=700mm
- Outlet diffuser diameter D_2=1500mm = fan diameter
- Diffuser length =6000mm
- The divergence angle is = θ = 7.6°
- Aspect ratio of diffuser AR = 4.527

When comparing the diffuser dimension with that in **Fig.** (3) for cone diffuser, the ratio will be (N/R1) =17 this mean the divergence angle will be equal to 7.25°. So it represents good approximation for dimensions. The losses at diffuser could be calculated numerically as mentioned previously and the results are:

```
TUNNEL DIFFUSER DIMENSION:-
=========================
L =        6.0000      m

W1=        0.7000      m
H1=        0.7100      m

D2=        1.5000      m
AR =       4.5270

INPUT PROPERTIES:-
==================
M_IN = 0.2022
V_IN = 70.0000           m/s
P_IN = 98510.0000        Pa
T_IN = 298.4000          K
RO_IN = 1.1503           Kg/m3
PO_IN = 101357.0715      Pa
TO_IN = 300.8390         K

OUTPUT PROPERTIES:-
===================
M_OUT = 0.0437
V_OUT = 15.1755          m/s
P_OUT = 101133.5630      Pa
T_OUT = 300.7244         K
RO_OUT = 1.1718          Kg/m3
PO_OUT = 101534.3830     Pa
TO_OUT = 300.8390        K
```

CONTRACTION LOSSES K:-
==========

K_d= 0.0629 This represents diffuser pressure losses.

It must be noted that the losses in contraction equal to 0.006 and in diffuser equal to 0.0629, in **(Pope and Harper 1966)** there is an experimental relation to find the losses in this section. In diffuser there are two types of losses, Friction (K_f) and expansion (K_{ex}) losses. The friction factor and density assumed constant along this section. The equations as in **(Pope and Harper 1966)** are,

$$K_f = \left(1+\frac{1}{A_R^2}\right)\frac{f}{8\times\sin\theta}$$

Friction factor could be calculated from moody diagram which its value at Re = $33*10^6$ is f = 0.01; K_f = 0.019. The expansion losses could be calculated from equation,

$$K_{ex}= K_e(\theta)\left(\frac{A_R-1}{A_R}\right)^2$$

K_e=0.1709-0.117θ - $0.0326\theta^2$ – $0.00178\theta^3$ – $0.00090076\theta^4$- $0.000013310\theta^5$ + $0.00001340\theta^6$

For θ = 3.8° and AR = 4.527 the expansion losses is K_{ex}= 0.0580 and total diffuser losses is,

K_d= K_e + K_{ex} = 0.019+0.0580 = 0.077

As show in calculations the two solutions are approximately same. The increase in losses is due to boundary layer, which is not considered in the previous calculations.

Settling Chamber and Straightener:-

The dimensions of settling chamber are,

- length of section = 1500 mm
- Entrance area (2000x2000) mm^2
- Three stage of screen

For strengthener the dimensions are,

- length = 450 mm
- Entrance is (700x700) mm^2
- One stage of screen

Screens are used to decrease the turbulence in the flow due to the fluctuating velocities in three components. So that the characteristics of screens are

- (8*8) 64 mesh pre cm^2
- The wire diameter of 0.39 mm

The losses in settling chamber may be calculated by taking the entrance velocity which is 8.4 m/s as calculated in contraction. The Reynolds number at this section is Re = 225.455 and from **(Pope and Harper 1986)** the losses calculation for Settling chamber and straitghtener are K = 2.2 with respect to local velocity of Settling chamber. For three stage the total losses in Settling chamber and straightened are K = 0.095 with respect to the dynamic pressure at the test section.

Entrance

The dimensions of entrance are:

- Inlet hydraulic diameter equal to 2000 mm (2000x2000) mm.
- The inlet bell mouth radius equal to 280 mm.
- Length of section 1200 mm.
- to enhance the flow enter to this section and decrease the flow velocity the dimension of entrance area increased 10 mm so that the dimension becomes 2100 mm height and 2100 width

Losses in this section becomes as,

TUNNEL ENTRANCE DIMENSION:-
==========

L = 1.2000 m

W1= 2.1000 m
H1= 2.1000 m

W2= 2.0000 m
H2= 2.0000 m
AR = 0.9070

INPUT PROPERTIES:-
==========

M_IN = 0.0220
V_IN = 7.6190 m/s
P_IN = 101300.0000 Pa
T_IN = 298.4000 K
RO_IN = 1.1828 Kg/m3
PO_IN = 101334.3358 Pa
TO_IN = 298.4289 K

OUTPUT PROPERTIES:-
==========

M_OUT = 0.0243
V_OUT = 8.4004 m/s
P_OUT = 101292.1583 Pa
T_OUT = 298.3938 K
RO_OUT = 1.1828 Kg/m3
PO_OUT = 101335.2135 Pa
TO_OUT = 298.4289 K

CONTRACTION LOSSES K:-
==========

K_E = 0.0003 This represents the entrance pressure losses.

Fan

A major work in designing fan is that it must provide a required velocity at test section (70 m/s) and to resist the decrease in pressure along the wind tunnel. The total pressure loss can be calculated as:

$TP = K_E + K_{SC} + K_N + K_{TS} + K_D =$
$0.0003+0.095+0.006+0.21+0.077 = 0.1993 \approx 0.2$

Usually a safety factor may be taken as 25% thus;

$K_T = 0.25$

$$\Rightarrow \Delta P = K_T \times 0.5 * \rho_0 \upsilon_0^{\,2} \Rightarrow \Delta P = 750.3125 \qquad Pa$$

So that, the total pressure loss at fan could be found by:

$A_{fan} = 1.767\ m^2$; $V_{fan} = A_{bs}V_{ts}/ A_{fan} = 1904.1$ m/s

$P_f = 0.5\ \rho_0\ V^2_{fan} = 0.5 * 1.225 * 19.41^2 = 230.75$ Pa

$\Delta P_T = \Delta P + P_f = 750.3125 + 230.75 = 981.0025$ Pa

The power required is :

Power $= A_F * V_F * \Delta P_T = 1.767 * 19.41 * 981.0025 = 33647.96$ W

Power (hp) = 33647/ 750 = 44.86 $\approx$ 45 hp

For BHP = 60% approximately then

EFF = power (hp)/ BHP $\Rightarrow$ BHP = 74.7667 $\approx$ 75 (hp)

This power is more than that needed, but for future work when velocity increases to 100m/s at test section it may give the required power.

The following are dimensions and characteristics of fan;

- Axial simple fan
- Hub diameter 500 mm
- Blade diameter 1500 mm
- Blade length is 450 mm
- Number of blades are 12
- Tilt angle of blade is 30°
- Length of convex shape of blade is 300 mm
- Outer diameter of fan is 1510 mm
- Number of revolution per minute is 1500 rpm.
- Steel sheets with thickness equal to 6mm are used in manufacturing the blades.

Wind Tunnel Simulation:

In recent years, **ANSYS** represents a good tool to find a mechanical and flow properties for complex configuration. Therefore it was used to simulate the flow inside wind tunnel of the present work.

The first step in simulation is to model the wind tunnel and to create its parts to apply the boundary conditions. These boundary conditions must be applied accurately to ensure good results. **Figs. (4, 5, and 6)** show **ANSYS** steps for the present wind tunnel (Modeling ,boundary condition, meshing and solving using **FLOTRAN** three dimensional solutions).

ANSYS solution shows that test section is approximately have a constant velocity near (70 m/s) along test section as shown in **Fig. (6),** which represents most important part of the wind tunnel. This indicate that our design is fair enough since there is no flow separation in velocity at test section or at least no thickening boundary layer at this region which may cause an error in measurement.

Wind Tunnel Construction

An open circuit wind tunnel was designed and constructed incorporating features discussed in previous articles. The following group figures show the construction of parts of the wind tunnel and its final shape.

Test Section

A test section was designed to give a velocity of 70m/s and size equal to (700x700) mm^2 inlet area and 1500mm long section. Transparent Plexiglas was used entirely in its construction to provide viewing of the model. A square cross section with upper and lower surface diverges along the section to balance the boundary layer growth. This may provide a constant pressure along test section and prevent error in measurements. A steel form was constructed and used to hold the Plexiglas's and prevent them to make convex shape due to low pressure at test section (less than atmospheric pressure).

Contraction and Settling Sections

The contraction shape and settling section were made of steel galvanized plate to prevent corrosion and it's strong enough to give safety work with velocity 70m/s. Both have square cross section. The contraction ratio is (8.16:1). The wall shape was designed using the previous equations. The settling section contains [(8x8)64 – mesh per cm^2 and diameter 0.39mm]. Both sections are mounted on stands held on the ground by bolts.

The contraction section is joined to test section by a mating flange which compresses an O-ring rubber there by sealing joints.

Inlet Section

Inlet section and bell mouth are made of galvanized steel. The bell mouth increases the efficiency of air inlet and prevents what is called vena contracta. All wall plate of inlet section made pyramid shape with inlet and outlet area. Flanges are constructed at ends of parts with O-ring sealing and lifted from ground by stand structure holder on the ground.

Diffuser

The diffuser was made of galvanized steel plate with circular cross section so that, there must be converting sections which convert the square section at test section to the circular cross section of the diffuser. So it was decided to make the diffuser and converter section in same part. This gives a gradually grading of transformation. The diffuser then has a square cross section at inlet and circular cross section at exit. A constant divergence angle of (7.6°) between upper and lower surfaces was made. The diffuser exit matches the fan inlet with (1510mm) diameter.

Four crosse shape plates placed inside diffuser before fan section and holder on the diffuser wall. These plats prevent the swirling action of the flow due to fan rotation and decrease losses in fan work

Power Plant:-

An axial fan driven by a (75hp) (1500rpm) amplitude lament motor provides the power to the tunnel. The fan is mounted at the end of tunnel and swallows the flow from tunnel inside and discharged it to outside. The power plant section mounted on the ground by a structure and connected with diffuser with a double sealing rubber to prevent vibrational motion during its operation. The fan manufactured by steel of 6mm thickness and 12 vanes with probability to change or maintenance.

Power Supply and Motor Speed Control:-

In order to have motor speed control from zero to 1500rpm a power supply and motor speed control were provided to the wind tunnel power plant.

CONCLUSIONS

An open circuit wind tunnel has been designed, simulated and constructed to obtain as speed of 70 m/s at test section of (0.7x0.7) m^2. The design procedure shows the wind tunnel losses are approximately equal to 0.25 with respect to the dynamic pressure at test section. A 75 HP AC motor with regulator are used to control its velocity from 0-70 m/s. The wind tunnel was simulated and solved using ANSYS commercial program. The results show that the test section has a constant velocity along it. The construction is then being done using the dimensions of the wind tunnel. The test work and calibration will be done in the next part of the paper.

ACKNOWLEDGEMENT

We would like here to acknowledge the (Research and Development (R & D) Office at the Iraqi Ministry of Higher Education and Scientific Research MOHESR), which adapted the present project as one of the pioneer projects, and supported it financially.

REFERENCES

Bradshaw P. and Mehta R. D., “Design Rules for Small Wind Tunnels”, Aeronautical Journal, November 1979, p.p. 443-449.

Frank, P. B., “Handbook Selection, Application and Design”, McGraw-Hill, 1997.

Milan Vilaginac, “Design, Construction and Evaluation of a Subsonic Wind Tunnel”, M.Sc. thesis, MIT, June 1970.

Pop a. and Harper j. j., “Low Speed Wind Tunnel Testing”, McGraw-Hill, 1986.

R. Allan Wallis, ”Axial Flow Fan and Ducts”, John Wiley and sons, 1983.

Raikan S. Dawas, “Proposal for Subsonic Wind Tunnel Suitable in Iraq”, M.Sc.Thesis, University of Baghdad, September, 2001

Schlichting, H., "Boundary Layer Theory", McGraw-Hill, 6th Edition, 1968.

Shapiro, A. H., "The Dynamic and Thermodynamic of Compressible Fluid Flow", Vol I, Ronald Press, New York, 1953.

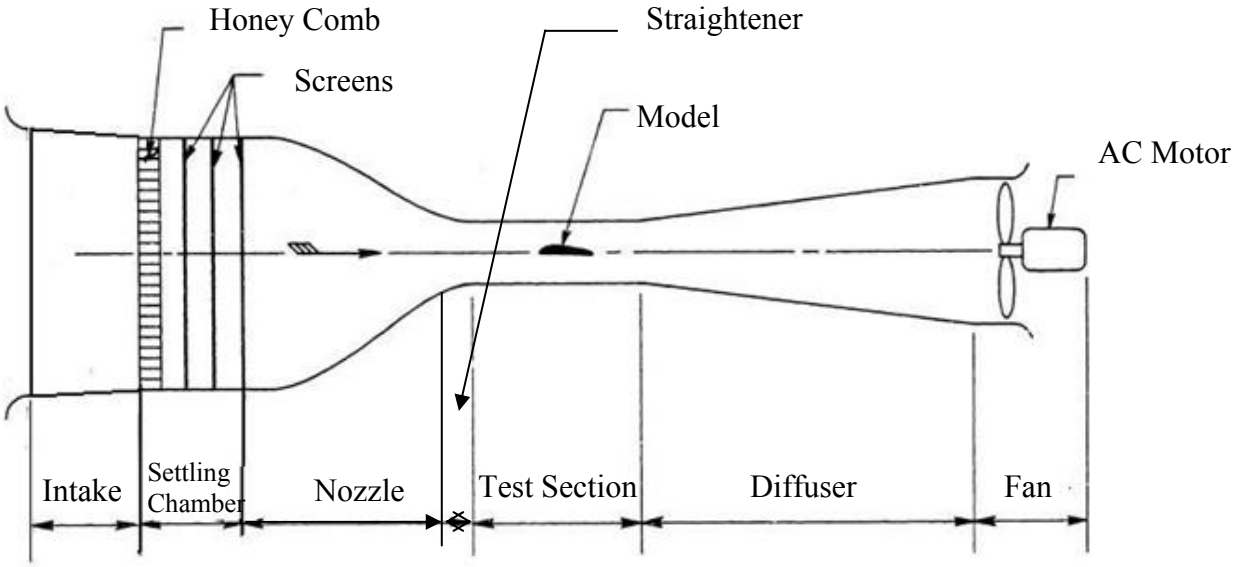

Fig.1: Wind Tunnel Parts.

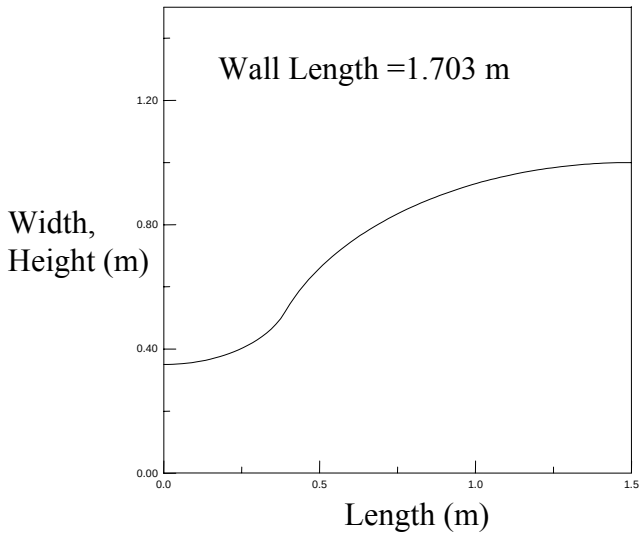

Fig.1: Contraction wall shape.

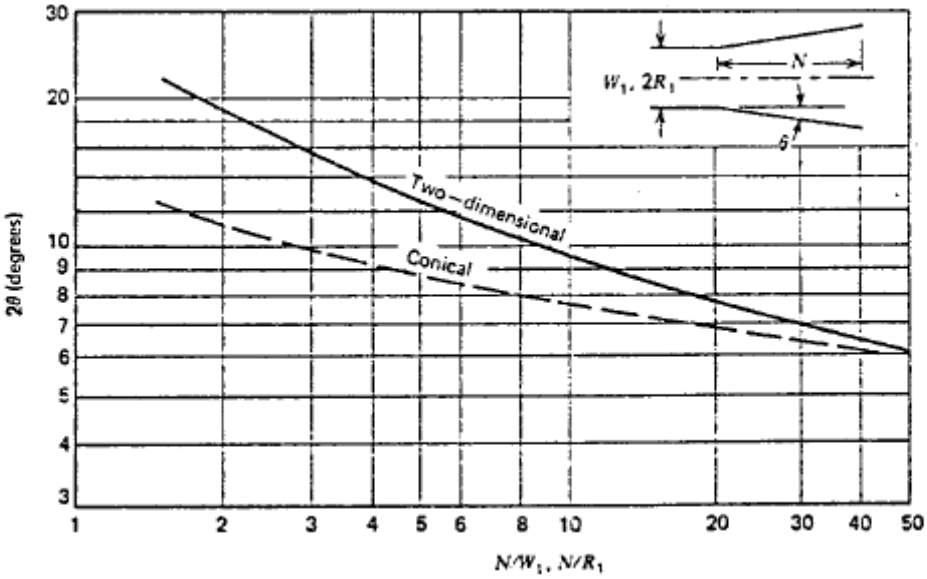

Fig.3: Diffuser Divergence Angle. (Wallis 1983)

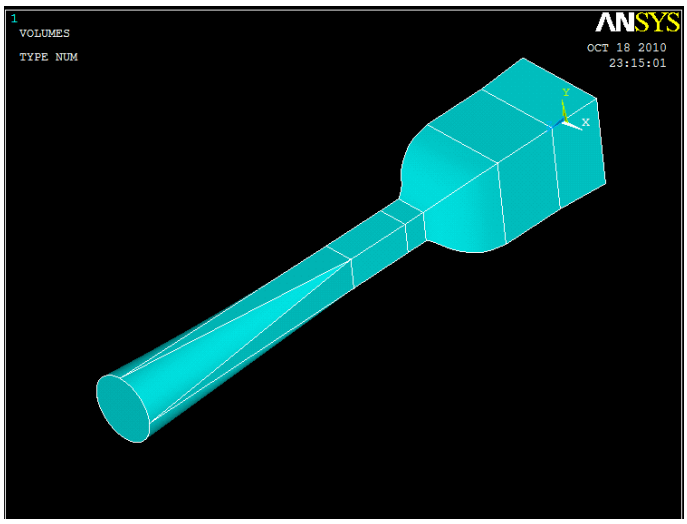

Fig.4: ANSYS Modelling of Wind Tunnel

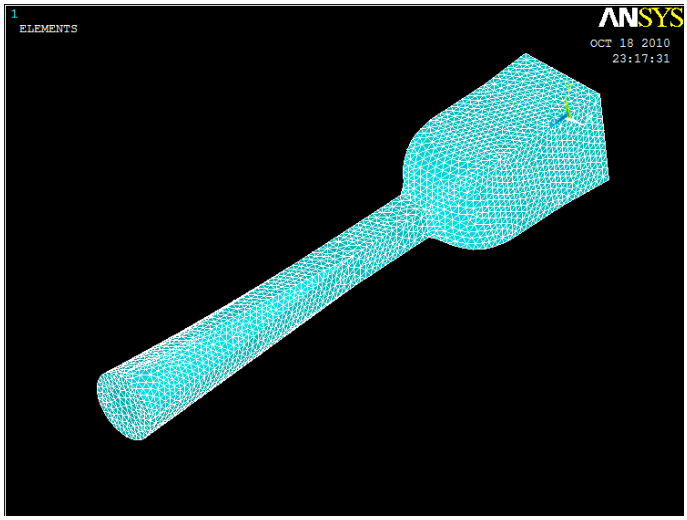

Fig.2: ANSYS Meshing of Wind Tunnel

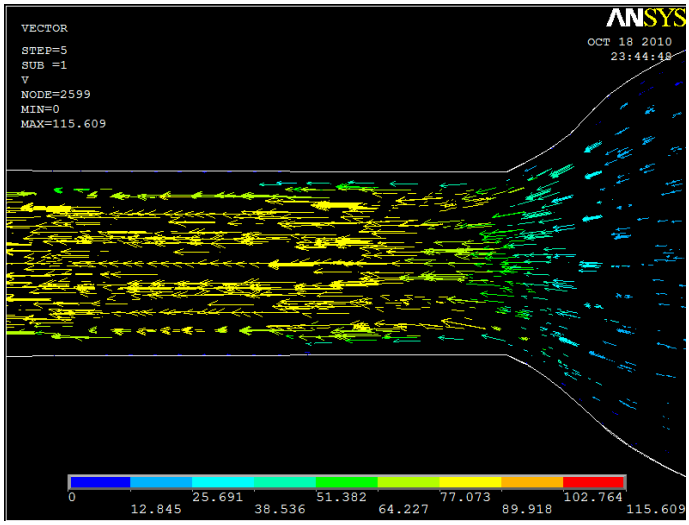

Fig.3: ANSYS Test Section Solution.

Fig.4: Wind Tunnel Construction.

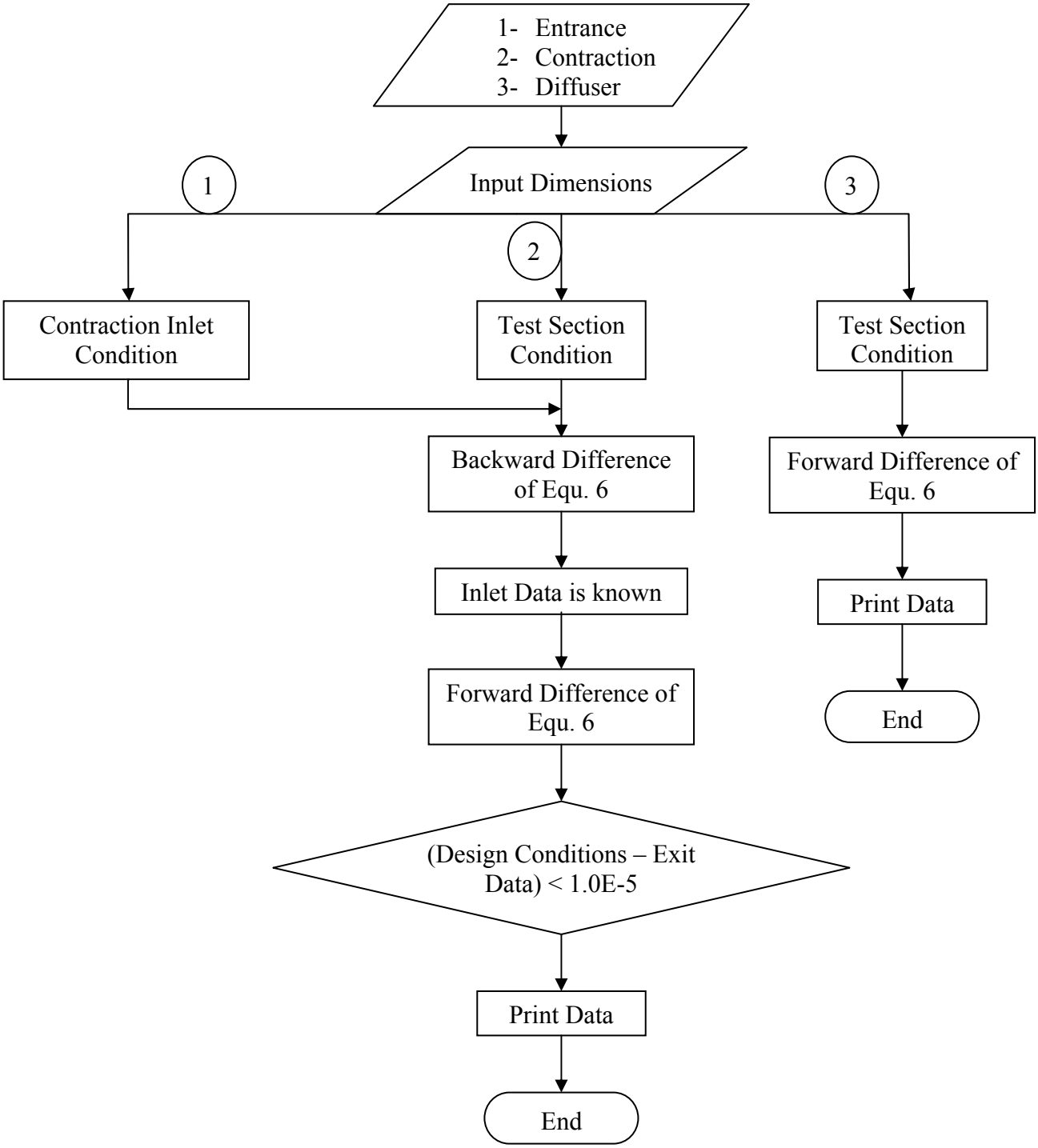

Fig.8: Flowchart of Computer Program.

Nomenclature:

Latin Symbols

A_0	Cross-section area test section	m^2
AR	Aspect ratio	
CD	Drag coefficient	
D_H	Hydraulic diameter	M
E.R	Energy ratio	
E_0	Energy at test section	W
f	Friction factor	
K_i	Pressure drop coefficient	
L	Length	M
M	Mach No.	
Re	Reynold No.	
v_0	Velocity at test section	m/s
ΔP	Pressure difference	Pa
ρ_0	Density at test section	Kg/m^3

Greek Symbols:

□	Power	W
δ^*	Displacement thickness	M
η	Efficiency	
θ	Divergence angle	Deg.
μ	Viscosity	Pa.s

The Effect of Shear on the Properties of Rigid PVC

Sawsan D. A. Shubbar

Dept. of Material Engineering
Engineering College – University of Kufa

ABSTRACT:

The rheological and fusion behavior of polyvinyl chloride (PVC) compounds plays a dominant role in the processing operations and in the development of physical properties in the processed material. A comprehensive study was made in this work to evaluate the effect of shear and thermal history on stability, mechanical and rheological properties of rigid PVC compounds. Different samples of Rigid Poly vinyl chloride including dry blend powder, granules, and bottles molded from both were examined. A study was also made on recycled RPVC where 25% of reclaimed material was continuously blended with fresh dry blend and processed for 15 cycles. Results showed that compaction of the PVC material took place in the brabender plastograph at constant temperature and shear stress. Correlations were given to explain results concerning residual stability and rheological behavior. Furthermore, it was seen that elongation and tensile impact are dependent on shear history.

KEYWORDS: stability, rigid polyvinyl chloride, rheology, apparent viscosity, recycling, and shear stresses.

تأثير قوى القص على خواص مادة متعدد (كلورايد الفاينيل) الصلب

م. م. سوسن ضياء احمد شبر

قسم هندسة المواد/ كلية الهندسة - جامعة الكوفة

خلاصة البحث :

حيث ان لخواص الانصهار والانسياب لبوليمرات متعدد (كلورايد الفاينيل) الصلب دورا حيويا في عمليات التصنيع وفي عمليات تطوير الخواص الفيزياوية للمنتج النهائي ؛ تمت اجراء دراسة شامله تناولت تاثير قوى القص والاجهاد الحراري المسبق على كل من الثبوتية وخواص الانسياب والخواص الميكانيكية لهذا البوليمر. شملت الدراسة اربع انواع من متعدد (كلورايد الفاينيل) الصلب هي : مسحوق البوليمر الجاف ، حبيبات مصنعة من نفس المسحوق، وقناني مصنعه من كلا الفقرتين السابقتين. كذلك تمت دراسة تاثير رفع نسبة (المثروم البلاستيكي للقناني : نسبة المسحوق الجاف) الى 25% وذلك باعادة تدويره 15 دورة متتالية .

اظهرت النتائج ان عملية الرص والانصهار للبوليمر حصلت في جهاز البرابندر بدرجة حراره واجهاد قص ثابتين. وكذلك تم اعطاء ارتباطات لتوضيح النتائج التي تتعلق بالاستقرارية وخواص الانسياب. علاوة على ذلك ، تبين ان الاستطالة والصدم تعتمد على قوى القص المسبقة.

INTRODUCTION:

Poly (vinyl chloride) (PVC) is one of the most explored polymers in the world, bearing a wide range of properties. It is very durable and strong, abrasion and moisture resistant; withstands rust and corrosion, is electrically nonconductive and has excellent fire resistance properties. Moreover, it is cheap, easily produced, and light weight [Charles, 2000].

In 1996, about 6.5 million pounds of post-consumer vinyl were recycled in the U.S. An estimated additional 300 million pounds of vinyl post industrial scrap was diverted from landfills and recycled into second-generation products. More than 3,500 communities accept vinyl products in their recycling programs, which is about 25 percent of all communities that recycle [PACIA & Nolan-ITU, 2004]. A recent directory published by vinyl institute lists nearly 50 companies that make commercial products out of recycled vinyl [Directory of Companies, 1994].

It is known that rigid PVC is the most sensitive thermoplastic to the effect of shear and heat [Owen et al, 1984 and Ivan et al, 1989]. Noticeable changes in the structure could occur and therefore some physical and chemical properties would consequently changes such as melt viscosity [Villemaire, 1983], mechanical properties and long term performance [Yarahmadi, 2001].

Rigid PVC microstructure strongly depends on processing conditions. Under both shear and heat influence, gelation process occurs, and the resulting morphology can be characterized by gelation level parameter [Fillot et al, 2007].

Hattori [1972], Marshall [1983], and Gilbert [1985] showed that PVC powder consisted of grains which were 50-150 microns in size. These grains were converted into smaller micro domains of 0.3-1.0 micron in diameter after the plastic material has melted. Sieglaff [1981] reported that the small grains of 100-1000°A network structure were developed during processing within the PVC micro grains. According to Truss [1985], these grains could not be destroyed completely in the melting process. Allsopp [1982] reported the predominance of Van Der Waals forces, entanglements and crosslinking could also contribute to couple these particles. Teriellus [1981] postulated the formation of crystallites and/or entanglements, which can be destroyed by increasing temperature, and stated that balancing the properties of rigid PVC products requires an optimization of the gelation level.

Furthermore and according to Summers et al [1996] the primary particles fused when the crystallites started to melt, freeing polymer chains for interdiffusion between the primary particles. Covasa and Gilbert [1992] studied the behavior of RPVC during single screw extrusion and observed both the breakdown and internal fusion of the grains, depending on the location of the material around the screw.

Moghri [2004] examined the effect of processing temperature on fusion in the Brabender Plasticorder. Chen et al [1995] pointed that the starting temperature of the brabender, rotor speed, and totalized torque are the three major factors that affect the fusion level of PVC compounds. Tomaszewska et al [2007] discusses the transitory stage between the minimum and the maximum of the torque, which corresponds to an inflection point on the torque curve.

Wenguang et al. [1996] compared the mechanical and processing properties of recycled polyvinylchloride from bottles and pipes with those of virgin pipe grade PVC, and concluded that recycled PVC didn't reduce the modulus and tensile strength.

Yarahmadia et al [2001] examined recycling RPVC profiles by re-extrusion and noticed an improvement of mechanical properties after the second extrusion, due to an increase in the degree of gelation of the PVC material.

Melt processing is one of the best methods of reutilizing plastics, but particular care is required in the recycling of PVC due its thermal and shear sensitivity [Scheirs, 1989]. There are several poly vinyl chloride plants which produce pipes, bottles, and containers from rigid PVC dry blend material. PVC compounds develop optimum bottle properties, impact and chemical resistance when they are highly fused (melted) during processing. These plants consume several thousand tons of this material. Hundreds of tons per year of processed PVC waste are accumulated. This waste is added to the fresh material at certain concentrations not exceeding 10%. In the present work, a comprehensive study was made to evaluate the effect of the shear and thermal history on stability, mechanical and rheological properties changes in three different probes, viz. rigid PVC dry blend, granules obtained thereof and bottles molded from both materials. Moreover, in order to

examine a higher recycling percent, 25% of a previously processed dry blend was mixed with fresh material and then reprocessed for 15 cycles to study and correlate rheological properties for industrial applications.

2. EXPERIMENTAL WORK:

2.1 Materials:

PVC resin (Geon) with K-value 57 was used in this study. Irgastab BC103 (Ciba-Geigy) (100:3 parts by weight) was used as a stabilizers and (Epolene E-20) (100:0.5) as lubricants.

2.2 Sample preparation:

The dry blend mixtures were prepared using a mixer type Henschell FM4, fitted with temperature indicator mounted inside the mixing chamber. An industrial pelletizer and blow molding machine were utilized for producing granules and bottles respectively.

2.3 Rheological properties:

The shear flow properties of polymers are frequently used to characterize polymer melts and to distinguish their processing performance. The measurements of RPVC systems were carried out using a Brabender torque plastograph heated at 190°C. Temperature of the melt was continuously measured and recorded using Fe/Co thermocouple, fitted in the test chamber. The speed of the rotors was 60 rpm. Density was measured for PVC during the Brabender measurements at several periods of time.

It is useful to mention that the measured torque is a function of the melt viscosity, which related to the flow property of the plastic melt

High pressure capillary rheometer, type Rheoscope 1000-CEAST, was also used. Flow properties were conducted at 190°C, the L/D of the capillary was 10.

2.4 Measurements of mechanical properties:

The mechanical properties were specified by measuring the tensile and tensile impact properties.

2.4.1 Tensile properties:

Specimens for mechanical testing were cut out from bottles and then tested according ASTM D-638 for tensile properties. A Zwick testing machine was used to perform the tensile strength test at a crosshead speed of 50 mm/min, and each test was performed until tensile failure occurred. The elongation was also measured [ASTM 1989].

2.4.2 Tensile impact:

Impact is a very important phenomenon in governing the life of a structure. This test was performed according to DIN 53448 (ASTM D1822). A tensile-impact test is a uniaxial tensile test with a high deformation speed. The pendulum device has a working capacity of 7.5 J, at maximum falling angle (150°). For the test, a specimen was fixed between a stationary clamp and a cross head. The pendulums hammer hit the cross head which is fixed to the specimen. In this way, the specimen is deformed in the direction of its longitudinal axis until fracture occurs.

2.5 Recycling evaluation:

For recycling experiments, 25% of already processed dry blend was mixed again with a fresh material and reprocessed. This procedure was repeated for 15 cycles in the same conditions, without adding new additives. Extrudate Samples from each cycle was tested in a high pressure capillary rheometer.

3. RESULTS AND DISCUSSION

The fusion rate plays an important role in the processing of RPVC, especially in blow molding technique, and is defined as the required time to convert a cold formulation of PVC when introduced in an extruder to a melt.

Plots of torque-time and temperature-time curve obtained from Brabender measurements for PVC dry blend and granules are represented in **Fig. 1**. It is seen that the thermal stability of the granules was reduced by 6% and the value of minimum torque was increased by ca.4%. This can be due to the heat and shear that the dry blend was subjected to in the pelletizing machine, therefore, stability and viscosity were slightly affected.

Point E in **Fig.1** represents the end of stability period. Behind this point, the polymer started to degrade and HCL – libration reaction come off very fast.

As shown in **Fig.1**, the melt took 10 minutes to obtain the set temperature and the minimum value of the torque. Thereafter, temperature and torque remained unchanged for about 14 minutes, after which they increased slightly. This could indicate an increase in melt viscosity of the system. In polymer melts, temperature increase is known to cause decrease in the viscosity, but in this work an opposite trend was obtained which could be due to the predominant effect of densification. This observation underlines the possibility that

crosslinking reaction took place. The consequent increase in density values supports such reaction (see density values in **Fig. 1**).

Compaction was attributed in literature [Truss, 1985] as a consequence of the increase in pressure and /or temperature. However, in this work, these parameters in the brabender were constant, yet compaction took place. Therefore, this could be due to the time dependency of the process where the following irreversible crosslinking reaction might occur:

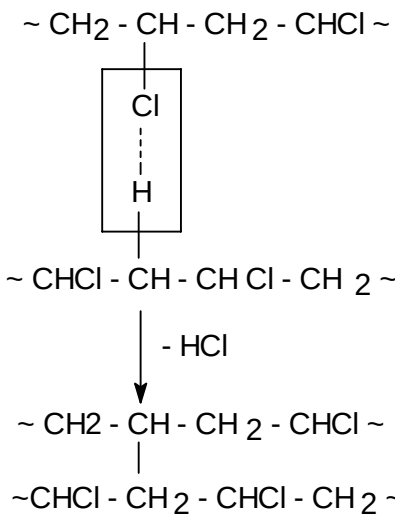

It is worth to mention, that mixing of the melt and metallic surfaces of the mixer would accelerate this reaction. IR data obtained for the samples taken near point E in **Fig. 1** showed no evidence to the presence of conjugated double bonds which give another support of a suggested formulation of the crosslinking reaction rather than dehydrochlorination according to zipper mechanism.

Table 1 shows data obtained from brabender measurements, namely: minimum torque, stability period, and percentage reduction in stability reference to the dry blend. These measurements were conducted on the dry blend, granules, bottles from both and a mixture of dry blend with 25% chips from reclaimed bottles. The bottles which were molded from granules showed the maximum reduction in stability period followed by the bottles molded from the dry blend. The addition of 25% reclaimed bottles to the dry blend caused 7.2% reduction in stability. These results proved that the blow molding process has stronger effect on the reduction of thermal stability than the pelletizing process.

Gelation involves the conversion of the initial PVC particle structure into an increasingly homogeneous melt and therefore the rheological properties of PVC at low temperatures are very different from those at higher ones.

Fig. 2 demonstrates the correlations between apparent viscosity and shear rate obtained from high pressure capillary Rheometer for the following system: PVC dry blend, granules produced thereof, and bottles molded from both materials. No noticeable differences in the values of apparent viscosity could be detected in the higher range of shear rates. On the other hand, the apparent viscosity values for the dry blend were a little lower than that of the bottles molded thereof. These results are in good agreement with the results obtained from the torque measurements in the Brabender.

Fig. 3 shows changes in apparent viscosity of the PVC system for 15 cycles, and at three different shear rates, namely: 608, 1216 and 2452 s^{-1}.

The reprocessing of dry blend containing 25% previously molded PVC indicated the feasibility of using a relatively higher percentage of industrial waste in recycling processes without effective deteriorating changes on specifications but would yield more economic revenue. These results coincide with those of Wenguang et al. [1998].

Table 2 represents data obtained from mechanical testing. A slight decrease in tensile strength for bottles molded from the granules could be seen, while elongation and tensile impact had a more pronounced differences, which probably was due to the shear and thermal history. That indicates that the last two properties are dependent on shear history, while the last cause has no big effect on tensile strength. These results are in agreement with previous studies [Covasa et al. 1992 and Tersilus and Janson 1981], while Fillot et al. [2007] noticed a decrease in impact strength and stated that it was attributed to partial disorientation of the PVC macromolecular chains and reduction of the molecular mobility.

4. CONCLUSIONS:

- The temperature increase in PVC melt caused increase in the viscosity possibly due to crosslinking reaction in the melt and that is proved by the consequent increase in density values.
- When comparing between the blow molding process and pelletizing process, it was noticed that the later had stronger effect on the reduction of thermal stability than the later.

- A correlations between apparent viscosity and shear rate obtained from high pressure capillary Rheometer, demonstrated no noticeable differences in the values of apparent viscosity could be detected in the higher range of shear rates between PVC dry blend, granules produced thereof, and bottles molded from both materials.
- The reprocessing of dry blend containing 25% previously molded PVC indicated the feasibility of using a relatively higher percentage of industrial waste in recycling processes without effective deteriorating changes on specifications.
- Elongation and tensile impact are dependent on shear history, while this cause has no large effect on tensile strength.

REFERENCES:

Allsopp, M.W. [1982]," Morphology of PVC", in: Burgress, R.H. Manufacturing and Processing of PVC. New York: Applied Science Publishers.215.

Annual Book of ASTM, [1989], Section 8, Vol. 08.01 Plastic, Amer. Soc. Test Mat. "M.V.S.A.", Philadelphia.

Charles H. A. [2000],"Modern Plastic Handbook."Mc-Graw Hill, New York.

Chen, C.H, Wesson R.D, Collier, J.R. and Lo, Y.W. [1995], "Studies of Rigid PVC Compounds IV: Fusion Characteristics and Morphology Analyses". Journal of Applied Polymer Science. 58: 1107-1115.

Covasa J. A.; Gilberta M. [1992], "Single Screw Extrusion of Poly (Vinyl Chloride): Effect on Fusion and Properties", Polymer Engineering and Science 32(11): pp. 743-750.

Directory of Companies Involved in The Recycling of Vinyl (PVC) Plastics [1994], Third Edition, The Vinyl Institute, a Division of the Society of the Plastics Industry, Inc,65 Madison Avenue, Morristown ,NJ 07960. May.

Fillot L -A, Hajji P, Gauthier C, Masenelli - Varlot K., [2007]," Thermomechanical History Effects on Rigid PVC Microstructure and Impact Properties", J. Appl. Poly. Sci. 104: pp.2009-2017.

Gilbert, M. [1985], "Fusion of PVC Compounds". Plastics and Rubber International.10 (3):16-19.

Hattori, T., Tanaka, K. and Matsuo, M., [1972]. “Fusion of Particulate Structure in PVC during Powder Extrusion". Polymer Engineering Science.12: pp. 199.

Ivan B., Kelen, T. T. F. [1989], in Degradation and Stabilization of Poly Vinyl Chloride; Vol. 2, Ed.; Jellinek, H. H. Ed.; Elsevier.

Marshall, D.E., Higgs, R.P. and Obande, O.P. [1983], "The Effect of Extrusion Conditions on the Fusion , Structure and Properties of Rigid PVC", Plastics and Rubber Processing and Applications. 3: 353-358.

Moghri M., Garmabi H., Akbarian M., [2004], "Effect of Processing Parameters on Fusion and Mechanical Properties of a Twin-Screw Extruded Rigid PVC Pipe", Journal of Vinyl and Additive Technology, 9 (2), pp 81 – 89.

Owen, E.D. [1989]. "Degradation and Stabilization of PVC". New York: Elsevier Applied Science Publisher.

PACIA & Nolan-ITU [2004], National Plastic Recycling Survey 2004-Main Survey Report, N. John & Plastics and Chemicals Industries Association (PACIA). Australia.

Scheirs, J., [1998],"Polymer Recycling, Science Technology and Applications", Wiley Series in Polymer Science, 1st Ed. Chichester: John Wiley & Sons, Ltd.

Sieglaff C.L. [1981]," The Morphology, Rheology and Processing Properties of Poly vinyl Chloride", Pure & Appl. Chem., Vol.53, pp. 509-520.

Summers J.W.,[1996]," Vinyl Polymers (PVC)", in Encyclopedia of Chemical Technology, 4th Ed. by John A. Davidson and Keith L. Gardner, BF Goodrish Co. ,September 16.

Terselius B., Janson J F., Bystedt J., [1981],"Gelatin of Rigid PVC-Pipes", Journal of Macromolecular Science, Part B, 20, (3), pp. 403-414.

Truss R W [1985]," Understanding Brittle Fracture of UPVC Pipes", Pure & Appl. Chem., 57(7), pp.993-1000.

Villemaire J.P., [1983],"Apparent Viscosity Measurements Using a Capillary Viscometer with Prehearing" Polymer Process Eng., 1 (13), pp221.

Yarahmadi, N., Jakubowicz, I. and Gevert, T. [2001]. "Effects of Repeated Extrusion on the Properties and Durability of Rigid PVC Scrap". Polymer Degradation and Stability. 73: 93-99.

Wenguang M., La Mantia F. P., [1998], "Processing and Mechanical Properties of Recycled PVC and of Homopolymer Blends with Virgin PVC", Journal of Applied Polymer Science, 59(5), pp 759 – 767.

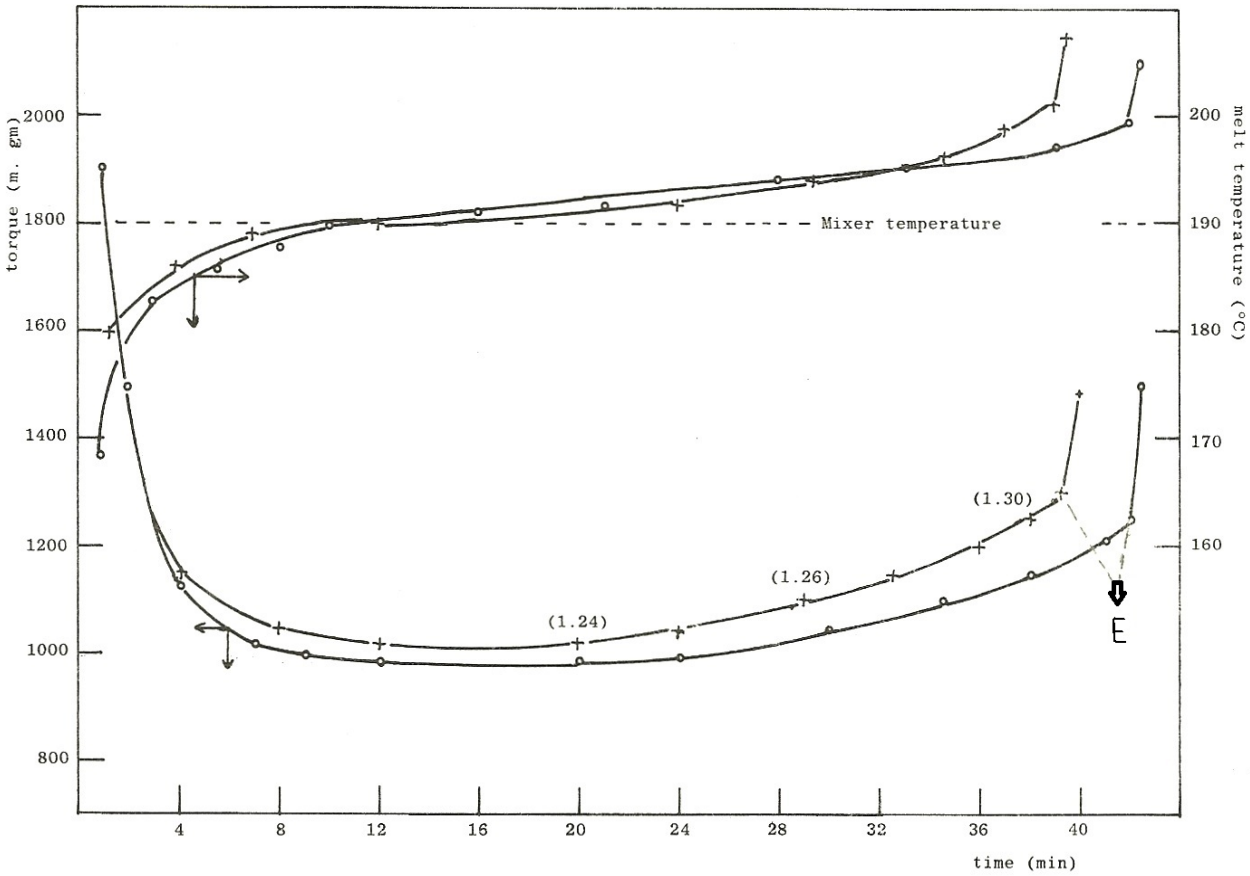

Fig. 1 Torque and temperature vs. time for PVC dry blend (°°°°) and granules (+++)

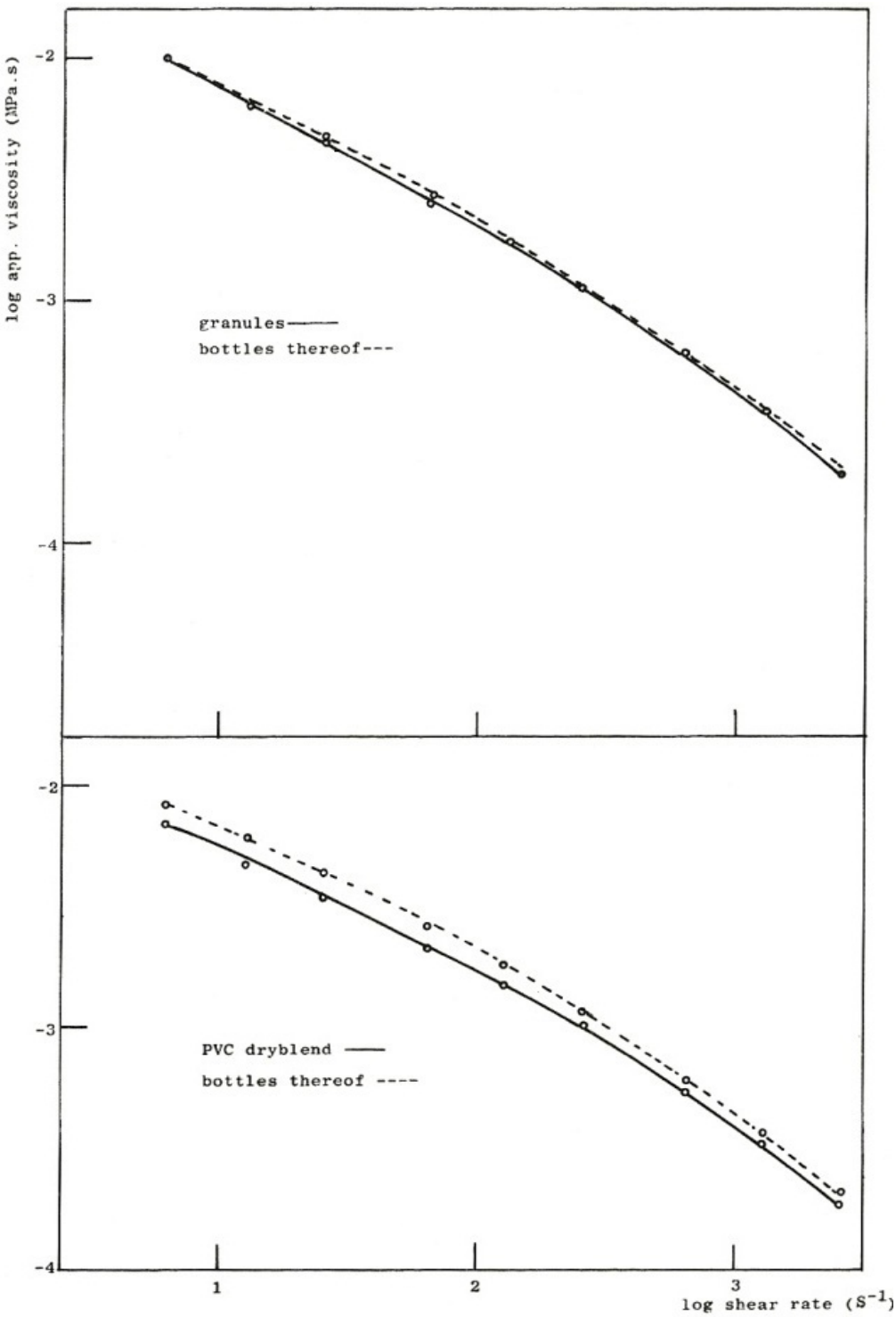

Fig. 2 Log apparent viscosity vs.log shear rate for dry blend, granules and bottles from both.

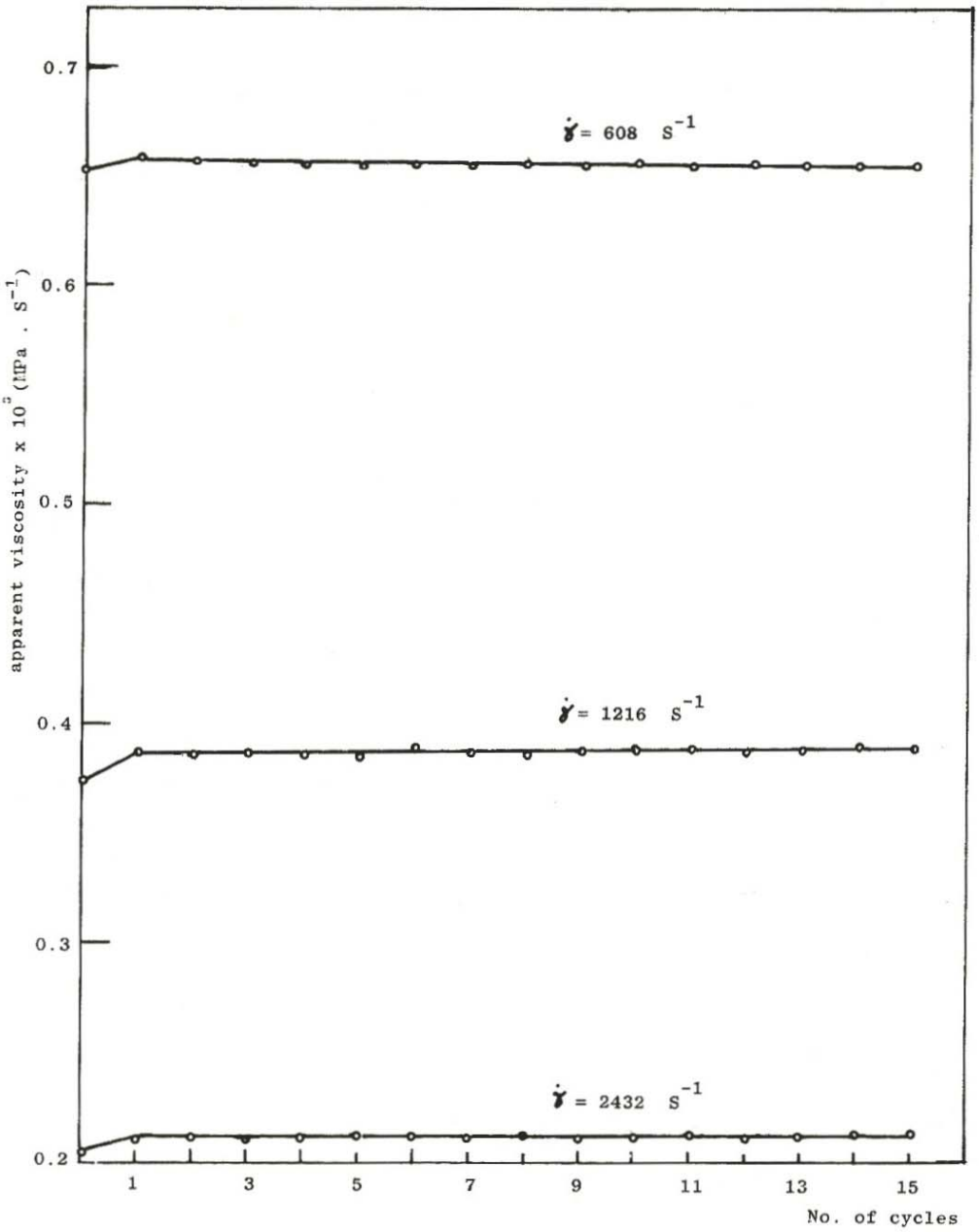

Fig. 3 Apparent viscosity vs. number of cycles at three constant shear rate using 25% waste

Table 1- Thermal stability and torque data on different PVC systems

System	Minimum torque (g .m)	Stability period (min)	Reduction in thermal stability (%)
PVC dry blend(I)	980	42	-
sGranule(Π)	1020	39.5	6
Bottles from(I)	980	37.0	12
Bottles from(Π)	1020	35.5	15.5
Dry blend + 25% reclaimed material	980	39.0	7.2

Table 2 - Mechanical properties of bottles molded from (I) and (Π)

System	Tensile strength (Mpa)	Elongation (%)	Tensile impact (J/mm^2)
Bottles from (I)	49.0	15	0.48
Bottles from(Π)	48.0	20	0.40

EFFECT OF COOLING RATE ON MECHANICAL PROPERTIES OF EUTECTIC AND HYPOEUTECTIC Al-Si ALLOYS

Dr. Zeyad D. Kadhim
Materials Engineering. Dep. College of Engineering.
University of Al-Mustansiriya- Baghdad-Iraq

ABSTRACT

In this research the effect of cooling rate and mold type on mechanical properties of the eutectic and hypoeutectic (Al-Si) alloys has been studied. The alloys used in this research work were (Al- 12.6%Si alloy) and (Al- 7%Si alloy).The two alloys have been melted and poured in two types of molds with different cooling rates. One of them was a sand mold and the other was metal mold. Mechanical tests (hardness, tensile test and impact test) were carried out on the specimens. Also the metallographic examination was performed.

It has been found that the values of hardness for the alloys(Al-12.6%Si and Al-7%Si) which poured in metal mold is greater than the values of hardness for the same alloy when it poured in a heated metal mold at different temperatures or in sand mold. The strength and impact resistance for the alloys (Al-12.6%Si and Al-7%Si) are greater when these were poured in a metal molds than that when it poured in a sand mold.

Furthermore, the higher cooling rates enhance the strength, hardness and impact resistance for the two alloys, while the low cooling rates reduces these mechanical properties.

The percentage of elongation and the amounts of formed porosity decreased when the cooling rates increased.

الخلاصة

درس في هذا البحث تأثير معدل التبريد ونوع القالب على الخواص الميكانيكية لسبائك (المنيوم – سليكون) اليوتكتيكية و تحت اليوتكتك. السبائك المستخدمة في هذا العمل البحثي كانت (سبيكة المنيوم –٦، ١٢% سليكون) و (سبيكة المنيوم – ٧ % سليكون). السبيكتين تم صهرها و صبها في نوعين من القوالب و بمعدلات تبريد مختلفة . أحدهما كان قالب رملي و الاخر كان قلب معدني . الاختبارات الميكانيكية (الصلادة ، أختبار الشد ، أختبار الصدمة) تم أجرأها على العينات. أنجز الفحص المجهري أيضا.

لقد وجد بأن قيم الصلادة للسبائك (المنيوم –٦، ١٢% سليكون و المنيوم – ٧ % سليكون) و التي صبت في القالب المعدني هي أكبر من قيم الصلادة لنفس السبائك عند صبها في قالب معدني مسخن عند درجات حرارية مختلفة أو في قالب رملي.

المقاومة ومقاومة الصدمة للسبيكتين هي أكبر عند صبها في قوالب معدنية من تلك المصبوبة في قالب رملي.

علاوة على ذلك ، معدلات التبريد العالية تحسن من المقاومة ، الصلادة و مقاومة الصدمة للسبيكتين بينما معدلات التبريد الواطئة تقلل من تلك الخواص الميكانيكية.

أن النسبة المئوية للاستطالة و كمية المسامية المشكلة تقل عندما تزداد معدلات التبريد.

Keywords: cooling rate, eutectic, hypoeutectic alloys, mechanical properties, molds.

1-Introduction

Alloys with silicon as the major alloying addition are the most important of the aluminum casting alloys mainly because of high fluidity imparted by the presence of relatively large volumes of the Al-Si eutectic. Other advantages of these castings are high resistance to corrosion, good weldability and the fact that silicon reduces the coefficient of thermal expansion. [1]

The static fracture toughness of a series of eutectic AI-Si casting alloy with different microstructural features has been evaluated by Hafiz and Kobayashi . Fracture toughness was found to be strongly associated with the size and morphology of silicon particles. [2]

One of the major problems associated with the casting of aluminum alloys is the formation of micrometer scale cavities called microporosity. Microporosity is a leading cause in the reduction of mechanical properties. Particularly, fatigue resistance, as well as a loss of pressure tightness and a degradation of the surface appearance in cast parts[3, 4]

For aluminum alloy A356 permanent mold castings, it was observed that local fatigue resistance varied substantially along the solidification path while tensile strength was little affected. The amount of Al–Si eutectic and the density of micropores are increased along the solidification path. [5]

Haizhi studied the fatigue and wear properties of Al-Si alloy. The silicon phase is important to both of these properties. Coarse silicon usually reduces fatigue life due to microcrack initiation. Higher silicon content usually increases the wear resistance of Al-Si alloy as it increases the alloy's hardness. Intermetallic precipitates and casting defects also influence fatigue and wear performance. Fine precipitates can usually strengthen the alloy while sharp and coarse precipitates degrade these two properties. Casting defects such as porosity and inclusion usually reduce the alloy's fatigue and wear resistance due to microcrack initiation. [6]

Taylor discussed the various sources of iron and how it enters aluminum alloys, the way that iron leads to the formation of complex intermetallic phases during solidification, and how these phases can adversely affect mechanical properties, especially ductility, and also lead to the formation of excessive shrinkage porosity defects in castings. [7]

It was found there are no differences in ultimate tensile strength as well as bulk hardness between the sulfurized alloy and normal A356; it is evident that yield strength and ductility of the A356 alloy are reasonably altered with the presence of sulfure. The A356 alloy containing sulfur exhibits greater ductility and lower yield strength in comparison with the normal A356 alloy. [8]

The effect of cast Al-Si-Cu alloy solidification rate on alloy thermal characteristics has been studied by L.A. Dobrzański et al. It was found that the solidification parameters are affected by the cooling rate. The formation temperatures of various phases are changed with an increasing cooling rate. Also increasing the cooling rate increases significantly the Al nucleate temperature, nucleation undercooling temperature, solidification range and decreases the recalescence undercooling temperature. These phenomena lead to an increased number of nucleus that affect the size of the grains and the Secondary Dendrite Arm Spacing (SDAS). [9]

Abdulwahab, et al. have made a comparative study of the hardness values and impact energy of as-cast and age-hardened Al-Si-Fe-MnCr alloy produced when various addition of MnCr (0.1-0.5%) were made to Al- Si-Fe alloy so as to give a series of alloys with constant composition of Si and Fe. The alloy was solution treated and aged at 490oC and 200oC respectively for six hours. These treatments introduced the formation of complex precipitates in the alloys. It was found that the reprocessed (age–hardened) alloys showed an excellent combination of hardness and impact energy values than the as-cast alloys. [10]

The effects of eutectic silicon particles on tensile properties and fracture toughness of three A356 aluminum alloys were investigated by Kyuhong Lee. et. al. These A356 alloys were fabricated by casting processes such as low-pressure-casting, casting-forging, and squeeze-casting, and their tensile properties and fracture toughness were analyzed in relation with microfracture mechanism study. Microfracture observation results showed that eutectic Si particles segregated along solidification cells were cracked first, but that aluminum matrix played a role in blocking crack propagation. The cast-forged alloy had the best hardness, strength, ductility, and

fracture toughness because of the matrix strengthening and homogeneous distribution of eutectic Si particles due to forging process. [11]

The strength and fracture studies of as-cast Al-Si-Cu alloys have been investigated. As cast alloys have been characterized using XRD and optical microscope. To evaluate the strength of these alloys, a tensometer has been employed and the fracture surfaces have been observed under SEM to understand the mode of fracture. It has been observed that the fracture surface of the alloys mainly shows brittle characteristics. The porosity and blowhole present in the cast alloy has been the dominating factor for low strength of the alloys. [12]

The influence of microstructure and process history on mechanical behavior of cast Al-Si alloys is reported. Metallographic and image analysis techniques have been used to quantitatively examine the microstructural parameters of the α-Al phase and eutectic silicon. The results showed that secondary dendrite arm spacing SDAS and length of eutectic silicon particles increase with section thickness, and consequently mechanical properties decrease. [13]

2- Experimental Procedure

In present work, the casting process was carried out by using sand and metal molds to cast the eutectic alloy (Al-12.6% Si) and the hypeoteutic alloy (Al-7%Si). These alloys have been prepared before casting process Table (1).

Table (1) Chemical compositions of the alloys studied

Alloys	Elements (Wt%)					
	Si	Mg	Fe	Cu	Mn	Al
Al-12.6%Si	12.6	0.75	0.86	0.85	0.11	Remainder
Al-7%Si	7	0.30	0.20	0.01	0.006	Remainder

After charging the crucibles with the alloys, it were put inside a resistance electric furnace and heated up to (650 ºC). The molten alloys were pouring in the molds, as soon as the mold cavity was filled with metals, it is allowed to cool and solidify. The metal molds have been previously heated for different temperatures (25°C, 100°C and 250°C) .So the cooling rate for the two alloys became (1°C/sec, 4°C/sec and 7°C/sec). In the case of sand mold, the cooling rate was (6 °C/sec).The samples that produced from the casting process have square cross sections with dimensions (20x20x200)mm³.A thermometer with chromel-alumel thermocouple (K-type) covered by a hastalloy was used to measure the temperature. The thermometer was put in the center of the mold cavity as shown in the figures below.

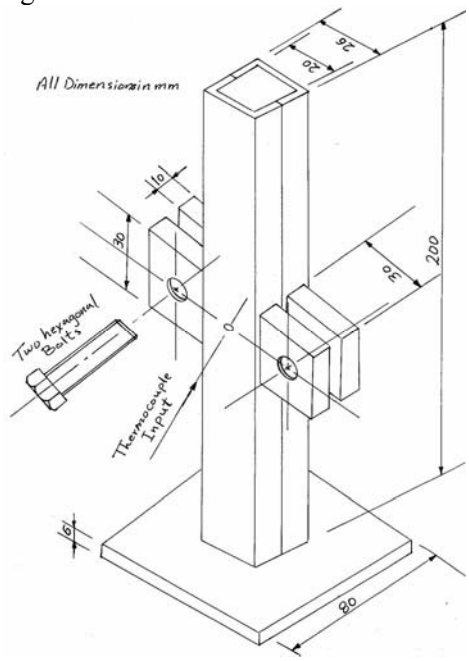

Fig(1) Metal mold

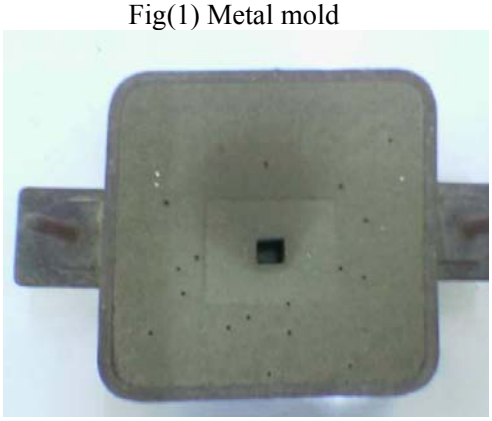

Fig (2) Green sand mold (upper part)

For metallographic examination, all castings were sectioned vertically across the centerline to observe the internal porosity; (see figs (1, 2)) their surfaces were grounded by using 250, 500 and 1000 SiC emery papers. Primary and final polishing was performed using alumina slurry with particle size of 50 µm and diamond paste with particle size of 1 µm. Finally all polished samples were cleaned by

water and alcohol and then dried. The samples were etched using 0.24% hydrofluoric acid (HF). Each sample was then observed and photographed at a magnification of X300.

The tensile test was performed using UTS apparatus with 200 kN loading capacity. The tensile flat test specimens were prepared with the gauge length section has the dimension of 12.5 mm width and 50mm gauge length according to ASTM designation: E8M-03. [14] The tensile test was achieved at room temperature in ambient air at a cross-head speed of 2 mm/min.

The hardness test was carried out by using the Vickers Microhardness technique with load (20 gm).

The impact test was carried out according to the recommended standard charpy V-notched method. The specimen is supported at each end and notched at the midpoint between the supports. The notch is on the face directly opposite to where the pendulum strikes the test piece. The specimen has a square cross-section of side 10mm and length 55mm.

The percentage porosity of specimen was calculated from the following relationship:-

$$\%\text{Porosity} = \frac{\rho_{\text{pfs}} - \rho_{\text{o}}}{\rho_{\text{pfs}}} \times 100$$

Where ρpfs is the density of the pore-free sample and ρo is the observed density of the sample.[15]

In order to obtain the maximum density or pore-free density of a sample, the sample was compressed to about 80% of its original thickness under a compressive load after which its density was evaluated using the common Archimedean method. [15]

3-Results and Discussion

It was found that strength of alloy Al-12.6%Si has changed when changing the cooling rate. It can be seen that the strength value reach to (194 MPa) when the cooling rate has a value (7 ºC/sec).Fig (5) the eutectic structure of this alloy can be observed from the microstructure Fig (13).

The strength of this alloy became (160 MPa) when the cooling rate is low (1ºC/sec). It can be seen that from the Fig (5). And this is due to the formed cavities. These cavities are bigger as a result of small porosity which join together to form big cavities Fig (10).

However, when the cooling rate is very low so there is an evolution of hydrogen gas bubbles due to a sudden decrease in hydrogen solubility during solidification (gas pores). Combined gas-shrinkage porosity may also exist. [3, 4]

The values of strength, microstructure and the formed porosity were differs when the (Al-7%Si) alloy was poured in molds.

It was found that the strength of Al-7%Si became (183 MPa) when the pouring of this alloy in a metal mold with cooling rate (7 ºC/sec).Fig (5) This is due to defects formation. However, the percentages of defects (porosity) were low, and have a small size; this can be seen from the metallographic. Fig (16)

The strength of this alloy was differing as result to the change in cooling rate. When the cooling rate became (1ºC/sec) the defects (cavity) size became big and the percentages of defects (porosity) were high. Fig (14)

The strength value of this alloy was (150 MPa) when the cooling rate was (1ºC/sec) and this is a less value of strength due to size of the formed porosity was too big , where the small porosity (microporosity) meet each other to form a big porosity (cavities). And this is also could be seen when pouring the alloy in a sand mold which the cooling rate (6ºC/sec).

The alloy (Al-12.6%Si) has a hardness value of 58 HV while the Vickers hardness value for the alloy (Al-7%Si) was 48 HV. These alloys were cast in sand casting process where the cooling rate was (6°C/sec).

These values were changed when the alloys casted in a metal mold as shown in Fig (6).It can be seen that the highest values were 64 HV and 52 HV for (Al-12.6%Si) and (Al-7%Si) alloys respectively.

From these results, it can be remarked that the values of hardness increased due to the big amount of the volume fraction for Si in matrix so the eutectic alloy (Al-12.6% Si) has a high value of hardness, However high cooling rate make high hardness value for these alloys. Also the percentage of porosity was less when the cooling rate was high.

The values of hardness for the two alloys were low when the cooling rate low due to the formation of cavities and porosities (microporosity and

macroporosity). The increment in cavities and porosities are as a result of joining the gas porosities to the shrinkage porosities inside the casting because there is no degasser has been used.

The solidification mode in the alloy (Al-7%Si) is a denderatic, so the formed porosity in this casting has small size but the amounts was high as compared with the casting (Al-12.6%Si) in which the solidification mode is planner. And the small amounts of the formed porosity in the alloy (Al-12.6%Si) make cavities which can be seen in the upper part of cast as pipe. Thus these modes have an effect on the formed porosity and the mechanical properties.

From the values of the absorbed energy to break samples by shock, it can be seen that the highest value was for the sample of (Al-12.6%Si) alloy which is casted in a metal mold with a cooling rate of (7°C/sec) and this is due to the formed porosity was low as compared with the other samples which have a different cooling rates. Fig (7)

Fig (8) shows the effect of cooling rate on the elongation of these alloys , it can be seen that the increments in cooling rates make the percentage of elongation low and this is because of the high cooling rates make an increments in defects ((point and line defects (dislocation)). So there is an increase in strains thus the extension will be low.

It can be Concluded that the ductility of these alloys are low. While the alloys that solidified with low cooling rates have high ductility.

However alloys having coarse eutectic exhibit low ductility because of the brittle nature of the large silicon plates. Fig (10) Rapid cooling greatly refines the microstructure and silicon phase assumes a fibrous form with result that the ductility is much improved. Fig (13) [1]

Microporosity formation is generally attributed to two factors: shrinkage, coupled with a lack of interdendritic feeding during mushy zone solidification (shrinkage pores), and evolution of hydrogen gas bubbles due to a sudden decrease in hydrogen solubility during solidification (gas pores). Combined gas-shrinkage porosity may also exist.

However, Fig (9) shows that the high cooling rates decrease the amounts of porosities. This is because there is no sufficient time for formation big amounts of gas porosity or joins this porosity with shrinkage porosity and makes cavities. So the percentage of porosity was high when the cooling rate low.

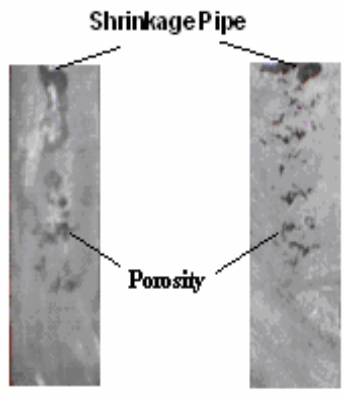

Fig (3) Shows Al-12.6% Si Casting after sectioning that cut from the centerline with cooling rate (1%°C/sec)

Fig (4) Shows Al-7%Si casting after sectioning that the cut from the centerline with cooling rate (1%°C/sec)

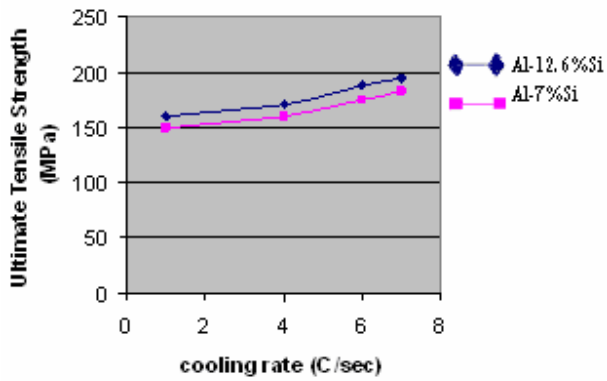

Fig (5) the effect of cooling rate on ultimate Tensile strength for two alloys a- Al-12.6% Si b- Al-7%Si

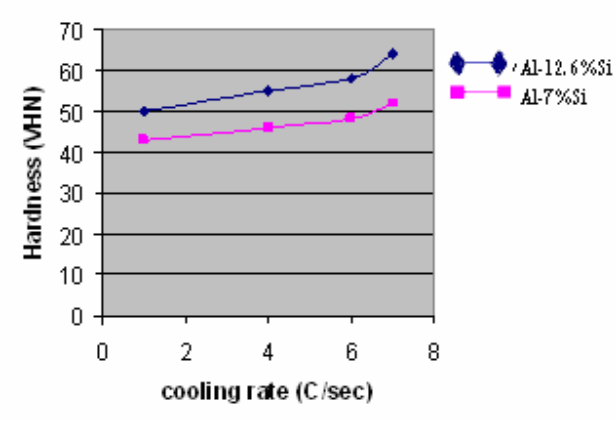

Fig (6) the effect of cooling rate on hardness for two alloys a- Al-12.6% Si b- Al-7%Si

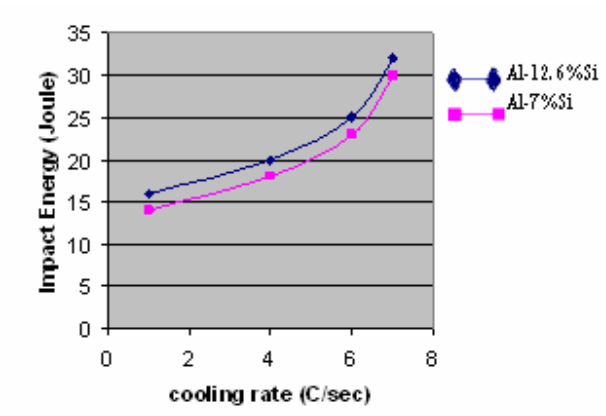

Fig (7) the effect of cooling rate on the impact energy for two alloys a- Al-12.6% Si b- Al-7%Si

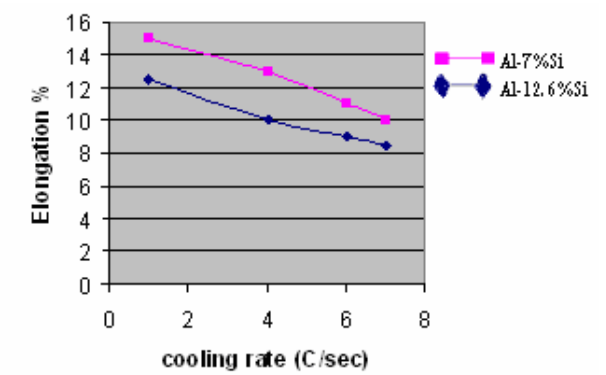

Fig (8) the effect of cooling rate on the percentage of elongation for two alloys a- Al-12.6% Si
b- Al-7%Si

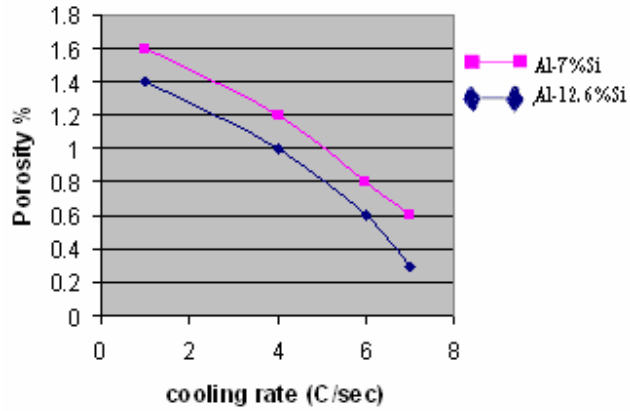

Fig (9) the effect of cooling rate on the percentage of porosity for two alloys a- Al-12.6% Si
b- Al-7%Si

Porosity
(Gas and Shrinkage)

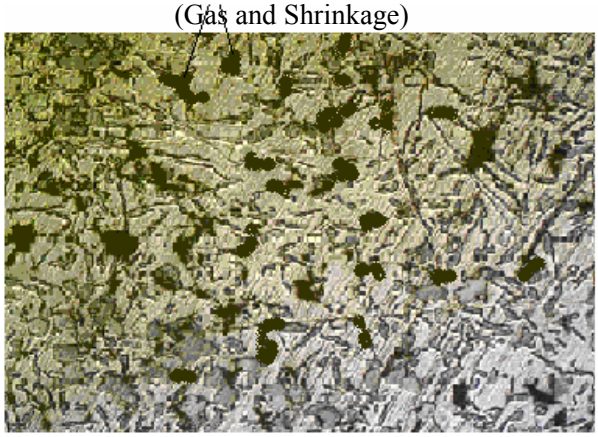

Fig. (10) The microstructure for cast Al-12.6%Si with cooling rate 1ºC/sec Magnification (300X), shows the porosity and the eutectic layers.

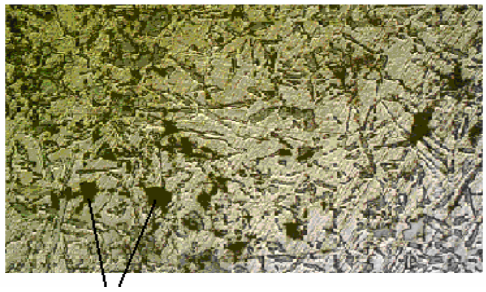

Porosity (Gas and Shrinkage)

Fig. (11) The microstructure for cast Al-12.6%Si with cooling rate 4ºC/sec Magnification (300X), shows the porosity and the eutectic layers.
Porosity (Gas and Shrinkage)

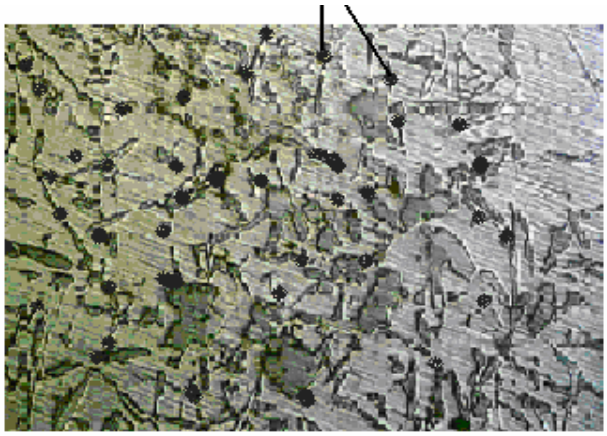

Fig. (12) The microstructure for cast Al-12.6%Si with cooling rate 6ºC/sec Magnification (300X), shows the porosity and the refining eutectic layers.

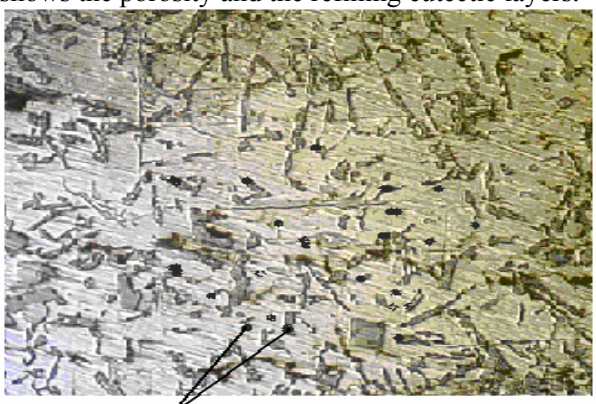

Porosity (Gas and Shrinkage)

Fig. (13) The microstructure for cast Al-12.6%Si with cooling rate 7ºC/sec Magnification (300X), shows the porosity and the refining eutectic layers.

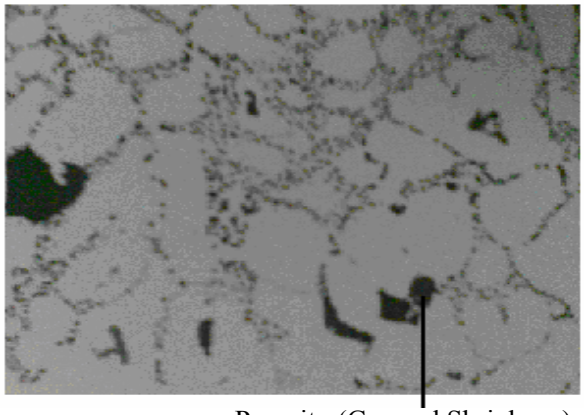

Porosity (Gas and Shrinkage)

Fig. (14) The microstructure for cast Al-7%Si with cooling rate 1ºC/sec Magnification (300X), shows the formed porosity.

Porosity (Gas and Shrinkage)

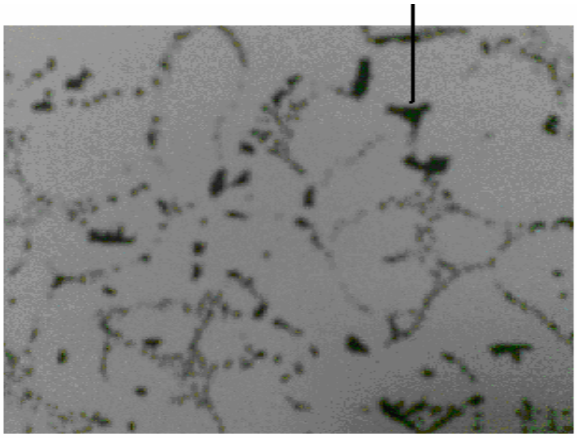

Fig. (15) The microstructure for cast Al-7%Si with cooling rate 4ºC/sec Magnification (300X), shows the formed porosity.

Porosity (Gas and Shrinkage)

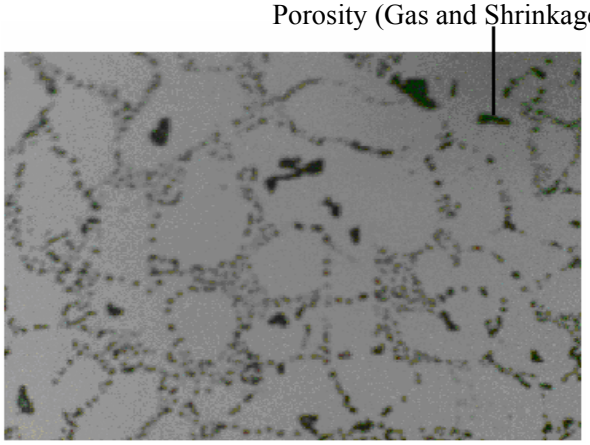

Fig. (16) The microstructure for cast Al-7%Si with cooling rate 7ºC/sec Magnification (300X), shows the formed porosity.

4-Conclusions

Investigating the mechanical properties of eutectic and hypoeutectic Al-Si alloys with different cooling rates yielded the following conclusions:-

1- It has been found that the following mechanical properties; ultimate tensile strength, hardness and the impact energy for the eutectic and hypoeutectic Al-Si alloys increases with increasing the cooling rates.

2- The values of ultimate tensile strength, hardness and the impact energy for the eutectic alloy (Al-12.6%Si) are greater than that for the hypoeutectic alloy (Al-7%Si) at the same cooling rates.

3-The percentage of the formed porosity increases with decreasing the cooling rate.

5- References

1- I. J. Polmear "Light Metals", Second edition, P(147-152), 1989. Routledge, chpman and Hall, Inc.
2- M. F. Hafiz and T. Kobayashi "Fracture toughness of eutectic Al-Si casting alloy with different microstructural features", J. Materials Science, V 31 p(6195-6200),1996.
3- J. P. Anson and J. E. Gruzleski " The Quantitive Discrimination between shrinkage and gas microporosity in cast aluminum alloys using spatial data analysis", Materials Characterization 43, p(319-335), 1999.
4- J. P. Anson and J. E. Gruzleski "Effect of Hydrogen content on relative shrinkage and gas microporosity in Al-7%Si casting", AFS Transactions, p(135-141),2000.
5- Mark E. Seniw, James G. Conley and Morris E. Fine "The effect of microscopic inclusion locations and silicon segregation on fatigue lifetimes of aluminum alloy A356 castings", Materials Science and Engineering, A285 (43–48), 2000.
6- Haizhi Ya "An Overview of the Development of Al-Si alloy based material for engine applications",J. Materials Engineering and Performance,V12, P(288-297),2003.
7- John A. Taylor "The effect of iron in Al-Si casting alloys", Cooperative Research Centre for Cast Metals Manufacturing (CAST), 2004.
8- J. Kajornchaiyakul,R. Sirichaivejakul, n. Moonrin "Solidification characteristics and mechanical properties of hypoeutectic aluminum – silicon alloy containing sulfur", la metallurgia italiana, V10,p(47-50),2005.
9- L.A. Dobrzański , R. Maniara , J.H. Sokolowski "The effect of cast Al-Si-Cu alloy solidification rate on alloy thermal characteristics", J. of Achievements in Materials and Manufacturing Engineering 17 p(217-220),2006.
10- Abdulwahab, M., Shehu, U. and Bello.K.A "Comparative Study of the Hardness and Impact Energy of As-cast and Age-hardened Al-Si-Fe-MnCr Alloy", J. of Applied Sciences Research, 3(9): p(823-827), 2007.
11- Kyuhong Lee , Yong Nam Kwon , Sunghak Lee "Effects of eutectic silicon particles on tensile properties and fracture toughness of A356 aluminum alloys fabricated by low-pressure-casting, casting-forging, and squeeze-casting processes", J. of Alloys and Compounds 461 p(532–541), 2008.
12- Abhishek Sharma "Strength and Fracture studies of as-cast Al-Si-Cu alloys", Ms.c. Thesis, School of physics and materials science, Thapar University, patiala, India, 2008.
13- F. Grosselle, G. Timelli, F. Bonollo, A. Tiziani, E. Della Corte "Correlation between microstructure and mechanical properties of Al-Si cast alloys", la metallurgia italiana, Alluminio e leghe, p (25-32) 2009.
14- Mathew Philip and Bill Bolton "Technology of Engineering Materials", first edition, P (46), 2002.
15-T.Uddin, PhD Thesis, University of Birmingham, UK, 1991.

Image Reconstruction Using Modified Hybrid Transform

By

Assist. Prof. Sulaiman Murtadha
Electrical Engineering Department
Baghdad University

Ali K.Ibrahee
Electrical Engineering Department
Baghdad University

ABSTRUCT:

In this paper, an algorithm for reconstruction of a completely lost blocks using Modified Hybrid Transform. The algorithms examined in this paper do not require a DC estimation method or interpolation. The reconstruction achieved using matrix manipulation based on Modified Hybrid transform. Also adopted in this paper smart matrix (Detection Matrix) to detect the missing blocks for the purpose of rebuilding it. We further asses the performance of the Modified Hybrid Transform in lost block reconstruction application. Also this paper discusses the effect of using multiwavelet and 3D Radon in lost block reconstruction.

Keywords: Modified Hybrid Transform, Lost Blocks, Detection Matrix

1. INTRODUCTION

The most important goal of any communication system is the sound and correct delivery of information between the source and the destination. General purpose images are most commonly compressed by lossy JPEG. JPEG divides the image into_blocks of 8× 8 pixels and calculates a two-dimensional (2-D)__discrete cosine transform (DCT), followed by quantization and_Huffman encoding, [1]. In common wireless scenarios, the image is transmitted over the wireless channel block by Block. Due to severe fading, we may lose an entire block, evenseveral consecutive blocks of an image. In [2] the authors report that average packet loss rate in a wireless environment is 3.6% and occurs in a bursty fashion. In the worst case, a whole line of image blocks might be lost. Note that JPEG uses differential encoding for storing the average (dc) value of successive pixels. Hence, even if a single block is lost, the remaining blocks in that line (or reset interval) might be received without their correct average (dc) value. Two common techniques to make the transmission robust are forward error correction (FEC) and automatic retransmission query protocols (ARQ). Of these, FEC needs extra error correction packets to be transmitted. ARQ lowers data transmission rates and can further increase the network congestion which initially induced the packet loss [3]. Instead, we show that it is possible to satisfactorily reconstruct the lost blocks by using the available information surrounding them. This will result in an increase in bandwidth efficiency of the transmission. The basic idea of this work is to detect the lost block and then fill it by the available surroundings by creating the (8×8×8) matrix from surrounding of the lost block and take the 3D transformation. The aim of reconstruction algorithms, is to heal wounded images that suffer from distortion as a result of losing information in some block locations, due to fading channels and traffic congestions and other transmission errors, which may cause this loss of information, and hence, emerging a reconstruction algorithm. The algorithm must manipulate such errors in order to ensure proper recovery to perform the reconstruction process effectively.

2. PREVIOUS RELATED WORK

Based on Walidlet transform, [4] proposed a new scheme for using walidlet transform of lost image blocks in wireless image transmission. This method employed a new approach of 2D-matrix manipulation. These methods of reconstruction consist of mainly generation of matrix manipulation, computation of the specified transformation and post processing to obtain the lost block. The manipulation matrix is of dimension (16 x 16), Formed from the 8 x 8 matrices that surround the lost block. Rane et al. [5], proposed a fast scheme for wavelet-domain interpolation of lost image blocks in wireless image transmission. The algorithm is designed to be compatible with the wavelet-based JPEG2000 image compression standard. In the transmission of block-coded images, fading in wireless channels and congestion in packet-switched networks can cause entire blocks to be lost. Instead of using common retransmission query protocols, lost blocks are reconstructed in the wavelet-domain using the correlation between the lost block and its neighbors. The algorithm first uses a simple method to determine the presence or absence of edges in the lost block. This is followed by an interpolation scheme, designed to minimize the block ness effect, while preserving the edges or texture in the interior of the block. The interpolation scheme minimizes the square of the error between the border coefficients of the lost block and those of its neighbors, at each transform scale. The performance of the algorithm on standard test images, its low computational overhead at the decoder. They [5] have also designed an algorithm for **Structure and Texture Filling-in of Missing Image Blocks in Wireless Transmission and Compression Applications. It was** an approach for filling-in blocks of missing data in wireless image transmission is presented in this paper. When compression algorithms such as JPEG are used as part of the wireless transmission process, images are first tiled into blocks of 8×8 pixels. When such images are transmitted over fading channels, the effects of noise can kill entire blocks of the image. Instead of using common

retransmission query protocols, the algorithm aims to reconstruct the lost data using correlation between the lost block and its neighbors. If the lost block contained structure, it is reconstructed using an image inpainting algorithm, while texture synthesis is used for the textured blocks. The switch between the two schemes is done in a fully automatic fashion based on the surrounding available blocks. The performance of this method is tested for various images and combinations of lost blocks [6]. Waleed and Atheer[7],proposed a new scheme for Lost Block Reconstruction in noisey environment The reconstruction is achieved using the Boundary Interpolation (BI) which is based on wavelet transform. The algorithm's performance is further improved through the modification of the Boundary Interpolation algorithm.

3. The Modified Hybrid Transform.

The main idea behind the 3D-Modified Hybrid transform is first to apply the three dimensions discrete cosine Transform (3-D DCT) to the three dimensions signal (image). Next, to map the 3D object into 2D-object using the 3D Radon transforms. Hence, it is required to take the two dimension inverse Discrete cosine Transform (2-D IDCT) of the produced two dimensions signal. Finally, perform the 2D Multicircularlet transform of the resultant two dimensions signal. Thus the structure of this transform consists of four fundamentals parts,

Three dimensions Discrete Cosine Transform (3-D DCT).

Three dimension Radon Transform (3D-RT).

Two Dimension Inverse Discrete cosine Transform (2-D IDCT).

Two Dimension Multicircularlet Transform (2-D MCT) .

Fig.1 illustrates the block diagram of the 3D-Modified Hybrid Transforms.

It is expected that this Transform will give a high performance and strong properties. This is because it combines together the good properties of the local transforms.

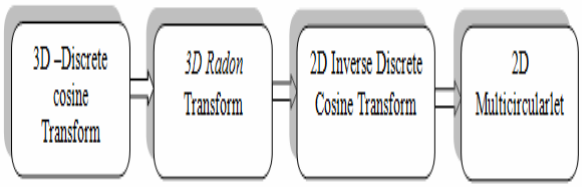

Fig. 1: block diagram of the 3D-Modified Hybrid Transforms

3.1 Algorithm for computing 3D Modified Hybrid Transform:

To compute 3D Modified Hybrid transform, the next steps should be followed:

i. Go to 3-D DCT:

Computing three dimensions discrete cosine Transform.

ii. Preprocessing: Here it is necessary to check for dimensions; matrix should be an N×N×N matrix, where N must be the prime number If the matrix is not of size N×N×N, a zero padding operation should be performed to the matrix (adding rows or columns or frames of Zeros to get a matrix of size N×N×N and they must be a prime number).

iii. Computing the best directions: To compute the best directions, the following steps should be followed:

Step1: Define (x, y, z) arbitrary vector.

Step2: Arrange vectors in volumes in different views X-view, Y-view, and Z-view

Step3: Calculate Φ and θ in Radian.

Step4: Convert X-view (Cart) to X-view (Spherical).

Step5: Convert Y-view (Cart) to Y-view (Spherical).

Step6: Round the X-view (Spherical) and Y-view (Spherical).

Step7: Rearrange the contain of data according to X-view (Spherical) and Y-view (Spherical).

iv. Compute the Fourier slices: Finding the Fourier slices

That must be taken. The resulting matrix after Fourier slices are (RR)

v. Back to the spatial domain:

Applying 2-D IDCT to resulting (RR) matrix.

vi. **Resizing:** resizing the resulting matrix into N×N where N must be of power 2

vii. **Applying 2D MCT:** Here it is apply the 2D dimensional discrete multicircularlet transform (2D MCT) [8].

3.2 The Inverse of the Proposed 3D – Modified Hybrid Transforms

In order to reconstruct the original 3-D signal (image) from the transformed matrix, an inverse 3D Modified Hybrid transforms steps must be followed. **Fig.2** illustrates the block diagram of the Inverse 3D-Modified Hybrid Transforms. The process starts by taking the Inverse Discrete Multicircularlet transform, using critically sampling scheme (1st order approximation of post processing). Then after preprocessing (resizing the resulting matrix) apply the two dimensional discrete cosine transform to the resulting matrix and then apply inverse 3D Radon transform and applying inverse 3D discrete cosine Transform and post processing. In the next sections a proposed algorithm to compute the inverse discrete multicircularlet transform using critical sampling preprocessing scheme.

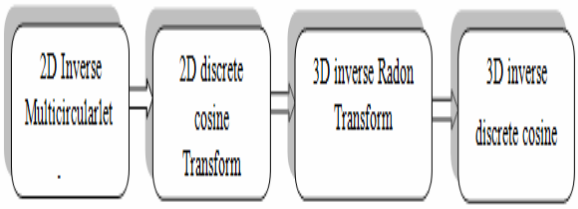

Fig.2 the Inverse 3D Modified Hybrid Transform

3.2.1 Algorithm for computing inverse 3D Modified Hybrid Transform

To reconstruct the original 3-D signal (N× N×N matrix) from the 3D Modified Hybrid transformed 3-D signal (N× N×N matrix), the Inverse 3D Modified Hybrid Transform should be used. The next steps exhibit the sequence of this algorithm:

1. Apply 2_D IMCT: Here it is required to apply the two dimension inverse discrete multicircularlet transform (2_DIMCT).

2. Inverse resizing: Check coefficients matrix length, length should be a prime number. If the coefficients matrix length is not a prime number, a zero padding operations should be performed to the coefficients matrix size, such as removing rows and columns from the coefficients matrix (which are added in the forward steps).

3. Apply 2-D DCT: Here it is required to apply the two dimensional discrete cosine transform.

4. Compute the best directions: The same geometrical algorithm of

Computing the best directions was applying in the forward steps and backward steps, described previously.

5. Compute the Fourier slices: Find the Fourier slices that must be taken.

6. Rearrang Fourier slices: Sort the Fourier slices according to the new positions, getting from compute the best sequence of directions is obtained.

7. Apply 3_D IDCT: Here it's required to apply 3D inverse discrete cosine transform.

4. The Main Structure of the Proposed Method Using 3D-Modified Hybrid Transform:

The reason for employing the 3D-Modified Hybrid transform instead of the 3D Radon or 3D- multiwavelet transforms is that, the 3D Modified Hybrid transform has the ability to

detect sharp areas in images edges. This is an advantageous over other transforms that failed in reconstructing such areas, therefore it is predicted that this transform will have the capability to upgrade the reconstruction performance significantly.

In addition, the 3D Modified Hybrid owns many other characteristics that can be summarized in:

1- Maintaining the effect of two transforms at the same time, which are: the three dimension discrete cosine transform (3D DCT), and the 2D Multicircular let Transform (MCT).
2- Using the 3D Radon Transform helps visualizing the image with different angles.
3- Cartesian information is transformed into spherical information which is very important due to the difficulty of transforming images from spatial domain into spherical domain.
4- It is possible to employ the reconstruction process in different angles, that is because of the transformation of information from 3-D into 2-D implicitly.

According to the above, a study has been developed to use the 3D Modified Hybrid transform to reconstruct lost blocks in images. Initially, the idea was to implement the reconstruction within the 3D DCT, or 3D radon, or the 3D multiwavelet transforms.

The block diagram of the system can be concluded as depicted in **Fig.3**

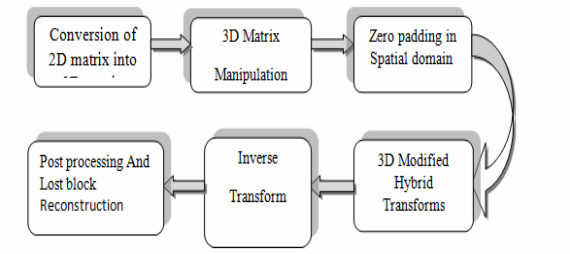

Fig.3 the proposed system using 3D Modified Hybrid Transform

It starts with zero padding in spatial domain and next 3D-matrix manipulation that is responsible of generating a (8×8×8) blocks matrix. This matrix (will be referred to as M matrix) will play the leading role in the reconstruction process.

The algorithm of the proposed system assumed a block of (8×8×3) is completely lost, and hence starts preprocessing to compute the Matrix from the lost block and the surrounding ones. The reason for selecting (8×8×3) size is the standardization that is followed in image compression. Knowing that it is impossible to transmit any image without compression due to its high size, hence the selection of (8×8×3) block size is beyond any dispute. The preprocessing start with zero padding in spatial domain and next 3D-matrix manipulation through which matrices of (8×8×3) that surrounds the lost block will be combined to create 3D matrix of size (8×8×8). Next, a transform computation will be applied which is either the 3D-Radon transform or the3D-multiwavelet transform. In this case a special method of computation was adapted for the application of the transformation. After arranging the (8×8×8) coefficient an inverse transformation will be followed. Finally the selection of the lost block will be according to a post processing depending on the manipulation followed before. The algorithm starts first by tiling the image into

8 x 8 blocks. Then iteratively, checking each block. If a lost block was detected, then start the Process of reconstruction according to the position of the lost block being Detection matrix method (DM), an easy to implement and efficient algorithm that can determine whether a block of an image has lost information or not. The next section will discuss in details of the detection matrix technique to give a comprehensive view of the reconstruction system proposed .

4.1 Detection Matrix for Lost Block Reconstruction

In order to perform the reconstruction process, a detection method should be enforced to find out the missing blocks. The proposed system presents a technique for lost block detection that is based on a specially generated matrix called the detection matrix. The idea is that, at any given block B of an image I, and after a quantization process Q (B) of presumed 16

levels. After several experimental tests it was found that for images of sizes 128 x 128 up to 512 x 512, the successful number of quantization levels was 16. The block B is said to be safe (no loss in its information) if each diagonal element in the detection matrix of the block B has a maximum value in its corresponding row. The main steps to compute the detection (DM) for a given image are illustrated in the following algorithm: The intensity image is quantized into 16 levels.

1) For the quantized image, the level **j** after level **i** is counted given that
i = 1…16, j = 1…16.

3) The counted value is put in a new matrix called detection Matrix (DM) in the location (i, j).

4) For the final matrix, if the image does not have any lost blocks then for each row, the diagonal element has the maximum value in that row. Otherwise, the image has lost blocks [6].

5. Experiment results.

The following examples have been tested after setting the (M) matrix for each given transform to its best arrangement, to compare the performance of the proposed system with these transforms. The performance of the system using 3D Radon Transform illustrated in **Table 1**, the performance of the system using Multiwavelet transform illustrated in **Table 2**, finally the performance of the system using 3D Modified Hybrid Transform illustrated in **Table 3**.

Table.1 reconstruction example using Multiwavelet transform

images	Data lost	PSNR	MSE
1	3%	53.98db	0.0168
2	3.5%	50.74db	0.0157
3	3.66%	46.39db	0.0171
4	5%	42.56db	0.023
5	2.5%	55.389db	0.01801
6	7%	38.19db	0.0283
7	7.8%	38.106db	0.0289
8	11%	27.45db	0.0397
9	8.5%	31.625db	0.0429
10	4.7%	42.65db	0.0295

Table 2 reconstruction example using 3D-Radon transform

images	Data lost	PSNR	MSE
1	3%	56.98db	0.0162
2	3.5%	51.74db	0.0153
3	3.66%	48.39db	0.0168
4	5%	43.56db	0.021
5	2.5%	57.389db	0.0172
6	7%	39.19db	0.027
7	7.8%	39.106db	0.0281
8	11%	28.45db	0.0393
9	8.5%	33.625db	0.0421
10	4.7%	44.65db	0.0285

Table-3 reconstruction example using 3D-Hybrid transforms

images	Data lost	PSNR	MSE
1	3%	58.437db	0.0131
2	3.5%	52.331db	0.0149
3	3.66%	51.4db	0.0158
4	5%	44.82db	0.0196
5	2.5%	59.51db	0.0168
6	7%	41.744db	0.024
7	7.8%	40.19db	0.0267
8	11%	31.43db	0.037
9	8.5%	37.26db	0.0321
10	4.7%	48.359	0.0213

6. Conclusions

In this paper, a new algorithm of lost blocks reconstruction in RGB transmitted images is proposed. The originality of the proposed algorithm comes from the following features:

1- The algorithm is based on a matrix manipulation technique that is responsible for generating a (8×8×8) matrix in a block by block fashion. This generated matrix will be responsible of reconstructing the lost block after applying certain transforms. The use of the (8×8×8) generation matrix operations exhibit a better performance than the generation of (16×16) methods that suffer from many deficiencies of time consumption and accumulated errors.

2- The association of this matrix manipulation technique and its matching with those transforms that are dominated most researches in the field of image processing. Namely the 3D Radon, 3D-Multiwavelet, and the recently developed 3D-Modified Hybrid transform.

3- The system proposes a lost block detection scheme for identifying the lost information in an (8×8×3) image block fashion. This is done through the use of a proposed method for the generation of a special detection matrix.

4- The quality of reconstruction achieved when using the 3D Modified Hybrid transform, was remarkably higher than those associated with the 3D- multiwavelet and 3D Radon transform, especially in the cases of sharp edges.

Finally, although the performance of the reconstruction algorithm when using the 3D Modified hybrid transform is noticeably the best comparing with the 3D- multiwavelet and 3D Radon transforms, yet, generally the performance of the two transforms is highly acceptable. This is due to the involvement of the fast 3D-matrix manipulation technique incorporated in the three reconstruction algorithms.

7. References

[1] G. K.Wallace, “The JPEG still picture compression standard,” *Commun. ACM*, vol. 34, no. 4, pp. 30–44, 1991.

[2] E. Chang, “An image coding and reconstruction scheme for mobile computing,” in *Proc. 5th IDMS*, Oslo, Norway, Sept. 1998, pp. 137–148.

[3] S. S. Hemami, “Digital image coding for robust multimedia transmission,” in *Proc. Symp. Multimedia Communications and Video Coding*, New York, 1995.

[4] Sarwa Amir,” Lost Blocks Reconstruction in Image Transmission Systems Using the Walidlet Transform” PhD thesis, Iraqi Commission for Computers and Informatics Institute of Postgraduate Studies, June 2006.

[5]Shantanu D. Rane, J.R, and Guillermo**,** S., "Wavelet-Domain Reconstruction of Lost Blocks in Wireless Image Transmission and Packet-Switched Networks", IEEE **ICIP(1)** , pp. 309-312, 2002

[6]Shantanu D. Rane, J.R, and Guillermo**,** S., "Structure and texture filling-in of missing image blocks in wireless transmission and compression", IEEE ICIP, pp. 317-320, 2002.

[7] waleed A .mahmoud,Atheer A.sabri." **Wavelet & Multiwavelet Lost Block Reconstruction in Noisey Environment"**Eng.&Tech .journal,Vol 27,No.4,2009.

[8] Iman Alubady,"image compression using mixed transform",M.SC, thesis ,university of Baghdad,2009.

OPTIMAL DESIGN OF MODERATE THICK LAMINATED COMPOSITE PLATES UNDER STATIC CONSTRAINTS USING REAL CODING GENETIC ALGORITHM

Dr. Majid H. Faidh-Allah
Dept. of Mech. Eng.
Baghdad University

Musaddiq A. M. Kadem
Dept. of Mech. Eng
Baghdad University

ABSTRACT

The objective of the current research is to find an optimum design of hybrid laminated moderate thick composite plates with static constraint.
The stacking sequence and ply angle is required for optimization to achieve minimum deflection for hybrid laminated composite plates consist of glass and carbon long fibers reinforcements that impeded in epoxy matrix with known plates dimension and loading. The analysis of plate is by adopting the first-order shear deformation theory and using Navier's solution with Genetic Algorithm to approach the current objective. A program written with MATLAB to find best stacking sequence and ply angles that give minimum deflection, and the results comparing with ANSYS.

الخلاصة:

ان .ان الهدف من هذا البحث هو ايجاد التصميم الامثل للصفائح المتراكبه الهجينه متوسطة السمك في ظل الظروف السكونيه التتابع الصفائحي وزاويه ميلان الالياف لكل صفيحه مطلوبه للحصول على امثل تصميم لصفائح متراكبه هجينه مكونة من ان تحليل الصفيحة . في الايبوكسي كمادة القالب والمعلومة الابعاد والقوة المسلطة الياف طويلة من الزجاج والكاربون مغموره لايجاد التتابع الطبقي MATLABكتب برنامج باستعمال . Navierتم باستعمال نظرية تشوه القص من الدرجة الاولى وحل ANSYS. وقورنت النتائج مع ال الافضل وزوايا الميلان التي تعطي اقل انحراف

Keywords: optimization, moderate thick plates, genetic algorithms, Navier's solution

1.INTRODUCTION

Structural optimization is a process by which the optimum design is aimed while satisfying all the defined constraints. In recent years, using of moderate thick hybrid laminated composite materials in fabrication of mechanical, airspace, marine and machine industries are of major concern, due to their high strength and light weight. The design variables could be stacking sequence, orientation, thickness and other design variables. The evolutionary optimization technique such as genetic algorithms is easier and reduces searching and solving time of optimization problem. The use of real coding genetic algorithm is easier to deal with than binary encoding and faster and it's used in this paper to find optima stacking sequence and ply angles of hybrid moderate thick laminated composite plates. The use of first order shear deformation theory in the analysis of moderate thick plates is widely used and acceptable as a very good solution from many authors and researchers, so it's used with modified genetic algorithms to find the objective of this research.

At **(1981 Stround, S. et al)**., developed a programming solution using Fortran77 based on linear programming to find the optimal design for composite laminates for buckling constraints. There is many researchers study the study of optimization of composite plates, **(Kim, S. J. and Goo, N. S. 1992)**, studied the use of Fuzzy Environment to find optimal design of laminated composite plates. There goal was minimize weight design for composite laminate plates. At (**1993 Kam, T. Y**.) et al. published their paper that deals with dynamic programming with finite element method to find the optimum aspect ratio for laminated composite plates that give maximum stiffness and low weight and find the natural frequencies for the plates. At **(2007, Paluch, B. et al)**, combine finite element method with genetic algorithm to optimize composite hybrid moderate thick and thick structures with variable thickness. **(Apalak, M. Kamel et al 2007)**, studied layer optimization and stacking sequence using a model of hybrid artificial intelligence method based on a genetic algorithm foundation and accelerated by use artificial neural network with use finite element method as a evaluation technique to find maximum fundamental frequency. They also made a numerical sequence to optimize layer sequences for maximum fundamental frequency using genetic algorithm with evaluation technique that Ritz-based layerwize.

2.MECHANICS OF MODERATE THICK LAMINATED PLATES

The static analyses of orthotropic plates have been topics of continued interest; a variety of analytical and discrete mathematical models based on different theories have been proposed. Generally, the models are based on classical plate theory in which plane sections remain plane and normal to the midsurface after deformation, and first order shear theory which includes the transverse shear deformation. The classical plate theory can be regarded as a special case of the first order shear theory. According to both theories, the displacements, $u(x,y,z), v(x,y,z)$ and $w(x,y,z)$, at an arbitrary point in the plate can be represented as functions of midsurface displacements and angular rotations

$$\begin{aligned} u(x,y,z) &= u^o(x,y) + z\Psi_x(x,y) \\ v(x,y,z) &= v^o(x,y) + z\Psi_y(x,y) \qquad (1) \\ w(x,y,z) &= w^o(x,y) \end{aligned}$$

It is well known that when the aspect ratio of the plate increases, the applicability of the classical plate theory becomes questionable. If, in addition, the plate material is with the magnitude of the transverse shear, the inadequacy of the classical plate theory is even more pronounced **(Ten, K. K. et al 1983)**.

As before the analysis of plates using classical laminated plate theory (CLPT) use for thin plate. The define of thin plates is not unique. There's a different standards use by researcher of different countries based on academic relations and actual needs of those countries, but the major characteristic that use to define thin or thick plates is the aspect ratio. This research use the scale of Dr. J. N. Reddy that consider aspect ratio over $(1/50)$ is thin plate, aspect ratio less than $(1/20)$ is thick plate and in between is so called moderate thick plate which is in this subject is used and studied.

In the First–order Shear Deformation plate Theory (FSDT), the Kirchhoff hypothesis is relaxed by assume that the transverse normal do not remain perpendicular to the midsurface after deformation**(Reddy, J. N. 2004)**. This amount to including transverse shear strains in the theory.

Under the same and restrictions as in the classical laminate theory, the displacement field of the first-order theory is

$$u(x,y,z) = u^o(x,y) + z\Phi_x(x,y)$$
$$v(x,y,z) = v^o(x,y) + z\Phi_y(x,y) \qquad (2)$$
$$w(x,y,z) = w^o(x,y)$$

Where ($u^o, v^o, w^o, \Phi_x, \Phi_y$) are unknown function to be determined, and (u^o, v^o, w^o) are denote the displacements of a point on plane z = 0 , and

$$\Phi_x = \frac{\partial u}{\partial z}$$
$$\Phi_y = \frac{\partial v}{\partial z} \qquad (3)$$

Which indicate that Φ_x and Φ_y are the rotation of a transverse normal about the y and x axis respectively.

Constitutive equations are that relate the force and moment resultants to the strain of laminate.

First, the resultants direct forces (not transverse) acting on a laminate are obtained by integration of the stresses in each layer of lamina through the laminate thickness.

As before

$$[N] = \sum_{k=1}^{n} \int_{z_k}^{z_{k+1}} [\sigma]\, dz \qquad (4)$$

Direct stresses made of direct and bending loads so

$$\begin{bmatrix} N_x \\ N_y \\ N_z \end{bmatrix} = \sum_{k=1}^{n} \int_{z_k}^{z_{k+1}} \begin{bmatrix} \overline{Q}_{11} & \overline{Q}_{12} & \overline{Q}_{16} \\ \overline{Q}_{12} & \overline{Q}_{22} & \overline{Q}_{26} \\ \overline{Q}_{16} & \overline{Q}_{26} & \overline{Q}_{66} \end{bmatrix}^{(k)} \begin{bmatrix} \varepsilon_x^{(0)} + z\varepsilon_x^{(1)} \\ \varepsilon_y^{(0)} + z\varepsilon_y^{(1)} \\ \gamma_{xy}^{(0)} + z\gamma_{xy}^{(1)} \end{bmatrix} dz \qquad (5)$$

Or in other words

$$\begin{bmatrix} N_x \\ N_y \\ N_z \end{bmatrix} = \begin{bmatrix} A_{11} & A_{12} & A_{16} \\ A_{12} & A_{22} & A_{26} \\ A_{16} & A_{26} & A_{66} \end{bmatrix} \begin{bmatrix} \varepsilon_x^{(0)} \\ \varepsilon_y^{(0)} \\ \gamma_{xy}^{(0)} \end{bmatrix} + \begin{bmatrix} B_{11} & B_{12} & B_{16} \\ B_{12} & B_{22} & B_{26} \\ B_{16} & B_{26} & B_{66} \end{bmatrix} \begin{bmatrix} \varepsilon_x^{(1)} \\ \varepsilon_y^{(1)} \\ \gamma_{xy}^{(1)} \end{bmatrix} \qquad (6)$$

Where $\varepsilon^{(0)}$ and $\varepsilon^{(1)}$ are vectors of the membrane and bending strains

$$\begin{bmatrix} \varepsilon_x^{(1)} \\ \varepsilon_y^{(1)} \\ \gamma_{xy}^{(1)} \end{bmatrix} = \begin{bmatrix} \dfrac{\partial \Phi_x}{\partial x} \\ \dfrac{\partial \Phi_y}{\partial y} \\ \dfrac{\partial \Phi_x}{\partial y} + \dfrac{\partial \Phi_y}{\partial x} \end{bmatrix} \qquad (7)$$

For moments it is not different from above so

$$\begin{bmatrix} M_x \\ M_y \\ M_{xy} \end{bmatrix} = \sum_{k=1}^{n} \int_{z_k}^{z_{k+1}} \begin{bmatrix} \sigma_x \\ \sigma_y \\ \tau_{xy} \end{bmatrix} z\, dz \qquad (8)$$

$$\begin{bmatrix} M_x \\ M_y \\ M_{xy} \end{bmatrix} = \sum_{k=1}^{n} \int_{z_k}^{z_{k+1}} \begin{bmatrix} \overline{Q}_{11} & \overline{Q}_{12} & \overline{Q}_{16} \\ \overline{Q}_{12} & \overline{Q}_{22} & \overline{Q}_{26} \\ \overline{Q}_{16} & \overline{Q}_{26} & \overline{Q}_{66} \end{bmatrix}^{(k)} \begin{bmatrix} \varepsilon_x^{(0)} + z\varepsilon_x^{(1)} \\ \varepsilon_y^{(0)} + z\varepsilon_y^{(1)} \\ \gamma_{xy}^{(0)} + z\gamma_{xy}^{(1)} \end{bmatrix} z\, dz \qquad (9)$$

$$\begin{bmatrix} M_x \\ M_y \\ M_{xy} \end{bmatrix} = \begin{bmatrix} B_{11} & B_{12} & B_{16} \\ B_{12} & B_{22} & B_{26} \\ B_{16} & B_{26} & B_{66} \end{bmatrix} \begin{bmatrix} \varepsilon_x^{(0)} \\ \varepsilon_y^{(0)} \\ \gamma_{xy}^{(0)} \end{bmatrix} + \begin{bmatrix} D_{11} & D_{12} & D_{16} \\ D_{12} & D_{22} & D_{26} \\ D_{16} & D_{26} & D_{66} \end{bmatrix} \begin{bmatrix} \varepsilon_x^{(1)} \\ \varepsilon_y^{(1)} \\ \gamma_{xy}^{(1)} \end{bmatrix} \qquad (10)$$

A_{ij} is called extensional stiffness matrix, B_{ij} the bending-extensional coupling stiffness matrix and D_{ij} is bending stiffness matrix.

A_{ij}, B_{ij} and D_{ij} matrices can be written as

$$A_{ij} = \sum_{k=1}^{n} \overline{Q}_{ij}^{(k)} (z_{k+1} - z_k)$$
$$B_{ij} = \frac{1}{2} \sum_{k=1}^{n} \overline{Q}_{ij}^{(k)} (z^2{}_{k+1} - z_k{}^2) \qquad (11)$$
$$D_{ij} = \frac{1}{3} \sum_{k=1}^{n} \overline{Q}_{ij}^{(k)} (z^3{}_{k+1} - z_k{}^3)$$

Now equations (6) and (11) can be written in a compact form as

$$\begin{bmatrix} [N] \\ [M] \end{bmatrix} = \begin{bmatrix} [A] & [B] \\ [B] & [D] \end{bmatrix} \begin{bmatrix} [\varepsilon^{(0)}] \\ [\varepsilon^{(1)}] \end{bmatrix} \qquad (12)$$

And the transverse force resultant across the lamina of thickness (h) be as

$$\begin{bmatrix} Q_x \\ Q_y \end{bmatrix} = \int_{-\frac{h}{2}}^{\frac{h}{2}} \begin{bmatrix} \tau_{xz} \\ \tau_{yz} \end{bmatrix} dz \qquad (13)$$

Since the transverse shear strains are represented as constant through the laminate thickness, it follows that the transverse shear stresses will also be constant. In composite laminated plates, the transverse shear stresses vary at least quadratically through layer thickness. This discrepancy between the actual stress state and the constant stress state predicted by the (FSDT) is often corrected in computing the transverse shear force resultants (Q_x, Q_y) by multiplying the integrals in equation (14) with a parameter K, called shear correction coefficient, so

$$\begin{bmatrix} Q_x \\ Q_y \end{bmatrix} = K \int_{-\frac{h}{2}}^{\frac{h}{2}} \begin{bmatrix} \tau_{xz} \\ \tau_{yz} \end{bmatrix} dz \qquad (14)$$

These amounts to modifying the plate transverse shear stiffness. The factor K is computed such that the strain energy due to transverse shear stresses in equation (15) equals the strain energy due to the true transverse stresses predicted by the three-dimensional elasticity theory (Reddy, J. N. 2004).

The constitutive equation for transverse shear forces be

$$\begin{bmatrix} Q_x \\ Q_y \end{bmatrix} = K \begin{bmatrix} A_{44} & A_{45} \\ A_{45} & A_{55} \end{bmatrix} \begin{bmatrix} \dfrac{\partial w_o}{\partial y} + \Phi_y \\ \dfrac{\partial w_o}{\partial x} + \Phi_x \end{bmatrix} \qquad (15)$$

3.ANALYSIS OF MODERATE THICK PLATES

The case that used here is simply supported plates with constraint load in the middle, and the objective is to find the best design that give minimum value of deflection.

Navier present a solution of bending of simply supported plates by double trigonometric series
(Ventsel, Edward et al 2001).

The aim of this section is develop analytical solution of rectangular laminates using (FSDT) using Navier solution and that analysis, what is used in this research.

For simply supported laminated plate with (FSDT) analysis and had $a*b$ area **Fig.(1)**, the boundary conditions be

$$u_o(x,0)=0 \qquad N_x(0,y)=0$$
$$u_o(x,b)=0 \qquad N_x(a,y)=0$$

$$v_o(0,y)=0 \qquad N_y(x,0)=0$$
$$v_o(a,y)=0 \qquad N_y(x,b)=0$$

$$w_o(x,0)=0 \qquad M_x(0,y)=0$$
$$w_o(x,b)=0 \qquad M_x(a,y)=0$$
$$w_o(0,y)=0 \qquad M_y(x,0)=0$$
$$w_o(a,y)=0 \qquad M_y(x,b)=0$$

$$\Phi_x(x,0)=0$$
$$\Phi_x(x,b)=0$$
$$\Phi_y(0,y)=0 \qquad \Phi_y(a,b)=0$$

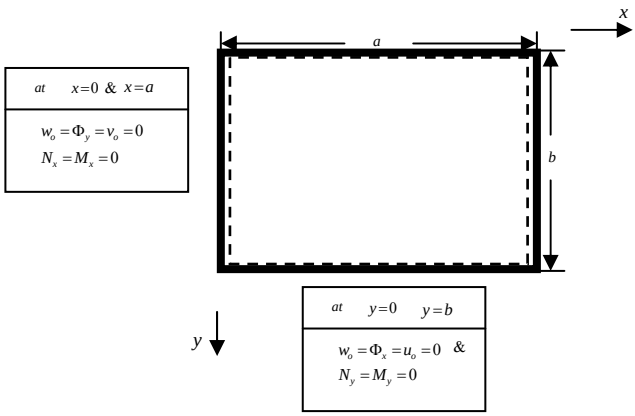

Fig. (1) Simply supported boundary conditions for laminated plate using FSDT

The boundary condition above are satisfied by the following excretions

$$u_o(x,y)=\sum_{n=1}^{\infty}\sum_{m=1}^{\infty} U_{mn}\cos\alpha x\sin\beta y$$

$$v_o(x,y)=\sum_{n=1}^{\infty}\sum_{m=1}^{\infty} V_{mn}\sin\alpha x\cos\beta y$$

$$w_o(x,y)=\sum_{n=1}^{\infty}\sum_{m=1}^{\infty} W_{mn}\sin\alpha x\sin\beta y$$

$$\Phi_x(x,y)=\sum_{n=1}^{\infty}\sum_{m=1}^{\infty} X_{mn}\cos\alpha x\sin\beta y$$

$$\Phi_y(x,y)=\sum_{n=1}^{\infty}\sum_{m=1}^{\infty} Y_{mn}\sin\alpha x\cos\beta y \qquad (17)$$

Where $\alpha = m\pi/a$ and $\beta = n\pi/b$

The mechanical load are also expanded in double Fourier sine series

$$q(x,y)=\sum_{n=1}^{\infty}\sum_{m=1}^{\infty}Q_{mn}\sin\alpha x\sin\beta y \qquad (18)$$

Where

$$Q_{mn}(t)=\frac{4}{ab}\int_0^a\int_0^b q(x,y)\sin\alpha x\sin\beta y\ dxdy \qquad (19)$$

The final form express as

$$\begin{bmatrix}\hat{S}_{11} & \hat{S}_{12} & 0 & \hat{S}_{14} & \hat{S}_{15}\\ \hat{S}_{12} & \hat{S}_{22} & 0 & \hat{S}_{24} & \hat{S}_{25}\\ 0 & 0 & \hat{S}_{33} & \hat{S}_{34} & \hat{S}_{35}\\ \hat{S}_{14} & \hat{S}_{24} & \hat{S}_{34} & \hat{S}_{44} & \hat{S}_{45}\\ \hat{S}_{15} & \hat{S}_{25} & \hat{S}_{35} & \hat{S}_{45} & \hat{S}_{55}\end{bmatrix}\begin{bmatrix}U_{mn}\\ V_{mn}\\ W_{mn}\\ X_{mn}\\ Y_{mn}\end{bmatrix}=\begin{bmatrix}0\\ 0\\ Q_{mn}\\ 0\\ 0\end{bmatrix} \qquad (20)$$

Where $\hat{S}_{ij}$ matrix is

$$\begin{aligned}
\hat{S}_{11}&=(A_{11}\alpha^2+A_{66}\beta^2)\\
\hat{S}_{12}&=(A_{12}+A_{66})\alpha\beta\\
\hat{S}_{14}&=(B_{11}\alpha^2+B_{66}\beta^2)\\
\hat{S}_{15}&=(B_{12}+B_{66})\alpha\beta\\
\hat{S}_{22}&=(A_{66}\alpha^2+A_{22}\beta^2)\\
\hat{S}_{24}&=\hat{S}_{15}\\
\hat{S}_{25}&=(B_{66}\alpha^2+B_{22}\beta^2)\\
\hat{S}_{33}&=K(A_{55}\alpha^2+A_{44}\beta^2)\\
\hat{S}_{34}&=KA_{55}\alpha^2\\
\hat{S}_{35}&=KA_{44}\beta\\
\hat{S}_{44}&=(D_{11}\alpha^2+D_{66}\beta^2+KA_{55}\\
\hat{S}_{45}&=(D_{12}+D_{66})\alpha\beta\\
\hat{S}_{55}&=(D_{66}\alpha^2+D_{22}\beta^2+KA_{44})
\end{aligned} \qquad (21)$$

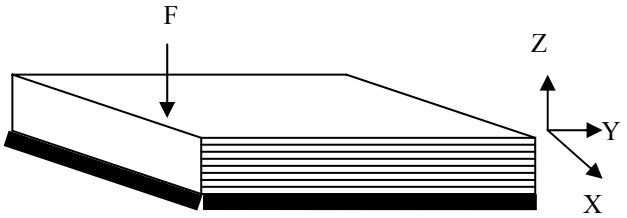

Fig. (2) Simply supported plate

4.GENETIC ALGORTHIM

Genetic algorithms are search and optimization algorithms that mimic the process of natural evolution, unlike conventional algorithms (Tabakov, P. Y. 2004), Genetic algorithms start from population of strings, each representing a solution in the search space. Moreover, there is no need of any derivative information and there is no requirement in terms of convexity of the search space. An evaluation function rates each string according to some kind of fitness measure. Starting from a population of strings, the successive application of so-called genetic operators (Crossover, mutation and reproduction, generates new populations. The search is performed, in such way that the best strings have increasing portability of being present, in the next generation. The algorithms stop at the end of the prescribed numbers of generations. The risk of the algorithms being trapped in a local minimal, since the research performed from a pool of points. In spite of using probabilistic transitional rule to perform the search, Genetic algorithms are distinct from a simple random walk, since the information embodied in the most successful strings, is passed to future generations.

The basic requirements for building Genetic algorithms are:

1.Encoding Technique
2.Evaluation Function
3.Initialization Procedure
4.Genetic Operators

Encoding Technique

The coding technique that used in this research is real coding, so it's used two kinds of fiber reinforcement, glass-fibers and carbon-fibers, embedded in polyester resin. The stacking sequence and ply angles are required. The material reinforcement types has the coding value (0 refers to glass-fiber and 1 refers to carbon-fibers) and ply angle for each laminate is vary from 0 to 180. The real coding of ply angle was done by putting the same real values of angles, and that making checking and evaluation easier.

A chromosomes made of material-ply angle sequence are selected from population. The case here taking as 8 (symmetry and unbalanced) stacking laminates, for example:

1	25	0	90	1	132	1	66

Evaluation Function

A function made from combining first-order shear deformation theory and Navier's solution is used as evaluation function. The case that taken in Navier's solution is concentrated load as said before.

Initialization Procedure

Genetic algorithm requires an initial population. This population is randomly

generated, and in the present work, its just random generation of bit strings.

Genetic Operators

The exploration of the search space is done through the successive application of the genetic operators. The most usual operators are crossover, mutation and reproduction.

Crossover

Crossover is one of the most important ways by which a genetic algorithm shuffles the information contained in the gene pool, in order to generate new chromosomes, i.e., new points in the search space. For example lets there are two chromosomes Selected randomly from the population, and the bit in between the two are randomly selected points in each strings, are swapped. That show below

1	25	0	90	1	132	1	66
0	156	1	22	1	12	0	45

The crossover operation here is by transfer some of bits between string 1 and 2, so let us transfer bits from bit 1 to bit 4. The new genes that generate is shown below

0	156	1	22	1	132	1	66

1	25	0	90	1	12	0	45

Mutation

The mutation operator selects a random position in the strings, and with a given probability, changes the corresponding bit. For example, the string that shows below

1	25	0	90	1	12	0	45

Be after mutation as in bit 5

1	25	0	90	0	12	0	45

As the search proceeds through the generations, the less fit members of the population are discarded. Thus, mutation prevents that some information is permanently lost. This occasional random change in the strings assures that new regions of the search space are explored, which could not be done exclusively with crossover and reproduction.

Reproduction

The strings for the next generation mating pool are copied with probability proportional to their fitness value. In the present case, let us consider four strings, representing different solution to the problem; the fitness value is evaluated through Navier's solution that based on first-order shear deformation theory.

In order to minimize the objective function, these solutions are ranked in suck way that, the best solution has the highest rank. Thus, the probabilities of each these strings being present in the next generation are, respectively, the ratio of the individual rank the sum of the ranks **(Brighenti, Roberto 2001)**. **Fig. (3)** Show structure of G.A.

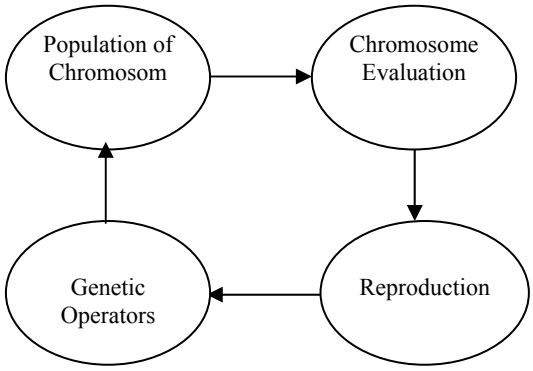

Fig. (3) Presents the general GA structure

5.THE PROGRAMING AND FINAL RESULT

Using MATLAP® version 7.4 to programming genetic algorithm program that use roulette wheel selection technique with real coding to reduce operation time, and with computer its hardware are: 2.4 gigabyte, 256 kilobyte cash processor, 1024 DDR1, bus 400 ram, Motherboard Gigabite SIS 651 and 80 gigabyte hard, and as said before the evaluation technique based on Navier's solution of FSDT (The window of programs shown in Fig. (4), and the flow chart of the program show in Fig. (5).

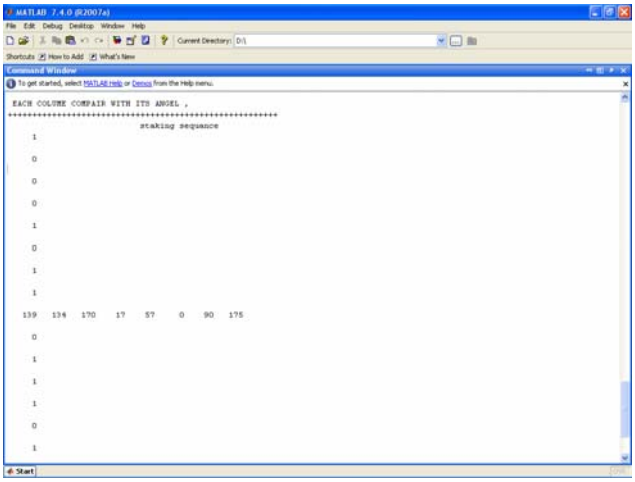

Fig. (4) MATLAP® Window that show the solution

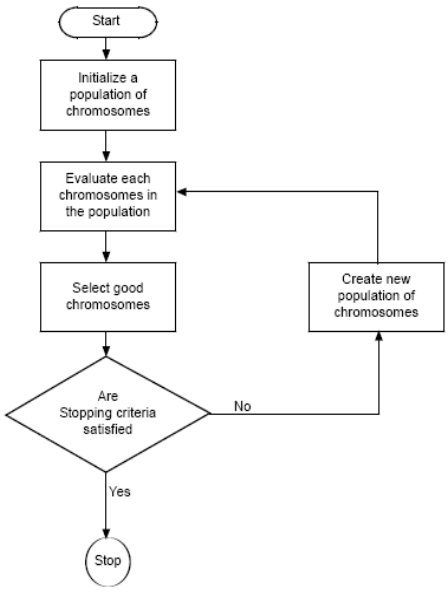

Fig. (5) Flow chart of G.A. program

For example use 500 Newton central load for simply supported moderate thick plate, and with the use laminates of epoxy-carbon fiber(see **Table1** and **Table2** for mechanical properties), and epoxy-glass fiber, taking there mechanical properties from [COMPOSITE MATERIALS HANDBOOK]that Published by Department of Defense, USA.]

Table (1) Show the properties of carbon-epoxy

E_x(N/m^2)	E_y(N/m^2)	E_z(N/m^2)	V_{12}	V_{23}	V_{31}	G_{12}(N/m^2)	G_{23}(N/m^2)	G_{31}(N/m^2)
181e9	10.3e9	10.3e9	0.3	0.29	0.28	7.17e9	7.17e9	10.1e9

Table (2) Show the properties of glass-epoxy

E_x(N/m^2)	E_y(N/m^2)	E_z(N/m^2)	V_{12}	V_{23}	V_{31}	G_{12}(N/m^2)	G_{23}(N/m^2)	G_{31}(N/m^2)
38.6e9	8.27e9	8.27e9	0.3	0.28	0.28	5.59e9	4.11e9	4.14e9

The final result is shown below for 8 unsymmetrical unbalanced plates.

1	139	0	90	0	75	0	149	1	57	0	7	1	90	1	175

and its deflection (Evaluation) 0.8072e-009 meter. **Fig. (6)** show minimization operation with genetic algorithm

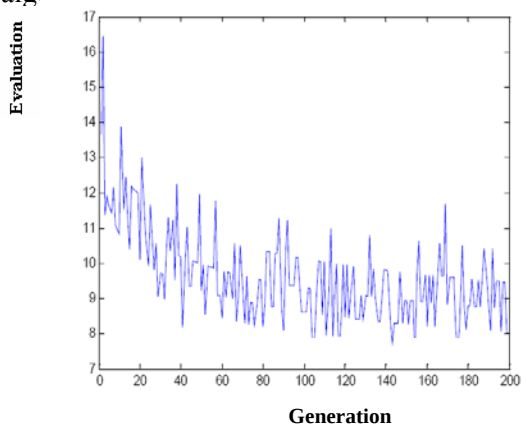

Fig. (6) Minimization operation with genetic algorithm

Using Finite element program *ANSYS* ® version 11.0 (**Fig.(7)**) for simulation of solution and comparing. **Table (3)** and **(4)** show eight cases of solution for six difference loads

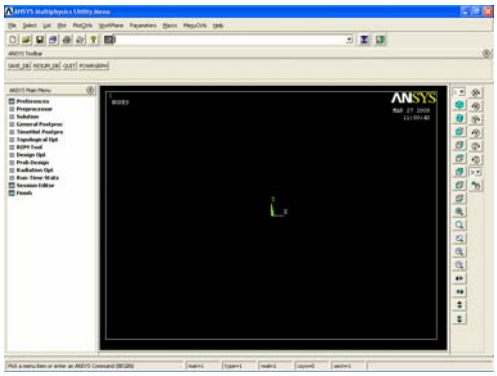

Fig. (7) ANSYS® Window that show the solution

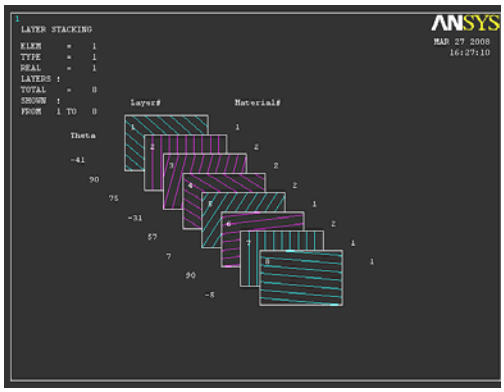

Fig. (8) ANSYS representation of the plate (the example**)**

The ANSYS resultant (Fig.(8)) is .78e-9 meter and its give a difference about .0372 from MATLAP program and that about 4%.

Table (3) Final results for some of cases (loads)

Load Value (N)	Load Condition	Area (cm^2)	Number of Stacking Laminate	G.A Best Displacement w(m)	ANSYS Test W(m)
1000	Central Load	225	8	1.3660 e-10	1.330 e-10
3000	-	-	-	4.0975 e-10	4.10 e-10
6000	-	-	-	8.1924 e-10	7.598 e-10
9000	-	-	-	1.2293 e-9	1.009 e-9
12000	-	-	-	1.5246 e-9	1.4e-9
15000	-	-	-	1.9057 e-9	2.02e-9
18000	-	-	-	2.4588 e-9	2.28 e-9
21000	-	-	-	2.6691 e-9	2.805 e-9

Table (4) Final results for some of cases (stacking sequence and angles)

loading	Material sequence								Angles							
1000	1	1	1	1	0	0	1	1	118	139	21	0	96	66	107	101
3000	1	1	1	0	1	0	1	1	141	68	142	52	40	37	123	145
6000	1	1	0	1	1	1	0	1	94	8	86	23	140	87	175	105
9000	1	1	1	0	1	1	0	1	6	8	48	19	95	100	72	177
12000	1	1	1	1	1	0	1	1	134	155	128	63	71	76	65	60
15000	1	1	1	1	1	0	1	1	64	102	136	160	108	11	70	98
18000	1	1	0	1	1	0	1	1	108	60	160	137	147	155	52	136
21000	1	1	1	1	1	0	1	1	168	131	126	147	162	101	112	171

6.DISCUSSION

It can be seen in **Fig.(6)**[as example] that the instability of evaluation of real coding genetic algorithm, an that notice by many authors and researchers like, M. Kemal Apalak et al., Mohammed Reza and Zafer Gurdal et al, but the real coding G.A. more quicker than binary coding so it's widely used. The analysis done by using data taking from [COMPOSITE MATERIALS HANDBOOK] that Published by Department of Defense, USA. The time that taking from GA program is about 7 hours according to hardware that used and that time depend on number of variables and the population of the case to e study. Another computer used to apply GA program and its hardware specification are: 2.2 Dual Core LGA processor and 2 gigabyte, DDR2, bus 800MHz, Mainboard 965 Intel chipset, hard SATAII 200 Gigabyte and that reduce time of working to 9 hours and then using 3.6 Dual core LGA processor and the same previous hardware it improve time saving so that it take 4 hours to do the process. The analysis of plates comparing with ANSYS shows a good match for the analysis of plates (about 4% and less difference).

7.CONCLUSIONS

It can be seen in Table (3) and (4) the final results of central loads for simply supported composite plates, and the final results gives the minimum deflection that can be found and design of laminated plates (stacking sequence and ply angle).The use of genetic algorithms is so effective than other methods of optimization, but the classical genetic algorithms more slow, so modifying GA to real coding strategy be more efficient and fast. Programming of GA is more suitable for many purposes, and form of functions than GA tool box that built in MATLAB but it is slower in finding solution, but the benefit of Varity of Evaluation function for classic programming making it more common. Using ANSYS to analyzed and optimized plates show a god approach in results. Most of authors used symmetric and balanced plates to reduce the population, but the final result be guided by their choices, here, in this research, the use of angles (0 to 180) make more chances to approach the best solution to have the requirements.

REFERENCES

– Apalak, M. K. et al., "Layer Optimization for Maximum Foundational Frequency of Laminated Composite Plates for Different Edge Conditions", Composite Science and Technology Journal, Vol. 68, pp 537-550, 2007.

- Bond, D. A., 1996, "Lecture Notes on Composites", lecture of University of Manchester.
- Department of defense publication "COMPOSITE MATERIALS HANDBOOK", USA, 1997.
- Faimum, F. et al., "Analytical Sensitivities of a Shear Deformation Laminate Composite Plates", Sixth World Congresses of Structural and Multidisciplinary Optimization, Brazil, Rio de Janeiro, 30 May-03 June 2005.
- Gilat, Amos, 2001, "MATLAB®, an Introduction with Applications", John Wiley & Sons, INC.
- Gurdal, Zafer et al., "Design and Optimization of Laminated Composite Materials", John Wiley & Sons, INC., 1999.
- Kam, T. Y. et al., "Design of Laminated Composite Plates for Optimal Dynamic Characteristic Using a Constrained Global Optimization Technique", Composite in Applied Mechanics and Engineering Magazine, Vol. 3, pp 389-402, 1993.
- Moaveni, Saeed, 1999, "Finite Element Analysis, Theory and Application with *ANSYS*", Prentice Hall.
- Pluch, B. et al., "Combining a Finite Element Programme and a Genetic Algorithm to Optimize Composite Structures with Variable Thickness", Composite and Structure Journal, Vol. 81, pp 284-294, 2007.
- Reddy, J. N., 2004, "Mechanics of Laminated Composite Plates and Shells, Theory and Analysis", CRC Press, Second edition.
- Reza, Mohammed et al, "A Hybrid Radial-Based Neuro-GA Multiobjective Design of Laminated Composite Plates Under Moisture and Thermal Action", International Journal of Computer, Information and Systems Science and Engineering, Vol. 1,No. 2, pp 109-116, 2007.
- Roberto, Brighenti , 2001, "Fiber Distribution Optimization in Fiber-Reinforced Composites by a Genetic Algorithm", Journal of Composite Structures, Vol.54, pp 349-354.
- Tabakov, P.Y., 2004, "Multi-Dimensional Design Optimization of Laminated Structures Using an Improved Genetic Algorithm", Journal of Composite Structures, Vol.71, pp 1-15.
- Ten, K. K. et al., 1983, "On the Three Dimensional Analysis of Thick Laminated Plates", Journal of Sound and Vibration Vol. 2, pp. 213-224.
- Townsend, A. A., 2003, "Genetic Algorithm, a Tutorial", lecture of University of Alabama.
- Ventsel, Edward et al, 2001, "Thin Plates and Shell, Theory and Application", Marcei Dekker, INC.

List of Symbols

a	Height of Plate	m
b	Width of Plate	m
E	Young's modulus	N/m^2
K	Shear correction factor	unit less
N	Force	N
M	moment	N.m
S_{ij}	Compliance matrix	unit less
Q	Shear force	N
u	Deflection in x direction	m
v	Deflection in y direction	m
w	Deflection perpendicular to the plate(z direction)	m
$\varepsilon^{(0)}$	Vectors of the membrane strain	unit less
$\varepsilon^{(1)}$	Bending strains	unit less
σ	stress	N/m^2

NUMERICAL INVESTIGATION OF NATURAL CONVECTION RADIATION AND MAGNETOHYDRODYNAMIC IN VERTICAL POROUS CYLINDRICAL CHANNEL

Manal H. AL-Hafidh
Ass. Prof. /University of Baghdad

Hayder I. Mohammed
Mechanical Engineer

ABSTRACT

A numerical study has been carried out to investigate heat transfer by natural convection and radiation under the effect of magnetohydrodynamic (MHD) for steady state axisymmetric two-dimensional laminar flow in a vertical cylindrical channel filled with saturated porous media. Heat is generated uniformly along the center of the channel with its vertical surface remain with cooled constant wall temperature and insulated horizontal top and bottom surfaces. The governing equations which used are continuity, momentum and energy equations which are transformed to dimensionless equations. The finite difference approach is used to obtain all the computational results using the MATLAB-7 programming. The parameters affected on the system are Rayleigh number ranging within ($10^2 \leq Ra \leq 10^4$), radiation parameter ($0 \leq Rd \leq 2$) and MHD (Mn) ($0 \leq Mn \leq 2$). The results obtained are presented graphically in the form of streamline and isotherm contour plots and the results show that heat transfer enhanced by radiation effect but decrease with the increase of magnetohydrodynamic. A correlation has been set up to give the average Nusselt number variation with Ra, Rd and Mn for which the results are found to be in good agreement with previously published researches which give maximum deviation of 3.73% when compared with the results of **(Prasad, 1989).**

دراسة عددية للحمل الحر والإشعاع والمغناطيسية الهيدروديناميكية في قناة عمودية مملوءة بوسط مسامي

الخلاصة

أجريت دراسة رقمية لإستقصاء إنتقال الطاقة الحرارية بالحمل الحر والإشعاع تحت تأثير المغناطيسية الهيدروديناميكية(MHD) لجريان طباقي مستقر ثنائي البعد في مجرى اسطواني عمودي مملوء بوسط مسامي مشبع. طاقة حرارية متولدة بإنتظام في مركز المجرى مع ثبوت درجة الحرارة الباردة على السطح العمودي للمجرى وعزل السطحان الأفقيان العلوي والسفلي. المعادلات التي أستخدمت هي الإستمرارية، الزخم ومعادلة الطاقة وتم تحويلها إلى معادلات لابعدية. أستخدمت طريقة الفروق المحددة للحصول على النتائج بإستخدام برمجية MATLAB-7. المتغيرات المؤثرة على النظام هي رقم رايلي بمدى ($10^2 \leq Ra \leq 10^4$)، تأثير الإشعاع ($0 \leq Rd \leq 2$) والمغناطيسية الهيدروديناميكية (MHD (Mn) $0 \leq Mn \leq 2$).

النتائج تم توضيحها برسم منحنيات مغلقة للخطوط الإنسيابية ومنحنيات درجات الحرارة الثابتة وبينت النتائج أن الإشعاع يعزز من إنتقال الطاقة الحرارية بينما تقل الطاقة الحرارية بزيادة المغناطيسية الهيدروديناميكية. والنتائج أعطت تمثيلاً لمعدل رقم نسلت ضد Ra, Rd وMn . المقارنة مع البحوث الأخرى أعطت نتائج دقيقة كفاية لإمكانية حساب معامل انتقال الطاقة الحرارية لحالة الجريان المذكورة آنفاً وكان الفرق بالنتائج 3.73% بالمقارنة مع نتائج **(Prasad, 199)**

KEY WORDS:- Natural convection, radiation, magnetohydrodynamic, vertical cylindrical channel, laminar flow numerical solution

INTRODUCTION

Various heat transfer mechanisms and geometries have been studied by some engineers and scientists purposely to augment heat transfer in heat exchangers and some other heat transfer equipments. A numerical investigation of natural convection was studied for vertical annulus. **(Prasad and Kulacki, 1984)** studied numerically free convection in a vertical annulus filled with saturated porous media whose vertical walls at constant temperatures and insulated horizontal wall. Convective velocities wrer higher in the upper half than the lower in the annulus and the local rate in the heat transfer much higher near the top edge of the cold wall and Nu was increase with the radius ratio. **(Prasad and Kulacki, 1985)** studied numerically and experimentally the free convection heat transfer in short cylindrical annuli filled with saturated porous media which was glass beads(3 and 6 mm). For an annulus whose inner wall heated with constant temperature and outer wall isothermally cooled, the top and the bottom being insulated. Heat transfer results have been obtained numerically and experimentally up to Ra = 10^4. **(Prasad and Chui, 1989)** studied numerically the natural convection inside a cylindrical enclosure filled with a volumetrically heated, saturated porous medium. Three cases were studied (i) both top and bottom adiabatic, (ii) insulated bottom and cooled top, and (iii) both top and bottom were cooled, and the vertical wall was cooled for all cases. The maximum temperature decreased significantly with the change in horizontal walls boundary conditions from adiabatic to isothermally cool. The lower is the aspect ratio and\or Rayleigh number, the larger the variation in maximum temperature. **(Shivakumara and Prasanna, 2002)** studied numerically the free convection in vertical cylinder annulus filled with fluid saturated porous medium with the inner wall heated to a uniform temperature, the outer wall cooled to a uniform temperature and maintaining top and bottom boundaries at adiabatic condition. The heat transfer rate and the flow field were obtained for $10^3<Ra<10^6$, Darcy number $10^{-1}<Da<10^{-3}$ and aspect ratio 1 to 2. The results show that the heat transfer rate decreased as the Darcy number decreased.

(Rashad, 2007) was studied the magneto-hydrodynamics and radiation effect in study laminar boundary layer flow of Newtonian. Viscous fluid over a vertical flat plate embedded in a fluid saturated porous media in the presence of thermophoresis particle deposition effect. The conclusion deduced that the velocity of the fluid decreased with increasing of magnetic field and buoyancy ratio.

MATHEMATICAL MODEL

The schematic drawing of the geometry and the Cartesian coordinate system employed in solving the problem is shown in **Fig.1.** The fluid flows naturally in the cylinder. This cylinder is symmetrical about z-axis (**∂/∂r=0**). Convection heat transfer through a saturated porous media with a fluid (liquid or gas) is based on a series of concepts; such concepts include porosity and permeability of the porous media, and the volume average properties of the fluid flowing through the medium. The governing equations for axisymmetric, steady flow through Darcy porous medium including the radiation and magnetohydrodynamic effect are:

Continuity Equation

$$\frac{1}{r}\frac{\partial}{\partial r}(rV_r) + \frac{\partial V_z}{\partial z} = 0 \qquad (1)$$

Momentum Equation

In z direction

$$V_z = -\frac{K}{\mu}\left[\frac{\partial p}{\partial z} + \rho g + \sigma\beta^2 V_z\right] \qquad (2)$$

In r direction

$$V_r = -\frac{K}{\mu}\left[\frac{\partial p}{\partial r} + \sigma\beta_o^2 V_r\right] \quad (3)$$

The density of the fluid assumed constant except when it's happened directly from flotation force **(Bejan, 1999).**

$$\left.\begin{aligned} \rho &= \rho_o[1-\beta(T-T_o)] \\ \beta &= \frac{1}{\rho}\left(\frac{\partial\rho}{\partial T}\right) \end{aligned}\right\} \quad (4)$$

From (4) & (2)

In z direction

$$V_z = -\frac{K}{\mu}\left[\frac{\partial p}{\partial z} + \rho_o g[1-\beta(T-T_o)] + \sigma\beta_o^2 V_z\right] \quad (5)$$

Energy Equation

According to the assumptions the energy equation and the radiation flux q_r are **(Prasad, 1989)**:

$$V_r\frac{\partial T}{\partial r} + V_z\frac{\partial T}{\partial z} = \frac{k}{\rho Cp}\left[\begin{aligned} &\frac{1}{r}\frac{\partial}{\partial r}\left(r\frac{\partial T}{\partial r}\right) \\ &+\frac{\partial}{\partial z}\left(\frac{\partial T}{\partial z}\right) \\ &-\frac{1}{r}\frac{\partial}{\partial r}\left(\frac{r q_r}{k}\right)\end{aligned}\right] + \frac{q^{\circ}}{\rho C_p} \quad (6)$$

$$q_r = -\frac{4\sigma_i \partial T^4}{3\beta_r \partial r}$$

NORMALIZATION PARAMETERS

The variables in the governing equations and boundary conditions are transformed to dimensionless formula by employing the following transformation parameters **(Prasad, 1989):**

$$\bar{r} = \frac{r}{R}, \quad \bar{z} = \frac{z}{H}, \quad \bar{T} = \frac{T-T_o}{\frac{q^{\circ}R^2}{2k}},$$

$$\bar{V}_z = \frac{V_z R^2}{H\alpha} \quad (7)$$

$$\bar{V}_r = \frac{V_r R}{\alpha}, \quad \bar{V}_z = \frac{1}{\bar{r}}\frac{\partial\psi}{\partial\bar{r}}, \quad \bar{V}_r = -\frac{1}{\bar{r}}\frac{\partial\psi}{\partial\bar{z}} \quad (8)$$

By using the relation above the eq. (3, 5 and 6) became

$$\left[A^2\frac{\partial}{\partial\bar{r}}\left(\frac{1}{\bar{r}}\frac{\partial\Psi}{\partial\bar{r}}\right) + \frac{\partial}{\partial\bar{z}}\left(\frac{1}{\bar{r}}\frac{\partial\Psi}{\partial\bar{z}}\right)\right] = \frac{Ra}{1+Mn}A\left[\frac{\partial\bar{T}}{\partial\bar{r}}\right] \quad (9)$$

$$\left[\begin{aligned} &-\left(\frac{1}{\bar{r}}\frac{\partial\Psi}{\partial\bar{z}}\frac{\partial\bar{T}}{\partial\bar{r}}\right)+ \\ &\left(\frac{1}{\bar{r}}\frac{\partial\Psi}{\partial\bar{r}}\frac{\partial\bar{T}}{\partial\bar{z}}\right)\end{aligned}\right] = \left[\begin{aligned} &\left(1+\frac{4}{3}Rd\right)\frac{1}{\bar{r}}\frac{\partial}{\partial\bar{r}}\left(\bar{r}\frac{\partial\bar{T}}{\partial\bar{r}}\right) \\ &+\frac{1}{A^2}\left(\frac{\partial^2\bar{T}}{\partial\bar{z}^2}\right)+2\end{aligned}\right] \quad (10)$$

And the boundary condition be

$$\left.\begin{aligned} &\bar{r}=0,\ \Psi=0,\ \frac{\partial\bar{T}}{\partial\bar{r}}=0 \\ &\bar{r}=1,\ \Psi=0,\ \bar{T}=0 \\ &\bar{z}=0,\ \Psi=0,\ \frac{\partial\bar{T}}{\partial\bar{z}}=0 \\ &\bar{z}=1,\ \Psi=0,\ \frac{\partial\bar{T}}{\partial\bar{z}}=0 \end{aligned}\right\} \quad (11)$$

Overall Heat Transfer

For the problem considered here, there is no well-defined characteristic temperature difference to express the heat transfer coefficient. However one can define an overall Nusselt number based on either the maximum temperature in the cylinder or the mean temperature in the centerline. When the heat transfer coefficient is defined in terms of

$(\bar{T}_{max} - \bar{T}_c)$, the overall Nusselt number is defined as **(Prasad, 1989)**

$$Nu_{max} = \frac{hR}{k} = \frac{1}{\bar{T}_{max}} \quad (12)$$

Nu_{max} It's Nusselt number meaning inverted maximum temperature, and not mean maximum Nusselt number. In a similar way, the average

Nusselt number based on the mean temperature difference $(\bar{T}_{mean} - \bar{T}_c)$ can be expressed as

$$Nu_{mean} = \frac{1}{\bar{T}_{mean}} \quad (13)$$

NUMERICAL SOLUTION

The new algebra equations system can easy be solved using some of known techniques, like relaxation method, to give approximate values of the dependent variables at a number of discrete points called (grid points or nodes) in the computational domain. A grid was established by subdividing the computational domain in the R and Z directions with indexes i and j that are integers describing the number of radial grid lines from the center of the cylinder and the number of axial grid lines from the lower to upper surface respectively. The spacing of the grid lines in the R-direction is uniform and given by (Δr) and that of the grid lines in the Z-direction is also uniform and given by (Δz). The number of the grid points will be [m×n] where (m) represents the number of gridlines in the R-direction and equals $[(1/\Delta\bar{r}) + 1]$ while (n) represents the number of gridlines in the Z-direction and equals $[(1 / \Delta\bar{z}) + 1]$.

The partial differential eq. (9) & (10) were finite-differenced using central difference schemes for all of the derivatives. In particular, let ξ represents Ψ and $\bar{T}$ then

$$\Delta\bar{r} = \Delta\bar{z} \quad , \quad \Delta\bar{r}_i = \Delta\bar{r}_{i+1} \quad , \quad \Delta\bar{z}_j = \Delta\bar{z}_{j+1}$$

$$\frac{\partial\xi}{\partial\bar{r}} = \frac{\xi_{(i+1,j)} - \xi_{(i-1,j)}}{2\Delta\bar{r}} \quad , \quad \frac{\partial\xi}{\partial z} = \frac{\xi_{(i,j+1)} - \xi_{(i,j-1)}}{2\Delta\bar{z}} \quad (13)$$

$$\frac{\partial^2\xi}{\partial\bar{r}^2} = \frac{\xi_{(i+1,j)} - 2\xi_{(i,j)} + \xi_{(i-1,j)}}{\Delta\bar{r}^2}$$

$$\frac{\partial^2\xi}{\partial z^2} = \frac{\xi_{(i,j+1)} - 2\xi_{(i,j)} + \xi_{(i,j-1)}}{\Delta\bar{z}^2}$$

In terms of the above expressions momentum and energy equations become

Momentum Equation

$$\frac{A^2}{\bar{r}_{(i)}}\frac{\Psi_{(i+1,j)} - 2\Psi_{(i,j)} + \Psi_{(i-1,j)}}{\Delta\bar{r}^2} - \frac{A^2}{\bar{r}_{(i)}^2}\frac{\Psi_{(i+1,j)} - \Psi_{(i-1,j)}}{2\Delta\bar{r}} + \frac{\Psi_{(i,j+1)} - 2\Psi_{(i,j)} + \Psi_{(i,j-1)}}{\bar{r}_{(i)}\Delta\bar{z}^2} = \frac{RaA}{1+Mn}\frac{\bar{T}_{(I+1,J)} - \bar{T}_{(I-1,J)}}{2\Delta\bar{r}} \quad (14)$$

Energy Equation

$$\frac{1}{\bar{r}_{(i)}}\frac{\Psi_{(i+1,j)} - \Psi_{(i-1,j)}}{2\Delta\bar{r}} * \frac{\bar{T}_{(i,j+1)} - \bar{T}_{(i,j-1)}}{2\Delta\bar{z}} - \frac{1}{\bar{r}_{(i)}}\frac{\bar{T}_{(I+1,J)} - \bar{T}_{(I-1,J)}}{2\Delta\bar{r}} * \frac{\Psi_{(i,j+1)} - \Psi_{(i,j-1)}}{2\Delta\bar{z}^2} = \left(1 + \frac{4}{3}Rd\right)\left[\frac{\bar{T}_{(I+1,J)} - 2\bar{T}_{(I,J)} + \bar{T}_{(I-1,J)}}{\Delta\bar{r}^2} + \frac{1}{\bar{r}_{(i)}}\frac{\bar{T}_{(I+1,J)} - \bar{T}_{(I-1,J)}}{2\Delta\bar{r}}\right] + \frac{1}{A^2}\frac{\bar{T}_{(i,j+1,J)} - 2\bar{T}_{(i,j)} + \bar{T}_{(I,J-1)}}{\Delta\bar{z}^2} + 2 \quad (15)$$

RELAXATION METHOD

As a solution method for the system of algebraic equations (9) and (10) obtained from the discretization of governing

differential equations, iterative relaxation method was used. In relaxation methods, the value of the variable to be used for obtaining the solution in the next iteration is the value in the current iteration plus a fraction of the difference between the current value and the predicted value as follows **(Massarotti et. al., 2003):**

$$\phi_p^{\zeta+1} = \phi_p^{\zeta} + \gamma\left(\frac{\sum(a_{\zeta b}*\phi_{\zeta b})+b}{a_p} - \phi_p^{\zeta}\right)$$

Where:
$\gamma > 0$ is the relaxation factor
$\phi_p^{\zeta+1}$ is the value of the state variable at node P to be used for the next iteration
ϕ_p^{ζ} is the value of the state variable at node P form current iteration
$\phi_{\zeta b}$ is the values of the variable at the surrounding nodes and ap and b are the constants from the discretized equation.

Relaxation method is a relatively simple method and can be easily altered when changing the grid structure or parameters affecting convergence but, the major disadvantage is the task of choosing the optimum relaxation coefficient (γ) for a given situation. The grid that used in this work was (41*61) for Ra=10^2&10^3, and (81*81) for Ra=10^4. The grid that used in present work showed in **Fig.(2)**. Generally, the temperature is over relaxed and/or the stream function is under relaxation

RESULTS AND DISCUSSION

The results of numerical modeling have been compared with the notable previously published studies. The results that obtained from these studies gave a good agreement where these results compared with **(Prasad, 1985)** maximum deviation was found (2.81%) and with **(Prasad, 1989)** the maximum deviation was found to be (3.73%). **Table 1 & 2** show the value of the mean Nu of the present work comparing with previous work, with explaining the deviation.

Table 1 Comparison of the present results with that of (Prasad, 1985)

ϵ	Ra	Nu. Prasad	Nu. Present	%Dev.
2.5	90	4.271	4.25	0.491
	30	2.275	2.211	2.81
3.333	105	5.071	5.005	1.3
	35	2.691	2.622	2.56
5	120	6.242	6.188	0.865
	40	3.384	3.41	-0.677

Table 2 Comparison of the present results with that of (Prasad, 1989)

A=1	Nu_{Mean} Prasad	Nu_{Mean} Present	%Dev.
Ra=100	3.155	3.0371	3.73
Ra=1000	7.639	7.5885	0.66
Ra=10000	19.841	19.3853	2.29

Centerline Temperature Distributions

Figs. 3, 4 and 5 show the effect of Rd, Mn and Ra on the centerline temperature distribution, **Fig. 3** shows the temperature variation along the cylinder centerline with increasing of the radiation parameter. Because heat diffusion in the system increase with increasing of Rd and the temperature value in the upper surface is higher than the lower surface the fluid will moved and collected near the upper surface. The temperature in the centerline increase with increasing of the MHD parameter as it is clear in **Fig. 4**, because the force which created from MHD acting in the opposite direction of the force that caused the motion of the fluid and this

behavior caused a low diffusion of the heat and increasing of the temperature. In **Fig.5** the dimensionless temperature in the centerline dropped with the increasing of Ra, because of the circulation between the layer of the flow which cause more heat diffusion.

Streamlines and Temperature Fields

The Rd Effect

The Rd effect is presented in **Fig. 6**. When Rd equal zero, that mean's no radiation effect on the system. In **Fig.6** (Ra=100, A=1, Mn=1) the warm region area limited between the centerline and the upper wall of the cylinder and the cold region was adjacent to the cold vertical wall, maximum temperature for internal cell was (0.4263) when the Rd was increased the warm region was contracted from the upper wall and more expanded in the centerline, maximum temperature for internal cell was (0.201) at Rd=1 and (0.124) at Rd=2. The change in the flow was not affected on the shape too much. This increasing in the hot region area is happen because of the increasing of the flow and heat diffusion in the system, and the value of the stream decrease because the molecular lose it's energy with losing the heat.

The Mn Effect

From **Fig. 7** it is clear that the dimensionless streamlines (Ψ) in the internal cell was dropped from (4.187) at Mn=0 to (2.11) at Mn=2, and the maximum dimensionless temperature line was increased from (0.133) at Mn=0 to (0.184) at Mn=2. From the foregoing it's clear that the streamlines value was dropped with the increasing of Mn at constant value of Ra, A & Rd, because the force which created from MHD acting in the opposite direction of the force that caused the motion of the fluid, and this behavior caused a low diffusion of the heat and increasing of the temperature.

The Ra Effect

From **Fig. 8** for (A=1, Rd=1 & Mn=2) it's clear that the temperature of the hotter region was decreased with the increasing of Ra, where this temperature equal to (0.196) at Ra=10^2 and (0.088) at Ra=10^4, taking part (b) of the last figures, it's clear that the streamlines value in the internal cell increased with the increasing of Ra, where this streamlines equal to (0.257) at Ra=10^2 and (8.151) at Ra=10^4. This behavior was happened because the increasing of the Ra cause an increasing in the velocity and more circulation between the layers of the fluid that caused the temperature to be dropped.

Mean (Nu) Number and Maximum Temperature

As can be expected the temperature is always maximum in the center of the upper surface. **Fig.9** illustrates the variation of (T_{max} and Nu_{mean}) with Mn respectively at Ra=10^4 and A=1 for different values of Rd, it's clear that the value of the maximum temperature was decreased with the increase of Rd at a certain value of Mn, and that the value of the mean Nusselt number (at a certain value of Ra and Mn) was increase with Rd increasing because the increase of the radiation caused increasing of the heat flux diffusion. **Fig.10** shows the variation of (T_{max} & Nu_{mean}) with Rd respectively at Ra=10^3 for different values of Mn, it's clear that the value of the maximum temperature was increased with the increasing of Mn at a certain value of Rd and that the value of the mean Nusselt number at a certain value of Ra and Rd, was decreased with Mn increasing.

A correlation was deduced from the numerical data for cases 1 and 2 which is given as:

$$Nu_{mean} = a\ Ra^{b}\ A^{c}\left(\frac{1}{1+Mn}\right)^{d}\left(\frac{1}{1+Rd}\right)^{e}$$

	a	b	c	d	e
Case 1	1.4	0.222	-0.282	0.2168	-0.6588
Case 2	2.68	0.252	-0.877	0.2391	-0.329

CONCLUSIONS

1. Isothermal lines and the streamlines are symmetric about vertical center line. The maximum temperature was appeared at the centerline of the top surface.
2. Temperature and stream were decrease, Nu_{mean} was increase, and the hot region area and inner streamlines cells was increased with increasing of Rd.
3. With increasing of Mn the temperature was increased and the streamline was dropped. Nu_{mean} was decreased with Mn increase.
4. Temperature was decreased and the streamline and Nu_{mean} was increased with increasing of Ra, for high values of Ra the warm region will be adjacent to the upper wall.
5. At a low Ra there are a little change of T_{max} and Nu_{mean} with Mn at constant Rd and A.

REFRENCES

Bejan A. and Nield D., (1999), "Convection in Porous Media", Springer

Massarotti N., Nithiarasu P. and Carotenuto A., (2003), "Microscopic and Macroscopic Approach for Natural Convection in Enclosures Filled with Fluid Porous Medium", Int. J. of Numerical Methods for Heat and Fluid Flow, Vol.13, No.7, pp. 862-886.

Prasad , V. and Kulacki, F. A., (1984), "Natural convection in a vertical porous annulus", Int. J. Heat Mass Transfer. Vol. 27 No. 2, PP (207-219).

Prasad, V. and Kulacki, F. A., (1985), "Natural convection in porous media bounded by short concentric vertical cylinders", Transaction of ASME, J. of heat transfer , Vol. 107, PP (147-154), February.

Prasad, V. and Chui, A., (1989), "Natural convection in cylindrical porous enclosure with internal heat generation", Transaction of ASME, J. of heat transfer, Vol. 111, PP (916-925), November,.

Rashad A. M., (2007), "Influence of radiation on MHD free convection from a vertical flat plate embedded in porous media with thermophoretic deposition of particles", Communication in nonlinear science and numerical simulation www.sciencedirect.com.

Shivakumara, I. S.,and Prasanna, B. M. R., (2002), "Numerical Study of Natural Convection in a Vertical Cylindrical Annulus Using Non-Darcy Equation", J. of Porous Media, Vol.5, No.2, PP.87-102.

NOMENCLATURE

Symbols	Description	Units
As	Dimensionless aspect ratio (A = H/R)	
C_p	specific heat at constant Pressure	J/kg.K
Da	Darcy number ($Da = K/R^2$)	
g	Acceleration of gravity	m/s^2
H	axial length of cylinder	m
h	Heat transfer coefficient	$W/m^2.K$
K	Permeability	m^2
k	Thermal conductivity	W/m.K
M_n	Magnetohydrodynamic parameter ($M_n = K\sigma\beta_0^2/\mu$)	m^3s/kg
Nu	Nusselt number (Nu=h.R/k)	
Nu_{mean}	Average Nusselt number	
Nu_{max}	Nusselt number resulting from inverted maximum temperature	
p	Pressure	N/m^2
$\dot{q}$	volumetric heat generation	W/m^3
q_r	Radiation flux	W/m^2
T	Temperature	ºC

$\bar{T}$	Dimensionless temperature ($\bar{T} = \frac{2k\,(T-T_c)}{q''R^2}$)	
T_o	Reference temperature	ºC
Tc	Cooled temperature for boundary	ºC
$\bar{T}_{max}$	Dimensionless maximum temperature	
$\bar{T}_{mean}$	Dimensionless mean temperature	
R	Radius of the cylinder	m
Ra	Rayleigh number ($Ra = \frac{K\rho g\beta\, q''R^3}{2\mu\alpha k}$)	
Rd	Radiation parameter ($Rd = \frac{4\sigma_i T_\infty^3}{\beta k}$)	
r	Radial coordinate	m
$\bar{r}$	Dimensionless Radial coordinate	
U	Average velocity of the flow	m/s
Vr	Radial velocity component	m/s
$\bar{V}$	velocity vector	
Symbols	Description	Units
$\bar{V}_r$	Dimensionless radial velocity component ($\bar{V}_r = \frac{V_r R}{\alpha}$)	
Vz	Axial velocity component	m/s
$\bar{V}_z$	Dimensionless axial velocity component ($\bar{V}_z = \frac{V_z R^2}{\alpha H}$)	
z	Axial coordinate	m
$\bar{z}$	Dimensionless axial coordinate	

GREEK SYMBOLS

Symbols	Description	Units
α	Convective thermal diffusivity	m2/s
β	Volumetric thermal expansion coefficient	1/K
β_o	Strength of magnetic field	
β_r	Roseland extinction coefficient	1/m
ε	Porosity	
$\forall$	Total volume of porous media	m3
$\forall_p$	Solid matter volume	m3
$\forall_o$	Difference between $\forall$ & $\forall_p$	m3
σ	Electrical conductivity of the fluid	
σ_i	Stephan Boltzmann constant	W/m2.K4
ψ	Dimensionless Stream function	
γ	Relaxation factor	
ξ	Represents ψ and $\bar{T}$	
ψ	Stream function	m2/s
Δ	Difference between two values	

μ	Dynamic viscosity	kg/m.s
∇	Laplacian in dimensionless cylindrical coordinates	
η	Actual value of the quantity of a point inside the sample volume	
ρ_o	Reference density at T_o	kg/m3
Φ_P	Value of the state variable at node	

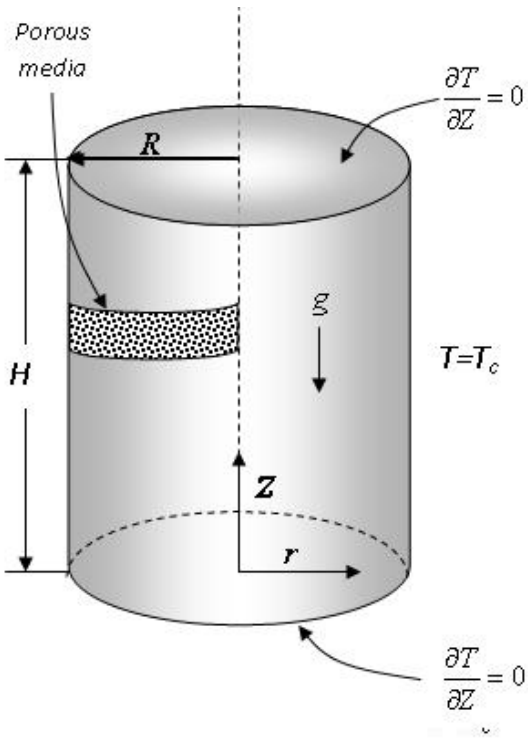

Figure (1) geometric configuration, coordinate system and the boundary conditions

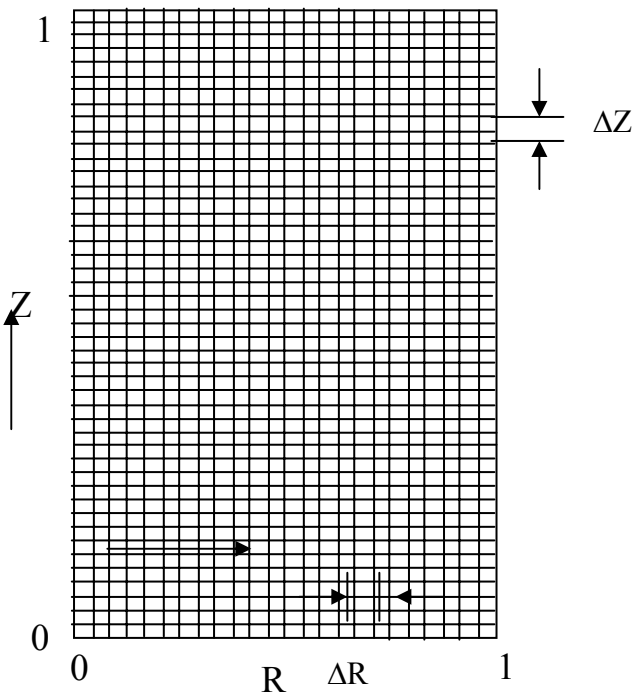

Figure (2) Domain Discretization in a cylindrical enclosure at A=1

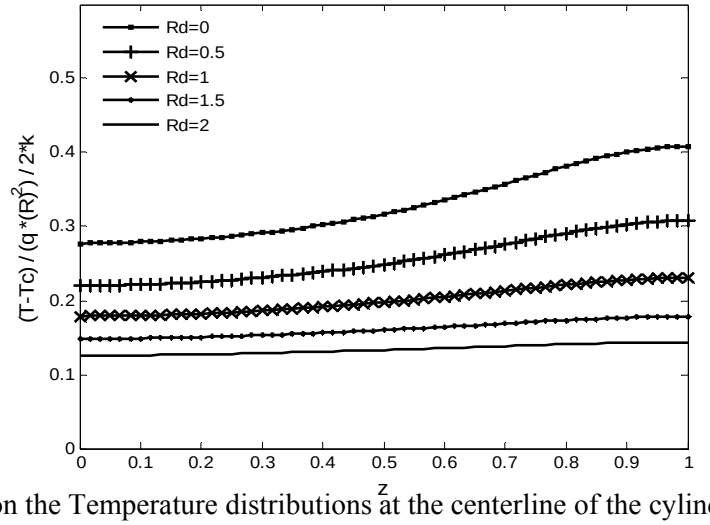

Fig. (3) Effect of Rd on the Temperature distributions at the centerline of the cylinder for (Ra=100, A=1 and Mn=0)

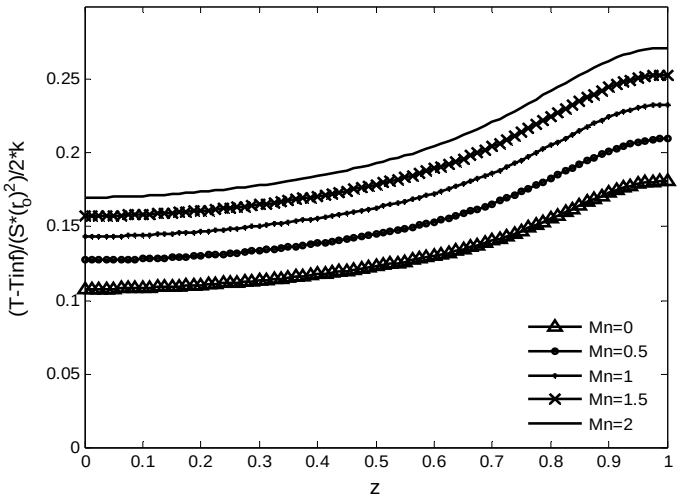

Fig. (4) Effect of Mn on the Temperature distributions at the centerline of the cylinder for (Ra=1000, A=1 and Rd=0)

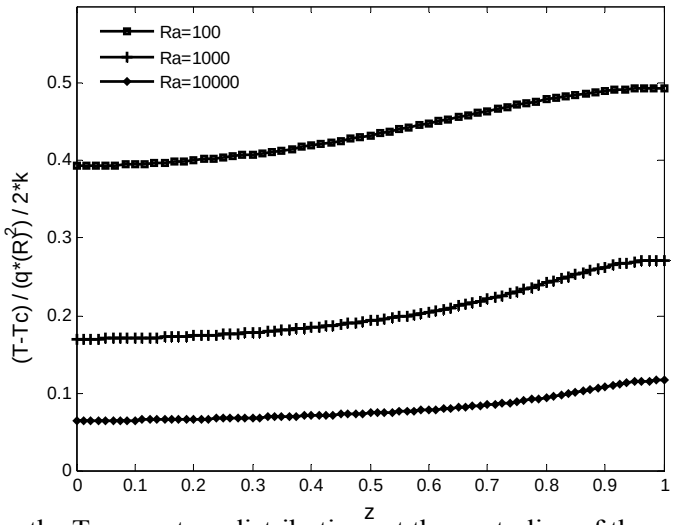

Fig (5) Effect of Ra on the Temperature distributions at the centerline of the cylinder for (Rd=0, A=1 and Mn=2)

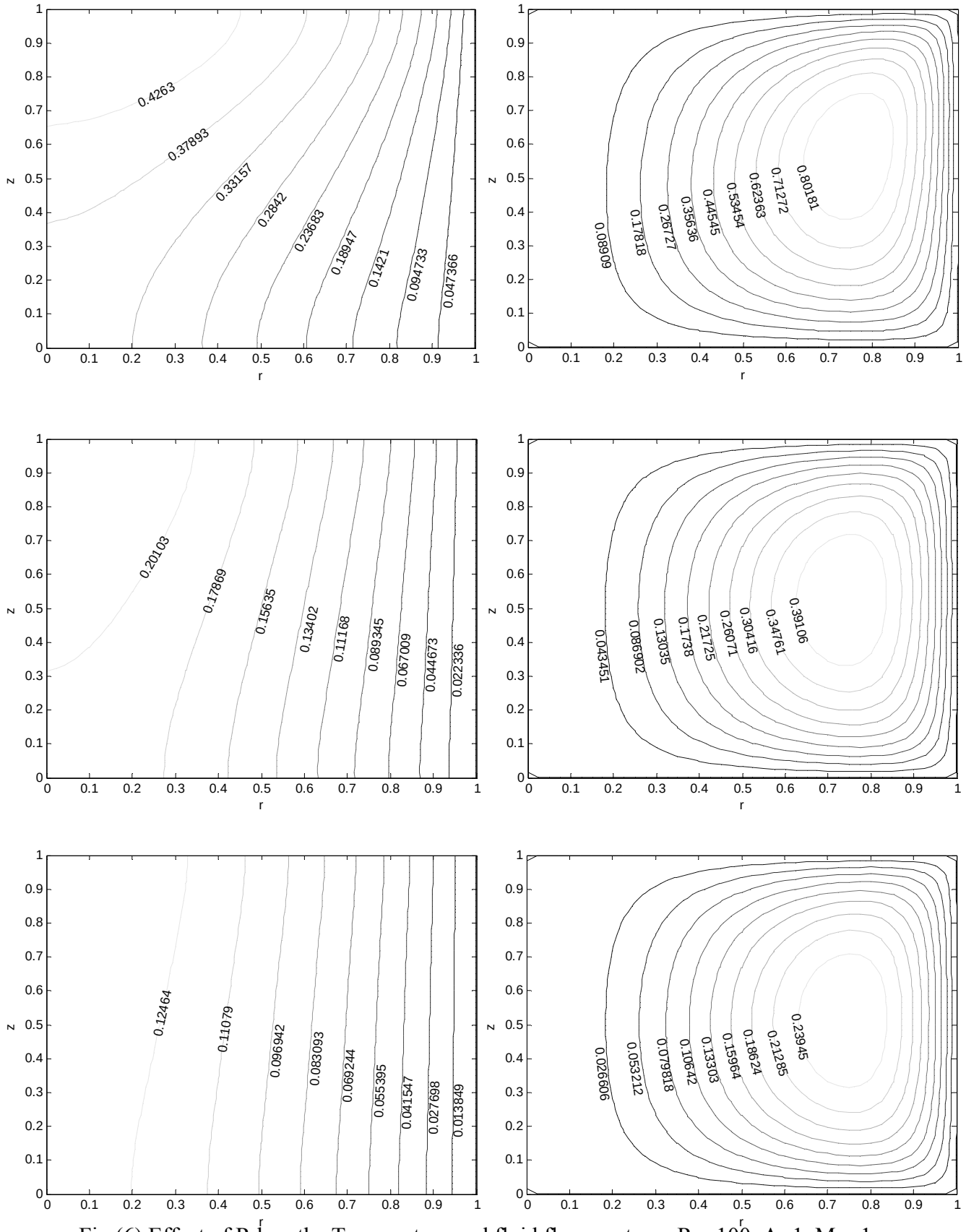

Fig (6) Effect of Rd on the Temperature and fluid flow contours Ra=100, A=1, Mn=1

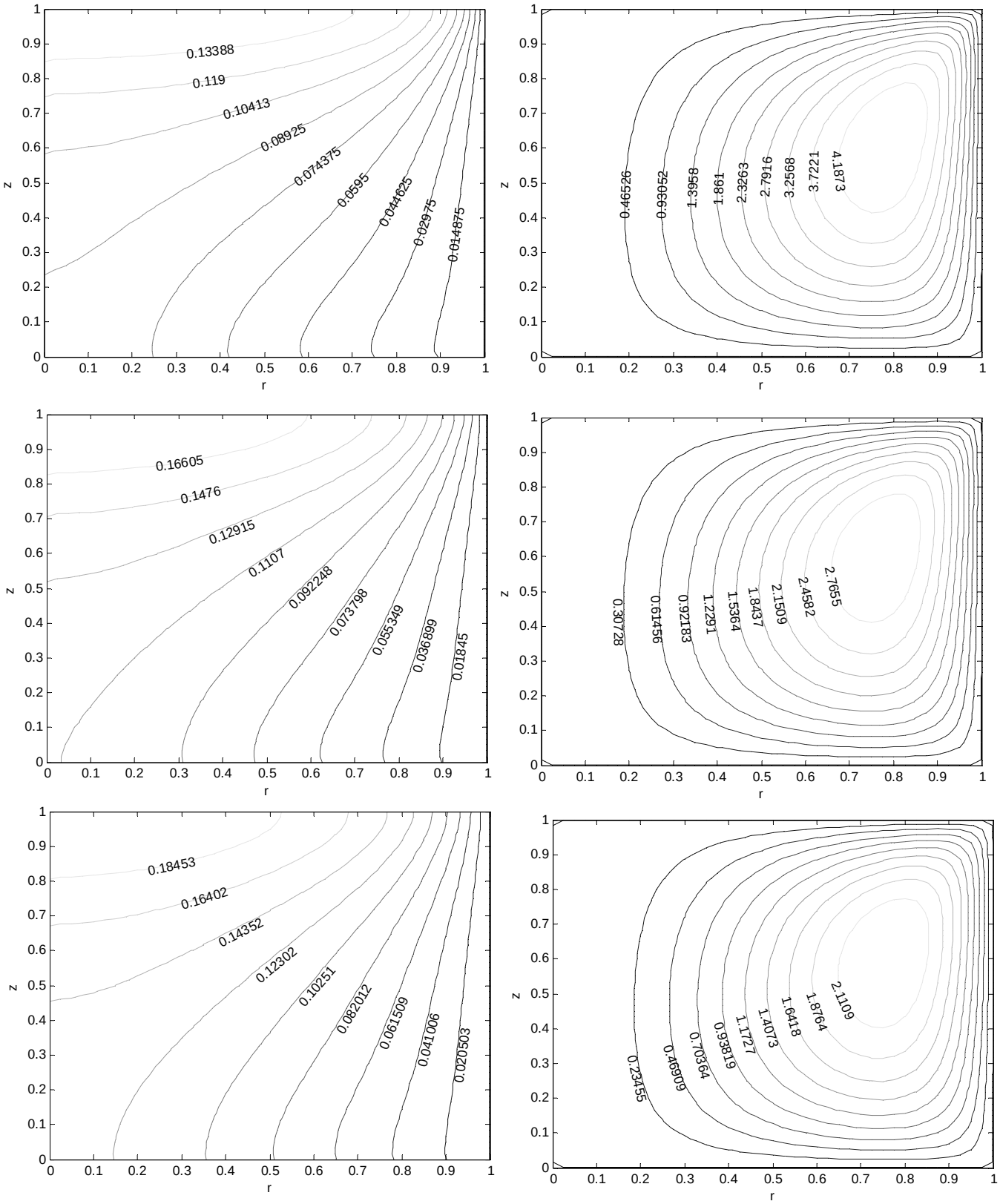

Fig (7) Effect of Mn on the Temperature and fluid flow contours Ra=1000, A=1, Rd=1

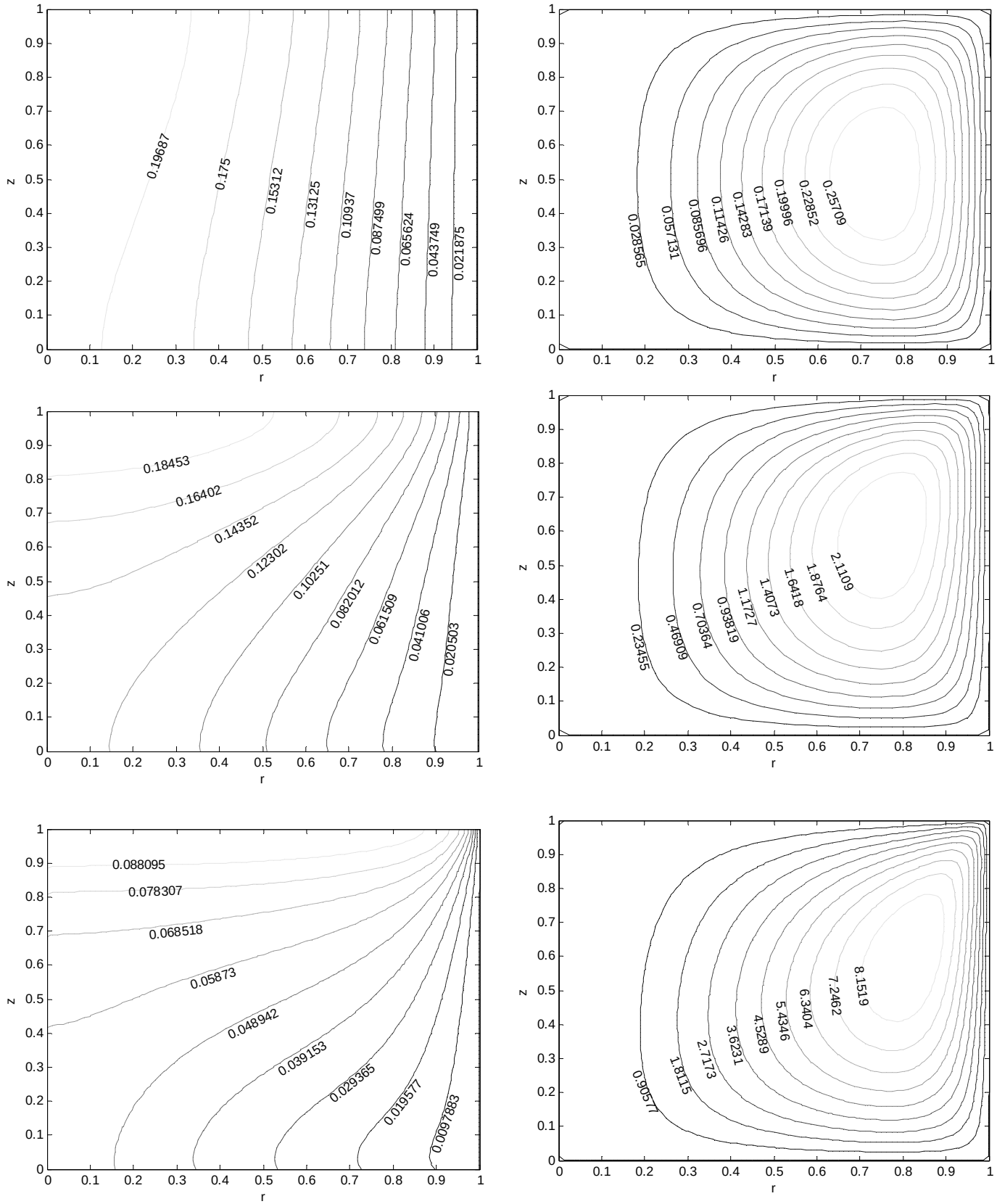

Fig (8) Effect of Ra on the Temperature and fluid flow contours Rd=1, A=1, Mn=2

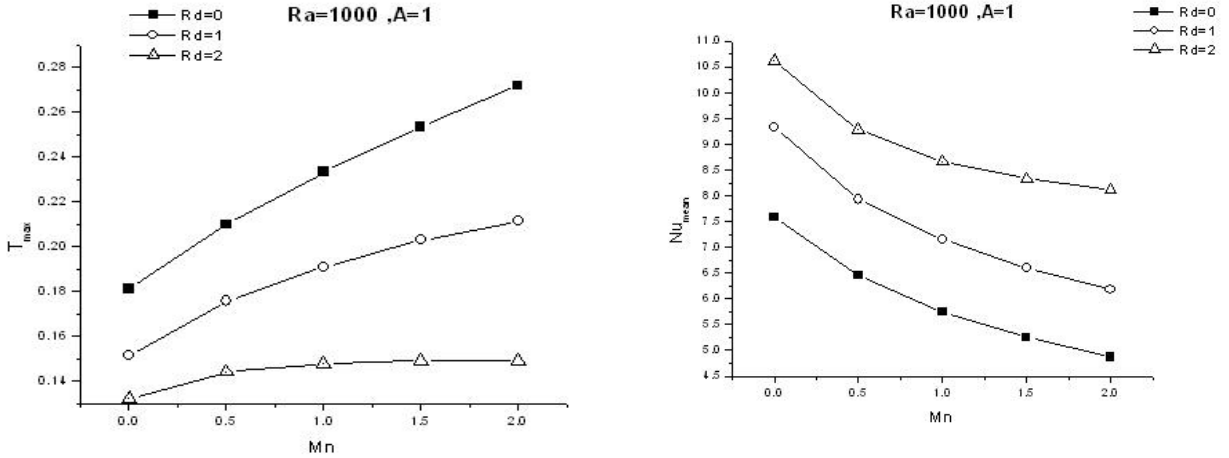

Fig. (9) Effect of Rd on the relationship between T_{max},Nu_{mean} with Mn at Ra=1000 & A=1

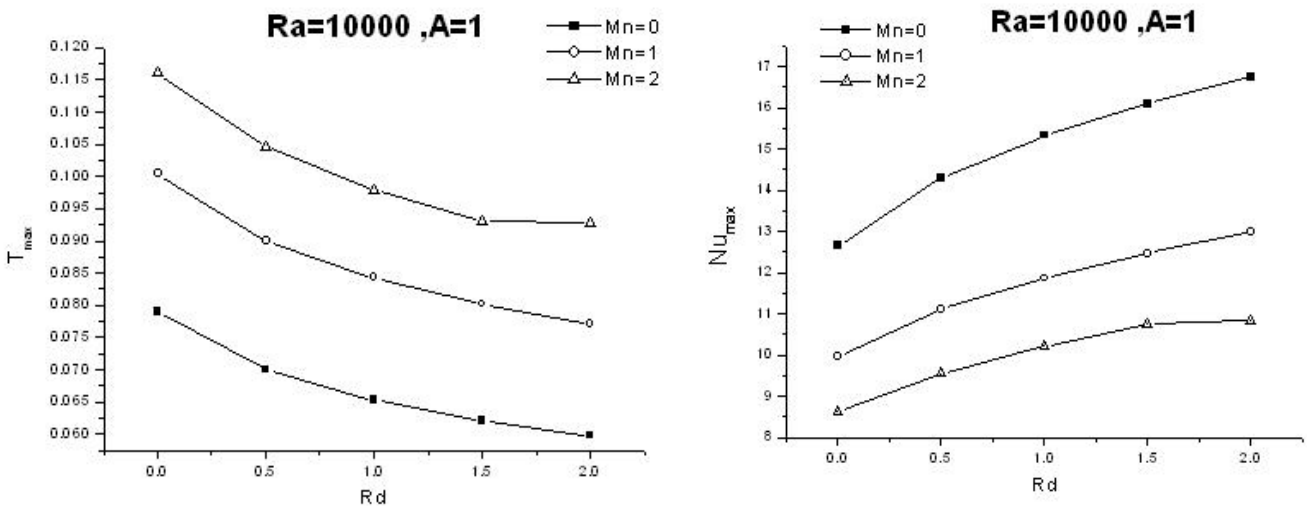

Fig (10) Effect of Mn on the relationship between T_{max},Nu_{mean} with Rd at Ra=10000 & A=1

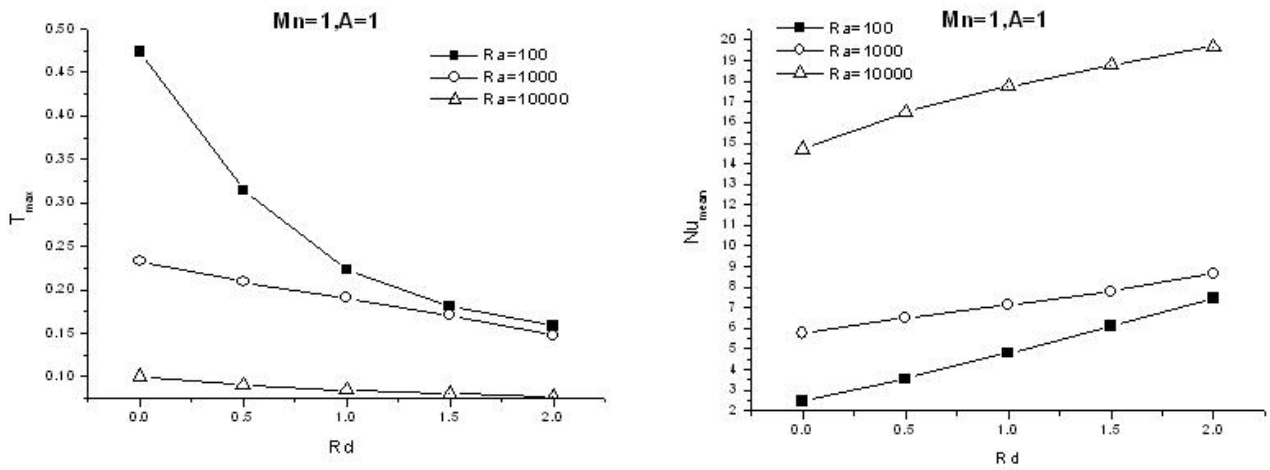

Fig. (11) Effect of Ra on the relationship between T_{max},Nu_{mean} with Rd at A=1 & Mn=1

A GENERAL VELOCITY PROFILE FOR A LAMINAR BOUNDARY LAYER OVER FLAT PLATE WITH ZERO INCIDENCE

Qussai J. Abdul-Ghafour*
Department of Machines and Equipment, University of Technology, Baghdad, Iraq

ABSTRACT
A general velocity profile for a laminar flow over a flat plate with zero incidence is obtained by employing a new boundary condition to the other available boundary conditions. The general velocity profile is mathematically simple and nearest to the exact solution. Also other related values, boundary layer thickness, displacement thickness, momentum thickness and coefficient of friction are nearest to the exact solution compared with other corresponding values for other researchers.

الخلاصة
تم ايجاد معادلة عامة للسرعة خلال الطبقة المتاخمة للجريان الطباقي فوق السطح المستوي من خلال توظيف ظرف محيطي جديد بالاضافة الى الظروف المحيطية المتوفرة. المعادلة العامة المستحصلة ذات صيغة رياضية بسيطة واقرب ماتكون من الحل التام. تم استخدام المعادلة العامة للسرعة لايجاد القيم ذات العلاقة، سمك الطبقة المتاخمة و سمك الازاحة و سمك الزخم و معامل الاحتكاك وكانت النتائج هي الاقرب للحل التام مقارنة مع القيم المناظرة لها والمستحصلة من الباحين السابقين.

Keywords: Laminar Boundary Layer, Flat Plate, General Velocity Profile

profile is a polynomial function of the vertical distance. Thus,

$$u = a + b(y) + c(y)^2 \qquad (6)$$

Where a, b and c are constants.
The boundary conditions which are used to find the values of these constants are:

at y=0 , u=0 (7)

at y = δ , u = u_∞ (8)

shear stress (τ) decreases linearly and becomes zero when y= δ (9)

Applying these conditions yields:

$$\frac{u}{u_\infty} = 2(\frac{y}{\delta}) - (\frac{y}{\delta})^2 \qquad (10)$$

Another velocity profile derived by Von Karman (Eckert 1959), by using four conditions. These conditions are:

at y = 0, u = 0 (11)

at y = δ u = u_∞ (12)

at y = δ, du/dy = 0 (13)

$d^2u/dy^2 = 0$
(for constant pressure condition) (14)

The simplest function used to satisfy these conditions is a polynomial with four arbitrary constants. Thus:

$$u = a + b(y) + c(y)^2 + d(y)^3 \qquad (15)$$

After applying these conditions, a velocity profile is obtained as:

$$\frac{u}{u_\infty} = \frac{3}{2}(\frac{y}{\delta}) - \frac{1}{2}(\frac{y}{\delta})^3 \qquad (16)$$

Noting that, the forth condition in eqn.14 which is used in deriving eqn.16 is not used in deriving eqn.10.

(Pohlhausen 1921), suggested that the velocity profile is a polynomial of forth order. The profile is changed due to the variation in pressure gradient along the flat plate. For zero incidence case, the velocity profile becomes:

$$\frac{u}{u_\infty} = 2(\frac{y}{\delta}) - 2(\frac{y}{\delta})^3 + (\frac{y}{\delta})^4 \qquad (17)$$

The most famous solution for the laminar boundary layer is obtained by (Blasius 1908), which is called the exact solution. This solution depends on obtaining new dependent and independent variables. A non-linear third order ordinary differential equation formed due to these variables then the solution achieved without the need of mathematical expression for the velocity profile. The result of this solution is agreed, and the results of other solutions are compared with it. **Table 1** shows the comparison between these solutions.

EVALUATION OF THE GENERAL VELOCITY PROFILE

The approach used in present work is a modified approach used by Von Karman (Eckert 1959). A new condition is employed in addition to the other four conditions described in eqn.11 to eqn.14. The new condition is,

At y = 0 $$\frac{\tau_w}{\mu} = \left(\frac{\partial u}{\partial y}\right)_{y=0} \qquad (18)$$

So the function which can be chosen to satisfy the five boundary conditions is a fifth order polynomial with five arbitrary constants. Thus,

$$u = c_1 + c_2(y) + c_3(y)^2 + c_4(y)^3 + c_5(y)^4 \qquad (19)$$

Applying boundary conditions yields:

$C_1 = 0$ (20)

2A - 3 = 0
Or
A = 3/2 (32)

Substituting this value in eqn.28, to get,

$$\frac{u}{u_\infty} = \frac{3}{2}(\frac{y}{\delta}) - \frac{1}{2}(\frac{y}{\delta})^3$$

Pohlhausen (Pohlhausen 1921) suggested that the velocity profile is a polynomial of forth order. It is clear that the coefficient of the forth power term in eqn.17 is equal to one. Equating the coefficient of the forth power term in eqn.17 and eqn.28, yields.
2A - 3 = 1
Or
A = 2 (32)

Substituting this value in eqn.28, to get,

$$\frac{u}{u_\infty} = 2(\frac{y}{\delta}) - 2(\frac{y}{\delta})^3 + (\frac{y}{\delta})^4$$

This is exactly the velocity profile obtained by Pohlhausen (eqn.17)

EVALUATING OF BLASIUS VELOCITY PROFILE

In the exact solution, Blasius (Blasius 1908) found a numerical expression for (δ), (δ*), (θ) and (C_f), with no explicit mathematical expression for the velocity profile. One of the consequences of Blasius solution is,

$$\frac{\delta\sqrt{Re_x}}{x} \approx 5 \qquad (33)$$

The result of the present work could be used for obtaining velocity profile agrees with exact solution. By comparing eqn.31 with eqn.33, simply result obtained:

$$\left(\frac{2A}{(0.11428 + 0.06187A - 0.03015A^2)}\right)^{0.5} \approx 5 \qquad (34)$$

Solving eqn.21 for (A), yields:

A = 1.67326 (35)

Substituting the value of (A) in eqn.28 to get the velocity profile for the exact solution,

$$\frac{u}{u_\infty} = 1.67326(\frac{y}{\delta}) - 1.01978(\frac{y}{\delta})^3 + 0.34652(\frac{y}{\delta})^4 \qquad (36)$$

Fig.3 shows the velocity profile for the present work and other profiles. It is clear that the profile of eqn.36 is the nearest one to the exact profile.

CONCLUTIONS

The result of this work is a new velocity profile for laminar boundary layer over a flat plate with zero incidence. This profile is nearest to the exact solution obtained by Blasius (Blasius 1908). Also the consequences of using the new profile in calculating (δ), (δ*), (θ) and (C_f) are mostly nearest to the corresponding values of the exact solution as shown in **table 1**.
The new profile is mathematically simple, accurate and including most conditions bounded the laminar boundary layer. Therefore it can be used in fluid mechanics and convective heat transfer fields.

REFERENCES

Duncan, W.J, Thomas, A.S. and Young, A.D. "Mechanics of fluid" Edward Arnold Ltd, (1970).

Eckert, E.R.G and, Drake, R.M "Heat and mass transfer" 2nd edition. McGraw Hill, Inc., (1959)

H. Blasius, Z. Math. Phys., 56, I (1908).

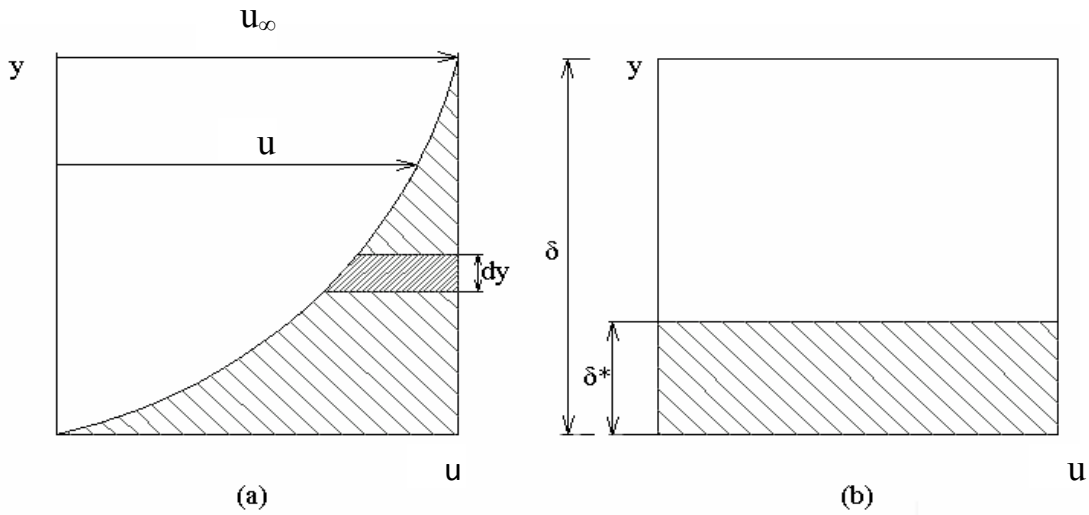

Figure 2: Observation of the displacement thickness (δ*)

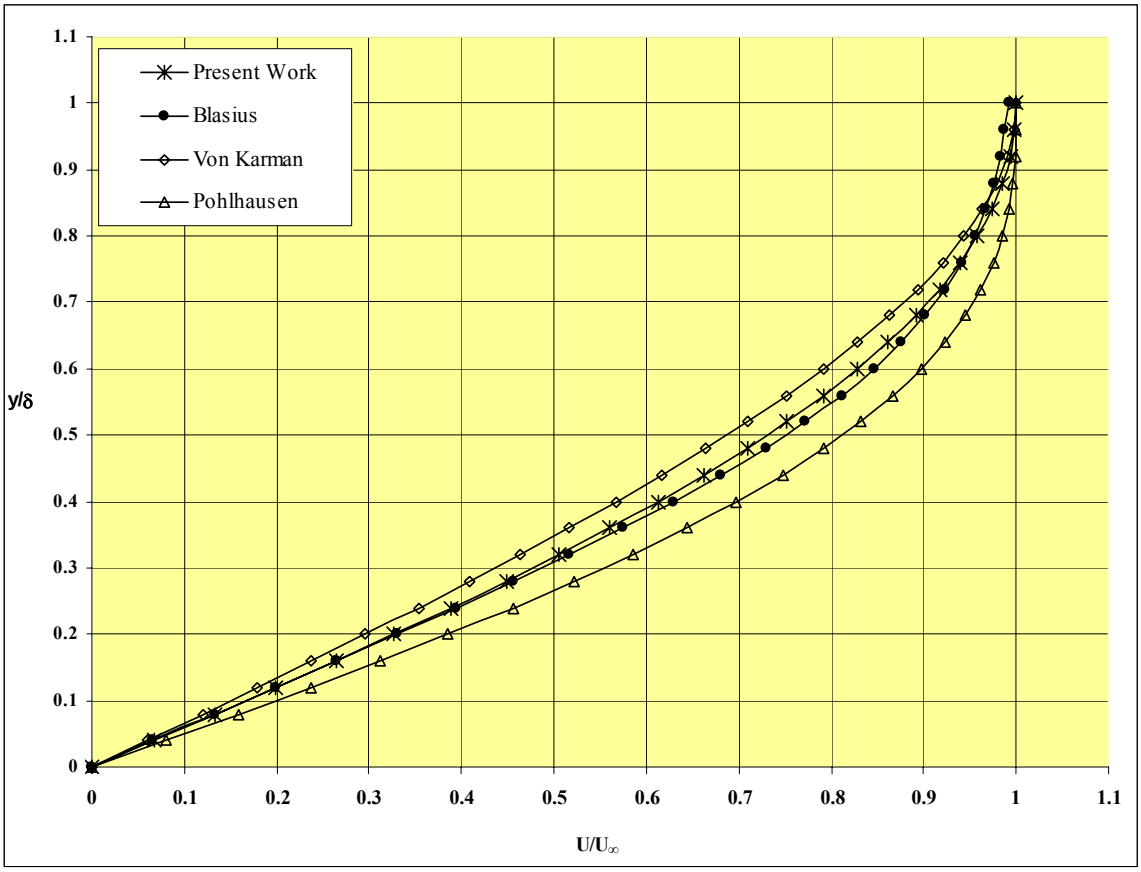

Figure 3: Velocity Profiles for the Present Work and Previous Studies Compared with Blasius Solution

THEORETICAL AND EXPERIMENTAL STUDY ON THERMAL PERFORMANCE OF CLOSED WET COOLING TOWER

Dr. Najim A. Jassim
Department of Mechanical Engineering, College of Engineering, University of Baghdad, Iraq

Abstract

Thermal performance of closed wet cooling tower has been investigated experimentally and theoretically in this work. The theoretical model based on heat and mass transfer equations and heat and mass transfer balance equations which are established for steady state case. A new small indirect cooling tower was used for conducting experiments. The cooling capacity of cooling tower is 1 kW for an inlet water temperature of 38°C, a water mass velocity 2.3 kg/m^2.s and an air wet bulb temperature of 26°C. This study investigates the relationship between saturation efficiency, cooling capacity and coefficient of performance of closed wet cooling tower versus different operating parameters such wet-bulb temperature, variable air-spray water flow ratio and cooling water inlet temperature. Results indicate that the capacity and saturation efficiency was found close to the related experimental results. Good agreement was obtained between the theoretical results and experimental measurements for the performance of small cooling tower.

الخلاصة

تم التحقق من الاداء الحراري لبرج التبريد المغلق والرطب. النموذج رياضي مبني على اساس معادلات انتقال الكتلة والطاقة ومعادلات موازنة الكتلة والطاقة للحالة المستقره. استعمل برج تبريد غير مباشر في اجراء التجارب. السعة التبريدية لبرج التبريد هي ا كيلو واط عند درجة حرارة مقدارها 38°م لماء التدوير، سرعة كتلة لماء تدوير مقدارها 2.3 كيلو غرام/ م2.ثا و درجة حرارة هواء رطبة مقدارها 26°م. تم التحقق في هذه الدراسة العلاقة بين كفاءة الاشباع ، السعة التبريدية ومعامل الاداء الحراري لبرج التبريد المغلق والرطب وعوامل مختلفة كدرجة هواء البصلة الرطبة عند الدخول، نسبة جريان الهواء- الماء المرشوش المتغيرة، درجة حرارة ماء التبريد عند الدخول. بينت النتائج بان سعة التبريد وكفاءة الاشباع مقاربة الى النتائج العملية ذات العلاقة. تم الحصول على تقارب جيد بين نتائج النظرية والنتائج القياسات العملية لاداء ابراج التبريد ذات السعات الصغيرة.

Keywords: Theoretical and Computational Analysis, Closed wet cooling tower, heat and mass transfer balance, Wet operation mode, variable air-spray water flow ratio.

1: Introduction

Cooling towers are increasingly used in buildings as a component of environmental cooling systems. The use of cooling towers to reject heat, cool buildings and reduce the temperature of water circulated through various heat rejection equipment have been also increased considerably in recent days. A closed circuit cooling tower maintains an indirect contact between the fluid and the atmosphere. Indirect contact cooling towers have been traditionally used to remove excess heat from various industrial process with hot water temperatures between 32 and 40C^o and a typical cooling capacities above 40 kW [1,2].

Cooling towers respectively are called wet tower when evaporative cooling is used, dry cooling tower when air blast cooling is utilized and the hybrid closed circuit cooling tower which is capable of working in wet-dry mode which has the simultaneous characteristics of both dry and wet towers[3,4]. The closed wet cooling tower is one applications of evaporative cooling and can be used to replace the vapour compression system in cooling of buildings. The cooling tower can be combined with chilled ceiling or beams. Highest potential for this concept is cool and dry climates but warm and dry maritime temperate climates offer a significant potential as well [5].

A number of numerical simulation and mathematical modes of cooling tower have been reported [5]. Most of the simplified models are built the basis of merkel's theory [6] assuming a Lewis number equal to unity and neglecting the losses due to water evaporation. The most important coefficient used in models are the mass transfer coefficient between spray water interface and air, and the heat transfer coefficient between tubes and spray water which are built on the basis of enthalpy potential [1]. Existing simplified models allow the prediction of cooling tower performance but using as input heat and mass transfer correlations which were experimentally obtained for large-size cooling towers [7,8]. Experimental studies have been carried on the wet cooling tower but the experimental results on hybrid closed circuit cooling tower is lacking on the relevant literature [9,10,11].

The aim of this paper is to adapt a simplified model for analyzing the combined heat and mass transfer in indirect cooling tower to evaluate the tower performing condition. The analysis of energy and mass balance for the tube element of bare type heat exchanger will define the mathematical equations for tower performance. Performance characteristics will compare with the experimental measurements.

2: Experimental setup

A new indirect cooling tower was modulated in order to be used for conducting experiments. Design conditions were a cooling capacity of 1 kW, for an inlet water temperature of 38 ^oC, a water mass velocity 2.3 kg/m^2.s and an air wet bulb temperature of 26 ^oC. The tower has a section of 0.15*0.15m and height of 0.8 m. The tube bundle has 72 inline tubes of 8 mm outside diameter and 73 mm inside diameter, with a horizontal pitch of 20 mm and vertical pitch of 25 mm, and with a total transfer area of 0.24 m^2. This corresponds to a much smaller size than usual towers.

The tower was manufactured by Gaunt company (Germany). A forced draft configuration was chosen with a cross flow fan located at air entrance. This arrangement has a lower noise level, and also leads to a lower pressure drop. It was also chosen to facilitate air flow measurements. **Figures (1)** and **(2)** shows schematically the cooling tower and main variables involved. A test facility was assembled at air conditioning lab of Mechanical Engineering Department, University of Baghdad to test this cooling tower. The thermal load was modeled with an electric heater located at a water tank. Tower inlet water temperature was controlled by varying heating power. Fan speed was also controlled by varying power supply, which allowed changing air flow rate. Spray and cooling water flow rates could be changed manually by using regulating valves.

The tower water inlet and outlet temperatures were measured with PT100 probe. Air flow rate was measured with Orifice meter at tower outlet section. In order to measure cooling water temperature evolution, thermocouples were connected to the tubes. The data acquisition system used a data logger and its software.

(1) Constant temperature bath (2) heater (3) cooling water circulation pump (4) cooling water flow meter (5) heat exchanger (6) spray nozzle (7) fan (8) spray water flow meter (9) spray water circulation pump (10) data acquisition.

Table (1): Experiment condition

Cooling water mass velocity	1.1 to 2.3 kg/m^2.s
Inlet temperature	34 to 46 ^oC.
Spray water mass velocity	0.66 to 2.1 kg/m^2.s
Air mass velocity	0.47 to 0.84 kg/m^2.s
Wet bulb temperature	21 to 26 ^oC.
Dry bulb temperature	33 to 45 ^oC.

3: Theoretical and computational modeling

In this section of the paper, the basic equations of heat and mass transfer which occurs in this type of cooling tower. The main assumptions are:

- The heat exchange between the cooling tower and the surroundings is negligible.
- The specific heats of the fluids are assumed to be constant.
- The heat and mass transfer take place only in the direction normal to the flow.
- The air and water flows are uniformly distributed in the test column.
- The water film covers the entire wall separating the air from the water.
- The interface temperature between water film and air is assumed to be equal to the water-film temperature.

3.1: Mass balance

The rate at which spray water is transferred between two phases using the overall mass transfer coefficient (ka) and referring to the humidity ratio of saturated air and water-vapor at the bulk water temperature ($H^{/}$) is:

$$GdH = dL = Ka\,(H^{/} - H)\;dz \qquad (1)$$

or $$\frac{Ka.dz}{G} = \frac{dH}{H^{/} - H} \qquad (2)$$

Multiplying both sides by $\frac{G}{L}$ gives:

$$\frac{Ka.dz}{L} = \frac{G}{L}\frac{dH}{H^{/} - H} \qquad (3)$$

Let del = $$\frac{Ka.dz}{L} \qquad (4)$$

Applying the backward finite deference method approximation, substituting equation (4) and rearranging equation (3) gives:

$$H(n+1) = H(n) + \frac{del\;\;L(n)}{G}\left[H'(n) - H(n)\right] \qquad (5)$$

3.2: Energy balance

3.2.1: Enthalpy balance of air-water film

The rate of heat transfer from the inter face to the air stream using the over all mass transfer coefficient (ka) and referring to the enthalpy of saturated air and water-vapor at the bulk water temperature (h'), neglected air and variation in humid heat is:

$$Gdh_a = Ka(h' - h_a)dz \qquad (6)$$

Which is known as Merkel equation [6].

Or $$\frac{Ka.dz}{G} = \frac{dh_a}{h' - h_a} \qquad (7)$$

The integration of equation (7) gives the NTU based on the air flow rate:

$$(NTU)_G = \frac{Ka.z}{G}\int_{ha_1}^{ha_2}\frac{dh_a}{h' - h_a} \qquad (8)$$

If the evaporation rate is ignored, then substituting for Gdh_a from equation (8) gives:

$$\frac{Ka.dz}{L} = \frac{C_L.dt_f}{h' - h_a} \qquad (9)$$

The integration of equation (9) gives the NTU based the spray water flow rate:

$$(NTU)_L = \frac{Ka.z}{L}\int_{t_{f1}}^{t_{f2}}\frac{C_L dt_f}{h' - h_a} \qquad (10)$$

Multiplying equation (7) by $\frac{G}{L}$ we have:

$$\frac{Ka.dz}{L} = \frac{G}{L}\frac{dh_a}{h' - h_a} \qquad (11)$$

Applying the backward finite difference method approximation, substituting equation (4) and, rearranging equation (11) gives:

$$h_a(n+1) = h_a(n) + \frac{delL(n)}{G}\left[h'(n) - h_a(n)\right] \qquad (12)$$

From definition of the enthalpy of air-water vapor mix true, the bulk air temperature, to and reference temperature = 273K can be written as:

$$t_a = \frac{h_a - h_{fg}H}{Cp_a + Cp_v H} \qquad (13)$$

Using finite deference substituting we have:

$$t_a(n+1) = \frac{h_a(n+1) - h_{fg}H(n+1)}{Cp_a + Cp_v H(n+1)} \qquad (14)$$

From the equation of conservation of mass equation (1) using the finite deference method we have:

$$L(n+1) - L(n) = G\left[H(n+1) - (H(n)\right] \qquad (15)$$

Rearranging equation (15) we have:

$$L(n+1) = L(n) + G\left[H(n+1) - (H(n)\right] \qquad (16)$$

Introducing the spray water enthalpy h_f in the enthalpy balance gives:

$$d\left[Lh_f\right] = d\left[Gh_a\right] \quad (17)$$

Or in the finite difference approximation:

$$L(n+1)h_f(n+1) - L(n)h_f(n) = G\left[h_a(n+1) - h_a(n)\right] \quad (18)$$

Rearranging equation (18) we have:

$$h_f(n+1) = L(n)h_f(n) + G\left[h_a(n+1) - h_a(n)\right] / L(n+1) \quad (19)$$

The spray water enthalpy is defined as:

$$h_f = C_L[t_f - 273] \quad (20)$$

Therefore

$$t_f = \frac{h_f}{C_L} + 273 \quad (21)$$

Or in the finite difference approximation:

$$t_f(n+1) = \frac{h_f(n+1)}{C_L} + 273 \quad (22)$$

3.2.2: Overall enthalpy balance

The rate of heat transfer from cooling water through the outside surface of heat exchanger to the interface of spray water-vapor film to the stream can be written as:

$$d[Wh_w] + d[Gh_a] = d[Lh_f] - dLdh_f \quad (23)$$

or

$$Wdh_w = d[Lh_f] - Gdh_a - dLdh_f \quad (24)$$

Or in the finite difference approximation:

$$Wh_w(n+1) - Wh_w(n) = [L(n+1)h_f(n+1) - L(n)h_f(n)] - [L(n+1) - L(n)][h_f(n+1) - h_f(n)] - G\left[h_a(n+1) - h_a(n)\right] \quad (25)$$

Rearranging equation (25) we have:

$$h_w(n+1) = h_w(n) + \{[L(n+1)h_f(n+1) - L(n)h_f(n)] - [L(n+1) - L(n)][h_f(n+1) - h_f(n)] - G\left[h_a(n+1) - h_a(n)\right]\} / W \quad (26)$$

The cooling water enthalpy is defined as:

$$h_w = C_L[t_w - 273] \quad (27)$$

$$t_w = \frac{h_c}{C_L} + 273 \quad (28)$$

Or in the finite difference approximation

$$t_w(n+1) = \frac{h_c(n+1)}{C_L} + 273 \quad (29)$$

Interface humidity ratio and enthalpy, the interface humidity ratio H' and enthalpy, h' should be know at the bottom boundary of the incremental volume (n). The bulk water temperature at this boundary is considered equal the interface temperature, a computer sub routine is prepared to evaluate H' and h'. This is done by, first using the Keenan-Keyes formula [1] to find the saturation water-vapor pressure (P_s) (in atmosphere).

$$\log_{10}\left[\frac{P_s}{218.167}\right] = -\frac{\beta}{T}\left[\frac{a + b\beta + C\beta^3}{1 + d\beta}\right] \quad (30)$$

Where: a, b, c and d are constants:
a = 3.2437814
b = $5.86826*10^{-3}$
c = $1.1702379*10^{-8}$
d = $2.1878462*10^{-3}$
T = absolute temperature, K
β = 647.27–*T*

From the perfect gas low, the saturation humidity ration (H_s) is defined by [1]:

$$H_s = 0.62198\frac{P_s}{1 - P_s} \quad (31)$$

But the interface enthalpy is defined as:

$$h^{/} = [Cp_a + Cp_v H_s]t_f + h_{fg}H_s$$

Substituting for H_s from equation (31), then:

$$h^{/} = Cp_a t_f + 0.62198\frac{P_s}{1 - P_s}[Cp_v t_f + h_{fg}] \quad (32)$$

Thus h' could be found and $H^{/}$ is H_s.

A basic computer program was written, all the measured parameters taken from experimental runs, such as: air inlet dry and wet bulb temperatures, air outlet dry and wet bulb temperatures, spray water inlet and outlet temperatures, cooling water inlet and outlet temperatures, air velocity, spray and cooling water flow rates, and heat exchanger dimensions. These data were fed the program as input data. All computed parameters taken from the output from the computer which are: The water to air ratio, performance coefficient, outlet air dry-bulb temperature and air humidity ratio, inlet and outlet cooling water temperature, air and spray water flux,

mass and heat transfer coefficients and the rejected heat. The flow chart of this program is presented in **Figures (13)**.

3.3: Results and Discussions

Under the standard experimental conditions given in **table (1)**, the experiment and computer program of computational model was repeated over and over changing the air and spray water mass velocities, air dry and wet bulb temperatures and cooling water inlet temperature.

The variation of saturation and cooling capacity efficiency with respect to air wet bulb temperature for different air mass velocities is shown in **figs.(1) and (2)**. The latent heat transfer between the air and the tube surface of heat exchanger is determinates by the density difference between them. Thus, when the wet bulb temperature of air increases the temperature difference between the cooling water and air at inlet decreases, therefore the rate of evaporation of spray water flowing at the outer surface of tubes decreases so that the temperature decrease of cooling water flowing inside the tubes deceases causing the cooling capacity to be significantly reduced. However, the saturation efficiency of the tower is increased slightly with the increasing of air wet bulb temperature, thus increase become linear at temperature higher than 23. Saturation efficiency increases with wet bulb temperature about 8 % for temperature between 22 and 26 ^{o}C.

The range of cooling water and the coefficient of performance behaves similarly versus air wet bulb temperature as shown in **figs.(3) and (4)**. The rate of increase of coefficient of performance is looks identical to the cooling capacity because the wet bulb temperature has no effects on the power consumption of both fan and spray water pump.

Fig.(5) shows almost linearity and a little increase of efficiency with the air dry bulb temperature due to the decrease in overall heat transfer coefficient sequencing by the less amount decrease in the approach of tower.

The air mass velocity affects the cooling tower characteristics represented by saturation efficiency, cooling capacity and coefficient of performance for different spray water mass velocities as shown in **figs (6), (7)** and **(8)**. Higher saturation efficiency and higher coefficient of performance can be obtained with higher air mass velocity. This mostly because when air mass velocity increases it becomes sufficient to accomplish the same transfer of heat and mass especially by evaporation, thus causing an increase of the range of cooling water leading to increase these characteristics.

Also these figures show the effect of spray water mass velocity on tower characteristics. It is clear that the cooling capacity is influenced slightly by the spray water mass velocity, that is mainly because when the spray water mass velocity increases, the rate of evaporation is augmented causing more heat transferred from the cooling water because the heat and mass transfer coefficients are affected by the spray water mass velocity. If **fig.(6)** compared with **fig.(7)** it can concludes that the effect of spray water mass velocity is relatively small compared to the effect of air mass velocity, this conforms well to Yeon Yoo et al [12]. Also it is clear that the coefficient of performance is increased slightly with increasing of spray water mass velocity. When the spray water mass velocity increases, both cooling capacity and power consumption of spray water and supply air fan increase which overcomes by the cooling capacity, thus conforms well to Riffat et al[13].

The saturation efficiency and cooling capacity while varying the cooling water inlet temperature for different air mass velocities are shown in **figs.(9), (10)** and **(11)**. When the temperature and density differences between the tube surface and the air increase according to the increase in water inlet temperature, the heat and mass transfer coefficients increase, thus the efficiency and cooling capacity is increased. However, as it could be noticed in this figure, the increase in efficiency is not significant compared to the increase in cooling capacity.

Finally **Fig.(12)** show a very little influence of spray water mass velocity on the cooling capacity.

3.4: Concluding Remarks

The performance characteristics of wet closed circuit cooling tower having a rated capacity of 1kw were investigated experimentally and theoretically in the present study. The following conclusion can be abstracted from results:

1- All the characteristics of cooling tower increase significantly with the increasing of air mass velocity and slightly increase with the increasing of spray water mass velocity.

2- Air wet bulb temperature has a significant influence on the cooling capacity and has no significant influence on the saturation efficiency.

3- The cooling water inlet temperature has a very little influence on the performance of cooling tower. The same the behavior for the effect of air dry bulb temperature.

4- There is a good agreement in cooling tower performance characteristics between the experimental and theoretical results.
5- Thermal computational model investigated during theoretical analysis is useful for designing and predicting cooling tower performance.

Refrences

1- ASHRAE, 1998, Hand-book of fundamentals, American Society Heating Refrigeration and Air Conditioning Engineering, USA.
2- R.T.I. Mizushina, H. Miyashita, 1968, Characteristics and methods of thermal design of evaporative cooler, International Chemical Engineering, Vol.8, No.3, 532-538.
3- Cooling tower, 2000, ASHRAE HVAC systems and Equipment, American society of heating, Refrigeration and Air conditioning, USA.
4- P. Stabat and D. Marchio, 2004, Simplified model for indirect-contact evaporation cooling-tower behavior, Applied, Energy No.78, 433-451.
5- Ala Hasan and kairen , 2002, Theoretical and computational analysis of closed wet cooling towers and its applications in cooling of buildings, Energy and Buildings, Vol. 34, No.5, 477-486.
6- Merkel, 1925, Verdunstungskuehlung, VDI Forrschungs Sarbiten, No.275, Berlin.
7- S.Y. Yoo, J. H. Kim and K.H. Han, 2010, Thermal performance analysis of heat exchange for closed wet cooling tower using heat and mass transfer analogy, Journal of Mechanical Science and Technology, Vol.24, No.4, 893-898.
8- A. Oliveira and J. Facao, 2002, Heat and mass transfer correlations the design of small indirect contact cooling tower, 1st International Conference on Heat Transfer, Fluid Mechanics and Thermodynamics, Kruger Park, South Africa.
9- J. Facao and C. Oliveira, 2000, Thermal behavior of closed met cooling towers for use with chilled ceilings, applied thermal Engineering, No.20, 1225-1236.
10- M.M.A. Sarker, C.G. Moon and J.I. Yoon, 2005, The cooling capacity and pressure drop in a hybrid closed circuit cooling tower, Proceeding of the International Conference of Mechanical Engineering, Dhaka, Bangladesh.
11- S. Riffat, A. Oliveira, J. Facao, G. Gan and P. Doherty, 2000, Thermal performance of closed wet cooling tower for chilled ceiling: Measurement and CFD simulation, International Journal of Energy Research, No.24, 1171-1179.
12- Yeon Yoo, S., Kim, J.H, and H, k.h., 2010, " Thermal performance analysis of heat exchanger for closed wet cooling tower", Journal of mechanical science and technology, Vol.24, No.4,. 29-34.
13- Riffat, S.,Oliveira, A., Facao,J.,Gan, G. and Doherty, P., 2000, " Thermal behavior of a closed wet cooling tower for chilling ceiling", Journal of energy research, Vol.24, 1171-1179.

Nomenclatures

Symbol	Definitions
a	Surface area per unit volume, m^2/m^3
A	Cross section area, m^2
C_L	Specific heat of water, kJ/kg.K
Cp_a	Specific heat of air, kJ/kg.K
C_V	Specific heat of moist air, kJ/kg.K
C_S	Specific heat of water vapor, kJ/kg.K
H	Humidity ratio, kg_a/kg_v
$H^/$	Humidity ratio at sat. mixture, kg_a/kg_v
h_a	Enthalpy of moist air, kJ/kg
$h^/$	Enthalpy of moist air at sat. mixture, kJ/kg
h_{fg}	Latent heat of evaporation, kJ/kg.K
G	Air flux, $kg/s.m^2$
K	Mass transfer coefficient, $kg/s.m^2$
K.a	Volumetric mass transfer coeff., $kg/s.m^2$
K.az/G	Performance coefficient based on G
K.az/L	Performance coefficient (NTU) based on L
L	Air flux, $kg/s.m^2$
m	Mass flow rate, kg/s
Q	Heat load, kW
t	Temperature, K
V	Coil volume / cross section, m^3/kg
Z	Coil height, m
W	Cooling water flux, $kg/s.m^2$

Subscript

f (L)	Spray water
a (G)	Air
w	Cooling water
v (m)	Humid air
1	Down tower section
2	Up tower section
i	Interface

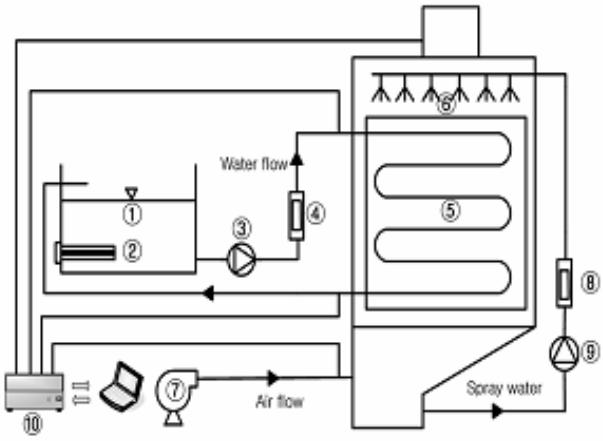

Fig.1. Schematic of closed wet cooling tower

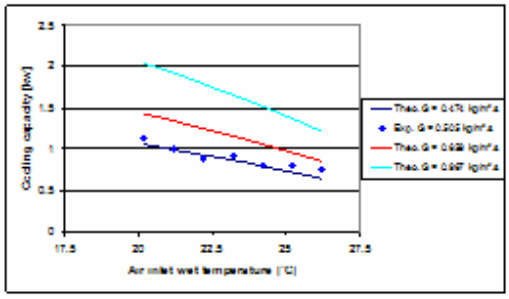

Fig 1: Cooling capacity w.r.t. air wet bulb temperature for different air mass velocity.

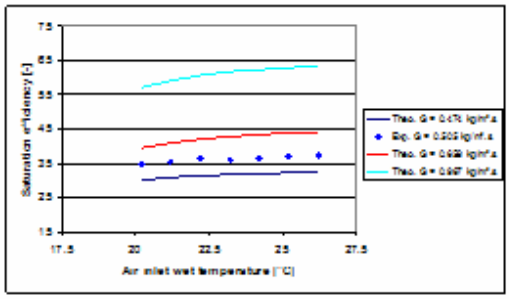

Fig 2: Saturation efficiency w.r.t. air wet bulb temperature for different air mass velocity.

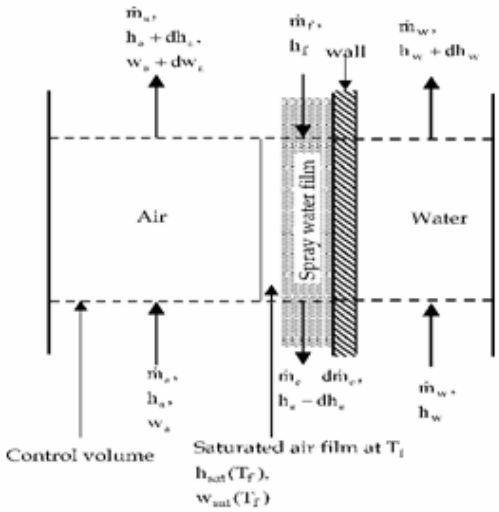

Fig. 2. Flow steams inside an element

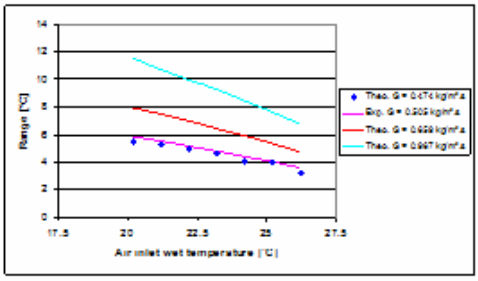

Fig 3: Range of cooling tower w.r.t. air wet bulb temperature for different air mass velocity.

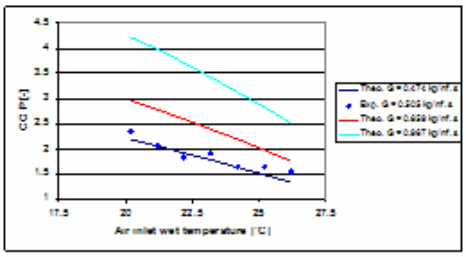

Fig 4: Coefficient of performance w.r.t. air wet bulb temperature for different air mass velocity.

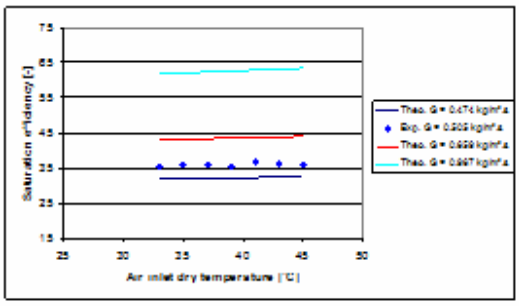

Fig 5: Saturation efficiency w.r.t. air dry bulb temperature for different air mass velocity.

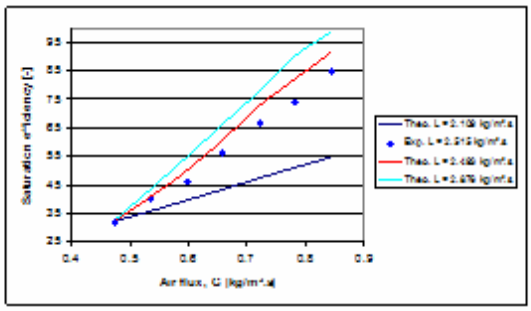

Fig 6: Saturation efficiency w.r.t. air mass velocity for different air mass velocity.

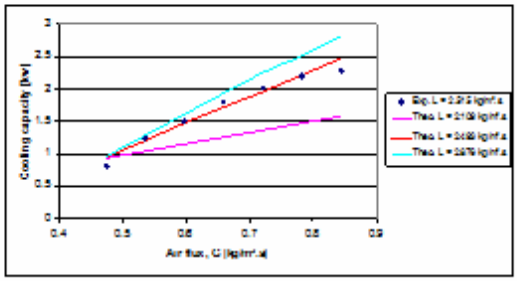

Fig 7: Cooling capacity w.r.t. air mass velocity for different air mass velocity.

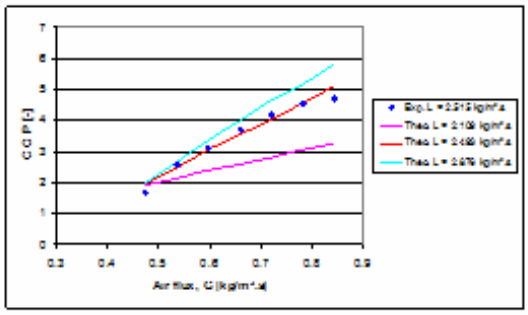

Fig 8: Coefficient of performance w.r.t. air mass velocity for different air mass velocity.

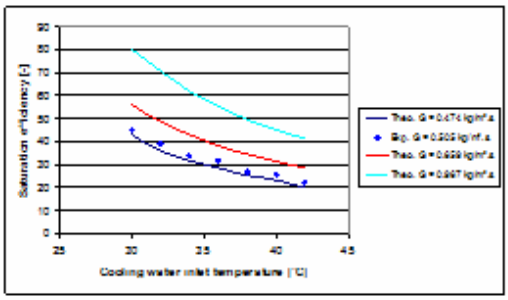

Fig 9: Saturation efficiency w.r.t. cooling water inlet temperature for different air mass velocity.

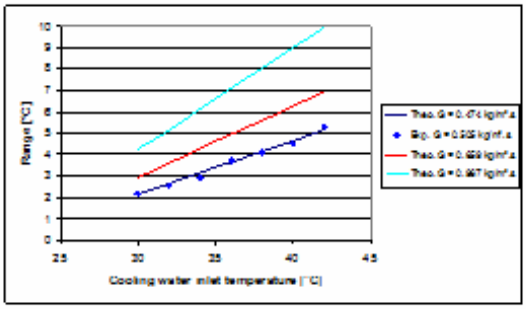

Fig 11: Range of cooling tower w.r.t. cooling water inlet temperature for different air mass velocity.

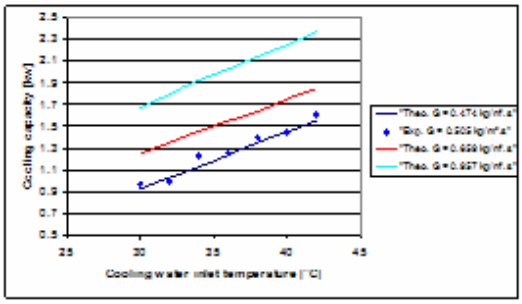

Fig 10: Cooling capacity w.r.t. cooling water inlet temperature for different air mass velocity.

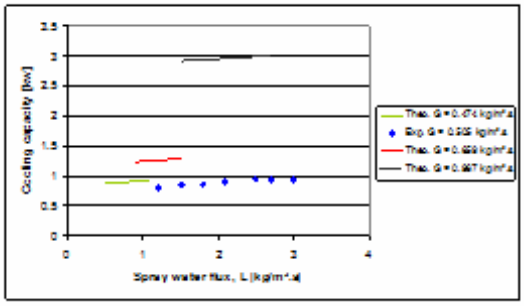

Fig 12: Cooling capacity w.r.t. spray water mass velocity for different air mass velocity.

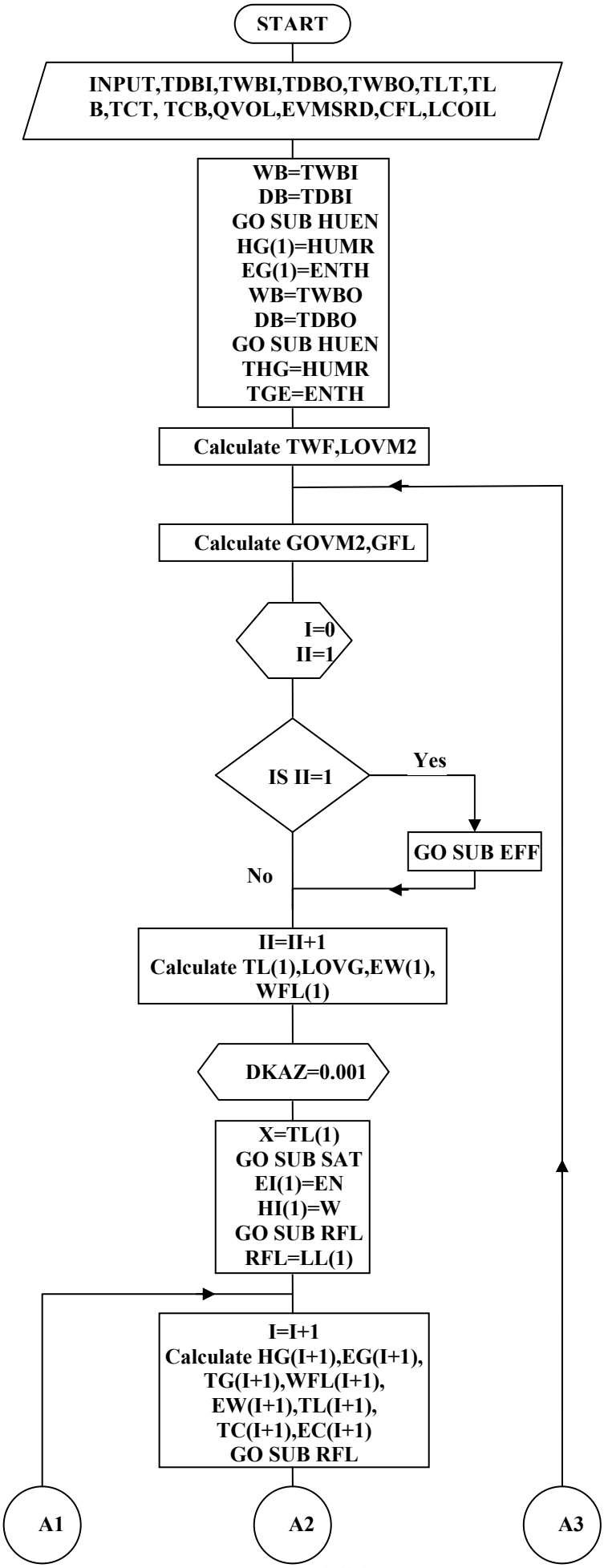
START
INPUT,TDBI,TWBI,TDBO,TWBO,TLT,TLB,TCT, TCB,QVOL,EVMSRD,CFL,LCOIL
WB=TWBI
DB=TDBI
GO SUB HUEN
HG(1)=HUMR
EG(1)=ENTH
WB=TWBO
DB=TDBO
GO SUB HUEN
THG=HUMR
TGE=ENTH
Calculate TWF,LOVM2
Calculate GOVM2,GFL
I=0
II=1
IS II=1
Yes
GO SUB EFF
No
II=II+1
Calculate TL(1),LOVG,EW(1),WFL(1)
DKAZ=0.001
X=TL(1)
GO SUB SAT
EI(1)=EN
HI(1)=W
GO SUB RFL
RFL=LL(1)
I=I+1
Calculate HG(I+1),EG(I+1),TG(I+1),WFL(I+1),EW(I+1),TL(I+1),TC(I+1),EC(I+1)
GO SUB RFL
A1
A2
A3

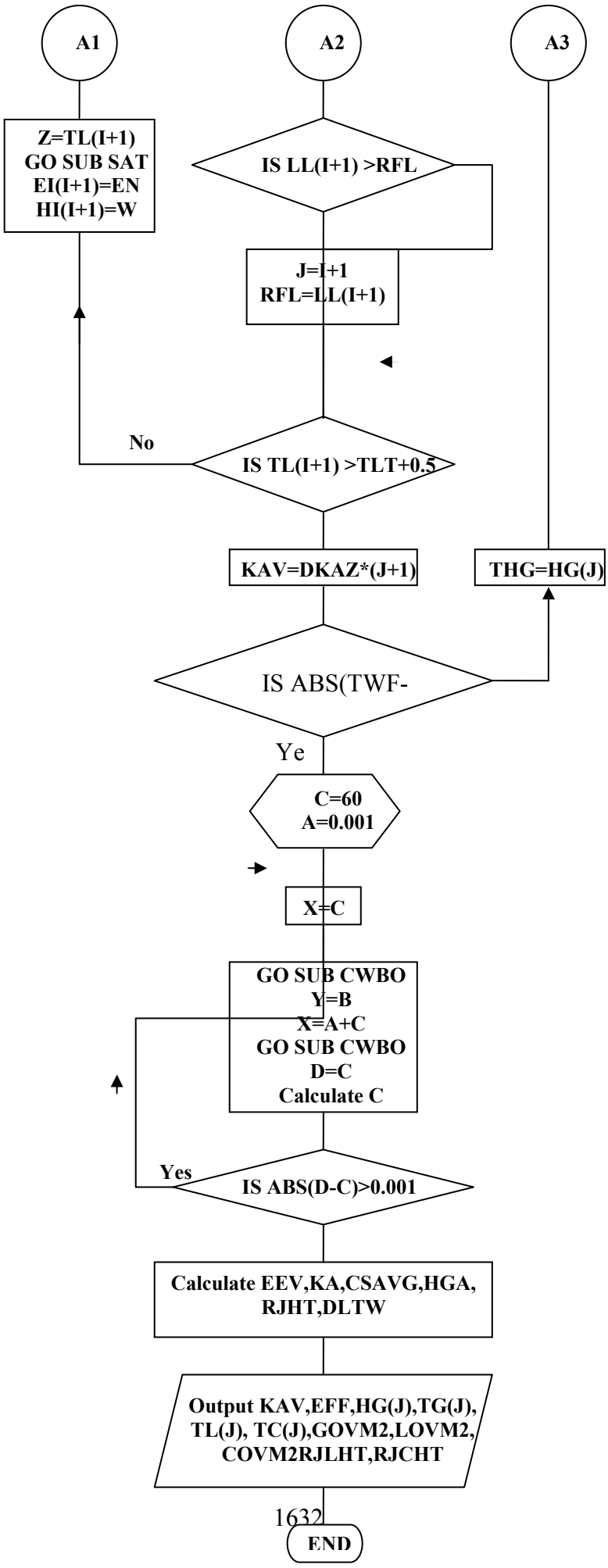
A1
A2
A3
Z=TL(I+1)
GO SUB SAT
EI(I+1)=EN
HI(I+1)=W
IS LL(I+1) >RFL
J=I+1
RFL=LL(I+1)
No
IS TL(I+1) >TLT+0.5
KAV=DKAZ*(J+1)
THG=HG(J)
IS ABS(TWF-
Ye
C=60
A=0.001
X=C
GO SUB CWBO
Y=B
X=A+C
GO SUB CWBO
D=C
Calculate C
Yes
IS ABS(D-C)>0.001
Calculate EEV,KA,CSAVG,HGA,
RJHT,DLTW
Output KAV,EFF,HG(J),TG(J),
TL(J), TC(J),GOVM2,LOVM2,
COVM2RJLHT,RJCHT
END

الفضاء المعماري في مملكة الحيرة والحكم الساساني أنذاك

بحث مستل مقدم من قبل

أ. د. غادة موسى رزوقي

د. شذى عباس حسن

الملخص

شهدت العمارة الرافدينية منذ بداياتها الاولى في حضارات وادي الرافدين المتعاقبة مرورا بالحضارة الاسلامية وحتى مطلع القرن العشرين سلسلة من الطرز المعمارية المتعددة خصها الباحثون والاثاريون والمؤرخون بدراسات وفيرة سواء على مستوى الحقب التاريخية او على مستوى الانماط الوظيفية او الطرز المعمارية وحتى على مستوى العناصر المكونة لتلك الطرز.

لكن يمكن تشخيص المشكلة البحثية محدودية في الدراسات التي ترصد العمارة الرافدينية خلال مملكة الحيرة والحكم الساساني المواكب لها.

لذا يهدف البحث الى توثيق وتحليل العمارة الرافدينية في مملكة الحيرة والمدن التي ظهرت في نفس الحقبة التاريخية وعلى مستوى

1- التشكيل الفضائي

2- العلاقات الفضائية

3- العناصر المعمارية

4- المعالجات التفصيلية.

يعتمد البحث الدمج بين المنهج الوصفي والمنهج التحليلي المقارن في تقصي عمارة المرحلة وتحليلها على المستويات الاربعة المكونة للفضاء المعماري انفة الذكر، ومن ثم بدأ البحث بالتقصي عن بدء ظهور المفردات المعمارية والتغيرات الحاصلة فيها واختفاء مفردات وظهور اخرى مع جداول تحليلية توضح الحقب وانواع الابنية ووظائفها.

وتوصل البحث الى استنتاج يخص كل مكون من مكونات الفضاء على مستوى التشكيل الفضائي، العلاقات الفضائية، العناصر المعمارية، المعالجات التفصيلية.

وشخص البحث تواصل كل من تلك المفردات مع مفردات واساليب معالجات العمارة الرافدينية القديمة وكما سيرد توضيح ذلك في الاستنتاجات النهائية للبحث.

كلمات رئيسية: (ايوان، قبة، فضاء معماري، تواصل، تشكيل فضائي، علاقات فضائية، عناصر معمارية، معالجات تفصيلية).

Architectural Space in Hera Kingdom and Sasanyain Empire

Prof. Dr. Ghada Musa

Dr. Shatha Abbas

Abstract

The research problem can be identified in the limitedness of the studies that allocate the comprehensive historic continuity of the Mesopotamian architecture during the Hera and sasanyain eras and at the architectural space level on the consideration that it is the heart of architecture in all its compositional and detailed items.

Thus, the research aims at clarifying if there were any continuity in the Mesopotamian architecture during the Hera and sasanyain eras, and consequently, clarifying the levels of this continuity if it were on the whole or part level in architecture, then, identifying the changes that it has been through in order to know how to achieve continuity of contemporary architecture along its historical course.

In order to verify this hypothesis, the architectural space has been studied. This study has managed to specify the items of the spatial continuity in the Mesopotamian architecture at the level:

1- The spatial formation 2- the spatial relations 3- the architectural elements 4- the detailed treatments

Moreover, the research has reached the general conclusions and it recommends a number of recommendations at the applicable, academic and epistemological level.

1- المقدمة

الحيرة مملكة عربية عراقية حظيت باهتمـام المـؤرخين والرحالة لكنها لم تحظى باهتمام كاف من قبـل البـاحثين المعماريين بشكل يوازي ماكان زاخرا بها من عمارة مهمة شملت قصورا وكنائس واديرة تركت بصماتها في التشكيل الفضائي لعمارة ما بعد الفتح الاسلامي.

من هنا برزت **المشكلة البحثية** فـي محدوديـة المعرفـة المعمارية عن فضاءات مملكة الحيرة والمدن المعاصرة لها زمانيا ومكانيا. **لهذا يهدف البحث**:

1- الى تسليط الضوء على العمارة العراقية فـي مملكـة الحيرة والمدن المعاصرة لها زمانيـا ومكانيـا كتكريـت والمدائن.

2- بيان خصائص الفضاء المعماري في المنطقة وبكافـة انماطه الوظيفية وعلى جميع مستويات هذا الفـضاء مـن التشكيل، فالعلاقات فالعناصر وصـولا الـى المعالجـات التفصيلية.

يفترض البحث ان الفضاء المعماري لعمارة مملكة الحيرة وتكريت والمـدائن وللحقبـة المحـصورة بـين سـقوط الامبراطورية البابلية وبداية الفتح الاسلامي. يعـد حلقـة الوصل بين الفضاء الرافديني القديم والفـضاء الرافـديني الاسلامي. وللتحقق من هذه الفرضية حاول الباحث القـاء الضوء على الفضاء المعماري الرافديني بعمارة المرحلـة قيد الدراسة.

وخرج البحث بمجموعة استنتاجات تـضمنت خـصائص الفضاء المعماري لعمارة المرحلة على مـستوى التـشكيل الفضائي والعلاقـات الفـضائية والعناصـر المعماريـة والمعالجات التفصيلية.

2- موقع مملكة الحيرة الجغرافي

تبعد الحيرة حوالي خمسة كيلومتر عن الكوفة على موضع النجف، وتقع الحيرة ما بين شطري نهر الفرات، (العلـي، صالح احمد، 1989، ص20)، الا انه من الواضـح بـان المدينة تقع مابين فضاء الحيرة ومدينتي الكوفـة والنجـف الحاليتين، لان معظم التلال والمكتشفات الاثرية تمت فـي المثلث الحاصل مابين الكوفة والنجف والحيـرة الحاليـة، (قديفة، 2006،ص95).

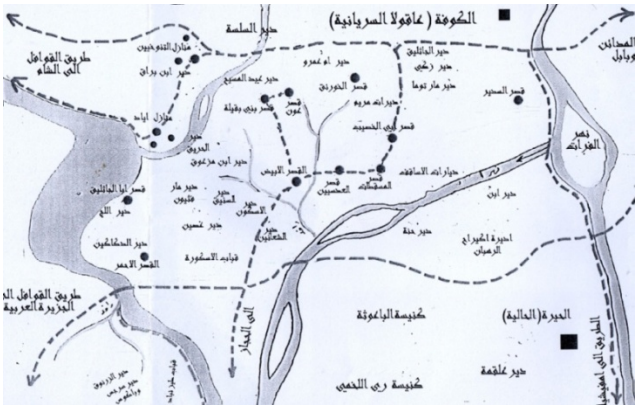

شكل (1) موقع ومخطط مملكة الحيرة

3- تاريخ مدينة الحيرة

يذكر التاريخ وجود قبائل عربية استقرت بعـد الهجـرات العربية الى الحيرة والانبار، وتؤكد المـصادر بـان تلـك القبائل بدأت تتدفق الى بادية العراق الشمالية من الغـرب والجنوب بعد سقوط نينوى عام (612 قبل الميلاد)، وكانت تتمتع بعلاقات تجارية وحضارية مختلفة مع بلاد الرافدين منذ الالف الاول قبل الميلاد، او ما قبلها، وانها كانت على احتكاك مع الحضارات الرافدينية القديمة في قمة تطورها.

وبعد سقوط الامبراطوريات الرافدينية الضخمة، السومرية والاشورية والبابلية، نزح عدد من القبائل العربية الى بلاد الرافدين واقامت فيها حضارات يشهد لها التاريخ بالعظمة والرخاء، واهمها مملكة الحيرة في جنوب وادي الرافدين، (جنان، 2000، ص302).

يعتقد ان تشييد مملكة الحيرة يعـود الـى عـصر الملـك نبوخذنصر الذي بنى حيرا على النجف وحـصنه ليـضم التجار العرب الذين كانوا يقدمون على بابل في عـصره، (سفر، مصطفى،1974،ص46). لقد كانت مملكة الحيـرة مملكة مستقلة في ظل الحكم الفرثي والساساني الذي اعقبه وقد ازدادت اهميتها لوقوعها على خط الهدنة بين الـروم والفرس فضلا عن اهميتها كمركز مهم للقبائـل العربيـة ومركز تجاري مهم.

انتشرت النصرانية في مملكة الحيرة منذ العصور المسيحية الاولى وازدهرت في القرنين الاول والثاني بعد المـيلاد، واصبح فيما بعد الدين السائد في مملكة الحيرة لغاية الفـتح الاسلامي.

4- عمارة مملكة الحيرة

اشتهرت مملكة الحيرة بقصورها وعمارتها التي لـم يبـق منها سوى كتابات الرحالة ووصفهم، وان قصور مملكـة الحيرة مشهورة في المصادر التاريخية لكن ايا منها لم يتم الكشف عنه بشكل مؤكد، وتذكر المصادر التاريخية قصور الخورنق والسدير (قصرالثلاث قباب)، وقـصر العـذيب والصنبر والقصر الابيض وقصر الزوراء وقصر العـين، وغيرها من القصور، (الشرقي، 1987، ص46).

وقد عرفت قصور مملكة الحيرة باواوينها ومـن وصـف المسعودي لاخرها والذي يعتقد بانه الخورنق وان الجـزء الرئيس فيه كان ذا تخطيط ثلاثي مؤلف من الصدر (الذي كان يجلس عليه الملك) والكمين علـى جـانبي الـصدر، (يوسف، 1982،ص22).

أ – قصر الخورنق

قصر الخورنق، (معنى الكلمة)، في اصل اللفـظ، ذهـب الخليل الى انه عربي الاشـتقاق مـن الخرنـق ومعنـاه الصغير من الارانب، وارتأى (نلدكه) الالماني، انه حرف من العبرية الربانية بمعنى المزرعة والعـريش، وذهـب (اندريا)، الى انه ايراني من (كوورنه) بمعنى ذي السقف الجميل، وفي البرهان القاطع انه معرب من (خورن كاه) أي موضع الاكل والشرب1، (يوسف رزق الله غنيمـة، 1936، ص19).

آخر من وصفه ابن بطوطه بقوله (**... وبه عمارة وبقايا قباب ضخمة في فضاء فسيح علـى نهـر يخـرج مـن الفرات**)، *(الشرقي،2001، ص47)*. وقال الدكتور جـواد علي، (ويظهر من وصف اهل الاخبار للخورنق انه كان قصراً كبيراً اعد للسكنى وليكون **حـصناً** يهـيمن علـى مشارف البادية)، *(عن المفصل في تاريخ العـرب قبـل الاسلام 3 : 202)*. وفي حديثه عـن الخورنـق، قـال الدكتور **ناجي الاصيل**، (واستطعنا ان نتتبع اسـس هـذا القصر بان قسنا (**ساحة مربعة**) منه، يحيط بها جـدران **مدعمة بابراج مستديرة**، فالفينا طول ضـلعها خمـسين متراً، وتفحصنا كسرات الفخار المبعثرة عليه فوجدنا انها من اواخر العهد الساساني في وادي رافدين. وعثرنا على عدد يسير من مسكوكات نحاس واجزائها، ظهرت الكتابة

في احـداها انهـا ضـربت فـي الكوفـة سـنة 143 هـ ،(*الشرقي، 2001، ص46*).

الخورنق اعلى وارفع بناءاً من السدير، وقد زاد من حسنه زهرة النقوش والفسيفساء المزركشة، والزخارف الملونـة محيطه بالمصابيح والاضوية العالية،يظهر مـن ذلـك ان الخورنق والسدير بناءان ان لم يقوما على اسـاس واحـد وانهما متجاوران، ويقترب من هذا برأي الدكتور علـي ابراهيم حسن في كتابـه (التـاريخ الاسـلامي العـام) ص63، قال ويغلب على الظن انهما كانا في مكان واحـد في مملكة الحيرة ويطلق عليهما معاً الخورنق ويفهم مـن قول المنشئ البغدادي ان الخورنق والسدير على بعـد 4 فراسخ عن النجف انهما متجاوران ولكنه لم يذكر الاتجاه وهذا يخالف الروايات التي تقول : ان الخورنق بعيد عن السدير مسافة غير قليلة. من القصائد الشعرية التي تغنت في وصف قصر الخورنق:

قول الشاعر علي بن محمد العلوي الكـوفي المعـروف بالحماني:

كم من وقفةٍ لك بالخورنق ما توازي بالمواقفِ

تلقى اواخرها اوائلها بالوان الرفارفِ

بحرية شتواتها برية منها المصائفِ

درية الصهباء كافورية منها (المشارف)

وله ايضاً،

وما بسط الخورنق من رياضٍ

مفجرة (بافنيةٍ فساح)

وقال الاسود بن يعفر، (الامير اسامة الكنـاني، المنـازل والديار، ص19):

اهل الخورنق والسدير وبارق

(والقصر ذي الشرفات) من سنداد

يقال ان الحيرة بنت الكوفة، لانها بنيت بأجرها، قال البلاذري (وجد في قراطيس هدم قصور الحيـرة التـي كانت لآل المنذر، ان المسجد الجامع بالكوفة بني بـبعض نقض تلك القصور)، (*الشرقي، 2001، ص47*).

الا ان الخورنق حظي بعناية الولاة وعمـال الدولـة حتى نهاية العصر العباسي، ثم نزله الرحالة العربي ابـن بطوطة في القرن الثامن الهجري، فشاهد **بقايا (قبابـه)،** وكان وصف ابن بطوطة له هو آخر عهد لذكر الخورنق بناءاً قائماً ببعض قبابه، وان كان ذكره باقيـاً حتـى الان وسيبقى على لـسان الكتـاب والـشعراء، والظـاهر ان الخورنق لم يسلم من ايدي الطامعين بآجره، لما ظهـرت الدولة العباسية اقتطع الخورنق الى ابـراهيم بـن سـلمه الخلاّل، واحدث فيه **قبه** ولم تكن قبل ذلك، وبقـي يقـاوم الزمن، (*يوسف رزق الله غنيمة، 1936، ص19*).

وهناك دليل على تكرار نمط تخطيط قصور الحيـرة في اماكن وعواصم اسلامية لاحقه، ومنها ما يشير اليـه المسعودي في مروج الذهب، بان (الخليفة المتوكل احدث في ايامه بناء، لم يكن الناس يعرفونه، وهـو المعـروف بالحيري والكمين والاورقة، وذلك لان بعض سماره حدثه في بعض الليالي ان بعض ملوك الحيرة فـي النعمانيـة احدث بنياناً ....)، فاعجب المتوكل ذلك ومدحـه النـاس بفعله هذا، (الصالحي، ج3، 1985، ص260).

ذكر في وصف التشكيل الفضائي لقصر الخورنق، شـكل (2)، بانه قائم على مجموعة اسس منها:

- **الطراز الحيري، (الصدر والكمين).**
- **عدد من القباب الضخمة**
- **افنية كثيرة**
- **سور مدعم بابراج مستديرة (حصن)**
- **ذو شرفات**
- **مساحة 50 x 50 م**
- **بينه وبين دار الامارة تشابهاً كبيراً**

فهو وفقاً لمبدأ الصدر والكمين وقد اضيفت خلـف ايـوان الصدر قبه في مراحل لاحقة، وبعض المصادر اشارت او اعتبرت (قصر الاخيضر)، الذي لايزال قائماً، ليس سوى قصر الخورنق، حيث ان عمر البناء يعود لمرحلة تاريخية بين القرن الخامس والسابع الميلادي وان وجد فيه مسجد.

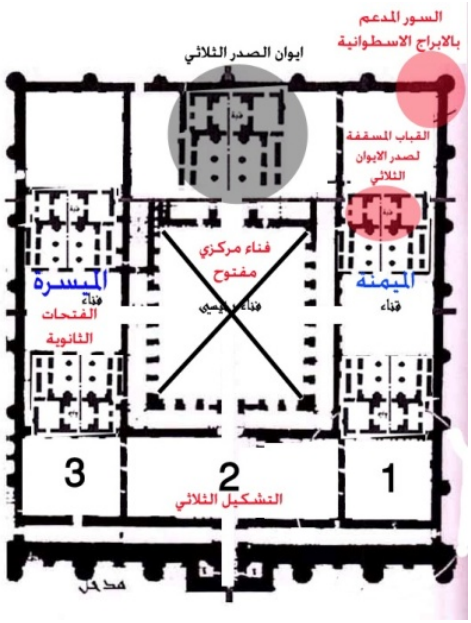

شكل(2) المخطط التخيلي لقصر الخورنـق (مـن اعـداد الباحث)

ب- قصر السدير

تسمية السدير تعريب (سادل) أي قبة في ثلاث قباب متداخلة، *(العلي، 1989،ص31)*، وهو بالفارسـية (سـه دلي)، أي ثلاث شـعب، او ثـلاث متـداخلات، وقـال الاصمعي، (السدير فارسية كان اصلها (سادل)، أي قبـة في ثلاث قباب متداخلة. وهي التي تسميها النـاس اليـوم (سدلي) فاعربته العرب فقالوا (سدير)، *(جواد علـي، 3، هامش ص202)*. ان هذا الرأي يسنده المـسعودي، فـي قوله (والابواب الثلاثة على الرواق)، *(الـشرقي،2001، ص48)*.

موقع القصر مثلما اختلف المؤرخون في موقع الخورنق، اختلفوا في موقع السدير، فـاليزدي ذكـر ان الخورنـق والسدير في مكان واحد، (الميـرزا فـضل الله اليـزدي، ص236)، وقال المنشئ البغدادي، (بعد اربعة فراسخ عن النجف يأتي قصر السدير)،(الشرقي،2001، ص48).

يبقى ان نلجأ الى ما اعتـاد عليـه بنـاة القـصور، فالغالب انها تشيد بالقرب من الماء وبذا يـضعف الـرأي القائل، (السدير في البرية، ويرجح الرأي القائل الـسدير يقع عن شمال نهر الغدير)، قال الشاعر الحماني:

سحم وقفةٍ لك بالخورنق ما توازي بالمواقف

بين الغدير الى السدير الى ديارات الاساقف

فالسدير اذن ليس بعيداً عن الخورنق، اما نهر الغدير فقد حدد الشابشتي موقعه حين حدد موقع ديارات الاساقف بقوله، بالنجف بظاهر الكوفة وهو اول مملكـة الحيـرة وبحضرتها نهر يعرف بالغدير عن يمينـه قـصر ابـي الخصيب وعن شماله السدير)، (الشرقي،2001، ص49).

وصف القصر، قال المسعودي، (ان بعض ملوك الحيـرة من النعمانية من بني نصر، احدث بنياناً في دار قـرارهِ وهي الحيرة، فكان الرواق فيـه مجلـس الملـك، وهـو الصدر، والكمان ميمنة وميسرة، ويكون في البيتين اللذين هما الكمان من يقرب منه من خواصه، وفي اليمين منهما خزانة الكسوة، وفي الشمال ما احتيج اليه مـن شـراب، والرواق قد عم فضاؤه الصدر والكمين والابواب الثلاثـة على الرواق، مسمي هذا البنيان الى هذا الوقت بـالحيري ذو الكمين اضافة الى النمط الحيري)، *(الـشرقي،2001، ص50)*.

وعقب الاب انستاس ماري الكرملي على مـا تقـدم بقوله، (وسمي بعضهم هذا النـوع مـن البنـاء الـسدلي والسدير، كما اشار اليه لغويو العرب)، وقال يوسف رزق الله غنيمه، (وهذا الوصف يلمح الى هيئة قصر الـسدير)، وقال ايضاً، (وقد تفـنن الحيريـون بـنقش عمـاراتهم وزخرفتها بالرسوم وبطلاء سقوفها بالفسافس والـذهب)، *(يوسف رزق الله غنيمة، 1936، ص86)*، وقـد وضـع الباحث مالك قديفة تصورا تخيليا لشكل قـصر الـسدير،

وفقا لما ورد عنه من شروحات، (قديفة، مالـك، 2006، ص124)، شكل (3).

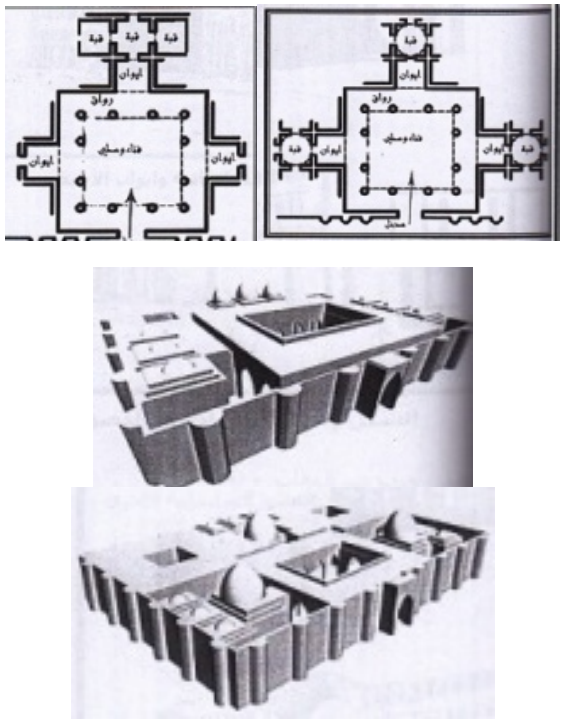

شكل(3) المخطط التخيلي لقصر السدير

ج- القصر المكتشف في مملكة الحيرة

مبنى واسع بني بطبقتين متشابهتين تماماً، الطبقة الـسفلى كانت بمثابة اسس او مصطبة على الارجح، واقيم فوقهـا البناء الرئيسي، والمبنـى مـستطيل ابعـاده (50x70)م، مدخله من جهة الجنوب، يتوسط القصر فنـاء مكـشوف يطل عليه مـن الجـانبين الـشرقي والغربـي ايوانـات بالاسلوب الحيري وعلى يمين ويسار كل ايوان غرفـة، (قديفة، مالـك، 2006، ص116)، **التـشكيل الفـضائي للقصر يعتمد مبدأ الانفتاح نحـو الـداخل علـى فنـاء مكشوف شيد على الجـدران الحاملـة، فيـه الاواويـن انتظمت حول الفناء بالاسلوب الحيري، شكل (4).**

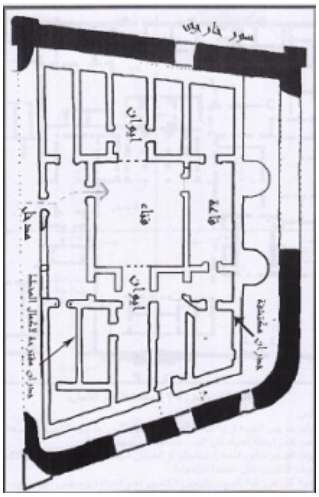

شكل(4) مخطط القصر المكتشف في الحيرة

د- الكنيسة المكتشفة في مملكة الحيرة

- ذات تشكيل فضائي ثلاثي Tripartite مشابه لما كـان عليه نمط المعبد الجنـوبي الاقـدم عهـداً فـي وادي الرافدين.
- احتوت على ثلاثة صوامع احتوت الوسطية منها علـى مصطبه المذبح.
- عند تحليل شكل اركان الصومعه الوسطيه وفقـاً لمـا يمكن ان يكون شكل السقف، فان الشكل الملائم **يكـون قبه**، لوجود الدعامات فـي الاركـان ولكـون شـكل الصومعه اقرب الى المربع الذي يمكن تسقيفه بقبة. كما امتازت الكنيسة بسمة وادي رافدينية اخرى هي المحاور المتعامدة للمداخل على محور المذبح وهي صفة لازمت معابد وادي الرافدين. انظر معبد في الوركـاء، شـكل (5).
- كما ان سمة البناء المصمت المعتمـد علـى الجـدران الحاملة هي سمة وادي رافدينية اخرى، تميزت الكنائس الحيرية بوجود القباب كعنصر في الفضاءات، وكـسمة عامة للابنية وقد ارتبطت بالكنيسة.
- العمود اصبح شائعاً سواء كان دائري المقطع ام مربع، (قديفة، مالك، 2006، ص128).

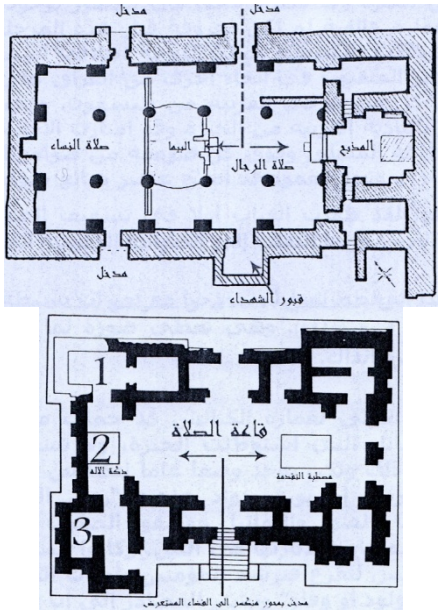

شكل (5) مقارنة كنيسة مملكة الحيرة مع معبد أنن في الوركاء للملك كرنداش الكيشي من الحقبة البابلية الوسيطة[1]

هـ - دير العبيد في تكريت

- يحيط بالدير سور خارجي مدعم بأبراج نصف اسطوانية تكون مع بعضها البعض وحدة بنائية اقرب الى الشكل المربع، احتوى المجمع على كنيسة، قاعات متعددة، فناء محاط برواق معمد، غرف صغيرة متعددة، (الحديثي، 2002، ص107)، شكل (6).
- المخطط مفتوح نحو الداخل In word Looking plan، احتوى على فناء عام محاط برواق معمد قرب المدخل، تشرف عليه الكنيسة وفناءات خاصة تقع بين المشتملات البنائية.
- مبدأ الجدران الحاملة هي السمة الاساس في فضاءات وادي الرافدين.
- يحوي المبنى على اروقه.
- محتمل وجود ايوان في الضلع الشرقي من الرواق المحيط بالفناء الرئيسي يؤكد ذلك:

1. ضخامة حجم الدعامتين المكتشفتين في وسط الرواق وهما لاتشبهان جميع اعمدة الرواق الاخرى.
2. الايوان يؤدي الى قاعتين ربما كانتا تمثلان صالة استقبال، او مكتبة الدير، حيث انهما عزلتا عن الساحات الخاصة والغرف الصغيرة التي تمثل صوامع الرهبان، (قديفة، مالك، 2006، ص136).

نجد على هذا الصعيد الرواق، والايوان، والدعامات، والاعمدة، هي سمات اصبحت تميز فضاءات المرحلة، وهي تماثل ما كان موجوداً في مدينة الحضر، الا ان الاختلاف هو في التوجه الداخلي لمخطط الدير، والذي يقترب من معابد الفناء المفتوح القديمة المعروفة في الاجزاء الجنوبية من وادي الرافدين، شكل (6).

قد تكون الكنيسة مسقفة بالقبة، لان المسافات المتساوية ما بين الاعمدة ترجح ذلك، اسوة بكنائس المرحلة، الطراز الحيري المعتمد على الوسط والكمين غير موجود في فضاءات دير العبيد، ربما يعود ذلك الى كون مجلس الحرب لا يتلائم مع المجالس الدينية المسالمة، (*العلي، 1989، ص31*).

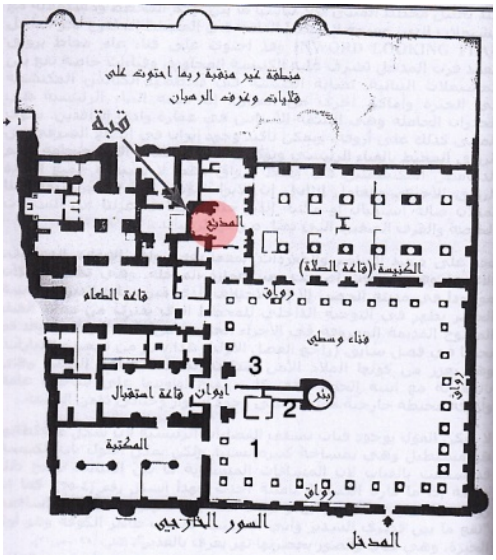

شكل(6) مخطط دير العبيد في تكريت، (قديفة، مالك، 2006، ص135)

من خلال ما تقدم نرى ان التشكيل الفضائي لعمارة مملكة الحيرة

- **اختفاء الزقورة في مملكة الحيرة وفي الحضر، لتغير العقائد الرافدينية القديمة، التي تشير الى هبوط الاله**

[1] المصدر: قديفة، مالك، 2006، ص129

من السماء، وقد كانت درجات الزقورة هـي الوسـيلة الى ذلك.

- **ظهور الاديرة التي كانت ضرورية لرهبان النصارى.**
- **ظهور الكنيسة (معابد النصارى).**
- **اشتهرت مملكة الحيرة بقصورها الكثيرة، وبنيت علـى شهرتها وطرازها ابنية لاحقة، في بغـداد وسـامراء، واكثرها شهره هما قصري (السدير والخورنق).**

نمط التشكيل الحيري الذي تواصل في العمارة الرافدينية بعد الفتح الاسلامي، وهو امتداد للنمط الفضائي في مملكة الحضر، (النمط الحضري). لكن مما لايمكن انكـاره، ان عرب مملكة الحيرة قد اضافوا الـى الـنمط الحـضري اضافات طرازية خاصة بهم، مستنبطة اساساً من الانماط الوادي الرافدينية المتوارثة في جنـوب بـلاد الرافـدين، وخاصة البابلية، وذلك من خلال احتكاكهم المبكر معهـم وكذلك لملائمة هذه الطرز للبيئة الطبيعية لجنـوب بـلاد الرافدين. ان النمط الحيري في الفضاءات يمكن ان نجده متجسداً في الانماط البنائية السائدة في مملكـة الحيـرة، اشتهرت مملكة الحيرة بكنائسها، لان الديانـة الاساسـية للمملكة هي المسيحية، ولكنها قد نشأت وتطـورت فـي المملكة العربية، (*الصالحي، 1985، ص260*).

كانت مملكة الحيرة عبارة عن مزيج بـين نمطـين رافدينيين اصليين، الاول هو (نمـط التـشكيل الثلاثـي للاواوين) والذي يمثـل الجـزء المخـصص للمحـراب وخدماته، اما الجزء الامامي للكنيسة فيمثل امتداداً، (لنمط التشكيل الثلاثي للمعابد الوادي رافدينية الاولى)، والـذي تواصل استخدامه في الفضاءات الرافدينية فـي تخطـيط المعابد، وخاصة المشيدة فوق الزقورات. وقد اسـتعيض عن الجدران الداخلية، والطولية في المخطط في الغالـب بصفين من الاعمدة.

اما قصور مملكة الحيرة فهي مـشهورة فـي المـصادر التاريخية ولكن اياً منها لم يتم الكشف عنه بشكل مؤكـد حتى ان مواقعها الحقيقية غير معروفة. عرفـت قـصور مملكة الحيرة (باواوينها)، ومن وصف المسعودي لاحدها، والذي يعتقد بانه الخورنق، (ان الجزء الرئيس فيه كان ذا تخطيط ثلاثي، مؤلفاً من الصدر، (الذي يجلس فيه الملك)، والكمـين علـى جـانبي الـصدر)، (*شـريف، 1982، ص221*).

ومن المؤكد ان التخطيط الثلاثـي للايـوان، هـو الـنمط الحضري الذي انتقل الى عرب مملكة الحيـرة اولاً عـن طريق العلاقات المتبادلة بينهما. امـا بالنـسبة للتـشكيل الفضائي الخاص بالبيت الحيري استمر محافظا على النمط الرافديني التقليدي السومري، مع التركيز علـى الاواويـن كفضاء استقبال رئيسي، مفتوحة علـى الفنـاء الوسـطي، (*جنان عبد الوهاب، 2000، ص332*).

العلاقات الفضائية

- تواصلت العلاقة ما بين الفراغ والكتلة بتوجهها نحـو الداخل في المخطط، ونمط التشكيل الثلاثي، المـداخل المنكسرة.
- الحقت الكنيسة بالدير بدلاً عن القصر، استمر الايوان والرواق بالظهور في مخططات ابنية مملكة الحيـرة كافة، كفضاءات انتقالية رابطة.

عناصر الفضاء الرئيسية

- شيدت قصور مملكة الحيرة من الآجر، وفي الغالب كان بعضها ذا طابقين او اكثر، واستخدمت فيهـا **الاروقـة المعمدة**، والاعمدة من الرخام والآجر، التي اقتلعت من ابنية مملكة الحيرة فيما بعد ونقلت الـى الكوفـة عنـد انشاءها في الازمنة اللاحقة.
- استخدام الاقواس والفتحات المعقودة ذات الشكل نصف الدائري، وظهر العقد المدبب.
- استخدام القباب بكثرة في التسقيف.
- استخدام الاواوين المطلة على الفناءات الوسطية.
- ظهرت في عناصر مملكة الحيرة الاعمـدة المركبـة، وهي مجموعة تتكون من عمود رئيسي وسطي تحيط به اربعة اعمدة اصغر، انفرد بهذا العنصر فضاءات مملكة الحيرة، (قديفة، مالك، 2006، ص140).
- القبة هي العنصر المعماري الاكثر حضوراً والذي يشار اليه في هذه المرحلة في العصور الوسيطة اذ ان وصف

القباب احتل جانباً مميزاً لدى الرحاله القدماء، ويعتقـد فليتشر ان القباب التي انتشرت في العصور الوسيطة في العراق هي حلقة الوصل بين العمارة الرافدينية القديمـة والبيزنطيـة التـي اشـتهرت بقبابهـا المفلطحـة، (Fletcher,1975,p82).

- تواصل نظام الجدران الحاملة، شكلت مفـردة الايـوان والرواق والفناء مفردات لطراز معماري جديد، سـمي بالطراز الحيري، واصبح المفردة الاساسية في التشكيل العمراني لمراحل تاريخيه لاحقه.

المعالجات التفصيلية

- الاستخدام الواسع لمادة الآجر كمادة بنائية وادي رافدينية متوارثه، وبمهارة في بناء الاسس والجـدران، وتبلـيط الارضيات، وبناء الاعمدة.
- استخدام الملاط الجصي كمادة رابطة، وهي تقنية عرب الحضر.
- استخدام الجص لتغليف السطوح، واستخدام القرميد على نطاق واسع، وهي مادة لم تكن معروفة من قبل علـى نطاق واسع.
- الاستخدام الواسع للزخارف الجصية البارزة، (اسـتخدم هذا النمط في الحضر)، وكانت الثيمـات والمواضـيع الزخرفية اقرب الى الهندسـية والبنائيـة منهـا الـى الشخوص والاشكال الآدمية.
- استخدام الرسومات الملونة على الجص المبلل، وهو ما يعرف بالفريسكو Fresco، وهو اسلوب وادي رافديني متوارث، مع اختلاف المواضيع التشكيلية.
- الانتشار الواسع للفسيفساء، وخاصة في معالجة السقوف وكذلك الطلاء بالذهب، (*سفر، 1974، ص15*).
- استخدام مادة المرمر في نحت الاعمـدة وفـي عمـل الجداريات التشكيلية.

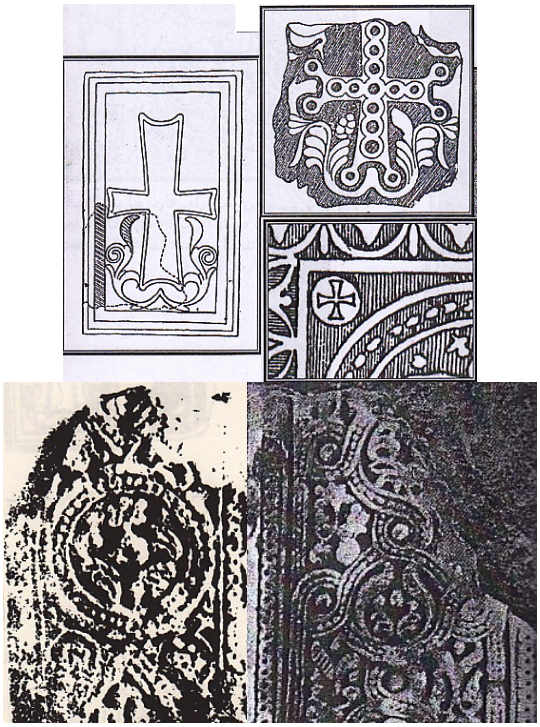

شكل (5) نماذج من الزخارف الجصية والرسوم الجدارية المكتشفة في مملكة الحيرة، (الطريحي، 1981، ص(22-37))

شكل (6) تصور تخيلي لكيفية بناء أحد قـصور مملكـة الحيرة

الفضاء الرافديني في العصر الوسيط: مملكة الحيرة والحكم الساساني المواكب لها (226 ق.م – 632 م)

المثال	نمط التشكيل الفضائي	نمط العلاقات الفضائية	عناصر الفضاء الرئيسة	معالجات الفضاء التفصيلية
بيت سكن من المدائن	بقي البيت محافظا على نمطه التشكيلي الرافديني القديم في توجهه نحو الفناء الداخلي، مع التركيز على الاواوين المطلة على الفناء كفضاء استقبال رئيس، وعند ملاحظة تلك الاواوين نراها متقابلة لتشكل نمطا تشكيليا اقرب الى الصليبي المركزي، اذ شوهد هذا النمط التشكيلي في القصر ذو الاواوين المتقابلة في اشور نرى بعض الفضاءات المربعة مدعمة زواياها والتي من المحتمل ان تكون مسقفة بالقبة، الجدران حاملة مع وجود بعض الدعامات	 قديفة، 2006 التوجه نحو الداخل، اطلالة الاواوين على الفناء الداخلي، التدرج العلاقة بين العام والخاص، مدخل رئيس مباشر نحو الفناء الموزع ومداخل ثانوية غير مباشرة، تناظر محوري حول محوري الفناء الوسطي	الايوان المطل على الفناء الداخلي، والجدران الحاملة، الدعامات المحيطة بفضاء المدخل (فضاء الاستقبال)، والقبة كعنصر تسقيف شاع استعمالها في فضاءات الحيرة، مع ان لها اصول رافدينية، كما في بيوت جرمو وتل حسونة لعصور ما قبل التاريخ، لكنها انقطعت كاحد اساليب التسقيف بسبب تطور النظام الانشائي المؤدي الى استخدام السقوف المستوية، لكنها لم تختف بالكامل فعاودت الظهور في بعض الفضاءات المربعة التي تدل على احتمالية تسقيفها بالقباب، كما في معبد ننكال السومري، لكنها لم تكن عنصر تسقيف شائع الاستعمال كما في فضاءات الحيرة 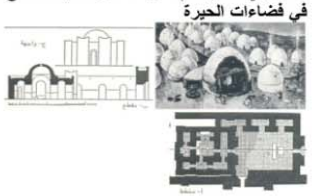	
دير العبيد في تكريت	ذو تشكيل مربع، ونمط مفتوح نحو الداخل، احتوى المجمع على كنيسة وقاعة وفناء محاط برواق معمد وغرف صغيرة، مبدأ الجدران الحاملة هي السمة الاساس في الفضاءات الرافدينية، يوجد ايوان في الضلع الشرقي من الرواق، الذي يدل على وجوده وجود دعامتين وصالة استقبال خلفه	 قديفة، 2006 التوجه نحو الداخل، الحاق الكنيسة بالدير،المدخل الجانبي، سيادة الايوان والرواق كفضاءات انتقالية رابطة، الكنيسة مطلة على الفناء الوسطي من خلال الرواق المعمد	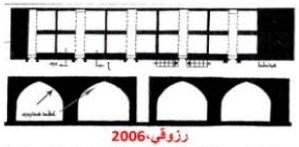 رزوقي،2006 شيوع الرواق المعمد المطل على الفناء الداخلي المفتوح في فضاءات الحيرة، والذي لوحظ في الفضاءات الرافدينية البابلية، وتحديدا في قصر عكركوف وقد تكون الكنيسة مسقفة بقبة التي شاعت في فضاءات تلك الفترة، الاسوار البرجية المحيطة بالدير وهو تقليد رافديني قديم 	 رزوقي، 2006 ظهور العقد المدبب في فضاءات الحيرة

كنيسة قلعة تكريت	شكل هندسي منتظم، ذو فناء وسطي مفتوح، يطل عليه فضاء الكنيسة، بينهما رواق معمد، وهو تشكيل رافديني قديم، انظر معبد عشتار في بابل 	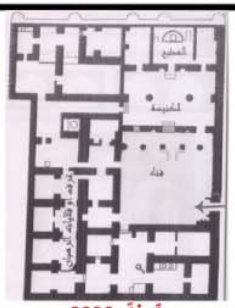 قديفة، 2006 التوجه نحو الداخل، الرواق كفضاء رابط بين العام والخاص، الدخول الجانبي المباشر الى الفناء الداخلي ومنه الى بقية الفضاءات، صلادة الكتلة الخارجية، التتابع الفضائي بين العام والخاص، فكلها علاقات رافدينية	الجدران الحاملة اسلوب انشائي، احاطة الكتلة بالسور المدعم، الرواق المطل على الفناء الداخلي
كنيسة في المدائن	اعتمدت الكنائس الاولى في العراق على تراكب نمطين رافديين، الاول هو النمط الثلاثي للاواوين والذي انتشر في فضاءات الحضر، المكون من ثلاث صوامع، الوسطية منها هي المذبح التي تسقف على الاغلب بقبة، وان شكل الجدران والدعامات التي في الاركان وشكل الصومعة المربع يدل على ذلك. والثاني نمط المعابد الثلاثية الرافدينية القديمة بعد استعاضة الدعامات بدل الجدران الداخلية الطولية المؤدية الى حنية المحراب. البناء المصمت المعتمد على الجدران الحاملة وهي سمة رافدينية قديمة 	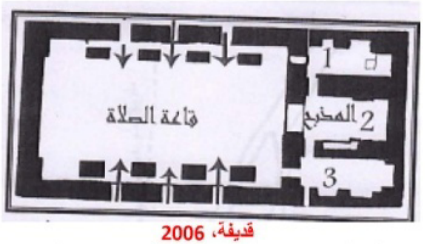 قديفة، 2006 محور الدخول عمودي على محور المذبح، وجود الدعامات في قاعة الصلاة يحدد الاتجاهية نحو المذبح وهي ليست اعمدة حاملة، بظهور الديانات الموحدة اصبح هناك فضاء داخلي تمارس فيه الطقوس الدينية (الصلاة)	وجود الدعامات في قاعة الصلاة، عنصر القبة الذي يسقف المذبح، نظام الجدران الحاملة الرافديني الاصل، انظر اولى الدعامات الرافدينية في المعبد الكلسي في الوركاء

5- الاستنتاجات

اولا- التشكيل الفضائي

- حافظ التشكيل الفضائي للبيت على نمطه الرافديني بالتوجه نحو الداخل والتشكيل الثلاثي المطل على الفناء الوسطي مع دخول الايوان كفضاء استقبال مفتوح على الفناء
- في حين نجد الاواوين متقابلة يمينا ويسارا نحو الفناء الوسطي في دور مملكة الحيرة ونجدها متقابلة باربع اتجاهات شبيهة بالتنظيم الصليبي في دور المدائن، اسوة بقصورها ذات النمط الصليبي المتاثرة بقصور اشور والحضر
- اعتمدت الكنائس الرافدينية الاولى تراكب نمطين رافدينيين، الاول هو الثلاثي للاواوين (الحضري)، بعد ان تحولت الصومعة الوسطية الى مذبح مسقف بقبة، في الغالب، والنمط الثاني هو المعابد الثلاثية الرافدينية، بعد الاستعاضة بالدعامات عن الجدران الداخلية المؤدية الى حنية المحراب، مع ان الدعامات لم تكن غريبة عن الفضاء الرافديني
- تواصل البناء المصمت المعتمد على الجدران الحاملة كسمة رافدينية

التشكيل الثلاثي لقصور مملكة الحيرة المعتمد على مبدا (الصدر والكمين)، المتوجه نحو الفناء الداخلي، المحاط بالرواق المعمد والاواوين المطلة عليه، والمؤدي الى فضاء الاستقبال المقبب، بقي هذا النمط محافظا على شكله وسمي (بالحيري)

ثانيا- العلاقات الفضائية

- تواصلت العلاقات الفضائية للادور والقصور الرافدينية في توجهها نحو الداخل، والفناء هو الموزع الرئيس للحركة، وتواصلت المداخل المنكسرة المؤدية اليه
- الحقت الكنيسة بالدير
- سيادة الاروقة والاواوين كفضاءات انتقالية رابطة بين العام والخاص
- اطلالة الطابق العلوي نحو الفناء الداخلي التي سادت في فضاءات مملكة الحيرة
- محور الدخول في الكنائس عمودي على محور المذبح، ووجود الدعامات يحدد الاتجاهية نحو المذبح، فاصبح هناك في الكنيسة فضاء داخلي تمارس فيه الصلاة
- الكتلة الخارجية الصماء المتاتية من السور المدعم بالابراج، وهي سمة رافدينية متواصلة
- انفتحت اواوين قصور المدائن نحو الخارج اسوة باواوين الحضر، اما اواوين مملكة الحيرة فهي مفتوحة على الفناء الداخلي

ثالثا – العناصر المعمارية

- بظهور الرواق المعمد المحيط بالفناء الداخلي والاواوين المطلة عليه والقباب التي تسقف صدر الايوان والسور الخارجي المدعم بالابراج اكتمل النمط الرافديني فترة العصر الوسيط والمستمد من الفضاء الرافديني القديم
- بالاضافة الى سيادة نظام الجدران الحاملة ووجود الدعامات واستخدام القبو نصف الاسطواني والبيضوي ذو الاصول الاشورية بالتسقيف
- الاعمدة المندمجة بالجدار والعقود الصماء هو تطوير لنظام الخسفات والبروزات الرافدينية
- الشرفات المتدرجة لتزيين الجزء العلوي من الجدران الخارجية تواصلا مع الواجهات الرافدينية
- التواصل في عنصر البوابات والتاكيد على المداخل
- ظهور الاعمدة المركبة (عمود مركزي يحيطه اربع اعمدة)
- ظهور العقد المدبب في الفتحات والعقود الصماء

رابعا –المعالجات الزخرفية

- الرسوم الملونة على الجص، اسلوب رافديني متواصل، مع اختلاف المواضيع لاختلاف المعتقدات الفكرية
- انتشار الفسيفساء في معالجة السقوف والطلاء بالذهب
- استخدام المرمر في نحت الاعمدة والجداريات
- انتشار استخدام مادة الاجر كمادة بنائية رافدينية
- استخدام الملاط الجصي كمادة رابطة (تقنية عرب الحضر)

- **استخدام الجص لتغليف السطوح**
- **استخدام الفرميد، حيث لم يكن شائعا من قبـل تيجـان اعمدة مزخرفة**

المصادر

1. الاحمد ،الدكتور سامي سعيد / العراق في التاريخ /الفصل الثالث/دار الحرية للطباعة والنشر /بغداد 1983/
2. باقر، طه، عبد العزيز، (طرق البحث العلمي في التاريخ والاثار)، وزارة التعليم العالي والبحث العلمي، مؤسسة دار الكتب في جامعة الموصل، 1980
3. ثويني، علي، (المدائن العراقية..النشأة والتسميات) (www.mesopotamia4374.com)، 2010.
4. الجابري، علي حسين، (الحوار الفلسفي بين حضارة الشرق وحضارة اليونان، سلسلة كتب شهرية مصدرة من افاق عربية، عدد 12، 1985
5. الدباغ، تقي، البيئة الطبيعية والإنسان، حضارة العراق، الجزء ألأول، دار الحرية للطباعة. بغداد 1985
6. الدباغ/الدكتور تقي / العراق في التاريخ-الفصل الأول – دار الحرية للطباعة والنشر/بغداد 1983/
7. سفر، فواد سفر، محمد علـي،(الحـضر مدينـة الشمس)، وزارة الاعلام، مديرية الاثار العامـة، العراق، 1974
8. سلمان ، عيسى وآخرون (العمـارات العربيـة الاسلامية في العراق) الجـزء الثـاني قـصور ومشاهد وزارة الثقافة والاعلام ، بغداد 1982
9. الصالحي، واثق اسماعيل، العمارة في العهدين السلوقي والفرثي، موسوعة حضارة العراق، 1985
10. الصالحي، واثق اسماعيل، العمارة قبل الاسلام، موسوعة حضارة العراق، بغداد، 1985
11. طالب الشرقي : القصور العربية والاسلامية في العراق، دار الـشوؤن الثقافيـة فـي العـراق، بغدد،2001
12. الطريحي، محمد سـعيد، الـديارات والامكنـة النصرانية في الكوفة وضواحيها، بيروت، لبنان، 1981
13. عبد الوهاب، جنان (جدلية التواصل في العمارة العراقية، دراسة استقرائية في طرز العمارة الوادي الرافدينية، اطروحة دكتوراه غير منشورة، جامعة بغداد، كلية الهندسة، 2000
14. العلي صالح الاحمد (معالم العـراق العمرانيـة) دراسة في المعـالم الجغرافيـة والـسكانية، دار الشوؤن الثقافية، بغداد، 1989
15. العلي صالح الاحمد ومجموعـة مـن المـؤلفين (العراق في التاريخ) دار الحرية للطباعة بغـداد 1983/ 119
16. قديفة، مالك صبري، (صورة العمـارة العراقيـة قبل الاسلام، رسالة دكتوراه غير منشورة، جامعة بغداد كلية الهندسة، 2006
17. محمد، مشتاق طالب، (مدن العراق القديم)، (www.mesopotamia4374.com)، 2010.
18. محمود، حسان الحـاج قاسـم، تـاثير التفاعـل الحضاري في العمارة العربية قبل الاسلام البتراء والحضر وتدمر، رسالة دكتوراه غير منـشورة، جامعة بغداد، كلية الهندسة، 2007
19. يوسف رزق الله غنيمة / الحيرة – المدينة والمملكة العربية ، مطبعة دنكور، بغداد،1936
20. يوسف شريف، تاريخ فن العمارة العراقية، دار الرشيد، بغداد، 1982

"التوجهات التكنولوجية الحديثة وتصميم محطات المطارات المعاصرة"

اشراف:أ.د. بهجت رشاد شاهين اعداد الطالبة:دنيا جمعة عبد الكريم
جامعة بغداد/كلية الهندسة/قسم الهندسة المعمارية

الخلاصة:

لا يخفى دور التكنولوجيا في تصميم محطات المطارات الحديثة والمعاصرة منها، فقد شهد النصف الثاني للقرن العشرين عددا غير قليل من المطارات تمثل فيها التكنولوجيا استعارة مجازية لثقافة العصر تؤثر على آلية التفكير والتصميم والانتاج معا. يهدف البحث الى تحديد وتمييز هذه التوجهات وطبيعة تطبيقاتها في محطات المطارات المعاصرة .

حيث لم يعد تصميم محطات المطارات_ والتي تعد احدى اهم انواع الابنية المتخصصة_ يعتمد على افكار تلبية الاداء الوظيفي او طروحات الشكل كعمليات منفصلة لإنتاج هذا النمط المتحدي من المباني ذو ادائية ورمزية عاليتين. يلاحظ التوافق التام بين قضايا التصميم المختلفة لمحطات المطارات المعاصرة والتكنولوجيا الحديثة، وهذا مايميز التوجهات الجديدة لجيل المطارات، وادى الى صياغة مشكلة بحثية تتعلق بوجود **نقص معرفي في تمييز دور التوجهات التكنولوجية الحديثة لمحطات المطارات المعاصرة وطبيعتها وابعاد تأثيرها على مفردات العملية التصميمية**، تعامل البحث مع المشكلة باشتقاق فرضيته " **توافق أسس التكنولوجيا الحديثة مع القضايا التصميمية لأبنية محطات المطارات المعاصرة وتكامل منظوماتها التصميمية الرئيسية، مما انتج توجهات جديدة متأثرة باستخدام البعد التكنولوجي كآلية للتفكير والانتاج وادوات للتعبير".**

Terminals' Modern Technological Approaches and Contemporary Airports" "Design

ABSTRACT :

It is not hidden the role of technology in modern and contemporary airport terminals design, the have a large number for airports in which technology represent a second half of the twentieth century metaphor for contemporary culture that modified the mechanism of thinking, designing and ways in contemporary airport 'production. This research aims to determine and its applications terminals design .

Then the design of airport terminals _which considered one of the most important building type_ is not only related to the ideas of functions performance or buildings shapes as separated processes to produce this challenging building type, which is charged by functional encumbrances and is a airport symbolic building . There is inclusive overlapping between design issues of contemporary terminals, and the new technology. which distinguished the new approaches of contemporary airport architecture, and has led to formulate a research problem considered about **the gab of knowledge in distinguishing the role of the new technological approaches for contemporary airport terminals, the "and its nature and its effect on design process**, the hypothesis formulated from this problem is**: compatibility of contemporary technology fundamentals and contemporary airport terminals main systems, that produces new approaches affected and the integration of its design issues by the use of the technological dimension as a method of thinking and producing and as a tool for expression".**

مقدمة :

يوصف النقل الجوي بانه وسيلة النقل المعرفة للقرن الحادي والعشرين ولا توجد اي وسيلة اخرى تنافسه من حيث السرعة، الراحة، المتعة والحجم والتشويق. تمثل المطارات المعاصرة مجمعات ضخمة تعكس الغنى الثقافي وتنوع الحياة المعاصرة، فأصبح المطار معلما عمرانيا متعدد الوظائف الاقتصادية والاجتماعية والترفيهية. تعكس المطارات صورة البلد بصورة مباشرة اكثر من اي نوع من انواع الابنية العامة، ويعد مبنى المسافرين العنصر الرئيسي في التصور العام فيعد رمزا تعكس عمارته سحر وغنى ومقياس التقدم التكنولوجي، فضلا عن دوره كبوابة تعكس قيم ومتطلبات المجتمع بأسره.

يتجاوز التعامل مع المطارات المعاصرة التعامل مع مبنى منفرد بإمكانية السيطرة على حلوله التصميمية والتقنية، بل تمثل المطارات مجمعات ضخمة لابد من ان تتكامل بادائيتها وبكفاءة عالية، تمثل التكنولوجيا الحديثة اهم الوسائل لتحقيق عملية الكفاءة التشغيلية وبأجواء بيئية متوازنة لمحطات المطارات المعاصرة.

المشكلة البحثية: النقص المعرفي فيما يتعلق بالتوجهات التكنولوجية الحديثة في تصميم محطات المطارات المعاصرة وامكانياتها التطبيقية وابعاد تأثيرها .

فرضية البحث: توافق أسس التكنولوجيا الحديثة مع قضايا ومفردات العملية التصميمية لمحطات المطارات، وبما يحقق تكامل المنظومات التصميمية الرئيسية للمبنى باعتماد التكنولوجيا كآلية للانتاج والتنفيذ واداة للتعبير.

هدف البحث: توضيح دور التكنولوجيا في تصميم محطات المطارات المعاصرة وماهي امكانية تطبيقها وتأثيرها من الناحية البيئية والتعبيرية والرمزية لهذه الابنية الوظيفية .

- يتعامل البحث مع **فرضيته الرئيسية** : توافق أسس التكنولوجيا الحديثة مع قضايا ومفردات العملية التصميمية لمحطات المطارات، وبما يحقق تكامل المنظومات التصميمية الرئيسية للمبنى باعتماد التكنولوجيا كآلية للانتاج والتنفيذ واداة للتعبير.

يمكن اشتقاق فرضيتين ثانوية :

1. تكامل المنظومات التصميمية الرئيسية للابنية باعتماد التكنولوجيا كآلية تدخل في مفردات وعناصر المبنى الرئيسية وبما يحقق تكامل منظومات المبنى الرئيسية بمستويات ودرجات التكامل المختلفة ويمكن تقسيمها الى: منظومات الغلاف الخارجي والهيكل المنشأي والغلاف الداخلي ومنظومة الخدمات .
2. اعتماد التكنلوجيا كاداة للتعبير، حيث يبرز دور التكنولوجيا في تحقيق المستويات التعبيرية والرمزية النابعة من طبيعة وظيفة الطيران، فضلا عن التعبير البيئي لمحطات المطارات المعاصرة.

- وفيما يأتي تحقيق فرضيات البحث :

1. تكامل المنظومات التصميمية لمحطات المطارات المعاصرة :

حيث ان اي مبنى يتكون من مجموعة من المنظومات البنائية يحقق ترابطها الشكل الفيزياوي للمبنى ، يتعرض البحث الى منظومات المبنى الرئيسية ومستويات التكامل فيها ودرجة التكامل التي تعتمد على طريقة ترابط هذه المنظومات،

ودور التكنولوجيا في تحقيق التكامل بين المنظومات للوصول الى مبنى ذكي في منظوماته ضمن بيئته المحيطة. حيث ان البيئة اصبحت مفهوما شاملا لكل المؤثرات المحيطة بالشكل العام للمبنى وان استخدام التقنيات التكنولوجية البيئية يعمل على تكيف المبنى مع البيئة الخارجية ويجعل البيئة الداخلية في حالة تكيف مع البيئة الخارجية عن طريق غلاف المبنى ويتم ذلك من خلال تصميم المبنى بطريقة تكاملية بين عملية التصميم والانظمة والفعاليات بطريقة تجعل المبنى عالي الادائية وغير مستهلك للطاقة ومتحسس بالبيئة والمناخ وبما حققته التكنولوجيا كآلية للانتاج والتنفيذ واداة للتعبير.

اما دور التكنولوجيا في مفردات العملية التصميمية فنجده متداخلا بتصميم كل من هذه المنظومات على حدة وتحقيق التكامل فيها بترابط هذه المنظومات وكالاتي :

1) النظام المنشئية والغلاف الخارجي
structural and envelope systems
:

تعد المطارات، وخصوصا الدولية منها، احد اهم المداخل لأي دولة وواجهتها الحضارية، فضلا عن كونها ابنية حديثة ذات خصوصية وظيفية عالية، هذه الاعتبارات ادت الى الاهتمام بالمطارات وبشكلها المعماري وادائها الوظيفي. وقد كان اختيار المنظومة الانشائية الملائمة احد الاساليب المتبعة لتحقيق **(Blow,1991,p127)**

- شكل معماري متميز.
- اداء وظيفي عالي يتميز بالمرونة .
- سرعة التنفيذ باعتبار ان المطارات مشاريع ضخمة تحتاج الى سنوات طويلة لانشائها.

ولان محطات المطارات اليوم مركز للعديد من الفعاليات الانسانية المتنوعة، السفر والمتعة، التسوق النوادي الصحية، المؤتمرات وغيرها. مثل هذا التنوع الوظيفي حد من سهولة وظيفة محطات المطارات وجعلها مسارح للفعاليات الانسانية التي اكسبتها صفة التعقيد. لذا فعناصر المنشأ والانشاء مثل ،الاعمدة والدعامات، الجسور الاقواس وغيرها اصبح لها دور اساسي في تنظيم واستيعاب الفضاءات الداخلية حيث انها **(Edwards,2005,153)** :

- تخلق حيوية وديناميكية ضمن الفضاءات.
- تساعد المسافر على فهم واستيعاب الاحساس بالاتجاهية.
- استيعاب سرعة الحركة خلال المبنى.
- استيعاب التدرج الوظيفي.

النظم المنشئية التي توظف في محطات المطارات اليوم نظم ضخمة "mega structure لكي تحتوي التنوع الوظيفي والفضاءات الواسعة للمطارات، اما تصنيف النظم المنشئية فهو كالآتي **(Sebestyen,2003,p80)**:

a) النظم الواسعة wide-span structure :

تتضمن الفضاءات الواسعة ذات السطوح الواسعة وبدون دعامات داخلية (أعمدة وجسور)، مثل القباب التي انشأت منذ زمن طويل ببحر لاكثر من 50 مترا ومع التقدم التكنولوجي يمكن اعتماد القباب لتغطية بحور فضائية ل300 متر. يتضمن هذا النظام نوعا من الهيكل الاسنادي وهناك جانب معين من التصنيف لهذا النظام يتم عن طريقه نقل الاحمال العمودية الى الارض وكالآتي :

- نقل الاحمال مباشرة بواسطة المنشأ، كما في حالة القبة، القبو،الشكل البيضوي "shape capsule" من ميزاته امكانية تغطية مساحات او فضاءات كبيرة تمنح الفضاءات الداخلية اكبر مساحة ممكنة باستغلال افقي وعمودي وبدون الحاجة لدعامات عمودية. كما في

مطار بانكوك الثاني/تايلند، حيث ان المبنى بشكل حرف " U" يتألف من مجموعة من الابنية المكررة ، يغطيها سقف من وحدات الستيل بشكل منحني تغطي المساحة الافقية الطولية لوحدات المبنى وتخلق فضاءات واسعة يتخللها الزجاج المنحني بين وحدات الستيل المنحني ليخلق واجهة زجاجية تغطي ارتفاع

- المبنى، الشكل (1) **(Gepford,2004,p12)**
- نقل الاحمال بواسطة دعامات خاصة :ابراج "pylons"،اعمدة او دعامات. قد يتضمن الهيكل الانشائي في هذه الحالة سندا واحدا، اثنين او اربعة او ثمانية او اكثر حسب طبيعة الفضاء. يمكن لهيكل السقف ان يأخذ مدىً واسعا من الاشكال قد يكون مسطحا، منحنيا، او قد تكون اشبه بالاجنحة glider wing، وغيرها من الاشكال الدراماتيكية المميزة .هذه السقوف تكون مستندة على دعامات عمودية باشكال مختلفة فقد تكون بشكل حرفV ، او اطر من الستيل او الالمنيوم، تتضمن هذه الدعامات اشكالا مختلفة او قد تكون بشكل اشجار" trees" كما في مطارStuttgart/ المانيا، الشكل (2) ،او قد تكون بشكل مربع (مظلات umbrella) مثل مطار ستانستيد/لندن **(Sebestyen,2003,p81)**.

b) نظام الأغشية والشد Membranes tension structure :

يتضمن هذا النظام أغشية الشد، السقوف المعلقة وسقوف الشد (مثل نظام الاغشية والخيام) . تعتبر الدعامات(السواري) اهم جزء ضمن هذا النظام تضم اعمدة او ابراج تقوم بنقل الاحمال والقوى العمودية الى الارض. فضلا عن ذلك هناك الكيبلات المعلقة واي دعم اخر (مثل الاقواس والمسنمات)، التي تدعم السقوف المعلقة :الصفائح المعدنية ،الانسجة ..الخ .

من ابنية المسافرين التي استخدم فيها نظام الشد، مبنى مسافرين الحاج /مطار الملك عبد العزيز(استخدم فيه نظام الخيم "tent structure" ،السعودية عام 1981 حيث ان تسقيفه يغطي مساحة 460000 متر مربع ويعتبر اكبر مساحة تسقيف في العالم. يتضمن 210 خيمة كل منها مع سقف بمساحة 2000 متر مربع ،الشكل (3) .

مثال آخر بنفس الأهمية هو مطار دنفر الدولي/الولايات المتحدة 1995، ايضا استخدم في تسقيفه نظام الخيام يتضمن التسقيف سلسلة من الخيام مدعومة بصفين من الدعامات بطول اجمالي 305 متر، السقف من أغشية telfoncoated fibreglass، السقف بوزن خفيف 10 كغم لكل متر مربع، ولكان وزنها اكثر ب50 مرة لوكان السقف من الستيل، غشاء التسقيف وعلى الرغم من وزنه الخفيف الا انه يتحمل احمال الثلج snow load، ويسمح بمرور كاف للضوء الطبيعي الى فضاءات المبنى الشكل(3) **(Robbin, 1996,p72) .**

c)الهياكل الفضائية space structure :

تطوير استخدام نظام المسنمات الفضائية ادى الى استخدام نظم المسنمات "truss systems" مع انواع مختلفة من العقد، بعلاقات سطحية ثنائية، ثلاثية او هرمية ..الخ.

النوع الاساسي لهذه الهياكل هي الشبكات الفضائية المسطحة "flat skeletal grid" والاشكال المنحنية مثل الاقبية المتوازية والقباب المدعمة. تتضمن نظم الشبكات الفضائية استخدام العناصر المنحنية او الانبوبية ، قد تكون عقدها عقد كروية صلبة او مجوفة، اسطوانية او منشوريه، او على شكل صفائح "plates" او قد تكون بدون عقد، يعطي هذا النظام امكانيات كبيرة في التشكيل **(Sebestyen,2003,p85)**. مثل مطار سان

فرانسيسكو/الولايات المتحدة، يتألف السقف من 5 وحدات من نظام المسنمات الفضائية (3d space truss) اثنين منها تمثل بروزات جانبية تنقل القوى العمودية الى الارض بواسطة الدعامات العمودية الشكل (4) **(Scodeck,2000,p12-14)**.

مع التطور التكنلوجي الذي طرأ النظم المنشأية وامكانيات وتقنيات المواد الحديثة، خلق امكانيات اكبر لنظم المطارات وفرتها امكانية التعامل مع المواد التكنلوجية منها الستيل، الالمنيوم، الزجاج ..الخ بنظم فضائية ومسنمات ثنائية وثلاثية .

2) منظومة الفضاء الداخلي :

تمثل عمارة محطات المطارات المعاصرة عمارة اللافضاء" spaceless "، تنساب فيها الفضاءات وتتابع مع بعضها البعض بصورة متداخلة .

ومن منطلق وظيفي لابد ان يحقق الفضاء الداخلي توافقا مابين الخصائص الرئيسية للفضاء، ومابين طبيعة الفعاليات التي يحتضنها، وبما يدعم الادائية الوظيفية للمكان، فالفضاء بنية تتأسس في التنظيم المنهجي للوظيفة **(Eizenman,1984,p70)**. وحيث ان محطات المطارات ذات فضاءات داخلية واسعة ومنسابة لابد ان يكون التعامل مع التصميم الداخلي لفضاءات المبنى بلغة مقروءة ومدركة للمسافرين لمعرفة توجههم " way finding"، يتم هذا بتكامل عناصر التصميم مع بعضها وكالآتي :

- **العناصر الفيزياوية (objects) :**

تتضمن مفردات التصميم الداخلي لأبنية المطارات والعناصر الاساسية لمحتوياته وتكويناته شاملة مناطق الجلوس، الاثاث، حركة المسافرين واكشاك الخدمة، وكاونترات الاستعلامات وتأكيد الحجوزات والخدمات المصرفية ومواقع الاسواق الحرة والمصاعد والسلالم المتحركة **(Blow,1996,p152)**.

تعامل هذه العناصر على انها عناصر لتوجيه الحركة، تقاطع الحركة او المشهد وتحدد حافات الفضاء وقد تضم وظائف معينة (مثل مكاتب الفحص والهجرة، الحمامات ..الخ). ففضلا عن وظيفتها لها وظيفة ادراكية في تنظيم فضاءات المبنى قد تعالج بطريقة نحتية لتحدد وترسم خطوط حركة المسافرين وتدرجها.

- **الاضاءة lighting :**

يمثل الضوء عنصرا ملموسا" tactile element" في تصميم الفضاءات الداخلية لأبنية المطارات، وسواء كانت اضاءة طبيعية او صناعية فانها تعتبر من العناصر المهمة في تنظيم الفضاءات الداخلية وتدرجها وتوجيه الحركة فيها، فضلا عن ذلك التلاعب بدرجة شدة الضوء يساعد في تعريف طبيعة الفعاليات فغالبا مانجد شدة الاضاءة اكثر في قلب المبنى حيث القاعات والفضاءات العامة، او قد يكون تركيز وشدة الضوء لمفصلة الفضاء ونقاط الحركة وتحريك العناصر الهيكلية للمبنى ويرفع الروح المعنوية وادراك المسافرين للمبنى **(De Neufville,2003,p132)** .

يمثل الضوء الصفة المميزة للتجربة الجمالية في تصميم الفضاءات الداخلية، فبالتحكم بالاضاءة الطبيعية او الصناعية من الممكن ان تزيد او تخفض التعقيد والغموض في بنية المكان من خلال التحكم بمستوى التحفيز المطلوب وحسب طبيعة الفعالية وخصوصيتها الوظيفية، يساعد الضوء ايضا

في التأكيد على الفعالية وجعل الفضاءات الحركية اكثر وضوحا وجاذبية، كما انه يساعد المسافرين في فهم وتحديد مواقعهم. يمكن للضوء والظل في الفضاءات الداخلية التزويد بتنوع عالي في الاحساس بحجم الفضاء وسعته، فضلا عن ذلك يلعب الضوء دورا كبيرا في خلق فضاءات بشفافية عالية وخفيفة_والتي تميز الجيل الحديث لمحطات المطارات_ حيث يدرك فيها الشخص تنوعا من الاحداث البصرية والحسية وبمستويات عدة وحسب خصوصية وطبيعة الوظيفة **(Edwards,2005,p97).**

- **<u>الهيكل المنشأي structure :</u>**

متضمنا الهيكل الانشائي لسقف المبنى، والعناصر الافقية والعمودية (الاعمدة والجسور والجدران .الخ)

تعكس هذه العناصر توجه الحركة، ويعكس مقياسها تدرج الفضاءات وتتابع الحركة فيها، نجد هذه الثيمة في مقاطع معظم محطات المطارات الحديثة حيث انها تمثل تتابع حركة المسافرين من الجانب الارضي الى الجانب الجوي مع مفصلة الحركة وحسب طبيعة الفعالية والوظيفة التي يمر بها المسافر**(Ibid,p98)** .

من اهم مايميز محطات المطارات وجود فضاءات رئيسية مهيمنة لتجمع المسافرين في كلا الجانبين الارضي والجوي، ضمن الجانب الارضي بهو المسافرين يمثل اول نقطة انتقالية تواجه المسافر اثناء دخوله الى مبنى المسافرين حيث يواجه فضاء كبيرا مكتظا، مفعما بالضوضاء والاحداث البصرية التي تمثل حجما من المحفزات الادراكية، وضمن الجانب الجوي الباحة الجوية او صالة المغادرة المركزية تمثل فضاء مهيمنا في وظيفته وتصميمه **(Dempsey,1999,p213)** .

3)المنظومات الخدمية (services):

a) الاضاءة "lighting":

مصادر الاضاءة ضمن فضاءات محطة المطار هي الاضاءة الطبيعية يوفرها ضوء الشمس، والاضاءة الصناعية. يعتبر الضوء عنصرا مهما ضمن تجربة التعبير المعماري فضلا عن كونه احد الاعتبارات التقنية المهمة، توجه المطارات المعاصرة نحو الحصول على كميات كبيرة من الاضاءة الطبيعية هو احد الوسائل لحفظ الطاقة، وتقليل مستوى الحرارة المتولدة من المصادر الصناعية ويساعد في توجيه حركة المسافرين. فنجد تصميم معظم محطات المطارات الحديثة على انها ابنية شمسية، حيث تساعد الشفافية في الحفاظ على الطاقة، لكن التزجيج المبالغ فيه يؤدي الى فقدان السعه الحرارية عن طريق نسيج المبنى. المطارات ذات المساحات المزججة وعلى الرغم من انها تقلل من استهلاك الطاقة والاضاءة الصناعية الا انها تقود حتما الى تكييف هواء جزأي او كلي، مما يحدد استخدام الزجاج فيها اعتمادا على طبيعة المناخ وتوجيه النوافذ. ويتطلب من المصممين عمل حسابات دقيقة فيما يتعلق بالعلاقة بين مساحة النوافذ، التوجيه، وبالتالي الحرارة المفقودة عبر نسيج المبنى **(Ashford,1991,p292)** .

الموازنة في استخدام الطاقة بين الاضاءة الطبيعية والصناعية عملية صعبة تعتمد على الظروف المحلية ففقدان الحرارة خلال النوافذ يجب ان يعوض من خلال اطلاق الطاقة المنبعثة من مصادر اخرى قد تكون معتمدة على الوقود الاحفوري .

اما مستويات الاضاءة في محطات المطارات مساوية لتلك المطلوبة في المكاتب والدوائر خاصة عند خدمة فحص وقراءة التذاكر وفي مناطق الفحص والتدقيق. فتكون 200 لوكس، يختلف هذا المقياس حسب درجة الامن والهدوء للفضاء مثل هذا الرقم يتطلب رفع معامل الانارة الطبيعية اكثر من 4% مما يعرض واجهات المبنى الى جهد قوي

(Edwars,2005,p166).

تمثل الاضاءة الاصطناعية في المطار المصدر الرئيسي في استهلاك الطاقة _متجاوزة بذلك الطاقة المستهلكة للتبريد والتدفئة _مصادر الضوء المستخدمة لها تأثير كبير على الراحة، الامان والاحاطة العامة .

القليل من ابنية محطات المطارات صممت بدون إنارة طبيعية، بحيث يكون الاعتماد على الانارة الصناعية من ناحية التصميم المعماري لذا بات من الضروري ان يكون هناك نمط معين من انماط الاضاءة المنظمة خلال فترات الليل والنهار بحيث لايختلف ادراك المسافرين لمسالك الحركة والفضاءات .

❖ دمج وتكامل مصادر الاضاءة الطبيعية والصناعية يعزز التجربة والفكرة التصميمية المعمارية بنفس الاهمية خلال اوقات اليوم بأكمله او24 ساعه بأكملها **(Fordham,1995,p80)** على سبيل المثال :

- في مطار ستانستيد /لندن، يعتمد نظام الاضاءة استخدام مجموعة من الوحدات المركبة على هيئة مجاميع بقوة 400 واط مجتمعة على شجرة الهيكل المستخدم ومشعة الى الاعلى بحيث ان الضوء ينعكس من السقف، فتكون الاضاءة الطبيعية من خلال السقف والاضاءة الصناعية مركزة على شجرة الهيكل، مما يعطي الاضاءة تأكيدا بصريا ضمن فضاءات المبنى فضلا عن التأكيد على فكرة الهيكل الانشائي نفسها والتي بدورها تساعد المسافرين على فهم تنظيم المبنى، الشكل (5).
- فلسفة مشابهة طبقت في تصميم الاضاءة في مطار كنساي/اليابان، حيث ان الاضاءة السقفية في الجزء الوسطي المركزي "الشارع canyon" تتمثل بمصادر اضاءة صناعية مركزه على طول الشارع تساعد في توجيه حركة المسافرين من خلال توحيد الفكرة التصميمية مع نظام الاضاءة الطبيعية والصناعية. نفس المبدأ طبق في اضاءة الجدران حيث ان النوافذ العمودية تسمح بدخول 40 % فقط من ضوء النهار بالنسبة للنوافذ الافقية السقفية، اختراق ضوء الشمس خلال النوافذ العمودية يضيف حيوية الى الفضاءات ،لكن الاشعة الشمسية المباشرة قد تكون غير مريحه خاصة للناس الجالسين او العاملين مباشرة ضمن الصفوف المجاورة للنوافذ. لذا فان الجدران المزججة يجب ان تكون محمية _من الخارج او الداخل _او ان يكون الزجاج منحنيا_(مثل مطار كنساي) والخ من لمعالجات، الشكل (6) **(Bunchanan,1994,p76).**

b) تكييف الهواء (HVAC air heating :,ventilation cooling)

معظم محطات المطارات بأي حجم وسعة كانت تعتمد على التكييف الصناعي خلال السنة باكملها او جزء منها، ولكل المبنى او لجزء منه. معظم الأنظمة تعمل على تدوير الهواء كوسيلة للتبريد او التدفئة ، وغالبا ما يكون شكل المقطع الجانبي للمبنى مساعدا في تدوير الهواء : على سبيل المثال السقوف المتموجة والمنحنية المشكلة لجانب مبنى مطار كنساي، اوسلو/النرويج، وجارلس

دي كول/باريس، كلها تأتي كاستجابة مباشرة لعملية توزيع الهواء **(Edwards,2005,p167)**.
شكل الفضاء عنصر مهم في درجة اختراق الهواء المندفع وطرز حركته ونظام تكييف الهواء هو الذي يحدد شكل سقف ابنية المطارات الحديثة اذا ماكانت متموجة او منحنية وليس الطراز المعماري، فالانحناء الطبيعي لحركة الهواء المندفع بدرجه حرارة وسرعة معينتين تنتج شكل الغلاف الخارجي المميز للمبنى، التكامل بين هذه النقاط مع هندسة الشكل والانشاء يعطي الصورة الحديثة التي نجد عليها ابنية محطات المطارات اليوم .

ولان حركة الهواء حسب درجه حرارته فان زوايا تصريف الهواء تحتاج الى تنظيم وضبط، في مطار كنساي على سبيل المثال، الفوهات تتموضع مباشرة تحت السقف وتوزع الهواء بزوايا واتجاهات مختلفة حسب الاحتياجات، ويتم التحكم بزوايا فوهات التصريف الكترونيا حسب الموسم، الشكل (7).

معظم المطارات لها انظمة رئيسية macro وانظمة ثانوية microمصغرة للتدفئة، النظام الاول يوزع الهواء المبرد او المسخن الى كل المبنى، اما النظام الثاني " المصغر" يوزع الهواء الى مناطق مخصصة ومعينة مثل مسارات حركة المسافرين **(Wang,2010,p240)**.

لكون محطات المطارات هياكل انشائية عالية فمن الممكن استغلال "المداخن stacks " لتشجيع التهوية الطبيعية ولتنظيم حركة هواء لتبقى مستمرة ومندفعة، بالإضافة لذلك فان ارتفاع المبنى يعني ان مستوى الاشغال على ارتفاع اقل من 3 امتار له خدمات ذات خصائص مختلفة عن بقية اجزاء الفضاء الداخلي. اي من الممكن توفير خدمات التبريد والتدفئة حسب المستوى الاشغالي الذي يستخدمه المسافرون اما بقية الفضاءات فمن الممكن معاملتها بمستوى خدمات مختلف.

مع الفضاءات الواسعة من الممكن استغلال انخفاض حرارة الجو بحدود ال 16 درجه مئوية. بحيث يمكن استغلالها في تدوير الهواء داخل المبنى مما يخفض درجة حرارة المبنى ويبقيه بدرجه حرارة ملائمة خلال النهار. انظمة التدفئة تضمن مثل هذا العمل خاصة اذا كانت مندمجة ضمن الهيكل الانشائي للمبنى مما يجعلها تعمل بكفاءة اكثر واناقة .

معظم ابنية المطارات تعتمد انظمة التخلص من الحرارة لتعالج الحرارة المتولدة من الهواء او الماء النافذ وبالتالي لتزيد درجة حرارة الهواء النقي، في مطار ستانستيد/لندن.

نظام التبريد المركزي يستخرج الحرارة من الماء المبرد للحفاظ عليه بدرجه ملائمة وبالتالي تصريف الحرارة الناتجة في نظام تدوير الماء بدرجه 40-50 درجه مئوية. حيث ان هذه الحرارة الناتجة تستغل فيما بعد في نظام تدوير الهواء الرئيسي .خلال معظم اوقات السنه الاحمال الحرارية من الممكن التخلص منها باستخراج الحرارة **(Edwards,2005,p168)**.

c) منظومة الحرائق"fire safety" :

محطات المطارات ابنية خطرة فيما يتعلق بالحرائق، حيث ان مخططاتها العميقة والفضاءات المغلقة فيها تعطي الاولوية لأمر التخلص من الدخان، فضاءات اصحاب العقود والامتيازات مثل المحلات، المطاعم والبارات معرضة لدرجة عالية من خطر الحرائق لأنها مشغولة من قبل عدد كبير من الناس وفي حالة حدوث حريق يكون عدد المعرضين للإصابة عددا كبيرا. على مستوى تنظيمي أبنية المطارات ذات درجه عالية من التنظيم بمسالك حركة منظمة ولكون هذه الابنية ذات انفتاحيه عالية، يسهل على المسافرين الانتقال من منطقة وقوع الحريق، بالإضافة لذلك المطارات لها كوادرها الموقعيه من فرق اطفاء

حرائق وفرق مدربة تكون في حالة استعداد في حالة حصول حريق **(Robbin,1991,p58)** .

❖ التصميم للحماية من خطر الحرائق يتضمن **(Edwards,2005,p165)**:

- تحديد الخطر النسبي في فضاءات المطار المختلفة .
- تحديد النظم المرجحة والملائمة للتخاص من الدخان وانتشار الحرائق .
- عمل افتراضات عن مستوى الاشغال في فضاءات المبنى .
- استخدام طريقة الجزر- الفصل بين الفضاءات - في استخراج الدخان ونظم المرشاة .
- تحديد موقع جهاز الانذار الخاص بالحرائق ونظام الكشف عن الحرائق .
- عمل احصائيات عن الوقت المستغرق لاستجابة فرق الاطفاء وكادر المطار الخاص .
- تحديد الاستجابة المحتملة للهيكل الانشائي للمبنى في حاله وقوع حريق .

❖ تصميم محطات المطارات اليوم للحماية من الحرائق يقوم على **(Robbin,1991,p40)** :

1. اعتماد انفتاحية الفضاءات مع تحديد الاكثر خطرا منها مثل المحلات، البارات، المساحات المخصصة لمقاعد الانتظار وخدمة الفحص والتدقيق محمية بأنظمة المرشاة او باستخدام انظمة الرغوة .
2. تشجيع توظيف حجوم الفضاءات الكبيرة والارتفاع العالي في الابنية لأنه يسهل استخراج الدخان من النوافذ السقفية، ولان الدخان وليس اللهب هو المسبب للتسمم والاختناق في حاله حدوث الحرائق لذا تفضل الفضاءات الواسعة لأنها تقلل من كثافة الدخان.
3. تحديد المناطق الاكثر خطرا وتقسيمها بكفاءة بفضاءات متباعدة لمنع انتشار الحرائق من منطقة لأخرى هي احدى السياسات الجديدة المتبعة في تصميم محطات المطارات مثل مطار كنساي . ففي فضاء ذو خطر كامن هناك نظام متكامل منفذ للدخان ونظم للمرشاة والتي تعمل بكفاءة عالية من معاملة فضاءات المطار بنفس المستوى. وبتعريف المناطق الاكثر خطرا كل منها يقيم حسب مستوى الخطورة من اختيار المواد، انظمة الرش وطرق التخاص من الدخان وكل من هذه الانظمة تحدد حسب مستوى الخطورة في الفضاء المعني **(Dempsey,2003,p224)** .
4. بسبب ارتفاع الحرارة والدخان في حالة حصول حريق فمن الممكن تحوير سقف المبنى للتخاص من المواد الكيميائية السامه الى خارج المبنى، مرة اخرى نجد الانفتاحية والشفافية الداخلية في مطار كنساي فمن الممكن في مبنى بحجم فوق ال 15 مليون متر مكعب معالجة مسألة الحريق بدون فواصل تقسم المبنى. فالتصميم الذي يشجع التخاص من الدخان بصورة طبيعية يساعد على توجيه حركة المسافرين في حال حدوث الحريق ولحين الوصول الى منافذ الخروج من مسالك وسلالم .
5. بعض الحرائق قد تنشب لأغراض مقصودة لذا لابد من توفر حماية من قبل الشرطة والامن في المطار وتجنب المواقع والفضاءات المخفية والمحجوبة عن النظر**(Ibid,p66)** .
6. معظم محطات المطارات المعاصرة هيكلها الانشائي هيكل حديدي لذا فإنها بحاجة

للحماية من الحرائق، المقياس الاعتيادي لهيكل المبنى بتحمل لفترة ساعة ونصف في الفضاءات العامة وبحدود الساعة في المكاتب، مع معالجة الهيكل الحديدي بمواد مثل السمنت المسلح لارتفاع يصل الى 4 او5 امتار(اي مستوى الطابق الارضي)، اما الهيكل المكشوف المتبقي يجب ان يطلى بطلاء جاف.

وبينما يسبب الدخان اختناق الناس، فان اللهب هو الاكثر ضررا بالنسبة لهيكل المطار، وعندما يكون خطر انتشار الحريق في المبنى عاليا خاصة في بعض الفضاءات مثل فضاء استلام الحقائب فمن الضروري ان تكون هناك جدران ذات حماية من الحرائق تباعد هذه الفضاءات عن القاعات العامة. **(Edwards,2005,p165)**.

7. اعتماد التقنيات الذكية في منظومة مكافحة الحرائق، تتكون هذه المنظومة من مجموعة من المكونات الكهربائية والميكانيكية المترابطة، تتكون من حاويات او اسطوانات لغاز ثنائي اوكسيد الكربون ثانيا: متحسسات حريق حرارية حسب منطقة العمل، ثالثا: جهاز كهروميكانيكي للسيطرة المركزية.

رابعا، مرشاة co2 او الماء موزعة حول الحيز المراد حمايته من الحريق، خامسا: صندوق متحسسات، سادسا: صندوق الاشارة، يتم نقل الاشارة اليه عن طريق المتحسسات الى صندوق الاشارة الذي يقوم بدوره بتوزيع الاشارة الى باقي النظم الاخرى المكملة في المبنى كنظم التكيف والاتصالات. مع وجود نظام رقمي للتحكم بستائر ذكية ضد الحريق موجودة على فتحات الطوابق المطلة بالسقوف والممرات **(Wang,2010,p235)**.

d)منظومة الاتصالات system Telecoms:

تعد هذه المنظومة من اهم المنظومات ضمن محطات المطارات لأنها ترتبط بمختلف نظم المبنى الاخرى فمن خلال هذه المنظومة يمكن تكامل باقي منظومات المبنى، وتبادل المعلومات والبيانات بين اجزاء المبنى مثل خدمة البريد الالكتروني والانترنيت وقاعدة المعلومات المركزية **(Bachman,2003,p40)** .

فضلا عن ذلك فإنها تضم نظما اخرى مثل الخدمات الصوتية، كخدمة الهاتف والبريد الصوتي، وخدمة النداءات عن بعد ونظم التلفزة الداخلية في المبنى، وخدمة الشبكات المحلية والعالمية للبريد الالكتروني والانترنيت والعمل عن بعد **(Wang,2010,p43)** .

لابد ان تكون شبكة الاتصالات متطورة لتدعم كل تطبيقات المبنى، ببناء شبكة معلوماتية عالية الجودة لضمان الترابط المادي بين النظم المختلفة وتحقيق تكاملها التقني والمعرفي، والسيطرة على مكوناتها المختلفة ضمن شبكة واسعة قابلة للتعديل والتغيير والاضافة المستقبلية لتقليل كلفة التشغيل ورفع مستوى راحة وفعالية مستعملي المبنى عن طريق نظم لمراقبة الفضاءات المختلفة، ومستشعرات مراقبة الاشغال لتعديل درجة الحرارة والاضاءة..الخ ونظم شبكة نقل المعلومات المتكاملة مع نظم الحاسوب **(Wang,2010,p49)**.

2. اعتماد التكناوجيا اداة تعبيرية بيئيا ورمزيا :

a)اعتماد نظم التكتونك كلغة منشأية تعبيرية رمزية :

يعتبر العديد من المعماريين مسألة التعبير باللغة التكنولوجية مهمة معنوية، وفيما يتعلق بتكنلوجيا المطار تعتبر بيئة المطار بيئة ملائمة لاختبار افكارهم، حيث ان العملية الانشائية فضلا عن المفهوم الشامل تتبناها وتعززها لغة التكتونك ، من هنا ينبثق عصر جديد اكثر اناقة ورشاقة يليق بعصر ابنية المطارات الحديثة **(Frampton,1995,p20)**. يعتبر بعض المعماريون التكتونك كشتالت العصر وتمثل ابنية المطارات الاداة الانسب للتعبير عنها **(Edwards,2005,p271)**:

"The tectonic is the Gestalt of the age and the terminal is the perfect vehicle for its expression"

حيث تستغل محطات المطارات المعاصرة امكانيات الهيكل المنشأي لإيجاد اشكال رائعة ونادرة من الافكار التكتونية tectonic idealالتي يعمل فيها المنشأ والنظام الانشائي على التقليل من الوزن الظاهري للمبنى، وتقليل الجاذبية لمثل هذه الابنية فتبدو عائمة على سطح الارض كأنها طائرة مستعدة للإقلاع.عمارة التكتونك تعكس ايقاع الاجزاء ومفصلة العناصر المفصلية، والتي اصبحت أهم سمة من سمات التعبير. فاستخدمت عناصر المفاصل، الخطوط، والعناصر قليلة السمك عوضا عن العناصر الثقيلة من جدران واعمدة، الزوايا تلاشت مع سقوف عائمة وارضيات عبارة عن سطوح افقية رقيقة **(Edwards,2005,p270)** .

قد يشكل التعبير التكتوني الفكرة المعمارية لجميع اجزاء المبنى مثل مطار جاراس دي كول/محطة2 ،او قد يقتصر على سقف المبنى فقط مثل مطار كنساي . الشكل(8) يوضح مفهوم التكتونك في عمارة عدد من المطارات الحديثة على مستوى الجزء والكل .

في عمارة ابنية المطارات التكتونية، تعد السقوف اهم الملامح الرئيسية المميزة لهذه الابنية فنجدها ببحور واسعة، البعض منها ذات معنى مستعار والبعض منها يعكس حركة الطائرات، او قد تكون حركتها لأغراض التفاعل الايجابي مع البيئة فقد تكون السقوف منحنية

باتجاه الرياح لسهولة التهوية الطبيعية، اوقد يكون انحناء السقف لمقاومة عوامل بيئية معينة (مثل مقاومة حدوث الزلازل والاعاصير في مطار كنساي) .

يعد مطار كنساي/اليابان، للمعماري رينزو بيانو 1994، اضخم مبنى مجازي، وهو اشبه بطائر ضخم يخبئ رأسه

تحت جناحيه. عند الدخول للمبنى نحس كأننا في متحف التاريخ الطبيعي لأضلاع ديناصور متكومة ومتوازية،)

اضافة منحنيات انابيب التكييف وتقليل انسيابيتها تعطي

اتجاهية داخل المبنى، حيث انها تعتمد تصميم الشكل المنحني للمبنى تأثرا بحركة الهواء ومراعاةً لأخطار الزلازل. يمتلك المبنى عظمة الصحراء وهدوء المحيط في نفس الوقت ويجسد المبنى مفهوم التقنية العضوية باعتماد عنصر المكان اولا، ثانيا علم البيئة وثالثا عنصر التشكيل الحي **(جينكس،2007 ،ص 100-101)** ،الشكل(9)

تعكس محطات المطارات تكنلوجيا البناء اكثر من اي نوع من انواع الابنية المتخصصة، فتكنلوجيا المطار تعتبر انعكاسا للتكنلوجيا المتقدمة والمستمرة للطائرات، والتعبير التكتوني هو احد الوسائل لهذا التعبير.

b) توافق البيئة والتكنولوجيا (التعبير البيئي والاستجابة البيئية) لمحطات المطارات المعاصرة :

ان استخدام التقنيات التكنولوجية البيئية يعمل على تكيف المبنى مع البيئة الخارجية ويجعل البيئة الداخلية في حالة تكيف مع البيئة الخارجية عن طريق غلاف المبنى ويتم ذلك من خلال تصميم المبنى بطريقة تكاملية بين عملية التصميم والانظمة والفعاليات بطريقة تجعل المبنى عالي الادائية وغير مستهلك للطاقة ومتحسس بالبيئة والمناخ وبما حققته التكنولوجيا كآلية للانتاج والتنفيذ واداة للتعبير**(Bachman,2003,p145)**.

تصميم الغلاف الخارجي لابنية محطات المطارات يستجيب للبيئة من خلال :

1) شكل السقف في المقطع roof profile الذي يأتي استجابة لحركة الهواء وتوجه الشمس.
2) تكيف الغلاف الخارجي للمبنى عن طريق : استخدام نظم الحماية مثل نظم التظليل ، كما في مطار زوريخ. في مطار كنساي، الواجهة الزجاجية مكونة من وحدات مكررة من الزجاج الماص للأشعة الحمراء وللحماية وتقليل الحرارة المتولدة على هذه الواجهة الزجاجية الواسعة تغطى كل وحدة من وحدات الزجاج باطار سليكون مطاطي كحماية ويساعد في تكيف الاشكال للانحناءات المطلوبة، فضلا عن الجدار الزجاجي الذي يحيط به اطار من الالمنيوم على شكل ribs، يمثل هذا الاطار مع الواجهة الزجاجية حماية من الماء والهواء **(Charleson,2005,p133)** الشكل (10) .
3) استخدام المواد الذكية التي تقلل من التأثيرات البيئية مثل الزجاج المحمي(الزجاج الماص للأشعة الحمراء استخدم في واجهة مطار كنساي المواجهة للشمس) او الزجاج المضاعف double skin، مثل مطار ميونخ/المانيا الشكل (11) ، حيث يعمل الزجاج بنظام تبريد وتدوير الهواء البارد بين طبقتي الزجاج واستخراج الهواء الحار لتقليل الحرارة المكتسبة عن طريق غلاف المبنى .
4) استخدام المواد الانشائية الطبيعية والمحلية في الفضاءات الداخلية وفي التغليف الخارجي للأبنية .
5) الاضاءة الطبيعية من خلال المناور السقفية والمناور الحدائقية التي تستحضر الطبيعة ضمن ابنية المسافرين مثل مطار كوالالمبور/ماليزيا، وجود حديقة صناعية تتوسط المبنى ،حيث يتكامل الضوء الطبيعي مع مساحات النوافذ الزجاجية والهيكل الانشائي ،الشكل (12) .
6) من خلال التفاصيل المنشئية التي تستجيب لعوامل

البيئة، مثل مفاصل التمدد مطار كنساي/اليابان، تمتد المفاصل على ارتفاع المبنى تقع ضمن 11 موقع تفصل بينها 150 متر، على طول واجهة المبنى ال 17كم، تعمل هذه المفاصل على امتصاص التشوه الناتج عن الانكماش والارتفاع في الحرارة او عند حدوث زلازل، تفصيل اخر عبارة عن حلقات متداخلة ضمن الهيكل الانشائي مثبتة على زجاج الجانب الارضي تعمل على امتصاص الحركة بنسبة 1.2 متر. الشكل (13) **(Buchanan,1997,p9)**. وكمثال تطبيقي للاستجابة البيئية، مركز النقل الجديد في مطار Inchon air transportation centre/Seoul يشخص العديد من معالم التكنولوجيا الخضراء الحديثة والمنبثقة من مشكلة تصميم خدمات المبنى في مناخ حار ،التصميم من قبل المصمم Terry Farrell &partners خفض استهلاك الطاقة بمعالجة بارعة لشكل وتوجه المبنى وفقا لاتجاه الشمس. احتياج البيئة الداخلية للتدفئة في الشتاء والتبريد في الصيف والتهوية خلال السنه كلها تتحقق باستثمار الطاقة الجارية في تصميم المبنى **(Pearman,2004,p167)**.

الحمل الشمسي واختراق ضوء النهار تمت باستخدام جدران مزججة وسقوف مزججة مع

حماية شمسية مجهزة بواسطة كاسرات شمسية متحركة .على العكس في اغلب ابنية النقل هذا المثال له درجه من التهوية الطبيعية مزوده باستلام الضوء من السقف ومن الجوانب.

التهوية الطبيعية لايمكن ان توفر الراحة خلال فصول السنه . يمكن تزويد مستوى واطئ وقليل من الهواء البارد في الاماكن المستغلة من قبل العامة. حيث جاء التركيز على معالجة المساحات المشغولة في مركز النقل اكثر من الفضاء باكمله للتغلب على الحرارة العالية المتولدة على طول المساحة المزججه وضع نظام من الثقوب موجهة باتجاه الزجاج والذي بدوره يخرج الهواء باتجاه الزجاج لتقليل حرارته .نفس هذا النظام من الثقوب وفتحات التهوية تستخدم شتاء لتعمل على تدفئة الهواء شتاء.

الواجهة الرئيسية تتضمن معالجه بنظام بيئي ذكي من زجاج مضاعف double glazing مع قنوات او دكتات متضمنة ضمن الاطار الزجاجي حيث توفر بالاضافة للظل الشمسي محيطا او قشرة خارجية مرنة ومسؤولة لحماية الفضاءات الضخمة في المبنى قادرة على الموازنة للتغيرات الموسمية في اكتساب وفقدان الحرارة والتكاثف والحاجه لضوء النهار .انشاء المبنى يجعل العناصر المختلفة منفصلة ومتباعدة بما يسمح لكوادر الادامة والصيانة بمراقبة الانجاز باستمرار **(Edwards,2005,p256)** الشكل(14) يوضح الانسيابية في تصميم الشكل الخارجي لمركز النقل في انشيون مع محطة نقل داخلية محلية ضمن المركز .

هدف Inchon في تقليل التأثير على البيئة نابع من اهداف محلية. كبوابة لكوريا هذا المطار يعطي مثلا واضحا في كيفية تكامل الطاقة والتكنلوجيا. الاستخدام الضخم لوسائل التهوية الطبيعية في القاعة الرئيسية لمركز النقل انتج تهوية طبيعة في المبنى بدون مداخن التهوية المشوهة على سطح المبنى. المنظر الجوي للمطار يمثل منظرا او سطحا قشريا منحنيا يستجيب للمتطلبات البيئية الشكل (15) يوضح الحدائق الكورية ضمن الفضاءات الداخلية لمركز النقل لتنقية وتحسين البيئة الداخلية .

معالجة بيئية اخرى تمثلت بتنقية او تصفية مياه الامطار واعادة استخدامها لعمليات الري ، والافادة من مساحات الحدائق المجاورة لمعالجة المياه المستخدمة بطريقة بيئية جديدة **(Ibid,p258)**.

تعد محطات المطارات مسرحا تلتقي فيه الامكانيات التكنولوجية المعاصرة، تكنلوجيا الملاحة الجوية والطائرات تعكسها افكار المصممين بلغة دراماتيكية تعبيرية، ادواتها امكانيات الهيكل الانشائي، انتجت جيلا من ابنية المطارات التكتونية حيث يستجيب شكل الابنية للقوى الفيزياوية المحيطة ويتفاعل معها، بفضاءات داخلية يتفاعل فيها الضوء مع الهيكل الانشائي بلغة ايقاعية هادفة . يلعب الهيكل الانشائي لأبنية المطارات الحديثة دورا كبيرا سواء بعناصره او بالتفاصيل الانشائية او الشكل المنشأي، وبإمكانيات وظيفية، رمزية وتعبيرية بيئية مختلفة .

الاستنتاجات :

1. تمثل التكنولوجيا لغة التعبير لمحطات المطارات المعاصرة حيث تدخل في مفردات العملية التصميمية لابنية المطارات، دور التكنلوجيا تمثل في نقاط عدة اثرت على العملية التصميمية من حيث الامكانيات التي اضافتها بامكانية التوسع والنمو والاستجابة للتغييرات الداخلية والخارجية، ومرونة في عملية وضع المخططات والنتاج الشكلي لابنية المطارات المعاصرة، حيث اصبحت

تكنولوجيا الطائرة والطيران متسارعة النمو والتغير هي السمة المميزة لمحطات المطارات الحديثة .

2. تكامل المنظومات البنائية والتكنلوجية لابنية المطارات، يحقق ترابطها الشكل الفيزياوي للمبنى صنفت هذه المنظومات الى اربع منظومات رئيسية هي :منظومة المنشأ، منظومة الغلاف الخارجي، منظومة الخدمات، ومنظومة الفضاء الداخلي .ترتبط هذه المنظومات فيما بينها ضمن مستويات معينة ، يتدرج مستوى التكامل من علاقات التكاملات الضعيفة الى التكاملات القوية اعتمادا على درجة الارتباط بين المنظومات.
3. تكامل منظومات محطات المطارات يرتكز على مبادئ التكنولوجيا في تحقيق عمل كل منظومة باجزائها ومكوناتها، فضلا عن تداخل وترابط هذه المنظومات مع بعضها بمستويات مختلفة تحددها التكنولوجيا المستخدمة . تلعب التكنولوجيا دورا مهما واساسيا في مفردات كل من المنظومات الرئيسية على حدة وفي تداخل عمل المنظومات معا (تكامل عمل الهيكل الانشائي مع الغلاف الخارجي ومع الخدمات) وبمستويات ودرجات مختلفة . يضمن تحقيق هذه المنظومات التصميمية حفظا للطاقة وكفاءة عمل المبنى وادائيته بالاستجابة للبيئة.
4. اختيار المنظومة الانشائية الملائمة هو احد الاساليب المتبعة لتحقيق شكل معماري متميز واداء وظيفي عالي يتميز بالمرونة والكفاءة. تتميز هذه النظم بكونها نظم ضخمة وواسعة " mega structure"، لكي تستوعب تنوع الفعاليات الوظيفية ضمن ابنية المطارات وطبيعة الحياة المتغيرة ضمنها .
5. التطور والامكانيات التكنولوجية سمحت بوجود عدة تصنيفات للنظم المنشئية لمحطات المطارات ،لكن اهم هذه النظم :<u>النظم الواسعة</u> ، تتضمن نقل الاحمال بصورة حرة وتخلق فضاءات واسعة ، او قد تستند الى نوع معين من الاسناد بدعامات او اعمدة باشكال مميزة تقوم بنقل الاحمال الى الارض، تسقف هذه الهياكل بمدى واسع من الاشكال قد تكون منحنية ، مسطحة وغيرها من الاشكال الدراماتيكية .

نوع اخرهو نظم الشد والاغشية التي تعطي امكانية عالية بخلق بحور واسعة ، مع تطور الامكانيات الانشائية في نقل القوى الفيزياوية ظهرت نظم اخرى تعطي مرونة عالية في التصميم هي نظم الهياكل والمسنمات الفضائية، التي تتضمن مجموعة من العناصر الافقية والعمودية وعناصر الدعم ،تخلق فضاءات ببحور واسعة فضلا عن الاشكال المميزة للسقوف وتعطي مرونة بامكانية تكامل منظومات اخرى ضمنها فغالبا ماتتخلل الاضاءة الطبيعية ضمن عناصر التسقيف ، فضلا عن امكانية تكامل منظومات اخرى مثل دكتات التهوية والتبريد ضمن هذا النظام الانشائي، الذي نجد اتباعه في تسقيف عدد غير قليل من محطات المطارات المعاصرة .

6. التكنولوجيا التي طرأت على النظم المنشئية وتقنياتها، المواد الانشائية مثل الستيل ، الالمنيوم ..الخ خلقت امكانيات اكبر لنظم المطارات ، فانتجت عمارة مطارات تعكس غنىً وتقدما تكنلوجيا على جميع الاصعدة.
7. عمارة المطارات الحديثة عمارة لافضاء spaceless ،تنساب فيها الفضاءات وتتابع مع بعضها،لابد ان تحقق البيئة الداخلية للمطارات توافقا حسب تنوع الفعاليات والوظائف، يمكن تحقيق هذا التوافق عن طريق تكامل مقومات هذه البيئة وهي

:العناصر الفيزياوية ، الهيكل المنشأي ، والضوء .

8. تتنوع الخدمات ضمن ابنية المطارات بين خدمات ميكانيكية تعمل على توفير معايير الراحة للمسافرين مثل منظومة الاضاءة : (التي تشمل الاضاءة الطبيعية والصناعية) ، تمثل عمارة المطارات الحديثة اليوم عمارة شمسية تميل للافادة من الاضاءة الطبيعية لتقليل استهلاك الطاقة، الا ان الموازنة بين استخدام الاضاءة الطبيعية والصناعية مسألة صعبة. دمج وتكامل الاضاءة بنوعيها وتكاملها ضمن منظومة الهيكل الانشائي يعزز من دورها في تعريف الفعاليات والفضاءات ضمن المبنى.

فضلا عن ذلك للتكنولوجيا دور مهم في الخدمات الاخرى في المبنى مثل منظومات التكييف، الحرائق،الاتصالات ..الخ .

9. تمثل التكنولوجيا آلية تفكير واداة تعبيرية رمزية وبيئية في عمارة محطات المطارات المعاصرة، حيث

اعتمدت عمارة الجيل الجديد لمحطات المطارات نظما انشائية مميزة ذات تعبيرية عالية هي نظم التكتونك التي تمثل اللغة التعبيرية الوظيفية والرمزية التي تشكل اجزاء المبنى وباستجابة وتفاعل ايجابي مع البيئة وحسب معطيات المكان . في حين سابقا اعتمدت محطات المطارات الهياكل الانشائية الساكنة staticالتي تراعي الوظيفة فقط لمبنى المطار وبدون خصوصية لطبيعة الحدث الوظيفي (الطيران) .

10. تمثل محطات المطارات المعاصرة جيلا جديدا تلتقي فيه الامكانيات التقنية والفيزياوية، تكنولوجيا صناعة الطيران والطائرات والتفاعل الايجابي مع البيئة يعكسها المصممون بلغة دراماتيكية تعبيرية اداتها لغة التكتونك (اعتبرها البعض كشتالت العصر) وتمثل ابنية المطارات اداتها التعبيرية وعلى مستوى الكل او الجزء .

11. تعمل التقنيات التكناوجية البيئية على تكيف المبنى مع البيئة الخارجية وتجعل البيئة الداخلية في حالة تكيف مع البيئة الخارجية عن طريق غلاف المبنى الذكي، مما يجعل غلاف المبنى عالي الادائية وغير مستهلك للطاقة ومتحسس بالبيئة، حصول الذكاء البيئي للمبنى يحققه اعلى درجة من التكامل المقام بين المنظومات والتكنولوجيا مقصودة الهدف.

12. تمثل محطات المطارات المعاصرة مصغرا لمدينة متكاملة، حيث العمل المتعه السفر والنظام البيئي المتحد في مبنى اونظام واحد، التحدي للمعماريين والمهندسين تحقيق ماهو اكثر انصافا بالنسبة للنظام الصناعي والتنظيمي والرغبات الثقافية للاقليم الذي تخدمه. مما يعطي موازنة افضل بين تصميم المطار والطبيعة في عمقها اي ايجاد توافق بين هندسة المبنى ،القيم الانسانية والمبادئ الايكولوجية وخلق محطة مطار اكثر مرونة وصداقه مع البيئة.

13. توافق البيئة مع التكنولوجيا من خلال تكامل المنظومات التصميمية ، من حيث :

- المنشأ :الشكل المنشأ يعكس القوى الفيزياوية والبيئية المحيطة .
- تفاصيل المنشأ تمثل استجابة للظروف المحيطة .
- استغلال القوى الفيزياوية في ايجاد شكل الغلاف الخارجي (شكل السقف) .
- نظم حماية الغلاف الخارجي (باستخدام التقنيات والمواد الذكية ..الخ).

- الانشاء من المواد الصديقة للبيئة ، المواد المحلية لتحقيق تصميم بيئي .
- تكامل المشهد الحدائقي ضمن الفضاءات الداخلية .
- تقليل استهلاك الطاقة (منظومات الاضاءة تبريد وتدفئة تتكامل مع المنشا).
- التأكيد على استخدام الطاقات النظيفة .

التوصيات :

1. تمثل التكنولوجيا لغة التعبير لمحطات المطارات المعاصرة، حيث انها تشكل اساسا في العملية التصميمية للمطار ولتكامل خدماته واستجابة غلافه الخارجي وشكله المعماري للبيئة في محاولة لتحقيق ابنية ايكولوجية اقل استهلاكا للطاقة وذات سمات كفاءة ادائية ووظيفية عالية .

   ومن هنا يوصي البحث بامكانية الافادة من التطبيقات التكنولوجية سابقة الذكر في التجارب العالمية والافادة بما يمكن تطبيقه من هذه التقنيات بما يلاءم البيئة المحلية وطبيعة مناخنا (الحار_ جاف)، وبما يمكن تطبيقه من هذه التقنيات كخطوات في تصاميم المطارات المحلية المستقبلية ، وبما يمكن تطبيقه من هذه التقنيات والتكنولوجيا في النهوض بواقع المطارات الحالية وتطويرها.
2. اصبحت التكنولوجيا لغة تعبيرية رمزية لمحطات المطارات الحديثة تدخل في مفردات العملية التصميمية وتعد السبيل لتحقيق كفاءتها. يوصي البحث ايضا بعمل دراسة للامكانيات التكنولوجية الممكن الافادة من لتحقيقها في تطبيقات لانواع اخرى من الابنية، مثل الافادة من تقنيات وامكانيات النظم الانشائية .

المصادر:

1. Ashford,Norman,1991"Airport Engineering", John Wiley and Sons, USA.
2. Aviation Symposium,"Sustainable Design of Airports",China/USA,2009.
3. Bachman, Leonard ,2003," Integrated Buildings: The Systems Basis of Architecture" ,John Wiley and Sons, USA, .
4. Blow,Christopher J,1991,"Airport terminals " , Butterworth Architecture.
5. Blow,Christopher, J,1996"Airport terminals," Butterworth Architecture .
6. Buchanan ,Peter ,Renzo piano workshop ,complete works volume 111 , new york ;phaidon press inc.,1997 (report)
7. Charleson, Andrew W.,2005 "Structure as architecture", Architectural Press, UK.
8. De Neufville,Richard,2003 "Airport system:planning,design,and management". McGraw-Hill Professional, USA.
9. Dempsey,Paul Stephen,1999," Airport planning and development", McGraw-Hill Professional, USA.
10. Edwards,Brian,2005," The Modern Airport Terminal: New Approaches to Airport Architecture ", Second Edition, Taylor & Francis, E & FN Spon, London.

11. Eizenman,Peter,1984,"The Futility of object",London,the institution of civil Engineers
12. Fordham, 1995,"Servicing the spaces ",The Architectural Review,May1995.
13. Frampton,K,1995,"Studies in Tectonic Culture":The Poetics of Construction in Nineteenth and Twentieth Centurey Architecture,MIT Press,Cambridge .
14. Gepford Stephanie,2005," SUVARNABHUMI AIRPORT", Air Transportation World .
15. Pearman, Hugh,2004," Airports: A Century of Architecture", Laurence King Publishing
16. Robbin, Tony , 1996," Engineering a New Architecture",Yale University Press.
17. Rush,Richard,1986,"the building systems integration handbook", John Wiley and Sons,New York, USA.
18. Sebestyen, Gyula, and Pollington, Chris, New Architecture and Technology, Architectural Press, UK
19. Wang,Shengwei,2010,"Intelligent Buildings and Building Automation",Spon Press,London
20. جينكس، تشارلز، "عمارة الكون الوثاب "(ترجمة رنا صبحي ناصر،2007)، دار علاء الدين للنشر والطباعة، دمشق- سوريا .

المواقع الالكترونية :

21. http://images.google.com/
22. www.SOM.com

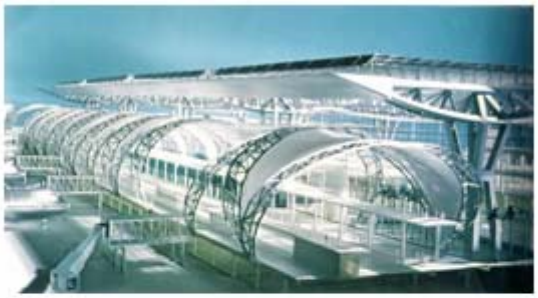

الشكل(١) مبنى مطار بانكوك الثاني/تايلند،
المبنى مغطى بشكل "capsule"
(Gepford,2004,p14)

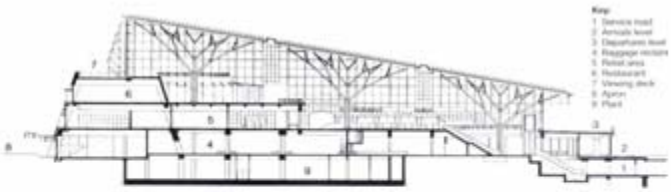

الشكل(٢) نظام الهيكل الانشائي بشكل اشجار مطار شتوتكارت/المانيا**(Edwards,2005,217)**

الشكل(٣) نظم الخيام في مطاري ١)مطار الملك عبد العزيز،السعودية، ٢)مطار دنفر/الولايات المتحدةwww.google images

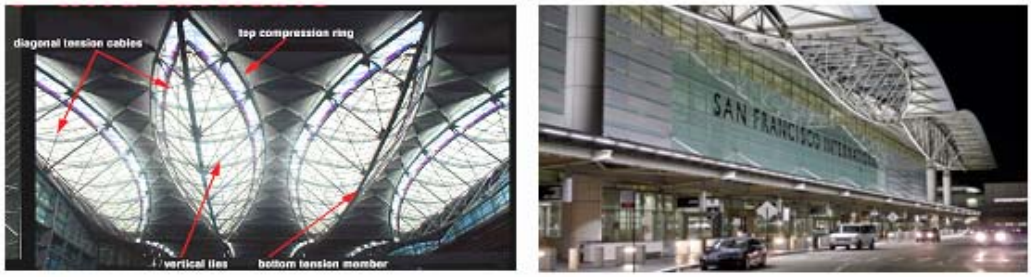

الشكل(٤) مبنى مطار سان فرانسيسكو،الولايات المتحدة،استخدام ٥ وحدات من نظام المسنمات الفضائيةwww.SOM.com

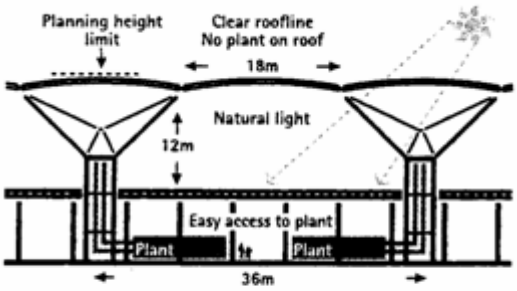

الشكل(5) تداخل الاضاءة الطبيعية والصناعية مطار ستناستيد لندن **(Edwars,2005,p117)**

الشكل(6) اعتماد الانارة السقفية في الجزء الوسطي canyonلمطار كنساي، واعتماد الانارة الصناعية مع الطبيعية في جانب الطيران boarding wing .(Bunchanan,1994,p77)

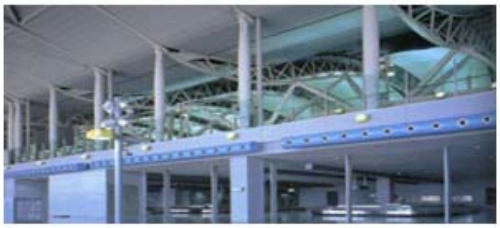

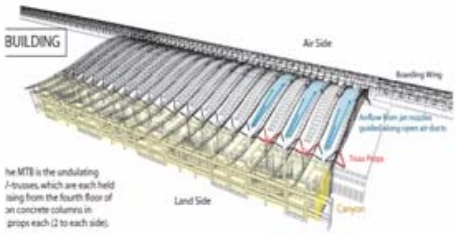

الشكل(7) تداخل دكتات التهوية مع نظام التسقيف، يدفع الهواء بواسطة فوهات توجه حركة الهواء الى دكت هوائي مفتوح على طول جناح المغادرة (Bunchanan,1994,p76)

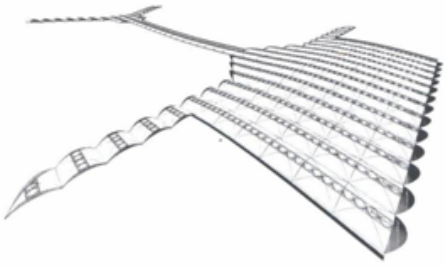

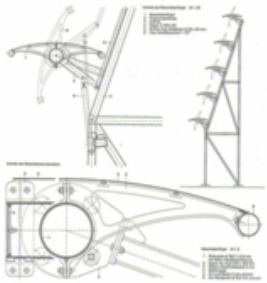

الشكل(8) الاجزاء المفصلية لنظام التظليل في مطار شتوتكارت،المانيا ، السقف العائم لمطار هونغ كونغ/الصين. (التعبير التكتوني على مستوى الجزء والكل)(Edwards,2005,p268)

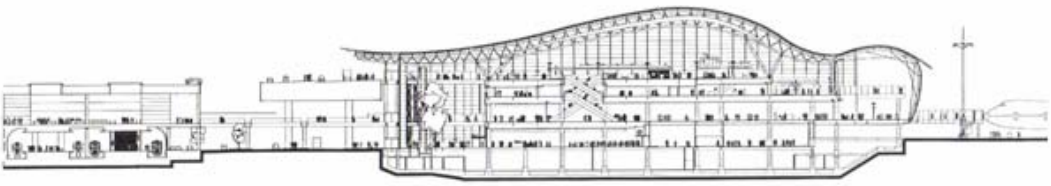

الشكل(9) مقطع مبنى مطار كنساي،اشبه بعمود فقري لاضلاع الديناصور، الفضاء الداخلي اشبه بفقرات متوازية (استعارة مجازية للتقنية العضوية) (**Edwards,2005,p170**)

الشكل(10)استخدم الزجاج المحمي واجهة مطار كنساي(**Aviation Symposium,2009,p10**)

الشكل(١٢) المناور الحدائقية مطار كوالالمبور،ماليزيا

www.google.imges

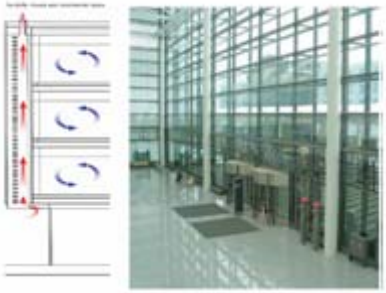

الشكل(11) تقنية الزجاج المضاعف مطار ميونخ(**Aviation Symposium,2009,p10**)

الشكل(13)مفصل التمدد مطار كنساي
(**Buchanan,1997,p9**)

الشكل(١٤) الشكل الانسيابي في التصميم الخارجي لمركز النقل **(Edwards,2005,p257)**

الشكل(١٥) التصميم الحدائقي(الحدائق الكورية) ضمن التصميم الداخلي لمركز النقل لتحسين البيئة الداخلية
www.google **images**

((الحلول المنشئية وجماليات الجسور المعاصرة))

اعداد :- ***أ.د صبا جبار نعمة الخفاجي*** ***المهندسة ازهار طارق احمد***

الخلاصة :-

باتت الجسور في السنوات الأخيرة من أصعب الإنجازات وأكثرها دقة من حيث التصميم ، يستخدمها المارة للعبور اوللاستمتاع بالمناظر المحيطة، بعضها اكتسبت أهميتها من تاريخها العريق وبعضها من التحول الذي ادخله تشيدها الى منطقة معينة ، والبعض الأخر من التقنيات التكنولوجية العالية التي تحملها ، حيث أصبحت رمزا للتطور والتقنية التي تتمتع بها منطقة معينة، وقد ساعدت انظمتها المنشئية في تحقيق التواصل وسمحت لهذه المنشآت بالامتداد إلى مسافات شاسعة تفوق الخيال ، وقد سلط هذا الدور الذي تلعبه الجسور بشكل واسع ومتزايد الأنظار الى هذه الهياكل ، مما جعلها مميزة بالنسبة لمصمميها ومستخدميها ليس من ناحية هندستها الإنشائية فحسب بل من ناحية هندستها المعمارية ايضا ، نتيجة هذا التميز اصبح لابد من دراسة تأثيراتها الجمالية على محيطاتها بشكل عام وعلى المتلقي بشكل خاص ، لذا ازدادت

الدراسات المتعلقة بجماليات الجسور واعتباراتها الفنية بعد ان اصبحت حاجة ومعلما في ان واحد ضمن الفضاءات المفتوحة . وعلى المصمم التعامل مع مجموعة من العوامل البصرية طوال عملية التصميم ، ويجب اختيارها بدقة عالية لخلق قطعة فنية تليق بهذا الدور الحيوي المتزايد ، مع التأكيد على تطبيق القيود الوظيفية للتصميم .

تطرق البحث الى التعريف بمفهوم الجمال في الجسور ومن ثم استعرض المفاهيم التطبيقية المتبعة عالميا المتعلقة بالموضوع وصولا الى تحديد بعض المفردات لأختبار الفرضية ، واستنتج البحث قاعدة عامة مفادها انه لا يمكن فصل المستوى الجمالي عن الأنشائي في عمارة الجسور لأن الجمال وفق كل المفاهيم التطبيقية (مفهوم الشكل والتشكيل المعماري والمفهوم الأنشائي والفني) متأت من المنشأ والشكل المنشئي .

Abstract :-

In recent years, bridges became one of the most difficult achievements and most accurate in terms of design, it's used to pass over, or to enjoy the surrounding scenery, some got its importance for its history and some for the changes it made to certain area, in addition to the high technology used in others in which it became a symbol to the development and technology of that specific area.

The structural systems helped to achieve connection and allowed them to extend to unbelievable distances.

This role played by Bridges grew attention to these structures and made them Special to its designers and users not only for its structural engineering but for its architecture too.

As a result of this distinction it became necessary to study their Aesthetic impacts on its surrounding in general and on the receiver in particular.

Therefore, studies on the bridges aesthetics and its artificial considerations have increased, as it became a need as well as a symbol within open spaces.

The designer would deal with a several optical elements during the designing process, which would be chosen with high accuracy to create a piece of art that fits the expandable vital role, in addition to applying the functional limitations of the design.

The research approaches the definition of Aesthetics in bridges and demonstrates the world wide applied concepts related to the subject to define some Hypothesis testing vocabulary, the research also

concluded a general rule that (Aesthetics cannot be separated from structure in bridge design because Aesthetics in all applied concepts is (a concept of form, architectural and artificial structure).

كلمات رئيسية :-
الجسور ، عمارة الجسور ، هندسة الجسور ، جماليات الجسور ، المستوى الأنشائي للجسور

مشكلة البحث :-

قلة توفر اطر معرفية حول الأعتبارات الجمالية لهندسة الجسور في الدراسات المعمارية المحلية وعن اهمية تحقيق التكامـل بـين المستويين الجمالي والأنشائي .

فرضية البحث :-

ان جماليات الجسور المعاصرة تنتج من مستواها المنشئي (على اعتبار انها اهم عامل في تصميم الجـسور) وبالتـالي تحقيـق التكامل بين المستويين الجمالي والأنشائي.

هدف البحث :-

توفير المعرفة حول جماليات الجسور المعاصرة ودراسة مدى وكيفية تحقيق التكامل بين المستوى الجمالي والأنشائي .

1- مفهوم الجمال في الجسور :-

جماليات الجسور(Bridge Aesthetics) :-

الجسور هي تلك المنشآت التي تؤدي وظيفتها في اجتياز العوائق بكفاءة انشائية فضلا عن امتلاكها قيمة جمالية، فهي تزاوج بين الهندسة الأنشائية والمعمارية **(Dock,1999, p1)**.

فالجسور هي اكثر من مجرد عنصر ضمن نظام النقل ، تخلق شعور بهوية المدينة او البلدة او المنطقة ، وبرغم ان الجسور المصممة بطريقة جيدة تجتذب كافة افراد المجتمع وليس الإنشائيين والمعماريين فقط ، الا ان مصمميها غالبا ما يركزون على وظيفتها الإنشائية مع إظهار عناية قليلة بتأثيراتها الجمالية ، فالجسر المصمم بدون عناية بجماليته يمكن ان يؤدي وظيفته في عبور العوائق ، لكن من جانب اخر فأنه قد يصبح عائقا بصريا وهيكلا مقحما غير جذاب ضمن بيئته . **(Ibid. ،p2) (Moon , p 738)**

كما ان الجسور هي عمارة لكنها عمارة من نوع خاص جدا فريدة في أهدافها ، حيث يكمن فن التصميم المعماري او تصميم الفضاءات المفتوحة في خلق وتشكيل الفضاء ، والمنشأ في النهاية هو الوسيلة للوصول الى هذه الغاية ، لكن بما ان وظيفة الجسر ببساطة هي استمرارية الطريق فوق فجوة لذا فان هيكله يمثل الوسيلة والغاية في ان واحد ، وحقيقته لا تكمن في تطويق الفضاء لكن في المنشأ نفسه **(Mock,1949,p7)** من هنا توصل البحث الى اشتقاق فرضيته الرئيسية .

2- المفاهيم التطبيقية لجماليات الجسور :-

ظهرت على مستوى العالم ثلاثة مفاهيم تطبيقية تتعامل مع تصاميم الجسور المعاصرة وجمالياتها هي :-

أ- مفهوم التشكيل المعماري .

ب- المفهوم الأنشائي (الفن المنشئي) .

ج - المفهوم الفني .

أ- مفهوم التشكيل المعماري :-

تعامل هذا المفهوم مع الجسور بمفهوم الأبداع في الشكل والتشكيل المعماري ، واعتمد على فكرة إن الإنشاء هو احد الجوانب الثلاثة الأساسية للعمل المعماري (وظيفة – شكل – انشاء) ، يقتصر دوره في كثير من الأحيان على تجسيد الشكل وضمان بقائه بما يحقق الوظيفة (مادية – ومعنوية) منه ، وفي بعض المنشآت (كما هو الحال في الجسور) يأخذ اهمية اكبر من ذلك بحيث يكون هدفا وخاصية مرئية (Visible Feature) في حد ذاته ، يصل ليكون هو الشكل نفسه **(عبد العظيم ،2003 ،ص130).**

وحيث ان الجسور تعد من الرموز والعناصر العمرانية التي ليس لها شبيه في العمران ،فأن تشكيلها يؤثر تأثيرا مباشرا وفعالا على المجتمع وتطور ثقافته وبيئته ، فالإبداع التشكيلي للطبيعة او للبيئة الحضرية (العمرانية) التي من صنع الأنسان يمثلان اهمية كبرى في الحفاظ على الصحة الجسمانية والنفسية للأنسان (حيث انه يحدث امتاعا عاطفيا وسموا بالأحاسيس واضافة الى فكر الأنسان الحضري) ، وبالتالي يجب التعامل مع الجسر كعمل معماري **(Leonhardt , 1984 , p 31)**

ورغم ان شكل الجسر في اغلب الأحيان هو نتاج صرف للنظم المنشئية ، فأن التصميم الأنشائي للجسر مستخدما أدواته ومعلوماته (قوانين اتزان - حسابات إنشائية - خواص مواد ..... الخ) او اهدافه (الكفاءة - الأمن - الأقتصاد) غير كافية لأنتاج تصميم يتميز بالأبداع والأبتكار والمتانة والأمن في نفس الوقت ، لأن القوانين الأستاتيكية والديناميكية لا تضمن وجود الأبتكار والتجديد وإبداعية الشكل ، رغم ان التصميم الإنشائي للجسر باستعمال أدواته الخاصة يحمي التشكيل من ظاهرة معمارية منتشرة الا وهي ((الشكل للشكل)) ، حيث في هذه الحالة يكون ((الشكل للأنشاء)) وهو امر معقول ومقبول وان لم يحسب في صف الأبداع .

ونظرا لأهمية التشكيل في تصميم الجسور فأنه يجب ان يكون هدف رئيسي (الى جانب الأهداف الهامة الأخرى المتمثلة بالكفاءة والأمن والاقتصاد) ، ويتوصل اليه من خلال الأنشاء لتحقيق الأبداع التشكيلي الإنشائي ، ليصبح الشكل الإنشائي للجسر عملا نحتيا معماريا يؤدي رسالة فنية بجانب

رسالته الوظيفية (أي تطويع وتطوير الشكل الإنشائي لخدمة الإبداع التشكيلي) **(Bennett , 1997 , p6)**

كما انه لا يوجد شكل في الطبيعة الا وكان مرجعه الى تفاعل القوى بدافع تحقيق الاتزان والبقاء والنمو (القوانين الطبيعية) ، و لا تستخدم قوانين الاتزان لتحقيق اتزان وبقاء

أ-1 مبادئ الجمال في التشكيل المعماري للجسور:-

كانت مبادئ الجمال موجودة في الأعمال المعمارية منذ القدم بصورة أو بأخرى ، ففي القرن الأول قبل الميلاد اهتم المعماري الروماني فيتروفيس بجانب مواد وطرق تشييد المباني بأهداف معمارية لخصت بعد ذلك في عصر النهضة الى ثلاثة اهداف هي :- الثبات (Firmness) والأقتصاديات (Commodity) و الشعور بالمتعة لدى المتلقي (Delight) أي ما يطلق عليه بالجماليات (Aesthetics) . **(Wadowski , 1971 , p15)**

وقد لاحظ المعماري (Le Corbusier) ان تأثر المنشأ بقانون الأقتصاد والحسابات الرياضية وضع المصممين في مواجهة قانون عالمي ، فالمنشأ

يسهم في إنتاج عمارة ، حيث انه يوظف الحسابات الرياضية المأخوذة من قانون الطبيعة لتحقيق شكل معماري يعطي الأحساس بالتواؤم او الأنسجام ، وبالتالي يظهر ان للأنشاء جماليات خاصة به **(Le Corbusier , 1970 , p 36)** ، واستنتج الإنشائي Nervi على نفس النهج بأن الجوهر الحقيقي للتصميم الجيد يتلخص في الأستيفاء الكامل للوظيفة و الثبات (Statical) والأغراض الأقتصادية ، ويؤدي استيفاء تلك الشروط في التصميم الى تشكيل معبر جماليا ، ولا يمكن ان يصبح مزعجا للمتلقي **.(Nervi, 1956 , p15)** ، وقد لخصت Elizabeth Mock فن تصميم الجسور الناجحة بقولها :- ((بما ان حقيقة الجسر تكمن في النظام او الشكل الأنشائي الخاص به ، فأن فن تصميم الجسور يكمن في معرفة وتطوير جمال تلك الاشكال التي تظهر قوة وخصائص المواد المستخدمة فيها بكفاءة عالية ، فالجمال ليس تلقائيا ، ولا تكفي الجودة التقنية وحدها لتحقيقه ، والمصمم الجيد ليس عبدا الشكل فحسب بل تحقيق ما يطلق عليه منطق الشكل، ومن منطق الشكل ينبثق الأنفعال بالجمال **(د. عبد العزيز، 1974 ، ص 112)** .

للمعادلات ، بل هو فنان يستخدم الحسابات كأدوات لخلق اشكال عاملة تتميز بالبقاء والتوافق والأنسجام في مظهرها مثل قوانين الطبيعة التي اوجدتها)) **(Mock , 1949 , p7)** ، كما قال Menn في ذلك :- ((كمبدأ عام تتحقق جماليات التشكيل في الجسور من خلال عنصرين غير معتمدين على بعضهم البعض هما :- أ- تكامل الجسر مع البيئة المحيطة به . ب- تصميم الجسر كمنشأ مستقل . **)) (Menn ,1991 , p 40)**

أي ان الجسور ذات التشكيل المعماري الجيد تتحقق من خلال اتحاد العلم والفن ، وبالتالي يحتاج مصمم الجسر الى الإلمام بالحس التشكيلي (الفني) بجانب الحس الأنشائي العلمي ، وقد اهتم عدد من المختصين بمبادئ الجمال في التشكيل المعماري للجسور وناقشوه وحددوا المتطلبات الأتية لتحقيق ذلك :-

1- اختيار الشكل الأكثر تعبيرا (Expressiveness) مع التمسك بالعامل الاقتصادي .
2-التماثل (Symmetry) .
3- البساطة (Simplicity) .
4-الانسجام والتضاد (Harming & contrast) .
5- التوافق مع البيئة .
6- الدمج الصحيح للمواد .
7- الاستخدام المناسب للزخرفة لأعطاء مظهر عام ممتع للمتلقي .

(Taly , 1998 ,p1226, 1229)

وبذلك يمكن تلخيص الجوانب الأساسية المعتمدة لتحقيق جسور ذات صفات جمالية وفق مفهوم الشكل والتشكيل المعماري للجسور في الشكل (1-1) :-

أ-1-1 جماليات المنشأ :-

اعتمد المفهوم على فكرة تطويع الشكل الأنشائي لخدمة الأبداع التشكيلي ، وان الحسابات الرياضية غير كافية لتحقيق ذلك ، اي ان

المصممين اتجهوا الى استثمار صفات جمالية للمنشأ بعيدة عن الجمال الناتج من الحسابات الرياضية الدقيقة (والذي سيظهر في المفهوم الأنشائي وكما سيتطرق اليه البحث في الصفحات القادمة).

كما ان للمنشأ جماليات خاصة به، لذا طبق المصممين اتجاهين لتحقيق جسور تمتلك صفات جمالية بالتعامل معها كتشكيل معماري يخلقه الشكل الأنشائي ، تمثل الأتجاهين بالاتي :- اتجاه الحركة الملفتة و اتجاه التفصيل المنشئي .

❖ ***اتجاه الحركة الملفتة :-*** يرى Jim Eyre [1] ان اهم مزايا العديد من الجسور في العالم الحديث هي حركتها الملفته ، والمقصود بالحركة الملفتة كثرة الأنحناءات في التشكيل ، مع التأكيد على المحافظة على التوازن (الأنشائي والبصري) الى ابعد حدودها .

(Hart,2004,p279)

يتعامل هذا الأتجاه مع مستوى النظام الأنشائي بأتجاه المخطط الأفقي والمقطع العرضي للنظام ، فضلا عن الشكل الكلي للجسر ، والمقصود بالحركة الملفتة على مستوى النظام الأنشائي هو التلاعب بالشكل الأنشائي للنظام ، حيث ان لكل نظام قواعده الخاصة ، رغم ذلك انتجت التصاميم المعاصرة وبمساهمة المعماريين نماذج تمتاز بحركة غير تقليدية في الشكل الأنشائي للجسر رغم اعتمادها على نفس مبدأ النظام ،وظهر هذا التأثير بشكل منطقي في المخطط الأفقي والمقطع العرضي للجسور المعاصرة.

فضلا عن ذلك فأن التلاعب بالنظام الأنشائي يؤثر بدوره على اضفاء حركة غير تقليدية الى الجسر كشكل معماري ، ويظهر ذلك في جسر Gateshead Millennium (1998 – 2001) شكل (1-2) يربط الجسر بين Gateshead في الضفة الجنوبية و Newcastle upon Tyne في الضفة الشمالية لنهر التاين ، انكلترا .

شيد الجسر باستخدام نظام العقود بأستخدام العقد المخترق ، حيث ان انتقال القوى في هذا النمط يكون من سطح الجسر عبر الاسلاك وصولا الى العقد ، ويسند الجزء الاخر من الجسر بالركائز ، ونفس هذا المبدأ الأنشائي مطبق في جسر كاتشيد ، لكن طريقة التطبيق مختلفة عن جسور العقود التقليدية وكما موضح في المخطط الأفقي للجسر (شكل1-2)، حيث تنتقل الأحمال من سطح الجسر الى العقد والى ركيزتين جانبيتين كما ان العقد نفسه يرتكز على هاتين الركيزتين ، فضلا عن ان العقد الرئيسي بعيد عن سطح الجسر المنحني بدوره ، نتج عن ذلك حركة ملفتة من خلال التلاعب بطريقة تطبيق المبدأ الأنشائي كما موضح في المقطع العرضي للمشروع (شكل1-3)، وظهر الشكل النهائي شبيه بالعين في المخطط الأفقي والمقطع العرضي .

http://www.galinsky.com/buildings/gatesheadbridge/index.htm

،

http://en.wikipedia.org/wiki/Gateshead_Millennium_Bridge

[1] Jim Eyre :- شريك في شركة Wilkinson Eyre للعمارة ، وهي شركة اعيد تجديدها بسبب تصاميم جسورها الراقية . **(Hart,2004,p279)**

❖ اتجاه التفصيل المنشئي :-

التفصيل المنشئي :- هو تحديد شكل وتشكيل وانهاء العناصر المنشئية ومفاصل ربطها مع بعضها البعض ، ويتضمن التفصيل المنشئي كعملية تصميم تصميم المقطع العرضي والواجهة الجانبية ومفاصل العناصر المنشئية ، من اجل تحقيق متطلبات الهندسة الأنشائية في الاستقرار والمتانة والصلادة . ويمكن ان يسهم التفصيل المنشئي المكشوف بشكل كبير الى عمارة أي هيكل بنائي ، حيث انه يمتلك القدرة على تحويل العناصر المنشئية النفعية الأعتيادية او النقية (ذات الوظيفة العملية البحتة) الى عناصر تعطي متعة جمالية ، كما انه يربط الأفكار التصميمية الرئيسة للمشروع مع الأفكار التفصيلية . وغالبا ما يتمكن المعماريون من اظهار تنوع هائل في الافكار التصميمية من خلال التفاصيل المنشئية ، حيث تظهر مجموعة من الصفات المعمارية التي يكون فيها التفصيل المنشئي قادر على المساهمة في التصميم والذي بدوره يؤدي الى نتائج مرضية جماليا . **(Charleson , 2005, p131)**

ويقول لويس كان في ذلك :- ((ان المبنى مثل الأنسان ، ولدى المعماري فرصة لخلق الحياة ، فالعمارة كالجسم البشري (مثل اليد) ، و ان طريقة اندماج البراجم [2] والمفاصل مع بعضها تجعل كل يد جميلة ومثيرة للأهتمام ، ولا يمكن اخفاء هذه التفاصيل في المبنى ووضعها داخل قفاز ، بل يجب العناية بها حيث ان الفضاء يكون معماريا عندما يكون دليل كيفية صنعه ظاهرا ومدركا)) **(Frampton , 1995 , p 227)** .

لكن عند اخفاء التفصيل المنشئي عن النظر تصبح أي اعتبارات اخرى بجانب الاداء المنشئي والأقتصاد وقابلية البناء غير ضرورية .

كما يجب ان يكون التفصيل ملائما منشئيا ومتناغما مع افتراضات الهندسة الأنشائية ، لهذا تتطلب الحلول الأنشائية الناجحة في الأبنية الكبيرة التي تتطلب خبير انشائي (منها الجسور) تعاونا كبيرا بين المعماري والأنشائي ، أي يجب ان يرضي التفصيل كل من فكرة التصميم المعماري والضرورة الأنشائية **.(Charleson , 2005,p132 -133) .**

- الصفات الجمالية للتفصيل المنشئي :-

للتفصيل المنشئي تنوع هائل من الصفات الجمالية ، ولتوضيح هذا التنوع يمكن وصف ازواج من صفات متعاكسة ضمن اربعة مجاميع رئيسه ، وان عملية التصنيف هذه غير دقيقة لأن بعض التفاصيل يمكن ان تناقش ضمن سياق مجاميع اخرى ، ولكن ليست الغاية من هذا التصنيف ترتيب تفصيلا معينا جماليا ، لكنه يوضح التنوع الكبير في اللغات المنشئية المختلفة وطرق التفصيل المنشئي ، ويساعد كل تفصيل على ايجاد قراءة معمارية خاصة به ويؤثر على الكيفية التي يدركه بها مستخدمي المنشأ ، وتقسم هذه المجاميع كالأتي :-

أ- التحسين مقابل المنفعة :- برغم انه من المتوقع ان يكون التفصيل ألمنشئي مصقولا في كل الأعمال المعمارية ، الا انه في بعض الحالات قد تقلل الميزانية او المدة الزمنية المحدودة لأنجاز العمل فرص التحسين والصقل في التفصيل ، او قد يلغى التحسين والصقل عمدا لضمان التناغم مع الفكرة المعمارية ، حيث قد يتطلب العمل جمالا صناعيا قاسيا او غير مصقول فنيا .

ب- **البساطة مقابل التعقيد :-** ليس المقصود من هذه المجموعة من الصفات غياب التحسين والصقل ، لكنها تشير الى ان كل عمل معماري يتضمن تحسينا بطريقة مختلفه تميزه عن المشاريع الأخرى ، فقد يتضمن بساطة الشكل وبساطة العناصر الأنشائية او التعقيد ، اذ ليس احد هذه الصفات صحيحا لكن كل منها يصح في موقع معين .

ج- الخفة مقابل الثقل :- عادة يميل المصممون الى استخدام عدد كبير من عناصر نحيفة بدلا من عدد قليل من عناصر ذات حجم كبير ، وقد تظهر في بعض الأحيان صفات الخفة والرشاقة في تصميم معين لكنها تكون اقل نجاحا من حيث المظهر اذا ما شوهدت من مواضع اخرى ، حيث ان المتلقي يختبر الشكل المنشئي من مواضع تختلف عن تلك المستخدمة لتصميم المخططات والمقاطع والواجهات ، كما تحث الحساسية للقرب البشري من العمل استخدام لمسة

[2] البرجمة (Knuckle) :- احدى البراجم وهي مفاصل الاصابع او العضام الصغيرة في الأيدي والارجل . (البعلبكي ، 1985 ، ص506)

من الخفة في التفاصيل ، مع ذلك يمكن تخفيف الخشونة والقسوة البصرية في العناصر وفي ادراك احجامها بأستخدام سطوح منحنية .

(Ibid. , p 151-156)

د- البساطة مقابل الزخرفة :- ان الفرق بين الزخرفة والجمال غير واضح بالنسبة لأغلب المصممين ، فتصميم جسر يتصف شكله بالجمال ليس معناه خلق جسر مزخرف ، بل تعد الزخرفة اضافات للديكوروالتزيين ، ويجب ان تكون الملجأ الأخير الذي يتجه إليه المصمم للحصول على قدر من جمال الشكل **(Taly , 1998 ,p 1221)**

وتعد الجسور انشاء نقيا ، بمعنى انها لا تحتوي على عناصر المبنى من جدران وابواب ونوافذ ..... الخ ، ويعد الشكل المعماري للجسر ترجمة طبيعية للنظام او الشكل الأنشائي ، ولتحقيق جمال الشكل يجب عدم وضع قناع يخفي النظام الإنشائي المستخدم ، لأن جمال الشكل ينتج عن فهم منطق

سادت المفاهيم الإنشائية في عمارة الجسور لمدة غير قليلة من الزمن بعد الانفصال الحاصل بين الفنون والعلوم، وهيمن عليها مفهوما الكفاءة المنشئية و الأقتصاد في الكلفة ، لكن اضيف المفهوم الجمالي ضمن هذه المفاهيم لعدة اسباب ذكرت مسبقا ، وبذلك اصبحت هذه المفاهيم الرئيسة الثلاثة اهم المعايير الواجب توفرها في كل جسر .

حيث نتجت جماليات الجسور في الحقول الأنشائية من الأختيارات اللاواعية للأشكال على يد مهندسين يبحثون عن تعبير المنشأ (expression of structure) فهي تمثل اما النتيجة الواعية للبحث عن الأقتصاد ، او نتيجة الدرجة القصوى من الحسابات الرياضية **(Chen ,& Duan, 2000, 3.2)**

يرى Billington بأن الهياكل الناتجة وفق هذا المفهوم ليست اعمالا نحتية ولا معمارية ، لكنها تعود الى وسط اخر مرتبط بكليهما معا ، و يبرز عن الأثنين الاخرين من خلال استخدامه لقواعد الكفاءة المنشئية كأسس اولية لخلق اشكال مرئية جديدة ومثيرة يطلق عليه ((الفن المنشئي)) **(Billington , 1983) نقلا عن (Gauvreau ,2003, p2)** ، فالفن المنشئي بالنسبة لـ Billington هو بنفس مستوى العمارة والنحت ولكنه يمتلك مميزاته الخاصة. الشكل **(Potyandy, 1969 , P 28)** ، فيجب ان لا تغطى الجسور بالزخارف ، حيث ان الغرض من الزخرفة (في حالة استخدامها هو تأكيد العناصر الأنشائية وبالتالي التأثير على المتلقي دون اخفاء الطبيعة الحقيقية للشكل الأنشائي والمادة (شكل 1-4) ، وفي ذلك وضع Ruskin قاعدة نشرت في كتاب بعنوان (Artistic Bridge Design) عام 1912 يقول فيها ((To decorate construction without constructing decoration)) ، فيجب ان لا تستخدم الزخرفة بغرض تعويض النقص الجمالي للشكل ، ومع ذلك يمكن ان تكون للزخرفة المقننة اهمية عندما يقترب المتلقي من الجسر ويطلع على تفاصيل المنشأ عن قرب (شكل1-5) **(Menn,1991 , p 15 , 31)**

ب- المفهوم الأنشائي (الفن المنشئي) :-

(Gottemoeller , 2004,p 49) ، ويعرف Thomas Telford [3] الفن المنشئي بأنه :- ((التعبير الشخصي عن

المنشأ ضمن قواعد ونظام الكفاءة والأقتصاد)) ، وقد وجد الفنانون المنشئيون ضمن هذه الحدود الوسيلة لأختيار الأشكال والتفاصيل التي تعبر عن رؤيتهم الخاصة **(Chen,& Duan ,2000)**

ويعتمد الفن المنشئي على ثلاث قواعد او معايير اساسية في العمل هي كالأتي :-

(أ) الكفاءة :- وتعني استخدام اقل ما يمكن من المواد مع امكانية السيطرة على توفير عامل الأمان .

(ب) الأقتصاد :- أي اقل ما يمكن من الكلف مع امكانية السيطرة على ادائها للوظيفة المطلوبة منها وامكانية المحافظة عليها لمدة طويلة .

(ج)الأناقة :- اي اقصى ما يمكن من التعبير عن شخصية المصمم مع ضمان تطبيق قاعدتي الكفاءة والأقتصاد .

(Gottemoeller , 2004,p 49)

---

[3] Thomas Telford :- هو مهندس بريطاني ، وكان اول من اشار الى الفن المنشئي عام 1812 **(Billington , 1983 , p 5)**

وتقدم اعمال الفن المنشئي في عصرنا الحالي ادلة بأن الحياة العامة يمكن ان تزدهر بشكل افضل عندما تتحقق اهداف الحرية مع تطبيق قواعد العمل بأتزان ، وتكمن حرية قواعد الفن المنشئي في انها تتيح الأمكانيات للمصمم للتعبير عن اسلوبه الشخصي بالبحث الجمالي الواعي عن الأناقة الهندسية . **(Billington , 1983 , p 5)**

واذا كان تصميم الجسور وسيلة فعالة للتعبير الجمالي بحد ذاته اذن فهو احد اكثر هذه الوسائل ارباكا وتشويشا ، لأن تصميم الجسور كشكل فني يترنح بين امكانيته الضخمة غير المستغلة بشكل كبير وبين الثقافة السائدة التي تكبح بقسوة خلق الأعمال المتميزة جماليا **(Gauvreau ,2003, p1)**

ب- 1 - مصادر الجمال في الجسور وفق المفهوم الإنشائي :-

ينتج التأثير الجمالي للجسور على المتلقي من اي جانب من جوانب الجسر ضمن هيئته الكلية واجزائه المنفردة وكما يراها المتلقي اثناء عبوره خلاله سواء من فوق او تحت الهيكل او مشاهدته من مسافة معينة **(Moore , C. & G. Allen ,1976) نقلا عن (Berk,2005,p 48)**. وحيث ان هيمنة المظهر الخارجي للجسور على مشهد المدينة ناتجة عن احجام واشكال عناصرها المنشئية ، وليس نتيجة التفاصيل والألوان والسطوح **(Berk,2005,p 51)** ، فهذا يعني أن التأثير الجمالي الأعظم ناتج عن :-

1 - العناصر المنشئية نفسها (الأسلاك ، العوارض ، والدعامات) ، حيث ان وجودها حتمي في كل جسر ، على سبيل المثال جسر Golden Gate(شكل 1-6) في الولايات المتحدة الأمريكية يدين بجماله وفتنته الى الشكل الرشيق لأبراجه واسلاكه وليس الى لونه المحمر . و لو كان تصميم الأبراج نفسها قبيحا فلن يجعلها الطلاء الأحمر جذابة بأي حال من الأحوال .

2-التصميم الجيد للعناصر المنشئية دون اضافة كلف غير ضرورية ، وغالبا ما يواجه هذا التحدي قيود في حالات المشاريع ذات الميزانية المضغوطة ، وافضل وسيلة لمواجهة ذلك هي اعتبار القيد نفسه تحديا واستخدامه لأيجاد الجمال المتأصل والمتضمن داخل المشكلة .
(Gottemoeller , 2004 ,p8,9,10,44)

اذن يكمن المبدأ الرئيس لتصميم جسور ذات قيم جمالية وفق قواعد العمل الثلاث(الفعالية والكلفة والخاصية الجمالية) في وضع كل هذه المقاييس مع بعضهاالبعض في نفس الوقت والعمل على تحسينها سويا دون التضحية بأحدها من اجل تحقيق الأخريات **(Berk,2005,p 52)** ،ويعتبر جسر Craigellachie لمصممه Telford مثالا جيدا لتوضيح هذا المفهوم (شكل 1-7)

حيث يتكون الجسر من عقد من حديد الصب كفوء منشئيا ، في حين اختار المصمم نموذجا ماسيا في قضبان السبندل (حيث تسمح الأعتبارات المنشئية في تلك النقطة من الجسر بالعديد من الخيارات) و كان اختيار المصمم اخذا بنظر الأعتبار المظهر الخارجي للجسر ووفق نظرته الشخصية لما هو جميل**(Chen,& Duan ,2000 , 3.2).**

ب-1-1 خصائص الجسور ذات الصفات الجمالية وفق المفهوم الأنشائي :-

تتلخص خصائص الجسور ذات الصفات الجمالية بالأتي :-

أ- انها ابسط :- بمعنى انها تمتلك عدد اقل من العناصر الفردية ، كما ان عناصرها المتشابهة في الوظيفة (كالعوارض مثلا) متشابهة من حيث الشكل والحجم .

ب- عوارضها انحف نسبيا :-(أي نسبة العمق الى الأمتداد اصغر) .

ج- خطوط المنشأ الرئيسة مستمرة :- أي ان امتدادات الجسر مستمرة مع بعضها البعض او تبدو للعيان بأنها مستمرة .

د- يعكس شكل العناصر المنشئية القوى الساقطة عليها :- أي يزداد سمك العنصر في المناطق التي تكون فيها القوى اكبر ويقل في المواقع التي تتحمل قوى اقل .

يظهر من هذه الخصائص بأنها جميعها صفات مرئية للكفاءة المنشئية ، أي ان تحسين الخاصية الجمالية في الجسور يزداد كلما زادت الكفاءة المنشئية ، وهذا ينطبق مع تفسير مصممي الجسور لمفهوم (الشكل يتبع الوظيفة)، حيث فهمت هذه العبارة ضمن سياق تصميم الجسور بأن السلوك الأنشائي الكفوء وكلف التشيد المنخفضة شروط كافية لتحقيق الأناقة البصرية . **(Gauvreau ,2003 , p4, 5)**

كما يظهر انها تمثل مجموعة من الصفات متمثلة بـ(البساطة، النحافة (thinness) ،الأستمرارية) ، ولا تتضمن مميزات او خصائص شكلية محددة ، مثل دعامات على شكل حرف (Y) مثلا وما شاكلها ، حيث ان الجسور كغيرها من الهياكل العمرانية تختلف عن بعضها البعض بنواحي مهمة ، منها متطلبات الموقع واختلاف تقنيات التشييد المتوفرة فضلا عن اختلاف الأجراءات التحضيرية اللازمة لموقع قادت وجهة النظر السابقة للتعامل مع جماليات الجسور وفق عبارة الشكل يتبع الوظيفة مع ميل المهندسين الى العمل مع الأرقام والحسابات الأنشائية الى اقتراح وتطوير طرق كمية للتعامل مع قضايا الجمال في الجسور ، على سبيل المثال طور Zuk نظام يتكون من 177 مفردة يتعلق بجماليات الجسور مستخلصة من نصوص متعلقة بالموضوع ، حيث وضع مقياسا لتقييم المظهر الخارجي للجسور (يبدأ من صفر بالنسبة للجسور الأكثر قبحا الى 10 بالنسبة للجسور ذات الجمال الراقي) وتمنح القيمة الأعلى للتصاميم المشابهة والأكثر انسجاما مع البيانات او التصريحات في قاعدة بيانات النظام ، لكن ادت هذه العملية الى انتاج مجرد نسخ من التصاميم المجربة والموجودة مسبقا ، وبذلك تحولت العناصر الأبداعية في تصميم الجسور الى عمليات اتباع فعلية للقوانين (Zuk ,1995) **نقلا عن** (Gauvreau , 2003 , p5) وان هذه التطبيقات معيبة بشكل اساسي لأنها جعلت المظهر الخارجي لأي جسر محدد بمجموعة قوانين دون اعتبارات خاصة لقضايا الجمال ، رغم ما اظهرته تصاميم ومؤلفات Maillart و Roebling و Ammann وغيرهم من عباقرة مصممي الجسور من اهمية ووضوح الصلة بين السلوك الانشائي والمدلول الجمالي ، لكن هذه العلاقة معقدة

ج – المفهوم الفني :-

بدأت تدرك امكانية تصميم الجسور كوسائل للتعبير الفني من قبل علماء الفن وتاريخ الفن والمهندسين ، حيث وضحت امكانية تصميمها كوسائل للتعبير الفني في روائع التحف الفنية لبعض المهندسين مثل جسر بروكلن لمصممه Roebling وجسر Salginatobel لمصممه Maillart وجسر Pont Isère ، وعرفت هذه الهياكل كاعمال ذات التشييد ، فأذا تطلع المصمم الى تحقيق الجمال كان عليه محاكاه او تقليد سمات الجسور الناجحة جماليا المذكورة اعلاه وتطبيقها وفقا لمعطيات الموقع **(Gottemoeller , 2004 ,p44)**

وبذلك يمكن تلخيص الجوانب الأساسية المعتمدة لخلق جسور ذات صفة جمالية وفق المفهوم الانشائي في الشكل (1-8) .

اكثر بكثير من مجرد تطبيق مفهوم الشكل يتبع الوظيفة ، حيث ان الكفاءة المنشئية والأقتصاد بحد ذاتها ليس لها مدلولات جمالية ، لكن يمكن ان تساعد قواعد عمل الكفاءة والأقتصاد على توليد اشكال مرئية ماكانت لتنشأ دون هذه القواعد بأيدي بعض المصممين الموهوبين **(Billington , 1983) نقلا عن(Gauvreau ,2003 , p5).**

لكن تطبيق مفهوم الشكل يتبع الوظيفة يسمح بأستثناء واحد فقط وهو ((الجسور الدلالية Signature Bridges)) ، تشمل هذه الفئة كل الجسور التي سعت الجهات المسؤولة فيها الى تحقيق نتاج ذي تعبيربصري فريد من نوعه ، حيث يكون المراد من هذه الجسور ان تكون دليلا (signature) او عنصر دلالة لمدينة او منطقة) ،و بدأت الجهات المسؤولة على مستوى العالم تدرك بأن الكفاءة المنشئية وحدها لن توفر مستوى صفة الجمال المطلوبة للجسور الدلالية ، فضلا عن وجود استعداد لتخصيص ميزانية عالية لمثل هذه المشاريع ، وبشكل عام هناك ميل للاستعانة بخدمات المعماريين في هذه المشاريع اكثر من غيرها ، حيث يلعب المعماري فيها دورا اساسيا في تحديد المظهر البصري للجسر . **(Gauvreau ,2003 , p7)**

مدلولات جمالية من قبل الباحثين في مهنة الهندسة وكذلك من قبل كتاب اخرين في حقول اخرى **(Gauvreau ,2003, p1)** ، مع ذلك تختلف مكانة الفن في الجسور عنها في الحقول الأخرى ، ويكمن الأختلاف الرئيس هذا في التقييد (restrictions) ، حيث ان فكرة الفن العامة هي اظهار العواطف والمشاعر القوية ونقلها الى الأخرين بمساعدة العنصر المبتكر ، وفي الجسور يظهر من ناحية ان هذه العواطف موجودة بشكل اساسي ومن ناحية اخرى هناك

متطلبات خاصة بالمنشأ يجب تطبيقها ليتمكن الهيكل من الوقوف والأستمرار لمدة طويلة ، فالجزء الأكثر تحديا في فن الجسور هو عكس احساس الفنان (المصمم) ضمن حدود القيود الموجودة مع اعطاء اولوية للوظيفة **(Berk , 2005 , 46)**

ج-1 الجسور وجوهر الفن :-

يقوم هذا الاتجاه على فكرة مفادها :- ((اذا ادرك تصميم الجسور كوسيلة متميزة وفعالة للتعبير الفني عندها يجب ان تعكس الجسور الحقائق التي تظهر الجوهر الأساسي المشترك بين كل الأعمال الفنية ، من غير التركيز على الوسيلة او التقنية المستخدمة للتعبير الفني))، ولتجسيد هذه الحقائق في الجسور يجب الأعتراف بوجود واهمية هذه الحقائق في اطر العمل الفكرية التي يستخدمها المصممون لتوجيه قراراتهم التصميمية .

ج-1-1 الخصائص الأساسية لجوهر الفن :-

الخاصية الاساسية لجوهر الفن هي تحدي الأفكار الموجودة من ثم تحدي النظريات الدوغماتية [4] (او النظريات العقائدية الجازمة) عن كيفية خلق اعمال فنية تتمتع بذوق رفيع ، ويظهر ضمن سياق الثقافة السائدة في جماليات الجسور ان اكثر هذه الخصائص اهمية هي :- ((ان الفن يتحدى الأفكار الموجودة بطرق ذات هدف ومعنى)) ، حيث ان الأشارة الى الأعمال الفنية بأستخدام كلمات مثل (ثوري) و (فتح افاقا) و (حالم) يعكس وعي وادراك بأن الأعمال الفنية يمكن بل انها تتحدى فعليا الأراء الشائعة والمتمسك بها ، وتؤكد عبارة (بطرق ذات هدف ومعنى) على استبعاد اخذ الأعمال الصادمة من دون مبرر بعين الأعتبار ، ويمكن توضيح التحدي ذي الهدف للأفكار الموجودة بأنه ذلك الذي يستطيع ان يحافظ على قدرته لتنبيه الأحاسيس والعواطف او يحافظ على قدرته على اثارة الأفكار بعد مدة طويلة من حدوث الصدمة وبعد ان تصبح بالية (بمعنى ان هذا التحدي يستطيع تحفيز افكار جديدة بعد مرور مدة زمنية طويلة على حدوث الصدمة) ، والدليل المنهجي على هذا الأفتراض هو ان الفن الذي يتحدى الأفكار الموجودة بطرق ذات هدف لا يتم التعدي عليه عادة ، بل عوضا عن ذلك تستخدم امثلة لتوضيح الطرق التي يمكن ان تثبت بها هذه الخصائص الأساسية نفسها ضمن الأعمال الفنية وفي كل من الأوساط الكلاسيكية وتصميم الجسور .

وبالنسبة للجسور ذات المدلولات الجمالية فأنها ايضا تجسد تحديات ذات اهداف نسبة الى الأفكار الموجودة ، على سبيل المثال يعتبر جسر Pont de la Tournelle في باريس (شكل1-9) شيد عام 1928 الصيغة الدلالية [5] للمثل الأعلى المعاصر لجماليات الجسور الممتعة ، ورغم انه مشيد من الخرسانة المسلحة الا انه مكسي بطبقة تزينية من الحجارة استخدمت لأضفاء تفاصيل تشبه الجسور التي تعود الى عصور سابقة ، لكن عندما جاء جسر Salginatobel تصميم Maillart فأنه اعتبر انحرافا راديكاليا عن الذوق الفني الشائع والمتمثل بجسر Pont de la Tournelle ، حيث انه استخدم المنشأ الخرساني نفسه ليكون وسيلته في التعبير ، حيث ان الأقتصاد في جسره كان اكثر اهمية لدى السلطات المحلية من الأختلاف بين تحقيق الجمال واتباع الأفكار السائدة . **(Gauvreau ,2003, p1-3)**

يظهر مما تقدم :-

أ- اذا كان جوهر الفن يتضمن انشاء او اظهار تحد للأفكار الموجودة في هذه الحالة لن يكون ذلك الفن نتيجة التطبيق المجرد للقواعد والتقاليد المحددة مسبقا والشائعة الاستعمال او للنظم المبدأية الأخرى .

ب- اذا اعتبر تصميم الجسور كوسط فعال ومتميز للتعبير الفني عندها يجب ان ينطبق الكلام المطروح في النقطة (أ) على الجسور ايضا .

وفي النهاية يظهر ان نجاح الجسر لا يأتي من اداءه لوظيفته فقط ، بل من جماله المرئي ، برغم اختلاف الأراء حول الجمال لدرجة انه لا يمكن ان يوجد فهم واضح ما اذا كان من الممكن اعتبار بناية او جسر معين جميلا او لا .

---

[4] **الدوغماتي (Dogmatic) :- مؤكد من غير بينة او دليل (البعلبكي ، 1985 ، ص 286) .**

[5] الصيغة الدلالية :- هي صيغة تظهر العمل او الحالة بوصفها حقيقة موضوعية لا مجرد شيء في الذهن . **(البعلبكي ، 1985 ، ص460)**

ومن المفاهيم الثلاثة السابقة توصل البحث الى الأستنتاج التالي فيما يتعلق بعلاقة المستوى الجمالي بالأنشائي في عمارة الجسور :- ((كقاعدة عامة لا يمكن فصل المستوى الجمالي عن المستوى الأنشائي في عمارة الجسور)) لأن الجمال وفق كل المفاهيم متأتي من المنشأ والشكل المنشئي وحسب المفاهيم الأتية :-

أ- مفهوم الشكل والتشكيل المعماري:- ان جماليات الجسور وفق هذا المفهوم متأتية من جماليات المنشأ وتتمثل بـ :-

- الحركة الملفتة .
- الصفات الجمالية للتفصيل المنشئي .

ب- المفهوم الأنشائي(الفن المنشئي) :- تنتج جماليات الجسور وفق هذا المفهوم من تطبيق القوانين والحسابات الرياضية (أي استثمار البعد العلمي للمنشأ) ، مع اظهار التعبير الشخصي للمصمم عن المنشأ .

ج- المفهوم الفني(الجسور وجوهر الفن) :- الجماليات ناتجة من تحدي الأفكار والتطبيقات التقليدية (تحدي الصيغ الرياضية الصارمة) .

3- مؤشرات الأطار النظري :-

أ- مؤشرات مفهوم الشكل والتشكيل المعماري :-

❖ الحركة الملفتة في النظام الأنشائي على مستوى :-
- المخطط
- المقطع العرضي
- الشكل الكلي .

❖ التفصيل المنشئي (الصفات الجمالية للتفصيل) :-
- التحسين مقابل المنفعة .
- البساطة مقابل التعقيد .
- الخفة مقابل الثقل .
- الزخرفة مقابل عدم التزيين .

ب- مؤشرات المفهوم الأنشائي :-
- بساطة التصميم (اقل عدد من العناصر الفردية) .
- تشابه عناصر التصميم من حيث الشكل والحجم .
- نحافة المنشأ (نسبة صغيرة للعمق الى الأمتداد) .
- استمرارية خطوط المنشأ .
- الوضوح المنشئي (عكس العناصر المنشئيه للقوى الساقطة عليها .
- التعبير عن شخصية المصمم .

ج- المفهوم الفني :-
- تجديد وتحدي الأفكار الموجودة .

4- الأمثلة التطبيقية :-

استخلص البحث من الأطار النظري المؤشرات الأتية لأختبار الفرضية على الأمثلة المختارة :-

اتجه البحث لأختبار الفرضية الى تحليل مجموعة من الأمثلة التطبيقية وفق مفردات الأطار النظري التي تم استخراجها، ومن ابرز الأمثلة التي تطرق اليها البحث :-

أ- جسر (Bach de Roda) تصميم المهندس المعماري و الأنشائي Santiago Calatrava Barchelona , Rpain(1985 – 1987) (شكل 1-10)

موقع المشروع :- يربط المشروع بين منطقتي Sant Andrea شمالا و San Marti جنوبا عند اطراف مدينة Cerda في برشلونا ، حيث كانت المنطقتان معزولتين عن بعضهما بخط سكة حديد ، والمطلوب ربطهما بهذا الجسر .

ظروف التصميم :- عام 1984 تم ترشيح مدينة برشلونا لتكون المدينة المضيفة لدورة الألعاب الأولمبية للعام 1992، لذا كثفت من برنامجها للتجديد الحضري اثناء استعداداتها لهذا الترشيح ، وقد كان من الأهداف الرئيسة للتجديد في المدينة هو تحسين البنى التحتية للنقل والتي من ضمنها الطرق وسكك الحديد ، و كان ينظر الى جسر Bach de Roda بأنه اول هذه المشاريع الرئيسة .

كان على كلترافا ان ياخذ بعين الأعتبار كيف يمكن ان يدمج ويكامل بين استخدام الجسر داخل الحدائق المحيطة والفضاءات الحضرية المفتوحة وجعله جزءا ايقونيا من برشلونا المتجددة ،فهو مصمم لتعزيز الفضاءات المدنية ، ونادرا ما تستغل الجسور لهكذا غرض ، لكن ميزة سنتياكو

في هذا المشروع وباقي جسوره هي انه يعمل على تحويل المهمة التصميمية البسيطة عند تصميم الجسور الى حدث لخلق مكان ، وبذلك أعطى برشلونا مطلبها بالتحديد (أي جسر ايقوني) .

يتكون الجسر البالغ طوله 128 مترا من ثلاثة اجزاء ، جزء مركزي بطول 45 مترا فوق خط سكة الحديد ، وجزءان جانبيان بطول 25 مترا ، تمر عبر الساحة ، الحركة على الجسر مفصولة الى جزئين ، جزء مركزي لحركة المركبات واقع بين العقدين الرئيسين ، بينما مسارات المشاة تمتد على طول الجانبين محصورة بين العقد الرئيس والثانوي المناظر له ،و ترتبط الأجزاء الجانبية للمشروع مع المساحات الخضراء بأربعة سلالم تبدأ بالأرتفاع عند قواعد الأقواس المائلة لتصل الى منصة للتجمع (للسابلة) على الطرفين .

المستوى الأنشائي :- استخدم المصمم في هذا الجسر نظام العقد المخترق ، وكان كلترافا واضحا جدا في تحديد منشأ الجسر، حيث ان هيكله قد استوفى وظيفته ، بمعنى ان الهيكل صادق في التعبير عن النظام الأنشائي والمادة البنائية التي تم اختيارها ، فسطح الجسر معلق من العقود الفولاذية بأسلاك فولاذية مما يظهر بوضوح المادة المستخدمة، كما انه من الواضح ان العقدين الرئيسيين مرتبطان مع بعضهما بواسطة عوارض سطح الجسر الرئيس ، هذا التحسين في ربط العقود ساعد على التقليل من المقطع العرضي للعقد وعناصر الأسناد المطلوبة .

ويستند الهيكل المركزي على اربع دعامات من الكونكريت المسلح ، وتم تثبيت كل عقد رئيس بواسطة عقد تقوية ثانوي من الفولاذ، يميل العقد الثانوي بزاوية مقدارها 60 درجة وتسند بواسطة اكتاف ، تعمل العقود الثانوية كمثبتات جانبية ، وبذلك استبعدت الحاجة الى استخدام مسنمات تربط بين العقدين الرئيسيين ، استخدم المصمم في هذا المشروع عقدا بشكل قطع مكافيء ، والذي ادى وظيفة جمالية لكن من جهة اخرى قلل المقطع العرضي الأنشائي المطلوب .

اما الجزء المضلل الوحيد في التصميم فهو ان العقدين يظهران كأنهما يعملان على اسناد سطح الجسر الكلي ، في حين ان العقد الرئيس هو الذي يقوم بأغلب العمل وحده (فعليا)، اما العقد الخارجي المائل فأنه يوفر استقرارا واسنادا للمماشي الجانبية فقط ، ومما زاد من هذا الخداع البصري كون العقد الخارجي مستمرا الى الأرض وصولا الى دعامات كونكريتية مائلة .

المستوى الجمالي :-

- ***النظام :-*** يجب ان يكون هناك نظام في خطوط وحافات المنشأ من خلال تحديد اتجاهها ، لكن لم يقم كلترافا بجهد مرئي لتقليل عدد الزوايا والخطوط المستخدمة ، مما نتج عنه هيكل انشائي معقد المنظر ومربك ايضا ، مع ذلك فأنه قد قام بتكرار شكل وحجم ركائز الأسناد الرئيسة لسطح الجسر مما وفر الأنتظام المطلوب في الهيكل الأنشائي ، كما أن التناظر هو تابع مهم للنظام ، والهيكل الأنشائي متناظر في مخطط واحد (المقطع العرضي) ، لكن قطع هذا التناظر في المخطط الأفقي الظاهر في الشكل.
- ***الظل والضوء :-*** تلاعب المصمم بالظل والضوء لتحقيق اهدافه الجمالية ، حيث جعل حافات السطح بزاوية معينة مما تسبب في تعتيم وتظليل الحافة السفلية للرافدة وجعل الجزء الظاهر على الواجهة منها اكثر لمعانا لأعطاء انطباع بأن سطح الجسر انحف مما هو عليه فعليا ، وذلك بسحب البصر الى السطح الأكثر نحافة (في الواجهة) بعيدا عن الجزء السفلي الأكثر سماكة .
- ***الخصائص المميزة للجسر :-*** يمتلك هذا المشروع شخصيته المميزة والبارزة ، حيث انه يتلاعب بالنحتية والهندسة المعمارية والأنشائية بطريقة نادرة لم تستخدم قبل هذا المشروع بنجاح كالذي حققه هذا المشروع ، حيث في ذلك الوقت وقبل ان يشيد كلترافا أي جسر اخر كانت هذه طريقة جديدة كليا وانتجت هيكل انشائي فريد من نوعه ، ويطلق السكان المحليين على هذا الهيكل اسم ((جسر كلترافا)) مما يدل على ان السكان المحلين لا ينظرون اليه كقطعة من البنى التحتية فقط ، بل كقطعة ايقونية جوهرية في المدينة .
- ***التعقيد في التنوع :-*** غالبا ما يشار الى ان التعقيد مرتبط بالشخصية المميزة لأي هيكل انشائي ، ويتحقق ذلك في هذا المشروع ، حيث كان بالأمكان استخدام جسر كونكريتي ذو روافد ليؤدي نفس وظيفة جسر كلترافا ، لكن كان هناك حاجة الى بعض التعقيد لتحقيق سمة مميزة للجسر وبالتالي

تحقيق الأيقونة المطلوبة التي رغبت بها برشلونا ، فالتعقيد هنا لم ينشأ من العقود المائلة والدعامات المنحوتة التي تبرز خطوط العقد ، بل من الطريقة التي صمم بها المشروع بحيث يكون مرئيا من جميع الجهات ومن أي زاوية دون اخفاق في أي جانب من جوانبه ، واستخدام العقود المائلة يعني ان المتلقي يختلف انطباعه عن الهيكل عند النظر اليه من أي زاوية .

• ***التحسينات :-*** كان للتحسينات التي استخدمت في الجسر اثر جزئي في جعله فريدا ، واكثر هذه التحسينات وضوحا في التصميم هي استخدام العقود المائلة لتوفير استقرار جانبي للعقود الأساسية ، حيث كانت هذه الفكرة جديدة في تصاميم الجسور ، والتحسين الأخر والأكثر اهمية في هذا المشروع هو الأستعانة بمصمم واحد معماري وانشائي مما سمح بتحقيق اعلى طاقاته الكامنة وتحقيق النجاح ، وان طريقة كلترافا في النظر الى العمل من وجهة نظر معمارية ونحتية تعني بأن الشكل لم يكن مقيدا بأي طريقة ، وان الأبتكار الهندسي الأنشائي الذي استخدمه ساعد فقط لأكمال العمل ولم يكن حجر الأساس فيه. **(Tzonis Caso , 2005, p 68 -77 &) (Thoume, 2009 , p 1-5)**

ب ***- جناح جسر(Zaragoza) ، المالك :- Expoagua Zaragoza 2008 ، المعماريين :- تصميم :- Zaha Hadid مع Patrik Schumacher[6] ، معماري المشروع :- Manuela Gatto (معاون) ، 2005 – 2008 ، شكل (1-11)***

القياسات :-

الطول :- 270 متر (185 مترا من الجزيرة الى الضفة اليمنى + 85 مترا من الجزيرة الى ضفة المعرض) .

مساحة سطح جسر المشاة :- 2500 مترا مربعا .

مساحة الطوابق الكلية :- 6415 مترا مربعا .

مساحة المعرض :- 3915 مترا مربعا .

تاريخ انتهاء التشييد :- 13 \ 6 \ 2008 .

موقع المشروع :- يقع جناح جسر سرقسطة في اسبانيا ، ويعبر فوق نهر Ebro .

البرنامج التصميمي :- تضمن برنامج المشروع تصميم مساحة للعرض تركز على الاستدامة المائية تشمل جسرا للمشاة يخدم كبوابة لمعرض سرقسطة عام 2008 .

مكونات المشروع :- يتكون الجزء الخارجي للمشروع من امتدادين،لا يوفران طريق منحني لعبور النهر فقط ، بل قاعات للعرض متعددة الأستخدام ايضا، يتضمن الجزء الجنوبي جيب واحد يربط ما بين ضفة النهر وجزيرة وسطية فيه ، في حين الجزء الشمالي يتكون من ثلاثة جيوب تمتد من الجزيرة الوسطية الى ضفة المعرض ، وبالتالي فأن المحصلة الكلية للجسر هي اربعة جيوب طولية متداخلة مع بعضها البعض (ظاهريا) ، ويقابل كل عنصر من هذه الجيوب فضاء عرض خاص ومحدد ، وقد استخدم الفضاء المثلث الناتج من الشكل الكلي لمقطع الجسر لأمرار الخدمات تحت مستوى الأرضية .

المستوى الأنشائي :- تؤدي الجيوب الأربعة انفة الذكر وظيفة انشائية فضلا عن توفير تطويقات مكانية للفضاءات الداخلية للمشروع ، وتتقاطع مع بعضها البعض ويدعم احدهما الأخر مما يسمح لوزن الجسر أن يتوزع على أربعة مسنمات بدلا من عنصر رئيس واحد ، وساهم ذلك في تقليص حجم عناصر التحميل .

جاءت الفكرة التصميمة الرئيسة للمشروع نتيجة دراسات وبحوث تفصيلية في امكانيات شكل مقطع الجوهرة الماسية ، حيث يوفر هذا الشكل خصائص انشائية وتخطيطة ، كما يمكن له ان ينشر القوى بفاعلية كبيرة على طول السطح (كما هو الحال في الهياكل الفضائية) ، يسير مقطع الجوهرة على طول مسار منحن ، هذا القذف للمقطع المعيني وعلى طول مسارات مختلفة هو الذي ولد الجيوب الأربعة المنفصلة ، وان تراص وتشابك هذه العناصر وفر معيارين رئيسين للتصميم هما :- (أ) جعل النظام الأنشائي اقرب ما يكون الى الكمال ،(ب) سمح بوجود اختلافات بين الفضاءات الداخلية لكل جيب بشكل طبيعي (بديهيا) . حيث ان كل الجيوب

---

[6] **Patrik Schumacher :- احد شركاء شركة زهاء حديد للعمارة ومدير مؤسس في مختبرات AA لبحوث التصميم (AA Design Research Lab) ، درس كل من علمي العمارة والفلسفة**
http://www.patrikschumacher.com/Texts/PATRIK'S%20BIO.html .

متراصة مع بعضها البعض وفقا لمعايير دقيقة تهدف كلها الى تقليل مقطع الجناح الى اصغر قدر ممكن عندما يكون الأمتداد طويلا (في الجانب الذي يصل طوله الى 185 مترا من الجزيرة الى ضفة النهر اليمنى) وتوسيع المقطع عندما يكون الأمتداد اقصر (في الأمتداد الثاني الذي بطول 85 مترا) .

المستوى الحمالي :-

- ***الأندماج مع البيئة المحيطة :-***

يلعب غلاف المبنى دورا رئيسا في تعريف علاقته مع البيئة المحيطة والتغيرات في الغلاف الجوي ، حيث ان شكل الجناح الديناميكي مغلف بقشرة مميزة وذات مقياس ضخم ، وتعتمد نفاذية الأغشية التي تولد مناخا داخليا خاصا على حركة الهواء الطبيعية ، وتقول زهاء حديد :- ((لقد صممنا غلافا يغلق فضاءات المعرض لجناح الجسر ، مع ذلك يمكن ان تتخلله عناصر طبيعية ، فالبيئة الداخلية المصغرة للجسر تختلف عن المناخ الخارجي وتتطلب الحد الأدنى من البنى التحتية للتبريد والتدفئة ، وخصوصا اننا اخذنا بنظر الأعتبار رياح Cierzo المحلية عند تصميم القشرة الخارجية ، وتوجد فتحات هواء مختلفة تنقل الهواء مباشرة الى داخل المبنى وتعمل على تبريد الزوار في حرارة الصيف)) .

اثناء التصميم كان هناك بحث متواصل عن سطوح طبيعية ليتم تصميم القشرة الخارجية بناءا عليها ، ووقع الأختيار على قشرة سمك القرش لما لها من جاذبية ساحرة من حيث مظهرها و فعاليتها في الأداء ، حيث يمكن لهذا النموذج ان ينعطف ويلتوي بسهولة حول منحنيات معقدة وبنظام بسيط يتكون من خطوط تقاطع مستقيمة ، وقد تم اثبات الكفاءة الوظيفة والأقتصادية والجمالية البصرية لهذا النموذج في مشروع جسر سرقسطة .

- ***هندسة الشكل :-*** يتبع السطح السفلي هندسة الاشكال الحرة والتي نتجت من مرونة مادة تشيده ، اما الأنحناءات في المستوى العلوي فقد نظمت بأستخدام مقاطع اسطوانية قسمت الى 26.500 لوحا مستطيل الشكل بأحجام متساوية .

وتقول زهاء حديد :- ((ان مشروع جناح جسر سرقسطة يعتبر النواة وشرارة الأنطلاق في ممارسة تصميم الجسور)) ، وتعتبر فكرة المشروع المكون من جناح المعرض المغلق لعبور النهر فكرة مثيرة كليا ، وقد عملت زهاء حديد على تطوير التصميم الذي يزاوج بين العمارة والهندسة الأنشائية، وجمع التصميم الفريد من نوعه رغبة العميل في بناء فضاءات عرض مغلقة ، كما يوفر اتصال بصري مباشر مع النهر وتوفير الظلال من اشعة الشمس ، ويمثل هذا المشروع ثلاثين سنة من الدراسات التفصيلية والأبحاث التي قامت بها زهاء حديد حول تصاميم الجسور .

Z A H A H A D I D A R C H I T E C T S,) 2008) ، (http:// www.arcspace.com)

1-4 نتائج تحليل الأمثلة التطبيقية :-

- ***جسر Bach de Roda :-***

وفقا لمؤشرات الأطار النظري توصل البحث الى ان الحركة الملفتة قد تحققت في هذا المشروع من خلال استخدام نمط العقد المخترق بطريقة غير تقليدية وذلك بأستخدام عقود ثانوية ساندة اثرت بدورها على اعطاء ميزة للمقطع العرضي والشكل الكلي (بصريا وانشائيا) ، وقد تطلب هذا المشروع تحسينا في تفاصيله المنشئية حيث كان الهدف منه ان يكون ايقونة للمدينة و برغم الشكل المعقد الظاهر بصريا للجسر الا ان عناصره الأنشائية واضحة وبسيطة وليس فيها أي تعقيد حيث جاءت طبيعة استخدام التفاصيل الجمالية للتفصيل المنشئي بما يخدم طبيعة المشروع وهدفه ، كما لوحظ ان الجسر لم يحتوي على أي عنصر تزييني يغطي النقاء الأنشائي فيه .

استوفى الجسروظيفته الأنشائية وكان صادق في التعبير عن النظام الأنشائي والمادة البنائية و عبر المصمم عن شخصيته من خلال اسلوبه الخاص في التعامل مع النظام الأنشائي لأعطاء نتيجة جمالية تختلف عن جسور العقود الأعتيادية ،كما تحدى المصمم فكرة العقد المخترق بأستخدام اسلوب جديد ، حيث استخدم العقود الساندة الجانبية المائلة .

وبذلك نستنتج ان الجمال متأتي من مفردات انشائية وذلك وفقا لمؤشرات الأطار النظري التي تم اختبارها ، فضلا عن ان الجمال تحقق من خلال التداخل بين المفاهيم ولم

يظهر الفصل في تطبيق احدهما دون الأخران ، وادى ذلك الى تحقيق نتيجة جمالية ناتجة من تفاصيل انشائية من حيث التعامل مع النظام بأسلوب متميز غير تقليدي .

- ***جناح جسر Zaragoza :-***

امتاز المشروع ببساطة التصميم حيث تمثلت العناصر الأنشائية بأربعة مسنمات و دعامة واحدة عند الجزيرة الوسطية ، وتشابه العناصر واستمراريتها ووضوح طريقة نقل الأحمال فيها ،وقد نتجت الحركة الملفتة من استخدام نظام متداخل من المسنمات مما اظهر مخطط غير تقليدي لهذا النمط الأنشائي من الجسور مما ادى الى اظهار حركة غير مألوفة في المقطع العرضي، وبالتالي الشكل الكلي .

بالنسبة للتفصيل المنشئي فأن الهيكل الانشائي المتمثل بالمسنمات الأربعة والدعامة المركزية يعتبر ثقيل ، حيث ان عدد العناصر قليل وذات احجام كبيرة ، في حين الهيكل الأنشائي للتسقيف يعتبر خفيف ، فقد تم استخدام عدد كبير من عناصر نحيفة نسبيا فيه .

كما تضمن المشروع تجديد بعدة نواحي اهمها :- أ- الجمع بين مبنى ومشروع بنى تحتية ، ب – نظام انشائي غير تقليدي ، ج – جسر يجمع بين فضاءات عرض تحتاج الى غلق تام مع فضاءات اخرى تتمتع بأنفتاحية عالية على البيئة المحيطة .

وبذلك نستنتج ان الجمال متأتي من المفردات الأنشائية ايضا ومن خلال تطبيق المفاهيم الثلاثة بشكل متداخل ، حيث تحققت خصائص الجمال فيه وفق كل مفهوم .

اي ان مفهوم التكامل بين المستويين الأنشائي والجمالي متحقق ، حيث ظهر ان الجمال متعلق ومرتبط بالأنشاء ارتباطا قويا ، وكل المشاريع ترجع الى الجانب الأنشائي فيها لتحقيق الجمال ، مما يؤكد على ما جاء به البحث كون العناصر الأنشائية هي اهم عنصر في اغناء عمارة الجسور ويعتمد عليها المستوى الجمالي ، وبذلك تحققت الفرضية التي مفادها ان المستوى الأنشائي يتكامل مع المستوى الجمالي في عمارة الجسور .

5- الأستنتاجات العامة:-

أ- يعد الهيكل الأنشائي اهم عنصر في عمارة الجسور ، حيث انه يمثل الشكل المعماري للجسر .

ب- لا يمكن فصل المستوى الجمالي عن الأنشائي في عمارة الجسور لأن الجمال وفق كل المفاهيم التطبيقية متأت من المنشأ والشكل المنشئي .

ج- لا يمكن اختزال السعي الى الصفة الجمالية في تصميم الجسور الى مجموعة من القواعد الصارمة او الى برنامج حاسوبي معين ، حيث تتطلب المواد والأفكار والتقنيات الجديدة او رغبات الجهة الممولة ابتكار طرق جديدة للوصول الى الجمال ، وقد يؤدي ذلك الى انتهاك او تغيير القواعد القديمة شائعة الأستخدام ، وعلى اساس ان الجسور اصبحت تعد وسيلة للتعبير الفني لذا فأن مثل هذه الأنتهاكات متوقعة ومقبولة .

د- اختلاف الجسور عن الأعمال المعمارية ناشيء من الأمكانيات الأبداعية المتميزة الناتجة من خصائص ومميزات كل حقل ، حيث من المهم ان يدرك مصمم الجسر (بغض النظر عن اختصاصه معماري او انشائي او نحات) الجانب الفعلي الذي يبرز به كل من هذين الفنين على حدة ، اضافة الى معرفة مدى تعقيد العوامل التي تميز كل واحد منهما عن الأخر ، مع ذلك فأن ادراك الأختلاف بين تصميم الجسور واشكال الفن الأخرى يجب ان لا يغير من حقيقة ان تصميم الجسور كشكل من اشكال الفن يجب ان يشترك مع الخصائص والمميزات الأساسية المحددة والمشتركة في كل حقول الأعمال الفنية بغض النظر عن نوع الحقل .

هـ- ان الجسور ليست وظيفية فحسب ،حيث انها يمكن ان تكون اكبر من ذلك بكثير ، فهي تملك القدرة على اثارة الأحاسيس والعواطف والمتعة المطلقة للشكل ، كما انها يمكن ان تكون اعمال فنية مدنية تضفي البهجة والحيوية على الرحلات اليومية لمستخدميها او المارين بالقرب منها .

و- يجب النظر الى المحددات الجمالية في الجسور كنوع من اللغة، يمكن ان تنظم بطرق لا تعد ولا تحصى للوصول الى اظهار تعبير ملائم وبنفس الوقت فريد ومميز لكل منشأ ،

أي يجب النظر الى الحلول الجمالية كأفتراضات قابلة للتنقيح والتغيير لكي تتماشى مع الأفكار التكنولوجية والحاجات الأجتماعية والجمالية المتغيرة.

6- التوصيات :-

نتيجة ما تقدم من الأستنتاجات يوصي البحث بالأتي :-

أ- استحداث تعاون بين الأقسام المعمارية والمدنية (على المستوى التدريسي) للتعريف بأهمية الموضوع واهمية تحقيق التكامل بين المستوى الأنشائي والجمالي للجسور .

ب- استحداث التعاون على المستوى التنفيذي وتوعية الحقول المعمارية والمدنية في الدوائر الرسمية المعنية بالموضوع حول ضرورة هذا التعاون للأرتقاء بمستوى البنى التحتية للبلاد .

ج- تحديد مواقع الرؤيا المهمة اثناء عملية التصميم وجعل العناصر الرئيسة للجسر مرئية من تلك المواقع اكثر من غيرها .

المصادر الأجنبية :-

1- Asensio , Francisco , Cerver , ((Arco Colour , Thematic Architecture , New Bridges)) , publishing director :- Paco Asensio , without publishing year .

2- Bennett, David , ((The Architecture of bridge design)) , by Thomas Tepford publishing , London . (1997)

3- Berk,Aysu,((Geometrical Analysis of Bridge Forms and Their Feasibility in Structural Design)) , M.Sc. Thesis ,Graduate School of Natural and Applied Sciences of Middle East Technical University , ,Turkey , 2005.

4- Billington , David P. , ((The Tower and The Bridge , The new Art of Structural Engineering)) . Princeton , NJ : Princeton University Press . 1983 .

5- Charleson , Andrew w. , ((Structure As Architecture , A source book for architects and structural engineers)) , Architectural Press is an imprint of Elsevier , 2005 .

6- Chen, Wai-Fah,& Duan , Lian , ((Bridge Engineering Handbook)) , Boca Raton: CRC Press , 2000 .

7- Delony , Eric . ((Landmark American Bridges, Historic american engineering record)) , A Bulfinch Press Book , Little , Brown And Company , Bostion , Toronto , London , 1993.

8- Dock , Frederick C. , ((Context Sensitive Design , an approach to: BRIDGE AESTHETICS)) , Office of Bridges and Structures , Minnesota Department of transportation , December 1999, Find in the Follow link :- http://www.cts.umn.edu/Education/ContextSensitive/documents/Session_12.pdf

9- Frampton, K. . Studies in Tectonic Culture ((The Poetics of Construction in Nineteenth and Twentieth Century Architecture)) . Massachusetts Institute of Technology, quoted from Louis Khan , (1995) .

10- Gauvreau , Paul ,((The Three Myths of Bridge Aesthetics)) , University of Toronto, Canada , (2003) .

11- Gottemoeller , Frederick , ((Bridgescape ,The Art of Designing Bridges)), WILEY ,John Wiley & Sons , Inc,2004 .

12- Hart,Sara, ((Architectural Record Magazine)) , 06 / 2004.

13- Le Corbusier, ((Towards a New Architecture)) , by Frederick A. praeger Inc. New York . (1970)

14- Leonhardt , Fritz , ((Bridges Aesthetics and Design)) , by MIT Press Cambridge . Massacrestt , Germany . (1984).

15- Menn ,c , ((Aesthetics Bridge design)) in Bridge Aesthetics around the world , committee on general structures, Subcommittee on Bridges Aesthetics, Transportation Research Board, Washington, Dc. (1991)

16- Mock, Elizabeth B. ,((The Architecture of Bridges)) ,Copyright , ,The Museum of Modern Art .New York .1949 .

17- Moon , Sie-young , ((Aesthetic Approach on Bridge Pier Design)) , Seoul National University, Yooshin Engineering Corporation , without publishing year , Find in the Follow link :- http://www.iasdr2009.org/ap/Papers/Orally%20Presented%20Papers/Aesthetics/Aesthetic%20approach%20on%20bridge%20pier%20design.pdf

18- MOORE, C. & G. Allen..((Dimensions: Space, Shape and Scale in Architecture)) . Architectural Record Book. New York. USA , 1976 .

19- Nervi P.L., ((Structures)) by F.W. Dodge Corp, New York . (1956)

20- Potyandy , J.G , ((Aesthetic problems in Bridge design)). ACI .U.S.A. (1969).

21- Taly , Narenda , Ph .D.P.E. , ((Design of modern Highway Bridges)) by the Mc Graw Hill companies inc . U.S.A.(1998)

22- Thoume , C. J. ((A CRITICAL ANALYSIS OF SANTIAGO CALATRAVA'S BACH DE RODA BRIDGE, BARCELONA)) Proceedings of Bridge Engineering 2 Conference 2009 April 2009, University of Bath, Bath, UK .

23- Tzonis ,Alexander . & Caso ,Rebeca ,Donadel .((SANTIAGO CALATRAVA , The Bridges)) , Universe Publishing , a division Of Rizzoli international Publication , Inc .2005.

24- Wadowski , Med ,S.J., ((Conceptual Design of Shells, in concrete thin shells)) , ACI pub. Sp. 28 . (1971).

25- Wells , Matthew ,((30 Bridges)) , Watson – Guptill Publications ,2002.

26- Z A H A H A D I D A R C H I T E C T S , ZARAGOZA BRIDGE PAVILION [ZARAGOZA, SPAIN] , PRESS RELEASE , 14 June, 2008 , For Immediate Release .

27- Zuk, William. ((A Rating Index for Bridge Aesthetics)) . Concrete International 17 (August 1995): 45-47.

المصادر العربية :-

1- د. عبد العزيز ، احمد ، عباس ، ((النحت بين العضوية والعمارة)) ، رسالة ماجستير (قسم النحت) كلية الفنون الجميلة ، جامعة حلوان ، القاهرة ، 1974 .

2- عبد العظيم ، فيصل ، ((الكباري بين التصميم المعماري والإنشاء دراسة تحليلية)) ، جامعة حلوان كلية الفنون الجميلة عام 2003 .

3- البعلبكي ، منير ، ((المورد)) قاموس انكليزي عربي ، دار العلم للملايين ، 1985 .

المواقع الألكترونية :-

1- . http://images.google.com

2- http://en.wikipedia.org/wiki/Gateshead_Millennium_Bridge

3- http://www.galinsky.com/buildings/gateshead bridge/index.htm

4-www. Suicide.org

5- http:// www.arcspace.com

6- http://www.patrikschumacher.com/Texts/PATRIK'S%20BIO.html

7- www.googleearth .com

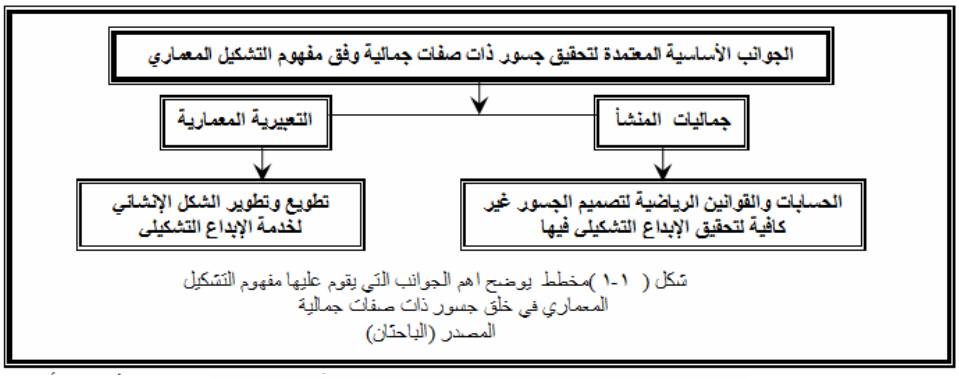

شكل (١-١)مخطط يوضح اهم الجوانب التي يقوم عليها مفهوم التشكيل المعماري في خلق جسور ذات صفات جمالية
المصدر (الباحثان)

شكل (١-٢)
جسر Gateshead Millennium ، تصميم مشترك بين شركتي WilkinsonEyre Architects و Gifford & Partners ، بمشاركة المعماري Keith Brownlie
(http://images.google.com)

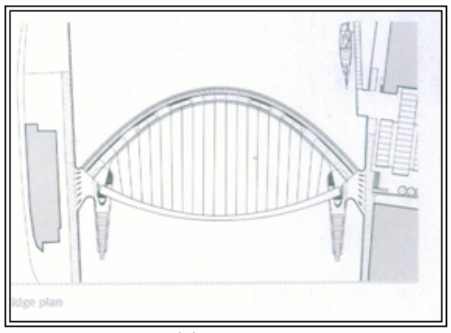

مخطط

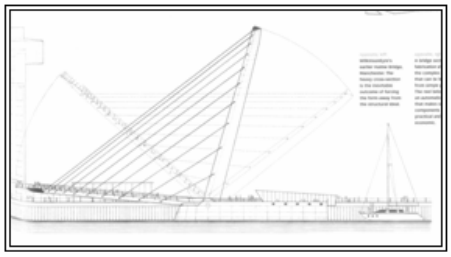

مقطع

شكل (١-٣)

مخطط افقي مقطع عرضي لجسر

Gateshead Millennium

(Wells ,2002 , p181 , 183)

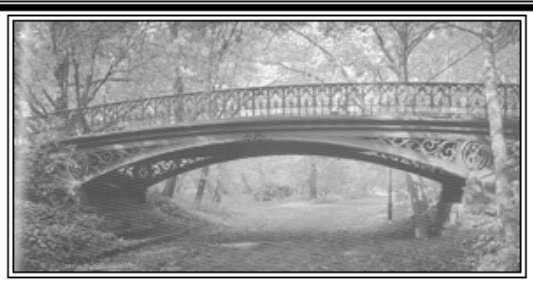

شكل (١-٤)

استخدام الزخرفة في تأكيد العناصر المنشئية / Reservoir Bridge Southwest

(١٨٦٤) Central Park ، New York ، المصممين

، Calvert Vaux &Jacob Wrey Mould

(Delony , 1993 , p49)

شكل (١-٥)
يوضح الفرق بين ضلوع العقد المزخرفة
وغير المزخرفة ، فالزخرفة المقننة يمكن
ان تكون لها اهمية في التشكيل
(عبد العظيم ، ٢٠٠٣ ، ص١٤٣)

شكل (١-٦)
جسر البوابة الذهبية (Golden Gate) / الولايات
المتحدة الأمريكية ، يربط بين San Francisco مع
(١٩٣٧) Marin Peninsula
(www. Suicide.org)

شكل (١-٧)
جسر Craigellachie تصميم Telford
(http://images.google.com)

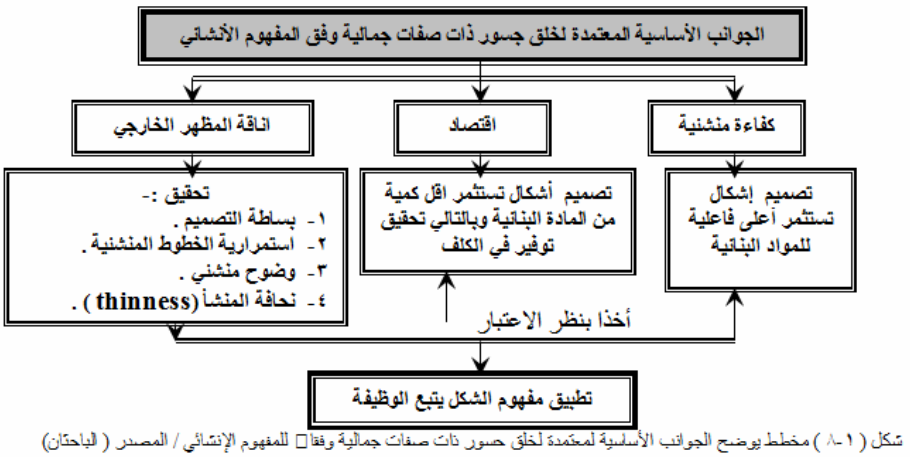

شكل (١-٨) مخطط يوضح الجوانب الأساسية لمعتمدة لخلق جسور ذات صفات جمالية وفقا للمفهوم الإنشائي / المصدر (الباحثان)

شكل (١-٩)
جسر Pont de la Tournelle /باريس
(Gauvreau ,2003,p3)

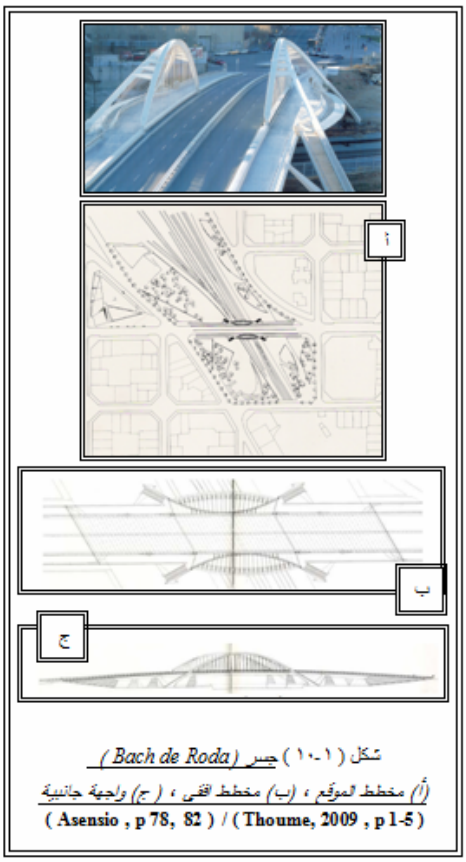

شكل (١-١٠) جسر (Bach de Roda)
(أ) مخطط الموقع ، (ب) مخطط افقي ، (ج) واجهة جانبية
(Asensio , p 78, 82) / (Thoume, 2009 , p 1-5)

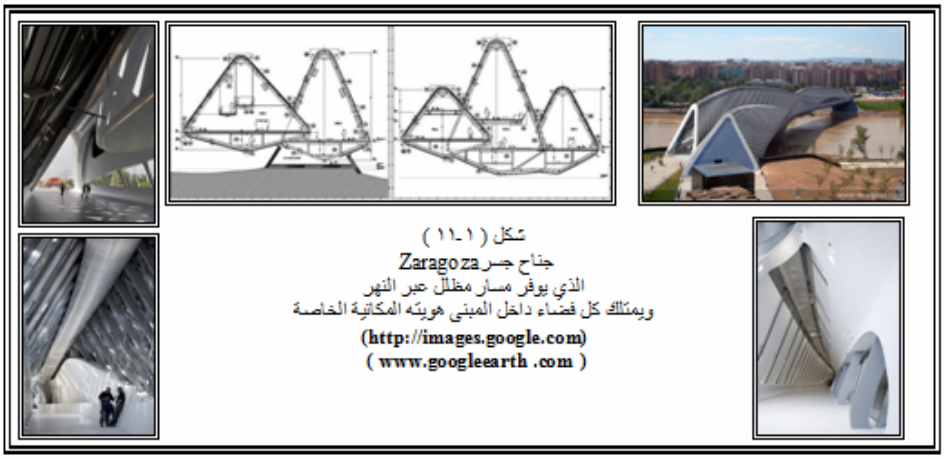

شكل (١-١١)
جناح جسر Zaragoza
الذي يوفر مسار مظلل عبر النهر
ويمتلك كل فضاء داخل المبنى هويته المكانية الخاصة
(http://images.google.com)
(www.googleearth .com)

الدال والمدلول بين الشكل وظله وإمكانية الفصل بينهما في المشهد الحضري

The signified and signifier between the object and its shadow and the possibility of their separation in the urban scene

Ammar Salim Dawood

Teacher assistant-Architectural department

Engineering college / Baghdad University.

People used to see shadow as an accidental result of light and object and as a sign of the object's existence .For example, when we see shadow we know an object exists. What happens if shadow is created without the object's existence?.

Dismantling the relation between the object and its shadow, in addition to the possibility of making the shadow as an independent design factor, constitute the research's problem.

The background relationship between the object and its shadow is presented according to the "signified – signifier" duality which has been extensively theorized by semanticists ,as it is made clear in Baflov's theory about the "conditional reflex" .This theory highlights the possibility that the "signified" has the same effect on the recipient as the " signifier". The research then focuses on the "shadow";its concept and characteristics ,and it specifies the main mechanisms by which the shadow could replace the original object .These mechanisms are employed to form what the research calls" shadow drawing elements";defined as design elements aiming at drawing shadows to provide formal richness by alternative means which would add beauty and interest to the urban scene in particular and the artistic work in general.

الملخص:

اعتاد كثير من الناس النظر إلى الظل على انه ناتج عرضي لوجود الضوء والشكل(الجسم)،مثلما اعتادوا ان يكون الظل دالة لوجود الشكل، فيكفي-مثلا- أن نرى ظل احد الأشكال لنوقن بوجوده، لكن، ماذا سيحصل لو قمنا باصطناع ذلك الظل مع غياب الشكل الأصلي؟؟.

محاولة تفكيك العلاقة بين الشكل وظله وإمكانية الارتقاء بالظل ليكون عنصرا تصميميا مستقلا غير مرتبط لزوما بوجود "شكل" مشابه له ،تلك هي مشكلة هذا البحث والتي سوف يحاول سبر أغوارها .

فمن خلال استعراض خلفيات العلاقة التي تربط بين الشكل وظله استنادا إلى ثنائية "الدال والمدلول" التي أسهب علم الدلالة في التنظير لها،مرورا بنظرية بافلوف في "الفعل المنعكس الشرطي " والتي كان احد نتائجها هو إمكانية ان يكون

للمؤثر من الدرجة الثانية "الدال " نفس التأثير في ذات المتلقي للمؤثر من الدرجة الأولى"المدلول "،وصولا إلى "الظل" مفهومه وخصائصه، تم في هذا البحث تحديد أهم الآليات التي يمكن من خلالها الاستعاضة بالظل عن الشكل الأصلي واستثمار ذلك لتكوين ما أطلق عليه البحث اسم "العناصر الراسمة للظل" والتي هي عبارة عن عناصر تصميمية غايتها الأساس هو رسم الظلال بما يوفره ذلك من ثراء شكلي يحقق بوسائل بديلة يمكن أن يضفي الكثير من الجمالية والتشويق على العمل الفني بشكل عام وعلى المشهد الحضري بشكل خاص.

1- المقدمة:

لا يستطيع الإنسان إعادة إجراء المسح البصري الشامل لكل الشكل المنظور في كل مرة يراه فيها،وهذا ما أطلق عليه "ابن الهيثم"((الإدراك بالمعرفة))(البصري-1983).فنحن نستطيع أن ندرك الكل من خلال إدراك احد الأجزاء كما تقرر ذلك نظرية "الجشتالت"(مولنار-1981)،فبالإضافة إلى الإدراك الحسي "الظاهر" الذي يدرك فيه الإنسان تفاصيل الأشكال،فان الإدراك العقلي الباطن يمكّن الإنسان من إدراك الشيء من خلال دواله أو آثاره (فخري-1980)،فقدرته على "التذكر" و"التخيل" تمكنانه من إدراك الكثير من الأشياء دون الحاجة الى التيقن من وجودها الفعلي،فيما تلعب الرؤية المسبقة " Pre Visibility " والقدرة على "التنبؤ" الدور الأكبر في إدراك الشكل ليس فقط في حالة الوجود والغياب،وإنما في إدراك مكانه وهيئته في المستقبل (مولنار-1981)،فهو يستطيع أن يدرك أن هذا الشكل مكعب ذو ستة أوجه من خلال رؤية ثلاثة أوجه فقط، وهو يستطيع ان يعرف ان هنالك سيارة قادمة نحوه فيتجنبها من خلال سماع صوت محركها فقط ،وهو لذلك أيضا يستطيع ان يدرك وجود احد العناصر من خلال رؤية ظله فقط.

إدراك الشيء من خلال إدراك جزء منه او من خلال إدراك آثاره او توابعه يعتبر مفصلا مهما يمكن من خلاله تفكيك بنية الشكل (كجوهر او معنى او كشكل مجسد) ومن ثم إعادة تركيبه لتوليد أشكال جديدة قد تكون أكثر "تشويقا" و "جمالا" في ذات الوقت الذي يمكن ان تكون فيه ارخص كلفة او اقل هدرا في الطاقة البشرية او "الكونية"،وعندما نتكلم عن "الشكل" فانه سيشمل بالتأكيد كل عناصره وتوابعه المادية وغير المادية التي يكون الظل احدها.

ربما كان القران الكريم من أوائل من أشار إلى وجود تلك العلاقة "الدلالية" بين الشكل وظله حينما قال في محكم آيه الكريم : ((أَلَم تَرَ إِلَى ربك كَيفَ مد الظل ولَو شَاء لَجعلَه ساكِناً ثُم جعلْنَا الشمس علَيهِ دلِيلاً)) [الفرقان : 45]، ورغم ان بعض الباحثين - من مجالات مختلفة - توقف عند هذه العلاقة "الدلالية" وفق بنيتها السطحية ليستشف من خلالها "أنواع "الظلال (الظل النافع والظل الضار) وطريقة حركة الظلال ومن ثم تخيل "اللا-متوقع " او المنفي من تلك العلاقة او ما يعرف بـ "الظل الساكن" (وزيري-2010)،فيما انبرت دراسات أخرى للاستدلال منها على حقيقة "ثبات الشمس ودوران الارض حولـ ـها"(المويل-2006)، فان دراسات أخرى متخصصة في العمارة ذهبت ابعد من ذلك عندما راحت تدرس العلاقة بين ثلاثية "الضوء والشكل والظل" وتأثير بعضها على بعض من حيث الإدراك والقيم التعبيرية (الامام-1989) او مناقشة تأثير تلك الثلاثية في تغيير الاستقطاب البصري واستخدام ذلك كأحد الآليات المعتمدة لمنع حدوث "الملل" ضمن المشهد الحضري (داود-1999)،فيما اقتنصت دراسات أخرى مصطلح "الدلالة" تحديدا لتضعه ضمن سياق النظرية "السيميائية" لتكتشف من خلاله علاقة أكثر عمقا الا وهي علاقة "الدال والمدلول" بين "الضوء" وبين "المعنى" الذي يشير

إليه،ليصاغ من خلال ذلك " منظومة دلالية للضوء" (البهادلي-1996)،أو أن يستقرؤوا منه " المستويات الدالة للمرئي والمحسوس" (الشاطيء-1996) ،ورغم ان هذه الدراسات اختصت تحديدا في دراسة الضوء كدالة للمعنى وليس الظل كدالة للشكل،ورغم انها اختصت في دراستها في حقل العمل المسرحي وليس العمارة وما يعتلي الفارق بينهما من اثر وخصوصية،وحيث انها حددت أهدافها بدراسة الضوء كـ"علامة مسرحية" وليس أي شيء آخر، ورغم إنها درست الضوء من حيث دوره" تقنيا" في إبراز الشخصية او إهمالها،أو إمكانياته في تغيير لون الأشياء او البيئة المسرحية ،فان هذه الدراسات ظلت تدور في فلك المعتاد من ان الظل مجرد ناتج عرضي لعلاقة الضوء بالشكل، لذلك أهملت التركيز عليه،مثلما أهملت أثره في تشكيل المشهد "الفني" عموما او المشهد المسرحي باعتباره مجال تخصصها، ولهذا ظلت تلك الدراسات بعيدة عن دراسة العلاقة الدلالية بين الشكل وظله ليس من خلال العلاقة"الرمزية" فقط،وإنما حتى على مستوى الدلالة البصرية بين الظل والشكل المكون له او بين الظل "كعنصر" وبين الشكل "الكل" (أي وفق الدلالة "الايقونية")،ولهذا فقد اشر البحث من خلال هذه العينة من الدراسات وجود الثغرة المعرفية كونها : عدم وجود دراسة مختصة في تحليل العلاقة الدلالية بين الشكل والظل ليس على مستوى العلاقة الرمزية فقط،وإنما ايضا باعتبار الظل عنصرا بصريا مستقلا غير خاضع بالضرورة للشكل المشكل له .

انطلقت فكرة هذا البحث من سؤال افتراضي وهو: **إذا كان الظل دالة للشكل،فماذا يحدث لو قمنا بالتلاعب بشكل الظل الناتج حتى لا يكون مشابها لشكل العنصر الذي شكله ؟؟.**

وكانت فرضية البحث الأولية هي :إمكانية الاستعاضة بالظل عن الشكل الأصلي لتحقيق الغاية الجمالية.

ووفقا لهذا فقد صنف البحث مشكلته العامة بأنها: **دراسة العلاقة بين الشكل وظله من منطلق ثنائية الدال والمدلول وإمكانية الفصل بينهما.**فيما حدد البحث مشكلته الخاصة بانها :**تفكيك العلاقة بين الشكل وظله ،وإمكانية الارتقاء بالظل ليكون عنصرا تصميميا مستقلا غير مرتبط لزوما بوجود "شكل" مشابه له.**

وبهذا كانت غاية البحث وهدفه هو: **وضع الآليات التي يمكن من خلالها فهم العلاقة "الدلالية" بين الشكل وظله وإمكانية التلاعب بهما لتوليد علاقات وتداعيات شكلية وضمنية جديدة تزيد في ثراء المشهد الحضري من جانب،وتزيد من قدرة المصمم في توليد أشكال جديدة من جانب آخر.**

شملت منهجية البحث الخطوات التالية:

-التطرق إلى مفهود الدال والمدلول الذي أفاضت الدراسات اللغوية السيميائية في التنظير له من اجل الوصول الى أهم العلاقات التي تربط بين الدال والمدلول والطرق التي يمكن من خلالها الفصل بينهما.

-التطرق إلى نظرية بافلوف في الانعكاس الشرطي والتي من خلالها يتم التعرف على مدى قدرة الدال على إحداث التأثير المطلوب بعد فصله عن المدلول.

-وضع الإطار النظري الذي يمكن من خلاله الفصل بين الظل وشكله.

-وضع الآليات التي يمكن من خلالها تطبيق الإطار النظري في الفصل بين الشكل وظله والتلاعب في مفصل العلاقة بينهما.

-طرح النتائج والتوصيات.

2-الدال والمدلول:

يعرف "الشريف الجرجاني" العلاقة بين الدال والمدلول بقوله ((هي كون الشيء بحالة يلزم من العلم به العلم بشيء آخر، والشيء الأول هو الدال، والثاني المدلول))(عبد الجبار-2001)،ومن قبله كان "أرسطو"قد أشار إلى أن ما يخرج بالصوت دال على الآثار التي في النفس، وما يكتب دال على ما يخرج بالصوت(عبد الهادي-2005)، وتحت نفس السياق يورد الإمام الغزالي القول((ان للشيء وجودا في الأعيان،ثم في الأذهان،ثم في الألفاظ،ثم في الكتابة،فالكتابة دالة على اللفظ،واللفظ دال على المعنى الذي في النفس،والذي في النفس هو مثال الموجود في الأعيان))(منقور-2001).

وقد صنف "الفارابي" الألفاظ الدالة إلى ثلاثة أقسام،هي الفعل والاسم والحرف، وفي ضوء حديثه عن"الحروف" يقول الفرابي بان الحروف ليست لها دلالة في ذاتها،إنما قيمتها الدلالية تتأتى مما تشير إليه،فيقول ((يستعمل "ما" في السؤال عن شيء ما مفرد،وقد يقرن باللفظ المفرد والذي للدلالة عليه أولا وهو الشيء الذي جعل ذلك الشيء دالا عليه))(منقور-2001)،ووفقا لهذا فهنالك "أشياء" ليس لها "دلالة" إلا فيما تشير إليه.

وقد قسم العرب الدلالة إلى:

دلالة عقلية: وهي أن يجد العقل بين الدال والمدلول علاقة ذاتية تنقله من أحدهما إلى الآخر، كدلالة العلة على المعلول(عبد الهادي-2005).

ودلالة طبيعية: وهي أن يجد العقل بين الدال والمدلول علاقة طبيعية تنقله من احدهما إلى الآخر كدلالة الحمرة على الخجل (عبد الهادي-2005)او دلالة الدخان على النار(منقور-2001).

والدلالة الوضعية: وهي أن يكون بين الدال والمدلول علاقة الوضع كدلالة اللفظ على المعنى (عبد الهادي-2005).

وفي ضوء حديثه عن "الإشارة" و"الإيماء" أثناء الخطابة حيث تنصرف الدلالة من المعنى الرئيسي الى المعنى الإيمائي يقول الغزالي ((وهي(أي دلالة الإشارة) ما يؤخذ من إشارة اللفظ لا من اللفظ،ونعني به ما يتبع اللفظ من غير تجريد قصد إليه،فكما ان المتكلم قد يفهم بإشارته وحركته في أثناء كلامه ما لا يدل عليه نفس اللفظ فيسمى إشارة فكذلك قد يتبع اللفظ ما لم يقصد به(....) وهذا ما قد يسمى إيماء و إشارة))(منقور-2001)،وهذا يعني ان هنالك ملحقات او توابع مع "الشيء" (او الشكل) تورد معه مع انها ليست من ضمن تركيبة الشكل نفسه.

بتحديده لطبيعة العلاقة بين الدال والمدلول، او ما يعرف حديثا بـ"القيم الحافة" والتي منها النظام الاشاري،والنظام النبري(النبر وهو الارتفاع والانخفاض في الصوت اثناء الخطابة)(النعيمي-1980)، والنظام الإيحائي،والنظام السياقي،ونظام المقام او الحالة،يحصي الجرجاني ثلاث دلالات،وهي دلالة الاقتضاء ودلالة الإشارة (التي أشار إليها الغزالي في أعلاه) ودلالة العبارة والتي يسميها الغزالي "فحوى الخطاب"، والتي هي عبارة عن النظام السياقي الذي عرفه الجرجاني بانه "المعنى الذي يتبادر الى الذهن من صيغة النص))(منقور-2001). ومن هنا نعرف بان فهم دلالة ما تقتضي معرفة مجمل "السياق" الذي وردت به،وان دلالة احد الدوال قد تتغير باختلاف "السياق" او المحيط الذي يوجد فيه.

2-1: إحلال الدال محل المدلول:

ذكر الدكتور "محمد حسان" في ضوء حديثه عن الرمز ودلالاته وإمكانية حذف احدهما او استبداله: ((هنالك طريقة أخرى للكشف عن هذه الرموز الطبيعية في الأدب،والطريقة هو عزل الدال عن المدلول او الشكل عن المضمون ثم النظر الى تأثير الدال في النفس))(منقور-2001).وتحت نفس السياق تنزع

التفكيكية إلى ان ((حضور الواقع على صورة متكررة يشحن بخصائص، الوعي بها لا ينهي إمكانية ميتافيزيقا الحضور على نبذ الأنموذج المؤسس كحضور مثالي. فالكتابة الصوتية عند دريدا بهذا المعنى تنزع إلى تذويب وجودها المادي تحت ضغط الحضور الواقعي إلى حضور المعنى، هذا الحضور المثالي الذي ينقلب إلى انتفاء الحضور وغيابه عن الإمكان.))،حيث يصب "دريدا" جلّ همه في إعادة الاعتبار للكلمة "المكتوبة" على حساب الكلمة "المنطوقة" بعد ان أصبح للأخيرة الدور الأكبر في إيصال المعنى فيما يوصف بـ"جينيالوجيا الكلام أو احتقار الكتابة "(ادريس-2010)، فـ((عندما تحقق الكتابة الصوتية حضورها كوعي على اعتبار أن الصوت يسمع ذاته داخل النص ولا يستمع إلى كاتبه، فمعنى ذلك أن غياب العالم، أو نسيان الدال، كنسق مادي للذات لا يبعد التفكيكية عن الميتافيزيقا.))،ولهذا فان ((ابتهاج وإعجاب الخطاب بالكلمة حال دون إيلاء الكتابة الاهتمام الذي تستحقه، من هنا يبدو أن هذا الاعتبار المطلق للكلمة يجب أن يكون حسب دريدا غير مقصود لذاته حتى تضمن المصادر الأولانية لثقافة ما شرعيتها المثالية وحتى يرتبط تأويل الموجودات بمنطق عقلاني، منطق الفكر المنتج لها كإحساسات متمركزة بـ"اللوغوس" أو خطاب أو عقل حاضر في قلب ذاته،لا ينفعل إلا بذاته،ولا يحتاج إلى سند أو ضمانة آتية من مرجع براني عليه))(ادريس-2010).

فالتفكيكية حسب دريدا كانت تعنى بالصورة"الكتابة" بنفس مستوى الاهتمام بالصوت"النطق" مع انه وحسب قول أرسطو الوارد أعلاه فان "ما يكتب دال على ما يخرج بالصوت"،ومن هنا تنزع التفكيكية الى أن يكون للدال"الكتابة" نفس مستوى المدلول -أي "الصوت"- باعتبار انه "إشارة لإشارة" كما يصفها "دريدا"(منقور-2001)،او إنها "دال باعتبار ومدلول باعتبار آخر" كما هي عند الغزالي(منقور-2001)، بمعنى آخر ان يتناوب الشكل صفة "الدال" او"المدلول" حسب السياق او الفعل.

حسب المدرسة الظاهراتية "الفينومينولوجيا" فان ((الإنصات إلى الذات وهي تتكلم مع اعتبار تفوق العوالم الداخلية على العوالم الخارجية يعكس الحضور القوي لأشكال الحديث الداخلي الذي لا يقيم وزنا للخارج إلا باعتباره دالا تقتضي ضرورة صياغته في انمحائه ونسيانه، من منطلق أن الكتابة لا تفترض الحضور المباشر للمتكلم فهي تتعالى عن التحيين، إذ العلامة المكونة لجسد النص تختلف عن الصوت أثناء التكلم إذ لا يمتلك النص خاصية البقاء، لانمحائه عند نهاية الحديث.))(ادريس-2010)،واذا ما أردنا القياس وفق منطوق العمل الفني "الصوري" وجدنا ان العلاقة بين الشكل والظل هي كالعلاقة بين الصوت والكتابة في هذا التفصيل تحديدا الا وهو ثبات الشكل واستقراره النسبي، مع تغير الظل وفناءه باستمرار حركة الزمن.

2-2:الأثر -الأساس:

حسب التفكيكية فان المفهوم الميتافيزيقي للزمن يحول من خلال منظور "الأثر- الأساس" archi-trace أي من المدلول إلى دال جديد يتجاوز التلقي البسيط إلى التلقي المركب. وحسب ذلك فان((تأويل التأويلات أشق من تأويل الأشياء)) (عبد الهادي-2005)،حيث أن الكثافة الدلالية للنص لا تجد صلابتها إلا في التأويل، ((فالصلابة أو الكثافة الدلالية المميزة للنص الميتافيزيقي مصدرها هو ذلك التراكم التكراري للتأويلات. يتعلق الأمر باستعارات مترسبة تسعى القراءة الجنيالوجية إلى اختراقها عبر خلخلة وتفكيك تماسك طبقاتها)) (عبد الهادي-2005)،وبهذا فان الأساس الواحد"المدلول" يمكن ان يكون له أكثر من دال يختلف تعقيدا او إدراكا حسب طبيعة المتلقي او مدى توغله في قراءة "النص" او "الشكل".

2-3:الغياب والحضور:

اهم ما ارتكزت عليه التفكيكية هي الإيمان بثنائية الحضور / الغياب ، و التي تعني أن الوجود لا يظهر حضوره إلا من خلال غيابه ، و هي محاوله منها لاستحضار الوجود المختفي(تاوريريت-2010)، الفلسفة الغربية منذ أفلاطون و حتى هيجل تعتبر فلسفة حضور فقط ، ولهذا هوجمت من قبل التفكيكية التي كانت تؤمن بالوجود الغائب الذي نسفته الفلسفة الغربية (فلسفة الحضور) ، فهي اعتبرت أن الشيء لا يحضر إلا بالاعتماد على الاختلافات و العلاقات الخارجية بوسائط مرجعيه أخرى(تاوريريت -2010) ،وجملة " أن الوجود لا يظهر حضوره إلا من خلال غيابه"،تزخر بكثير من التأويلات التي يكون احدها هو إمكانية أن "يحضر" الدال فيستعاض به عن المدلول"الغائب"،حيث لا يمكن ان يكون للغائب حضور إلا بوجوده بذاته أو بـ"دالة" له او عليه .

2-4:المطابقة والمفارقة والمغايرة بين الدال والمدلول :

يقول علماء الدلالة بان((الكلام اما يساق ليدل على تمام معناه،وإما ان يساق ليدل على بعض معناه،واما ان يساق ليدل على معنى اخر خارج عن معناه"(منقور-2001)،ووفقا لذلك قالوا ان علاقة الدال بالمدلول تقع على ثلاثة أصناف هي : دلالة المطابقة ودلالة التضمين ودلالة الالتزام،((فدلالة اللفظ على تمام معناه الحقيقي والمجازي هي دلالة المطابقة،ودلالة اللفظ على بعض معناه الحقيقي او المجازي هي دلالة التضمين،ودلالة اللفظ على معنى آخر خارج عن معناه لازم له عقلا او عرفا هي دلالة الالتزام))(منقور-2001).

وتحت نفس السياق صنف أصحاب النظرية السيميائية العلامة الى "الإيقونة والمؤشر والرمز"،فتكون ((العلاقة "ايقونية" عندما تكون العلاقة بين الدال والمدلول "تطابقية"،أي ان الدال لا بد ان يحيلنا الى مدلول واحد بالتشابه بينهما))(البهادلي-1996)،مثلا ان صورة الطائرة هي "أيقونة" للطائرة،واما المؤشر فتكون العلاقة بين الدال والمدلول سببية((فالإشارة دلالة تحددها مادتها الديناميكية وفقا للعلاقة الحقيقية بين الدال والمدلول،فيدل ارتفاع درجات الحرارة على المرض ويدل ضوء الشمس على النهار)) (البهادلي-1996).اما "الرمز" فيعرفونه على انه ((علامة تحيل الى الشيء الذي تشير اليه بفعل قانون غالبا ما يعتمد على التداعي بين افكار عامة))،ويضربون لذلك الأمثلة باللغة او التحية ،فمثلا في المسرح الياباني القديم ((فان الخطوط الحمراء على وجه الشخصية تدل على شهامة ونُبل البطل،أما الخطوط الزرقاء فتدل على الطابع الشرير للشخصية))(البهادلي-1996).

وبصورة عامة فإننا نستشف من الدراسات السابقة ان العلاقة بين الدال بالمدلول تتخذ ثلاثة احتمالات لا غير وهي :

المطابقة:وهي ان يكون الدال صورة طبق الأصل للمدلول (مثلا فان صورة لطائرة "دال" تطابق الطائرة"المدلول" بالكامل).

المغايرة (التضمين):ان الدال يغاير المدلول في بعض الأشياء ويشابه في بعضها(مثلا فان صورة لمقطع جناح الطائرة "دال" قد يدل على الطائرة رغم انه لا يمثل سوى جزء من الطائرة"المدلول").

المفارقة(الالتزام):أي ان الدال يفارق صوريا المدلول بالجملة رغم انه لازم له ضمنيا (مثلا فان صورة دوامات الهواء الحازونية المتشكلة خلف أطراف أجنحة الطائرة يمكن ان تكون "دالة" على الطائرة "المدلول" رغم انها لا تشبه شكل الطائرة في أي شيء).

3- نظريـــة بافلوف والفعل المنـعكس الشرطي:

في نظريته في "الفعل المنعكس الشرطي"،وضع بافلوف خصائص الاستعاضة عن المثير الحقيقي بالمثير الرمزي او الدلالي (المثير من الدرجة الثانية) لإحداث نفس الاستجابة ،فكانت التجارب التي أجراها على بعض الكلاب تتضمن تعويد الكلاب على تقديم الطعام لها بعد ضرب الجرس،حيث كان لعاب الكلاب يسيل بشدة (فعل منعكس لا شرطي) كلما رأت الكلاب الطعام وهو قادم إليها او شمت رائحته(حافز لا شرطي)،وحيث انه اعتاد ان يقدم لها الطعام بعد ان يدق الجرس،فقد لا حظ بافلوف ان لعاب الكلاب أصبح يسيل تدريجيا وبنفس الشدة بمجرد ان يدق الجرس حتى بدون ان ترى الكلاب الطعام او حتى ان تشم رائحته !،وحينها أدرك بان دق الجرس أصبح "رمزا"(او دالة) للطعام استطاع إحداث نفس الأثر "الفيسيولجي" الذي كان يمكن ان يحدثه ملامسة الطعام لفم الكلاب ، فسمى تلك الاستجابة بـ"الفعل المنعكس الشرطي" وسمى الجرس بـ"الحافز الشرطي"،واستنتج من تلك التجربة أن الاستجابات العصبية للفعل المنعكس الخاصة بسيلان اللعاب لا ترتبط بالعوامل الفيسيولوجية الخاصة فحسب بل ترتبط بعوامل نفسية أيضا،ليصل من بعد ذلك الى **ان المؤثر "من الدرجة الثانية (الشرطي او الثانوي) كان بإمكانه أن يؤدي إلى إحداث نفس الاستجابة او ردة الفعل التي يمكن ان تنتج لو استخدم المؤثر من الدرجة الأول (اللاشرطي او الأصلي)**.(تودز-2009) (وطفة-1996).

لكن هل تغدوا تلك السلوكيات (الانعكاسات الشرطية) دائمة وثابتة مع تغير الزمن عند من تستحدث عنده،ام انها قابلة للتغير و"الانطفاء" اذا ما تم مغايرتها؟؟،تجيب عن ذلك الجداول الإحصائية التي كان بافلوف قد دونها أثناء التجارب، والتي استطاع من خلالها ان يحدد ثلاث مفاهيم وهي:

1-التعزيز: لقد كانت تجارب بافلوف تقتضي قياس عدد قطرات اللعاب التي تسيل من فم الكلب كلما تعرض للمثير الشرطي(دق الجرس)،ومن خلال جداول الإحصائيات الخاصة بالتجارب وجد ان عدد قطرات اللعاب التي تسيل من فم الكلب خلال مدة محددة(ثلاثين ثانية) تزداد كلما زاد عدد مرات اقتران تقديم الطعام بدق الجرس،وسميت تلك العملية بعملية "التعزيز"السلوكي (وطفة-1996).

2-الانطفاء:في مقابل عملية التعزيز توجد عملية "الإطفاء" السلوكي، و((يشير هذا المفهوم إلى اضمحلال وتلاشي الاستجابة الشرطية حين تتوقف عملية التعزيز السابقة بصورة مستمرة ، ويعني ذلك أن المثير الشرطي يجب أن يعزز دائما أو بصورة متقطعة ليحافظ على فعاليته في إحداث الإرتكاس أو الاستجابة الشرطية))(وطفة-1996)، وقوام هذه التجربة هو تعريض الكلب لرنين الجرس دون تقديم الطعام له،مما أدى تدريجيا إلى "إطفاء" الاقتران الدلالي بين الجرس والطعام،مما أدى تدريجيا الى فقدان "المؤثر الثاني" او "الدال" لقدرته على توليد الاستجابة المطلوبة.

3-التعميم: لاحظ بافلوف في هذا السياق أنه عندما يتم إثارة اللعاب وفقا لصوت جرس معين فإن الأصوات المقاربة للذبذبة الصوتية المعينة يمكنها أن تؤدي إلى النتيجة نفسها وهذا ما يطلق عليه بافلوف مفهوم التعميم (وطفة-1996).وهذا يعني مثلا ان الحيوان الذي كانت تقترن لديه حركة أوراق الشجر باختفاء الذئب وراءها،فانه سيعتبر كل حركة لاوراق الشجر او سماعه لاي حركة لاوراق الشجر سوف يعتبر لديه مثيرا يستدعي الاستجابة(تودز-2009).وهذه النقطة مهمة جدا في تحليل الكثير من سلوكيات الانسان وخاصة فيما

يتعلق بالادراك السريع الذي لا يتطلب التحقق من حقيقة الشيء وهو الذي تعتمد عليه في الغالب ما يعرف بـ "الخدع البصرية "لتحقيق اهدافها.

3-1-المؤثر الثاني والاستجابة الأولى:

وفقا لتجاربه السابقة،فقد عرف بافلوف النظام الاشاري وفق ثنائية "المؤثر الاستجابة" فوصفها بانها ((نسق من المثيرات البيئية المباشرة والمسئولة عن إثارة سلوك الانسان او الحيوان))(عاقل -1977)،وتبعا لتجاربه على الكلاب ونظريته في "الفعل المنعكس الشرطي" فقد صنف بافلوف المؤثرات ضمن مستويين،"النظام الدلالي الأول" ويتضمن خصائص المؤثرات الطبيعية،و"النظام الدلالي الثاني" والذي وضع من ضمنه "الكلمات" باعتبارها مؤثر من الدرجة الثانية بإمكانها استفزازنا او تحريضنا او إحباطنا بنفس مستوى الفعـ ـل المادي(عاقل-1977)،حيث بإمكان الكلمات التعزيرية ان يكون لها نفس اثر السياط في جسد الإنسان مع انها مجرد كلمات.

4-الشكل وظله :

جاء في المعاجم اللغوية أن الظّل هو عتمة الفجر حتى طلوع الشمس ، أما الظّل بمعناه العام فهو يشمل الخيال الناتج عن الشخص أو الشاخص في اتجاه سقوط أشعة الشمس .والظل يكون غُدوةً وعشيةً ، ومن أول النهار إلى آخره ، وأما الفيء فلا يكون إلا بعد الزوال ولا يقال لما قبل الزوال : فيء ، وإنما سمي بعد الزوال فيئاً ، لأنه ظل فاء من جانب إلى جانب ، أي: رجع ،والفيء : الرجوع اما الظل فمعناه : الستر ،وظل الشمس : ما سترته الشخوص من مسقطها (شحرور-2010).

عندما يسقط الضوء على جسم غير شفاف تنشأ منطقتان :الأولى منورة وهي تقابل الضوء مباشرة , والثانية داكنة وهي التي لم يصلها الضوء وتسمى منطقة الظل الحقيقي .أما الظل الذي ينشره الجسم على السطح الموجود عليه فانه يسمى الظل الخيالي . وهذا الأخير يطول او يقصر طبقا لموقع المصدر الضوئي(عبد القادر-2009)،وهندسيا يمكن تحديد أربع أنواع من السطوح الدارجة في موضوعة الظل ،وهي:

1- أسطح النور :وهي الأسطح التي يصل الأشعة الضوئية مباشرة من المصدر .

2- أسطح الظلام:وهي الأسطح التي لا يصل إليها ولا تعكس أي كمية من الإشعاع الضوئي سواء المباشر او غير المباشر.

3- أسطح الظليل(Shade):وهي الأسطح التي تصلها الأشعة الضوئية المنعكسة فقط بسبب انحراف وجهتها عن توجه الضوء الساقط.

4- أسطح الظلِ(Shadow):وهي أسطح تقع ضمن اتجاه أسطح النور لكن حجبت عنها الأشعة الضوئية من المصدر بسبب وجود العوائق(داود-1999).

من جانب آخر فان شكل الظل الناتج عن شكل ما والساقط على سطح ما يعتمد على عدة عوامل وهي :

1- هيئة الشكل(حدوده الخارجية).

2- طبيعة الشكل(شفافيته ومدى صلادته).

3- طبيعة السطح المستقبل للظل(الذي يسقط عليه الظل).

4- الزاوية الأفقية والعمودية للأشعة الضوئية المشكلة للظل.(داود-1999)

5- شدة الضوء.

6- طبيعة الأسطح المجاورة للظل الساقط.(الامام-1989)

4-1: الدال والمدلول بين الشكل وظله:

((ألم تر إلى ربك كيف مد الظل ولو شاء لجعله ساكنا ثم جعلنا الشمس عليه دليلا * ثم قبضناه إلينا قبضا يسيرا)) [الفرقان : 45-46]،ربما كانت هذه الآية الكريمة أول من أشار الى العلاقة الدلالية بين الضوء والظل،فالكلمات التي وردت فيها والمقابلات وأضدادها التي تستدعيها كلمات مثل "الشمس(وتستحضر الضوء عموما)و"مد"(تستحضر نقيضها وهو القبض والتقصير) و "الظـ ـل"(وتستحضـ ـر الشكل المشـكل لـ ـ ـ ـ ـه) ، و"ساكنا"(وتستحضر تخيل سكون الظل وتداعيات ذلك امام صورته الحركية الحالية) ثم "دليلا" (وهي التي تحدد نوع العلاقة بين الضوء والظل)،كلها كانت كافية في الإشارة الى العلاقة الدلالية بين الشكل وظله.

وفي شرح هذه الآية تورد التفاسير القرآنية ان ((من هاهنا شرع تعالى في بيان الأدلة الدالة على وجوده ، وقدرته التامة على خلق الأشياء المختلفة والمتضادة ، فقال : "ألم تر إلى ربك كيف مد الظل"، (قال ابن عباس ، وابن عمر ، وأبو العالية ، وأبو مالك ، ومسروق ، ومجاهد ، وسعيد بن جبير ، وإبراهيم النخعي ، والضحاك ، والحسن البصري ، وقتادة ، والسدي ، وغيرهم : (هو ما بين طلوع الفجر إلى طلوع الشمس) . "ولو شاء لجعله ساكنا " (أي : دائما لا يزول ، كما قال تعالى : "قل أرأيتم إن جعل الله عليكم الليل سرمدا إلى يوم القيامة" (،) قل أرأيتم إن جعل الله عليكم النهار سرمدا إلى يوم القيامة] (القصص : 71 - 72 . [وقوله : (ثم جعلنا الشمس عليه دليلا) أي : لولا أن الشمس تطلع عليه ، لما عرف ، فإن الضد لا يعرف إلا بضده . وقال قتادة ، والسدي :دليلا يتلوه ويتبعه حتى يأتي عليه كله . وقوله" ثم قبضناه إلينا قبضا يسيرا" (أي : الظل ، وقيل : الشمس . "يسيرا " أي : سهلا . قال ابن عباس :سريعا . وقال مجاهد :خفيا . وقال السدي ; قبضا خفيا ، حتى لا يبقى في الأرض ظل إلا تحت سقف أو تحت شجرة ، وقد أظلت الشمس ما فوقه.وقال أيوب بن موسى " ثم قبضناه إلينا قبضا يسيرا " أي : قليلا قليلا ....)).(الدمشقي-2002).

يقول "ابن منظور":((يقال للرجل إذا مات وبطَلَ: ضحا ظِله. يقال: ضحا الظلُّ إذا صار شَمساً، وإذا صار ظِل الإنسان شَمساً فقد بطَلَ صاحِبه وماتَ.)) و((يقال للرجل إذا ماتَ ضحا ظِله لأنه إذا مات صار لا ظِل له.وفي الدعاء: لا أَضحى الله ظِلك؛ معناه لا أَماتَك اللهُ حتى يذْهب ظِل شَخْصِك.))(ابن منظور-2007)، ونقيضها قولهم "مد الله في ظلك" ،أي أطال الله في عمرك .

وفي الميثولوجيا الصوفية يحدد ابن عربي خمسة ادوار للظل (الظل حسب الميثولوجيا الشرقية عموما والميثولوجيا الصوفية تحديدا يوصف به الظل المادي الذي نتكلم عنه والظل المعنوي المتعلق بالغيبيات) وهي كما يلي :-

أولا: ارتباطه بالمصدر العلوي الذي عنه يحدث الفيض والظهور في صور محسوسة(أي ارتباطه بالضوء ان كان حسيا وبالنور ان كان معنويا).

ثانيا :ارتباطه بالصورة(أي الشكل المؤسس له)، وهو يؤكد أن الظل تابع للصورة المنبعث عنها حساً ومعنى . ومن هنا جاء تقسيمه للظل المعنوي والظل الحسي.

ثالثا:حاجة الظل إلى التموضع حسياً ومكانياً(أي الحاجة لوجود السطح الذي سيسقط عليه الظل)، ومن هنا يرتبط حديث ابن عربي عن الظل بالمكان (فالظلالات عمرتْ الأماكن) وعنده أن (لا خلاء في العالم) فالظل امتلاء، مقابل الإصرار على أن لا خلاء في العالم، ولذلك كلما تحدث عن الظل تظهر مفردات الحيز والامتداد والموضع.

رابعا :ارتباط الظل بالمكان مرتبط بمقولته أن لا خلاء

في العالم، ومن هنا تأتي مفردة (عمر) واشتقاقاتها ملازمة لمفهوم الظل، و كلمة "عمر" هنا تعني : إن كل منفصل عن شيء فقد كان عامراً للذي انفصل عنه، وبما أنه لا خلاء في العالم حسب مفهومه فإن الشيء المنفصل يعمر موضع انفصاله. وهذا يعني أن كلمة "عمر مرادفه لملأ، وان كان معنى عمر أيضاً مرتبط بمعنى الانفصال.

خامسا :ارتباط مفهوم الظل بمفهوم الانفصال، ويلاحظ هنا تلازم حضور كلمة الانفصال مع حديث ابن عربي عن الظل أو عما يسميه الوجود ألانبعاثي يقول: ابن عربي: "فعمر الشيء المنفصل موضع انفصاله بظله، إذ كان انفصاله إلى النور، وهو الظهور. فلما قابل النور بذاته، امتد ظله، فعمر موضع انفصاله، فلم يفقده من انفصل عنه. فكان مشهوداً لمن انفصل إليه. ومشهوداً لمن انفصل عنه.. فمن أسرار العالم أنه ما من شيء يحدث إلا وله ظل يسجد له.. سواء كان ذلك الأمر الحادث مطيعاً أو عاصياً.." (الوهيبي-2004).

اللافت من كل ما سبق في ثلاثية "الضوء الشكل الظل" ان كل منها هو دال للآخر ومدلول في نفس الوقت،فالشمس هي دليل الظل كما ورد في الآية الكريمة أعلاه ،لكنه في نفس الوقت دال عليها،فمن خلال طول الظل واتجاهه نستطيع أن نحدد اتجاه الشمس وارتفاعها،وكذلك الشكل هو دال على شكل الظل المنسوخ عنه،لكن الظل هو أيضا دال على شكل الجسم المسقط له ،وبالتالي كان كل منهما دال على الآخر ومدلول له.

4-2:الملازمة والمفارقة والمغايرة بين الشكل وظله:

جاء في تفسير قول الله تعالى ((ولله يسجد من في السموات والأرض طوعاً وكرهاً وظلالهم بالغدو والآصال)) [الرعد : 15] قولهم أن الكافر يسجد لغير الله وظله يسجد لله عز وجل.. وفي حديث ابن عباس: الكافر يسجد لغير الله وظله يسجد لله (الوهيبي-2004).وفي كل ذلك ما يشير إلى إن "الظل" يستخدم كدالة نيابة عن الشكل الأصلي"المدلول" من حيث إن "اختفاءه" او مفارقته للجسم الأصلي "المدلول" تشير الى موت الإنسان او "عدم" وجوده،ومن حيث "مغايرته" لفعل الإنسان،فحيث يستكبر الإنسان السجود لله يغايره ظله فيسجد رغما عنه،فيما تكون "الملازمة" بين الإنسان وظله حين يكون كلاهما "ساجدا" فيلتقيان في نفس نقاط التماس على سطح الأرض.

وهذه المطابقة والمغايرة،والمفارقة،هي مجمل العلائق التي يمكن ان تتشكل بين الشكل وظله والتي يمكن من خلالها التلاعب بالمشهد المنظور.وهي ذات العلائق التي تربط أي دال بمدلوله في أي مجال وكما ورد في سياق الحديث عن الدال والمدلول في اللغة.

4-3:ثبات الشكل وتغير الظل:

أهم ما يميز الظل عن الجسم هو اقتران اتجاه الظل ليس فقط بالشكل المشكّل له والسطح الساقط عليه،وإنما أيضا باتجاه مصدر الضوء الناسخ له،ولهذا فان أي حركة تعتري أي من هذه الثلاثة (الشكل والسطح الحامل للظل و مصدر الضوء)،فانه سوف يؤدي إلى تحرك الضوء او تغيره،فان كان مصدر الضوء متحركا فانه سيرسم للظل صورا دائمة التغير رغم ثبات الشكل الأصلي.هذا التغير رغم انه قد يكون قليل التأثير في بعض الأحيان،إلا انه في أحيان أخرى يكون له عظيم الأثر خصوصا عندما ينجح في تغيير مخطط الاستقطاب البصري لدرجة تختلف فيها مخططات الإدراك بصورة كبيرة،او حين ينجح ذلك التغير في تغيير تسلس استقبال الشكل مما قد يؤدي الى قراءة مختلفة جذريا عن القراءة الأولى(داود-1999).

4-4:الإطار النظري لعلاقة الظل بالشكل:

استنادا لما سبق يتحدد الإطار النظري لمجمل الاحتمالات التي تربط بين الشكل وظله استنادا الى علاقة الدال بالمدلول بانها:

1- **المطابقة:** وهو تطابق الظل مع الشكل حتى يعرف احدهما بالآخر بدون الحاجة الى دليل آخر.

2- **المغايرة:** وهو الاختلاف البين بين الشكل وظله،وهو يتدرج من الاختلاف اليسير الذي لا يدرك إلى الاختلاف الكبير حتى لا يعرف احدهما بالآخر الا بوجود بينة اخرى.

3- **المفارقة:**وهو وجود الظل مع انعدام الشكل، او وجود الشكل مع انعدام الظل.

5-آليات الاستعاضة بالظل عن الشكل الأصلي:

بعد ان بينا الإطار النظري لعلاقة الدلالة بين الشكل وظله، وكيف يمكن ان يكون للظل(الدالة او المؤثر الثاني) دور قد يغني عن وجود "المدلول"(او المؤثر الأصلي) نفسه ،فإننا سنبين هنا مجموعة الطرق او الآليات الممكنة او المستخدمة في توليد الأشكال المفارقة او المغايرة للشكل الأصلي والتي يمكن ان تولد نفس الأثر وهي كما يلي :

5-1:تكوين عناصر شبه ثنائية الأبعاد لتكوين الظل :

لعل أشهر وأقدم ما عرف في استخدام الأشكال الثنائية لتسقيط الظلال هو ما يعرف قديما وحديثا بـ"خيال الظل"،حيث كان الصينيون القدامى أول من ابتكر هذه الطريقة حين كانوا يضيئون مصباحاً زيتياً، ثم يضعون أمامه قطعة من قماش حريري مشدودة، وبين المصباح والقماش قطعة من الجلد المقسى، مقصوصة بشكلٍ معين لتشابه الشكل الذي يريدون الإيحاء به .فلا يرى الناظر من الجهة الأخرى سوى خيال هذه القطعة (اليسوعي2010).

شكل رقم (1)،نماذج من "خيال الظل" حيث تستخدم اشكال ثنائية الأبعاد لتشكيل ظلال توحي وكأنها ناتجة عن أشكال ثلاثية الأبعاد.(المصدر:اليسوعي-2010).

أهم ما يميز الظل الذي ترسمه الأشكال الثنائية الأبعاد عن الظل الذي ترسمه الأشكال الثلاثية الأبعاد هو ان الاخيرة يكون شكل الظل فيها مطابق تماما لشكل الجسم ثنائي الأبعاد،لان عملية التسقيط تجري داخل منظومة ثنائية الأبعاد أيضا (حيث يجري التحويل من الشكل الثنائي الأبعاد"الأصل" إلى شكل ثنائي الأبعاد أيضا الا وهو الظل)،وهذا على خلاف التسقيط الناتج عن الشكل ثلاثي الأبعاد حيث يكون الخلاف بين الشكل و ظله كبيرا نوعا ما وحسب اتجاه سقوط الضوء،فكلما تغير اتجاه سقوط الضوء تغير شكل الظل بدرجة كبيرا تبعا لطبيعة الشكل وهذا ناتج عن كون الشكل الثلاثي الأبعاد له اكثر من شكل ثنائي الابعاد عند التسقيط.

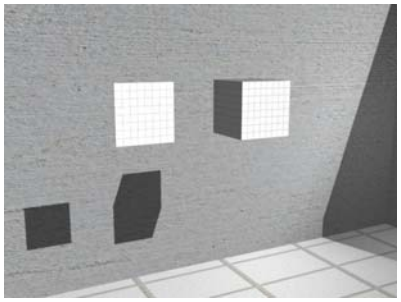

شكل رقم(2) ،الظل هو صورة ثنائية الأبعاد مسقطة عن شكل أحادي او ثنائي او ثلاثي الابعاد،لذلك فان التطابق بـين الشكل الثنائي وظله يكون اكبر بكثير من تطابق الظـل مـع الأشكال ثلاثية الأبعاد بسبب انتمائهم لنفس النظام ألبعدي،وهذه الصورة توضح تطابق الظل مـع الـشكل الثنـائي"المربـع" واختلافه مع الشكل الثلاثي"المكعب".(المصدر:الباحث).

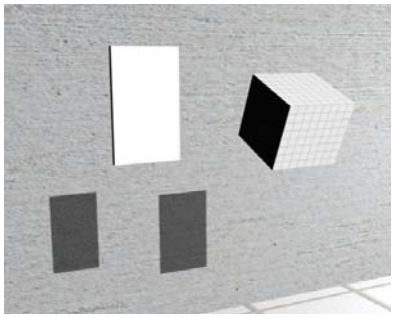

شكل رقم(3)،ويظهر كيف يمكن ان يكون للشكل ثلاثـي الأبعاد"المكعب" نفس ظل الشكل ثنائي الأبعاد"المربع" (انظـر كيف يتشابه الظلان مع اختلاف أصلهما).(المصدر:الباحث).

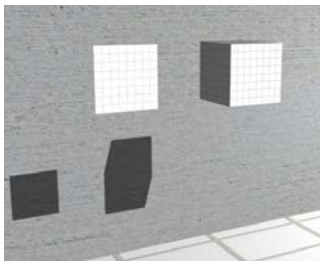

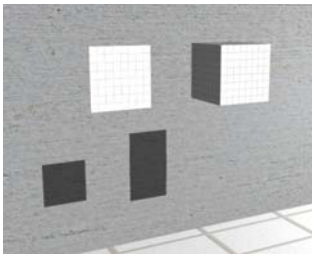

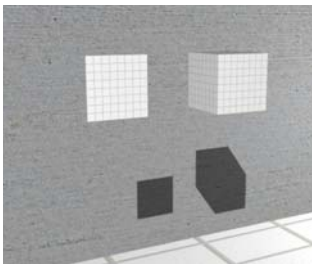

شكل رقم(4) ويشمل مقارنة بين طبيعة تغير شكل الظل المسقط من جسم ثلاثي الأبعاد"مكعب" وجسم ثنائي الأبعاد"مربع"،حيث تكون نسبة الاختلاف بين الظل وبين الشكل الثنائي الأبعاد المسقط له قليل حتى مع اختلاف زوايا أشعة الضوء،بينما نجد إن الاختلاف كبير جدا بين أشكال الظلال التي يسقطها نفس الجسم الثلاثي الأبعاد باختلاف زوايا أشعة الضوء(لاحظ ثبات ظل الشكل المربع نسبيا مقارنة بتغير شكل الظل للمكعب).(المصدر:الباحث).

5-2:اصطناع الظل بواسطة المرشحات(الظل الأبيض):

اشتهر في القرن التاسع عشر استخدام ما يعرف بالظلّ الأبيض،حيث تستعمل في هذه الطريقة ورقة معتمة،تُفرغ بطريقة يظهر فيها الشكل من خلال الظلّ الأبيض ،وحين توضع على سطح المصدر الضوئي او قريبة منه فسوف ترسم ذلك الشكل على السطح الذي يسقط عليه الضوء(اليسوعي-2010)،وقد استخدمت هذه الطرق حديثا بكثرة فيما يعرف باستخدام المرشحات، حيث توجد مجموعة كبيرة من "المرشحات" تركب على المصابيح الخاصة بالعروض الظلية او المسرحية،وعندما تضاء تلك المصابيح ترتسم صورة الظل على السطوح المضاءة(حديثا هنالك ما يعرف بجهاز "ماكلندلس" وهو عبارة عن كشاف "Projector" ذو عدسة مركزة للإضاءة يوضع أمام فتحة العدسة قرص شفاف عبارة عن شريحة زجاجية رسمت عليها صورا للمؤثرات المطلوبة كالمطر او الثلوج او البحر ،وعندما يدور ذلك القرص بواسطة محرك كهربائي فانه يرسم تلك المؤثرات على سطح المسرح او خلفيته(البهادلي-1996)).

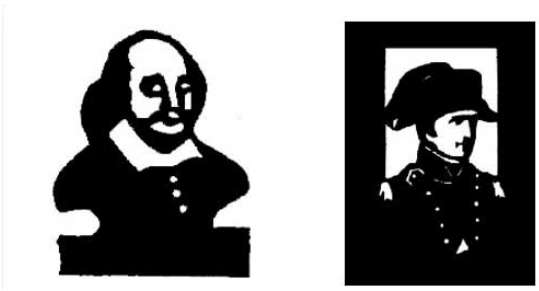

شكل رقم(5)،تقنية "الظل الأبيض" يقـصد بهـا تخـريم الصورة المراد عرضها على لوح ثنائي الأبعاد وعند تـسليط

الـضوء عليهـا ترتـسم الـصورة بواسـطة الظـل (المصدر:اليسوعي-2010).

3-5: الظل المستعار :

اشتهر في بداية القرن التاسع عشر أيضا أسلوب تشكيل الظلال بواسطة أصابع اليد،وفي الشكل رقم (6) يبرز مقدار "المغايرة" الكبيرة بين الشكل الحقيقي لليد،وبين الظل الذي يمكن ان ترسمه،لا يوجد تسمية علمية لهذه الطريقة من تسقيط الظل،لذلك أطلق البحث على هذا النوع من الظل اسم "الظل المستعار" والذي يعرفه البحث على انه **عملية تكوين ظلال لإشكال معروفة عن طريق عناصر لها ظلال مختلفة**.وسمى البحث هذه الطريقة بـ"الظل المستعار" لان الأشكال التي ترسم ذلك الظل إنما "تستعير" شكل الظل من أشكال حقيقية يوجد لها ظل مشابه كانت تُعرف به ،فمثلا قد يكون للأرنب ظلا مميزا له يمكن أن يعرف به ،لكن عندما نستطيع ان نشكل ظلا يشبه ظل الأرنب بواسطة أشكال لا تشبه الأرنب في حقيقتها(كاستخدام أصابع اليد) ،فهذا يعد "استعارة" لظل الأرنب تمت بواسطة أشكال أخرى(أصابع اليد) ، وهكذا لباقي الظلال.

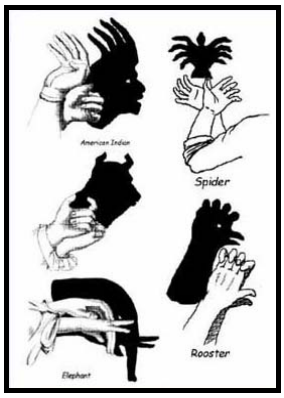

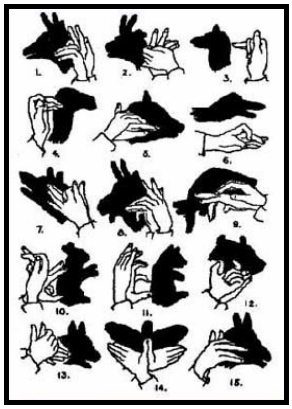

شكل رقم (6) ويمكن من خلاله ملاحظـة احـد نمـاذج "استعارة الظل" حيث تستعير اليد ظلال مجموعة من الأشـياء التي يمكن تشخيصها من خلال ظلهـا(المـصدر:اليـسوعي-2010).

ولعل في الأعمال الفنية التي انتجـ ـ ـها الفنانـ ـان SueWebster وTim Noble خير مثال على تقنية استخدام "الظل المستعار"، حين استخدم الفنانان مجموعة من المواد البالية "الخردة" لإنتاج(استعارة) ظلال لإشكال معروفة وذات قيمة عالية لتعطي الانطباع وكأنها مسقطة عن أشكال شبيهة فعلا(شكل رقم (6)).

فباستخدام مواد بالية ورخيصة الثمن تم إنتاج أشكال ظلية "دالة" لأشكال ذات قيمة عالية "مدلول" (كصورة المنحوتة في الشكل رقم (9))، وكانت المفارقة او "المتعة الجمالية" أو "الإثارة" تحدث عندما يتم الاكتشاف بان هذه الظلال ليست ناتجة عن الأشكال التي "توقعها" المتلقي والتي حاول الفنان استعارة ظلها، وإنما هي ناتجة عن مجموعة من العناصر التي لا تمت بأي رابط الى الشكل الذي أراد الإيحاء بوجوده من خلال دالة "الظل".

ولعل في هذه الأعمال ما يكفي لإثبات مغايرة الدال للمدلول تلك المغايرة التي قد تتعدى حد "المغايرة" إلى حد "المفارقة".

شكل رقم (7)،قد توحي هذه الظلال وكأنها مسقطة عـن نموذج مـصغر لمدينـة حديثـة(إحـدى أعمـال الفنانـان SueWebster وTim Noble المصدر:obvious-2007).

شكل رقم (8) ،لكن المفاجأة تحدث عندما نعرف ان هـذه الظلال إنما ناتجة عن مجموعة من المواد الخردة رتبت بشكل اسـتطاع الفنـان مـن خلالـه "اسـتعارة" ظـل لمدينـة حديثة(المصدر:obvious-2007)

شكل رقم (9) قد توحي هذه الصورة بأنها "ظل" إحـدى المنحوتـات المـشهورة للفنـان "مايكـل انجلـو" (المصدر:obvious-2007).

شكل رقم (10) لكن المفاجأة تظهر عندما يتبين ان هـذا الظل ناتج عن مجموعـة مـن الأنابيـب والخـردة،لينـتج "الدال"(الظل) ليغاير تماما حقيقة "المدلول" الذي نتوقعه،فتحدث الصدمة في عدم تطابق الدال مع المدلول "المتوقع" وتلك إحدى نتائج آلية استعارة الظل. (المصدر:obvious-2007)

6-العناصر الراسمة للظل:

استنادا لما سبق من حيث اعتبار الظل دالة للشكل وإمكانية تفكيك العلاقة بينهما ،واعتمادا على نظرية بافلوف في إمكانية الاستعانة بالمؤثر الثاني لإحداث نفس الاستجابة في نفس المتلقي،واعتمادا على آليات الاستعاضة بالظل عن الشكل الأصلي التي وردت أعلاه ،فان البحث يوجد بناءا على ذلك ما نستطيع ان نطلق عليه اسم "العناصر الراسمة للظل " والتي يضع البحث تعريفها بالقول بأنها: عبارة عن عناصر تصميمية تكون غايتها الأساس "رسم" الظل باعتباره احد عناصر التكوين الأصلية للاستفادة منه في خلق المشهد التصميمي . وهي بذلك تختلف عن باقي العناصر المعروفة كالمظلات او كاسرات الشمس او حتى الزخارف والمشربيات "الشناشيل"،لان غاية هذه العناصر الأساسية هو رسم الظل كعنصر بصري وليس تكوين الظل من اجل الحماية من حرارة الشمس او أي غرض اخر.وقد تستخدم هذه العناصر احد الآليات الواردة أعلاه لتحقيق هدفها،فقد تستخدم آلية الظل المستعار لرسم ظلال لإشكال معروفة بأدوات وعناصر مغايرة، أو أن تستخدم أسلوب "التخريم" أو مرشحات الضوء لرسم الظلال على أوجه البنايات (ويعزز دور هذه الآلية في المشهد الليلي عندما تستخدم الإضاءة الاصطناعية تحديدا)،أو أن نستخدم الأشكال الثنائية الأبعاد لتشكيل الظلال ورسمها على سطوح الأبنية .

شكل رقم (11) مجموعة مـن أعمـال SueWebster " وTim Noble " نلاحظ فيها مفارقة الدال"الظل" عن المدلول بشكل كبير حتى لا يكاد يصدق فعلا بان هذه الظلال ناتجـة عن هذه الخردة التي أمامها! (المصدر:obvious-2007).

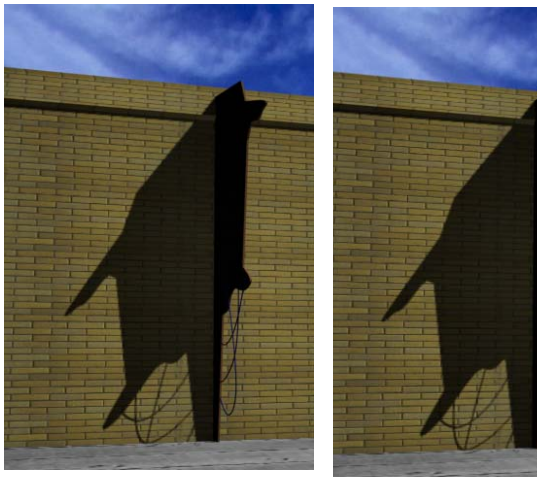

شكل (12)،الصورة في اليمن تظهر وكأنها صورة ظـل لأحد الشناشيل التقليدية،لكن في الصورة علي اليـسار يظهـر بان توليد ذلك الظل لم يكن بفعل "شنشول" حقيقي،وإنمـا تـم استعارة ظل الشنشول بواسطة لوح ثنائي الأبعاد قطع بحيـث يكون الظل الناتج منه مـشابه لظـل الشنـشول.(المـصدر: الباحث).

شكل رقم(13)،وهو عبارة عن عنصر ظلي "كتابي" حيث تستخدم لوحة ثنائية الأبعاد محفور فيها الكلمة المراد ان يظهر ظلها على الجدار، ثم تعلق اللوحة على الجدار عموديا وبشكل معكوس بحيث يكون أعلى الكتابة ملامس لسطح الجدار،وعندما يسقط ضوء الشمس عليها فانها سوف تعكس ظل الكلمة على الجدار فتظهر وكأنها خطت عليه بطريقة غير مألوفة.(المصدر:الباحث).

شكل(14) رسم توضيحي للشكل السابق يوضـح كيـف يمكـن وضـع لوحـة مخرمـة بالكلمـة المـراد إظهـار ظلها.(المصدر:الباحث).

6-1-وظائف العناصر الراسمة للظل:

يمكن تحديد أهم وظائف العناصر الراسمة للظل بما يلي:

1-إضافة عناصر جديدة للمشهد قد يكون له من التأثير ما يضاهي تأثير العنصر الأصلي وحسب مهارة المصمم في طريقة استخدامه.

2-حذف كل او أجزاء من العناصر الحقيقية،فقد يعمل الظل على التعمية او تغطية عناصر لها وجود حقيقي مما يعدم أي اثر حقيقي لها في المشهد،خصوصا اذا كان ذلك الظل شديد العتمة،وبما يحقق ذلك من تغيير في طريقة استقبال المشهد من قبل المتلقي.

4-التغيير من القيمة الضوئية واللونية لبعض العناصر الحقيقية مما يؤدي إلى تغيير صفاتها الحقيقية الظاهرية.

5-الإيهام والتشويق،فبإمكان العناصر الظلية أن تعطي انطباعات غير حقيقية تؤدي الى قراءة متوهمة للمشهد قد تكون أكثر تشويقا وجمالية من استخدام العناصر الحقيقية ،فرؤيتنا لظل احد الأشكال دون تمكننا من رؤية العنصر الحقيقي أكثر تشويقا بالتأكيد من رؤيتنا لذلك العنصر وظله كما هو في الطريقة المعتادة.

7-محددات استخدام العناصر الظلية في المشهد الحضري:

يعتبر التغير المستمر لحركة الشمس احد أهم العوامل التي بالرغم من إنها يمكن ان تولد أشكالا ظلية متغيرة لنفس العناصر مع تغير حركتها،إلا إنها في ذات الوقت تضع مجموعة محددات لعملية استخدام ما أطلقنا عليه في البحث اسم "العناصر الراسمة للظل"،وتلك المحددات تنطلق من جانبين الأول هو ان على المصمم ان يضع في حساباته ان شكل الظل الذي ينوي رسمه سوف يتغير اعتمادا على تغير زاوية سقوط الأشعة الشمسية مما يعني ان الشكل المحدد الذي يرغب في رسمه سوف لا يظهر إلا في أوقات معينة وذلك حسب زاوية سقوط أشعة الشمس(وقد تكون هذه النقطة إحدى الايجابيات خصوصا اذا ما عرفنا بان ذلك التغير قد يسهم في منع الملل من المشهد الحضري)،والعنصر الثاني هو إن حركة الشمس محددة بزوايا معينة لا يمكن تغييرها ،وبالتالي يجب ان تتوافق تصاميمه مع هذا المحدد ، وهذا على خلاف استخدام الإضاءة الصناعية والتي تتيح للمصمم تغيير زوايا سقوط الأشعة الضوئية من خلال التحكم باتجاه المصدر الضوئي حتى انها لتسمح له بإسقاط الظل إلى الأعلى وليس الى الأسفل دائما كما في الإضاءة الطبيعية(الظل الناتج عن الإضاءة الطبيعية يكون غالبا تحت الجسم او مواز له في حالات قليلة،لان الشمس تكون دائما أعلى الجسم،أما في الإضاءة الاصطناعية فبإمكاننا ان نضع المصدر الضوئي أسفل الجسم مما يتيح لنا إنتاج الظل أعلى الجسم).

8-الاستنتاجات:

1- الظل هو دالة للشكل في نفس الوقت الذي يكون فيه الشكل دالة للظل.

2- دراسة العلاقة بين الشكل وظله وفق مبدأ "الدال والمدلول" قادت إلى طرح فكرة الفصل بين الشكل وظله استنادا إلى نفس الإطار النظري الخاص باحتمالات الفصل بين الدال والمدلول الوارد في الحقول الثقافية الأخرى.

3- نظرية بافلوف في إمكانية أن يحل المؤثر الثاني محل المؤثر من الدرجة الأولى لتحقيق نفس الاستجابة أثبتت إن من شان الاستعاضة بالظل عن الشكل الأصلي تحقيق نفس الأثر او الاستجابة عند المتلقي،إن لم يكن أكثر إثارة وتشويقا انطلاقا من فكرة "اللا- متوقع" و"اللا- مألوف" ودوره في إحداث الانبهار او الإثارة و زيادة المتعة الجمالية.

4- تفكيك العلاقة بين الشكل وظله قادت إلى إن العلاقة بين الشكل وظله لا تقتضي دائما إن تكون علاقة "مطابقة" او علاقة التابع للمتبوع او ان يكون الظل مجرد ناتج عرضي للشكل والضوء،وان "المغايرة" و"المفارقة" في العلاقة بين الشكل وظله يمكن استخدامها لتوليد أشكال وعناصر جديدة تضفي على النتاج الفني -ومن ضمنه المشهد الحضري- الكثير من التشويق والجمالية.

5- هنالك عدة آليات يمكن استخدامها لتحقيق الفصل بين الشكل وظله أحداها هو استخدام أشكال ثنائية الأبعاد لتسقيط ظلال لأشكال ثلاثية الأبعاد،او استخدام المرشحات، فيما كان أبرزها هو آلية الظل المستعار .

6- استعارة الظل من أشكال معروفة ذات قيمة فنية عالية عن طريق استخدام أشكال رخيصة "القيمة" يمكن ان يكون احد الوسائل المبتكرة لإنتاج عمارة ذات قيمة فنية عالية وتكاليف مادية منخفضة،بما يسهم ليس فقط في فتح أبواب جديدة للابتكار الفني والتقني فقط،وإنما ايضا في المساهمة في تعزيز فكرة "الاستدامة" من باب لم يكن مطروقا من قبل باعتبار ان احد جوانب الاستدامة هو استخدام مواد غير مكلفة اقتصاديا(رخيصة) لإنتاج عمارة قيمة، او ما يعرف بالعمارة الفقيرة(او عمارة الفقراء).

7- التوجه نحو إشاعة استخدام العناصر الراسمة للظل قد يسهم في إنتاج "اسلوب" او "نزعة" معمارية جديدة يكون لتلك العناصر الدور الأكبر في تشكيل مفهومها وسياق عملها،وذلك سوف يندرج ضمن نفس السياق العام للعمارة الإسلامية ونظريتها في استثمار قوى الطبيعة بأقصى كفاءة من اجل خلق عمارة ممتعة و شيقة، وتحديدا في مجال استخدامها للظل والضوء واستثمار خصائصهما البيئية والجمالية.

9- التوصيات:

يوصي البحث في ختام طرحه ما يلي:

1- ضرورة الاهتمام بالظل باعتباره عنصرا تصميميا لا يقل أهمية عن باقي العناصر "المادية" خصوصا إذا ما اقترن استخدامه بطرق مبتكرة قد تؤدي الى ظهور نزعة معمارية (طرازا او أسلوبا) يمكن ان يضيف الى العمارة الكثير من الجمال والتشويق.

2- يوصي البحث بضرورة البحث عن آليات او "تقنيات" جديدة يمكن استخدامها لتوليد الظلال،قد يكون استخدام الليزر احد تلك التقنيات التي يوصي البحث باستخدامه لتوليد ظلال بعيدة عن وجود الشكل الأصلي.

3- يوصي البحث بضرورة التنظير لهندسة مختصة بدراسة الظل وطرق تسقيطه لما في ذلك من أهمية في اغناء المشهد الفني عموما والمشهد الحضري تحديدا بالكثير من المتعة والتشويق بوسائل رخيصة الثمن وسهلة التنفيذ،خصوصا اذا ما تم التوصل الى طريقة هندسية يمكن من خلالها معرفة شكل الظل الناتج مسبقا.

4- استنادا الى الفقرة أعلاه فان استخدام آلية "الهندسة العكسية" في إنتاج الإشكال انطلاقا من الظلال التي تولدها وليس إنتاج الظلال اعتمادا على الإشكال التي تسقطها، قد يؤدي ذلك الى إنتاج حقل معرفي جديد متخصص في "هندسة الظل" تكون احد نتائجه هو اغناء المعجم المعماري بكثير من العناصر الجديدة والمبتكرة اعتمادا على الظل الناتج وليس اعتمادا على الشكل المؤسس له .

-المراجع :

- obvious، Tim Noble and Sue Webster :2011\2\18 تمت زيارة اخر ،(2007) http://obviousmag.org/en/archives/2007/07/tim_noble_and_sue_websters_trash.html
- الامام.غسان:"النور والظل،فلسفة تعبيرية في العمارة التقليدية"،رسالة ماجستير،القسم المعماري،الجامعة التكنلوجية،بغداد،1989.
- الباهلي،رياض شهيد:"الضوء منظومة دلالية في العرض المسرحي"،اطروجة دكتوراه،كلية الفنون الجميلة،جامعة بغداد،بغداد،1996.
- البصري،حسن ابن الهيثم:"كتاب المناظر-المقالات1-2-3"،تحقيق :عبد الحميد صبرة،السلسلة التراثية،الكويت،1983.
- الدمشقي،اسماعيل بن عمرو بن كثير القرشي:"تفسير القران العظيم"،تحقيق سامي بن محمد السلامة،دار طيبة،الرياض،2002.
- الشاطيء،رعد عبد الجبار:"المستويات الدالة للمرئي والمحسوس في النص الضوئي"،اطروحة دكتوراه،كلية الفنون الجميلة،جامعة بغداد،بغداد،1996.

- المكتبة الاسلامية،القرطبي،محمد ابن احمد الانصاري(بلا):"الجامع لاحكام القران"،اخر زيارت تمت في (2011\2\14): http://www.islamweb.net/newlibrary/display_book.php?idfrom=2533&idto=2533&bk_no=48&ID=1972

- النعيمي،حسام سعيد:"الدراسات اللهجية والصوتية عند ابن جني"،دار الرشيد للنشر،العراق،1980.

- الوهيبي،فاطمة بنت عبد:" الظل في الميثولوجيا والمدونة التراثية والدينية والصوفية"،مجلة التراث العربي،العدد 95،اتحاد الكتاب العرب،دمشق،2004.

- تودز،دانيال:"ايفان بافلوف ،استكشاف الالة الحيوانية"،ترجمة هشام الدجاني،الهيئة العامة السورية للكتاب،دمشق،2009..

- داود،عمار سالم:"الضوء واثره في تغيير الاستقطاب البصري للمشهد الحضري"،رسالة ماجستير،الجامعة التكنلوجية،القسم المعماري، بغداد، 1999.

- شبكة "النبا" المعلوماتية،عبد الهادي،سعيد(2005):" من علم الدلالة إلى علم العلامات "،اخر زيارة في (2011\2\14): http://www.annabaa.org/nbahome/nba79/029.htm

- عاقل، فاخر :"معجم علم النفس"،بيروت،دار العلم للملايين،1977.

- عبد الجبار،منقور:"علم الدلالة،اصوله ومباحثه في التراث العربي"،اتحاد الكتاب العرب،دمشق،2001.

- فخري،ماجد:"ابعاد التجربة الفلسفية"،دار النهار للنشر،بيروت،1980.

- مدونة "forlive"،تاوريريت،بشير و سامية راجح(2010):" التفكيكية في الخطاب النقدي المعاصر"،اخر زيارت تمت في (2011\2\14): http://www.forlive5.com/?p=199

- مدونة "الحرية"، مسلم،حامد حماد،(2008):"الظل"،اخر زيـــــــــــارة تمـــــــــــت فـــــــــــي :2011\2\51، http://hamed.nireblog.com/post/2008/12/14/%D8%A7%D9%84%D8%B8%D9%84

- منبر التربية التشكيلية في الجزائر،عبد القادر،بوزيدي(2009):"الظل والنور"،منبر التربية التشكيلية،اخر زيارة تمت في (2011\2\14): http://tachkilia-mosta-algerie.maktoobblog.com/922958/%D8%A7%D9%84%D8%B8%D9%84-%D9%88%D8%A7%D9%84%D9%86%D9%8/8%D8%B1

- منتدى "صيد الفوائد"،شحرور،عبد القادر(2010):"المنتخب من ايات الظلال في القران"، ،اخر زيارة تمت في (2011\2\14): http://www.saaid.net/bahoth/tf.htm

- موسوعة الاعجاز العلمي،وزيري،يحيى(2010):" إعجاز وصف الظل والظلال في القران الكريم"،اخر زيارة في (2011\3\12): http://quran-m.com/container.php?fun=artview&id=964

- موقع "سلطانة الحبل بلادنس"،اليسوعي،سامي حلاق(2010):"مسرح خيال الظل"،اخر زيارة تمت في (2011\2\14): http://www.peregabriel.com/aveomaria/article.php?id=1341

- موقع الباحث العربي،ابن منظور(2007):"لسان العرب"،اخر زيارة تمت في (2011\2\14): http://baheth.info/

- موقع الدكتور كمال الموبل،موبل،كمال (2006):" التفسير التربوي لسورة الفرقان".اخر زيارة للموقع قي (22011\12): http://almowil.com/tafser%205.htm#%D8%A7%D9%84%D8%AA%D9%81%D8%B3%D9%8A%D8%B1_%D8%A7%D9%84%D8%AA%D8%B1%D8%A8%D9%88%D9%8A_%D9%84

%D8%B3%D9%88%D8%B1%D8%A9_%D8%A7%D9%84%D9%81%D8%B1%D9%82%D8%A7%D9%86.

- موقع"حكمة"، ادريس -عبد النـور (2010):" تفكيـك جاك دريـدا بـين الكتابـة والكـلام "،اخـر زيـارة فـي (2011\2\12):
http://www.hekmah.org/portal/%D8%AA%D9%81%D9%83%D9%8A%D9%83%D9%8A%D8%A9-%D8%AC%D8%A7%D9%83-%D8%AF%D9%8A%D8%B1%D9%8A%D8%AF%D8%A7-%D8%A8%D9%8A%D9%86-%D8%A7%D9%84%D9%83%D8%AA%D8%A7%D8%A8%D8%A9-%D9%88%D8%A7%D9%84%D9%83%D9%84%D8%A7/

- مولنار،فرانسو:"الوحدة والكل"،ترجمة نجلة فتي،مقال منشور في مجلة "فنون عربية"،العدد "2"،سنة "1981"،دار واسط للنشر،لندن.

- وطفة،علي اسعد:" تأملات في الجوانب العبقرية لنظرية بافلوف"،**مجلة المعلومات**، العدد 40، كانون الثاني، الكويت،1996.

تم بحمد الله

10

SIMULATION MODEL FOR THE ASSESSMENT OF DIRECT AND INDIRECT GEOREFERENCING TECHNIQUES IN ANALYTICAL PHOTOGRAMMETRY

H. Alwan, B. Saleem, and L. Khalid
Engineering of Surveying University of Baghdad

ABSTRACT

This paper compares between the direct and indirect georeferencing techniques in Photogrammetry bases on a simulation model. A flight plan is designed which consists of three strips with nine overlapped images for each strip by a (Canon 500D) digital camera with a resolution of 15 Mega Pixels.

The triangulation computations are carried out by using (ERDAS LPS) software, and the direct measurements are taken directly on the simulated model to substitute using GPS/INS in real case. Two computational tests have been implemented to evaluate the positional accuracy for the whole model and the Root Mean Square Error (RMSE) relating to (30) check points show that the indirect georeferencing is more accurate than the direct georeferencing. The computed RMSE of indirect georeferencing technique are (±0.0686 m., ± 0.0402 m.±, 0.3583 m.) in (X, Y, Z) respectively, while by direct georeferencing technique are (±0.1274 m., ± 0.1220 m., ± 0.5132 m.) in (X, Y, Z) respectively. Finally, the aim of this paper can be summarized as investigating the possibilities of using a simulation model to evaluate the applicability of direct and indirect georeferencing and analyzing the accuracy of both techniques.

الخلاصـة

يقارن البحث بين تقنيتي الإرجاع الأرضي (georeferencing) المباشر وغير المباشر في المسح التصويري اعتمادا على موديل محاكاة، حيث صممت خطة الطيران لتضم ثلاثة خطوط طيران بواقع تسع صور في كل خط وبتداخل أمامي وجانبي بين الصور الملتقطة باستخدام كاميرا رقمية نوع (Canon 500D) ذات دقة تمييز صورية (15 Mega Pixels) . إن حسابات التثليث أجريت باستخدام برنامج (ERDAS LPS) في حين أخذت القياسات على نموذج المحاكاة مباشرة للتعويض عن استخدام (GPS/INS) في الحالة الواقعية.
لتثمين الدقة الموقعية لكل النموذج تم حساب جذر معدل مربع الخطأ (RMSE) اعتمادا على (30) نقطة تدقيق وبتطبيق اختبارين حسابيين ، وجد أن تقنية الإرجاع الأرضي غير المباشر أدق من تقنية الإرجاع الأرضي المباشر. لأن نتائج جذر معدل مربع الخطأ في التقنية غير المباشرة كانت (±0.0686 m., ± 0.0402 m. , ± 0.3583 m.) في (X, Y, Z) على التوالي ، بينما كانت النتائج في التقنية المباشرة (±0.1274 m., ± 0.1220 m., ± 0.5132 m.) في (X, Y, Z) على التوالي أيضاً.
وبذلك يتلخص الهدف من البحث في إمكانية استخدام نموذج المحاكاة لتقييم تقنيتي الإرجاع الأرضي المباشر وغير المباشر عن طريق حساب جذر معدل مربع الخطأ(RMSE) بكلا التقنيتين ومقارنة دقتيهما.

KEY WORDS: Bundle Adjustment, Direct Georeferencing (DG), GPS/ INS, Indirect Georeferencing.

1. INTRODUCTION

Photogrammetry may involve rigorous mathematical calculations of ground coordinates by computer [Wolf, 2000], these computations require georeferencing: which occupy scaling, rotating, and translating processes to match a particular size of image with a position on ground area [Wing, 2005].

To carry out that, two quantities must be known: the coordinates of the camera lens perspective centers (Xo, Yo, Zo) "the position of exposure point" and the orientation elements (ω, φ, κ) of the image "the rotation matrix", as shown in **Fig.1**

Where (Xo, Yo, Zo) and (ω, φ, κ) are called the Exterior Orientation Parameters (EOP).

The georeferencing methods can perform by two different ways to derive (EOP) of an image:

- Indirect georeferencing
- Direct georeferencing

It is obvious that the camera orientation is a basic geometric problem that leads to determine the (EOP).

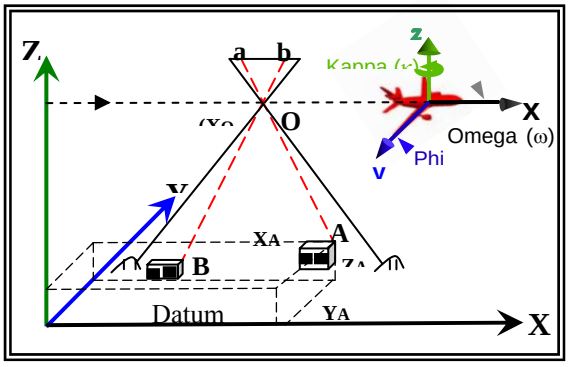

Fig. 1: the Exterior Orientation Parameters[Salama, 1980]

2. INDIRECT GEOREFERENCING

The **indirect** georeferencing approach uses conventional Aerial Triangulation (AT) that used a block of images with well-distributed sufficient number of (GCPs) for estimating the (EOP) and applying geometric constraint such as collinearity equations between the image points and object points. [Ebadi, 2006]

The Aerial triangulation is applied to the process of determining (X, Y, Z) ground coordinates of individual points based on measurements from photos, as shown in **Fig.2**

When the Image orientation is known, it is the key elements in any photogrammetric project to determine the three-dimensional coordinates of all points from images.

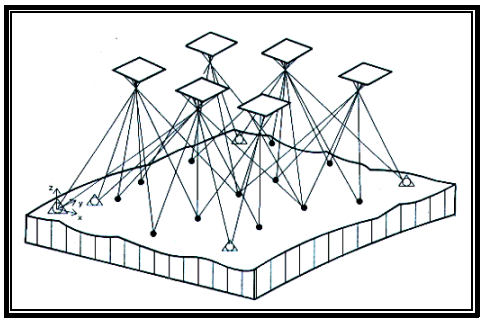

Fig. 2: Aerial Block Triangulation

3. DIRECT GEOREFERENCING

For **direct** georeferencing, EOP of an image can be determined directly by Differential Global Position System (DGPS) integrated with an Inertial Navigation System (INS).This allows the mapping to move from traditional aerial triangulation (AT) to direct georeferencing (DG) techniques.

Direct georeferencing is certainly one of the most significant applications of new technology in the mapping area. This approach combines the technologies of airborne GPS for determining the position of the plane and the camera. In addition, the velocity, with the abilities of (INS) for provides attitude, or orientation of the sensor with respect to the ground. Thus, the system that used in direct georeferencing contains the following:-

- Differential Global Position System Receiver (DGPS).
- Inertial Navigation System (INS).
- Camera.

As illustrated in **Fig. 3**

Fig. 3: Flight System (clockwise from upper left: aircraft, sensor head with camera and INS, data

logger with display and keyboard, data logger) [David, 2001]

4. COMPARISON BETWEEN DIRECT & INDIRECT GEOREFERENCING

As presented in earlier sections, the indirect georeferencing approach uses (AT) requires GCPs. When the availability of ground control points is in question, such as within forests, snow-covered grounds, desert, or along a coast line, the ability to resolve the EOP indirectly is limited. [Wing, 2005]

Also the time consuming ground control points have been reduced when using a block adjustment assisted by relative kinematics GPS derived coordinates of projection center.

In addition, some projects only require a single strip or single photo orientation. For instance, in the case where there are an existing Digital Elevation Models (DEM), the use of traditional AT to determine the EOP is unpractical because it requires excessive GCPs and additional overlapping photos.

Hence in many applications DG georeferencing is either the only practical solution, or the most cost effective solution [Schwarz and El- Sheimy, 2004].

The DG provides substantial benefits over AT. However, the accuracy achieved when using DG is limited by the accuracy achievable by DGPS, INS, and any remaining residual camera calibration error, which is not sufficient for some large scale mapping applications. At the same time, the stable geometry provided by direct EOP can reduce the number of required GCPs and tie points to a minimum.

5. EXPERIMENTAL WORK

To evaluate direct and indirect georeferencing, a simulation model is used to investigate the possibilities, then evaluating the accuracy of both techniques by analyzing the Root Mean Square Error (RMSE). The experiment consists of the following steps:-

- Establishing a lab simulation model.
- Preparing the suitable flight plan.
- Manufacturing a metal structure of flight plan.
- Establish and measure control and check points.
- Photo exposure stage.
- Block triangulation by ERDAS LPS 9.2.
- Comparison between the results of RMSE for the check points.

5-1. Establishing a lab Simulation Model

Building a model that used in the practical experience, which is an urban area, contains structures and features, varying in height like buildings, trees and river.

This is designed within a scale of (1/1000) with the dimensions of (156.5 cm. * 115 cm.) as shown in **Fig. 4**

Fig. 4: the simulation model

5-2. Prepared Flight Plan

The flight plan was designed on a scale of 1/25000, overlap 65%, and side lap 35%. After the transformation of the model values to the actual values in meters (m.), the air base become (B =140 m.), and spacing between adjacent flight lines (W = 390 m.). The simulated covered area dimensions are (1565*1150) m., which results in a block that contains three flight lines, and each one contains **nine** photos. The plan of flight is shown in **Fig. 5**

5-3. Manufacturing a Metal Structure for the Simulation Flight Plan

A metal structure is designed according to the flight plan to expose the photos.

The structure consists of an iron table with dimensions (120 * 160 cm.) and height (120 cm.) and equipped with iron carriers moveable on cushions fixed with screws to the table. This movable carrier is for the purpose of control the required flying height as shown in **Fig.6**. This designed metal stand can accommodate and modified for different flight plans.

The adjacent flight paths positions were determined on the cushion with a space of (39 cm.) according to the designed (W) measurement and exposure stations established on the moveable carriers every (14 cm.) according to the designed air base (B) measurement.

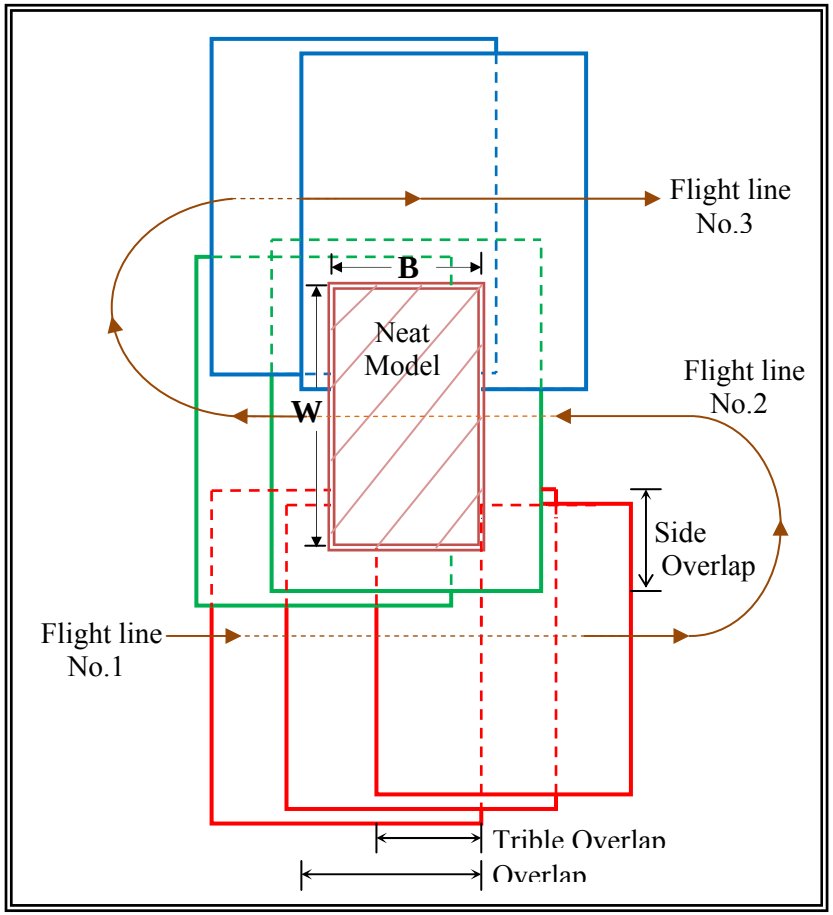

Fig. 5: details of flight plan [Wolf, 2000]

Fig. 6: metal structure of flight plan

5-4. Measured Control Points

The selection of points, which are suited to represent the ground control and check points need a careful procedure. Several artificial points were fixed to represent the full ground control points. The coordinates are measured by utilizing the sliding ruler in the metal framework as shown in **Fig. 7** and **Fig. 8.** The origin of the coordinate system was chosen at the lower left corner of the model, and the x-axis represents the edge of the horizontal model and the y-axis represents the vertical edge of the model while the z axis represents the direction of the plumb line. The measurement results listed in the **Tables (1) and (2)**.

Fig. 7: measurement of points coordinates

Fig. 8: fixing the GCPs coordinates

Table 1: the control points coordinate

No	Point ID	X (m.)	Y (m.)	Z (m.)
1	2	406.000	281.900	87.000
2	11	737.600	384.800	100.900
3	29	1219.000	147.500	110.500
4	56	892.000	1029.000	92.000
5	69	1307.000	590.000	87.800
6	78	1431.000	931.400	92.000
7	110	511.000	853.000	92.000
8	112	410.000	525.000	92.000

Table 2: the coordinate of thirty checkpoints

No	Point ID	X (m.)	Y (m.)	Z (m.)
1	57	893.200	750.300	96.000
2	61	946.200	712.500	96.200
3	62	1057.900	601.600	96.700
4	3	449.000	140.800	91.200
5	70	1292.200	632.500	89.200
6	71	1197.500	604.000	96.100
7	43	406.800	868.400	82.600
8	91	1372.500	206.600	88.500
9	92	680.000	553.700	129.700
10	95	444.000	335.600	90.700
11	98	1058.000	553.000	97.200
12	73	585.800	217.000	92.000
13	104	1198.600	549.500	94.700
14	106	459.100	281.100	90.200
15	107	603.000	495.500	115.600
16	108	444.000	413.000	91.900
17	94	1008.200	130.500	113.200
18	96	1090.900	136.200	111.300
19	109	1193.400	226.000	112.500
20	50	738.000	769.400	98.000
21	111	567.100	873.200	89.500
22	20	978.800	75.700	88.500
23	116	449.100	191.000	94.100
24	117	449.000	174.500	93.400
25	118	448.800	169.300	93.200
26	119	496.900	190.700	93.700
27	27	651.200	671.600	99.200
28	35	651.400	481.400	101.500
29	36	548.000	464.200	97.200
30	93	460.800	909.000	82.700

The distribution of the full ground control points, checkpoints, and photos in the simulated block is shown in **Fig. 9.**

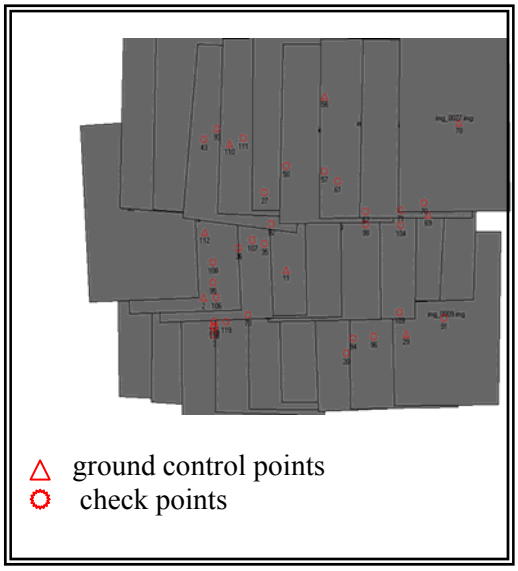

Fig. 9: distribution of ground control points and checkpoints in the simulated aerial block

5-5. Photo Exposure

Exposure was done by a digital camera of type (Cannon EOS 500D EF-S 18-55 mm)) as shown in **Fig. 10.** The pre-calibration of the camera was done by using Photo Modeler software; **Table 3** illustrates the calibration results.

The results according to the designed flight plan were twenty-seven photos which are illustrated in **Fig. 11.**

Table 3: the camera calibration report

Camera Parameter	Value (mm.)
Focal Length	26.075762
Xp - principal point x	11.278399
Yp - principal point y	7.565733
Fw - format width	22.590848
Fh - format height	15.0622
K1 - radial distortion 1	1.584e-004
K2 - radial distortion 2	-2.480e-006
P1 - decentering distortion 1	4.339e-006
P2 - decentering distortion 2	-3.129e-005
Pixel size	0.00475
Principal point shift xo	-0.1284
Principal point shift yo	-0.1157

5-6. Block Triangulation by ERDAS-LPS

The block triangulation computations were done by using ERDAS LPS 9.2. The direct georeferencing has done without the need for ground control points (the exterior orientation parameters supposed to be known) as illustrated in **Table 4** from the direct measurements on simulated model, substitution there from the GPS and INS measurements.

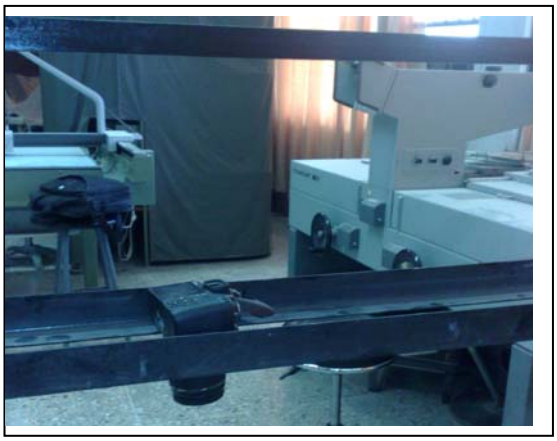

Fig. 10: photos exposure

Fig. 11: the simulated aerial block

The results of adjusted Aerial Block by direct and indirect georeferencing and their residuals are listed in the following **Tables 4 to 8**

Table 4: the fixed exterior orientation parameter

Strip No.	Image ID	Xo (m.)	Yo (m.)	Zo (m.)	Omega (degree)	Phi (degree)	Kappa (degree)
Strip 1	1	181.700	174.200	845.400	4.103	-6.999	-89.85
	2	333.000	166.000	857.300	3.265	-5.950	-91.043
	3	481.000	155.500	859.600	1.305	-3.776	-89.832
	4	630.200	156.600	864.300	1.846	-2.948	-90.330
	5	779.200	161.500	867.100	2.580	-1.804	-90.028
	6	929.600	168.700	868.300	3.898	-0.134	-89.781
	7	1088.400	165.400	862.700	2.190	1.273	-88.528
	8	244.000	166.100	862.600	2.489	2.419	-90.285
	9	1391.800	152.300	844.100	3.679	1.111	-89.808
Strip 2	10	1384.400	563.500	852.700	2.229	7.258	88.544
	11	1240.600	565.100	861.700	2.282	6.115	87.162
	12	1084.600	547.500	870.500	-0.914	3.066	88.962
	13	926.000	553.600	875.200	-1.612	2.159	90.311
	14	764.700	558.800	874.500	-1.387	1.882	90.280
	15	613.700	568.300	872.900	-1.586	1.315	90.959
	16	462.800	563.700	870.200	-2.141	0.688	91.775
	17	299.300	574.100	857.200	-1.032	-1.628	92.485
	18	135.100	585.800	843.600	0.924	-1.364	92.950
Strip 3	19	192.600	981.100	839.300	-3.079	-7.188	-90.826
	20	337.300	978.400	848.100	-3.168	-6.328	-90.479
	21	498.000	958.000	853.600	-4.582	-5.128	-94.526
	22	642.900	980.000	855.300	-3.867	-3.282	-90.932
	23	792.200	983.200	858.500	-2.826	-1.942	-89.649
	24	944.400	969.300	855.100	-4.746	0.622	-89.738
	25	1100.200	968.300	853.100	-3.322	0.625	-89.297
	26	1266.000	963.900	845.800	-3.263	0.618	-90.367
	27	1420.500	961.800	840.100	-1.555	0.808	-89.995

Table 5: the adjusted coordinate of checkpoints by direct georeferencing and their residuals

No	Point ID	X (m.)	Y (m.)	Z (m.)	V_x (m.)	V_y (m.)	V_z (m.)
1	3	449.040	140.885	90.781	0.040	0.085	-0.419
2	20	978.924	75.791	88.646	0.124	0.091	0.146
3	43	406.891	868.500	83.593	0.091	0.099	0.993
4	50	738.031	769.541	99.058	0.031	0.141	1.058
5	57	893.296	750.344	96.918	0.096	0.044	0.918
6	61	946.238	712.583	97.008	0.038	0.083	0.808
7	62	1057.954	601.742	97.239	0.055	0.142	0.539
8	70	1292.315	632.637	89.500	0.115	0.137	0.300
9	71	1197.638	604.086	96.414	0.138	0.086	0.314
10	91	1372.653	206.691	88.214	0.153	0.091	-0.286
11	92	680.030	553.918	130.131	0.030	0.218	0.431
12	95	444.100	335.769	90.631	0.101	0.169	-0.069
13	98	1058.326	553.117	97.680	0.326	0.117	0.480
14	73	585.849	217.208	92.026	0.049	0.208	0.026
15	104	1198.704	549.585	94.966	0.104	0.085	0.266
16	106	459.279	281.139	90.291	0.179	0.039	0.091
17	107	603.069	495.635	115.721	0.069	0.135	0.121
18	108	444.179	413.241	91.900	0.179	0.241	0.0
19	94	1008.359	130.644	113.469	0.159	0.144	0.269
20	96	1091.066	136.321	111.654	0.166	0.121	0.354
21	109	1193.522	226.047	112.593	0.122	0.047	0.093
22	111	567.216	873.301	90.641	0.116	0.101	1.141
23	116	449.229	191.037	93.785	0.129	0.037	-0.315
24	117	449.061	174.546	93.094	0.061	0.046	-0.306
25	118	448.953	169.347	92.941	0.153	0.047	-0.259
26	119	496.921	190.808	93.747	0.021	0.108	0.047
27	27	651.177	671.604	99.702	-0.023	0.004	0.502
28	35	651.544	481.612	101.919	0.144	0.212	0.419
29	36	548.167	464.208	97.777	0.167	0.008	0.577
30	93	460.931	909.101	83.405	0.131	0.101	0.705

Table 6: adjusted exterior orientation parameters by indirect georeferencing

Strip No.	Image ID	δ Xo (m.)	δ Yo (m.)	δ Zo (m.)	δ Omega (degree)	δ phi (degree)	δ kappa (degree)
Strip 1	1	3.025	3.037	1.049	0.2238	0.2223	0.0455
	2	1.571	2.858	0.774	0.2128	0.1158	0.0253
	3	1.473	2.802	0.744	0.2095	0.1061	0.0207
	4	1.425	2.858	0.858	0.2131	0.1030	0.0215
	5	1.411	2.470	0.757	0.1831	0.1009	0.0195
	6	1.797	2.369	0.792	0.1753	0.1290	0.0187
	7	1.892	2.325	0.897	0.1740	0.1377	0.0188
	8	3.178	2.885	1.316	0.2169	0.2403	0.0335
	9	6.990	6.704	3.686	0.5228	0.5109	0.1255
Strip 2	10	1.963	2.853	0.651	0.2146	0.1470	0.0303
	11	1.714	2.450	0.528	0.1834	0.1258	0.0189
	12	1.497	2.316	0.440	0.1713	0.1083	0.0136
	13	1.387	2.416	0.497	0.1777	0.0999	0.0136
	14	1.192	2.396	0.602	0.1762	0.0864	0.0135
	15	1.187	2.427	0.737	0.1783	0.0860	0.0147
	16	1.561	2.485	0.873	0.1820	0.1136	0.0184
	17	2.529	2.533	1.131	0.1869	0.1879	0.0260
	18	4.715	3.336	1.628	0.2422	0.3485	0.0520
Strip 3	19	3.817	3.862	2.635	0.2848	0.2726	0.0745
	20	1.937	3.102	2.374	0.2331	0.1414	0.0355
	21	1.608	2.830	2.102	0.2138	0.1171	0.0254
	22	1.746	2.902	2.041	0.2191	0.1247	0.0280
	23	2.201	3.037	1.988	0.2288	0.1587	0.0286
	24	1.484	2.755	1.759	0.2086	0.1053	0.0227
	25	1.728	2.865	1.641	0.2165	0.1238	0.0238
	26	1.963	2.857	1.500	0.2164	0.1424	0.0290
	27	2.771	3.084	1.469	0.2313	0.2034	0.0419

Table 7: The accuracy of exterior orientation parameters by indirect georeferencing

Strip No.	Image ID	Xo (m.)	Yo (m.)	Zo (m.)	Omega (degree)	Phi (degree)	Kappa (degree)
Strip 1	1	181.638	174.122	845.292	4.1006	-6.9966	-89.8390
	2	332.908	165.915	857.134	3.2626	-5.9478	-91.0320
	3	480.893	155.419	859.329	1.3023	-3.7737	-89.8215
	4	630.116	156.464	864.103	1.8437	-2.9456	-90.3197
	5	779.122	161.350	866.998	2.5779	-1.8013	-90.0177
	6	929.492	168.621	868.117	3.8957	-0.1312	-89.7701
	7	1088.292	165.262	862.547	2.1875	1.2701	-88.5177
	8	1243.873	165.912	862.415	2.4869	2.4160	-90.2747
	9	1391.655	152.189	843.998	3.6766	1.1089	-89.7977
Strip 2	10	1384.269	563.491	852.515	2.2266	7.2552	88.5336
	11	1240.484	564.964	861.550	2.2794	6.1121	87.1519
	12	1084.503	547.404	870.387	-0.9112	3.0632	88.9512
	13	925.915	553.503	875.039	-1.6092	2.1561	90.3005
	14	764.628	558.702	874.327	-1.3849	1.8792	90.2692
	15	613.639	568.160	872.796	-1.5831	1.3126	90.9482
	16	462.691	563.619	870.052	-2.1387	0.6856	91.7646
	17	299.151	573.974	857.022	-1.0297	-1.6259	92.4746
	18	134.984	585.654	843.450	0.9218	-1.3613	92.9396
Strip 3	19	192.484	981.014	839.151	-3.0764	-7.1858	-90.8157
	20	337.163	978.273	847.972	-3.1653	-6.3260	-90.4688
	21	497.944	957.907	853.492	-4.5799	-5.1259	-94.5155
	22	642.839	979.945	855.136	-3.8643	-3.2795	-90.9214
	23	792.111	983.090	858.303	-2.8240	-1.9398	-89.6385
	24	944.336	969.196	855.103	-4.7435	0.6198	-89.7276
	25	1100.176	968.212	852.948	-3.3197	0.6224	-89.2870
	26	1265.893	963.761	845.603	-3.2609	0.6160	-90.3565
	27	192.484	981.014	839.151	-3.0764	-7.1858	-90.8157

Table 8: the adjusted coordinates of the check points and their residuals by the indirect georeferencing

No	Point ID	X (m.)	Y (m.)	Z (m.)	V_x (m.)	V_y (m.)	V_z (m.)
1	3	448.914	140.784	90.785	0.086	-0.016	-0.415
2	20	978.846	75.635	88.403	0.046	-0.065	-0.097
3	43	406.811	868.390	83.189	0.011	-0.006	0.589
4	50	738.000	769.406	98.742	0.000	0.006	0.742
5	57	893.274	750.282	96.717	0.074	-0.018	0.717
6	61	946.219	712.499	96.835	0.019	-0.001	0.635
7	62	1057.945	601.669	97.154	0.045	0.069	0.454
8	70	1292.296	632.538	89.303	0.096	0.038	0.103
9	71	1197.608	604.003	96.270	0.108	0.003	0.170
10	91	1372.539	206.570	88.176	0.039	-0.031	-0.324
11	92	680.010	553.717	130.072	0.010	0.017	0.372
12	95	443.955	335.613	90.568	-0.045	0.013	-0.132
13	98	1058.226	553.041	97.457	0.226	0.041	0.257
14	73	585.728	217.044	91.923	-0.072	0.044	-0.077
15	104	1198.634	549.489	94.930	0.034	-0.011	0.230
16	106	459.133	281.091	89.969	0.033	-0.009	-0.231
17	107	602.940	495.451	115.596	-0.060	-0.049	-0.004
18	108	444.034	413.074	91.824	0.034	0.074	-0.076
19	94	1008.273	130.499	113.239	0.073	-0.001	0.039
20	96	1090.979	136.188	111.335	0.079	-0.012	0.035
21	109	1193.418	225.910	112.415	0.018	-0.090	-0.085
22	111	567.165	873.190	90.133	0.065	-0.010	0.633
23	116	449.094	190.925	93.784	-0.006	-0.075	-0.316
24	117	448.929	174.437	93.094	-0.071	-0.063	-0.306
25	118	448.822	169.240	92.941	0.022	-0.061	-0.259
26	119	496.801	190.682	93.650	-0.098	-0.018	-0.050
27	27	651.150	671.614	99.646	-0.050	0.014	0.446
28	35	651.411	481.426	101.815	0.011	0.026	0.315
29	36	548.035	464.128	97.369	0.035	-0.032	0.169
30	93	460.825	909.023	83.104	0.025	0.023	0.404

Table 9: comparison between the RMSE of check points

Ground Coordinate	RMSE by Indirect Georeferencing	MSE by Direct Georeferencing
X	±0.0686	±0.1274
Y	±0.0402	±0.1220
Z	±0.3583	±0.5132

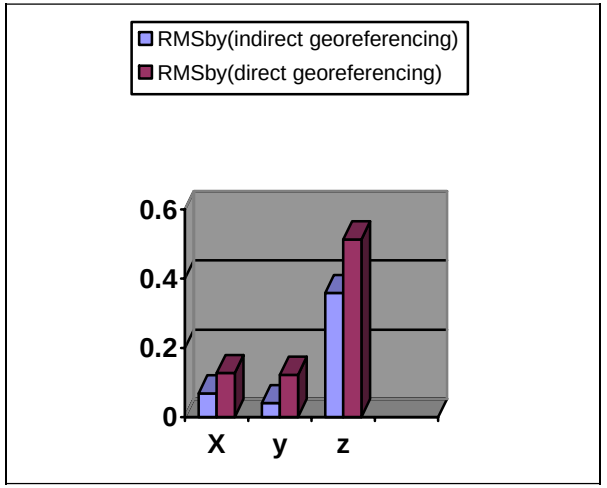

Fig. 12: the chart represented the statistical test

6- RESULTS DISCUSSION

By using ERDAS LPS and applying the direct and indirect georeferencing, the block triangulation leads to compute the coordinates of all points, which are tie points, check points, and other unknown points.

Then by computing the RMSE of each technique, the comparison results will be obvious that the indirect georeferencing gives a better positional accuracy when compared to the direct georeferencing technique as expected.

Table 9 represents the results that obtained from block triangulation in the two procedures. **Fig 12** explains the results from the statistical test.

7- CONCLUSION

From the experimental results obtained in this research the following conclusions are:-

1. The indirect georeferencing is more accurate than the direct georeferencing technique. The computed RMSE of indirect georeferencing are (±0.0686 m., ± 0.0402 m.±, 0.3583 m.) in (X, Y, Z) respectively, while by direct georeferencing are (±0.1274 m., ± 0.1220 m., ± 0.5132 m.) in (X, Y, Z) respectively.

2. The direct georeferencing gives an acceptable accuracy which is suitable for many engineering applications, like real time mapping and in the natural hazard conditions.

3. Simultaneous bundle adjustment using ERDAS LPS has sufficient accuracy level for large-scale mapping. Automatic tie point generation using exterior orientation parameters produced by GPS made dense and high accurate tie points and the block geometry were noticed to be better.

4. Direct georeferencing gives the exterior orientation parameters, projection center coordinates and attitude data, as the result of navigation process with GPS and INS observations without using control points in the navigation solution for airborne imagery and that will save the cost, time and efforts.

5. The Base/Height ratio of 0.25 is found to be sufficient when using digital cameras.

8- REFERENCES

▪ Alan Wing Lun Ip (2005), "Analysis of Integration Sensor Orientation for Aerial Mapping", MSc. Thesis, the University of Calgary, Department of Geomatics Engineering.

▪ David B., Alison B., Mark N.and Dan S., "GI-Eye II GPS/Inertial System For Target Geo-Location & Image Geo-Referencing", NAVSYS Corporation 14960 Woodcarver Road, Colorado Springs, CO 80921 August 2001.

▪Ebadi H., (2006), "Advanced Analytical Aerial Triangulation", 1st edition

▪ LPS, (2008). Leica Photogrammetry Suite Project Manager Version 9.2 Printed in the United States of America.

▪ Schwarz, K.P. (1995)"Integrated Airborne Navigation Systems for Photogrammetry", Proc. Photogrammetric Weeks '95, Stuttgart, pp. 139-153, September 11-14.

▪ Slama,C.,(1980)," Manual of Photogrammetry, 4th edition, American Society of Photogrammetry.

▪ Wolf R., Dewitt A., (2000) "Elements of Photogrammetry with Application in GIS", 3rd edition.

9- LIST OF ABBREVIATION

AT: Aerial Triangulation.

B: the air base

DEM: Digital Elevation Models

DG: Direct Georeferencing.

DGPS: Differential Global Position System.

E.O.P: Exterior orientation Parameter.

GCPs: Ground control points.

INS: Inertial navigation system.

RMSE: Root mean square error

تقليل كمية الحرارة المنتقلة من سقف المبنى المعرض للبيئة باستخدام تقنية المسطحات الخضراء أو المائية (دراسة تجريبية)

عاطف علي حسن/ أستاذ مساعد / معهد التكنولوجيا/ بغداد

الملخـــص :-

يهدف البحث الى دراسة السلوك (الأداء) الحراري للمبنى المشيد مسبقاً بعد تغطية سقفه المعرض للظروف الخارجية بالمسطحات الخضراء (استخدام تراب بسمك 50 ملم لزراعة الثيل الامريكي مع الرش بالماء بمعدل 0.0004 لتر/ثانيـة/م^2). لذلك تم تشييد غرفة أبعادها (4.5 x 4.5 x 3) م ، تقع في الطابق الثالث لمبنى في مدينة بغداد (خـط عـرض 33.2 درجـة شمالاً) مع استخدام عازل حراري نوع الستايريور سمك 200 ملم لتغطية الجدران والأرضية مـن الـداخل لتقليـل التـسرب الحراري وتم تزويد الغرفة بمكيفة هواء سعة 1 طن تبريد لتوفير الظروف الحرارية القياسية، وتم قيـاس درجـات الحـرارة للسطح الخارجي والداخلي لسقف المبنى ودرجة حرارة الظل من الساعة 5:00 صباحاً الى 10:30 مساءاً (18 سـاعة/يـوم) وخلال أشهر الصيف (الشهر الخامس (ايار) ولغاية الشهر التاسع (أيلول))/ 2009 .

تبين من خلال البحث أن استخدام المسطحات الخضراء ستوفر طاقة كهربائية تعادل 53% ممـا يـستهلكه الـسقف الاعتيادي (بدون تغطية) بينما استخدام المسطحات المائية سيوفر 38.0 % مما يستهلكه السقف الاعتيادي وخلال فترة الصيف.

الكلمـات الرئيسيـة : تقليل الحرارة المنتقلة من السطح الخرساني – اسـتخدام تقنيـات المـسطحات الخضراء والمائية – تقليل تأثير البيئة على درجة حرارة الحيز – تقليل الطاقة المستهلكة داخل المبنى.

The Heat Transferred Reduction From Building Roof Which Exposed to Environmental by using Grasses and Water (Experimental Study)

Atif Ali Hasan/ Assist Prof./ Institute of technology/ Baghdad

Abstract :

The object of this paper, is to study the thermal behavior of building roofs which covered by grass (used 50 mm sand as a base for American grasses and watered weeds by 0.0004 L/sec.m^2 for growth) or sprinkle the water (0.0004 L/sec.m^2) on that roofs, therefore , a room of dimensions (4.5 x 4.5 x 3) m was build in 3rd floor in building at Baghdad city (33.2°N) with thermal insulation of 200 mm thickness for other room sides and using Air – conditioner 1.0 ton of refrigeration to afford the standard thermal comfort, and measured the roof surfaces temperature from 5:00 Am to 10:30 Pm (18 hr/Day) during May to September month, it was found that, the grasses in roofs building was saved 53% from electrical energy for cooling purpose, while sprinkle the water on roofs saved 38 % only.

Key Words : Heat transferred reduction from concrete roofs, using grasses and sprinkle the water – effect environmental reduction on space temperature – building energy consumption reduction .

المقدمـــــة :

أن كمية الطاقة الكهربائية التي تـستهلكها الأبنية في العراق عموماً تقدر بحوالي (70)% من إجمالي الطاقة المنتجة في العراق عـام (2006) (علي حسن، مثنى– 2008)، بينما نـسبة الطاقـة الكهربائية المستهلكة لأغـراض تكييـف المبنـى المكعب الشكل والذي يتراوح حجـم (500-1000) m^3 ولا يزيد عدد طبقاته عن الثلاث، تكون فـي حدود (20-50) % من إجمالي الطاقة المستهلكة (علي حسن–2009)، فلذلك نجد أن للسقف تـأثير واضح في تغيير درجة حـرارة هـواء المبنـى وخصوصاً وهو يستلم طاقة شمسية تقارب 20% من إجمالي ما يستلمه المبنى. يمكن أن نميز جهود الباحثين في هذا المجال الى اتجاهين رئيـسيين : اعتماد الأول منها على زيادة مقدار قيمة المقاومة الحرارية للمقطع الانشائي للسقف باستخدام عوازل حراريـة بـسمك (70-100)mm (Hasan– 1984)، أو تغليف السطح الخارجي للسقف بمواد متوفرة محلياً (علي حسن – 2009). بينما الاتجاه الثاني يتمحور حول تقليل كمية الطاقة الحراريـة التي تصل الى السقف بامتصاصها باستخدام تقنية المواد ثنائية الطور (Amori– 2009)، أو جعـل السقف الأفقي يميل بزاوية قليلة (حسن – 2009). أو زيادة مقدار معامل انعكاس الطاقة الشمسية من السقف نفسه بتغيير درجة لونه وخشونته (الدوري وآخرون 1989).

مما تقدم يتضح بضرورة دمج الاتجـاهين في محور واحد، لذلك تم استخدام تقنية المسطحات الخضراء أو المائية والتي تعمل على تقليل كميـة الطاقة الممتصة وكذلك تلك المنتقلة خلال السقف.

الأبنية والبيئة:-

يقع العراق في المنطقة شبه المدارية الحارة الجافة والتي يغلب عليها المناخ الصحراوي، حيث يستمر فيها فصل الصيف لأكثر من سبعة أشـهر، تسطع الشمس خلاله فترات طويلة (لأكثر من (12) ساعة/اليوم)، وتصل درجة الحرارة الظل إلى أكثر من45م°) وبهذا تتعرض القشرة الخارجية للمبنـى إلى موجات حرارية تتناسب شدتها مع تغير الوقت وكما موضح في الشكل(1) مسببة أحـداث فـروق كبيرة بين درجتي حرارة الهواء الملامس (الطبقـة المتاخمة) للقشرة الخارجيـة والداخليـة للمقطـع الإنشائي للمبنى خلال ساعات اليوم الواحد، إضافة إلى المدى اليومي الكبير نسبياً لتغير درجات حرارة البيئة والذي يصل لأكثر من20م. (كامل شـعبان-1975). إن الكـسب الحـراري خـلال القـشرة الخارجية للمقطع الإنشائي للمبنى يتألف من مجموع كميات الحرارة المنتقلة في حاله الاستقرار (والذي ينشأ عن اختلاف درجتي حـرارة الهـواء داخـل وخارج المبنى) والحالة غير المستقرة (الناتجة عن اختلاف كثافة الإشعاع الشمسي الساقط على أسطح المبنى) وتتعقد عملية انتقال الحرارة خلال الـسقف لامتلاكه سعة حرارية (تعتمد قيمتها على كلاً مـن مقدار الموصلية الحـرارية، الحـرارة النوعيـة والكثافة لمكونات السقف). (Jones-87)، يجعلهـا تخزن جزءاً من الحرارة المنتقلة خلالها، حيـث لا تظهر تقلبات درجة حرارة السطح الخارجي (To)

لمقطع السقف بصورة سريعة بتقلبات مماثلة لدرجة حرارة السطح الداخلي (Ti) لمقطع السقف ، إي إن المواد الإنشائية المؤلف منها مقطع السقف ستزيد من قيمة المقاومة الحرارية للسقف نفسه (R) وبالتالي ستزيد من مقدار التأخير الزمني لانتقال الحرارة خلاله ، إضافة إلى تخميد ترددها العالي وكما موضح في الشكل (2) (الباحث)، ولكن بالرغم من ذلك فان درجة حرارة القشرة الداخلية لسقف المبنى سترتفع بعد فتره (قد تطول) ومما يؤدي إلى رفع درجة حرارة هواء الحيز الداخلي للمبنى لمستوى أعلي مما مؤشر في مستويات الراحة الحرارية المتناسبة مع طبيعة استخدام ذلك المبنى، مما يتطلب استخدام معدات التكييف على مدار ساعات اليوم الواحد لامتصاص هذه الأحمال الحرارية حال وصولها وتخفيض درجة حرارة هواء الحيز إلى ذلك المستوى المحدد مسبقاً، أي إن استهلاك الطاقة الكهربائية لأغراض تشغيل معدات التكييف يكون مرتبطا بكمية الحرارة المنتقلة خلال سقف المبنى، فتقليل تلك الحرارة سيقود إلى تقليل فترة تشغيل مكيفات الهواء وبالتالي تقليل كمية الطاقة الكهربائية المستهلكة لأغراض التكييف وبالتالي تقليل كمياتها المستهلكة.

الجانب التجريبي :

لغرض تحقيق هدف البحث في تقليل السريان الحراري خلال السقف الخرساني المسلح الشائع في التراكيب الانشائية للأبنية في عموم العراق، تم دراسة السلوك الحراري للسقف بعد زراعته بالثيل الأمريكي ومقارنته بالسلوك الحراري للسقف نفسه عند تغطيته بنفس كمية الماء المطلوبة لرش الثيل لتحديد أفضلها في تقليل تأثير البيئة على مقدار درجة حرارة هواء حيز المبنى، بثبوت المتغيرات التالية :

1. منطقة البحث/مدينة بغداد–خط عرض 33.2 درجة شمالاً (باعتبارها متوسط خطوط العرض المارة بالعراق.
2. الغرفة التي استخدمت للدراسة التجريبية أبعادها (3x4.5x4.5) م وكما موضحة في الشكل (3)، تقع في الطابق الثالث من مبنى، لتأمين عدم حجب أشعة الشمس من قبل الأبنية المحيطة
3. لغرض تقليل انتقال الحرارة من خلال جدران وأرضية الغرفة المعرضة للبيئة جهد الامكان، تم تغليفها من الداخل بمواد عازلة حرارياً (ستايربور) سمك 200mm ، لتثبيت السريان الحراري المؤثر من خلال السقف الى حيز الغرفة دون غيره.
4. مادة الانهاء الخارجية لسقف المبنى المحيط بالغرفة – البلاطات الخرسانية (الشتايكر) رصاصية اللون (40 x 800 x 800) ملم .
5. لون مادة انهاء الجدران الداخلية للغرفة والسقف هو اللون الأبيض.
6. تم الاعتماد على البيانات المتوفرة في (الدوري – 1992) لتقدير المعامل الاجمالي لانتقال الحرارة خلال مقطع السقف.
7. تم الاعتماد على البيانات الموضحة (1973–Rohsenow– Harthnelt)

لتقدير معامل انتقال الحرارة بالحمل الحر خلال هواء بيئة الغرفة (h)، تم افتراض أن سطح الغرفة مربع ساخن متجه للأسفل، وعليه فان العلاقة التقريبية لحساب المعامل (h) بدلالة فرق درجات الحرارة Δt ستكون $h = 1.52\ (\Delta t)^{1/3}$.

8. الظروف القياسية المطلوب تثبيتها داخل غرفة الاختبار (26.5 °م بصلة جافة،65% رطوبة نسبية) صيفاً لأن درجة حرارة البيئة تكون في حدود (50) °م (Arrora – 2007) .
9. استخدام تثبيت مكيفة هواء جدارية سعتها (1.0) طن تبريد لتوفير الظروف الحرارية القياسية داخل الغرفة، وربط مقياس الطاقة الكهربائية لتحديد مقدار استهلاكها اليومي.
10. تم استخدام مقياس الكتروني متعدد النقاط لتسجيل درجات الحرارة ومصنع من قبل شركة (Intelligent Auto Digital Thermometer by Victor Company) .

أما متغيرات البحث التي تم دراستها فهي تأثير زراعة سقف الغرفة بالثيل الامريكي على الأداء الحراري للسقف ومقارنته بالسلوك الحراري للسقف عند استخدام نفس كمية الماء المطلوبة لسقي الثيل لتوفير رذاذ ماء على السطح وفي كل حالة يتم تسجيل درجات الحرارة للهواء الخارجي (الظل) و درجتي حرارة سطح السقف (الداخلي والخارجي) وكمية الطاقة الكهربائية المطلوبة لتكييف الغرفة خلال يوم واحد / شهر .

نتائج الدراسة :

لمعرفة مقدار التوفير في كمية الطاقة الكهربائية المستهلكة لأغراض تكييف الغرفة نتيجة تغليف سقف الغرفة، تم رسم علاقة تغير درجات حرارة هواء الغرفة والبيئة خلال ساعات اليوم الواحد/ شهر وبتغير الأشهر وبتغيير المواد المستخدمة للتغليف وكما موضح في الأشكال (6-4)، بينما الجدول (1) يوضح مقدار متوسط درجة حرارة الأسطح ومقدار الحمل التبريدي للغرفة وكمية الطاقة الكهربائية المستهلكة لأغراض التكييف والنسبة المئوية للتوفير المتحقق.

المناقشة :

في أدناه مناقشة المتغيرات المؤثرة :

*** متطلبات سطح المبنى :**

ان استخدام سطح المبنى بمثابة سطح أخضر يتطلب تهيئة مسبقة لهذا السطح وكما موضح في الشكل (3) لكونه يتطلب عملية سقي باستمرار ، لذلك يتطلب منع وصول الرطوبة الى السقف أولاً، وثانياً يتطلب حجز طبقة الرمل التي تستخدم لزرع الثيل عليها، إضافة الى توفير ميل لسطح الرمل بحدود 2° عن الأفق للتخلص من الماء الزائد .

*** طبيعة زراعة المسطح الأخضر :**

يتطلب اختيار نبات لا تمتد جذوره كثيراً، أي أن تكون جذوره قريبة من السطح، لتقليل سمك الرمل المستخدم لاعتباره أوزان ميتة مسلطة على هيكل المبنى، وبزيادة سمك طبقة الرمل يتطلب تقوية سطح المبنى، إضافة الى كون النبات

المطلوب اختياره للزراعة يكون سريع النمو ودائم الخضرة ويتمتع بمنظر ناعم وجميل وعلى هذا الأساس تم اختيار الثيل الامريكي.

*** الماء المطلوب للسقي :-**

ان كمية الماء المطلوبة لسقي المسطح الأخضر المشيد على سطح الغرفة قيد البحث (4.5x4.5) م ستكون24 لتر/ساعة، وبمعدل (5) مرات/ يوم، لذلك فأن كمية الماء المطلوبة خلال يوم واحد ستكون في حدود 120 لتر لاستمرار النمو والاحتفاظ باللون الأخضر باستمرار، وأرخص وسيلة يعتقدها الباحث لتوفير الماء هي استخدام المياه الجوفية (بعد حفر بئر) لعملية سقي المسطح الأخضر.

*** استخدام المسطحات الخضراء :**

ان توفير مسطحات خضراء على سقف المبنى، يوفر مكان مناسب ومريح تجتمع فيه العائلة خلال فترة المساء أو الليل وتكون بعيدة عن ضوضاء الشارع إضافة الى ما يصاحب ذلك من تحسين المعايير البيئية.

*** السلوك الحراري للسقف :**

لمعرفة السلوك الحراري للمبنى المغطى سقفه بالثيل يتطلب تحييد مصادر انتقال الحرارة الأخرى (باستثناء السقف) لذلك تم عزله باستخدام عازل حراري (الواح البولي ستايرين الكثافة 20 كغم/م^3 ومعامل التوصيل الحراري 0.03 واط/م.ك سمك 200ملم).وتم قياس درجات الحرارة لأسطح السقف (الخارجي والداخلي) وكذلك درجة حرارة الهواء في الظل خلال فترة زمنية 18ساعة/اليوم (من الساعة :5 صباحاً ولغاية 10:30 مساءاً) وخلال أشهر الصيف (آيار ولغاية أيلول).وكما موضحة في الشكل(5) بينما تغيرمتوسط درجة الحرارة موضحة في الشكل(7)

*** تأثير الماء على السطح :**

بما أننا اقترحنا استخراج الماء من بئر يحفر خصيصاً، لذلك تم قياس السلوك الحراري للسقف بعد رشه برذاذ الماء وبنفس المعدل المطلوب لسقي المسطحات الخضراء وتغير درجات الحرارة لسقف الغرفة موضحة في الشكل (6) وخلال فترة الصيف بينما متوسط درجات الحرارة موضحة في الشكل (7).

*** أفضلية المسطحات الخضراء عن المائية :**

عند مقارنة السلوك الحراري للسقف في الحالتين، استخدام المسطحات (الخضراء أو المسطحات المائية) من خلال معرفة متوسط درجة حرارة أسطح السقف وخلال فترة الصيف وكما موضح في الشكل(7) والجدول(1) يوضح نتائج البحث ونسبة التوفير المتحقق، أي أن متوسط درجة حرارة طبقة الإنهاء الداخلية للسقف في حالة وجود المسطحات الخضراء كانت (28.58،26.6، 25.39،27.81) م للأشهر (8،7،6، 9) على التوالي بينما أصبحت عند استخدام رذاذ الماء ولنفس الفترة (29.9، 31.36،30.67، 25.53)م بينما كانت للسقف العادي ولنفس الفترة (44.75،35.81،45.81،37.67)م. حيث يتضح منها أن استخدام المسطحات الخضراء سيقلل من تأثير البيئة على مقدار ارتفاع درجة حرارة هواء الغرفة، وبالتالي يقلل كمية التبريد المطلوب توفيره وهذا سينعكس على تقليل كمية الطاقة الكهربائية التي تستهلكها مكيفات الهواء للوصول بدرجة حرارة الغرفة الى ما هو مصمم عليه.

أي أن نسبة التوفير في الطاقة الكهربائية سيكون 53% من الطاقة التي تستهلكها الغرفة (التي تحتوي على سقف خرساني) لأغراض التكييف صيفاً. بينما استخدام الماء لرش السطح سيوفر طاقة أقل وبحدود 38% .

* **القدرة المطلوبة لتشغيل المضخة :**

بما أن معدل جريان الماء المطلوب سواءاً لسقي المسطحات الخضراء أو تلك المائية، قليل، فان قدرة المضخة المطلوبة ستكون قليلة أيضاً وفي الحالة قيد البحث ستكون في حدود 0.17kw وتستهلك قدرة كهربائية في حدود 0.3kw وبمعدل (1.2 kw-hr) فيمكن توفيره أما يدوياً، أو باستخدام خلايا شمسية تجهز الطاقة المطلوبة لمضخة ماء (وخصوصاً أن السقي يكون خلال فترة وجود الشمس بالسماء).

الاستنتاجات :

وفي النهاية ، ومن خلال مناقشة النتائج المتحققة يمكن للباحث أن يوصي بما يلي :

1. لغرض تحقيق خفض ملحوظ للحرارة المتسربة من السقف يتطلب حماية السقف من تأثير البيئة وإحدى السبل الفعالة هي زراعة السقف بالثيل .
2. ان استخدام المسطحات الخضراء في السقوف يحسن من الكفاءة الحرارية والوظيفية لسقف المبنى، ويوفر مساحات جيدة لالتقاء افراد العائلة صيفاً خلال ساعات المساء أوالليل .
3. بالإمكان استخدام اسلوب آخر هو رش السقف برذاذ الماء (بنفس كمية الماء المطلوبة للمسطحات الخضراء) ، ولكن لا يحقق الكفاءة الحرارية والوظيفية التي تحققها المسطحات الخضراء.

المصـــادر :-

1- Amori, Dr. Kerima E. & Baqir Ameer K. (Analysis of Thermal Energy Storage System with Two Phase Flow) the 6th engineering conference, College of Eng., University of Baghdad, Iraq–2009 .

2- Arora, S. Domkundwar (A Course in Refrigeration and Air–Conditioning) Dhanpat Rai & Sons – Delhi – 2007.

3- Hasan – Atif Ali (Optimum Insulation Thickness for Iraqi walls & roofs)9Symposium of thermal insulation in hot climates – Scientific research Council – Iraq 1984.

4- Jones–W.P.(Air–Conditioning Eng.) Edward Amold. London –1987 .

5- Rohsnow , Warren & Hartaeti, James f. (Hand Book of Heat Transfer) Mc Graw–Hill book Company, N.Y. USA–1973.

6- الدوري – د. مجيد، حسن، عاطف علي وآخرون (معاملات انعكاس الطاقة الشمسية من أسطح مواد الانهاء المستخدمة في العراق)المؤتمر العلمي الخامس/مجلس البحث العلمي(الملغى)–العراق 1989

7- الدوري – د. مجيد، حسن، عاطف علي وآخرون (الصفات الحرارية لمواد البناء المحلية) المؤتمر العلمي الأول للطاقة / وزارة النفط – العراق 1992.

8- حسن ، عاطف علي، (تقليل التسرب الحراري من السقوف الخرسانية للأبنية السكنية بتغير زاوية ميلها) / المجلة العراقية للهندسة الميكانيكية وهندسة المواد/ كلية الهندسة/ جامعة بابل – 2009 .

9- علي حسن – عاطف ، لطيف – مثنـى (تحليـل مسارات الطاقة المستهلكة في القطاع السكني فـي العراق) المؤتمر العلمي الأول – الكلية التقنيـة – النجف – العراق/ 2008 .

10- علي حسن – عاطف (تقليل الطاقـة الحراريـة المتسربة من سقف خرسـاني سـمك 150 ملـم والمستخدم في سقوف الأبنية السكنية في العراق)/ المؤتمر الهندسي السادس – جامعة بغداد – كليـة الهندسة (4-7/4/2009).

11- كامل شعبان – عوني ، الجودي – مقداد (التحليل الناخي للعراق وأثره على العمارة) تقريـر مـن منشورات مركز بحوث البناء – مجلـس البحـث العلمي (الملغي) العراق – 1973.

جـدول (1) متوسط درجة الحرارة خلال فترة الصيف والنسبة المئوية لتوفير الطاقة الكهربائية المستهلكة من المبنى قيد الدراسة نتيجة تغطية سقف المبنى

النماذج التي تم دراستها	حالة السقف	Tsh درجة متوسط حرارة الظل	متوسط فرق درجات الحرارة على طرفي سقف الغرفة	متوسط فرق درجات الحرارة بين السطح الداخلي وهواء الغرفة	الحمل التبريدي خلال فصل الصيف طن تبريد	الطاقة الكهربائية (المسجلة) المستهلكة من قبل مكيفة الهواء kw-hr	مقدار الطاقة الكهربائية المستهلكة من قبل المضخة kw-hr	النسبة المئوية لتخفيض الحمل الكهربائي المستهلك نتيجة تغطية سقف المبنى %	
								بوجود مضخة	عدم وجود مضخة
النموذج الأول	الاعتيادي	36.5	3.07	10.6	176.22	132.5	—	—	—
النموذج الثاني	تغطية السقف بالحشائش الخضراء	36.5	5.5	5.91	82.8	62.3	38	24.3	53.0
النموذج الثالث	رش السقف برذاذ الماء	36.5	4.65	7.34	109.8	82.56	38	9	37.7

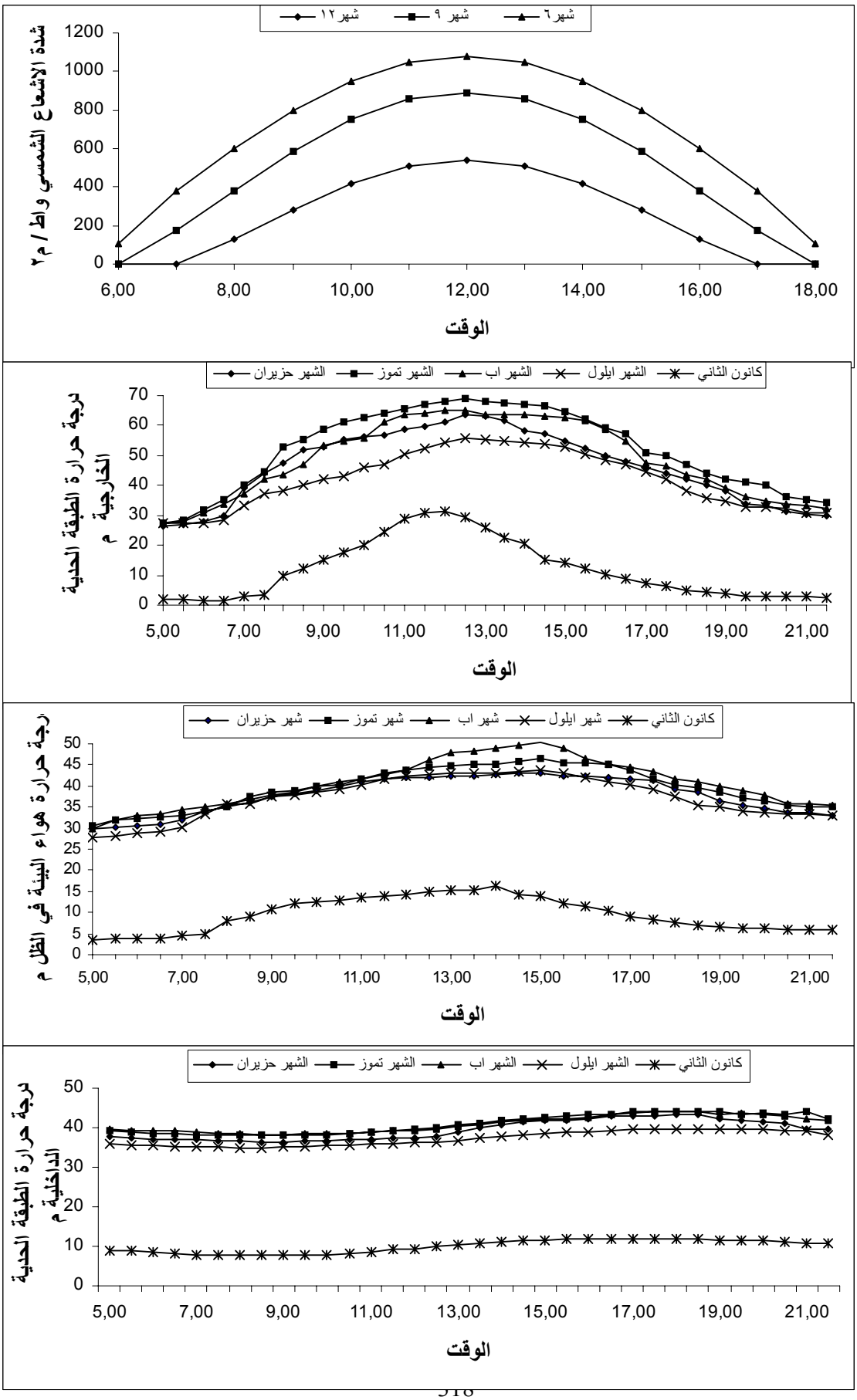

شكل (1) تغير الإشعاع الشمسي ودرجة حرارة السطوح والظل بتغير الوقت (الباحث /

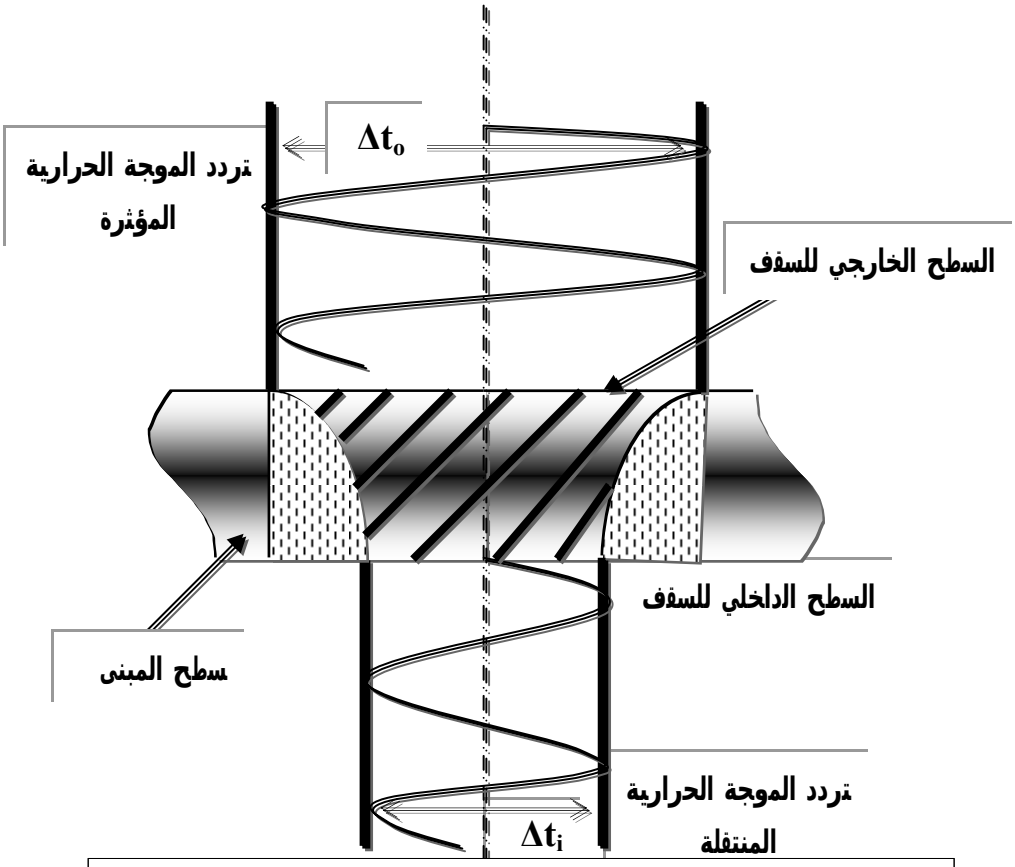

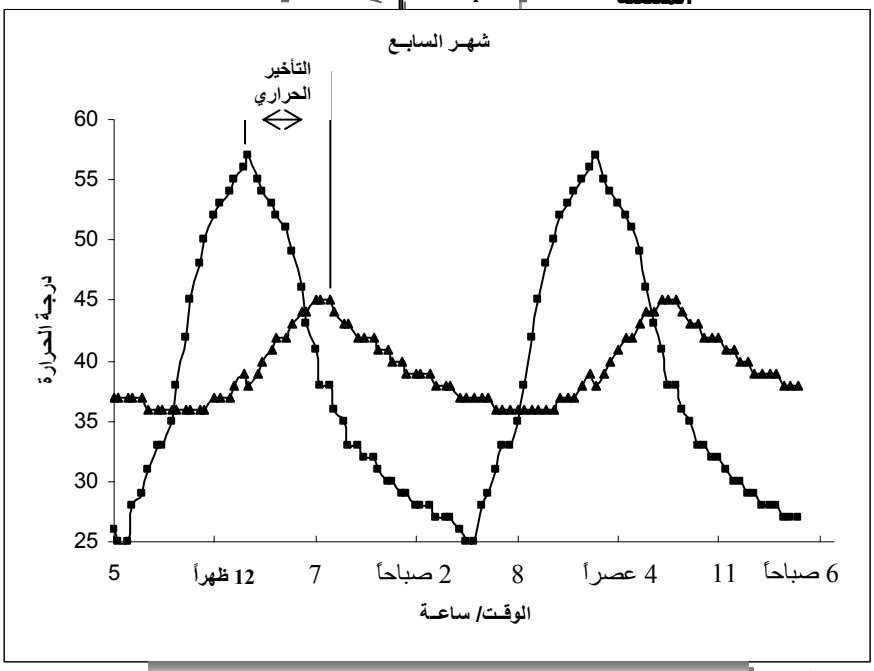

Ti درجة حرارة السطح الداخلى للسقف (المعرضة للغرفة)

To درجة حرارة السطح الخارجى للسقف (المعرض للبيئة)

شكل (2) تردد الموجة الحرارية الخارجية المؤثرة على السقف والموجة المنتقلة الى الداخل (الباحث)

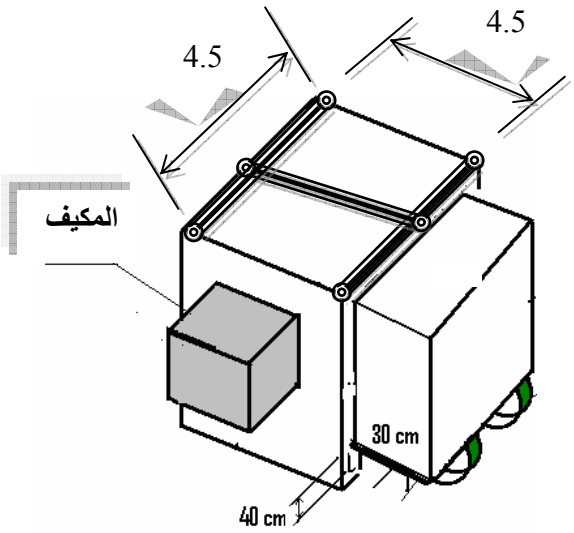

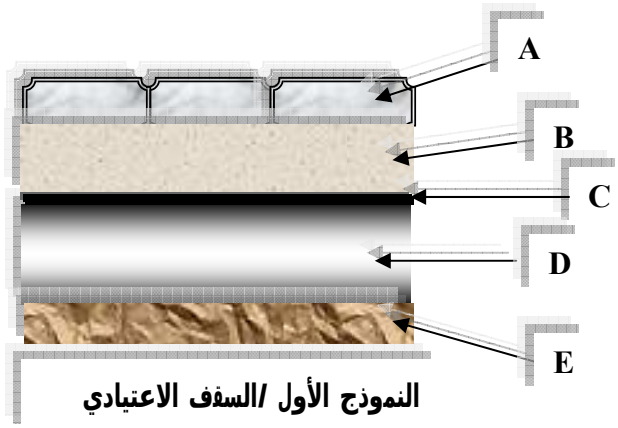

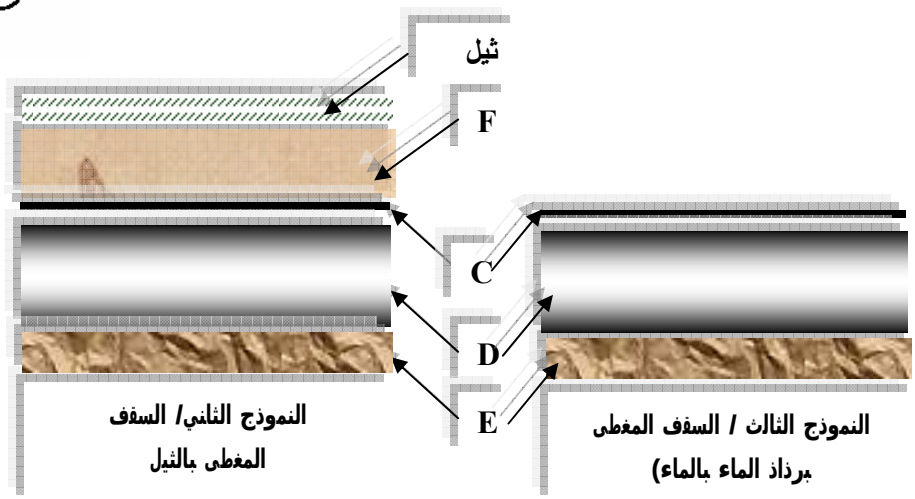

A = الشتايكر (الخرسانة) سمك (40) ملم

B = تراب تهوير سمك (100) ملم

C = فلانكوت سمك (1.5) ملم

D = الخرسانة المسلحة سمك (150) ملم

E = جص سمك (20) ملم

F = تراب سمك (50) ملم لأغراض الزراعة

شكل (3) تفاصيل نماذج انهاء السقوف التي تم دراستها بالبحث وغرفة البحث

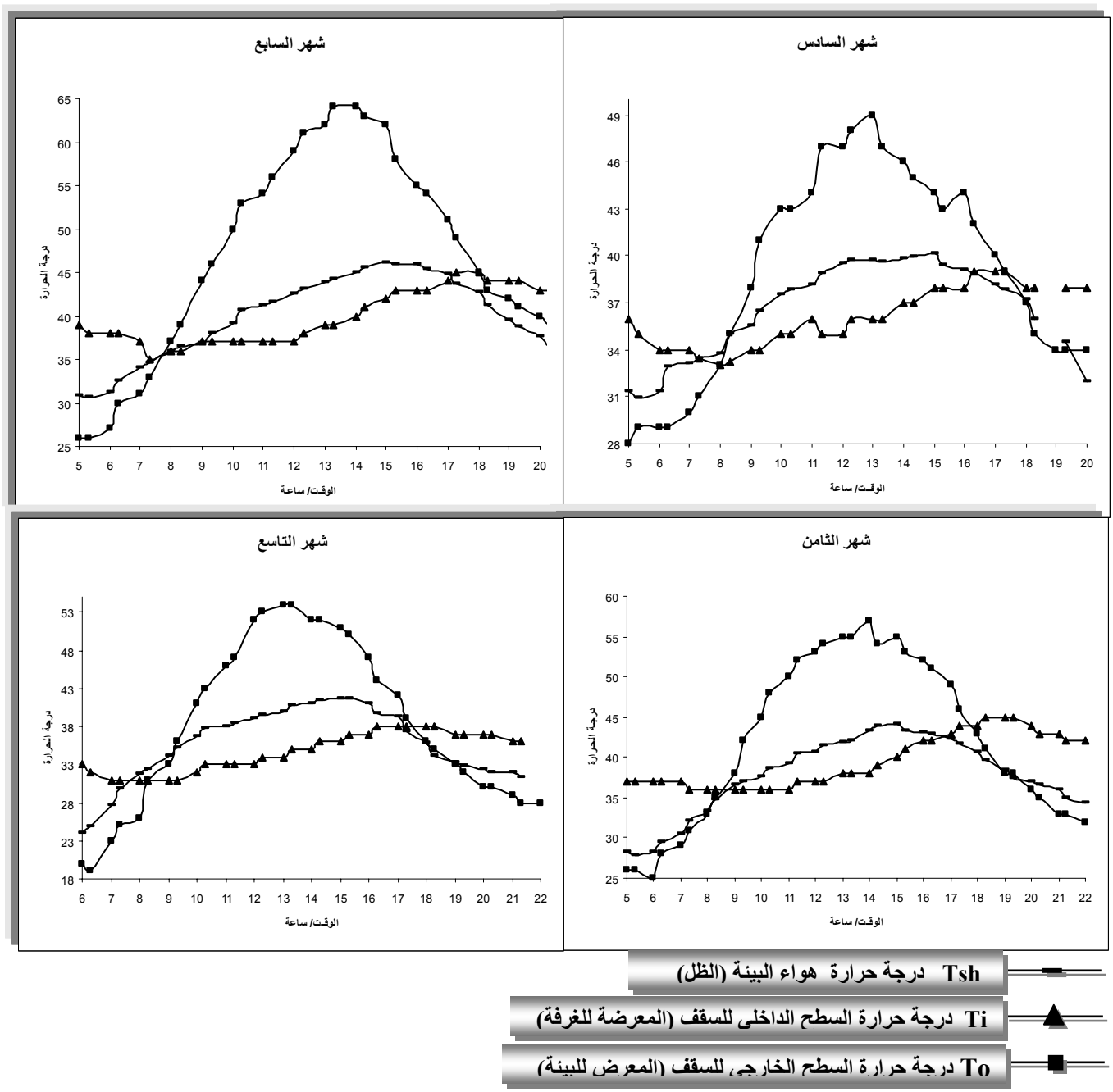

شكل (4) السلوك الحراري للنموذج الأول / السقف الخرساني الاعتيادي بتغير ساعات اليوم الواحد خلال فترة الصيف/ (2009)

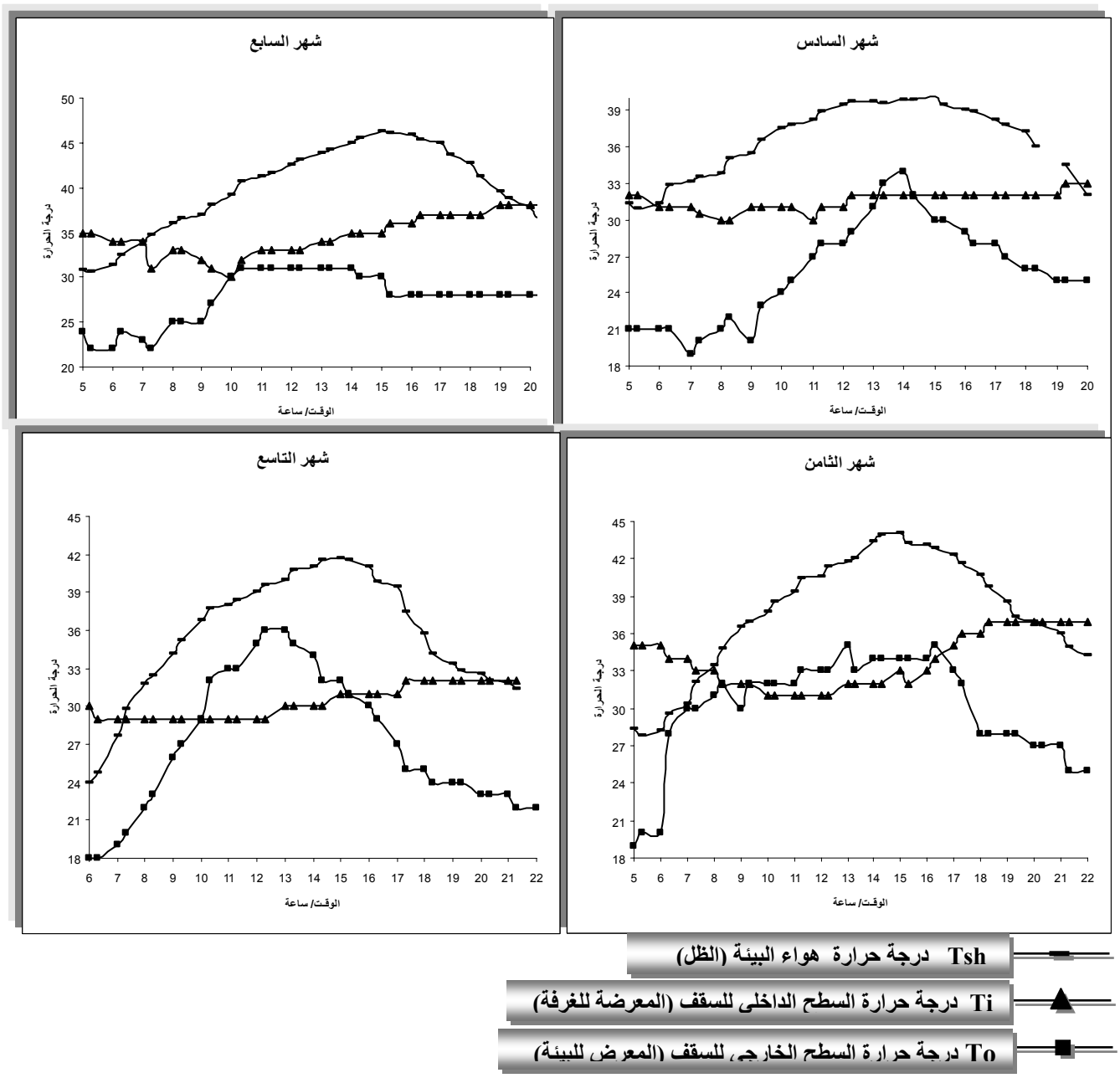

شكل (5) السلوك الحراري للنموذج الثاني / السقف الخرساني المغطى بالثيل بتغير ساعات اليوم الواحد خلال فترة الصيف / (2009)

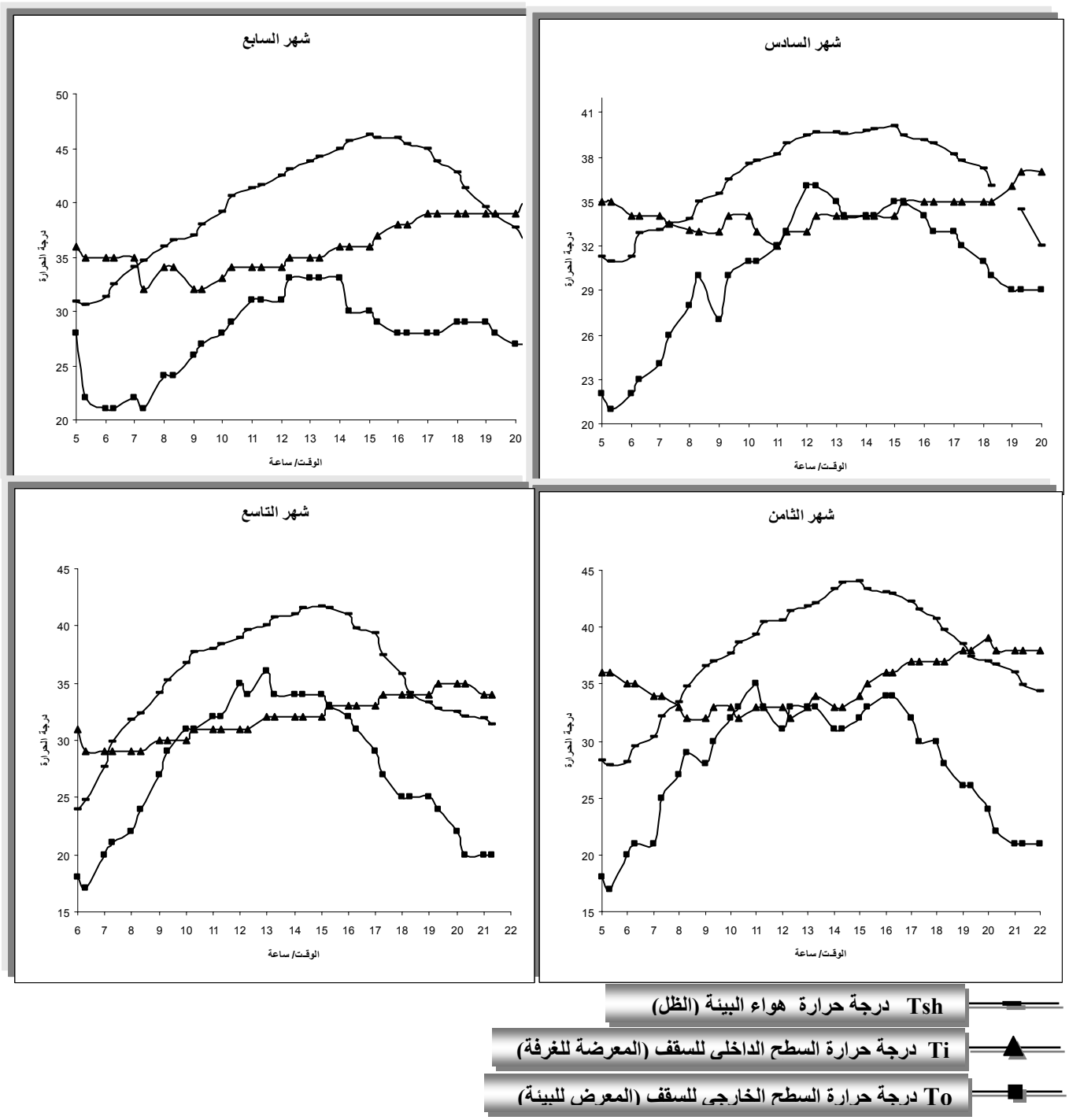

شكل (6) السلوك الحراري للنموذج الثالث / السقف الخرساني المعرض لرذاذ الماء بتغير ساعات اليوم الواحد خلال فترة الصيف/ (2009)

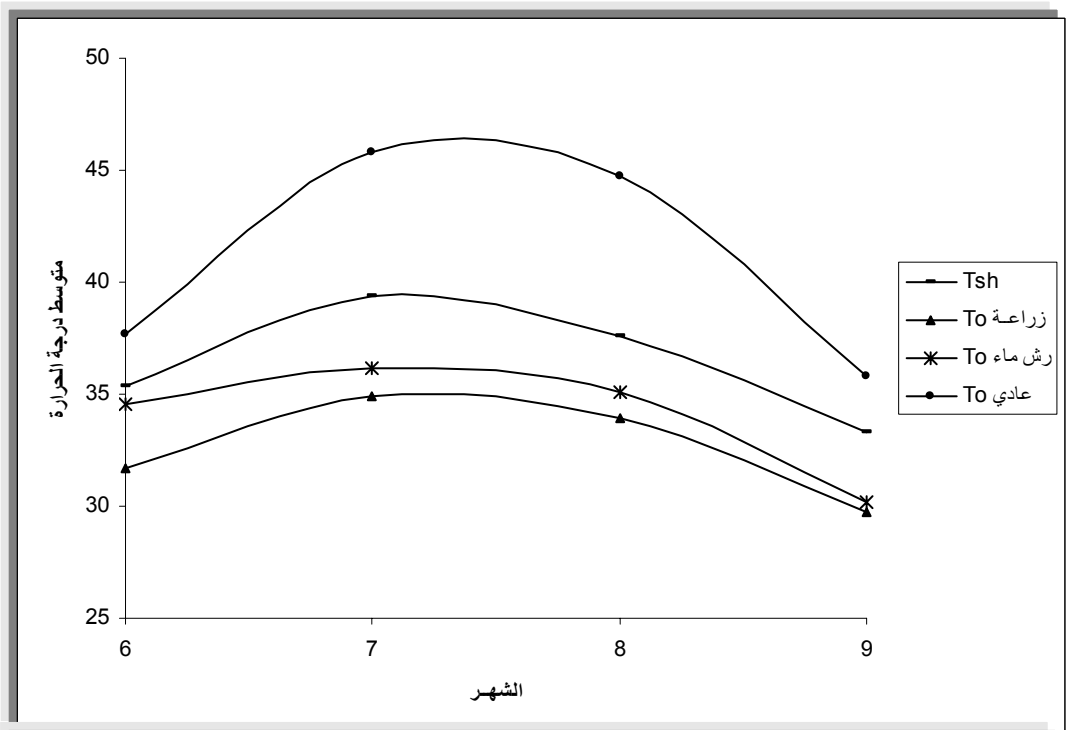

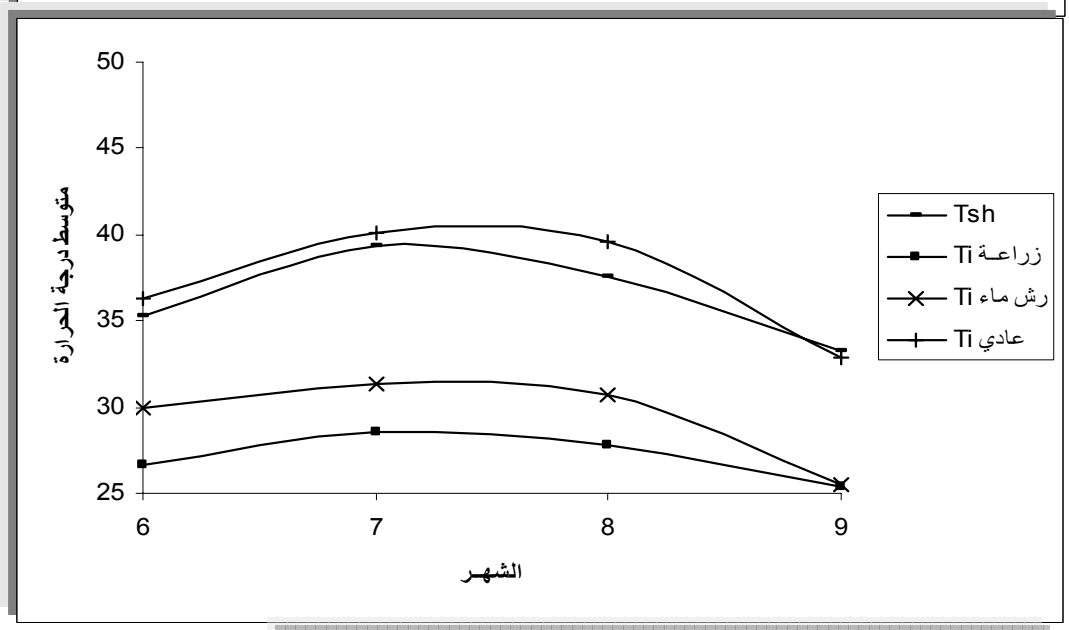

To : درجة حرارة طبقة الإنهاء الخارجية للسقف المعرض للبيئة

Ti : درجة حرارة طبقة الإنهاء الداخلية للسقف المعرض للغرفة

Tsh : درجة حرارة هواء البيئة (الظل)

شكل (7) متوسط درجة حرارة السطح الخارجي والداخلي للسقف باختلاف أسلوب التغطية

Effect of Kerosene and Gasoline on Some Properties of High Performance Concrete

Dr. Nada Mahde Al-Jalawi[1], and Asis.Lec. Dalia Shakir Atwan[2]

[1)] College of Engineering / University of Baghdad/Email:naljalawi@yahoo.com
[2)] College of Engineering / Al-Nahrain University/Email:msc.dalia@yahoo.com

ABSTRACT

During the last quarter century, many changes have taken place in the tanks industry and also in the materials that used in its production، while concrete is the most suitable material where concrete tanks has the benefits of strength, long service life and cost effectiveness. So, it is necessary improvement the conventional concrete in order to adapt the severe environment requirements and as a result high performance concrete (HPC) was used. It is not fundamentally different from the concrete used in the past, although it usually contains fly ash, ground granulated blast furnace slag and silica fume, as well as superplasticizer. So, the content of cementitious material is high and the water/cement ratio is low. In this study, the silica fume and superplasticizer were used for obtaining HPC. This paper is an attempt to provide some information about effect kerosene and gasoline on some properties of HPC which can be used as storage tanks for petroleum products. The experimental work in this research including; slump test, weight loss test and compressive strength test were performed. The results of these investigations indicated that the petroleum products have unacceptable effects on the properties of concrete.

Keywords: high performance concrete, kerosene, gasoline, silica fume, superplasticizer, weight loss, compressive strength

الخلاصة

في الربع الاخير من هذا القرن، حدثت العديد من التغييرات في ما يتعلق بصناعة الخزانات وايضا في المواد المستعملة في انتاجها، الا ان الخرسانة تعتبر من افضل المواد المناسبة لهذا الغرض كونها مفيدة من ناحية القوة والعمر الخدمي الاطول اضافة الى الكلفة. لذا كان من الضروري تحسين الخرسانة التقليدية لكي تتكيف مع متطلبات البيئة القاسية وكنتيجة لذلك تم استخدام الخرسانة عالية الاداء. حيث انها لاتختلف كثيرا عن تلك الخرسانة المستخدمة في الماضي بالرغم من احتوائها عادة على مواد بوزولانية فضلا عن المادنات المتفوقة. وعليه فأن محتوى المواد السمنتية يكون مرتفعا ونسبة الماء الى السمنت تكون منخفضة. في هذا البحث تم استخدام ابخرة السليكا والمادن المتفوق للحصول على الخرسانة عالية الاداء. ويمكن اعتبار هذا البحث كمحاول لتوفير بعض المعلومات عن تأثير النفط الابيض وزيت الغاز على بعض خصائص الخرسانة عالية الاداء التي بالامكان استخدامها كأحواض لخزن تلك المنتجات. تضمن العمل المختبري اجراء فحص الهطول، وفحص فقدان الوزن وفحص مقاومة الانضغاط. واشارت نتائج تلك الفحوصات بان للمنتجات النفطية تأثيرات غير مقبولة على خصائص الخرسانة.

INTRODUCTION

Concrete is the most commonly used material in construction industry. There are a number of reasons for this such as high strength, ease of production, low cost, good compatibility with other materials, especially with steel, durability under aggressive conditions(Hanh, P., 2008). But, when used in the petroleum environment, concrete has some special requirements compared to the conventional concrete. Nowadays, high performance concrete (HPC) is considered to be a major research and development strategy in many countries in the world. If the main requirement of high strength concrete is the value of compressive strength, HPC is required not only the value of compressive strength but also some other special properties as durable life, Low maintenance cost, Variety of structural configuration, Excellent resistance to temperature, Better resistance to fatigue and buckling, Stronger resistance against accidents of missile attack, fire and explosion (Hanh, P., 2008).

The versatility, economy, water-tightness, and long-term durability of HPC make it ideal for environmental structures. Environmental structures are classified as those used for petroleum products storage. HPC can be cast into tanks of any shape required to fit the site or the process. Its higher strength allows for thinner tank floors, walls, and roofs. Furthermore, the high recoating costs that are periodically required for steel tanks are unnecessary when using HPC. Construction joints, particularly those in the tank floor, can be eliminated, ensuring maximum water-tightness. Another benefit is that HPC can be made shrinkage-crack free, which helps protect the conventional reinforcement(Close, S.,2004).

Recently, the addition of silica fume has been used to produce concrete of increased strength and durability. Silica fume increases the strength of concrete due to pozzolanic reactions and increased particle packing density(De Larrad, F., 1994). In addition to higher strength, the addition of silica fume to concrete has been proposed as one method to substantially reduce the permeability of concrete due to reduced pore size(Hooton, R. 1993). Because of these and other advantages, HPC is gaining popularity among owners and engineers who are interested in new solutions to an old problem-leaking, maintenance-laden tanks (Gambhir, M. 1998).

OBJECTIVES AND SCOPE

The oil had and still great importance in all fields of life. It is basic source of energy all over the world. Therefore, the storage of petroleum products in concrete tanks has been offered more benefits compared with other materials such as safety, serviceability and maintenance costs.

The essential objective from this paper is to study the effect of kerosene and gasoline on the properties of HPC until 90 days exposure period. Besides, the research discusses the relationship between that properties.

PERFORMANCE−BASED SPECIFIC-ATIONS FOR HIGH PERFORMANCE CONCRETE

HPC is a concrete in which certain characteristics are developed for a particular application and environment, so that it well give excellent performance in the structure in which it will be placed, in the environment to which it will be exposed, and with the loads to which it will be subjected during its design life. Its includes concrete that provides either substantially improved resistance to environ-mental influences (durability in service) or substantially increased structural capacity while maintaining adequate durability. It may also include concrete, which significantly reduces construction time without compromising long-term serviceability. It is, therefore, not possible to provide a unique definition of HPC without considering the performance requirements of the intended use of the concrete. Examples of characteristics that may be considered critical in an application requiring performance enhancement are; ease of placement and compaction without segregation, early-age strength, long-term mechanical properties, permeability, density, heat of hydration, toughness, volume stability, and long life in severe environments (Gambhir, M. 1998).

Concretes possessing many of these characteristics often achieve higher strength. Therefore, HPC is often of high strength, but high strength concrete may not necessarily be of high performance. Thus, in practical applications of this type of concrete, the emphasis has in many

cases gradually shifted from the compressive strength to other properties of the material, such as a high modulus of elasticity, high density, low permeability, and high resistance to same forms of attacks. The cost and other benefits derived may include less material, light and fewer structural elements, reduced maintenance, extended life cycle and aesthetics (Gambhir, M. 1998).

The replacement of some Portland cement by one or a combination of supplementary cementitious materials is very often beneficial from a rheological point of view when making HPC. Experience shows that sometimes, it is difficult to fully control the rheology of the mixture for 1 h 30 min when using some combinations of pure Portland cement and superplasticizer. In fact, currently, most cement manufacturers optimize the characteristics of their clinker and the gypsum content and fineness of their cement to obtain a high early cube strength at a w/c of about 0.50. Consequently, they favour high C_3A and C_3S content for their clinker and a high fineness for their cement, which is the opposite of what should be done if the objective of their optimization process is to improve the rheological characteristics of low w/b ratio concrete. At the present time, binary, ternary and quaternary binders are commonly used to produce HPC (Aïtcin, P. 1998)

In recent years, the use of pozzolanic materials becomes an important strategy for obtaining HPC. In this study, the use of highly reactive pozzolans, such as silica fume combined with superplasticizer addition, let to prepare HPC.

BACKGROUND OF CONCRETE STORAGE TANKS

Tanks fulfill an important role in supplying mankind with essential products. They are used for storing liquids or solids which may be either intermittently produced but consumed at a fairly uniform rate, or continuously produced at a fairly uniform rate but consumed in an irregular manner. A further important aspect is that the locations of origin and consumption are frequently appreciable distances apart. These circum stances necessitate the provision of appropriate storage capacities. The building of tanks in concrete offers several advantages such as: (VSL International LTD 1983)

a. Concrete tanks are economical to construct and maintain (they require virtually no maintenance). Construction is relatively inexpensive because the basic materials for making concrete are usually locally available and suitable special building methods make rapid construction possible.
b. Concrete tanks are relatively insensitive to mechanical influences, whereas steel tanks, for example, when used for storing environ mentally polluting or dangerous substances have to be surrounded by protective concrete walls to assure the required degree of safety.
c. Concrete tanks are eminently suitable for the storing of a very wide variety of substances; for example, if provided with a suitable liner, they may even be used for low temperature liquefied gases.

Since the turn of this century, concrete tanks have been in use to store crude oil and its products. The critical shortage and cost of steel during the second world war expanded progressively the use of concrete for the construction of oil tanks. Striking development in this field, however, occurred in the early seventies, whenever giant concrete rostrums were built in the north sea for excavating crude oil which including temporary storage for large quantities from crude oil in submerged concrete tanks. Contained this mass rostrums more than 140000 m3 concrete, its weight about 350000 ton and designed to resist the effect of marine waves to height 30 m and winds with speed 250 km/hrs.. The basis of this cells was based on deep reach more than 200m. during 1973-1986, achieved 15 another cells and began of thinking to carry out cells on deeps over than 350m (Moufaq, J. 1998).

In 1975 VSL international LTD. prepared a design for a 20 000 m3 capacity fuel oil tank, consisting of an outer tank in post-tensioned concrete and a double layers, plasticized PVC inner tank. The concrete tank is designed to fulfill two functions: firstly to serve as a support for the PVC tank and secondly as a collecting basin for any leakages which might occur in the inner tank. The tank has an internal diameter of 36.00 m, a wall height of 20.00 m and wall thickness of 250 mm. It has a bottom slab at least 150 mm thick with an edge beam at least 400 mm thick. The roof consists of a reinforced concrete dome with post-tensioned ring beam. The minimum concrete thickness of the roof is 60 mm. There are sliding bearings between the ring beam and the tank wall. As a transition between the bottom slab and the wall, a sliding bearing with an internal seal or a

continuous neoprene bearing is installed. To improve the tightness of this joint, a proportion of the vertical tendons of the wall are continued through the joint and anchored in the base slab. This transition between base slab and wall would today be constructed monolithically.

In 1997, Al-Lami investigated the structural behavior of ferrocement exposed to petroleum products. It was observed that the oil soaking does not prevent shrinkage of ferrocement. Also, the results indicated that the final shrinkage of ferrocement depends on their initial drying shrinkage and the shrinkage occurred in during the petroleum soaking period which affected by aggregate content, reinforecement and thichness elements. The ferrocement exposed to petroleum products showed reduction in flexural first cracking, ultimate moments and direct tensile cracking strength ranging from (3.33% to 20.1%), (2.07% to 14.53%) and (5.13% to 16.27%) respectively. Finally, the ferrocement–reinforced brick beams exposed to gas oil demonstrated reduction in first cracking and ultimate moment ranging from (4.75% to 8.75%) and (12.8% to 16%) respectively. Besides, the ferrocement-reinforced concrete beams showed reduction in ultimate moment capacity about 11.9% versus no reduction in the first crack moment.

In 1999, Al-Geryawee and Al-Rahame studied the permeability characteristics and mechanical properties of concrete exposed to oil products. Six types of liquids were used in this study (water, gas oil, Kuwait crude oil, north sea crude oil, Basrah crude oil and Kirkuk crude oil). It was found that the oil product storage losses per day depended on the coefficient of permeability and type of stored liquid. It was concluded that tanks containing crude oil are more successful more and cost saving than gas oil tanks.

In 2001, Al-Zaidi studied the influence of oil products on the physical and electrical properties of concrete. The work involves reinforced and plain concrete samples. Physical test results revealed an increase in the compressive and tensile strength for specimens after 7 days of exposure to petroleum liquids compared with that cured in water. On the other hand, the exposure to petroleum liquids has produce an increase in permeability and electrical resistance of concrete specimens.

INTERESTS OF USING CONCRETE TANKS

Tanks are available in a wide range of materials including steel, concrete, fiberglass or plastic. All of these materials can be suitable providing the tanks have been manufactured specifically for the storage of petroleum products. But, It has been found that concrete tanks are very well suited to these requirements where concrete tanks offers significant advantages over other materials such as; (VSL International LTD 1983)

- Endless color options
- Minimal shrinkage
- Easily takes any shape
- The lower damage of water
- High durability
- Fire resistance
- Lower thermal conductivity
- Low effect for climate changes
- High safety
- Low maintenance
- No hazardous
- No staining
- Greater resistance to abrasion and impact
- Resistance to leakage
- Corrosion resistance
- Cost effectiveness

EXPERMENTAL WORK

Materials

Cement

Ordinary Portland cement type I used in this work. The percentage oxide composition and physical properties of the cement indicate that the adopted cement conforms to the Iraqi Specification No.5/1984 as illustrated in Tables 1 and 2.

Fine Aggregate

Local sand was used as fine aggregate. The sieve analysis and the grading curve of fine aggregate used conformed to the ASTM C33-03 as shown in Table 3 and Figure 1. The specific gravity and absorption of the fine aggregate were typically 2.62 and 0.72%, respectively as listed in Table 4.

Coarse Aggregate

Crushed gravel with a maximum aggregate size 20 mm was used as coarse aggregate. The sieve analysis and the grading curve of coarse aggregate

used corresponds to the ASTM C33-03 as illustrated in Table 5 and Figure 2. The average values of specific gravity and absorption of the coarse aggregate were typically 2.65 and 0.57%, respectively as listed in Table 6.

Silica Fume

As a pozzolainc material, silica fume was used in this study. The chemical analysis of silica fume illustrated in Table 7. The specific gravity of silica fume used was 2.16 as described in Table 8.

Superplasticizer

Superplasticizer combined with a retarding effect was used. Its has a trade name "EUCOBET SUPER VZ" and used to promote good workability for a long period due to retarding effects. The specific gravity of the superplasticizer as given by the supplier is 1.1 and without chloride content as described in Table 9.

Water

For mixing and curing tap water was used.

Composition of Trial Mixes and Their Fresh Properties

In this work, the trial mixes were designed to give minimum compressive strength of 50 and 60 MPa according to ACI Committee 211.1-95 classification and considered by varying the quantity of superplasticizer, while keeping the water content constant. Two trial mixes were prepared by using a fixed contents of binder (cement+silica fume) equal to (562 kg/m^3), sand (750 kg/m^3) and gravel (882 kg/m^3). Two levels of the superplasticizer 3 and 5 L/m^3 were used for preparing and testing. For each trial mix, a constant water content of 174 kg/m^3 of concrete was taken. By using the slump test, the workability of the fresh concrete mixes was measured according to ASTM C143-89. The mix proportions used are provided in Table 10.

Preparation, Compaction and Curing of Test Specimens

All molds were cleaned and oiled in order to prevent their from bonding to concrete. After that, the concrete was placed into the molds and compacted on a vibrating table. Then, the surface of the top layer is leveled. Follows, a polyethylene sheet was used to cover the molds for a period of 24 hours in the laboratory. After 24 hours, the specimens for strength test were removed from the molds and placed in a water tank for curing until measurement dates. Besides, two tanks were prepared, one filled with kerosene and another with gasoline. The specimens for testing durability in petrochemicals materials were placed in these tanks after 28 days curing in water tanks; this was done because the moisture of specimens placed in water tended to acquired strength.

Tests

Weight Loss Test

After 28 days of curing, the initial weight of the cubic specimens of 15x15x15 cm^3 was determined before immerging in the tanks of kerosene and gasoline. Then, the specimens were kept continuously immersed in these tanks for 12 weeks as recommended by ASTM C267-97. During the test period, the cubic specimens were removed weekly from curing tanks, rinsed with tap water, without brushing, and left to dry for 30 min before weighing and visual inspection. The kerosene and gasoline were renewed with each new weighing to maintain constant concentr-ation(ASTM C192-07). Cumulative weight change (WCt) for each specimen was determined as follows:

$$WCt\ \% = [(W_0-W_i)/W_0]*100 \qquad \text{Eq.(1)}$$

Where:

W_0 is the initial weight of saturated surface dry specimen before exposure to petroleum products (kg).

Wi (i=1,2,3, ,12) is the weight after I weeks of exposure to petroleum products (kg).

The percentage of strength change was calculated in the same way as the weight change equation.

Compressive Strength Test

This test was carried out According to B.S.1881: part 116: 1989 at ages of 7, 28 and 90 days on 150mm cubes by using a compression testing machine of 1814.882 kN capacity. For each age three samples were tested and the average of the three test results was reported.

RESULTS AND DISCUSSIONS

1. The results of workability test for mixes are shown in Table 10. The data results indicate that the increase of dosage of SP causes an increase in the slump of concrete mix.
2. The results of weight loss for specimens exposed to kerosene and gasoline tanks are shown in Fig. 3, and 4. The specimens with high addition of SP present the greatest weight loss in comparison with reference concretes (3.5% and 2.9% for K5and G5 respectively compared with 1.82 % for K3 and 1.7 % for G3 at 28 days curing age). This was probably due to the fact that the petroleum products as it is known is primarily related to the actual cement contents in these concretes.
3. Compressive strength results shown in Table 11 correspond to the average values obtained on at least three cubes samples 150 mm. The results show increasing in compressive strength with increase of dosage SP added in concrete mix as presented in Fig. 5. The main reason is attributed to that the extra dosage of SP may be caused more dispersion into smaller agglomerates of cement particles which predominate in the cement paste of the concrete mix. As a result to dispersion of cement agglomerates into individual particles; a greater rate of cement hydration can be achieved in the well dispersed system. So that, W5 specimens exhibited increase in compressive strength about 19.50% at 28 curing age compared to their corresponding W3 specimens.
4. The results also demonstrate that the concrete specimens immersed in kerosene and gasoline tanks show reduction in compressive strength compared to their corresponding specimens curing in water as represented in Fig. 6 and 7. The reduction in compressive strength at 28 days were 12.80% and 8.53% for K3 and K5 respectively compared to 9.70 % and 6.47 % for G3 and G5. This due to penetrate those materials into structure construction of cement and caused extending gel pores and spreading solid hydration components which caused weakly adhesion and cohesion forces in cement and easily slip of internal grains. In addition to rise the internal hydraulic pressure. Besides, happen reduction in surface power as a result to absorption these liquids and adhesion on gel surfaces caused reduction in compressive strength (Moufaq, J.1998)
5. The relationships between compressive strength loss and weight loss as a percentage of their initial values before exposure to kerosene and gasoline are illustrate in Fig. 8 and 9. The results reveal that there is not a direct relationship between the compressive strength loss and the weight loss for the concrete specimens immersed in kerosene tanks (Fig. 8). In the same way, for the results of the gasoline tanks, represented in Fig. 9, the external state of the degradation of the samples after exposure to the kerosene is not a good indicator of their compressive strength; in fact, there is a divergence between the loss of weight and the loss of the compressive strength. The observed trend of the compressive strength change after 1 week of exposure to kerosene and gasoline is affected by multiple factors. After exposure to these products, concrete specimens had a softened surface zone underlain by a sound part, which represents the bulk cross-section of specimens. The observed compressive strength reduction after exposure depends on the ratio of deteriorated-to-sound cross-section (Bassuoni M.,2007) Conversely, the occurrence of this zone can increase strength loss results since it has weak mechanical properties, as shown by different studies in the literature (Bernard F.,2008 and Nyugen V.,2007) .

CONCLUTION AND RECOMMEND-ATION

Based on results obtained from the basic investigation on HPC , several conclusions are drawn as follows:

1. Workability of HPC mixes was dependent on the content of SP. Where, the slump was 170 mm at the addition 3 liter from the admixture compared to 186 mm at the addition 5 liter at the same mix proportion.
2. The concrete specimens curing in water exhibited increasing in weight and compressive strength at all ages with rise addition of SP. The percentage increase in weight and compressive strength at 28 day were 0.5 % and 19.50% respectively for W5 specimens compared to their corresponding W3 specimens.
3. The weight loss was more with increasing of dosage of SP for specimens exposed to kerosene and gasoline. The reduction in weight were 1.24% and 0.74% for K5 and G5 respectively

compared to their corresponding K3 and G3 at 28 days.

4. The specimens exposed to kerosene and gasoline showed reducing in compressive strength at all ages with compared to their corresponding reference specimens. The reduction in compressive strength were 12.80% for K3 and 8.53% for K5 compared with 9.70 % and 6.47 % for G3 and G5 respectively at 28 days.
5. The size of the concrete samples was large enough to allow testing of concrete containing large aggregate.
6. The test apparatus and the procedures used for testing were carefully designed in order to provide high precision determination of loss in weight and the compressive strength.
7. In the future, HPC will be specified for characteristics other than its 28-day compressive strength because there are cases where another characteristic is more important for the designer or the owner than the 28-day compressive strength. Consequently, it is becoming imperative to understand better hydration reaction and its consequences as well as the role of the different materials used when making HPC to specify properly the most efficient and economical HPC.

REFERENCES

Aïtcin, P., (1998), High Performance Concrete, E and FN SPON, London, pp.592.

Al-Geryawee, A. and Al-Rahame, A., Properties of Concrete Exposed to Oil Products, Higher Diploma, Thesis, University of Technology, 1999.

Al-Lami, M., Structural Behaviour of Ferrocement Exposed to Petroleum Products, PHD, Thesis, University of Technology, 1997.

Al-Zaidi M., Influence of Oil Products on The Physical and Electrical Properties of Concrete, M.Sc, Thesis, University of Technology, 2001.

American Concrete Institute. ACI Committee 211.1-95, Standard Practice for Selection Proportions for Normal, Heavy Weight and Mass Concrete, ACI Manual of Concrete Practice, Part 1-1995.

ASTM C33-03, Standard Test method for Grading of crushed rock coarse aggregate, Annual Book of ASTM Standard, Vol.04.02.

ASTM C143-89, Standard Test Method for Slump of Hydraulic Cement Concrete, Annual Book of ASTM Standard, Vol.04-02, 1989, pp. 85-86.

American Society for Testing and Materials, Standard Practice for Making and Curing Concrete Test Specimens in the Laboratory, ASTM International, West Conshohocken, PA, USA. ASTM C 192, 2007.

American Society for Testing and Materials, Standard Test Methods for Chemical Resistance of Mortars, Grouts, and Monolithic Surfacings and Polymer Concretes, ASTM International, West Conshohocken, PA, USA, ASTM C 267, 1997.

Bassuoni, M. and Nehdi, M., Resistance of Self-Consolidating Concrete to Sulfuric Acid Attack with Consecutive pH Reduction, Cement and Concrete Research, 2007, pp. 1070–1084.

Bernard, F., Kamali, S. and Prince, W. ,3D Multi-Scale Modelling of Mechanical Behaviour of Sound and Leached Mortar, Cement and Concrete Research, 2008, pp. 449–458.

B.S.1881, Part 116, 1989, Method for Determination of Compressive Strength of Concrete Cubes, British Standard Institution, pp.3.

Close, S. and Gangliu, Z., Concrete for Environmental Structures, Concrete International, April 2004.

De Larrad, F., Acker, P., and Le Roy, R. "Chapter 3- Shrinkage Creep and thermal Properties" in High Performance Concrete and Applications, ed. Shah, S.P., and Ahmad, S.H., Edward Arnold, Great Britain, 1994, pp. 65-114.

Gambhir, M., Concrete technology, Third Edition, Civil Engineering Series, 2004.

Hanh, P. and Tuan, N., High Performance Concrete Used for Marine Gravity Concrete Works, The 3rd ACF International Conference ACF/VCA 2008.

Hooton, R., Influence of Silica Fume Replacement on Physical Properties and Resistance to Sulfate Attack, Freezing and Thawing, and Alkali-Silica Reactivity, ACI Materials Journal, Vol. 90, No. 2, March-April 1993, pp. 143-151.

المواصفة القياسية العراقية رقم (5) لسنة 1984
"الاسمنت البورتلاندي"الجهاز المركزي للتقييس والسيطرة النوعية.

Moufaq, J., Effects of Petroleum Products on Civil Engineering Structures, Editor, National Center for Construction Labs, July 1998.

Nyugen, V., Colina, H., Torrenti,J., Baulay, C.and Nedjer, B., Chemo-Mechanical Coupling of Leached Concrete Part 1: Experimental Results, Nuclear Engineering and Design, 2007, pp. 2083–2089.

VSL International LTD, Concrete Storage Structures, Berne/ Switzerland,use of the VSL special construction methods, may 1983.

Table 1 Chemical composition of cement

Physical properties	Fineness (m^2/Kg)	Setting time (hrs:min)		Compressive strength (MPa)		Expansion (%)
		Initial set.	Final set.	3 days	7 days	
Test result	341	2:35	4:45	18.8	23.3	0.03
Limits of I.S. No.5/1984	≥ 230	≥ 00:45	≤ 10:00	≥ 15.00	≥ 23.00	≤ 0.8

Table 2 Physical properties of cement

Oxide composition	CaO	$Si0_2$	Al_20_3	Fe_20_3	MgO	$S0_3$	I.R	L.O.I	L.S.F	C_3S	C_2S	C_3A	C_4AF
% by weight	60.78	20.54	5.88	3.28	1.93	1.87	0.15	3.31	0.89	41.74	27.48	10.04	9.97
Limits of I.S. No. 5/1984					≤ 5.0	≤ 2.8	≤ 1.5	≤ 4.0	0.66-1.02				

Table 3 Sieve analysis of sand

Sieve size (mm)	10	5	2.36	1.18	0.60	0.30	0.15
Cumulative % passing	100	97.44	91.65	78.37	37.21	19.08	3..01
ASTM C33-03	100	95-100	80-100	50-85	25-60	10-30	2-10

Table 4 Physical properties of sand

Physical properties	Specific gravity	Sulfate content	Absorption
Test results	2.64	0.05%	0.80%
Limits of I.S. No.45/1984	-	≤ 0.5%	-

Table 5 Sieve analysis of gravel

Sieve size (mm)	25	20	10	5	2.36
Cumulative % passing	100	94.26	37.35	2.87	1.12
ASTM C33-03	100	90-100	20-55	0-10	0-5

Table 6 Physical properties of gravel

Physical properties	Specific gravity	Sulfate content	Absorption
Test results	2.65	0.1%	0.72%
Limits of I.S. No.45/1984	-	≤ 0.1%	-

Table 7 Chemical analysis of silica fume

Oxide composition	Oxide content %	ASTM C1240-03
SiO_2	88.3	≥ 85%
Al_2O_3	0.35	
Fe_2O_3	1.17	
MgO	2.4	
CaO	1.25	
SO_3	0.91	
Na_2O	1.37	
L.O.I	3.78	≤ 6%

Table 8 Physical properties of silica fume

Property	Result
Specific gravity	2. 16
Fineness	16 m^2/g
Physical form	powder
Colour	grey

Table 9 Technical description of superplasticizer

Appearance	Liquid
Colour	Brown
Specific gravity	1.1
Chloride content	nil
Air entraining	Does not entrain air
Compatibility with cement	all types of Portland cement
Shelf life	Up to 2 years

Table 10 Mix proportions used

Symbol Mix	W/B (%)	Unit Weight (Kg/m^3)					SP (L/m^3)	Slump (mm)
		Water	Binder		Fine Aggregate	Coarse Aggregate		
			Cement	Silica Fume				
HPC3	31	174	533.9	28.1	750	882	3	170
HPC5	31	174	533.9	28.1	750	882	5	186

Table 11 Results of weight and compressive strength test for concrete specimens

Mix	Symbol	Weight (Kg)			Compressive strength (MPa)		
		7 days	28 days	90 days	7 days	28 days	90 days
HPC3	W3	8.07	8.26	8.35	44.46	51.91	59.53
	K3	7.92	8.11	8.14	41.34	45.27	48.11
	G3	7.98	8.12	8.19	42.25	46.88	49.60
HPC5	W5	8.13	8.30	8.42	56.56	62.02	69.70
	K5	7.79	8.01	8.15	52.21	56.73	59.79
	G5	7.96	8.06	8.16	54.97	58.01	60.08

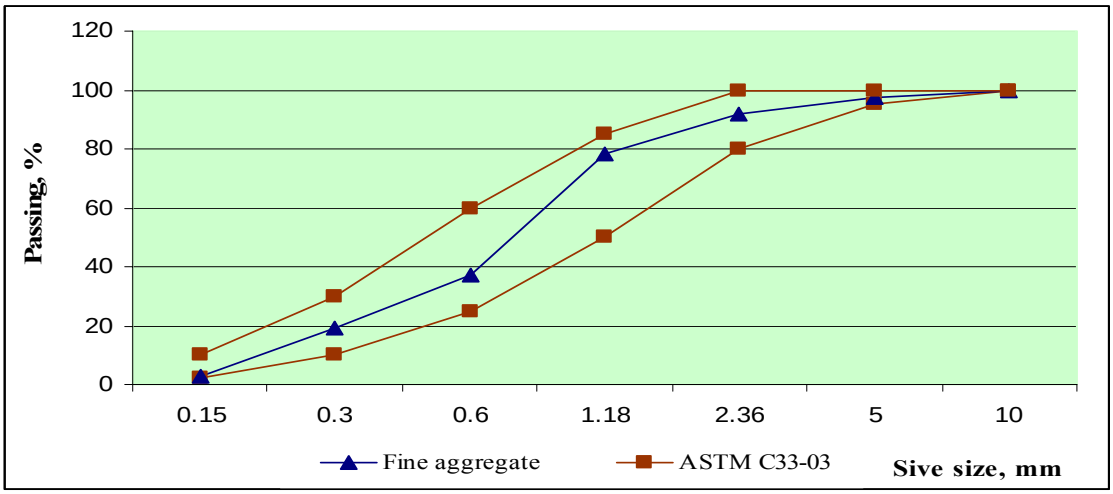

Fig.1 Grading curve for fine aggregate

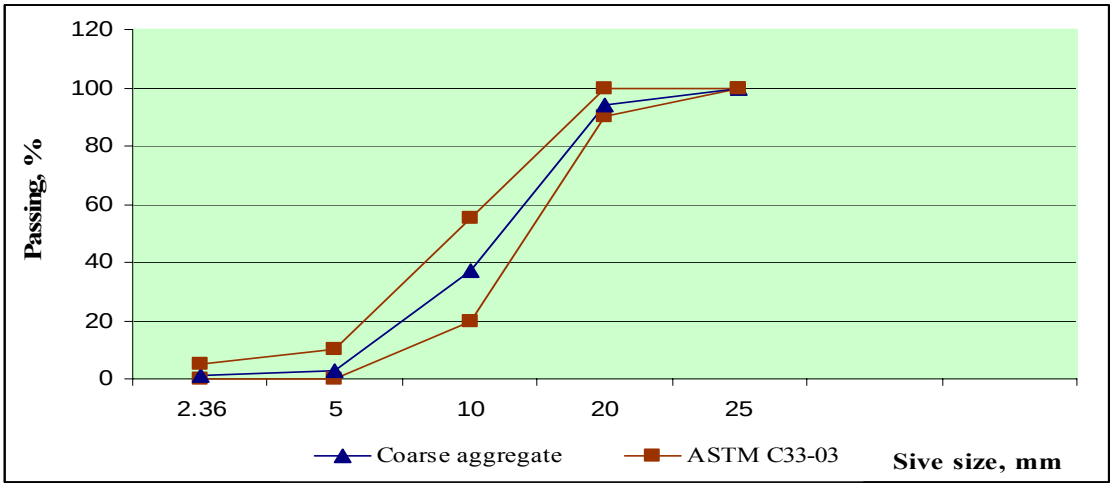

Fig.2 Grading curve for coarse aggregate

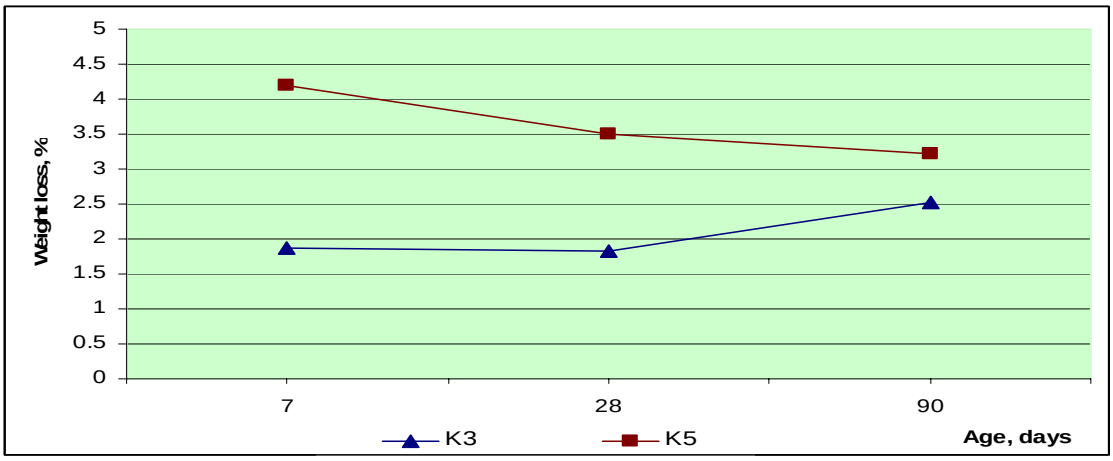

Fig. 3 Weight loss of concrete specimens immersed in kerosene as a percent to their corresponding specimens cured in water

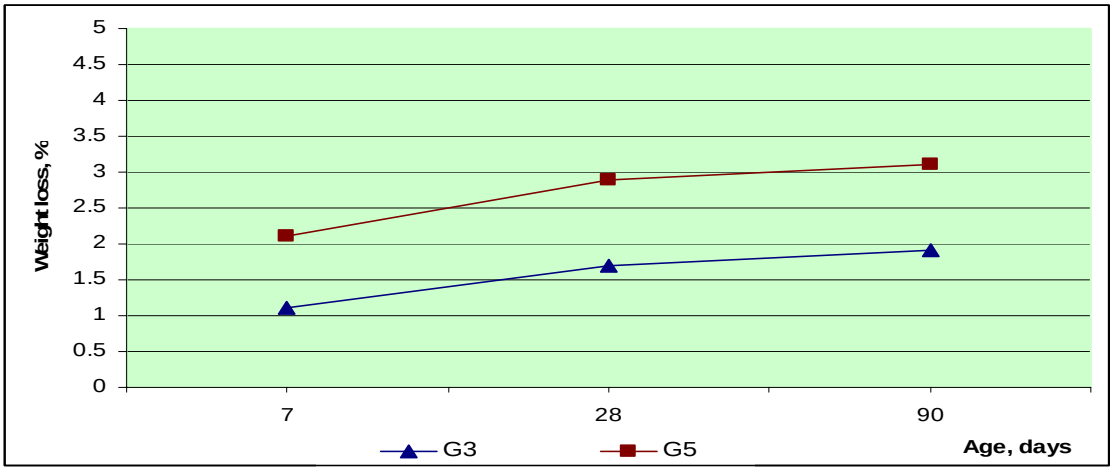

Fig. 4 Weight loss of concrete specimens immersed in gasoline as a percent to their corresponding specimens cured in water

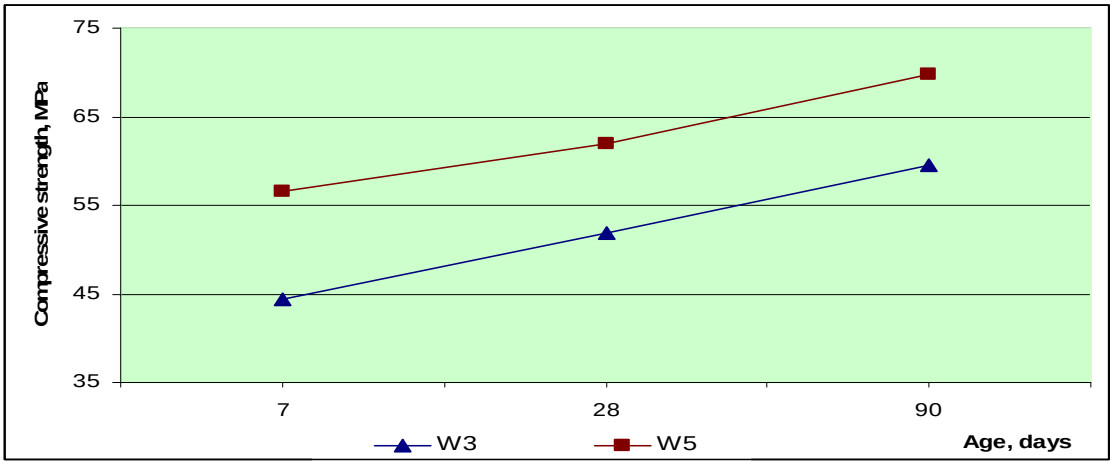

Fig. 5 Effect of SP on compressive strength of concrete specimens cured in water

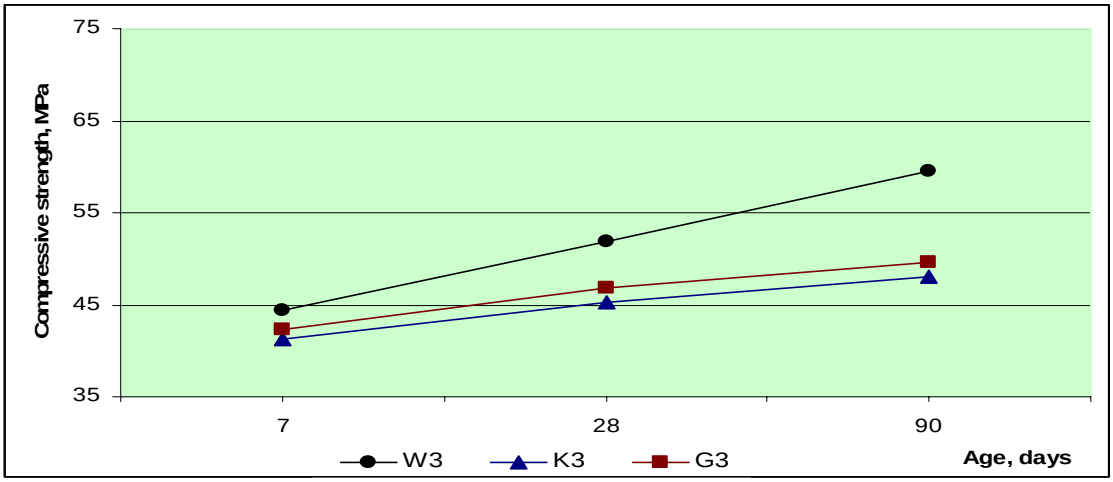

Fig. 6 Effect of kerosene and gasoline on compressive strength of HPC3

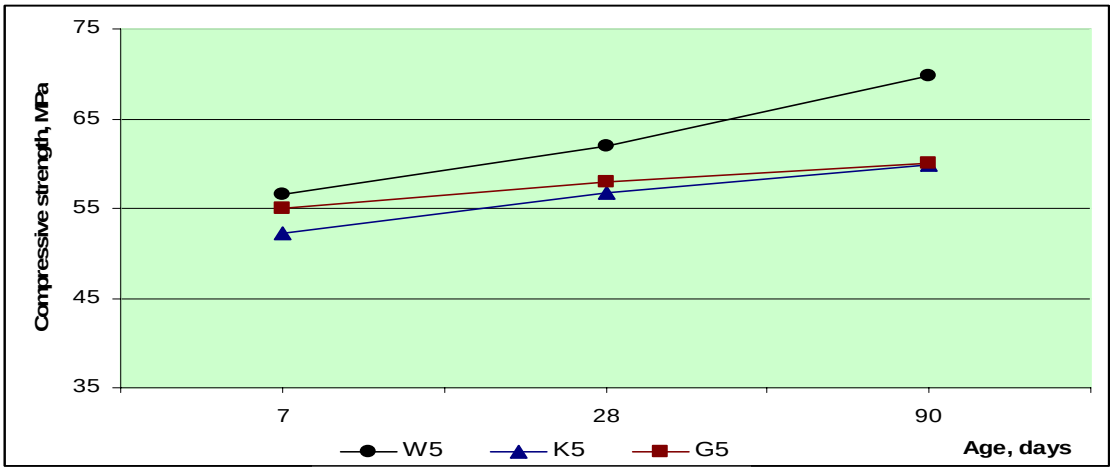

Fig. 7 Effect of kerosene and gasoline on compressive strength of HPC5

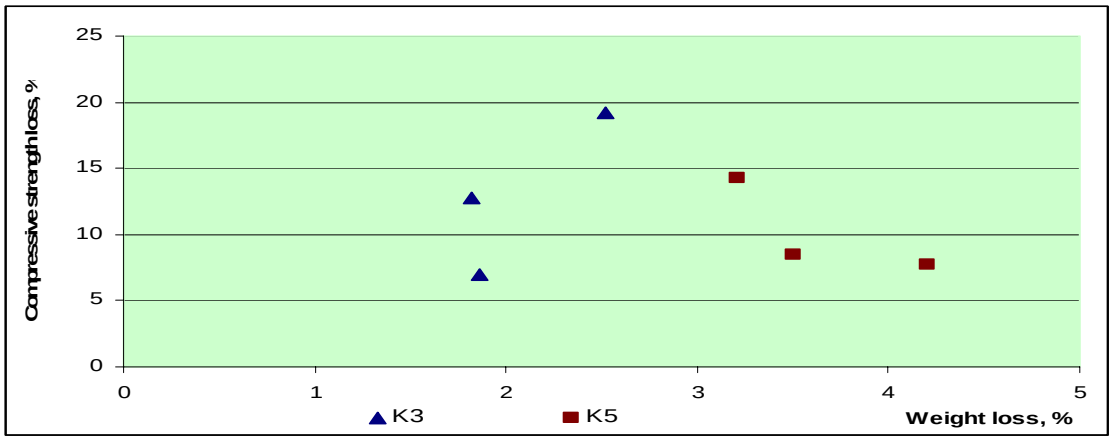

Fig. 8 Compressive strength loss versus weight loss after 12 weeks of exposure to kerosene as a percent to their corresponding specimens cured in water

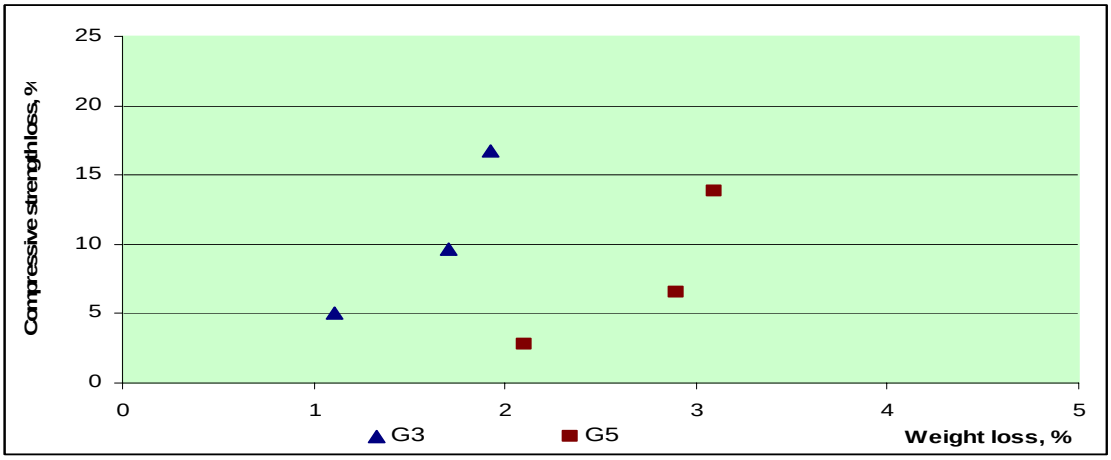

Fig. 9 Compressive strength loss versus weight loss after 12 weeks of exposure to gasoline as a percent to their corresponding specimens cured in wate